# Remote Sensing as a Precision Farming Tool in the Nile Valley, Egypt

**By**

**Adel Mohamed Helal Elmetwalli**

Submitted to the School of Biological and Environmental Sciences

University of Stirling

November 2008

For the degree of Doctor of Philosophy

Supervisors: Dr. A.N. Tyler and Dr. C.A. Salt

UNIVERSITY OF STIRLING

This research was undertaken at the School of Biological and Environmental Sciences, University of Stirling, Stirling, FK9 4LA, UK

# STATEMENT OF ORIGINALITY

The work in this thesis is to the best of my knowledge, original. The author hereby declares that the contents of this thesis have not been submitted, either in whole or in part, for a degree of any kind at this or any other academic institution.

Adel Elmetwalli

November 2008

# DEDICATION

My father and mother, Mohamed and Fouzia

My beloved wife, Rasha

My lovely boys, Mohamed and Omar

# ABSTRACT

Detecting stress in plants resulting from different stressors including nitrogen deficiency, salinity, moisture, contamination and diseases, is crucial in crop production. In the Nile Valley, crop production is hindered perhaps more fundamentally by issues of water supply and salinity. Predicting stress in crops by conventional methods is tedious, laborious and costly and is perhaps unreliable in providing a spatial context of stress patterns. Accurate and quick monitoring techniques for crop status to detect stress in crops at early growth stages are needed to maximize crop productivity. In this context, remotely sensed data may provide a useful tool in precision farming. This research aims to evaluate the role of *in situ* hyperspectral and high spatial resolution satellite remote sensing data to detect stress in wheat and maize crops and assess whether moisture induced stress can be distinguished from salinity induced stress spectrally.

A series of five greenhouse based experiments on wheat and maize were undertaken subjecting both crops to a range of salinity and moisture stress levels. Spectroradiometry measurements were collected at different growth stages of each crop to assess the relationship between crop biophysical and biochemical properties and reflectance measurements from plant canopies. Additionally, high spatial resolution satellite images including two QuickBird, one ASTER and two SPOT HRV were acquired in south-west Alexandria, Egypt to assess the potential of high spectral and spatial resolution satellite imagery to detect stress in wheat and maize at local and regional scales. Two field work visits were conducted in Egypt to collect ground reference data and coupled with Hyperion imagery acquisition, during winter and summer seasons of 2007 in March (8-30: wheat) and July (12-17: maize). Despite efforts, Hyperion imagery was not acquired due to factors out with the control of this research.

Strong significant correlations between crop properties and different vegetation indices derived from both ground based and satellite platforms were observed. RDVI showed a sensitive index to different wheat properties ($r > 0.90$ with different biophysical properties). In maize, $GNDVI_{br}$ and $C_{green}$ had strong significant correlations with maize biophysical properties ($r > 0.80$). PCA showed the possibility to distinguish between moisture and salinity induced stress at the grain filling stages.

The results further showed that a combined approach of high (2-5 m) and moderate (15-20) spatial resolution satellite imagery can provide a better mechanistic interpretation of the distribution and sources of stress, despite the typical small size of fields (20-50 m scale). QuickBird imagery successfully detects stress within field and local scales, whereas SPOT HRV imagery is useful in detecting stress at a regional scale, and therefore, can be a robust tool in identifying issues of crop management at a regional scale. Due to the limited spectral capabilities of high spatial resolution images, distinguishing different sources of stress is not directly possible, and therefore, hyperspectral satellite imagery (e.g. Hyperion or HyspIRI) is required to distinguish between moisture and salinity induced stress.

It is evident from the results that remotely sensed data acquired by both *in situ* hyperspectral and high spatial resolution satellite remote sensing can be used as a useful tool in precision farming in the Nile Valley, Egypt. A combined approach of using reliable high spatial and spectral satellite remote sensing data could provide better insight about stress at local and regional scales. Using this technique as a precision farming and management tool will lead to improved crop productivity by limiting stress and consequently provide a valuable tool in combating issues of food supply at a time of rapid population growth.

# ACKNOWLEDGEMENT

First of all, I would like to thank Allah for supporting me throughout my life. Secondly, I am very grateful to my main supervisor Dr Andrew Tyler for all his guidance, encouragement, friendship and support throughout my research project. Dr Andrew has given tremendous support, encouragement and mentoring for this study, and my professional development. A big thank you to Dr Carol Salt for her guidance, encouragement and support, it is very much appreciated. I am also grateful to the Egyptian Government for funding my research project. I would like to extend my appreciation to Dr Peter Hunter for all his help during the course of my Ph.D particularly analysing and processing satellite data.

I would like also to thank the wonderful team of technicians within the department of School of Biological and Environmental Sciences, at the University of Stirling, in particular Scot, and John MacArthur for solving computer problems over the last four years, Bill Jamieson for solving problems with cartographic, Stuart Bradley, for helping with my greenhouse experiments, Helen for helping in labs, and James for setting up the darkroom in the greenhouses.

Also, I should say thank you to all my friends, colleagues at the School of Biological and Environmental sciences in particular all my formal and current office mates; special thanks to Tory Milner for her friendship and help during my Ph.D, Joe, Richard, Crona, Stuart, and David for all their help, friendship and encouragement during my research project.

Last not least, I would like to express my appreciation to all my family particularly to my supportive parents, Mohamed and Fouzia, my beloved wife, Rasha for her love, support, patience and encouragement during my Ph.D. Finally, I would like to say thank you to my lovely boys Mohamed and Omar who made me happy all the time.

# TABLE OF CONTENTS

# LIST OF FIGURES

# LIST OF TABLES

# LIST OF ABREVIATIONS

| | |
|---|---|
| **ANN** | Artificial Neural Network |
| **ANOVA** | Analysis of Variance |
| **ASD** | Analytical Spectral Device |
| **ASTER** | Advanced Spaceborne Thermal Emission and Reflection Radiometer |
| **AVHRR** | Advanced Very High Resolution Radiometer |
| **AVIRIS** | Airborne Visible-Infrared Imaging Spectrometry |
| **AWC** | Available Water Content |
| **CASI** | Compact Airborne Spectrographic Imager |
| **CCD** | Charge Couple Device |
| **CIMMYT** | Centre Internacional de Mejoramiento de Maiz Y Trigo |
| **DAS** | Days After Sowing |
| **DVI** | Difference Vegetation Index |
| **EC** | Electrical Conductivity |
| **EO-1** | Earth Observing 1 |
| **EOC** | Electro Optical Camera |
| **EOS** | Earth Observation System |
| **FAO** | Food and Agricultural Organization |
| **FC** | Field Capacity |
| **FOV** | Field of View |
| **FPAR** | Fraction of Incident Photosynthetically Active Radiation absorbed by vegetation |
| **GNDVI** | Green Normalized Difference Vegetation Index |
| **GMT** | Greenwich Mean Time |
| **GPS** | Global Positioning System |
| **GVI** | Green Vegetation Index |
| **GIS** | Geographical Information System |

| | |
|---|---|
| **GCP** | Ground Control Point |
| **HPLC** | High Performance Liquid Chromatography |
| **HRV** | High Resolution Visible |
| **IPVI** | Infra-red Percentage Vegetation Index |
| **IRT** | Infrared Thermometer |
| **K** | Potassium fertilizer |
| **LAD** | Leaf Angle Distribution |
| **LAI** | Leaf Area Index |
| **LMI** | Leaf Moisture Index |
| **MDC** | Minimum Distance Classification |
| **MERIS** | Medium Resolution Imaging Spectrometer |
| **METI** | Ministry of Economy Trade and Industry |
| **MISR** | Multi-angle Imaging SpectroRadiometer |
| **MLC** | Maximum Likelihood Classification |
| **MODIS** | Moderate Resolution Imaging Spectrometer |
| **N** | Nitrogen |
| **NASA** | National Aeronautics and Space Administration |
| **NDVI** | Normalized Difference Vegetation Index |
| **NDWI** | Normalized Difference Water Index |
| **NIR** | Near Infrared |
| **NNI** | Nitrogen Nutrition Index |
| **NOAA** | National Oceanic and Atmospheric Administration |
| **NPCI** | Normalized Pigment Chlorophyll Index |
| **OSAVI** | Optimized Soil Adjusted Vegetation Index |
| **PCA** | Principle Component Analysis |
| **PRI** | Physiological Reflectance Index |
| **PSR** | Pigment Simple Ratio |

| | |
|---|---|
| **PWC** | Plant Water Content |
| **r** | Coefficient of correlation |
| **$R^2$** | Coefficient of determination |
| **REP** | Red Edge Position |
| **RMSE** | Root Mean Square Error |
| **RDVI** | Renormalized Difference Vegetation Index |
| **RVI** | Ratio Vegetation index |
| **SAR** | Sodium Adsorption Ratio |
| **SAVI** | Soil Adjusted Vegetation Index |
| **SAVI2** | Second Soil Adjusted Vegetation Index |
| **SeaWiFS** | Sea-Viewing Wide Field-of-View Sensor |
| **SI** | Stress Index |
| **SIPI** | Structural Independent Pigment Index |
| **SLAVI** | Specific Leaf Area Vegetation Index |
| **SPOT** | Satellite Pour L'Observation de la Terre |
| **SWIR** | Shortwave Infrared |
| **SZA** | Sun Zenith Angle |
| **TDS** | Total Dissolved Salts |
| **TIR** | Thermal Infrared |
| **TM** | Thematic Mapper |
| **VARI** | Visible Atmospheric Resistant Index |
| **VIS** | Visible range of the spectrum |
| **VNIR** | Very Near Infrared |
| **WBI** | Water Band Index |
| **WI** | Water Index |
| **YI** | Yellowness Index |

# 1 INTRODUCTION

## 1.1 Research Rationale

The shortage of good quality water resources has become an important issue in arid and semi-arid regions. For this reason the availability of water resources of marginal quality such as drainage water, wastewater, saline ground water and agricultural drainage water has become an important consideration in supplementing supply. The efficiency of water usage within irrigated sectors is generally low and significant savings could be achieved through more careful management of water resources. Jones (1999) reported that the major limiting factor in crop productivity is water. Crop water needs must, therefore be satisfied (Penuelas *et al*., 1992).

Water is becoming a major topic of discussion on national and international scales. Globally, 73% of all fresh water used is for irrigation, another 21% is used by the industrial sector and the remaining 6% used is for domestic purposes (Gonzalez, 1998). To emphasise its importance in regions such as Middle East water may become synonymous with power. The population density of Egypt doubled in the last three decades with an average annual growth rate of 1.8% without increasing in land and water resources (Hamza and Mason, 2004). The River Nile is the main source of water in Egypt providing more than 95% of the total water used. Egypt's annual quota of the Nile water is 55.5 billion cubic meters (El-Wakeel and El-Mowelhi, 1993) distributed across a range of requirements including agriculture, domestic and industry. Besides a rapidly increasing population, Egypt's water requirements have further increased as a result of new irrigation networks required by land reclamation projects and a new valley project where water will be pumped from Lake Nasser and transported hundreds of miles away to its Western Desert.

In the future, the demand for water will increase and it is predicted that the quantity of Nile water will no longer be sufficient to meet the demand within the next 25 years in terms of industrial development and agricultural expansion that together consume the highest proportion of more than 85% of the water withdrawal from the Nile (Hamza and Manson, 2004). The pressure is therefore on the Egyptian Government to look for other sources of water even low quality water, or use new techniques to use the limited resources more efficiently. Irrigation is vital to insure the essential moisture

for plant growth. In addition, Egypt is a unique case concerning irrigation as most agricultural lands are under irrigation because rainfall is not sufficient for growing crops. Cereal crops occupied approximately 670 million hectares worldwide during the year 2000 (FAO, 2005). Current increases in area under agriculture occur at the expense of natural ecosystems. Thus, increasing agricultural productivity without substantial modifying the natural ecosystem is a top priority. As successful plant biotechnologies have been developed; around the world researchers are examining a wide range of possibilities for improving the productivity of crops, ranging from developing crops with resistance to herbicides and insect pests, to crops with an increased ability to withstand drought, frost or salinity. In addition, new techniques (remote sensing and precision agriculture) are leading to better methods of producing and managing agricultural products, but primarily within the developed world.

Remote sensing has been used to monitor vegetation for a few decades. It provides timely information over large areas of economic importance for example wheat and maize crops (Penuelas and Inoue, 1999; Osborne *et al*., 2002a; Ozturk & Aydin, 2004; Sclemmer *et al*., 2005; Clay *et al*., 2006; Hong *et al*., 2007). Crop health and productivity can be estimated by almost instantaneous non-destructive data acquisition over vast areas (Clevers, 1997). Also, the innovative technique of airborne remote sensing can provide valuable information in crop stress management (Steven 1993, Reyniers *et al*., 2004). Such timely information concerning crop productivity is of vital importance for decision makers, from small-scale farmers to the national government, providing a potential way forward for increasing crop productivity whilst using water resources more efficiently.

Salinity and drought are major inhibitors to agronomic production and increasing efforts to remotely detect the effects of both moisture and salinity induced stress for irrigation management are needed since few studies have quantitatively assessed the ability of remote sensing technology to characterise simultaneous water and salinity stress on crop yields (Poss *et al*., 2006). Irrigation and water salinity management practices need to be adjusted to decrease the excessive losses of water and control the salinity in the root zone at the optimum level by adding proper application rates of water. Monitoring water and salinity status has traditionally been based on destructive sampling. Furthermore, monitoring plant status using sample-point technique is

tedious, laborious and a costly process. A promising alternative is the use of remotely sensed measurements as a quick, reliable and non-destructive tool that integrates the plant response to water and salinity stresses.

Remote sensing technology (aircraft-based) is currently being used as a management tool in precision farming. However, there is a need for a ground-based remote sensing system to provide quick and accurate prediction of water and salinity stresses. Quantitative estimations of plant biochemical and biophysical variables can be achieved by the measurement of reflected radiation from plant leaves and canopies (Carter, 1994; Penuelas *et al*., 1994). The pattern and the intensity of plant canopy reflected radiation, especially in the visible (VIS) and NIR, depend mainly on the biochemical content and vegetation amount of the plant (Fernandez *et al*., 1994).

Vegetation indices based on remote sensing have been acquired with ground, airborne and satellite systems (Penuelas and Filella, 1998). Narrow-band (hyperspectral) indices were shown to be more accurate than broad band indices in terms of correlating with plant biochemical data, because small physiological changes are mostly detectable at specific wavelengths (Penuelas *et al*., 1994). These indices can contrast reflectance from the same range, or from two different ranges mainly the VIS and NIR via different mathematical formulae. Normalized Difference vegetation Index (NDVI), Simple Ratio (SR), Soil Adjusted Vegetation Index (SAVI) and Water Band Index (WBI) have been widely used by remote sensing scientists to quantify green biomass, health status and water content etc. (Penuelas *et al*., 1994; Gamon *et al*., 1995).

Spectral reflectance between 680-780 nm, defined as the red edge spectrum has been used to assess chlorophyll concentration, nitrogen and water stress (Filella and Penuelas, 1994). It has been found that the NIR bands at 900 and 970 nm are sensitive to crop moisture conditions and were used for early water stress detection (Penuelas *et al*., 1996). Therefore, the relative change in the reflected light energy from the plant canopy could be used as a key link between various combinations of stress. However, little work has been done on the influence of salinity induced stress on the expected properties of vegetation and whether its influence can be distinguished from moisture induced stress.

## 1.2 Aims and objectives

The overall aim of this study is to investigate the potential of *in situ* hyperspectral and satellite remote sensing in detecting stress in wheat and maize to help manage limited water and land resources to maximise crop production. The study examines the crop response to moisture and salinity induced stress through controlled greenhouse based experiments followed by field visits in Egypt coupled with RS acquisition. The following objectives are set out to achieve the aims of this research.

The objectives of this study:

- To grow wheat and maize crops in controlled greenhouse conditions with sufficient number of replications to demonstrate whether moisture or salinity induced stress has a distinguishable influence on plant health (biophysical and biochemical properties).

- From time series hyperspectral measurements of a sample of the greenhouse wheat and maize crops, simulate broad band and hyperspectral satellite remote sensing capabilities to evaluate the ability to measure plant health and differentiate moisture and salinity induced stress.

- Undertake ground reference data collection in Egypt of wheat (March 2007) and maize (July 2007) crops including *in situ* hyperspectral measurements, soil sample collection for determining moisture, salinity, nitrogen concentration, pH, GPS coordinates, biometric measurements and total chlorophyll concentration.

- Apply the empirically determined/calibrations to satellite images to evaluate the capability of monitoring crop health status and causes of stress (moisture and salinity).

- Evaluate the potential effectiveness and value of implementing remote sensing technologies for precision farming and effective resources management in Egypt.

# 2 LITERATURE REVIEW

## 2.1 Introduction

This chapter mainly focuses further on the issues of crop production in Egypt and the remote detection of plant and crop stress. Remotely sensed data can be acquired at different levels including *in-situ*, airborne and satellite remote sensing. Much research has utilised remote sensing techniques for monitoring vegetation and plant health including crop productivity, biophysical properties such as aboveground biomass, leaf area index, grain yield and biochemical properties such as chlorophyll *a* concentration and other pigments. This chapter's aim is to investigate the factors causing stress in crops in particular wheat and maize in the Egyptian context and draws together the possibility of using both *in situ* hyperspectral measurements and high spectral and spatial resolution satellite remote sensing in detecting crop stress.

## 2.2 Cultivated land and crop production in Egypt

### 2.2.1 Overview

Population in Egypt is growing very rapidly as Egypt's population density has doubled during the last three decades (Hamza and Manson, 2004). The total agricultural land in Egypt is estimated at 3.5 million hectare which presents around 3.3 percent of the whole land mass of Egypt (FAO, 2005). As at present 5.4% of land resources in Egypt is qualified as excellent, while about 40% of either poor or of low quality, mainly due to issues of salinity, water logging and sodicity. Crop productivity for some crops such as maize has improved during the last three decades by 82% (FAO, 2005), relying on the introduction of the earlier maturing varieties of different crops, mechanization, modern irrigation techniques and new monitoring systems for plant status.

In Egypt, the main field crops are maize, rice and cotton during the summer season and wheat, clover and bean during the winter season. Cereal production represents about 50% of the value of field crops, occupying about 2.72 million ha of the whole cropped area. Wheat occupies approximately 1.26, maize 0.88, rice 0.59, sorghum 0.15 and barley 0.19 million ha (FAO, 2005). Wheat is considered the most important crop and the Egyptian Government gives priority to wheat production providing farmers with varieties which tolerate different types of stress. Wheat production has

improved a lot during the last three decades. Despite these improvements in wheat production, new techniques are still needed to increase crop productivity to sustain rapid population growth. The government also supplies farmers with high yielding varieties of maize such as Single Cross 10 which is imported from the USA.

### 2.2.2 Production of wheat

Wheat is a very adaptable crop grown from the Arctic Circle to the equator, from sea level to 3000 m, and in areas with between 250 to 1800 mm of annual rainfall. Wheat is, however, best suited to areas between $30^{o}$ and $50^{o}$ N, and $25^{o}$ and $40^{o}$ S latitude (Stoskopf, 1992). Despite the substantial increases in wheat production achieved globally over the last 50 years, further increases are required to meet the demands of the rapid population growth. An average projection is for world population to reach 8.3 billion by the year 2025, before possibly stabilizing at about 10 billion towards 2100 (Gooding and Davis, 1997). With constant per capita food consumption, therefore, yield needs to be 57% higher in 2025 compared with 1990 (Gooding Davis, 1997).

According to Klapp (1967) the most favourable climate for wheat would be a mild winter followed by a warmer summer with high radiation without excessive cooling summer rains and the optimum temperature for growth is usually within the narrow range of 20-25 $^{o}$C (min 2 $^{o}$C – max 30 $^{o}$C). Ideal annual rainfall can vary widely, between 250-1000 mm depending on season and stage of growth (Stoskopf, 1992). The optimum sowing depth of wheat is, like that of most crops, a compromise and commonly ranges from about 2.5-10 cm. Wibberley (1989) suggests that 3 cm is ideal for cereals for most temperature soil conditions. Sowing deeply reduce the risk of the seed being eaten, particularly by birds.

There are several published scales of cereal development that describe particular developmental stages defined by the external appearance and usually supplemented by a diagram. These include Zadoks scale, Feeks scale and Agricultural Development and Advisory scale (Zadoks *et al*., 1974; Wibberley, 1989). Among these scales, Zadoks is the most commonly used scale. Table 2.1 shows the Zadoks scale for identifying wheat developmental stages.

**Table 2-1**The decimal growth stage score for cereal development (Zadoks *et al*., 1974).

| Zadoks Scale | Growth Stage | Zadoks Scale | Growth Stage |
|---|---|---|---|
| | **Germination** | | **Booting** |
| 0.0 | Dry seed | 4.1 | Early booting |
| 0.1 | Start of water imbibitions | 4.3 | Mid booting |
| 0.3 | Complete imbibitions | 4.5 | Late boot stage |
| 0.4 | Radical emerged from caryopsis | 4.7 | Flag leaf sheath opening |
| 0.7 | Coleoptile emerged from caryopsis | 4.9 | 1st awns visible |
| 0.9 | Leaf at coleoptiles tip | | **Ear emergence** |
| | **Seedling development** | 5.1 | 1st spikelet visible |
| 1.0 | 1st leaf through coleoptile | 5.3 | ¼ of ear emerged (10.2) |
| 1.1 | 1st leaf unfolded | 5.5 | ½ of ear emerged (10.3) |
| 1.2 | 2nd leaf unfolded etc. i.e | 5.7 | ¾ of ear emerged (10.4) |
| 1.n | nth leaf unfolded (where n<9) | 5.9 | Ear completely emerged (10.5) |
| 1.9 | 9 or more leaves unfolded | | **Anthesis** |
| | **Tillering** | 6.1 | Beginning of anthesis |
| 2.0 | No tillers | 6.5 | Halfway through anthesis |
| 2.1 | Main shoot and one tiller | 6.9 | Anthesis complete |
| 2.2 | Main shoot and two tillers | | **Milk development** |
| 2.n | Main shoot and n tillers (n<9) | 7.1 | Water ripe |
| 2.9 | 9 or more tillers unfolded | 7.5 | Mid milk ripe (11.1) |
| | **Stem elongation** | | **Dough development** |
| 3.0 | Pseudo stem erect(4-5) | 8.5 | Early dough (11.2) |
| 3.1 | 1st node detectable (6) | 8.7 | Late dough |
| 3.2 | 2nd node detectable (7) | | **Ripening** |
| 3.n | nth node detectable (n<7) | 9.1 | Grain hard (difficult to divide) |
| 3.7 | Flag leaf just visible (8) | 9.2 | Grain hard (11.4) |
| 3.9 | Flag leaf ligule just visible (9) | | Grain loosening in daytime |

### 2.2.3 Production of maize

Besides wheat and rice, maize is considered the world's third most important cereal crop. In Africa maize is grown over a wide range of environmental and geographical regions ranging from lowland (Niger's northern Sahel), mid altitude and Ethiopia's sub-tropical high land environments to converted frost lands of Sierra Leone (Zaidi, 2004). Maize is mainly grown in Egypt in the summer season between May and September at small scales by most farmers in the Nile Delta and Valley. Maize production has increased from 3.35 million tonnes in 1982 to 6.1 million tonnes in

2002 (FAO, 2005) as a result of using high yielding varieties and hybrids exported from other countries such as USA. At a very small scale some farmers grow maize between August and December following vegetable crops like tomato, melon and watermelon.

**Maize growth stages and development**

There are several systems for identifying maize growth stages, the most common being Iowa State's system (Ritchie *et al*., 1992). This system divides plant development into vegetative (V) and reproductive stages (R). Subdivisions of the V stages are designated numerically as $V_1$, $V_2$, $V_3$, etc. through $V_n$, where n represents the last leaf stage before $V_T$ for the specific hybrid under consideration. The first and last V stages are designated as $V_E$ (Emergency) and $V_T$ (Tasseling). The n will fluctuate with hybrid and environmental differences. The six subdivisions of reproductive stages are designated numerically with their common names (Table 2.2)

**Table 2-2** different growth stages for maize crop (Ritchie *et al*., 1992).

| Growth stage | Description |
|---|---|
| *Vegetative stages* | |
| VE, emergency stage | Coleoptile emerges from soil surface |
| V1, first leaf stage | The collar of the first leaf is visible |
| V2, second leaf | The collar of the second leaf is visible |
| V3, third leaf | The collar of the third leaf is visible |
| V6, sixth leaf | The collar of the sixth leaf is visible |
| V9, ninth leaf | The collar of the ninth leaf is visible |
| V12, twelfth leaf | The collar of the twelfth leaf is visible |
| V15, fifteenth leaf | The collar of the fifteenth leaf is visible |
| V18, eighteenth leaf | The collar of the eighteenth leaf is visible |
| VT, tasseling stage | The last branch of the tassel is completely visible |
| *Reproductive stages* | |
| R1, silking stage | Silks are visible on 50% of the plants |
| R2, blister stage | Kernels are filled with clear fluid and the embryo can be seen |
| R3, milk stage | Kernels are filled with a white, milky, fluid |
| R4, dough stage | Kernels are filled with a white paste |
| R5, dent stage | The top part of the kernels are filled with solid starch |
| R6, physiological maturity | The back layer is visible at the base of the grain, grain moisture is usually 35% |

### 2.2.4 Socioeconomic pressure on crop production

Wheat provides a major source of energy, protein and dietary fibres in human nutrition. Despite successful attempts to increase local wheat production as mentioned previously, Egypt continues to import wheat from amongst the USA, Australia and

Russia due to rapid population growth. The Egyptian Government has undertaken a massive effort to improve wheat production by supplying farmers with high yielding stress-tolerant varieties (drought, salinity, disease, etc.) but the country is still only 40% self-sufficient. The reasons are: a) the limited cultivated area as the land cultivated with wheat in Egypt estimated at almost 1.26 million hectare and that is to rise by an additional 150 thousands, which represents nearly half of the cultivated land in Egypt, b) the rapid population growth particularly in the second half of the twentieth century with nearly the same cultivated area. Given the need to increase wheat production, it is important to use limited water and land resources very efficiently by using highly productive varieties, modern irrigation systems, stress tolerant varieties, expanding the cultivated area by using ground water and agricultural drainage water, which has been estimated at 17 billion cubic meter and using new techniques for monitoring crops such as remote sensing.

### 2.2.5 Climate change and crop production

Agricultural production and climate are closely linked, which means any change in climate will affect agricultural production. Climate change will affect the production directly and indirectly, for example, increasing temperature in a specific region will increase evapotranspiration, and therefore, the water requirements of crops especially summer crops. The length of the growing seasons and tolerance to pests and diseases will also be affected. Egypt is located in an arid region and climate change reduces crop production due to increased demand for water. Moreover, with increasing temperature, the amount of water delivered by the Nile will most likely decrease. Although agricultural production per unit area has increased substantially over the last few decades, further increases are limited by the availability of water and energy resources, land degradation and desertification, which affect the fertile lands for agricultural production.

Many researchers studied the climate change impacts on crop production in Egypt. El-Raey *et al*. (1995) reported that land losses of 12 to 15% of Egypt's current arable land as a result of a one meter sea-level rise. Nicholls and Leatherman (1995) estimated that a mean of 1 meter global sea-level rise by 2100 would give rise to a 0.37 meter sea level rise at the Nile Delta. Increased temperature as a result of climate change would increase evapotransipiration for most crops, which is likely to increase

crop water requirements and lower crop yields (Eid and Saleh, 1992). In addition, water flows from the Nile could be affected by upstream development in countries within the Nile basin such as Sudan and Ethiopia.

### 2.2.6 Limiting factors for crop production

Globally, water is regarded as the major limiting factor that reduces crop productivity especially in arid and semi-arid regions (Jones, 1999). Paolo and Rinaldi (2008) investigated maize yield response to irrigation and nitrogen fertilization and concluded that maize productivity is highly dependent on irrigation supplies in particular in areas with water limited conditions. They also reported that irrigation was more effective than nitrogen in increasing grain yield in two successive years. Barnabas *et al*. (2008) reported that drought is one of the major limitations to food production worldwide. High temperature causes high evapotranspiration making it difficult to meet water requirements of crops (Penuelas *et al*., 1992). Drought reduces the final crop yield of maize by 36% in the low land areas and 21% in sub-tropical areas (CIMMYT, 1988). Drought at any growth stage reduces crop yield but maximum reductions occurs at the flowering stage but early growth stage and mid to late grain filling stage are also sensitive (Claasen and Shaw, 1970). Edmeades *et al*. (1992) estimated that in the developing world, annual yield losses due to drought may approach 24 million tonnes, equivalent to 17% of a normal year's production.

The second major limiting factor is salinity as the accumulation of dissolved salts in the soil water inhibits plant growth (Gorham, 1992). Flowers *et al.* (1997) reported that approximately 7% of the world's total land area is affected by salinity. Few crops are tolerant of high salinity. Most agricultural land in arid and semi-arid regions depends on irrigation for growing crops, which enhances salinity problems.

The third limiting factor is the availability of nutrients. Drought and low soil fertility are the most stresses threatening maize production in eastern and southern Africa (Banziger and Diallo, 2004). Nitrogen (N) is the most important element affecting crop grain yield and is the most limiting nutrient in crop production as cropping practices become more intensive, other nutrients will likely become limiting as well (Osborne *et al*., 2002a). Nitrogen, because of its high plant demand and variability within the soil, is the most intensively managed plant nutrient in crop production (Schlemer, *et al*., 2005). They also concluded that stresses that involve deficiencies of

nitrogen and water will adversely affect the amount of chlorophyll plants produce as well as cell turgidity.

In addition to drought, salinity and nutrients stressors, there are some biotic factors that are limiting wheat and maize production. For example in Africa maize grain yield is affected by some of these factors including; the spotted stem borer (*Chilo parellus*), Africa stem borer (*Sesamia calamistis*), stalk borer (*Busseola fusca*), and the pink stem borer (*Sesamia cretica*). The most important diseases that affect maize production are turcicum leaf blight (*Exserohilum turicicum*), common rust (*Puccinia sorghi*), gray leaf spot (*Cercospora zeae-maydis*) and the maize streak virus transmitted by Cicadulina leaf hoppers.

### 2.2.7 Water resources and use

Egypt's climate is characterized by hot dry summers and mild winters. It is a predominantly arid country and agriculture in Egypt depends on irrigation from the River Nile. The necessary increase in food production to support the annual population growth (1.8%) compels the country to use all sources of water (drainage water, groundwater and treated sewage water) for the expansion of irrigated agricultural land. Rainfall is very low, irregular and unpredictable as annual rainfall ranges from a maximum of about 200 mm in the northern coastal region to a minimum of nearly zero in the south, with an average of 51 mm.

**Agricultural water use:**

While the amount of water used for agriculture has declined slowly during the past decade, it still accounts for the largest share (85.4%). This amount does not include an annual estimated loss of 2 billion $m^3$ due to evaporation from the irrigation system (FAO, 2005). Surface irrigation system is used in most cultivated lands of the Nile Valley and Delta. Its efficiency is considered to be low as a result of deep percolation and evaporation. Excess application of water to crops contributes to problems of salinity and high water tables. It must also be noted, however, that excess irrigation water contributes to ground water, a good part of which is pumped or partially reused through cycling. The measured drainage water out of the system amounted to about 17 billion $m^3$. In the newly reclaimed lands, modern irrigation systems such as drip and sprinkler irrigation systems are used to increase the efficiency of irrigation

systems. The government does not give permits for new water to lands unless evidence is given of the use of new irrigation technologies.

**Re – use of agricultural drainage and treated waste water**

The policy of the Egyptian Government is to use drainage water (up to salinity of 4.5 dS $m^{-1}$) after it is blended with fresh Nile water. Reuse of drainage water, returned to the Nile in irrigation is estimated at 4.84 billion $m^3$ per year in 2001-2 (FAO, 2005). In fact, direct use of drainage water for irrigation with salinity from 2 to 3 dS $m^{-1}$ is common in the district of northern Delta, where there are no other alternatives or in areas of limited better water quality supply. Farmers in Beheira, Kafr-Elsheikh, Damietta and Dakhlia regions have successfully used drainage water directly for periods of 25 years to irrigate over 10000 ha of land, using traditional farming practices. The major crops include clover, rice, wheat, barley, sugar beet and cotton. Yield reduction of 25 to 30% is apparently acceptable to local farmers. Yield reductions observed are attributed to water logging and salinization resulting from over-irrigation and other forms of poor agricultural, soil and water management (Rhoades *et al*., 1992).

Agricultural drainage water in Upper Egypt is discharged back into the Nile; this affects the quality of the Nile water, where its salinity increases from 0.4 dS $m^{-1}$ in Aswan to 0.6 dS $m^{-1}$ in Cairo. Hamza and Manson (2004) reported that because of the increased food needs in Egypt, two basic strategies are possible: importing food or growing more food. They also mentioned that reuse and efficient water utilisation have the highest priorities of the Egyptian Government. According to Egyptian estimates, they state that an additional 20.9 $km^3$ $year^{-1}$ could be made available through recycling water by changing irrigation techniques, adopting water efficient crops and cropping patterns, this is equal to 30% of the water that used at present.

### 2.2.8 Water quality

The first priority when using water for irrigation is salinity levels because salinity affects both soil structure and yield productivity in the same time. Many parameters are usually used to define irrigation water quality to assess salinity hazards and determine appropriate management strategies. A complete water quality analysis will include the following:

- The total concentration of the soluble salts.
- The relative proportion of sodium to the other cations and anions.
- The bicarbonate concentration as related to the concentration of calcium and magnesium.
- The concentration of specific elements and compounds.

Table 2.3 shows different elements that always found in irrigation water and the level of these elements.

**Table 2-3** The common elements found in irrigation water (Longenecker and Lyerly, 1994).

| Element | Chemical symbol | Approximate proportion |
|---|---|---|
| Sodium chloride | NaCl | Moderate to large |
| Sodium sulphate | $Na_2SO_4$ | Moderate to large |
| Calcium chloride | $CaCl_2$ | Moderate |
| Calcium sulphate (gypsum) | $CaSO_4\ 2H_2O$ | Moderate to small |
| Magnesium chloride | $MgCl_2$ | Moderate |
| Magnesium sulphate | $MgSO_4$ | Moderate to small |
| Potassium chloride | KCl | Small |
| Potassium sulphate | $K_2SO_4$ | Small |
| Sodium bicarbonate | $NaHCO_3$ | Small |
| Calcium carbonate | $CaCO_3$ | Very small |
| Sodium carbonate | $Na_2CO_3$ | Trace to none |
| Borates | $BO^{-3}$ | Trace to none |
| Nitrates | $NO^{-3}$ | Small to none |

A simple approach to evaluate the suitability of irrigation water is to observe the long term influence of water with similar chemical composition on soils and crops in a zone where other factors and conditions are similar to those of the project area. However, it is not always possible to apply this approach, and therefore, some kind of water classification may be required.

The salt effects on plant physiological process resulting from lowering of the soil water potential and the toxicity of specific anions (Bresler *et al*., 1982). However, it has been repeatedly reported that non-toxic highly saline water has an agricultural potential. If irrigation can be managed in a way which provides a high soil moisture content, and consequently high soil water potential within the whole root zone, the osmotic effects will be dampened (Michelakis *et al*., 1993). Moreover, when saline water is skilfully used for irrigation, it can be beneficial for agricultural production,

particularly in orchards (Hoffman *et al*., 1986). Saline water used for agricultural production offers several additional benefits:

- Re-use (instead of disposal as with fresh water) during the entire year, with minimal environmental risk of ground water deterioration (Oron, 1993).
- Enlarge the cultivated area with crops.

Table 2.4 shows the classification of water of different origins which allow a comparison among the salinity of drainage water, ground water and surface water.

**Table 2-4** Classification of water of different origins (Rhoades *et al*., 1992).

| Type of water | EC (dS/m) | TDS (g/l) | Water class |
|---|---|---|---|
| Drinking and irrigation water | < 0.7 | <0.5 | Non saline |
| irrigation water | 0.7 – 2 | 0.5 - 1.5 | Slightly saline |
| Primary drainage water and ground water | 2 - 10 | 1.5 - 7 | Moderately saline |
| Secondary drainage water and ground water | 10 - 20 | 7 - 15 | Highly saline |
| Very saline groundwater | 20 - 45 | 15 - 35 | Very highly saline |
| Seawater | >45 | > 35 | Brine |

TDS - Total Dissolved Salts; EC - Electrical Conductivity

In 1976, the FAO developed new guidelines for a rapid evaluation of the suitability of water for irrigation. These guidelines were slightly modified by Ayers and Westcot (1985). The relationship between the chemical composition of the water and the soil salinity, the effect of sodium on the infiltration rate, the specific toxicity of several ions and other specific effects are taken into account in these guidelines (Table 2.5).

These guidelines can be widely applied in the irrigated lands of the arid and semi-arid regions and cover the range from sandy loam to permeable clay loam soils. Drainage conditions have to be good using the most efficient system. It is assumed that there is a deep water table or it can be controlled by a subsurface drainage system. Furthermore, losses of water through percolation are at least 15% of the applied water. This assumption is valid for surface and sprinkler irrigation methods. If water is applied more frequently by localized irrigation a different approach is recommended.

**Table 2-5** Guidelines for interpretation of water quality for irrigation (Ayers and Westcot, 1985).

| Potential irrigation problem | Units | None | Slight to moderate | Severe |
|---|---|---|---|---|
| *Salinity (affects crop water availability)* | | | | |
| $EC_i$ | dS $m^{-1}$ | <0.7 | 0.7-0.3 | >3.0 |
| TDS | Mg/l | <450 | 450-200 | >2000 |
| ***Infiltration(affects infiltration rate of water into the soil, evaluate using EC and SAR together)*** | | | | |
| *SAR* | | | *EC (ds $m^{-1}$)* | |
| 0-3 | | >0.7 | 0.7-0.2 | <0.2 |
| 3-6 | | >1.2 | 1.2-0.3 | <0.3 |
| 6-12 | | >1.9 | 1.9-0.5 | <0.5 |
| 12-20 | | >2.9 | 2.9-1.3 | <1.3 |
| 20-40 | | >5.0 | 5.0-2.9 | <2.9 |
| ***Specific ion toxicity (affects sensitive crops)*** | | | | |
| Sodium (Na) | | | | |
| Surface irrigation | SAR | <3.0 | 3.0-9.0 | >9.0 |
| Sprinkler irrigation | meq/l | <3.0 | >3.0 | |
| Chloride (Cl) | | | | |
| Surface irrigation | meq/l | <4.0 | 4.0-10.0 | >10.0 |
| Sprinkler irrigation | meq/l | <3.0 | >3.0 | |
| Boron (B) | Mg/l | <0.7 | 0.7-3.0 | >3.0 |
| ***Miscellaneous effects (affects susceptible crops)*** | | | | |
| Nitrogen ($NO_3$ – N) | Mg/l | <5.0 | 5.0-30 | >30.0 |
| Bicarbonate ($HCO_3$) | meq/l | <1.5 | 1.5-8.5 | >8.5 |
| **(Overhead sprinkling only)** | | | | |
| pH | normal range 6.5-8.4 | | | |

For Egypt, El-Lakany *et al*. (1986) reported that the reduction in production of soils affected by salinity is about 30%, threatening the livelihoods of the poor farming and having a significant negative impact on the food production of Egypt. Recently, the Egyptian Government has tried to overcome the salinity problem in irrigated areas by establishing new efficient drainage systems such as sub-surface drainage system, but the annual average net income from crops grown with drainage systems is more limited than for those grown without drainage systems (Amer *et al*., 1989). Therefore, new techniques should be followed to solve this problem such as using genetic engineering technique to have high tolerant crops and using large-scale monitoring techniques (e.g. satellite remote sensing) to predict stress on plants at early stages.

## 2.3 Sources of plant and crop stress

There are many factors that affect the growth of any crop including water stress, salinity, disease, nutrients, pollution and heat stress and these factors affect the grain yield of both wheat and maize. In this research project we are mainly focusing on moisture and salinity stress due to their importance for Egypt. The term of plant stress is considered to be a condition that deviates significantly from the condition required for optimal plant growth and thus could cause harmful effects when the limit of a plant's ability to adjust is reached (Larcher, 1995).

### 2.3.1 Water stress

When plants are subjected to water stress, it affects the availability of water to plants, and therefore, water content of plant cells is lower than the optimum level and causes some degree of metabolic disturbance, hence, a plant is said to be suffering water stress (Fitter and Hay, 1981). Leaf curling, wilt or drastic decrease of leaf area expansion is generally symptoms of water stress (Alscher *et al*., 1990). Plants subjected to water stress reduce stomatal conductance, causing a decrease in transpiration rate, this affects the leaf energy balance and ends with increasing leaf temperature (Jones, 1999). Water stress affects leaf area and leaf angle distribution (LAD) in many plant species. Ehleringer and Forseth (1989) reported that several plant species have shown the ability to adjust leaf angle in response to limited soil moisture. The extent of moisture stress impact on plant leaves depends on the occurrence of the water stress relative to the phenological stage of the plant and severity of water deficit (Chaney, 2000).

Researchers have concluded that water availability is one of the major factors limiting maize production. Eck (1986) found that stress imposed on maize at vegetative stages of growth for 14 and 28 days reduced yields by 23 and 46% respectively. However, maize is very sensitive at specific periods of the growing season to moisture stress; during tasseling and continuing through grain filling (Musick and Dusek, 1980). They also reported that soil moisture stress during periods of tasseling and silking was most detrimental to yield, and that soil moisture stress during the time of grain filling was more harmful to yield than during vegetative growth. Schneider and Howell (1998) compared the yields of maize at different watering regimes, which were five levels in 25% increment ranging from 0 to 100% AWC (available water content) through the

growing season. Yields were highest when AWC of soil was held close to 100% throughout the growing season.

The availability of soil water is a major factor limiting wheat production in most regions of the world especially under semi arid and arid environments (Ozturk and Aydin, 2004). They also reported substantial losses in grain yield are caused by water deficiency depending on the developmental stage at which water stress occurs.

### 2.3.2 Salinity stress

Plant growth is hindered by salinity especially in sensitive plant species; salinity affects plant growth in three major ways (Greenway and Munns, 1980): (i) water deficit arising from the more negative water potential (elevated osmotic pressure) of the soil solution, (ii) specific ion toxicity usually associated with either excessive chloride or sodium uptake and (iii) nutrient ion imbalance when the excess of $Na^+$ or $Cl^-$ leads to a diminished uptake of $K^+$ , $Ca^+$ , $NO_3^-$ or $PO_4^-$, or to impaired internal distribution of one or another of these ions.

Excess salinity within the plant root zone has a general deleterious effect on plant growth since water with high salinity is toxic to plants and poses a salinity hazard (University of Texas, 2007). High concentrations of salt in the soil can result in a physiological drought condition-that is, even though the field appears to have plenty of moisture, the plants wilt because the roots are unable to absorb water. They also reported that this effect is primarily related to total electrolyte concentration and is largely independent of specific solute composition. The hypothesis that best seems to fit observations is that excessive salinity reduces plant growth primarily because it increases the energy that must be expended to acquire water from the soil of the root zone and to make the biochemical adjustments necessary to survive under stress. This energy is diverted from the process which leads to growth and yield. Larcher (1995) reported that plants are under salinity stress when salt content in the root zone exceeds the capacity of plants to cope. Plants try to adapt with high salinity in the root zone by reducing leaf size, scorching of leaf tips or margins, and premature discoloration and abscission of the leaves.

Salinity reduces the rate of leaf expansion therefore the total leaf area of the plant is reduced (El-Hendawy, 2004). The common decrease in leaf expansion is associated

with a loss in cell turgor pressure rather than a salt specific effect. This is supported by the evidence that $Na^+$ and $Cl^-$ are always below toxic concentrations in the growing cells themselves. In a study on wheat, Hu and Schmidhalter (1998) reported that irrigating wheat with water containing 120 Mm NaCl decreased the growth rate by 25%. However, Ball (1988) found that the common decrease in leaf expansion is not related to a loss in turgor pressure and is most likely a result of a change in hormonal signalling from roots to leaves.

Generally, salinity significantly decreases tiller numbers and their appearance in wheat (Mass and Poss, 1989). Salinity significantly reduces the total dry matter yield and the degree of reduction in total dry matter depending on genotypes and salt concentrations (Pessarkali and Huber, 1991). Aloy (1992) found that 1000-seed weight in barley was more strongly affected by salinity than grain number per spike and spikes per plant. Furthermore, the response of phenological aspects of plants to salinity changes with plant development stages (Neumann, 1995). Many plants show a reduced tolerance to salinity during the germination period (early stages) but show greater tolerance during later growth stages whilst other crops show the opposite. Research has shown that wheat, sorghum and cowpea were the most sensitive during the vegetative and early growing stages, less sensitive during flowering, and least sensitive during the grain filling stage (Mass and Poss, 1989).

### 2.3.3 Heat and chilling stress

Heat and cold stress depending on their intensity and duration can impair the metabolic activity, growth and variability of plants and thus limit the distribution of a species. When the critical temperature threshold of a species is exceeded, cell structures and cellular functions may be damaged (Larcher, 1995). Plants under heat stress are darker when compared with non-stressed plants and plants that suffer from this type of stress have dry or yellow – dry spots on their leaves (Staub, 1990). Physical and/or physiological changes that are induced by exposure to very low temperature include loss of chlorophyll, apparent as leaf yellowing, and purpling as a result of photo-oxidation (Saltveit and Morris, 1990).

It is predicted that increases in greenhouse gas concentration will result in increasing mean temperatures of about 2°C by the middle of the 21$^{st}$ century (Kattenberg *et al*., 1996). The growth stage of wheat most likely to be affected is the grain filling stage

as the duration of grain filling in cereals is determined principally by temperature (Wheeler *et al*., 1996). They also reported that high temperature episodes occurring near to anthesis can reduce the number of grains per ear and the subsequent rate of increase in harvest index, resulting in smaller grain yields.

### 2.3.4 Nutrients stress

Nitrogen deficiency is the most common and widespread nutrient deficiency (Larcher, 1995). When plants are subjected to nitrogen stress the first symptom tends to be yellowing of leaves. Most maize crops in African countries suffer from nitrogen deficiency because of intensive cropping system as most farmers grow at least three crops per year which leads to lack of soil fertility. Also, due to increasing chemical fertilization prices, farmers can not afford enough fertilizer to compensate for the loss of nitrogen in intensive cropping systems. In addition to grain yield reduction due to the lack of nitrogen, nitrogen deficiency may result in reducing ear biomass at flowering and under drought conditions (Edmeades *et al*., 1992).

## 2.4 Plant morphological responses to stress

Every part of a plant may be affected by any type of stress although in most cases one or some parts of a plant are affected first. Leaf responses to different stresses are very important when taking into account remote sensing techniques in detecting plant stress particularly the decrease in the rate of leaf expansion and consequent decrease in the total leaf area. The decrease in leaf expansion is generally thought to be due to a drop in cell turgor pressure. However, Ball (1988) suggested that it was more likely a result of a change in hormonal signalling from roots to leaves.

In maize crops suffering drought, the maize grain yield is decreased as a result of decreasing plant stand during the seedling stage, by decreasing leaf area development and therefore, decreasing photosynthetic rate as a result particularly during the pre-flowering stage, by decreasing ear and kernel set during the two weeks bracketing flowering, and by inducing early leaf senescence during the grain filling stage. At the cellular level, drought results in accumulating abscisic acid mainly in the roots where it simulates plant growth. Under severe drought, cell division is inhibited and therefore a lack of cell expansion results.

## 2.5 Remote sensing of Vegetation

### 2.5.1 Introduction

Remote sensing is the acquisition of information about our environment by devices not in direct physical contact with the objects or phenomena being sensed, i.e., non contact sensing. In the broadest sense this definition includes sensors and capabilities as old as human himself. However, in a more restricted sense, the term is commonly used to mean acquisition with various auxiliary devices human has designed to extend his natural sensory capabilities. Remote sensing provides the ability to collect information concerning large areas at frequent intervals through satellite remote sensing techniques and the monitoring capability for agricultural and hydrology has improved greatly during the last decade (Ambast *et al*., 2002).

The remote sensing task is taken to include the experimental plan, the selection of sensors to be used, the reception, recording and processing of data from these sensors, and equally important, the extraction and interpretation of useful and timely information from that data. Such remote sensing information is derived from data gathered through the measurement of force fields with the gravimeters magnetometers; the measurement of acoustical energy by seismograph, sonar or microphones; more commonly, the measurement of electromagnetic radiation by ground–based, airborne or satellite cameras, radar, infrared and multispectral scanners. These remote sensing instruments provide two kinds of information: basic scientific information on the earth and its environment (including the other planets or astronomical observations on a universal scale), and applied scientific information useful for the intelligent management of earth resources or the solution of specific problems. Recently there are many satellite sensors including high spatial and high spectral resolution satellites. Table 2.6 shows some of these satellites characteristics including the spectral and spatial resolution, revisit period and the application of these satellites. In 1980s and 1990s, it was not common to use satellite remote sensing in detecting stress in crops due to limited spectral and spatial resolutions. However, with launching the first generation of high spectral and spatial resolution (e.g. Hyperion, IKONOS and QuickBird) at the beginning of 21$^{st}$ century, it is now possible to use these platforms to detect stress and even distinguish sources of stress.

**Table 2-6** The spatial and spectral specification of some satellite remote sensing instruments.

| satellite | Spatial Resolution | Spectral Resolution | Revisit Period | Primary Applications |
|---|---|---|---|---|
| IKONOS | 4 m | Multispectral 4 bands 0.45-0.88 μm | 1-2 days | Terrestrial mapping |
| ALI | 30 m | Multispectral 10 bands 0.4-2.4 μm | unspecified | Designed to replace the landsat instrument |
| MODIS | 0.25-1 km | Multispectral 36 bands 0.4-14.4 μm | 2-4 days | Terrestrial oceanography and atmospheric |
| ASTER | 15 m | Multispectral 14 bands 0.52-0.86 μm | 16 days | Vegetation mapping and thermal applications |
| AVHRR | 1.1 km | Multispectral 5 bands 0.58-12.5 μm | 1 day | Large scale vegetation mapping |
| Hyperion | 30 m | Hyperspectral 220 bands 0.4-2.5μm 10 nm bandwidth | variable | Varied applications |
| ARIES | 10 m | Hyperspectral 32bands 0.4-1.05 μm 10 μm bandwidth | 7 days | Mineralogical and vegetation mapping |
| Landsat TM7 | 30 m | Multispectral 5 bands 0.5-1.1 μm | 16 days | Geological and vegetation |
| MERIS | 300 m | Multispectral 15 bands 0.39-1.04 μm | 3 days | Oceanography |
| SeaWiFS | 1.1 km | Multispectral 8bands 0.4-0.885 μm | 1 day | Ocean colour |
| Orbwiew-4 warfighter | 4-8 m | Hyerspectral 200 bands 0.4-2.5 μm 10 nm bandwidth | N/A | N/A |
| QuickBird | 2.4 m | Multispectral 5 bands 0.44-0.9 μm | 1-3.5 days | Terrestrial mapping |
| SPOT 5 | 20 m | Multispectral 5bands 0.5-0.89 μm | 2-3 days | Terrestrial mapping |
| AHS | Dependent on flying height | | | |

### 2.5.2 Principles of stress detection by remotely sensed data

Remote sensing provides information about objects through the analysis of data acquired by a device that is not in contact with the target (Lillesand and Kiefer, 2000). Detection of plant stress by remote sensing is mainly dependant on the assumption that stress factors that interfere with photosynthesis process or the physical structure of the plant affect the absorption of light energy and thus alter the reflectance spectrum by reliably measuring the reflectance spectrum of the status of plant health. Leaf reflectance is affected by different factors including leaf internal structure, surface properties, the concentration and distribution of biochemical components such as chlorophyll *a* and water content. Remote sensing analysis of reflectance has been used by many researchers to predict stress in plants by predicting yield, biomass, chlorophyll concentration, leaf water content and protein content (Penuelas *et al*., 1997a; Lu *et al*., 2005). Basically, leaf chlorophyll concentration is one of the main factors that affect reflectance from plant canopies particularly in the visible (VIS) and near infrared (NIR) wavelengths (500-900nm). Also, leaf water content is one of the primary factors that affect the reflectance in the region between 1300 and 2500 nm (Carter, 1991). Moran *et al*. (1994) reported that plants subjected to water stress have higher leaf temperature than normal plants and other types of crop stress related to water uptake by plant roots or translocation of water to the leaves for evaporation also have similar symptoms.

Attempts have been made by many researchers to investigate the reflectance from canopies of stressed plants. It has been reported that plants under stress show a decrease in reflectance of the near infrared region, a reduced red absorption in the chlorophyll active band (680 nm), and a consequence shift of the red edge (Malthus and Madeira, 1993; Carter, 1993).

### 2.5.3 Factors controlling the spectral responses of vegetation

Reflectance measurements are affected by many climatic parameters such as atmosphere, soil background, wind, viewing angle, the height of the sensor from plant canopies and light intensity. These factors affect the spectral signature from vegetation and consequently reduce the efficacy of remotely sensed data in monitoring specific features (e.g. plant health status).

**Soil background:**

Soil background has a great effect on reflectance measurements particularly at the very early growth stages because of the low density of plant shoots and leaves. Elvidge and Lyon (1985) found that the NIR and red based indices have pronounced soil background influences at low vegetation cover. Mickelson *et al*. (1998) reported that Green Vegetation Index (GVI) values were much less influenced by soil background. Little changes in soil reflectance ratios as soil moisture changed because a change in soil reflectance due to water concentration is similar in the visible and near-infrared (NIR) regions of the whole spectrum (Jackson *et al*., 1983). This fact demonstrates that soil moisture might not have a big effect on some derived vegetation indices. They also found that dark and low reflecting soils influence vegetation indices less than high reflecting and light coloured soils. Huete *et al*. (1984) reported that the spectral differences between soils may be closely associated with variations in surface moisture, particle size distribution, soil mineralogy, soil structure and surface roughness. Rainey *et al*. (2000) showed the importance of mineralogy in the maintenance of soil and sediment moisture in response to drying conditions. Clay rich sediment maintained low reflectance for longer whilst drying compared with silt and sand rich sediment. Huete (1988) proposed the Soil Adjusted Vegetation Index (SAVI) to minimise the effects of soil background on the quantification of greenness by incorporating a soil adjustment factor (L) in the basic NDVI equation. This factor is determined by the relative percentage of vegetation and whether the soil is light or dark; Huete gave the value of L at different growth stages as follow: 1.0 for emergent crops, 0.5 for the intermediate stage, and 0.25 for the final, pre tassel stage.

**Wind**

Wind has also a great effect on the reflectance from plant canopies as it affects the structure of canopies and leaf inclination angle, and therefore, the reflectance. Lord *et al*. ($1985_b$) carried out a study to investigate the effects of wind on spectral reflectance; they reported that within the windy and calm periods, extreme values of spectral reflectance differed by 60% and 12%, respectively, in the red and by 40% and 8% in the NIR for the barley canopy. The plant canopy architecture, the wind

conditions and the spectral regions all affected the magnitude of the influence of wind on the spectral reflectance of the canopy.

**Atmosphere**

Conditions in the atmosphere, i.e. the amount of incident sunlight and the percentage of water vapour affect reflectance from plant canopies. Many attempts have been undertaken to investigate these effects. Lord *et al*. (1985a) investigated the potential of using reflectance data collected under both cloudy and sunny conditions; they found that the reflectance measured under cloudy conditions with relatively constant irradiance values was constant and approximately 10% higher than the values measured at similar sun angles during sunny conditions. This suggests that it would be better to measure reflectance under cloudy conditions to minimise the impact of atmosphere. Gao and Goetz (1992) stated that it is important to minimise the length of time between the measurement of the reflectance panel and the target in order to reduce the error due to water vapour variability. Therefore, during reflectance measurements if a reference panel is used and the atmospheric conditions are changeable, the time between them should be a minimum as variability of atmospheric water vapour between the time when the reference panel and target measurements are acquired may affect the obtained spectrum.

**Solar angle:**

The effects of solar angle on reflectance measurements have been studied by some researchers. Pinter *et al*. (1987) reported that the NIR/red ratios of winter wheat were significantly influenced by changes in solar angles. They reported that the NIR/red ratio was highest in mid-morning and mid afternoon and lowest at the highest solar position near midday. Increasing solar zenith angle led to increasing NDVI values and with small sun zenith angle (SZA) improved the NDVI contrast between green vegetation and soil and also the land cover discrimination in all bands, except for those placed in the 750-1100 nm range (Galvao *et al*., 2004). Lord *et al*. (1988) investigated the relationships between daily variations in sun angles and both red and near infrared reflectance measured throughout a growing season over different types of crop canopies; they found that for wheat canopies visible reflectance is approximately constant throughout the day and infrared reflectance increases when

angle from solar azimuth increases. Therefore, reflectance measurements should be undertaken near the solar zenith (at noon) to decrease the effects of solar angle on canopy reflectance (Asrar *et al*., 1985; Serrano *et al*., 2000).

**Viewing angle:**

The ratio of off-nadir to nadir radiance increases or decreases as view zenith angle increases depending on view azimuth angle. Galvao *et al*. (2004) reported that at large solar zenith angles, this spectral interval was useful to separate primary forest/old woody vegetation re-growth from most of the other surface components due to enhancement in the shade fraction associated with the arboreal covers. Ranson *et al*. (1985) reported that the position of the sensor relative to the sun was an important factor for determining the angular reflectance characteristics of crop canopies. Pinter *et al*. (1987) reported that off-nadir viewing significantly influenced spectral band ratios. Thus, the nadir is a very popular viewing angle selected for reflectance measurements.

### 2.5.4 Satellite sensor specification

Generally sensors collect the sun radiation of the electromagnetic spectrum which basically comprises the entire range of the radiant energies or wave frequencies of solar radiation from the shortest wavelengths to the longest wavelengths. The electromagnetic spectrum is divided into seven portions including; visible, infrared, radio, microwave, ultraviolet, x-ray, and gamma ray radiation (NASA, 2005). Remote sensing instruments are characterized by their resolutions including; spatial resolution, spectral resolution, temporal resolution and radiometric resolution. Remote Sensing sensor's spectral resolution is determined by the bandwidth of the electromagnetic radiation of the channels used. High spectral resolution is achieved by narrow bandwidths which collectively are likely to provide a more accurate spectral signature for discrete objects than broad bandwidth. Temporal resolution is determined as the repetitive coverage of the ground by the remote sensing system. Radiometric resolution of a satellite remote sensing sensor's is defined by the number of discrete levels into which signals may be divided. The spatial resolution describes the geometric properties of the imaging system. Three types of satellite datasets were evaluated in this research project including ASTER (Advanced Spaceborne Thermal Emission and Reflection Radiometer), QuickBird, and SPOT (Satellite Pour l`

Observation de la Terre satellite) which are high spatial resolution satellites, Tables 2.7-2.9 show technical characteristics of these three satellites.

**ASTER satellite**

ASTER is a cooperative effort between NASA and Japan's Ministry of Economy Trade and Industry (METI), with the collaboration of scientific and industry organizations in both countries. The ASTER instrument provides the next generation in remote sensing imaging capabilities compared with the older landsat Thematic Mapper (TM). It captures high spatial resolution data in 14 bands, from the visible to the thermal infrared wavelengths. ASTER instrument consists of three separate instrument subsystems. Each subsystem, operates in a different spectral region, has its own telescope(s). ASTER's three subsystem are: the Visible and Near Infrared (VNIR), the Shortwave Infrared (SWIR) and the Thermal Infrared (TIR). The VNIR subsystem operates in three spectral bands at visible and NIR wavelengths, with a spatial resolution of 15 m. The SWIR subsystem operates in six spectral bands in the Near Infrared region through a single-nadir pointing telescope that provides 30 m spatial resolution. The TIR subsystem operates in five bands in the thermal infrared region using a single, fixed-position, and nadir looking telescope with a resolution of 90 m. Table 2.7 shows an overview of ASTER technical specifications and Figure 2.1 shows the ASTER satellite instrument.

**Figure 2-1** ASTER satellite instrument (www.satimagingcrop.com).

**Table 2-7** Technical specifications of ASTER satellite instrument.

| Characteristics | VNIR | SWIR | TIR |
|---|---|---|---|
| Spectral range | Band 1: 0.52-0.60 µm Nadir looking<br>Band 2: 0.63-0.69 µm Nadir looking<br>Band 3: 0.76-0.86 µm Nadir looking<br>Band 3: 0.76-0.86 µm Backward looking | Band 4: 1.6-1.7 µm<br>Band 5: 2.145-2.185 µm<br>Band 6: 2.185-2.225 µm<br>Band 7: 2.235-2.285 µm<br>Band 8: 2.295-2.365 µm<br>Band 9: 2.36-2.43 µm | Band 10: 8.125-8.475 µm<br>Band 11: 8.475-8.825 µm<br>Band 12: 8.925-9275 µm<br>Band 13: 10.25-10.95 µm<br>Band 14: 10.95-11.65 µm |
| Ground resolution | 15 m | 30 m | 90 m |
| Data rate (Mbits/sec) | 62 | 23 | 4.2 |
| Cross-track Pointing (deg.) | +/-24 | +/-8.55 | +/-8.55 |
| Cross-track Pointing (km) | +/-318 | +/-116 | +/-116 |
| Swath Width (km) | 60 | 60 | 60 |
| Detector Type | Si | PtSi-Si | HgCdTe |
| Quantization (bits) | 8 | 8 | 12 |

## QuickBird satellite

QuickBird is the second generation of the earlybird satellites launched by Digital Globe. This satellite launched on October 18$^{th}$ 2001, QuickBird is one of the first commercial remote sensing satellites capable of gathering sub-meter resolution data over a very wide swath. The QuickBird satellite incorporates an ITT – designed and built sensor subsystem, consisting of the focal plane array, image compression and electronics. The subsystem captures 0.61 meter-resolution panchromatic imagery, and 2.4 meter multi-spectral imagery. It produces 11 x 11 km snapshots to 11 x 225 km strip maps. In addition to green, red and near infrared wavelengths, the multispectral image sensor can also process a blue channel, enabling true colour imaging from space. Table 2.8 shows the technical specification of the QuickBird satellite and Figure 2.2 shows the QuickBird satellite instrument.

**Figure 2-2** QuickBird satellite instrument (www.satimagingcrop.com).

**Table 2-8** Technical specifications of QuickBird satellite instrument.

| Characteristic | Specification |
|---|---|
| Launch Date | October 18, 2001 |
| Launch Vehicle | Boeing Delta II |
| Launch Location | Vandenberg Air Force Base, California, USA |
| Orbit altitude | 450 km |
| Orbit Inclination | 97.2°, sun-synchronous |
| Speed | 7.1 km/second-25,560 km/hour |
| Equator Crossing Time | 10.30 a.m. (descending node) |
| Orbit Time | 93.5 minutes |
| Revisit Time | 1-3.5 days depending on latitude (30° off-nadir) |
| Swath Width | 16.5 km x 16.5 km at nadir |
| Metric accuracy | 23-meter horizontal (CE90%) |
| Digitization | 11 bits |
| Resolution | Pan: 61cm (nadir) to 72 cm (25° off-nadir) |
| | MS: 2.44 m (nadir) to 2.88 m (25° off-nadir) |
| Image bands | Pan: 450 – 900 μm, Blue: 450 – 520 μm, Green: 520 – 600 μm, Red: 630 – 690 μm, NIR: 760 – 900 μm |

## SOPT satellite

SPOT satellite is a joint venture between French, Swedish, and German organization and operated by the French-based company in Toulouse. SPOT 1 was launched in February 1986 by the French Government Agency, Centre National d`Etudes Spatials (CNES). Thereafter, SPOT 2, 3, 4 and 5 were launched. The SPOT sensors have the ability to image from vertical viewing (nadir) up to plus or minus 27 degrees off-

nadir. SPOT satellite has two sensors and when used in dual mode, both sensing instruments can be pointed to cover adjacent ground areas, while viewing the earth from the vertical (nadir) position. Table 2.9 shows the technical specifications of the SPOT satellite and Figure 2.3 shows the SPOT satellite instrument.

**Figure 2-3** SPOT 5 satellite instrument (www.satimagingcrop.com).

**Table 2-9** Technical specification of SPOT 5 satellite instrument.

| **Characteristic** | **Specification** |
|---|---|
| Launch Date | May 3, 2002 |
| Launch Vehicle | Ariane 4 |
| Launch Location | Guiana Space Centre, Kourou, French Guyana |
| Orbit altitude | 822 km |
| Orbit Inclination | 98.7°, sun-synchronous |
| Speed | 7.4 km/second-26,640 km/hour |
| Equator Crossing Time | 10.30 a.m. (descending node) |
| Orbit Time | 101.4 minutes |
| Revisit Time | 2-3 days depending on latitude |
| Swath Width | 60 km x 60 km to 80 km at nadir |
| Metric accuracy | <50 m horizontal position accuracy (CE90%) |
| Digitization | 8 bits |
| Resolution | Pan: 2.5 m form 2 x 5 m scenes; Pan: 5 m (nadir) |
| | MS: 10 m (nadir); SWI: 20 m (nadir) |
| Image bands | Pan: 480 – 710 µm, Green: 500 – 590 µm, Red: 610 – 680 µm, NIR: |
| | 780 – 890 µm, Short-Wave IR: 1,580 – 1,750 µm |

**Hyperion satellite**

Hyperion satellite was launched by NASA in November 2000 on board the EO-1 as the first satellite based hyperspectral imager. Hyperion is a pushbroom imager with 220 spectral bands in the range 400-2500 nm, a 10 nm bandwidth, a 30 meter pixel size and a 7.5 km swath. This platform provides a new class of earth observation data for improved earth surface characterisation and can image 7.5 km by 100 km land area per image. The standard scene width and length are 7.7 and 42 kilometres respectively, with an optional increased scene length of 185 kilometres.

The Hyperion instrument includes; system fore optics design based on the Korea Multi-Purpose Satellite (KOMPSAT) Electro Optical Camera (EOC) mission. A focal plane array provides separate Shortwave Infrared (SWIR) and Visible and Near Infrared (VNIR). Hyperion imaging has a wide range of applications including; agriculture, forestry, environmental management, mining and geology. Using shortwave infrared range in Hyperion could provide better understanding and accurate crop stress detection. Moreover, high spectral resolution of Hyperion imagery could enhance the ability to distinguish sources of stress such as moisture and salinity induced stress. Table 2.10 details the technical specifications of the Hyperion satellite instrument and Figure 2.4 shows a photograph of Hyperion satellite instrument.

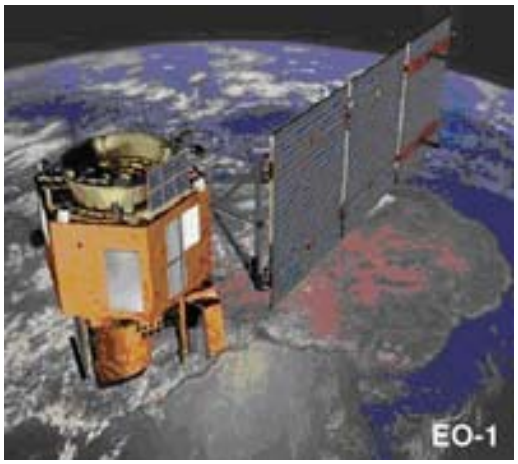


**Figure 2-4** Hyperion instrument on board EO-1 (www.satimagingcrop.com).

**Table 2-10** Technical specification of Hyperion satellite instrument (www.satimagingcrop.com).

| Characteristic | Specification |
|---|---|
| Launch Date | November 21, 2000 |
| Spectral range | 0.40-2.40 μm |
| Spatial resolution | 30 m |
| Swath width | 7.6 Km |
| Spectral resolution | 10 nm |
| Spectral coverage | Continuous |
| Pan band resolution | N/A |
| Number of spectral bands | 220 |
| Revisit frequency | 16 days |
| Sensor type | MSI |

### 2.5.5 Application of remote sensing to plant and crop stress detection and mapping

Estimates of biophysical and biochemical properties of crops and related traits from remotely sensed data are crucial especially if there is a disease or any type of stress, which leads to low crop productivity. The latest generation of high spectral and spatial resolution was launched by NASA at the beginning of 21$^{st}$ century. These platforms have high spatial and high spectral capabilities and are suitable for mapping vegetation cover. Many studies demonstrated the potential of remotely sensed data in mapping vegetation. Monitoring plant status using sample-point technique in large areas is tedious, laborious and a costly process, alternatively, non-destructive techniques such as remote sensing are quick, easy and cheap to perform. Davis and Tyler (2003) reported that remote sensing has the potential of providing a valuable monitoring technique for assessing the ecological impact of radionuclide contamination in vegetation. They stated that changes in leaf pigments (chlorophyll *a* and *b*, carotenoids) and biomass as a result of water and nutrient deficiency and other environmental influences can be detected through spectral reflectance characteristics of plant leaves. Jago *et al*. (1999) used field and airborne satellite spectrometry measurements to predict chlorophyll concentration in grassland affected by soil contamination and wheat field affected by different levels of nitrogen fertilization. They reported that the use of remotely sensed estimates of the red edge position

(REP) for estimating chlorophyll concentration has the potential for inferring both land contamination and grain yield.

**Remote sensing and precision agriculture:**

Precision agriculture uses information technologies acquired from global positioning systems (GPS), geographical information systems (GIS) and remote sensing (RS). Precision farming is the term used to describe the goal of increased efficiency in the management of agriculture. It is a developing technology that modifies existing techniques and incorporates new ones to produce a new set of tools for the manager to use (Rains and Thomas, 2000). The aim behind precision agriculture is to increase the productivity of grain yields under limited resources while decreasing production costs and minimising environmental impacts (Barnes *et al*., 1996). Precision farming basically aims to develop spatially varying crop management strategies to enhance the economic efficiency of crop production. It also aims to optimise agricultural practices by managing fields according to the measured within-field variability in soil and crop conditions: the economic margin from crop production may be increased by improving yield or reducing unnecessary inputs; the risk to the environment is mitigated because inputs are adjusted to match specific crop requirements, avoiding waste; the greater quality assurance is available to the food supply chain through improved traceability from precise recording of field applications. Whilst precision farming can provide economic benefits, increasing pressure towards environmental responsibility will most likely be the main factor driving the uptake of precision farming in the future.

Remote sensing imagery provides a visual method for observing the effects of managed inputs such as chemicals, fertilizers and cultural practices such as tillage (Casady and Palm, 2002). It is also useful in understanding the impact of environmental factors such as disease infestation (Yang *et al*., 2005). In contrast to yield maps, which affect only future decisions, remotely sensed images may be collected several times throughout the growing season and allow timely management decisions to correct problems or deficiencies in the current crop. Therefore, remote sensing can provide a robust technique for precision agriculture of crops. Inventions of many modern technologies made it easier to precisely apply spatially-variable

inputs to agricultural fields (Rawlins, 1996) and provided the inputs for research in this area. Some of these new technologies are as follows:

- Global positioning system (GPS) that provides the ability to identify locations precisely within a field.

- Grain monitoring sensors mounted on combine harvesters to provide measures of grain yield (Patty *et al*., 2001).

- The high capacity of modern computers, which provides the ability to store a huge dataset on very small devices.

During the last three decades, cameras and digital image scanners on satellite systems and airplanes have been improved greatly. The development of these digital devices has the most profound impact on the efficiency of remotely sensed data (Congalton and Green, 1999). Clevers (1986) has proven that reflectance measurements can be used to estimate LAI and field spectroscopy can be used to monitor field trails and provide information instantaneously and non-destructively. Remote sensing instruments have been widely used to collect reflectance data using broad band spectra collected from aircrafts and satellites. Both systems have the ability to provide images and data with high spatial and spectral resolution. These techniques have been largely applied in precision agriculture, in which crop management is performed in small units, on a local basis, rather than field wide. This requires the ability to detect and identify spatial distribution of crop stress in precise locations within a field in a way that allows management decisions to vary in those diverse locations (Thirkawala, 1999). In this context, many agricultural practices such as irrigation, seeds, herbicides and fertilizations may be applied in precise location and amount, based on the spectral data output. This innovative technique can maximise crop productivity at low cost. Spectral imagery together with soil maps collected by aircraft based systems have been widely used in precision agriculture for assessing spatial variability in crops, which make it easier for farmers to obtain detailed spatial information about their crops and therefore take the right decision to avoid crop yield reduction and maximise crop productivity.

**Natural vegetation**

Satellite images have become an important source of information for monitoring vegetation and mapping land cover and land cover change on regional, continental, and global scales (Teillet *et al*., 1997). Many vegetation indices have been developed for qualitative and quantitative assessment of vegetation using remote spectral measurements (Bannari *et al*., 1995). Sensors with spectral bands in the red and NIR are very useful in monitoring vegetation since the difference between the red and NIR bands has been shown to be a strong indicator of the amount of photosynthically active green biomass (Tucker, 1979). Therefore, the Ratio Vegetation Index (RVI) and the Normalized Difference Vegetation Index (NDVI) are now the most commonly used vegetation indices. Starks *et al*. (2006) developed canopy reflectance algorithms for real-time prediction of bermudagrass pasture biomass and nutritive values. They concluded that biomass was correlated linearly with the reflectance ratios of $R_{605}/R_{515}$, $R_{915}/R_{975}$ and $R_{875}/R_{725}$.

However using datasets for current generation of earth orbiting satellite carrying broad band sensors such as Landsat Thematic Mapper (TM), SPOT and High Resolution Visible (HRV) have limitations in providing accurate estimates of biophysical characteristics of agricultural crops (Thenkabail *et al*., 1995) and natural vegetation (Friedle *et al*., 1994). Therefore, reliable high spectral resolution satellite remote sensing such as Hyperion is important for predicting different types of stress and even distinguishing between different sources of stress. Hyperion imagery has more than 200 spectral bands which in turn enable researchers to define wavelengths sensitive to a particular kind of stress.

**Crop production**

Crop production is highly affected by many factors which are considered as limiting factors such as water, salinity, nutrients, diseases, pests and weeds stress. In most cases the aboveground biomass is mainly affected and the effect appears for example on leaves in terms of tone, colour, orientation and leaf area (Inoue, 2003). These changes of plant leaves result in changing reflectance from plant canopies which might be detected by remotely sensed data, and therefore, allow accurate and timely assessment of the extent of damage and identifying management units for time critical

material applications (Inoue, 2003). Prasad *et al*. (2007) showed the potential of spectral reflectance indices as a selection tool for wheat grain yield; they concluded that vegetation indices were strongly related to wheat grain yield in a linear fashion confirming the effectiveness for determining the higher yielding genotypes. They also reported that indices based on the minor water absorption band consistently provide the best relationship with grain yield.

Toler *et al*. (1981) carried out an investigation to detect Phymatotrichum root rot of cotton and wheat stem rust by using false colour NIR photography. Malthus and Madeira (1993) reported that fungal and mildew infected leaves of Faba have been detected using remotely sensed data before symptoms were visible to the human eyes. Moreover, spectral properties can be used to detect stress caused by pests such as insects' damage in wheat fields (Riedell *et al*., 2000). Remote Sensing data have been widely explored as a useful tool for monitoring, detecting and mapping of weeds in agricultural crops (Moran *et al*., 1997a; Lamb and Brown, 2001). However, some researchers mentioned that monitoring weeds in agricultural crops is a very difficult task so many researches used classification algorithms to delineate weed patches based on statistical variability in the spectral response of soil, crop and weed canopies.

### 2.5.6 Measuring stress from different platforms

When sun light touches plant surfaces, it is reflected in the form of radiations having characteristics of intensity and spectral range. This spectral radiance is commonly measured by many sensor-based systems in the visible, NIR and thermal infrared to assess and compare plant biochemical properties under healthy and stressful conditions. Green plants absorb most of the red light and most of the NIR light. Reflectance decreases in the NIR region of the spectrum and increases in the VIS part in stressed plants. Remotely sensed measurements can be acquired by different platforms and every type of platform has its own specifications. In general, there are three different types of platforms: ground-based, airborne and spaceborne.

**Spectroradiometers measurements**

Spectroradiometry is a commonly used ground-based remote sensing technique for a wide range of industrial applications (Yang *et al*., 2007). Spectroradiometry measurements are a quantitative measure of radiance, irradiance, reflectance or transmission of objects by using hand-held spectroradiometers, radiometers or infrared thermometers (IRT) above plant canopies. It measures both radiance and irradiance of an object and correlates them to the biological, chemical and physical attributes of the object. These above canopy sensors are always hand-held or mounted on a tripod, tower, tractor etc. Radiometers are used for this purpose to acquire reflectance from above canopies and these radiometers are often used with broad band similar to those of satellite sensors. Red and NIR ranges have been used mainly to calculate vegetation indices correlated with canopy structure parameters such as LAI.

Many researchers have used spectroradiometry data to assess broad band and hyperspectral vegetation indices (Blackburn, 1998; Serrano *et al*., 2000; Sims and Gamon, 2003; Gitelson *et al*., 2005; Franke and Menz, 2006; Li *et al*., 2008). For example, in a maize experiment Schlemmer *et al*. (2005) employed specroradiometry measurements to detect chlorophyll concentration in maize leaves. They concluded that remotely sensed data is a useful tool in determining a wide variety of physiological properties of plants in a large area and established a strong correlation between chlorophyll concentration and the ratio 600/680 nm. Therefore, ground-based spectroradiometry sensors can be used to collect data about plant surfaces for comparison with data acquired by aircrafts or satellite sensors. Hong *et al*. (2007) employed ground-based remote sensors to predict maize biomass under nitrogen stress conditions; they established strong relations between vegetation indices derived from different hand-held spectral sensors and maize biomass.

**Aircraft measurements**

Airborne measurements have been used to monitor vegetation and crop health by many scientists (Goel *et al*., 2003; Yang *et al*., 2006a and 2006b). There are different types of airborne observation platforms such as balloons and powered and high altitude sounding rockets. Aircrafts airborne sensors have been used in different research areas such as water quality, plant monitoring, and climate. Generally,

airborne sensors have been used in a development study phase leading to their subsequent deployment on satellite platforms. In airborne remote sensing, downward or sideward looking sensors are mounted on an aircraft to obtain images of the earth's surface. This has provided a very high spatial resolution images (20 cm or less), which are comparable to the images obtained by satellite sensors.

Previous studies showed the effectiveness of airborne imagery for monitoring Earth's features such as detecting stress in plants. For example, Goel *et al*. (2003) showed the potential of hyperspectral airborne remote sensing to detect weed infestation and nitrogen stress in maize. Yang *et al*. (2006a and 2006b) established a strong relationship between grain sorghum and cotton yields with vegetation indices derived from airborne imagery data.

However, obtaining airborne images is very costly per unit area of ground cover. Also, the coverage area is low in comparison to the satellite sensors and airborne missions are often carried out as one time operations, but satellite missions offer the possibility of continuous monitoring of the earth. The Canadian CASI (Compact Airborne Spectrographic Imager) was the first available airborne hyperspectral scanner, which contains a two-dimensional CCD array-pushbroom imaging spectrograph. CASI collects data in 288 programmable bands between 400 and 900 nm. Due to the high cost for continuous monitoring of crops, using airborne remote sensing in management applications is difficult. Airborne imagery faces some problems including the cost of obtaining frequent measurements and the problems associated with geometric correction.

**Satellite level**

Although using *in-situ* and airborne remote sensing have been successfully used to monitor different aspects on the ground, using airborne data has some difficulties associated with geometric correction and the high cost of obtaining frequent measures. Using high spatial and spectral resolution satellite remote sensing to monitor aboveground features such as vegetation and crops can be a robust technique. For example, Tyler *et al*. (2006) investigated the potential of remote sensing of water quality in shallow lakes; they stated that satellite remote sensing has the potential to provide truly synoptic views of water quality in particular the spatial distribution of

phytoplankton. Recently, there has been big interest among researchers for estimating of biophysical and biochemical properties of vegetation. A massive effort is under way to obtain large spatial and temporal scale estimates of LAI and fPAR (fraction of photosynthetic active radiation) absorbed by plant canopies, key state variables in most of these models (Buermann *et al*., 2001). AVHRR (Advanced Very High Resolution Radiometers) on board the NOAA (National Oceanic and Atmospheric Administration) is one of the most commonly used satellites for estimating canopy structure (Buermann *et al*., 2001). Thematic Mapper (TM) on board the Landsat satellite also used for estimating canopy structure (Fassncht *et al*., 1997; Tian *et al*., 2000).

Although, satellites are very important to observe earth's surface particularly agriculture, higher spatial and spectral resolution and low revisit period may have to be accomplished. The improvements and advances in satellite sensor technology providing higher spatial resolution (e.g. QuickBird and Ikonos sensors) enhance the ability of using satellite in precision farming. The advantage of these satellites is the revisit period (1-3 days), which was difficult to be accomplished with many other satellite systems (Moran, 2000). High spatial resolution satellite sensor imaging, such as Ikonos imagery, processed with standard remote sensing algorithms, offers a basis for mapping and updating habitat information (Mehner *et al*., 2004). Others used QuickBird satellite for detecting biochemical and biophysical properties in crops (Wu *et al*., 2007a; Wu *et al*., 2007b). Yang *et al*. (2006a and 2006b**)** investigated the potential of QuickBird satellite images to predict and map cotton and grain sorghum yield patterns; they established strong correlations between vegetation indices derived from QuickBird images and both crop yields.

Recently, hyperspectral satellite imagers such as Hyperion have been used in monitoring vegetation; this satellite has more than 200 spectral bands, which enable the construction of effective continuous spectra for every pixel in the scene. This will enable researchers to develop new vegetation indices for detecting stress in crops and facilitate the process of distinguishing different sources of stress in crops such as moisture induced stress from salinity induced stress. Bannari *et al*. (2008) developed several spectral chlorophyll indices to quantify chlorophyll concentration of wheat crops at both the canopy and the leaf scales using remotely sensed data. These

chlorophyll indices were derived from Hyperion imagery and the results demonstrated that Nomalized Difference Pigment Index (NDPI) is the best index for estimating wheat chlorophyll content.

Some new satellites such as VENUS and HyspIRI are launching in the next five years. These satellites are supposed to be more advanced than the pervious satellite generations in terms of revisit period, spatial and spectral capabilities. For example, the new micro satellite, VENUS, will carry a unique super spectral space camera, and will have an advanced plasma-thruster engine for propulsion. VENUS will provide farmers with accurate information about their crops, and consequently, take informed decisions to better treat their crops and maximise crop productivity. It can also be used for fishing and locate the places of large quantities of fish in mid sea.

HyspIRI is also a new hyperspectral satellite imager, which is proposed to be launched sometime around 2013. HyspIRI satellite instrument will have a TIR scanner and a hyperspectral imager that will cover UV, VIS, SWIR, and TIR ranges. The TIR range will have 8 bands between 3.9 and 12.7 μm with 45 m pixel resolution. HyspIRI data will provide useful information in the analysis of surface temperature, geology, surface morphology, natural resources, drought, soil and vegetation. The SWIR range of the HyspIRI may provide better understanding about crop stress at a regional scale.

### 2.5.7 Spectral vegetation indices

Reflectance is the ratio between the amount of energy reflected from an object and the amount of energy incident on the same object. Generally, plants have low reflectance in the blue and red portion of the spectrum because of chlorophyll absorption, with a slightly higher reflectance in the green, thus plants appear green to our eyes. Plants reflect approximately half of the incident radiation in the NIR portion of the electromagnetic spectrum. Some studies have found that measurements in the short-wave infrared can be correlated to leaf water content due to water absorption of SWIR radiation; however, these correlations are strong only for an extreme range of leaf water contents.

Reflectance characteristics depend on the absorption of light at specific wavelengths, and are indicators of plant traits. The amount of energy reflected from a plant in the

visible (VIS) and near infrared (NIR) portion of the spectrum has been correlated to many crop characteristics including biophysical and biochemical properties; chlorophyll concentration, biomass, height, LAI and canopy density. Reflectance in the VIS part of the spectrum depends on the absorption of light by leaf chlorophyll and other pigments such as lutein and carotenoids. It is relatively low in the VIS as a result of high absorption of light by these pigments. In contrast reflectance in the NIR region is relatively low since it is not absorbed by these plant pigments, but scattered by plant tissue (Knipling, 1970).

The most common application of reflectance data is the generation of vegetation indices (VIs). Vegetation indices are linear combinations and/or ratios of spectral bands designed to enhance the vegetation signal of pixels and spectral measurements. The most widely used vegetation indices for plant status are the Normalized Difference Vegetation Index (NDVI), Ratio Vegetation Index (RVI), Soil Adjusted Vegetation Index (SAVI), Physiological Reflectance Index (PRI), Water Index (WI) and Simple Ratio (SR). Spectral reflectance indices were developed on the basis of simple mathematical formulae such as ratios or differences between the reflectance at given wavelengths (Araus *et al*., 2001). SR and NDVI were the first $SRI_s$ developed, using information from the VIS and NIR ranges of the magnetic spectrum. These vegetation indices have been employed to predict different vegetative traits such as LAI or green biomass (Tucker and Seller, 1986). Some researchers have been used $VI_s$ based on VIS, PRI is one of these indices used to assess radiation use efficiency by plants (Penuelas *et al*., 1995), some others have used $VI_s$ based on the NIR, such as WI to assess water status of canopy (Penuelas *et al*., 1993).

NDVI is one of the commonly used vegetation indices, which has been correlated to many variables such as crop nutrient efficiency, final yield in small grains and long term water stress. Although NDVI has been successfully used for vegetation monitoring, it is very likely that the physical characteristics actually being detected by the index are related to some measure of canopy density or total biomass since NDVI values change over the growing season. Due to the effects of soil background on reflectance measurements, Huete (1988) suggested SAVI to minimize the effects of soil background on the quantification of greenness by incorporating a soil adjustment factor (L) in the basic NDVI equation.

Additionally, different combinations of the VIS and /or the NIR bands have been used to develop some other vegetation indices to assess various crop parameters. Normalized Pigment Chlorophyll Index (NPCI) and Pigment Simple Ratio (PSR) were used to classify different crops based on the assessment of their nutrient status (Filella *et al*., 1995). Penuelas *et al*. (1994) developed a new NPC based on the VIS range of the electromagnetic spectrum; to assess physiological changes in nitrogen limited sunflower. Gamon *et al*. (1997) used the PRI to estimate short-term variation in photosynthetic activity by optically measuring the xanthophyll cycle. Most researchers investigate the relationships between different vegetation indices and plant biochemical parameters under controlled conditions of viewing angle. However, vegetation indices were found to be sensitive to the viewing geometry.

The spectral reflectance in the NIR region is determined by leaf internal structure, dry matter content and two minor water-related absorption bands at 970 nm and 1200 nm (Campbell, 1996). Penualas *et al*. (1993, 1994, 1996 and 1997) investigated the reflectance in the 950-970 nm region as an indicator of plant water content. The results showed that the ratio of the reflectance at 970 nm, one of the weak water absorption bands, to the reflectance at 900 nm as reference wavelength ($R_{970}/R_{900}$) or Water Index (WI) was closely linked the changes in relative water content. In addition the Normalized Difference Water Index (NDWI) used two NIR channels; one centred at 860 nm and the other at 1240 nm, was proposed to evaluate vegetation liquid water from space by Gao (1996).

Absorption of radiation by water in the leaf is the primary effect of water content on reflectance. All the above methods for evaluating vegetation water content were based on the spectral reflectance ratios, combinations of spectral features within water-related absorption bands. Unfortunately, the absorption spectrum related to foliar water is also affected by the atmospheric vapour, and it is very difficult to distinguish the contribution of foliar liquid water and atmospheric vapour to the water-related absorption spectrum.

Besides the primary effect of water content on the reflectance, secondary effects of water content on reflectance occur that can not be explained by the radiative properties of water. Some of the secondary effects of water content on leaf reflectance are influenced by the transmissive rather than absorptive properties of water, and the

refractive indices in air and cellulose are different, therefore, the multi reflection inside the leaf is different due to cell turgor with different water content, and so reflectance in 700-1300 nm region varies with water content due to its effect on the leaf internal structure (Carter, 1991).

Previous studies showed that narrow band spectra are more efficient than broad spectra in accurately detecting physiological changes at specific wavelengths, which makes the utilisation of spectral indices more efficient (Gitelson *et al*., 2005). Narrow spectral bands also allow derivative analysis that decreases noise effects on the spectral signals and minimise variation related to soil reflectance background and illumination conditions (Filella and Penuelas, 1994; Blackburn, 1998).

Many derivative indices have been revealed in the literature. First derivatives have been used to minimise the spectral effects of leaf structure, soil background and resolve overlapping spectra (Filella and Penuelas, 1994; Filella *et al*., 1995). The red edge position (REP) defined as the maximum slope of spectral reflectance transition between the red around 680 nm and reflected radiations in the NIR around 780 nm, has been used as a good indicator of chlorophyll concentration at the leaf and canopy levels (Filella and Penuelas, 1994; Penuelas and Filella, 1998). Filella and Penuelas (1994) concluded that a slight shift of the REP towards the visible is an indication of a decrease in chlorophyll concentration. They also stated that the shift toward the longer wavelengths (NIR) accompanied with an increase in NIR reflectance is an indication of the increase in leaf chlorophyll concentration. Table 2.11 gives an overview of some of the previously published vegetation indices.

Some studies have shown the effectiveness of vegetation indices to predict crop yield at early growth stages. Prasad *et al*. (2007) employed different vegetation indices to predict wheat grain yield at early stages. They developed two new vegetation indices (NWI-3 and NWI-4) and established a strong relationship between wheat grain yield and vegetation indices. In another wheat experiment, Babar *et al*. (2006) showed strong correlations between wheat yield and NIR based indices and concluded that at booting stage the correlations were very low. Royo *et al*. (2003) used vegetation indices as indirect estimation for wheat crop yield and found that vegetation indices produced higher correlations at reproductive growth stages in comparison to early vegetative growth stages.

Despite many studies having shown the possibility of vegetation indices in detecting changes in plants physiological status as a result of different stressors, some others have shown poor relationship with plant properties. For example, Aparicio *et al*. (2002) investigated the relationship between growth traits and spectral vegetation indices in durum wheat; they concluded that the suitability of NDVI and SI as predictive tools for LAI within a group of genotypes being compared at a specific growth stage was poor, probably because genetic variability was not large enough to create wide LAI differences. Many studies have shown the ability of vegetation indices to predict wheat grain yield under stressful conditions. However, under well water conditions the relationships between wheat grain yield and ongoing vegetation indices are weak (Babar *et al*., 2006).

It is therefore evident that most researchers in the past decades focused on the stress resulting from water and nutrient stress and a very limited number focused on the potential for using spectral indices as a useful tool for predicting stress resulting from salinity. Hence, it is necessary to investigate different areas of the spectrum to detect wavelengths sensitive to salinity induced stress in existing of moisture induced stress. Moreover, most studies in the literature undertook their studies at the leaf scales ignoring the effects of canopy structure on reflectance at the canopy scale. Additionally, some previous studies showed the possibility of vegetation indices to predict crop properties at the canopy scale using solar radiation, which is not consistent especially in winter season. The research presented here was undertaken at the canopy scale under controlled illumination conditions.

**Table 2-11** previously published vegetation indices collected from literature.

| Notation | Name | Formulae | reference |
|---|---|---|---|
| NDVI | Normalized Difference Vegetation Index | $NDVI = \frac{NIR-RED}{NIR+RED}$ | Rouse *et al*., 1974 |
| RVI | Ratio Vegetation Index | $RVI = \frac{NIR}{\mathrm{Re}\,d}$ | Pearson & Miller, 1972 |
| DVI | Difference Vegetation Index | DVI = NIR-Red | Tucker, 1979 |
| SLAVI | Specific Leaf Area Vegetation Index | SLAVI = NIR/(Red + NIR) | Lymburner *et al*., 2000 |
| SAVI2 | Second Soil Adjusted Vegetation Index | $SAVI2 = \frac{NIR}{\mathrm{Re}\,d+b/a}$ | Major *et al*., 1990 |
| TVI | Triangular Vegetation Index | $TVI= 60(\rho_{NIR} - \rho_{Green})-100(\rho_{Red} - \rho_{Green})$ | Broge & Leblanc, 2001 |
| NPCI | Normalized Total Pigment-Chlorophyll a ratio Index | $NPCI = \frac{(R430-R680)}{(R430+R680)}$ | Penuelas *et al*.,1997b |
| WBI | Water Band Index | $WBI = \frac{R950}{R900}$ | Riedell and Blackmer, 1999 |
| OSAVI | Optimized Soil Adjusted Vegetation Index | $OSAVI = \frac{NIR-\mathrm{Re}\,d}{NIR+\mathrm{Re}\,d+L}(1+L),\ L=0.16$ | Rondeaux *et al*., 1996 |
| VI1 | Vegetation Index one | $VI1 = \frac{NIR}{(green-1)}$ | Vina, 2003 |
| VI2 | Vegetation Index two | $VI2 = \frac{R800}{(R694-1)}$ | Vina, 2003 |
| LMI | Leaf Moisture Index | $LMI = \frac{R1650}{R830}$ | Parkes, 1997 |
| SIPI | Structural Independent Pigment Index | $SIPI = (R_{800} - R_{450})\,(R_{800} - R_{680})$ | Penuelas and Inoue, 1999 |
| YI | Yellowness Index | $YI = (R_{580} - 2R_{630} + R_{680})/\Delta^2,\ \Delta = 50$ nm | Adams *et al*., 1999 |

| | | | |
|---|---|---|---|
| VARI | Visible Atmospheric Resistant Index | $VARI = \frac{green - Red}{green + Red - blue}$ | Gitelson *et al*., 2002 |
| RDVI | Renormalized Difference Vegetation Index | $RDVI = \sqrt{NDVI \times DVI}$ | Reujean & Breon, 1995 |
| GNDVI | Normalized Difference Greenness Vegetation Index | $GNDVI = \frac{NIR - green}{NIR + green}$ | Osborne *et al*., 2004 |
| SI | Stress Index | $SI = \frac{Red}{NIR}$ | Jiang *et al*., 2003 |
| NPCI | Normalized Pigment Chlorophyll Index | $NPCI = \frac{R680 - R430}{R680 + R430}$ | Filella *et al*., 1995 |
| PSR | Pigment Simple Ratio | $PSR = \frac{R680}{R430}$ | Filella *et al*., 1995 |
| IPVI | Infra-red Percentage Vegetation Index | $IPVI = \frac{NIR}{NIR + Red}$ | Crippen, 1990 |
| NWI-1 | Normalized Water Index 1 | $NWI\text{-}1 = \frac{(R970 - R900)}{(R970 + R900)}$ | Babar *et al*., 2006 |
| NWI-2 | Normalized Water Index 2 | $NWI\text{-}2 = \frac{(R970 - R850)}{(R970 + R850)}$ | Babar *et al*., 2006 |
| WI | Water Index | $WI = \frac{R900}{R970}$ | Penuelas *et al*., 1996 |
| SAVI | Soil Adjusted Vegetation Index | $SAVI = \frac{NIR - Red}{NIR + Red + L}(1 + L)$ | Huete, 1988 |
| PRI | Physiological Reflectance Index | $PRI = \frac{(R550 - R531)}{(R550 + R531)}$ | Penuelas *et al*., 1994 |
| NDWI | Normalized Difference Index | $NDWI = \frac{(R865 - R1204)}{(R865 + R1204)}$ | Gao, 1996 |

### 2.5.8 Using spectral indices for plant stress detection

Water, salinity, heat, disease, pollution and nitrogen are factors affecting plant health and therefore affecting canopy properties in terms of aboveground biomass, leaf area, chlorophyll concentration and leaf temperature. The magnitude of these effects

depends mainly on the amount of stress imposed, the crop type, variety, growth stage, soil and climatic factors. Measuring reflectance from plant canopies through detectors of remote sensing systems has been investigated as an indicator of plant status. Spectral data from remote sensing platforms are usually analysed based on the absorption/reflectance or fluorescence features of monitored plants or canopies. The fluorescence technique is best suited for chlorophyll characterisation in the blue, red and NIR fluorescence spectrum (Gitelson *et at*., 1999).

All growing plants reflect very little light energy in the red region due to high absorption features of chlorophyll pigments, but reflect high amount of NIR light due to leaf internal structure characteristics. The amount of reflected radiometric energy from plant canopies is a function of the amount of their tissue biochemical contents. Strong correlations between spectral reflectance and many plant biochemical and physiological variables such as plant dry biomass, chlorophyll concentration, nitrogen content, water content and leaf area index have already been established ( Carter and Miller, 1994; Penuelas *et al*., 1994; Blackmer *et al*., 1996; Carter *et al*., 1996; Penuelas and Filella, 1998). Hence variation in spectral reflectance has been related to specific changes in vegetation characteristics and growth due to several stress factors such as water deficiency (Moran *et al*. 1994, Graeff and Claupein 2007), nutrient deficiency (Carter, 1994) and diseases infestation (Penuelas *et al*., 1995; Xu *et al*., 2007). Other investigations have shown that reflectance measurements can be used to estimate foliar chemical content. This technique assumes that a foliar spectrum is the sum of the absorption features of each chemical weighed by its concentration (Curran, 1989).

**Spectral reflectance and water stress detection**

Many researchers studied the relationship between leaf water content and spectral reflectance. Carter (1993) studied the effects of water content on leaf reflectance and found that spectral reflectance centred at 1450, 1490 and 2500 nm bands showed the greatest sensitivity to water content. Tian *et al*. (2001) concluded that reflectance spectra of wheat leaves in the 1650-1850 nm region were dominated by water content. Absorption by water was expected to be very strong in the thermal region of the spectrum, so the infrared bands were considered inadequate for measuring the water concentration of whole plants or canopies. However, water absorption features were

found to dominate spectral reflectance in the NIR region of the spectrum. Sims and Gamon (2003) tested two field portable spectrophotometers and identified three wavelength regions (950-970, 1150-1260 and 1520-1540 nm) that established better correlations with water content from canopies of 23 plant species.

Plant water content was also related to vegetation indices based on the combination of two spectral bands in the NIR of the spectrum. Gao (1996) proposed a water index similar to NDWI and stated that it could be used for canopy water content estimation. Guiducci *et al*. (1993) report trends of LAI of well watered and droughted treatments for several field crops.

However, remote sensing of plant water content is difficult because the absorption band sensitive to foliar liquid water is also sensitive to the atmospheric vapour (Liu *et al*., 2004). Strong positive correlations were observed between plant water content (PWC) of wheat and spectral reflectance in 740-930 nm region in all of six different growth stages, which indicates that the NIR spectral reflectance increases due to the effect of PWC on the leaf internal structure. This mechanism also affects the red edge spectrum in 680-740 nm region (Liu *et al*., 2004). They also concluded that the spectral reflectance increases rapidly and the red edge becomes steeper if PWC is higher. The spectral reflectance of the green vegetation in 1300-2500 nm region is dominated by liquid water absorption, and also weakly affected by absorption due to other biochemical components, such as protein, lignin and cellulose (Carter, 1991).

**Spectral reflectance for Nitrogen stress detection**

Nitrogen is an essential element for plant nutrition and because of its high demand in the plant and high variability within the soil; it is the most intensively managed plant nutrient in crop production. Stresses that involve deficiencies of N and water will adversely affect the amount of chlorophyll plants produce as well as cell turgidity (Schlemmer *et al*., 2005). Most researchers often use the chlorophyll concentration as an indicator of nitrogen deficiency. Remotely sensed measurements of chlorophyll could provide information about the status of plants without the use of destructive sampling. Reflectance in the visible part of the spectrum (particularly at 550 nm and 675 nm) is highly indicative of chlorophyll *a* concentration and nitrogen status of various growing plants (Buschmann *et al*., 2000).

Recently, remote sensing has been used in precision farming to assist nitrogen management in agriculture. Because of the close link between leaf chlorophyll and leaf N concentration, remote sensing techniques have the potential to evaluate the N variability over large fields quickly (Daughtry *et al*., 2000). Reflectance spectroscopy has been used effectively to estimate tissue nitrogen concentration in various crops (Blackmer *et al*., 1994; Rodriguez and Miller, 2000). Assessing N crop status requires development of a direct relationship between spectral data at specific wavelengths and leaf N status or an indirect relationship between spectral data and plant chlorophyll status. Many studies have shown a close correlation between chlorophyll concentration of plants and N availability (Blackmer *et al*., 1994; Filella and Penuelas, 1994; Clay *et al*., 2006). Cutler (2000) investigated the relationship between remotely sensed data and canopy chlorophyll concentration of wheat under various regimes of fertilization, pesticide/fungicide application and found a strong correlation between reflectance measurements and canopy chlorophyll concentration.

Plants under N deficiency will have decreased photosynthetic activity and chlorophyll concentration, which will affect other physiological variables and hence the overall spectral signal from the plant. These changes could be optically detected in the red region of the spectrum (increase in red reflectance) and the NIR (decrease in NIR reflectance). Thus, reflectance measurements assessing chlorophyll could also be used to indirectly characterize the N status. Green reflectance peak at 550 nm and red reflectance at 700 nm were found to be strongly correlated to chlorophyll *a* concentration (Schepers *et al*., 1996). However, reflectance sensitivity was found to be higher at 550 nm for medium to high chlorophyll concentration, whereas for low concentration, reflectance sensitivity was higher at 675 nm. Blackmer *et al*. (1994) studied the effect of different nitrogen treatments on the spectral reflectance of maize leaves in the 400 to 700 nm region, and found that reflectance measurements near 550 nm could be used to detected N deficiencies in maize leaves, and thus predict grain yield. In another maize experiment, Blackmer *et al*. (1996) noticed that reflectance measurements at 550 nm and 710 nm were highly correlated with various N treatments.

The NIR spectral region has also been used for predicting N deficiency in many crops. GopalaPillai *et al*. (1998) employed digital aerial imagery to detect nitrogen

stress from reflected maize canopies in the infrared channel. Strong correlations between canopy reflectance and applied nitrogen amounts were established. Spectral bands between 780 nm and 810 nm were found to be sensitive to the presence of amino acids ($R\text{-}NH_2$), which are the building blocks of proteins (Stone *et al*., 1997). Gitelson *et al*. (1996) reported that there is a good correlation between near infrared range of the spectrum (700-750) and total leaf chlorophyll concentration of different tree species. Broad band vegetation indices acquired from various crops showed good correlations with vegetation (Fernandez *et al*., 1994; Stone *et al*., 1997). Other studies proposed hyperspectral indices for direct variable estimation, For example, for wheat Stone *et al*. (1996) showed a strong correlation between NDVI calculated at 660 nm and 780 nm and N uptake. In another wheat experiment, Reyniers *et al*. (2006) employed NDVI derived from Ikonos imagery and multispectral data and established a strong relationship between NDVI derived from both platforms and nitrogen status.

Bausch and Duke (1996) used a range of N fertilization treatments on maize and reported that differences in LAI of about 1 were significant at 0.05 only between the zero N and all the other treatments. Zero N LAI began to differ from the other treatments only after the $10^{th}$ leaf (V10) stage, but the greatest difference with the other treatments occurred after the onset of leaf senescence. The yield difference between the Zero N and the 102 kg N $ha^{-1}$ treatment was 22%, but there was also a difference of 14% between the latter and the 220 kg N $ha^{-1}$, between which visible LAI differences appeared only during senescence. In a maize experiment, Wu *et al*. (2007b) showed the possibility of estimating LAI using broad band vegetation indices derived from QuickBird satellite imagery. They also reported that among all broad band vegetation indices MSAVI was the best LAI estimator. Other studies showed the possibility of remotely sensed data to predict grain yield under different nitrogen levels (Raun *et al*., 2001; Royo *et al*., 2003; Babar *et al*., 2006; Prasad *et al*., 2007). For example, Raun *et al*. (2001) established a strong relationship between wheat grain yield and NDVI.

Pattey *et al*. (2001) showed significant differences in LAI (as assessed by 95% confidence) between low nitrogen (17 kg $ha^{-1}$) and high nitrogen (155 kg $ha^{-1}$) maize treatments at much earlier growth stages. The absolute differences were of about 0.5 LAI, corresponding to 25 - 40% differences according to the growth stage. In this

case, LAI was different in the period between 35 and 50 days after emergence, after which no significant differences appeared until the start of senescence. The yield difference assessed using a yield monitor, was statistically significant. A more standardized assessment of the effect of N stress on LAI can be carried out by considering the nitrogen nutrition index (NNI) the ratio of actual biomass dry weight N concentration to the critical N concentration required to produce maximum dry matter (Lemaire and Gastal, 1997). Nitrogen deficiency occurs when NNI<1. Using such an approach Vouillot *et al*. (1998) demonstrated that wheat at NNI of 0.6 had an LAI of about 70-75% of that of the unstressed control (which had a NNI not significantly different from 1).

Regarding the interaction between water and nitrogen, Fernandez *et al*. (1994) reported that for wheat at anthesis, LAI was about 3 for non-fertilized non-irrigated treatment, 3.5 for the irrigated non-fertilized, 4.5 for non-irrigated fertilized (200 kg N $ha^{-1}$) and 5.3 for the irrigated fertilized treatment. Clutterbuck and Simpson (1978) showed differences of about 0.5 maximum LAI between irrigated and non-irrigated potato at a fertilization level of 200 kg N $ha^{-1}$, which increased to differences of about 1.5 at 300 kg N $ha^{-1}$.

**Spectral reflectance to predict plant disease**

Using remotely sensed data to detect stress in plants is based on the assumption of a strong relationship between stress and photosynthesis or the physical structure of the plant and affects the absorption of light energy, and thus changes the reflectance spectrum of the plants (Moran *et al.*, 1997b). Hyperspectral remote sensing using remotely sensed reflectance for many contiguous narrow bands has been documented in crop management such as distinguishing various plant species, predicting crop yield, aboveground biomass, chlorophyll concentration and predicting damage caused by plant diseases such as pests and fungal infestation ( Pinter *et al*., 2003). Riedell and Blackmer (1999) investigated the effects of sucking insects on wheat leaf reflectance by infesting wheat seedlings with aphids (*Diuraphis noxia Mordvilko*) or greenbugs (*Schizaphis graminum Rondani*). Comparing reflectance from these infested plants with healthy plants, they reported that the leaves from infested plants had lower chlorophyll concentration and displayed significant changes in reflectance spectra at certain wavelengths (500-525, 625-635, and 680-695 nm). Nilsson (1991) used a

hand-borne radiometer to monitor plant growth and predict yield and yield reduction caused by plant disease. He reported that there is a good correlation between spectral reflectance data and plant growth, green biomass and grain yield as well as infection by various diseases at various levels of N fertilization and irrigation. A number of reflectance ratios proposed by Carter (1994) can be used as indicators of plant stress including competition, herbicides, pathogen, mycorrhizae, senescence, and dehydration. These ratios were significantly greater in stressed compared with non-stressed leaves for all stressors.

Wheat production is greatly affected by many different diseases among which are pests and fungal diseases. Severe damage happens to wheat production in some areas caused by greenbug (*Schizaphis graminum*) feeding, combined with its abundance. Yang *et al*. (2005) concluded that wheat damage by greenbug feeding was the most important insect pest of wheat in much of the great plain region of the United States. They also characterized greenbug-induced stress in wheat using a hand-held radiometer concluding that using radiometers to detect greenbug-induced stress is possible. The band centred at 694 nm and the vegetation indices derived from bands centred at 800 and 694 nm were identified as most sensitive to damage due to greenbug infestation. In addition, they mentioned that broad Landsat TM bands and derived vegetation indices also showed the potential for detecting stress in wheat caused by greenbug infestation.

Other researchers have attempted to characterize stress caused by plant diseases, Malthus and Madeira (1993) used the hyperspectral data acquired by a spectroradiometer to detect the fungus *Bortrytis faba* (chocolate spot) infection of beans in the field by scanning at 2 nm intervals over the range 400 – 1100 nm. They mentioned that the most significant change of reflectance was a flattening of the response in the visible region and a decrease in the near infrared reflectance at 800 nm. Genc *et al*. (2008) shown the possibility of vegetation indices derived from spectroradiometry measurements to detect the damage to wheat crops by sunn pest (*Eurygaster integriceps*). Xu *et al*. (2007) employed reflectance measurements to assess the damage to tomato leaves by leaf miner. They concluded that spectral reflectance decreased significantly with increasing severity level at short wavelengths of the NIR and the most sensitive wavelengths to the damage by leaf miner were

centred at 1450 and 1900 nm. In another wheat experiment, Franke and Menz (2006) monitored the heterogeneity of fungal diseases within agricultural sites using multispectral QuickBird satellite images. They found that high resolution multispectral data are generally suitable to detect in-field heterogeneity of vegetation, but they are not effective enough to detect stress factors.

**Spectral reflectance and salinity stress**

Drought and salinity are major inhibitors to agronomic production (Poss *et al*., 2006). Distinguishing salinity from other types of stress is very important particularly in areas located in arid and semi-arid regions. Few studies have shown the possibility of using reflectance measurements as a useful tool in predicting salinity stress in crops. Irrigation management may address salinity stress detected indirectly by remote sensing of biomass reduction (Pinter *et al*., 2003). Poss *et al*. (2006) used canopy reflectance spectra obtained in the 350-1000 nm region from two viewing angles (nadir view and 45° from nadir) to predict stress in alfalfa and wheat. They reported that the ability of narrow-band remote sensing of canopy reflectance to detect the effects of salinity and water stress was determined for alfalfa and wheatgrass forage crops.

Predicting biochemical properties of plant canopies such as chlorophyll concentration might be useful. One of the primary biochemical parameters that affect canopy reflectance in the visible domain is the concentration and total amount of leaf chlorophyll (Wang *et al*., 2002b). Other studies showed the potential of reflectance measurements to detect salinity induced stress in terms of temperature, LAI, plant height and chlorophyll. Wang *et al*. (2002a) investigated the potential of reflectance measurements to assess salinity stress on production of elephant grass; they concluded that canopy spectral reflectance in the NIR region was reduced incrementally with increasing levels of salinity stress. Salinity effects on different plant biophysical variables related to canopy development can be determined with remote sensing techniques (Penuelas *et al*., 1997a). Wang *et al*., (2002a) investigated also the potential of reflectance measurements to interpret salinity and irrigation effects on soybean, stating that canopy reflectance in the NIR was significantly and consistently reduced by the salinity treatments. They attributed this decrease to increases in leaf mass caused by salinity and found a relationship with the simple ratio vegetation

index (SRVI), with 660 and 830 nm as the most sensitive waveband combination. They also mentioned that reflectance in the visible domain did not show a salinity effect or any correlation to leaf chlorophyll changes from salinity stress.

It is therefore suggeseted that vegetation indices can be used as indirect tool to detect stress in crops including moisture, salinity, nitrogen deficiency, pollution and diseases. However, there is no single vegetation index to correlate well with a plant property over the growing season and therefore more work is needed to validate the results obtained using this technique to detect stress in crops.

## 2.6 Summary

This chapter provides an introduction to the agricultural context of Egypt in terms of land and water resources, population growth and crop production, factors influencing crop production including moisture, salinity, nutrients, disease and heat stress. Through reviewing the potential capability of remote sensing, we are now able to formulate testable hypothesis upon which to evaluate the role of satellite based remote sensing in increasing crop productivity.

This chapter has demonstrated the efficacy of monitoring agricultural crops by assessing aboveground biomass, grain yield, chlorophyll concentration and total leaf area, through remote sensing. Vegetation indices have been widely used to detect plant status. Broad band and narrow band based vegetation indices have been widely used for predicting plant status. Many studies have been undertaken to use remotely sensed data to detect nitrogen, disease and moisture induced stress in crops, but few studies have been undertaken to detect salinity induced stress by remotely sensed data. In this case, increased efforts to remotely detect the effect of salinity hazard and water stress for irrigation management are needed since few studies have quantitatively assessed the ability of remote sensing technique to characterize simultaneous water and salinity stress on plant yields (Poss *et al*., 2006).

Ground based sensors such as spectroradiometers and radiometers have been widely used for predicting stress on plants subjected to different types of stress such as moisture, salinity, disease and nutrient stresses. Most of these studies have been undertaken at the leaf scale (apical leaves) ignoring the effects of canopy structure. Also, from previous studies it is noted that airborne remotely sensed data have been

used in many fields monitoring vegetation in wetlands, water quality and forestry, but are still very expensive in the field of agriculture for monitoring crop health. Using satellite data in particular high spatial resolution satellites (QuickBird, SPOT and ASTER) and high spectral resolutions (Hyperion) is promising in monitoring crop status in terms of yield, biomass and chlorophyll. The following hypotheses have been deduced to provide the focus for this research:

1. *Moisture and salinity stress greatly affect wheat and maize productivity.*

2. *In situ hyperspectral measurements are able to detect stress in wheat and maize resulting from moisture and salinity stress.*

3. *Moisture induced stress can be distinguished from salinity induced stress spectrally.*

4. *High spatial resolution satellite remote sensing imagery can detect stress in wheat and maize at local and regional scales at early growth stages, and therefore, maximise crop productivity*.

# 3 MATERIALS AND METHODS

## 3.1 Introduction

This chapter describes the generic methodologies and equipment used during this research project, necessary to underpin the experimental approach to address the hypotheses derived at the end of chapter 2. This chapter will cover details of soil and vegetation sample collection, preparation and analysis. The spectroradiometry acquisition is described here, but details of their specific use are covered in the experimental Chapters 4 and 5. Satellite data acquisition and analysis will be described in Chapter 6.

## 3.2 Vegetation Sampling

During both greenhouse-based experiments and field work campaigns, plant samples were collected for identifying different biophysical and biochemical measurements including plant height, leaf area index, total aboveground biomass, chlorophyll *a* concentration. Care was taken to ensure that the sampling of leaves for chlorophyll determination was done as early as possible before sun rise during field visits in Egypt to minimise the influence of the climate extremes.

### 3.2.1 Vegetation sampling strategy for greenhouse experiments

After measuring spectral reflectance, plant samples were collected from an area of 0.15 $m^2$. Samples were collected three times for biomass and leaf area index over the growing season of the Scottish winter wheat including harvesting and two were concurrent with spectroradiomtry measurements. Plant height was measured at the same time as spectroradiometry measurements were made. Leaf samples were collected over the growing season, immediately following the acquisition of reflectance measurements. Samples were analyzed for leaf pigments and chlorophyll *a* concentration. During the first two experiments of Scottish wheat (winter season 2005-6) the timing of the reflectance measurements was dependent upon the weather and lighting conditions. To avoid the problems associated with the limitations of the Scottish climate, a darkroom was constructed behind the greenhouse experiments in which the lighting conditions could be controlled. This enabled much greater control over the timing of data collection and sampling for later experiments.

The whole plants were cut with a pair of scissors just above the soil surface, separated into leaves, stalks and spikes and each component weighed to determine fresh weight. Following oven drying at 70$^{o}$ C for 72 hours the dry weight was determined, then the leaf water content was calculated as follows:

$$LWC = \frac{FW - DW}{FW} \quad \text{.....3.1}$$

Where:

LWC is the leaf water content

FW is the fresh weight of the sample and

DW is the dry weight of the sample

From every treatment a sample of 10 youngest fully developed leaves was taken for further analysis of chlorophyll *a* during the first two wheat experiments (Scottish wheat 2005-6 and Egyptian wheat, spring season of 2006). In the last two experiments of Scottish and Egyptian wheat varieties in winter season of 2006-7 the samples were split for chlorophyll *a* determination and estimation of the pigment concentrations through HPLC analysis.

At harvesting time the spikes were cut and threshed manually to determine grain yield and derive grain yield in kg m$^{-2}$. Two hundred grains were randomly collected from the harvested pots from different replicates to estimate *the thousand grain weights*.

For maize crop, biomass samples were collected at four different stages over the growing season at V6 (sixth leaf), V12 (twelfth leaf), R1 (silking stage) and at harvesting. Two plants were sampled from one pot from each treatment to determine aboveground biomass, plant height, leaf area index, plant water content and chlorophyll *a* concentration as explained above.

### 3.2.2 Vegetation sampling in the field

Two field work visits were undertaken in south-west Alexandria, Egypt, one for winter wheat and the other for maize to collect ground reference data coupled with satellite image acquisition. The vegetation sampling was timed to be within a few days of Hyperion image acquisition for both field visits. For each investigated field

with a typical size of 0.25-0.50 hectare, reflectance measurements were taken at five random locations closely followed by crop sampling at the same locations. Three samples were collected for determining different crop properties. Crop biomass was cut at ground level from 0.25 $m^2$ and placed in a sealed plastic bag then taken for biometric analysis (leaf area index, plant height, total biomass, spikes weight). Plant height was the only agronomic parameter that was measured at each location within the same field (non-destructive measure). To determine chlorophyll concentration, 20 apical leaves were sampled from each field then put in an ice box before sun rise and quickly transferred to a lab (Alexandria University, Egypt) for chlorophyll analysis using SPAD chlorophyll meter. Care was taken to ensure that all vegetation samples were collected at the spectra locations within a field. For maize the same approach was followed, but sampling three plants at each location. Figure 3.1 shows vegetation sampling for wheat in the field during field work in Egypt. At a number of 4 sites, vegetation sampling was prohibited by the farmer.

**Figure 3-1** Collecting vegetation samples of wheat crop in the field during field visit in 2007.

## 3.3 Vegetation pigment analysis

### 3.3.1 Chlorophyll *a* analysis through laboratory based spectrophotometry

#### Spectrophotometer instrument

A digital Cecil spectrophotometer was used to measure the absorbance of the extracts at different wavelengths (480,510, 630, 647, 664, 665 and 750 nm). Table 3.1 shows the technical specifications of the Cecil spectrophotometer.

**Table 3-1** The technical specification of the digital spectrophotometer employed in determining chlorophyll *a* concentration in wheat and maize leaves.

| Parameter | Description |
|---|---|
| Model | CECIL, CE 1021 |
| Optical system | Littrow monochromator using 1200 lines/mm holographic grating; coated optics. Accommodates 100 mm cells |
| Optical bandwidth | 8 nm |
| WI range | 200-1000 nm; CE1021 and 325-1000 nm; CE1011 |
| WI Accuracy | +/- 1 nm |
| WI Reproducibility | +/- 0.1 |
| Scan Speed | 1-4000 nm/min |
| Stray light | Less than 0.05% at 220 nm and 340 nm |
| Photometric accuracy | +/- 0.005A or 1% |
| Start up wavelength | 400 nm |
| Lamp change wavelength | 355 nm (default) |

#### Sample preparation

A sub-sample from each treatment consisting of 10 leaves was selected randomly among the youngest fully developed leaves for analysis. Using a corer, twenty leaf discs of 0.4 cm in diameter were taken from each treatment and pooled. Three leaf discs were chosen randomly, cut into small pieces and ground up in a mortar and pestle. Four ml of 90% acetone solution was used initially to extract chlorophyll. The extract was transferred to a 10 ml plastic centrifuge tube. The mortar and the pestle were rinsed with 4 ml of 90% acetone solution which was then added to the centrifuge tube and the total volume made up to 10 ml. The centrifuge tubes were sealed, left in the dark for 2-4 hrs then centrifuged at 3000 rpm for 5 minutes.

**Sample analysis using spectrophotometer**

To measure the absorbance, a volume of 3 ml of extract was transferred from the upper half of the supernatant to a spectrophotometer cuvette. The absorbance of the blank solution (90% acetone) was measured first and then the extract was measured at 480 nm to check how concentrated the extract was. The absorbance of the extracts and blank solution was measured at specific wavelengths (510, 630, 645,646, 663, 664, 665, and 750 nm). The concentration of chlorophyll *a* was determined according to Lichtenthaler (1987) using the following equation:

$$\textbf{Chl } \boldsymbol{a} \textbf{ = 12.21 } A_{663} \textbf{ – 2.81} A_{646}$$

Where:

Chl *a* is the chlorophyll *a* concentration in μg $cm^{-3}$ of the 90% acetone solution

$A_{646}$ and $A_{663}$ are the absorbance at 646 and 663 nm wavelengths respectively. To convert the concentration of chlorophyll *a* to μg $cm^{-2}$ of leaf the chlorophyll amount was related to the amount of acetone and the leaf area, which was used for the extraction. The chlorophyll *a* concentration was also determined using HPLC instrument and different pigments were also measured.

## 3.3.2 Pigment analysis using HPLC

**HPLC instrument**

The HPLC (High Performance Liquid Chromatography) system used in this study consists of a Dionex quaternary gradient pump which connected to a Spherisorb TM OSD2 reverse-phase C-18 column (25 cm x 4.6 mm, 5μm particles, 90-100 000 plates $m^{-1}$) and a lab Alliance UV6000LP photodiode array detector (PDA). An oven was used to maintain the Spherisorb TM OSD2 reverse phase C-18 column at 30$^{o}$C during analysis. Pigments for RP-HPLC analysis were extracted from maize and wheat leaves using the method described in section 3.3.1.

**Sample preparation**

Samples of apical leaves were collected from each treatment by cutting leaves at the base, placing them in a sealable plastic bag and refrigerating as quickly as possible.

Discs of 0.7 cm in diameter were taken from different locations on each leaf replicated five times for wheat and three times for maize. Three discs were chosen randomly, cut into small pieces and transferred to a mortar. The pigments were extracted using 90% acetone solution following the same method described in section 3.3.1.

**Sample analysis using HPLC**

Using a syringe, a volume of 500 µl of the extract was injected into the RP-HPLC system; the injection value was interfaced with a 100 µl Dionex stainless steel LC sample loop. The chromatic conditions for pigment separation followed the protocol of Wright *et al*. (1991), which employs three mobile-phase solvents in a linear gradient programme (Table 3.2): the protocol includes three solvents: solvent A, 80:20 methanol:0.5 M ammonium acetate (v/v); Solvent B, 90:10 acetronitrile : water (v/v); and solvent C, 100% ethyl acetate. A constant flow rate of 1 ml $min^{-1}$ was used. Pigment peaks were quantified using absorbance (mAU) at 436 nm. The pigment peaks were identified through comparisons with standard reference pigments obtained from the water quality institute (VKI), Horsholm, Denmark and via comparisons with published pigment PDA absorption spectra, elution sequences and retention times (RTS). The solvents used were HPLC grade and de-ionized water was purified using a Milli-Q system. Ammonium acetate was A.R. grade.

**Table 3-2** The RP-HPLC solvent system used in the (a) start-up, (b) analytical and (c) shut down protocols employed in the analysis of wheat and maize leaves pigment signatures (Wright *et al.*, 1991).

| Time (min) | Flow rate (ml $min^{-1}$) | Solvent A (%) | Solvent B (%) | Solvent C (%) | Conditions |
|---|---|---|---|---|---|
| ***(a) Start-up protocol*** | | | | | |
| 0 | 1.0 | 0 | 0 | 100 | Start-up |
| 3 | 1.0 | 0 | 0 | 100 | Washing |
| 6 | 1.0 | 0 | 0 | 100 | Linear gradient |
| 16 | 1.0 | 0 | 100 | 0 | Linear gradient |
| 17 | 1.0 | 100 | 0 | 0 | Ready for analysis |
| ***(b) Analytical gradient protocol*** | | | | | |
| 0 | 1.0 | 100 | 0 | 0 | Injection |
| 4 | 1.0 | 0 | 100 | 0 | Linear gradient |
| 18 | 1.0 | 0 | 20 | 80 | Linear gradient |
| 21 | 1.0 | 0 | 100 | 0 | Linear gradient |
| 24 | 1.0 | 100 | 0 | 0 | Linear gradient |
| 29 | 1.0 | 100 | 0 | 0 | Equilibrium |
| ***(c) Shut down protocol*** | | | | | |
| 0 | 1.0 | 100 | 0 | 0 | Analysis complete |
| 3 | 1.0 | 0 | 100 | 0 | Linear gradient |
| 6 | 1.0 | 0 | 0 | 100 | Linear gradient |
| 16 | 1.0 | 0 | 0 | 100 | Washing |
| 17 | 1.0 | 0 | 0 | 100 | Shut down |

### 3.3.3 Total chlorophyll through SPAD meter

For measurement of chlorophyll concentrations during field work in Egypt, a hand-held SPAD 502 meter (Minolta, Osaka, Japan) was used due to difficulties accessing laboratory equipment. SPAD provides a convenient means of making relative determinations of the leaf chlorophyll concentration (dimensionless). Chlorophyll has absorbance peaks in the blue (400-500 nm) and red (600-700 nm), with no transmittance in the NIR. The SPAD determines the relative amount of chlorophyll presented by measuring the absorbance of the leaf in two wavelength regions (red and NIR). Using transimittance in these two regions, the meter calculates a numerical value, which is a proportional to the amount of chlorophyll in a leaf. Twenty apical leaves were sampled before sun rise to avoid high temperature, sealed in a plastic bag and kept cool in an ice box. Leaf samples were taken from different locations within each field as close as possible to locations of *in situ* spectroradiometry measurements.

In the laboratory (Faculty of Agriculture, University of Alexandria, Alexandria, Egypt) chlorophyll concentration was measured using SPAD chlorophyll meter. To reduce the variability, the meter readings were taken at three different locations on each leaf from the leaf tip to the leaf base and the average of these three readings was calculated. Also, readings from twenty leaves of each location were averaged to reduce variability to a minimum. Chlorophyll concentration was not determined for the third study site (Bangar site) due to availability of SPAD meter.

## 3.4 *In situ* Spectroradiometry measurements

### 3.4.1 Instrument

An ASD FieldSpec Pro spectroradiometer from Analytical Spectral Devices Inc. (Boulder, Co 80301 USA) was used to measure reflectance from plant canopies using both solar radiation and artificial illumination. This instrument can detect reflected light from the canopy ranging from 350 nm to 1050 nm, covering the visible near infrared (VNIR) portion of the magnetic spectrum. The Visible/Near Infrared (VNIR) portion of the spectrum is measured by a 512 channel silicon photodiode array overlaid with an order separation filter. Each channel, an individual detector itself, is geometrically positioned to receive light within a narrow bandwidth (1.4 nm). The VNIR spectrometer has a spectral resolution of approximately 3 nm at around 700 nm. Table 3.3 shows the specifications of the ASD FieldSpec instrument.

**Table 3-3** The specifications of the ASD FieldSpec TH spectroradiometer.

| parameter | Description |
|---|---|
| Model | ASD FieldSpec Pro Inc. (Boulder, Co 80301 USA) |
| Spectral range | 350 – 1050 nm |
| Sampling interval | 1.6 nm @ 350 – 1050 |
| Spectral resolution | 3 nm @ 700 |
| Typical data collection rate (solar illumination) | 0.7 spectra/second |
| Detector | 512 channel Silicon photodiode array 350 – 1050 |
| Field of view (FOV) | $25^{o}$ (FOV) |
| Calibration | Wavelength, reflectance, radiance, irradiance. All calibration are NIST traceable |
| Noise Equivalent Radiance (NER) | UV/VNIR 5.0 x 10 -9 , W $cm^{-2}$ $nm^{-1}$ $Sr^{-1}$ @700nm |

**Field use**

An ASD FieldSpec Pro spectroradiometer was used to measure the spectral reflectance from plant canopies at a specific height from the soil surface. Each reflectance spectrum was the average of a number of scans (which was adjusted and calculated by the spectroradiometer). The spectroradiometer was mounted at the end of a support telescope pole at a specific height from the soil surface to maximise the scanning area. A foreoptic was aligned vertically (nadir) with a field of view (FOV) of 3.5$^{o}$ and a FOV of 25° without using the foreoptic. In all greenhouse experiments the height of the spectroradiometer was kept at 1.7 m from the pot soil surface and it was adjusted to cover most of the (whole) canopy of each pot. The spectroradiometer was connected to a computer, which stores the individual scans for subsequent processing. Reflectance spectra (350 nm-1050 nm) of the plant canopies were acquired regularly with solar radiation during clear days (free-cloud days) from 11am to 3 pm over the first two experiments of the Scottish and Egyptian wheat experiments. Spectra collection was started at early growth stages before applying different treatments, and continued over the growing season until harvest time. Five scans for each pot were acquired to obtain the average, and therefore, reduce variations within pots.

During field work in Egypt, care was taken to keep a constant distance of 2 m between the spectroradiometer and soil surface using an iron stand (see Fig. 3.2). The instrument was used without the foreoptic during field work, providing a FOV of 25° and notes were taken during the daily work about weather conditions including light intensity, time and cloud cover. Also, the reflectance was measured as quickly as possible to cover many fields within a short period of time (around noon) before sun angle changes to reduce variability. Care was taken to minimise the influence of shadow and the white Spectralon reference panel was used before acquiring reflectance at each location within the same field during the field work. A combination of visual inspection and distance from irrigation channels was used to try and encompass a gradient of crop stress across the study area. Figures 3.2 and 3.3 show examples of measuring reflectance from wheat canopies using natural solar radiation and artificial illumination source (two 300 W halogen lamps). Figure 3.4 shows reflectance measurements at the leaf scale under darkroom conditions.

**Figure 3-2** Measuring reflectance from wheat canopy in the field.

### Darkroom measurements

For the greenhouse experiments reflectance measurements were also made in a darkroom to avoid changing light intensity from solar radiation and to have a constant light incident on the plant canopy. The darkroom measured 3.9 x 2.75 x 2.35 m (length x width x height). To minimise the reflectance from the floor and walls a non-reflective black cloth with a very low reflectance (reflectance < 5%) was used to cover the walls to prevent reflectance from them and the floor was painted with a non-reflective black paint. The spectroradiometer and two 300 W halogen lamps were mounted on the ceiling at a height of 2 m to cover the maximum possible area from each pot. The instrument was calibrated using a white Spectralon reference panel (reflectance ≈ 100%). Fig. 3.3 shows the darkroom during reflectance measurements from wheat canopies. The distance between the spectroradiometer and pot surface were kept constant over the whole growing season.

**Figure 3-3** Measuring reflectance from wheat canopy in the darkroom using artificial illumination.

**Figure 3-4** Measuring spectral reflectance at the leaf scale under darkroom conditions using artificial illumination.

### 3.4.2 Physical Characteristics of Plants

### 3.4.3 Biometric properties

**Leaf area index (LAI)**

Leaf area was measured three times for the Scottish wheat experiments and five times for the Egyptian wheat experiments during the growing season immediately after spectroradiometry measurements from wheat and maize crops. The number of replicates of each treatment was larger for Egyptian wheat. Ten wheat plants were sub sampled and all leaves were removed, weighed and the fresh weight was recorded. Twenty discs of 1 cm in diameter were taken from different leaves randomly of the sub-sample at different locations on each leaf from leaf tip to leaf base. Five discs were taken randomly to determine leaf area for each treatment. To calculate the whole leaf area the weight and the area measured for the five discs were used according to the following equation.

$$\text{The whole leaf area} = \frac{WT \times DA}{DW} \quad \text{…….3.2}$$

Where WT is the weight of the whole sample,

DA is the area of a specific number of discs

DW is the weight of these discs

After calculating the leaf area for each treatment, the Leaf area index can be calculated by dividing the total leaf area for each sample by the area occupied by these plants as follows:

$$\text{LAI} = \frac{LA}{SA}$$

Where:

LAI is the leaf area index

LA is the leaf area per sample

SA is the occupied land area

**Plant height**

Plant height was recorded bi-weekly during the first two experiments of Scottish and Egyptian wheat (winter 2005-6 and spring 2006). Additionally, plant height was measured immediately after measuring reflectance from plant canopies. During the last three experiments using the darkroom, it was measured immediately after measuring reflectance since reflectance measurements were independent of weather conditions.

### 3.4.4 Grain yield

Wheat plants were harvested at the end of June for winter season 2005-6, early September for spring wheat 2006. In the third experiment for Egyptian and Scottish winter wheat 2006-7, Egyptian wheat reached maturity (end of May) before Scottish wheat (mid June). The maturation of grain was observed visually depending on the colour as plants turned completely yellow and also some spikes were threshed manually to make sure that all seeds were dry. At harvesting, there were three pots for each treatment and plants were cut just above soil level and separated into leaves, stems and spikes. Spikes for each pot were threshed manually and the total grain yield was recorded. The grain yield was converted to kg $m^{-2}$ by relating the yield from an area of 0.15 $m^2$ to an area of 1 $m^2$.

## 3.5 Soil Sampling

### 3.5.1 Soil sampling for greenhouse experiments

The soil used in the greenhouse pot experiments was taken from the walled garden area at the University of Stirling. Soil was collected from surface and sub surface levels (10-30 cm) and mixed thoroughly to be representative of the soil used in the pot experiments. Soil samples of approximately 1 kg each were sub-sampled to characterise the soil properties (electrical conductivity, pH, chemical analysis-anions and cations and particle size distribution). Samples for analysis were oven dried at 105°C for 24 hours then ground and sieved to < 2 mm.

### 3.5.2 Soil sampling for field work

In June 2006 and before the two field work visits were undertaken, soil samples were collected from the study area (south-west Alexandria, Egypt). Sample sites were chosen randomly from surface (0-20 cm) and sub-surface levels (20-40 cm). A soil

sample of approximately 1 kg was collected and immediately put in a sealed plastic bag for analysis. Twenty three soil samples were collected covering three different areas; Kahr, Hewaihy and Bangar sites within the study area. To determine soil characteristics, some soil chemical analysis such as salinity, pH, anions, cations and nitrogen concentration were determined. During the two field work visits in March and July 2007 to collect ground reference data for wheat and maize, three soil samples were collected from each field at different locations and placed in a sealed plastic bag then taken as soon as possible to a laboratory belonging to the ministry of agriculture in Egypt for analysis.

## 3.6 Soil Analysis

### 3.6.1 Soil pH

Three oven dried soil samples were taken to determine the pH. Soil paste extracts were prepared and the pH measured according to Rowell (1994). A WPA analogue pH meter model C14/16/18 was used to measure soil pH. The pH values were also determined in the presence of calcium chloride ($CaCl_2$).

### 3.6.2 Soil Salinity

The soil salinity in oven dried soil samples was determined using soil paste extract according to Rowell (1994). Soil samples were weighed to determine the wet weight then oven dried for 24 hours at 105°C and passed through a 2 mm sieve. A weight of about 300 g of oven dried soil was put into a weighed 500 ml plastic beaker. Distilled water was added to the soil sample with stirring until nearly saturated. The paste was allowed to stand for several hours to wet thoroughly, and then more water was added to form a saturated paste. In this state the paste glistens as it reflects light, flows slightly when the beaker is tipped, slides freely and cleanly off a spatula and is consolidated easily by tapping the beaker after a trench has been formed in the paste with a spatula. The beaker was covered and allowed to stand overnight and then the condition of the paste was checked. More distilled water or more dried soil was added depending on the paste condition. After that the saturated paste was transferred on to a toughened filter paper in a Buchner funnel, the extract was collected in a sample glass after applying suction to the filtering unit. Before measuring the electrical conductivity of the soil paste, the instrument was calibrated against NaCl solutions as

recommended. Finally, the electrical conductivity of the sample was measured and recorded at 25°C.

### 3.6.3 Organic matter and particle size distribution

Particle size distribution aims to determine different particles of sand, silt and clay to provide a soil classification. Three sub-samples of oven dried soil were taken from the greenhouse experiment soil for determining particle size distribution. Organic matter determined by loss on ignition at 375$^{o}$C (Ball, 1964) was very low (0.09%). Ten grams from each sample were suspended in 25 ml of distilled water and 2 ml of Calgon (Sodium hexametaphosphate) was added for dispersing. The suspension was left for 10 minutes to ensure that the soil was fully saturated and then shaken for 10 more minutes to give a homogenous suspension. Before injecting the sample into the instrument (Coulter LS 230), an automatic stirrer with a magnet was used for stirring the suspension and finally a pipette was used to take a volume of the suspension then injected into the instrument for analysing particle size distribution. The instrument gives the percentage of clay, silt and sand (see Table 3.4), which were recorded to use it on the triangle diagram to determine soil texture. These three percentages then used to identify soil texture.

### 3.6.4 Exchangeable Anion and Cation concentration

Sub-samples of oven dried soil sieved to < 2 mm diameter were used to determine cations and anions. To quantify the concentration of anions and cations, an amount of 0.5 g oven dried soil was weighed and transferred to a 50 ml beaker then a volume of 20 ml KCl (1.0 M) from a measuring cylinder was added and the mixture was stirred to ensure complete wetting of the soil (Rowell, 1994). The suspension was filtered through a no. 2 filter paper into a 100 ml volumetric flask, and then the soil was leached with another four 20 ml portion of KCl. Two volumes of 50 ml of the extract were taken for determining different cations using atomic absorption (UNICAM 989 AA Spetrometer) and anions using dionex (DX-120 ION Chromatography). All standards for different elements were bought from Ficher Scientific International Company. Table 3.4 shows some soil specifications including anions ($CO_3$, $HCO_3$, $SO_4$ and Cl), cations (Ca, Mg, Na and K), organic matter, percentage of silt, sand and clay, electrical conductivity, pH and field capacity. Anions and cations were also

determined in water samples collected during greenhouse experiments using same routine.

**Table 3-4** some physical and chemical properties of the soil used in the greenhouse experiments.

| | |
|---|---|
| Field capacity (%) | 30.10 |
| Sand (%) | 58.48 |
| Silt (%) | 36.79 |
| Clay (%) | 4.73 |
| pH | 4.90 |
| Electrical Conductivity, EC, (ds $m^{-1}$) | 1.20 |
| Organic matter (%) | 0.09 |
| Calcium, Ca, mg/kg | 88.00 |
| Magnesium, Mg, mg/kg | 13.20 |
| Sodium, Na, mg/kg | 6.68 |
| Potassium, K, mg/kg | 7.46 |
| Carbonate, $CO_3$, mg/kg | 0.50 |
| Bicarbonate, $HCO_3$, mg/kg | 57.0 |
| Sulphur, $SO_4$, mg/kg | 30.70 |
| Chloride, Cl, mg/kg | 27.48 |

## 3.7 Statistical analysis

Analysis of variance was performed in MINITAB v.15 to analyse yield and aboveground biomass data for both wheat and maize under moisture and salinity stressors. Salinity, moisture and salinity/moisture were used as predictor variables, and yield and biomass data as the response variables. Data were checked for normality using Anderson- Darling method with 95% significance level.

Where necessary residual diagnostics were performed to ensure compliance with the assumptions of the regression. The Pearson Product Moment correlation coefficient was used to test the association between different vegetation indices and crop properties and to identify optimum vegetation indices. Simple linear and multiple regression analysis were used to derive regression equations to the retrieval of grain yield and biomass under moisture and salinity stressors.

The differences in the spectral signatures from healthy and stressed treatments were also investigated using the Principle Component Analysis (PCA) in MINITAB v.15. The spectral datasets from each experiment were examined individually and the best results were chosen to identify the optimum time to distinguish between moisture and salinity induced stress. The advantage of using PCA is to reduce the dimensionality of

large datasets such as spectroradiometry. Prior to performing the PCA and to reduce the dimensionality of the 0.5 nm of the instrument spectral resolution, the original spectral datasets were averaged to 10 coarser resolution datasets. Moreover, the five scans obtained from each pot or location was averaged to reduce variability within each pot or location. The spectra between 400 nm and 900 nm were used in this analysis to avoid noise extremes at either ends of the spectrum.

## 3.8 Summary

This chapter describes the methodologies used to collect and prepare vegetation, characterise their spectral properties and soil samples for analysis to achieve the objectives of this research project, previously mentioned in Chapter 1. The techniques and the instruments used to determine the soil characteristics are described in this chapter. The design of the greenhouse experiments and the specific implementation of *in situ* spectroradiometry are described in Chapters 4 and 5. More specific, remote sensing acquisition details, data processing and analysis will be described in Chapter 6. The next chapter will investigate the potential of *in situ* hyperspectral measurements in detecting stress in wheat crops when subjected to moisture and salinity stress.

# 4 IN SITU SPECTRORADIOMETRY MEASUREMENTS IN MONITORING WHEAT

## 4.1 Introduction

Chapter 3 outlined the generic methodology and equipment used in this research project. This chapter explores the potential for *in-situ* hyperspectral remotely sensed data to predict stress in wheat when subjected to a combination of various salinity and moisture stresses and addresses the following hypotheses: (i) *in situ* hyperspectral measurements are able to detect stress in wheat crops and (ii) moisture induced stress can be distinguished from salinity induced stress spectrally.

In order to control factors influencing the response of wheat crops, reflectance measurements from the plant canopies and leaves are collected to evaluate the response of both broad band and hyperspectral vegetation indices to predict biophysical and biochemical properties of wheat including; aboveground biomass, plant height, leaf area index, final grain yield and chlorophyll *a* concentration. This chapter focuses on wheat crops and contrasts the behaviour of Scottish and Egyptian wheat varieties in response to salinity and moisture induced stress. Wheat has been chosen specifically for this research as it is the most important agricultural crop in Egypt.

## 4.2 Aims and objectives

The specific aim of the research presented in this chapter is to evaluate the potential of *in situ* hyperspectral measurements for detecting stress in Scottish and Egyptian wheat varieties when subjected to both salinity and moisture induced stress. The specific research objectives are:

- Under controlled greenhouse conditions grow wheat and subject plants to moisture and salinity induced stress over ranges known to have an effect on plant response.
- Use reflectance measurements to detect stress in wheat under controlled conditions through using different vegetation indices.

- Establish whether salinity induced stress can be distinguished spectrally from moisture induced stress.
- Identify which spectral indices are sensitive to different crop properties.
- Identify wavelengths sensitive to stress and biochemical properties of wheat crops.
- Consider implications for remote sensing for wheat stress.

## 4.3 Experimental design and methods

### 4.3.1 Greenhouse experiment

The greenhouse-based experiments were undertaken at the gardens of the University of Stirling, Stirling, United Kingdom (latitude 56°8`46.25``, longitude 3°55`4.54``) during winter season of 2005-6, spring season of 2006 and winter season of 2006-7. The experimental soil was a sandy loam with low organic matter (0.09%), a pH of 4.9 and an EC of 1.2 dS $m^{-1}$. The particle size distribution consists of 58.48% sand, 36.79% silt and 4.73% clay (see Table 3.4 for a more detailed breakdown of soil properties). About 2500 kg of soil was collected from the University of Stirling's Estates Garden Centre to fill pots. To ensure soil homogeneity, the soil was mixed thoroughly and three sub-samples were collected for chemical analysis, including pH, electrical conductivity (EC), cations ($K^+$, $Na^+$, $Mg^{2+}$, $Ca^{2+}$) and anions, ($Cl^-$, $SO_4^{2-}$, $CO_3$, $HCO_3$).

The Scottish wheat variety Gladiator was grown initially in the 2005-6 winter growing season. This variety has a lower tolerance to salinity and thus examines the ability to distinguish salinity and moisture induced stress spectrally. Scottish and Egyptian wheat varieties were used in three successive growing seasons (see Table 4.1). Winter wheat was sown in the second week of October 2005 and during the last week of October 2006. Spring wheat was sown in the last week of March 2006. Wheat seeds were sown at a depth of 3-5 cm at a seed rate of 200 seeds $m^{-2}$; a specific mesh was designed for this purpose to ensure that plant spacing was constant and uniform for all pots. Nitrogen, phosphor and potassium were applied to the pots at

levels of 100, 60 and 60 kg $ha^{-1}$ respectively. In all growing seasons the total amount of phosphor and potassium was applied during soil preparation. The total dose of nitrogen was applied in the first week of March in all seasons for winter wheat and at the middle of May for the spring wheat.

**Table 4-1** Different growing seasons for Scottish and Egyptian wheat varieties.

| Season | Variety | Sowing date | Harvest date |
|---|---|---|---|
| Winter 2005-6 | Scottish (Gladiator) | 12 October | 25 June |
| Spring 2006 | Egyptian (Sakha 8) | 24 March | 4 September |
| Winter 2006-7 | Scottish (Gladiator) | 25 October | 15 June |
| Winter 2006-7 | Egyptian (Giza 93) | 25 October | 28 May |

To subject plants to different levels of moisture and salinity stress, eleven different treatments were used including: one control (tap water with an average salinity of 0.05 dS $m^{-1}$ with 90% FC (Field Capacity) moisture regime, three moisture regimes at 75%, 50% and 25% FC, three water salinity levels at 2, 4, and 6 dS $m^{-1}$, and four combinations of both moisture and salinity (a complete list of the treatments is given in Table 4.3). Tap water was salinized with sodium chloride (NaCl) and Calcium chloride ($CaCl_2$) mixture at 1:1 volume ratio; concentrations were used to generate EC values of about 2, 4 and 6 dS $m^{-1}$. A large container was used to mix tap water with the salinization solution. Samples of tap water were collected for chemical analysis including cations and anions (see Table 4.2). To achieve a high germination rate, tap water was used for the first two irrigations in all treatments. During the first experiment (Scottish wheat, winter growing season 2005-6) the watering regime was set as intervals of 20, 30 and 40 days and one control at 10 days. The watering regime was changed for the remainder of the experiments to fractions of field capacity.

**Table 4-2** Chemical analysis of tap water samples from the greenhouse.

| Sample | pH | EC, ds $m^{-1}$ | Cations, mg/l | | | | Anions mg/l | | | |
|---|---|---|---|---|---|---|---|---|---|---|
| | | | Ca | Mg | Na | K | Cl | $SO_4$ | $NO_3$ | P |
| 1 | 6.31 | 0.083 | 9.31 | 0.98 | 1.93 | 0.263 | 4.11 | 11.67 | 0.62 | 2.63 |
| 2 | 6.09 | 0.072 | 9.73 | 0.98 | 2.23 | 0.277 | 4.16 | 11.7 | 0.61 | 2.75 |
| 3 | 6.21 | 0.068 | 9.72 | 0.97 | 2.11 | 0.262 | 4.12 | 11.76 | 0.61 | 2.85 |

**Table 4-3** Moisture, salinity and moisture/salinity treatments applied to the crops (five replicates).

| Treatment | Salinity | Watering regime (% FC) | | | |
|---|---|---|---|---|---|
| | | 0.90 | 0.75 | 0.50 | 0.25 |
| $T_1$ | 0.05 | + | | | |
| $T_2$ | 0.05 | | + | | |
| $T_3$ | 0.05 | | | + | |
| $T_4$ | 0.05 | | | | + |
| $T_5$ | 2 | + | | | |
| $T_6$ | 4 | + | | | |
| $T_7$ | 6 | + | | | |
| $T_8$ | 6 | | + | | |
| $T_9$ | 6 | | | | + |
| $T_{10}$ | 2 | | + | | |
| $T_{11}$ | 2 | | | | + |

Temperature was monitored in the greenhouses using a Grant, Squirrel SQ 800 data logger at 15 minute intervals and downloaded into MS Excel in order to calculate average daily and monthly values. Figure 4.1 shows the average monthly temperature in the 2005-6 and 2006-7 growing seasons.

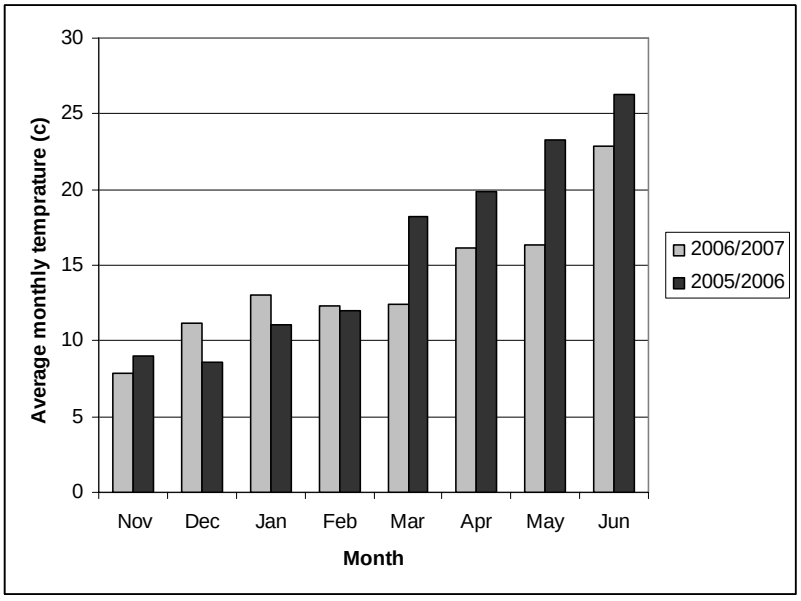


**Figure 4-1** Average monthly temperature inside the greenhouse in the 2005-6 and 2006-7 growing seasons.

### 4.3.2 Spectral data analysis

The spectral reflectance data was measured using an ASD FieldSpec Pro spectroradiometer, then downloaded to PC and pre-processed with ASD software. The *in situ* hyperspectral and laboratory darkroom spectral data were interpolated to a final spectral resolution of 0.5 nm then truncated between 300 and 1000 nm. Finally the

reflectance was smoothed to further reduce the noise at the start and the end of the magnetic spectrum by passing a 5 nm running mean filter over the whole spectrum.

To use reflectance in detecting stress in plants, 55 previously published narrow and broad band spectral vegetation indices were calculated (Tables 4.4 and 2.11). Blue, green, red and NIR bands were calculated from hyperspectral measurements using QuickBird bands, and then these bands were used to calculate different vegetation indices. The reflectance values for each band were averaged in Excel to have the mean. The calculated vegetation indices were used to predict changes in plant physiological responses to salinity and moisture stressors. Figure 4.2 shows the typical vegetation spectral response of the wheat canopy under clear sky conditions obtained in the 2005-6 growing season. To distinguish between moisture and salinity induced stress, Principle Component Analysis (PCA) was used to analyse the spectra in the 400-900 nm range; this eliminated the noise at either end of the spectrum. PCA were performed on all datasets collected over the growing season in each experiment to choose the optimum time to differentiate between these two stressors.

To investigate the effects of moisture, salinity and moisture/salinity on different biophysical and biochemical properties of wheat crops, analysis of variance (ANOVA) was applied to the data. Furthermore, simple and multiple regression analysis were carried out to predict wheat properties as a function of moisture and salinity stress levels.

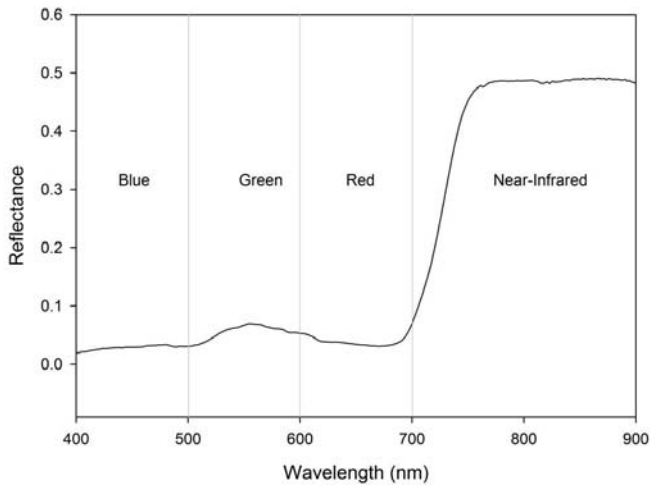


**Figure 4-2** An example of typical vegetation spectral reflectance measured from wheat canopy under solar radiation obtained from a control sample of healthy Scottish wheat.

**Table 4-4** Different spectral reflectance indices calculated from *in situ* and laboratory darkroom spectroradiometry (le Mair *et al*., 2004).

| Vegetation Index | Formula | Intended scale | Reference |
|---|---|---|---|
| $NDVI_{broad}$ | $(R_{NIR}-R_{Red})/(R_{NIR+}R_{Red})$ | Canopy | Rouse *et al*., 1973 |
| $NDVI_{hyper}$ | $(R_{800}-R_{680})/(R_{800}+R_{680})$ | | |
| Green $NDVI_{broad}$ | $(R_{NIR}-R_{green})/(R_{NIR+}R_{green})$ | Canopy | Gitelson *et al*., 1996 |
| Green $NDVI_{hyper}$ | $(R_{750}-R_{550})/(R_{750}+R_{550})$ | | |
| SIPI | $(R_{800}-R_{445})/(R_{800}+R_{680})$ | Leaf | Penuelas *et al*., 1995 |
| TCHVI | $[(R_{red}-R_{green})+(R_{NIR}-R_{red})]/$ $[(R_{red}-R_{green})+(R_{NIR}-R_{red})]$ | Canopy | Yefremenko *et al*.,1998 |
| NPQI | $(R_{415}-R_{435})/(R_{415}+R_{435})$ | Leaf | Barnes *et al*., 1992 |
| SRPI | $R_{415}-R_{680}$ | Leaf | Penuelas *et al*., 1994 |
| NPCI | $(R_{680}-R_{430})/(R_{680}+R_{430})$ | | |
| PSSRb | $R_{800}-R_{635}$ | Leaf | Blackburn, 1998 |
| PSNDb | $(R_{800}-R_{635})/(R_{800}+R_{635})$ | | |
| $R_{shoulder}$ | Mean $R_{750-850}$ | Canopy | Strachan *et al*., 2002 |
| PRI | $(R_{531}-R_{570})/(R_{531}+R_{571})$ | Leaf | Gamon *et al*., 1992 |
| C420 | $R_{420}/R_{695}$ | Leaf | Carter, 1994 |
| $R_{800}/R_{550}$ | | Leaf | Buschmann & Nagel, |
| $R_{800}-R_{550}$ | | | 1993 |
| NDI | $R_{800}R_{680}$ | Canopy | Jordan, 1969 |
| $R_{695}/R_{760}$ | | | |
| $R_{605}/R_{760}$ | | | |
| $R_{710}/R_{760}$ | | Leaf | Carter, 1994 |
| $R_{695}/R_{670}$ | | | |
| $R_{550}$ | | | |
| $R_{675}/R_{700}$ | | Leaf | Chappelle *et al*., 1992 |
| $R_{675}/(R_{700}Xr_{650})$ | | | |
| $R_{672}/(R_{550}Xr_{708})$ | | | Datt, 1998 |
| $R_{672}/R_{550}$ | | Leaf | |
| $R_{860}/(R_{550}Xr_{708})$ | | | |
| $R_{750}/R_{550}$ | | | Gitelson & Merzlyak |
| $R_{750}/R_{700}$ | | Leaf | ,1994 |
| $R_{725}/R_{675}$ | | | |
| $(R_{850}-R_{710})/(R_{850}+R_{680})$ | | Leaf | Datt, 1999 |
| $(R_{780}-R_{710})/(R_{780}+R_{680})$ | | Leaf | Maccioni *et al*., 2001 |

## 4.4 Results and discussion

### 4.4.1 Effects of moisture and salinity stress on biophysical properties of wheat

**Grain yield**

ANOVA analysis was used to assess the effects of both moisture and salinity on wheat grain yield. The results are listed in Table 4.5 and depicted in Figures 4.3 and 4.4. The results show that both moisture and salinity significantly affected wheat grain yield in all seasons of winter 2005-6, spring season of 2006 and winter 2006-7 on both Egyptian and Scottish wheat varieties. Moisture stress treatments highly affected the yield ($R^2$ = 0.96 and p = 0.000 in the 2005-6 growing season). A significant decrease in grain yield was observed with increasing water stress level. The highest grain yield of 1.17 and 1.03 kg $m^{-2}$ were recorded with the control treatments in the 2005-6 and 2006-7 growing seasons in Scottish wheat. The Egyptian wheat varieties followed the same trend with the highest grain yields of 0.66 and 0.62 kg $m^{-2}$ recorded in the control treatments of the winter season 2006-07 and spring season 2006 respectively.

**Table 4-5** P values of analysis of variance (ANOVA) results for the effects of moisture, salinity and moisture/salinity on grain yield of Scottish and Egyptian wheat crops in different seasons. Highlighted values are significant (P<0.05).

| Season | Source of variation | | | $R^2$ | $R^2_{adj}$ |
|---|---|---|---|---|---|
| | Moisture | Salinity | Moisture/ salinity | | |
| Winter 2005-6 | 0.000 | 0.000 | 0.000 | 96.9 | 95.5 |
| Spring 2006 | 0.000 | 0.000 | 0.000 | 98.5 | 97.9 |
| Winter 2006-7 (Scottish) | 0.000 | 0.000 | 0.000 | 99.0 | 98.6 |
| Winter 2006-7 (Egyptian) | 0.000 | 0.000 | 0.000 | 96.9 | 95.5 |

Salinity also significantly affected wheat grain yield in all seasons for both the Scottish and Egyptian wheat varieties. Significant decrease in wheat grain yield was observed with increasing water salinity levels. The highest grain yield was recorded with the control treatments of tap water. The lowest grain yields of 0.22, 0.17, 0.36 and 0.21 kg $m^{-2}$ for Scottish winter wheat in 2005-6, Egyptian spring wheat 2006, Scottish winter wheat 2006-7 and Egyptian winter wheat 2006-7, respectively were recorded with low watering regime and high salinity levels.

Figures 4.3 and 4.4 show that wheat grain yield was affected by increasing salinity levels; this may be due to the main function of good water quality in building new cells and their growth. Results also showed that the effects of moisture regime on grain yield was higher than the effects of salinity in all growing seasons, this may be attributed to the low rate of photosynthesis as a result of small leaf area. The interaction between moisture regime and salinity level also had a significant effect on wheat grain yield in all growing seasons.

Simple and multiple linear regressions were performed to investigate the relationship between wheat grain yield and both salinity and moisture levels. The multiple regression equations below were developed to describe this relationship. A simple regression analysis was applied first to assess the relationship between grain yield and moisture levels. The results showed that a significant linear relationship was found between grain yield and moisture regime in all growing seasons for both Scottish and Egyptian wheat varieties. This indicated that yield reductions were highest in treatments with low watering regimes (25% FC or 40 days interval in the first experiment with Scottish wheat, 2005-6 growing season). A further significant linear relationship was found between wheat grain yield and water salinity levels indicating that reductions in grain yield were higher with high salinity levels (6 dS $m^{-1}$).

Multiple regression analysis showed a significant relationship between wheat grain yield and both moisture and salinity stress ($R^2$ = 0.80, 0.87, 0.88 and 0.89 for Scottish wheat in 2005-6, Egyptian wheat in spring 2006 and both Scottish and Egyptian wheat in 2006-7 respectively).

The following are the multiple regression equations for the relationship between Scottish and Egyptian wheat grain yield and both moisture and salinity stress treatments in different growing seasons:

Scottish wheat in winter season 2005-6

Equation 4.1: $Y = 1.09 – 0.021\ F – 0.028\ S$ $\quad R^2_{adj} = 78.3\%$

Scottish wheat in winter season 2006-7

Equation 4.2: $Y = 0.285 – 0.74\ W – 0.041\ S$ $\quad R^2_{adj} = 82.6\%$

Egyptian wheat in spring season 2006

Equation 4.3: $Y = 0.046 - 0.51\ W - 0.005\ S$ $\quad R^2_{adj} = 85.8\%$

Egyptian wheat in winter season 2006-7

Equation 4.4: $Y = 1.8 - 0.49\ W - 0.027\ S$ $\quad R^2_{adj} = 88.1\%$

Where Y was the total grain yield (kg $m^{-2}$), F the watering frequency (days), S the water salinity level (dS $m^{-1}$) and W the watering regime (% FC). For all regression equations, p values were always 0.000 associated with high values of coefficient of determination ($R^2$) and the difference between $R^2$ and adjusted $R^2$ was always less than 1.5%. Some relationships may not be conclusively linear, but useful for the first approximation. For example, Fig 4.4 shows linear relationship in the first graph and non-linear in the third graph.

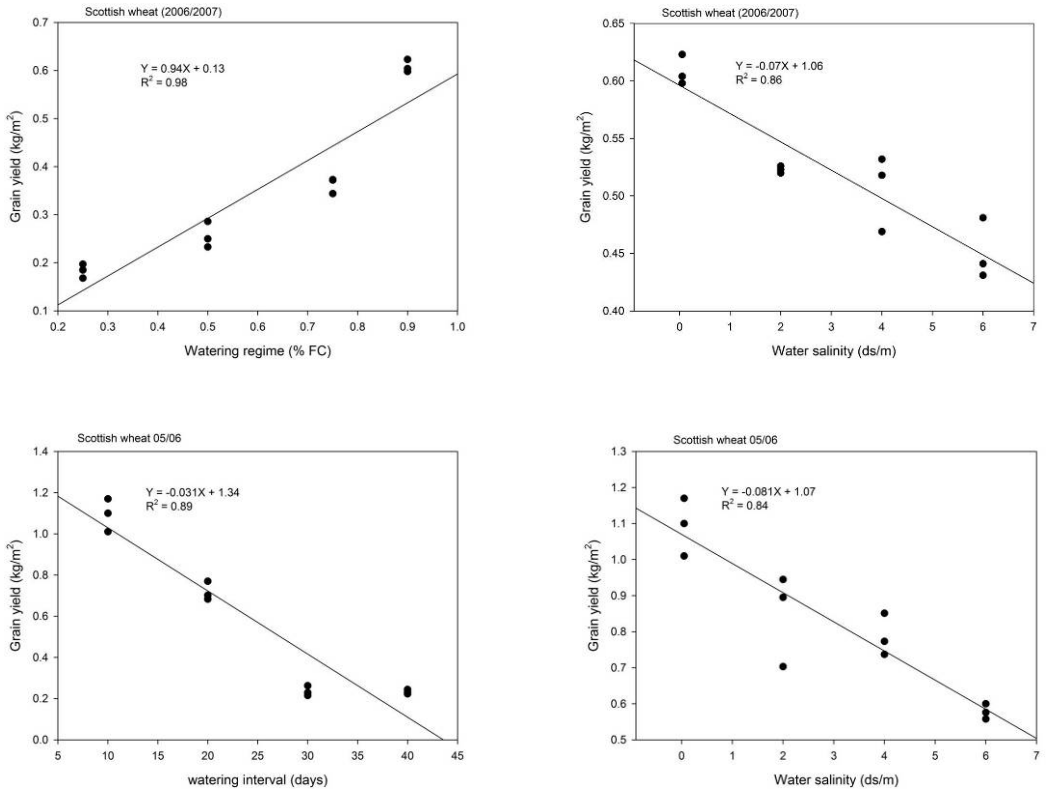


**Figure 4-3** The effects of moisture and salinity stress on total grain yield of Scottish wheat in the 2005-6 and 2006-7 growing seasons (n = 12).

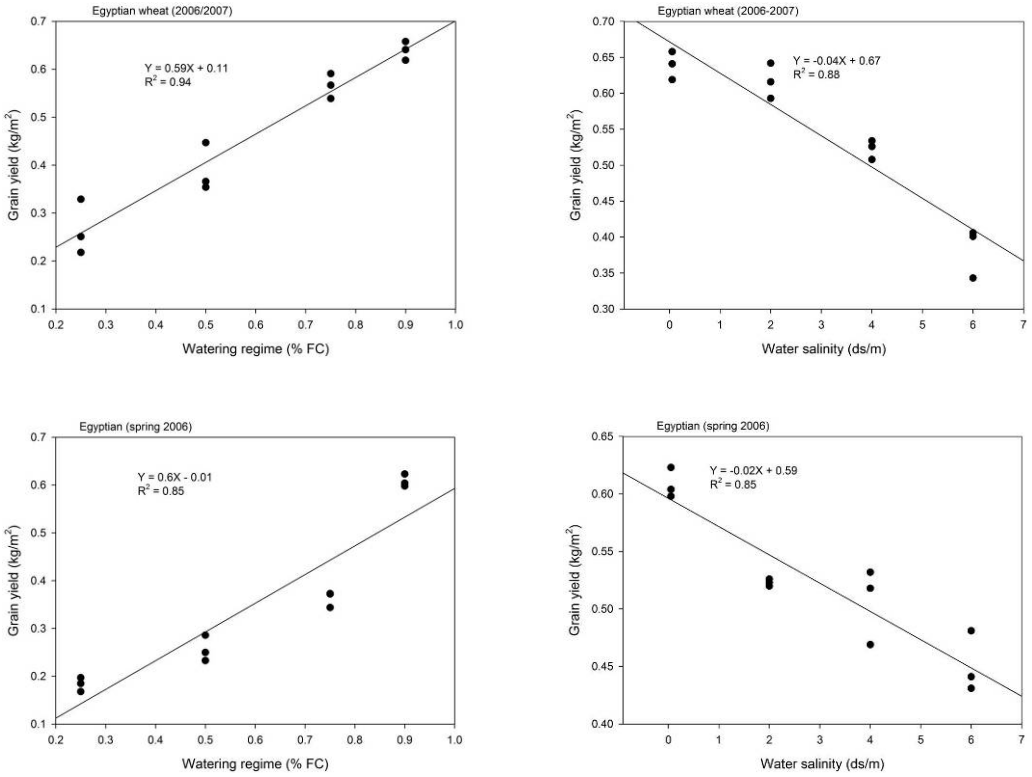


**Figure 4-4** The effects of watering regime and water salinity on total grain yield of Egyptian wheat in the spring season of 2006 and winter season of 2006-7 (n = 12).

## Aboveground biomass

The analysis of variance was performed to assess the relationship between aboveground biomass and both moisture and salinity stress. Results detailed in Table 4.6 show that the aboveground biomass has been greatly affected by moisture stress in all growing seasons of Scottish and Egyptian wheat varieties. Results illustrated in Figures 4.5 and 4.6 show that there is a noticeable reduction in total biomass with decreasing moisture levels. The highest production of aboveground biomass was recorded with the control treatment (tap water at 90% FC). The aboveground biomass was negatively correlated with decreasing watering regime level. This data also showed that grain yield was negatively correlated with increasing water salinity level.

It was further observed that the total aboveground biomass was not affected by different treatments of salinity and moisture stress over the first three months (November-January) of the winter wheat growing seasons. This may be due to the low evapotranspiration during this time, which affects the rate of photosynthesis in plants.

**Table 4-6** P values of analysis of variance (ANOVA) results for the effects of moisture, salinity and moisture/salinity on aboveground biomass of Scottish and Egyptian wheat varieties at harvesting in different growing seasons. Highlighted values are significant (P<0.05).

| Season | Source of variation | | | $R^2$ | $R^2_{adj}$ |
|---|---|---|---|---|---|
| | Moisture | Salinity | Moisture/salinity | | |
| Winter 2005-6 (Scottish) | 0.000 | 0.000 | 0.000 | 95.9 | 94.1 |
| Spring 2006 (Egyptian) | 0.000 | 0.000 | 0.000 | 99.0 | 98.6 |
| Winter 2006-7(Scottish) | 0.000 | 0.000 | 0.000 | 98.7 | 98.1 |
| Winter 2006-7 (Egyptian) | 0.000 | 0.000 | 0.000 | 96.5 | 94.9 |

Simple and multiple regressions were performed to investigate the relationship between total aboveground biomass and moisture and salinity stress. The simple regression equations showed significant differences for both stressors between control and different salinity and moisture levels. This significant linear relationship between biomass and both factors indicating that biomass is highly reduced with saline water and low watering regime, and therefore, multiple regression analysis has been performed to develop a regression equation to predict total aboveground biomass. Following are the multiple regression equations for all winter and spring growing seasons of Scottish and Egyptian wheat varieties.

Scottish wheat in winter season 2005-6

Equation 4.5: $B = 2.18 - 0.03\ F - 0.036\ S$ $\quad R^2 = 86.6\%;\ R^2_{adj} = 85.7\%$

Scottish wheat in winter season 2006-7

Equation 4.6: $B = 0.731 + 1.26\ W - 0.083\ S$ $\quad R^2 = 82.1\%;\ R^2_{adj} = 81.0\%$

Egyptian wheat in spring season 2006

Equation 4.7: $B = 0.36 + 0.95\ W - 0.012\ S$ $\quad R^2 = 89.9\%;\ R^2_{adj} = 89.2\%$

Egyptian wheat in winter season 2006-7

Equation 4.8: $B = 0.5 + 1.17\ W - 0.065\ S$ $\quad R^2 = 86.4\%;\ R^2_{adj} = 85.5\%$

Where B was the total aboveground biomass (kg $m^{-2}$), F the watering frequency (days), S the water salinity level (dS $m^{-1}$) and W the watering regime (% FC). It is clear from regression equations that both moisture and salinity stressors greatly affected aboveground biomass of wheat in all experiments. The strongest relationship

was observed in spring season 2006, which may have been a result of weather conditions during this time (high temperature, and therefore, high evapotranspiration).

Total biomass also was negatively correlated with salinity levels in all experiments of Scottish and Egyptian wheat varieties. Results obtained from the first and last experiments showed similar relationship (both Scottish wheat). Figures 4.5 and 4.6 showed positive linear relationship between the measured aboveground biomass and both moisture and salinity stress levels.

Because grain yield and aboveground biomass are closely linked, it can be further noticed that the coefficient of determination derived from regression equations for both crop parameters are approximately similar in all experiments. It is therefore important to estimate biomass at early growth stages to avoid crop reductions.

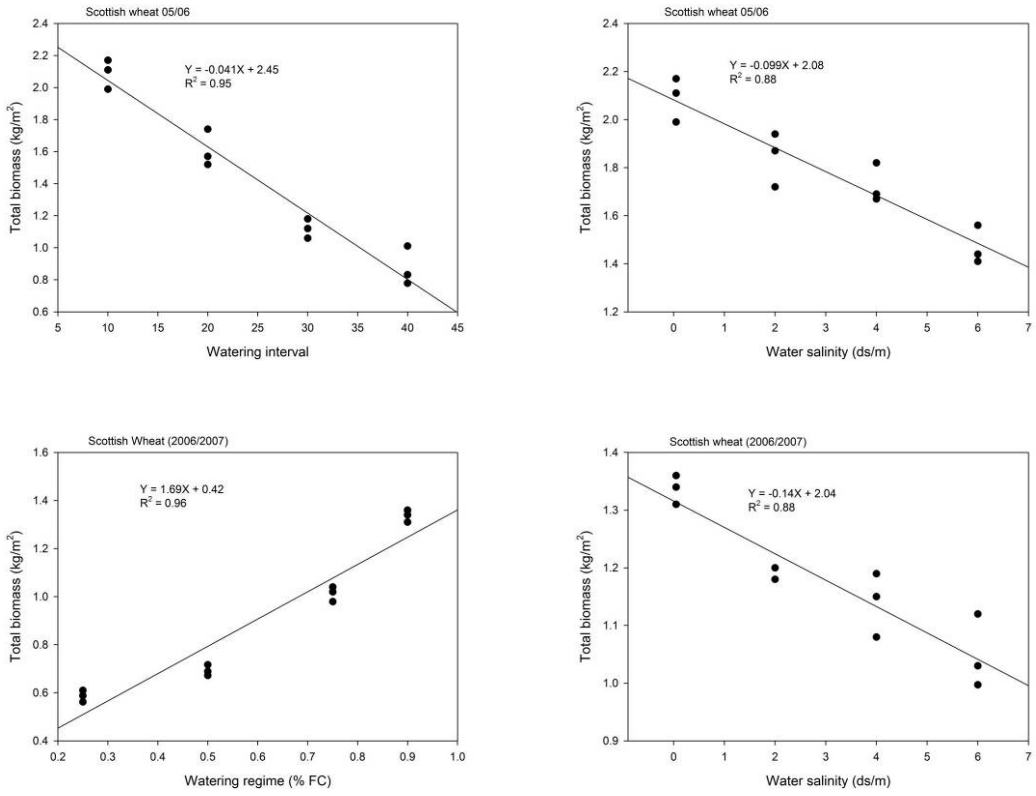


**Figure 4-5** The effects of watering regime and water salinity on total aboveground biomass of Scottish wheat in 2005-6 and 2006-7 growing seasons (n = 12).

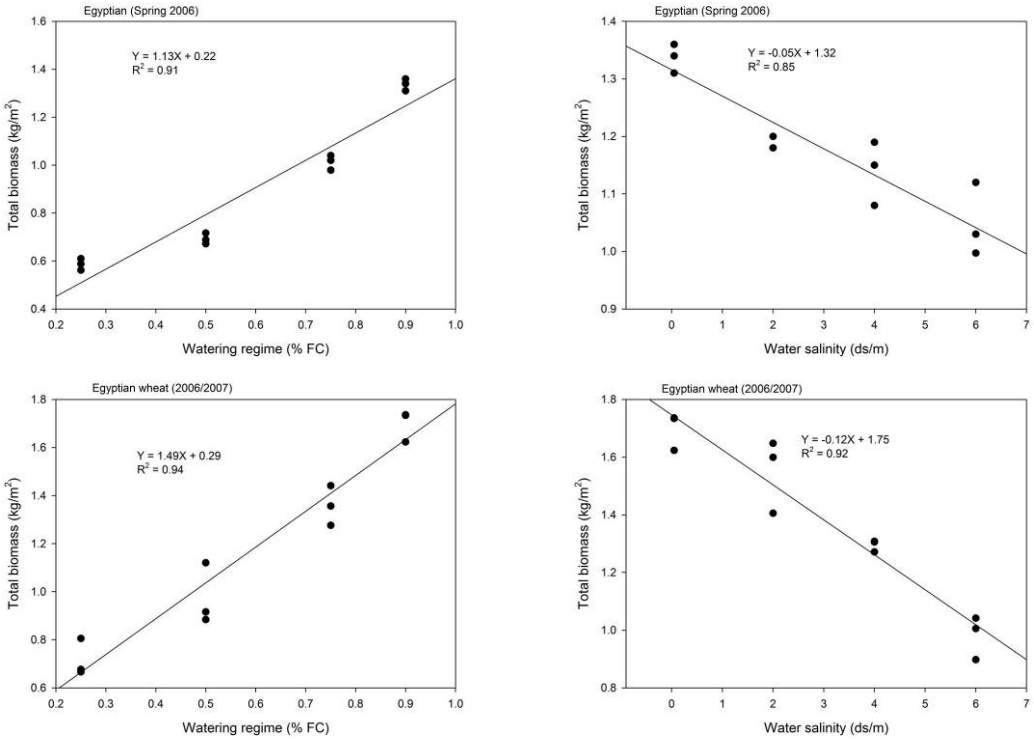


**Figure 4-6** The effects of watering regime and water salinity on total aboveground biomass of Egyptian wheat in the 2006 and 2006-7 growing seasons (n = 12).

## Plant height

Plant height was recorded concurrently with the reflectance measurements. Over the first two experiments with the Scottish wheat variety (winter season of 2005-6) and Egyptian wheat variety (spring season of 2006) the plant height was recorded every two weeks in addition to the immediate measurement after reflectance measurements were taken. This was because reflectance measurements during the first two experiments were affected by ambient light levels. In later experiments the darkroom was used to ensure consistent light intensity. Results detailed in Table 4.7 show the relationship between moisture, salinity and moisture/salinity and the plant heights of Scottish and Egyptian wheat varieties in three successive seasons of winter 2005-6, spring 2006 and winter 2006-7.

Generally, both moisture and salinity significantly affected wheat plant height in all wheat experiments at most measuring dates ($R^2 > 0.85$; $p = 0.000$). The interaction between these two stressors also showed significant effects on wheat plant height at most measuring dates. At early growth stages moisture, salinity and moisture/salinity did not show any significant effects on wheat plant height in all experiments.

**Figure 4-7** P values of analysis of variance (ANOVA) for the relationship between moisture, salinity, moisture/salinity and plant height of Scottish and Egyptian wheat varieties at different DAS over the four experiments. Highlighted values are significant (P<0.05).

| Season | Source of variation | | | $R^2$ | $R^2_{adj}$ |
|---|---|---|---|---|---|
| | Moisture | Salinity | Moisture/Salinity | | |
| **Scottish 05/06** | | | | | |
| 73 DAS | 0.705 | 0.603 | 0.662 | 0.19 | 0.00 |
| 125 DAS | 0.000 | 0.000 | 0.000 | 0.89 | 0.84 |
| 181 DAS | 0.000 | 0.000 | 0.000 | 0.89 | 0.84 |
| 207 DAS | 0.000 | 0.000 | 0.000 | 0.99 | 0.99 |
| 225 DAS | 0.000 | 0.000 | 0.000 | 0.99 | 0.98 |
| **Egyptian 2006** | | | | | |
| 57 DAS | 0.738 | 0.106 | 0.150 | 0.56 | 0.36 |
| 78 DAS | 0.000 | 0.030 | 0.000 | 0.95 | 0.93 |
| 91 DAS | 0.000 | 0.120 | 0.000 | 0.95 | 0.93 |
| 103 DAS | 0.000 | 0.006 | 0.000 | 0.94 | 0.92 |
| 127 DAS | 0.000 | 0.002 | 0.000 | 0.91 | 0.87 |
| **Scottish 06/07** | | | | | |
| 97 DAS | 0.762 | 0.481 | 0.317 | 0.29 | 0.00 |
| 135 DAS | 0.183 | 0.959 | 0.817 | 0.23 | 0.00 |
| 177 DAS | 0.000 | 0.000 | 0.006 | 0.96 | 0.94 |
| 198 DAS | 0.000 | 0.000 | 0.030 | 0.96 | 0.94 |
| 223 DAS | 0.000 | 0.000 | 0.000 | 0.98 | 0.97 |
| **Egyptian 06/07** | | | | | |
| 83 DAS | 0.123 | 0.715 | 0.100 | 0.60 | 0.52 |
| 108 DAS | 0.354 | 0.931 | 0.796 | 0.18 | 0.00 |
| 130 DAS | 0.000 | 0.000 | 0.000 | 0.93 | 0.91 |
| 149 DAS | 0.000 | 0.000 | 0.000 | 0.96 | 0.94 |
| 197 DAS | 0.000 | 0.000 | 0.000 | 0.98 | 0.97 |

### 4.4.2 Effects of moisture and salinity stress on chlorophyll *a* concentration of wheat leaves

The relationship between chlorophyll *a* concentration in wheat leaves and different salinity and moisture treatments is presented in Table 4.8 and illustrated in Figures 4.8 and 4.9. These show that both moisture and salinity treatments have significantly reduced the chlorophyll *a* concentration at the highest salinity and lowest watering regime level. There is a strong negative correlation between moisture stress and total chlorophyll *a* concentration. A significant correlation was also observed between the measured chlorophyll *a* and salinity levels, especially after applying the nitrogen dose in March in both winter growing seasons (2005-6 and 2006-7) and in May in the spring growing season of 2006.

Analysis of variance results for the first experiment demonstrated that up to 125 DAS the relationship between chlorophyll *a* concentration and salinity/moisture was not significant as p values ranged from 0.100 to 0.880. From 181 DAS, moisture, salinity

and moisture/salinity significantly affected the concentration of chlorophyll *a*. At 225 DAS the effects of moisture and moisture/salinity were non-significant; this may be due to chlorophyll *a* degradation prior to and during ripening.

Results obtained from the second experiment show that the effects of moisture were higher than the effects of salinity on chlorophyll *a* concentration in the plants. The effects of moisture started to be significant from 78 DAS. Moisture/salinity did not show any significant effects over the whole experiment. The early stress detection in this experiment (Egyptian wheat variety, spring season of 2006) may be attributed to the high temperature and the long days during this time of the year (April-August). Results obtained from the last two experiments of Scottish and Egyptian wheat in the 2006-7 growing season showed the same trend as the first two experiments with no significant effects detected. This is a result of the static period of growing (November–February), which may be attributed to very short days at this time of the year. At 177 and 130 DAS for Scottish and Egyptian wheat respectively, results showed that salinity, moisture and salinity/moisture had significant effects on the concentration of chlorophyll *a*.

The highest correlation between moisture and salinity stress and chlorophyll *a* concentration was observed just prior to flowering in May in both the 2005-6 and 2006-7 winter growing seasons for Scottish wheat variety ($r = 0.95$ and $-0.92$ for the 2005-6 growing season and 0.95 and -0.94 for moisture and salinity in the 2006-7 season). The results obtained from Egyptian wheat experiments (winter wheat season 2006-7) demonstrate that the highest correlation between chlorophyll *a* concentration and different moisture and salinity stress treatments were recorded around the flowering stage at the end of April ($r = 0.85$ and $-0.87$ for moisture and salinity stress respectively). Figures 4.8 and 4.9 showed the effects of moisture and salinity on chlorophyll *a* concentration extracted from wheat leaves in different seasons for the Scottish and Egyptian wheat varieties. It can be noticed that in all experiments both moisture and salinity stressors did not significantly affected wheat chlorophyll *a* concentration at early growth stages particularly winter seasons of Scottish and Egyptian wheat varieties.

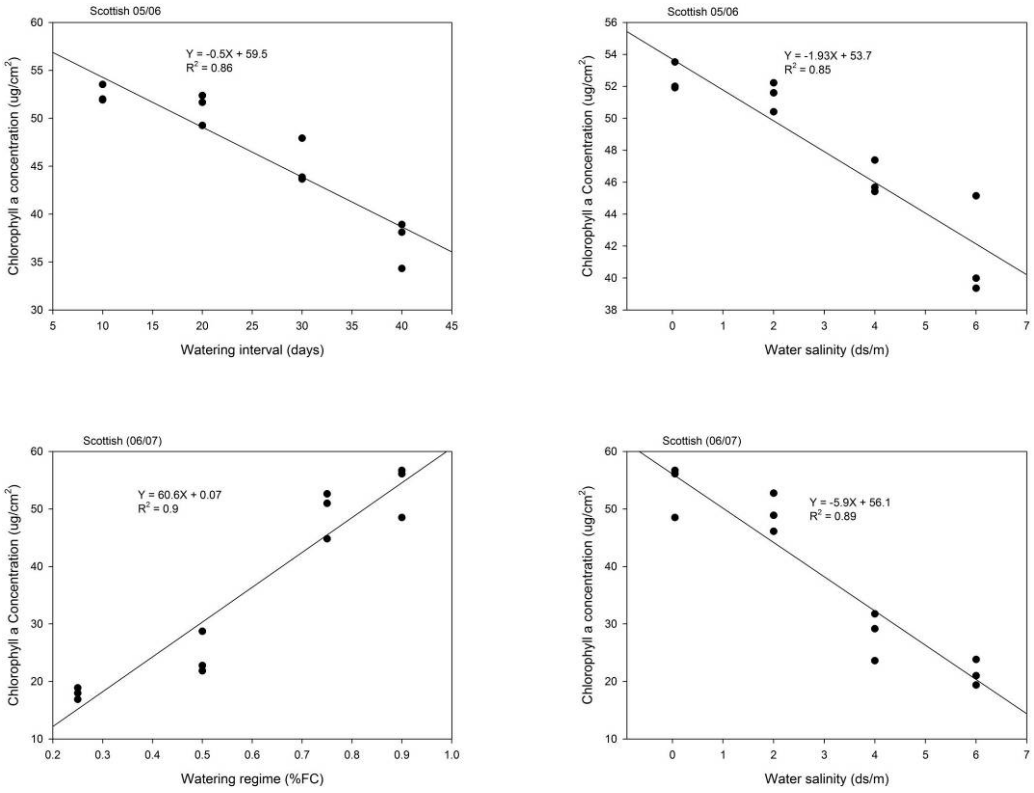


**Figure 4-8** Effects of moisture and salinity treatments on chlorophyll *a* concentration in Scottish wheat leaves at flowering stage in the 2005-6 and 2006-7 growing seasons (n = 12).

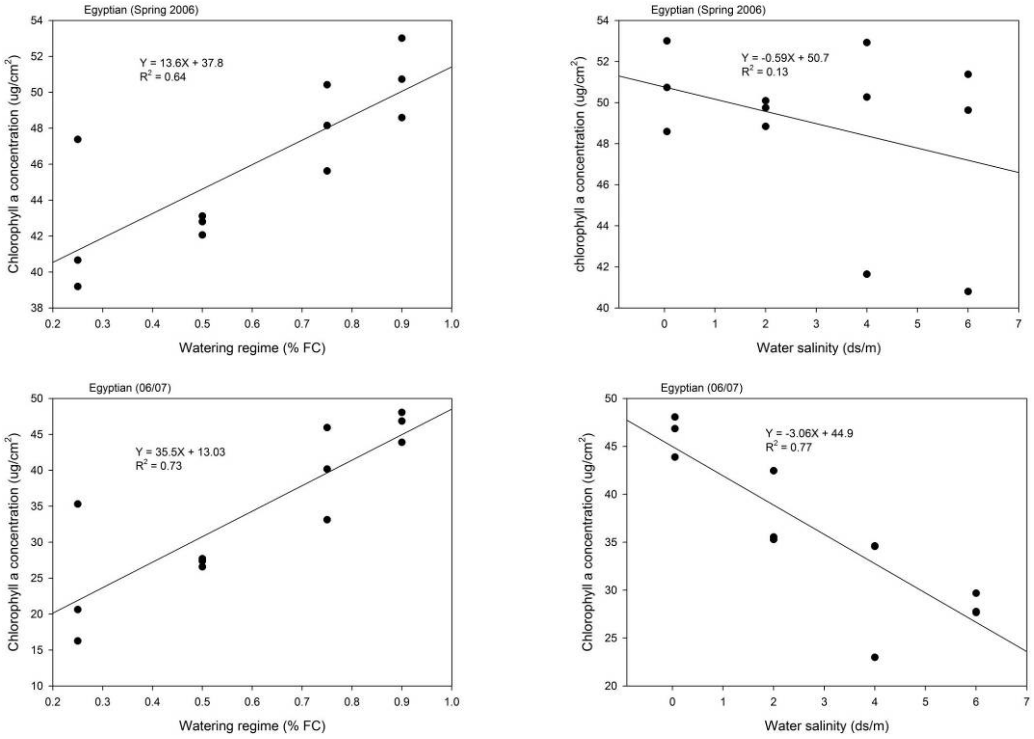


**Figure 4-9** Effects of moisture and salinity treatments on chlorophyll *a* concentration in Egyptian wheat leaves in the spring season of 2006 and winter season of 2006-7 (n = 12).

It is evident that the effects of salinity on chlorophyll *a* concentration over the second experiment (Egyptian variety) was not high in comparison to all other experiments and this may be attributed to the short growing season and consequently the lower amount of accumulated salts.

**Table 4-8** P values of analysis of variance (ANOVA) for the relationship between moisture, salinity and moisture/salinity and the concentration of chlorophyll *a* extracted from Scottish and Egyptian wheat leaves in different seasons. Highlighted values are significant (P<0.05).

| Season | Source of variation | | | $R^2$ | $R^2_{adj}$ |
|---|---|---|---|---|---|
| | Moisture | Salinity | Moisture/salinity | | |
| **Scottish 05/06** | | | | | |
| 73 DAS | 0.201 | 0.157 | 0.000 | 0.73 | 0.61 |
| 125 DAS | 0.215 | 0.882 | 0.579 | 0.26 | 0.00 |
| 181 DAS | 0.000 | 0.000 | 0.000 | 0.95 | 0.93 |
| 207 DAS | 0.001 | 0.001 | 0.008 | 0.77 | 0.67 |
| 225 DAS | 0.067 | 0.024 | 0.151 | 0.56 | 0.37 |
| **Egyptian 2006** | | | | | |
| 57 DAS | 0.223 | 0.324 | 0.211 | 0.40 | 0.13 |
| 78 DAS | 0.002 | 0.100 | 0.286 | 0.62 | 0.45 |
| 91 DAS | 0.000 | 0.495 | 0.895 | 0.64 | 0.48 |
| 103 DAS | 0.001 | 0.05 | 0.913 | 0.63 | 0.46 |
| 127 DAS | 0.001 | 0.06 | 0.922 | 0.63 | 0.46 |
| **Scottish 06/07** | | | | | |
| 97 DAS | 0.353 | 0.952 | 0.110 | 0.63 | 0.47 |
| 135 DAS | 0.215 | 0.882 | 0.579 | 0.27 | 0.00 |
| 177 DAS | 0.070 | 0.020 | 0.151 | 0.56 | 0.37 |
| 198 DAS | 0.000 | 0.000 | 0.000 | 0.93 | 0.90 |
| 223 DAS | 0.000 | 0.000 | 0.000 | 0.97 | 0.96 |
| **Egyptian 06/07** | | | | | |
| 83 DAS | 0.498 | 0.005 | 0.180 | 0.56 | 0.36 |
| 108 DAS | 0.201 | 0.157 | 0.000 | 0.73 | 0.62 |
| 130 DAS | 0.000 | 0.000 | 0.326 | 0.84 | 0.76 |
| 149 DAS | 0.000 | 0.000 | 0.000 | 0.96 | 0.95 |
| 197 DAS | 0.000 | 0.001 | 0.183 | 0.75 | 0.65 |

## 4.5 Reflectance measurements as a potential for predicting stress in Scottish and Egyptian wheat

### 4.5.1 The association between spectral reflectance and biochemical properties

The relationship between reflectance measurements and both moisture and salinity stress is depicted in Figure 4.10 which shows whole spectra measured from the wheat plant canopy under both stressors using solar radiation. The spectra collected from healthy plants (control treatment) show low values of reflectance in the blue region as a result of strong absorption by chlorophyll and other pigments. In the green region

the spectral reflectance from the wheat canopy increases up to the peak that is referred to as the 'green peak'. After the reflectance has reached this peak it decreases between about 625 and 680 nm as a result of chlorophyll *a* absorption. The behaviour of the spectral reflectance changes in the NIR region as the spectral reflectance increases rapidly forming the rededge (680-730 nm).

However, the spectral reflectance from stressed plants is different from the spectra obtained from healthy plants. Moisture stress greatly affects the signature as spectral reflectance increases in the blue, green and red regions. This may be due to the effects of different pigments and chlorophylls (*a* and *b*). The reflectance decreases in the NIR region in comparison to spectral signatures obtained from healthy plants (Serrano *et al*., 2000). The curves show that the green peaks from the spectra obtained from moisture induced stress treatments were shifted positively in comparison to spectra obtained from healthy and salinity stressed plants; this may be attributed to the dryness of leaf edges. The moisture stress had higher effects on the spectral signature in comparison to salinity effects (Figure 4.10).

(a) (b)

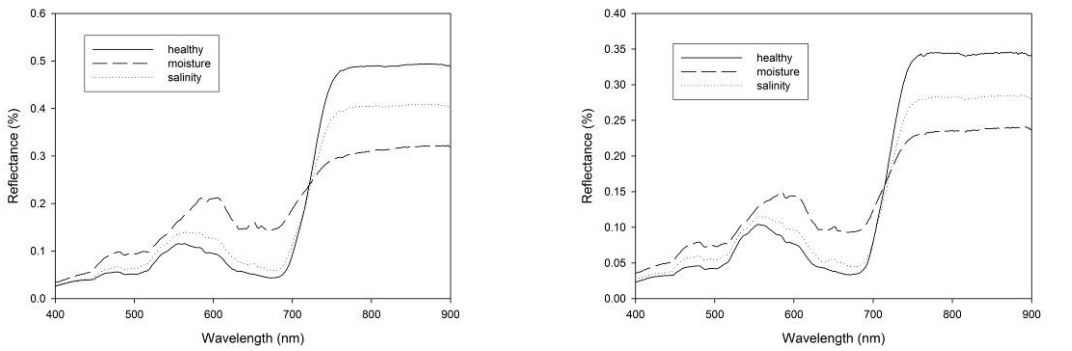


**Figure 4-10** Typical spectral signatures obtained from (a) Scottish wheat canopies and (b) Egyptian wheat canopies at the grain filling stage under moisture and salinity stress using solar radiation.

## 4.5.2 Simple broad band spectral indices

### Wheat grain yield

Twelve broad band spectral vegetation indices have been examined in this research project. Results in appendix A (Tables A2, A8, A14 and A20) show the correlation coefficient for the relationship between these twelve indices and the measured wheat

grain yield. Correlation coefficients have been used to investigate the possibility of predicting grain yield of Scottish and Egyptian wheat varieties using these indices. The coefficient of correlation for the relationship between wheat grain yield and different spectral vegetation indices was calculated at different growth stages from early growth through to harvest time. Results demonstrate that the majority of the twelve broad band indices had significant relationships with the measured wheat grain yield for all experiments (winter and spring seasons).

In the first experiment (Scottish wheat, winter season 2005-6) at early growth stages it is not possible to predict wheat grain yield as the coefficient of correlation values ranged from -0.08 to 0.19. This may be attributed to the similar spectral response from different treatments. At 181 DAS the relationship became stronger and the coefficient of correlation values increased into the significant range. The strongest correlation was recorded at 225 DAS with RVI, $GNDVI_{br}$, SR and RDVI ($r = 0.91$).

Results obtained from the second experiment (Egyptian wheat, spring season of 2006) gave the highest relationship between different spectral vegetation indices and wheat grain yield at 91 DAS. The strongest correlation was recorded with RVI and SI ($r = 0.96$). During this experiment the temperature and day length were considerably different in comparison to the winter season; days were longer and the temperature higher. The early prediction of grain yield may be attributed to the shorter growing season, which was approximately 5 months from sowing date to harvest (approximately 9 months for the winter season). The growing season for Egyptian wheat varieties is also slightly shorter than for the Scottish wheat and therefore the maturation more rapid.

Results obtained from the third experiment (Scottish wheat variety, winter season of 2006-7) show that at 97 DAS it is possible to predict wheat grain yield (an early growth stage). The results from this experiment demonstrated that the strongest correlation recorded at 198 DAS with $GNDVI_{br}$ ($r = 0.92$). The early prediction of grain yield in this experiment may be due to the high level of moisture control as fractions of field capacity were used.

Results for the correlation coefficient obtained from the fourth experiment are listed in Table A20. The results demonstrate that at early growth stages the spectral

vegetation indices did not show high correlations for predicting wheat grain yield. This may be attributed to the similar spectral signature from different treatments. At 108 DAS eight out of twelve spectral vegetation indices had a significant relationship with wheat grain yield. The strongest correlation was observed between OSAVI and wheat grain yield at 197 DAS (r = 0.94). In addition, NDVI, SLAVI, RDVI and IPVI had high significant correlations with the measured grain yield (all > 90).

The results from all experiments with Scottish and Egyptian wheat showed that the highest correlations between wheat grain yield and different vegetation indices were observed after the flowering stage. This is because at late stages of the growing season some old leaves started to dry, especially in the stressed treatments (moisture and salinity induced). RDVI, RVI and SR gave the highest significant correlation figure for predicting wheat grain yield observed in the second experiment (Egyptian wheat, spring season 2006) as early as 91 DAS (r = 0.97 and 0.96). Overall RVI was the best at predicting grain yield with both Scottish and Egyptian wheat varieties. Some other indices (NDVI, SR, RDVI, OSAVI and SLAVI) also produced high significant correlation for predicting wheat grain yield in all experiments. Figure 4.11 shows the relationship between RVI and Scottish and Egyptian wheat varieties in different seasons. The graphs show strong significant relationships between RVI and wheat grain yield in all experiments ($R^2 > 0.75$; p = 0.000).

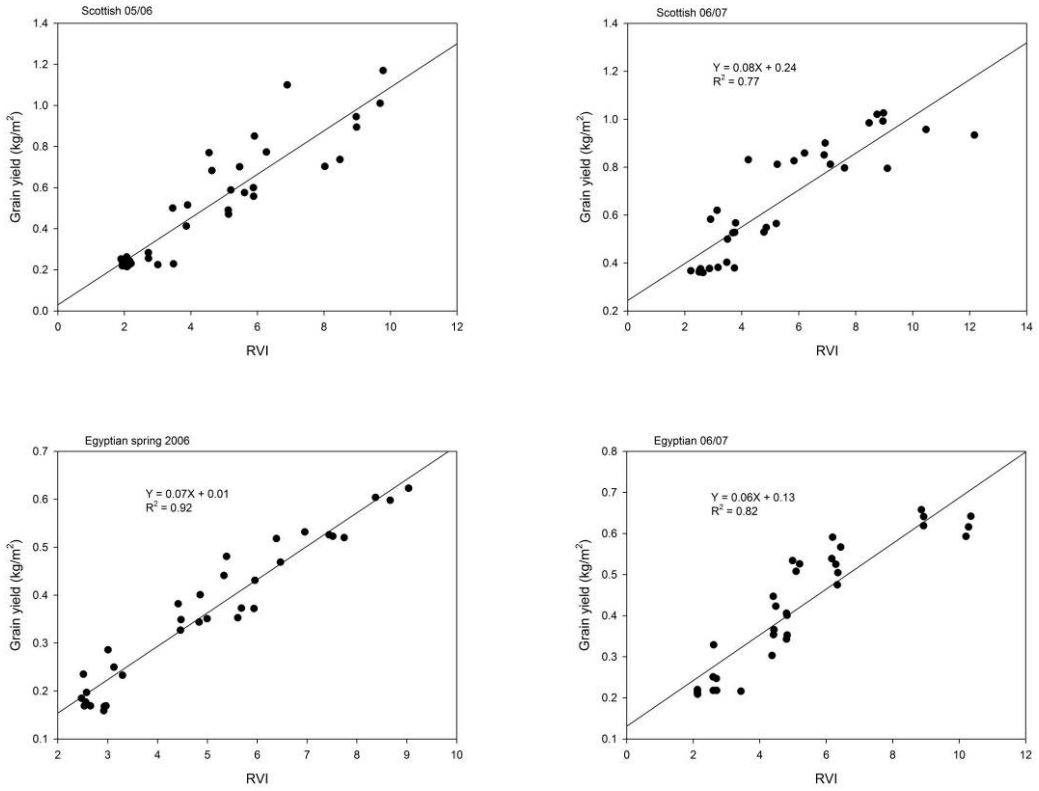


**Figure 4-11** The relationship between the Ratio Vegetation Index (RVI) obtained using natural and artificial illumination and wheat grain yield at the grain filling stage in different growing seasons (n = 33).

## Aboveground biomass

Aboveground biomass and grain yield are closely linked and, therefore, both moisture and salinity treatments greatly affected aboveground biomass. The coefficient of correlation for the relationship between the measured aboveground biomass and different broad band ratio indices is given in Tables A3, A9, A16 and A21 (appendix A). The results demonstrate that the effects of moisture stress were higher than the effects of salinity on aboveground biomass. From the time series hyperspectral spectroradiometry measurements, collected over the growing season, it can be seen that at early growth stages none of the tested broad band vegetation indices were significantly correlated with the measured aboveground biomass (all experiments). The correlation values for the relationship between different broad band indices and the measured aboveground biomass of Scottish wheat variety in winter season of 2005-6 are given in Table A3 (appendix A). The results show that all broad band vegetation indices produced a significant correlation with the measured aboveground biomass at late growth stages. At 181 DAS all tested broad band indices had

significant correlations with the measured biomass and the strongest correlation values were recorded at 225 DAS with $GNDVI_{br}$ and RDVI (r = 0.92). NDVI, RVI, SR, SLAVI, and IPVI also gave a highly significant correlation with the measured aboveground biomass (all 0.91).

In the second experiment (Table A9), at the early growth stage (57 DAS), none of the tested broad band vegetation indices had significant correlations with the measured aboveground biomass. At 78 DAS most of the tested indices had high significant correlations which ranged from -0.68 to -0.72 for the negative values and from 0.72 to 0.80 for the positive values. The strongest correlation was observed at 91 DAS with RDVI (r = 0.98). NDVI, RVI, SR, SLAVI and IPVI also gave high significant correlation (r = 0.97) with the measured aboveground biomass. Correlations obtained from the 91 DAS were higher than those obtained at 103 and 127 DAS which may be a result of early senescence.

In the third experiment (Table A16), at 177 DAS, all tested spectral vegetation indices had significant correlation with the measured aboveground biomass. The strongest correlation was observed at 198 DAS with $GNDVI_{br}$ (r = 0.90). NDVI, RVI, OSAVI, RDVI and IPVI also had exhibited strong correlations (r = 0.88-0.89). At 223 DAS most of the correlation coefficient values were significant but less than at 198 DAS. This can be attributed to the senescence that occurs in late growth stages which leads to a decrease in chlorophylls and other pigments in the leaves.

In the fourth experiment (Table A21) the correlations between different broad band spectral vegetation indices and the measured aboveground biomass were very low at the early growth stage (r < 0.3). At 108 DAS, eight out of the twelve indices had a significant correlation with the measured aboveground biomass. The strongest was at 197 DAS with RDVI and OSAVI (r = 0.94). NDVI, RVI, OSAVI, RDVI and IPVI also had a high significant correlation (r = 0.91-0.92). Figure 4.12 shows the relationship between RDVI and the measured aboveground biomass in different growing seasons; the strong linear relation can be clearly observed in these diagrams. It is evident that in all experiments VI1 always produced poor correlations with different biochemical and biophysical crop properties.

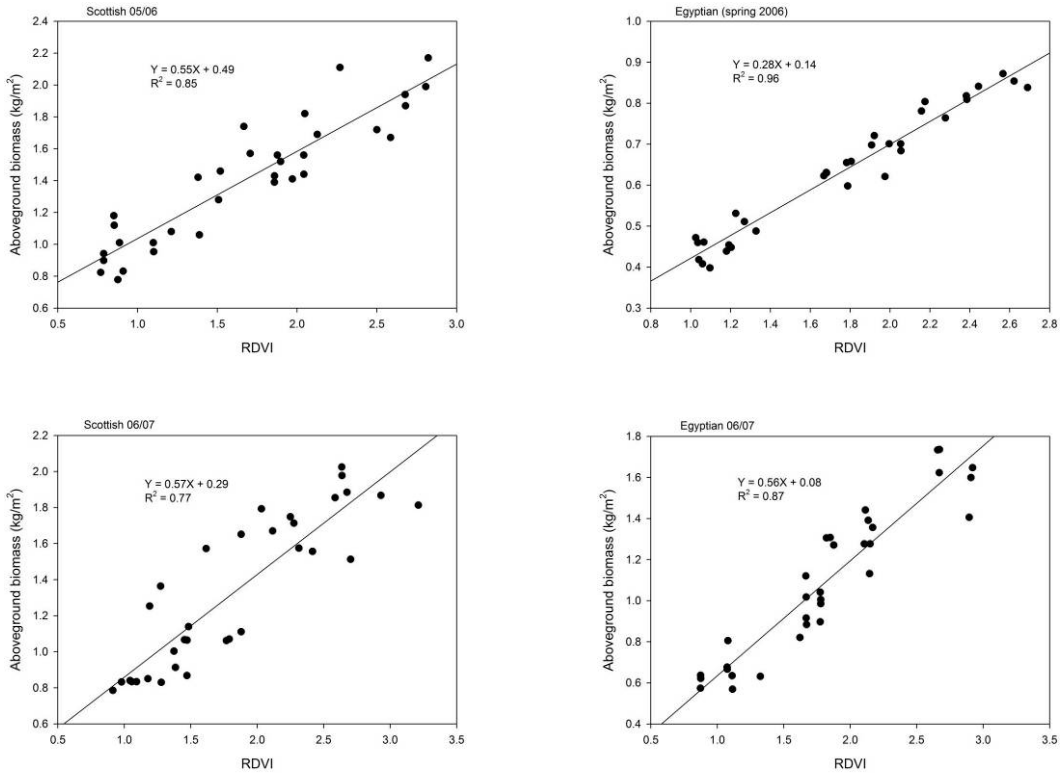


**Figure 4-12** The relationship between Red Difference Vegetation Index (RDVI) obtained using natural and artificial illumination and aboveground biomass of Scottish and Egyptian wheat in different growing seasons (n = 33).

## Leaf Area Index (LAI)

LAI was measured three times during the two Scottish wheat experiments due to low number of replicates (5) but it was measured five times with the Egyptian wheat variety (6 replicates). The correlations between LAI and the different broad band vegetation indices are given in Tables A4, A12, A18, and A24 (Appendix A). The results obtained from the first experiment showed that at 181 DAS all the tested indices had significant correlation with the measured LAI. At 207 DAS the values had increased to ($r > 0.7$). The strongest correlation was recorded with $GNDVI_{br}$ at 225 DAS ($r = 0.90$). The poorest correlation was recorded with VI1 (all experiments) in both Scottish and Egyptian wheat varieties.

Table A12 (appendix A) shows the relationship between LAI and the broad band indices in the second experiment. At the early growth stage (55 DAS) none of the tested broad band indices was significantly correlated with LAI. From 78 DAS onward most of the tested broad band indices had significant correlations with the measured LAI ($r > 0.6$). The strongest correlation was recorded with NDVI, SAVI,

SLAVI, OSAVI, SI and IPVI at 91 DAS (r = ±0.96). The correlations started to decrease after 91 DAS as a result of early maturation (the leaves began to yellow).

The third experiment (Table A18) had the same trend as the first experiment - both are Scottish wheat. All tested broad band indices were significantly correlated with the measured LAI on all measurement dates. The correlation coefficient between broad band indices and the measured LAI was significant and increased with time, reaching a maximum value at 223 DAS with $GNDVI_{br}$ (r = 0.90).

Correlation values for the relationship between broad band indices and the measured LAI obtained from the fourth experiment showed that at 83 DAS none of the broad band indices was significant with LAI (r < 0.30). From 108 DAS most of the tested broad band indices were significantly correlated with the measured LAI. The strongest correlation was recorded at 197 DAS with NDVI, SLAVI and IPVI (r = 0.96). $GNDVI_{br}$ and SI also produced high significant correlations with the measured LAI (r = 0.95 and -0.95 respectively).

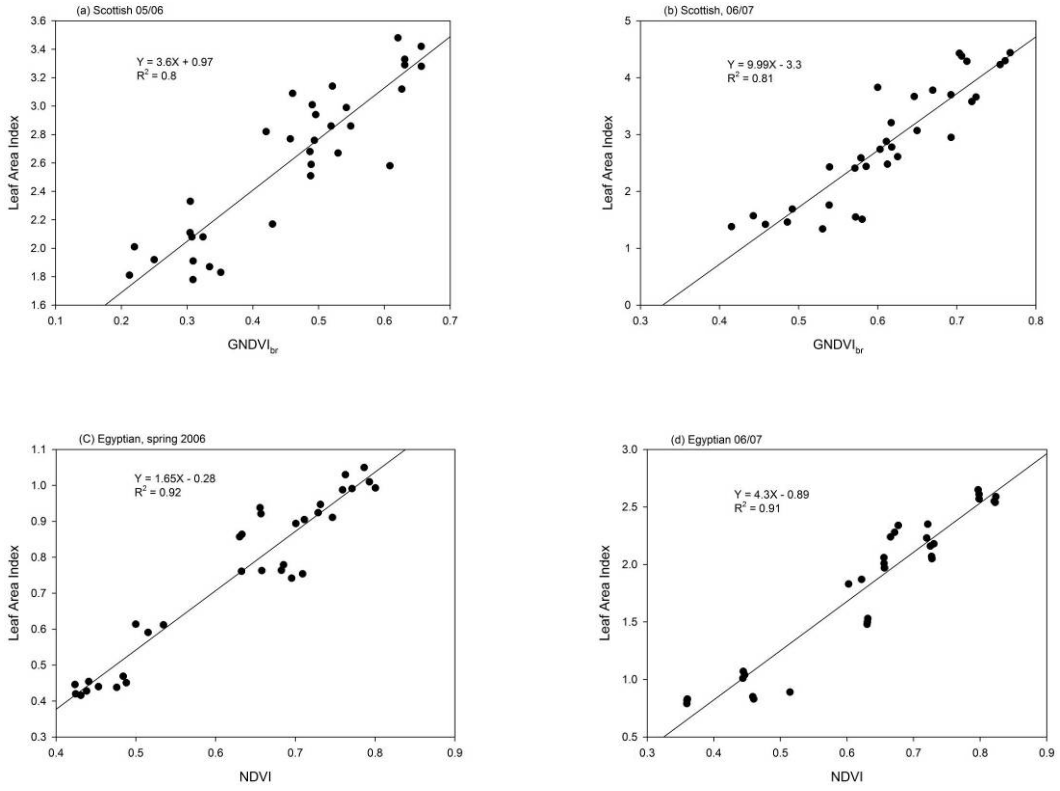


**Figure 4-13** The relationship between NDVI and $GNDVI_{br}$ obtained using natural and artificial illumination and leaf area index of Scottish and Egyptian wheat varieties in different growing seasons (n = 33).

**Chlorophyll *a* concentration**

In all experiments the spectral signature from stressed plants was different from those obtained from healthy plants. This is a result of changes in levels of chlorophyll *a* and other pigments caused by the stress factors. The regression equation and correlation coefficient for the relationships between different broad band vegetation indices and the measured chlorophyll *a* concentration have been investigated. The correlation values are given in Tables A1, A7, A13 and A19 (appendix A). There is no significant correlation between the measured chlorophyll *a* concentration and different broad band spectral vegetation indices at early growth stages. Data obtained from the first experiment show that up to 125 DAS all tested broad band indices had non-significant correlation values. This may be attributed to the low difference in chlorophyll *a* concentration and other pigments. The strongest correlation was observed at 181 DAS with RVI, SR and RDVI ($r = 0.57$). The majority of the twelve broad band indices gave a significant correlation with chlorophyll *a* concentration at 207 and 225 DAS.

Correlation values from the second experiment (Egyptian wheat, spring season of 2006) are detailed in Table A7. Most of the twelve broad band indices gave significant correlation with the concentration of chlorophyll *a* at 78 DAS. At early stages all tested broad band vegetation indices had a low correlation with the measured chlorophyll *a*. The strongest correlation was recorded at 127 DAS with SAVI and OSAVI ($r = 0.69$); this may be a result of the low aboveground biomass caused by the short growing season.

The same trend was observed in the third experiment (Scottish wheat, winter season of 2006-7); results are given in Table A13. At early growth stage the relationship between different spectral vegetation indices and the measured chlorophyll *a* was non-significant with all tested indices. Correlation values became significant at 177 DAS with eight out of the twelve broad band indices producing significant correlations ($r > 0.35$). At 198 and 223 DAS all twelve broad band indices produced a significant correlation with chlorophyll *a* ($r > 0.55$ with the majority of the indices). The strongest correlation was recorded at 198 DAS with SAVI and OSAVI ($r = 0.84$).

In the fourth experiment (Table A19) up to 130 DAS the correlation coefficient was non-significant with all vegetation indices. This may be attributed to dormancy during

early winter months (November- January). At 149 DAS half of the broad band indices produced significant correlations with the concentration of chlorophyll *a* (r > 0.45). At 197 DAS all tested indices had significant correlations with the measured chlorophyll *a* with the strongest correlation recorded with OSAVI (r = 0.79). Chlorophyll *a* concentration was also measured using HPLC, and similar results to those obtained using spectrophotometer were observed. Other pigments such as chlorophyll *b* and lutien were also measured by HPLC. Chlorophyll *b* demonstrated a similar trend to chlorophyll *a* with both moisture and salinity induced stress. However, the relationship between lutien and both stressors was poor. The results suggest that OSAVI is a good indicator for predicting chlorophyll *a* concentration; it gave the strongest correlation in three of the four experiments. SAVI, RVI and SR also gave good results with strong correlations in all experiments. Figure 4.14 shows the relationship between OSAVI and the concentration of chlorophyll *a* in different seasons for Scottish and Egyptian wheat varieties.

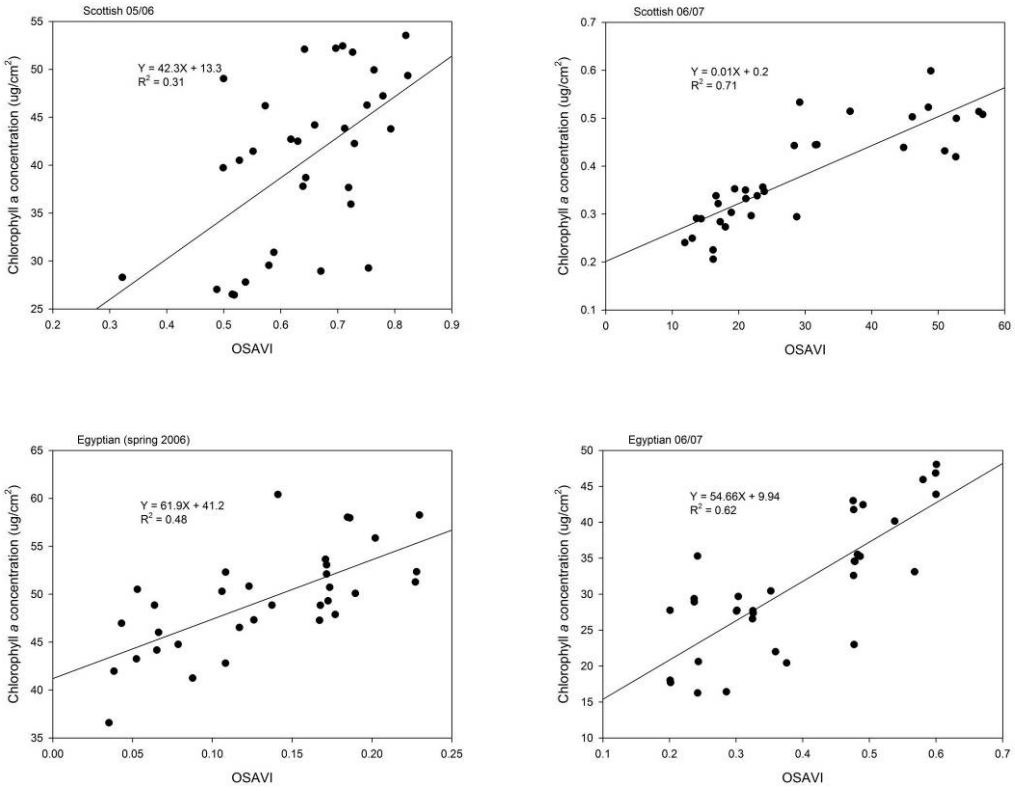


**Figure 4-14** The relationship between OSAVI (using natural and artificial illumination) and chlorophyll *a* concentration for Scottish and Egyptian wheat varieties in different growing seasons (n = 33).

### 4.5.3 Hyperspectral indices

**Wheat grain yield**

Forty three hyperspectral vegetation indices were examined to detect stress in wheat during this research. Results given in Tables A2, A8, A14 and A20 (appendix A) show that the majority of the tested vegetation indices are good predictors of wheat grain yield, particularly at the flowering stage. Results obtained from the first experiment showed that at the early growth stage (<125 DAS) most of these indices showed low correlations with the measured wheat grain yield. At 181 DAS the correlation values were significant with fifteen spectral indices ($r > 0.34$). At 207 and 225 DAS, the majority of the indices had significant correlation with the yield ($r > 0.45$). The strongest correlation was recorded at 225 DAS with the band ratio $R_{750}/R_{550}$ ($r = 0.93$). $GNDVI_{hy}$, $SR_{hy}$ and $R_{800}/R_{550}$ were also good at predicting wheat grain yield ($r = 0.90$).

Results obtained from the second experiment (spring season) showed that the grain yield can be predicted at the early growth stage. At 78 DAS more than half of the hyperspectral indices had significant correlations with the measured grain yield ($r > 0.4$). At 91 DAS the majority of the hyperspectral indices gave highly significant correlations, the strongest correlation was recorded with the band ratios of $SR_{hyper}$ and $R_{725}/R_{675}$ ($r = 0.97$). The early prediction of wheat grain yield in this experiment may be attributed to the shorter growing season. In addition, the temperature was higher; this accelerates plant growth and consequently decreases maturation time.

In the third experiment (Table A14), results showed that grain yield can be predicted successfully using hyperspectral vegetation indices. At 97 DAS almost half of the indices gave significant correlations with the measured grain yield ($r > 0.4$). The strongest correlation between the vegetation indices and wheat grain yield was observed at 198 DAS with 5 indices; $GNDVI_{hyper}$, $R_{800}/R_{550}$, $R_{750}/R_{550}$, $C_{green}$ and $C_{NIR}$ ($r = 0.92$). The decrease in correlation between different indices and wheat grain yield at the last measurement may be attributed to senescence and the decreased concentration of chlorophyll *a*.

In the fourth experiment (Table A20) $GNDVI_{hyper}$, $R_{800}/R_{500}$, $R_{750}/R_{550}$, $C_{rededge}$ and $C_{green}$ gave a high significant relationship with the measured wheat grain yield. The

strongest correlation was recorded At 197 DAS with $NDVI_{hyper}$ (r = 0.94). Results also further showed that up to 108 DAS the correlation between grain yield and vegetation indices was non-significant for more than half of those assessed. Seventeen indices gave significant correlations for predicting yield. Similar results were also obtained at 130 DAS; thirteen indices gave significant relationships with grain yield.

It is evident that most of the spectra obtained from the wheat canopy (using both solar radiation and artificial illumination inside the darkroom) show a strong relationship with the measured wheat grain yield. Some of the indices had non-significant correlations with the grain yield (e.g. WI, WBI and NPQI). The band ratio $R_{750}/R_{550}$ gave the strongest correlation for predicting yield in two experiments and therefore is a good predictor for wheat grain yield. Figure 4.15 demonstrates the relationship between the band ratio $R_{750}/R_{550}$ and the measured wheat grain yield in different growing seasons including winter and spring. The figure shows that there is a positive linear relationship between the band ratio and grain yield in all seasons ($R^2$ = 0.86, 0.84, 0.76 and 0.86) for Scottish and Egyptian wheat.

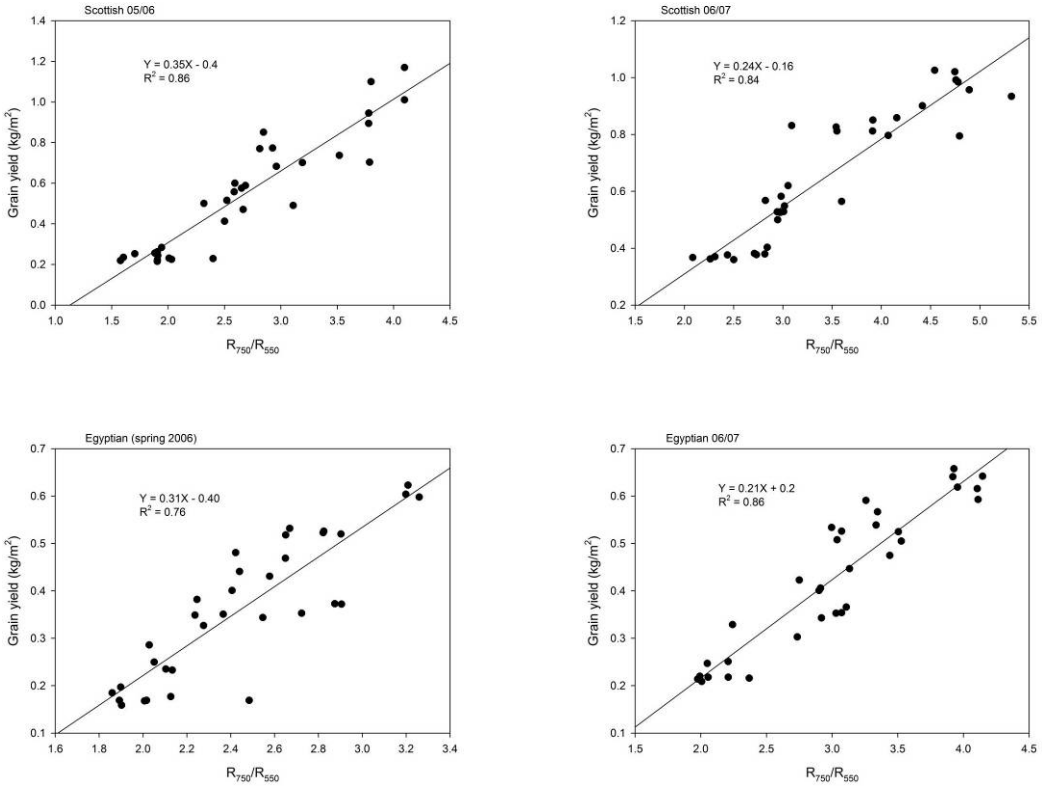


**Figure 4-15** The relationship between $R_{750}/R_{550}$ (using natural and artificial illumination) and wheat grain yield for Scottish and Egyptian wheat varieties in different growing seasons (n = 33).

The results show that the majority of the hyperspectral indices examined in this research have strong relationship with the measured wheat grain yield. This may be used to predict other biophysical and biochemical properties of wheat. Comparing the results obtained from both broad band and hyperspectral indices for predicting wheat grain yield, it can be seen that there is no great difference between the strongest correlations obtained using the two methods. This is a good indicator that it should be possible to extrapolate the results at a large scale using high spatial resolution satellite remote sensing such as QuickBird imagery.

**Aboveground biomass**

The correlation coefficient for the relationship between the forty three hyperspectral vegetation indices and the measured aboveground biomass is given in Tables A3, A9, A16 and A21 (appendix A). At early growth stages, the majority of the tested hyperspectral indices did not show strong correlations with the measured aboveground biomass. Results obtained from the first experiment show that at 181 DAS 29 indices showed significant correlations with the measured aboveground biomass, with the strongest correlation observed at 225 DAS with 5 indices; $GNDVI_{hy}$, SIPI, $R_{800}/R_{550}$, $R_{750}/R_{550}$ and $C_{green}$ ($r = 0.92$). Over the three measurement dates in this experiment the relationship gradually increased, with the highest correlation values at 225 DAS. Very few indices did not show any significant correlation (e.g. PSI and $R_{700}/R_{670}$ produced the lowest values < 0.30).

In the second experiment (Table A9) the results showed that at 57 DAS none of the tested hyperspectral indices were significantly correlated with the measured aboveground biomass; the correlation coefficient values ranged from -0.28 to 0.31. At 78 DAS the relationships were more significant with twenty eight indices having significant correlations with the measured aboveground biomass ($r > 0.35$). At 91 DAS the majority of the tested indices produced highly significant correlations with the measured biomass ($r > 0.45$). The strongest correlation observed was with the band ratio $R_{750}/R_{700}$ ($r = 0.98$), this gave one of the earliest strong correlations observed over the whole set of wheat experiments. $NDVI_{hy}$, $PSND_b$, $SR_{hy}$, $R_{675}/R_{700}$, RNDVI and $C_{rededge}$ gave almost identical results ($r = 0.97$). At 103 DAS and 127 DAS the correlation values decreased in comparison to those from 91 DAS; this may

be due to the senescence occurring at late stages during which chlorophyll *a* and other pigments decrease towards a minimum at harvest time.

The results obtained from the third experiment (Scottish wheat 2006-7) are detailed in Table A16. At 177 DAS most hyperspectral vegetation indices showed high significant correlations with the measured aboveground biomass. At 198 DAS thirty nine indices were significantly correlated with the aboveground biomass ($r > 0.38$) with the strongest correlation observed at 198 DAS with $C_{NIR}$ ($r = 0.92$). $GNDVI_{hy}$, $R_{800}/R_{550}$, $R_{750}/R_{550}$ and $C_{green}$ gave higher correlations in comparison to the other indices ($r = 0.90$). At 223 DAS nearly two thirds of the indices gave significant correlations with the biomass. As in the other experiments, WI, WBI and NPQI did not show any significant correlations with the measured biomass ($r < 0.25$).

The results obtained from the fourth experiment had the same trend as the previous experiments. It should be mentioned that both hyperspectral and broad band indices derived from the darkroom were much more controlled and the dates of measuring reflectance were close to specific growth stages (tillering, booting, flowering, heading, and grain filling stages). Results are detailed in Table A21. Roughly half of the tested hyperspectral indices did not show any significant correlation with the measured aboveground biomass except at the final date of measurement. The strongest correlation derived from the experiment was observed at 197 DAS with $NDVI_{hy}$, $SR_{hy}$, $R_{800}/R_{550}$, $R_{695}/R_{670}$ and $R_{750}/R_{550}$ ($r = 0.93$). The results obtained from all experiments showed that there was no great difference between hyperspectral and broad band vegetation indices in predicting aboveground biomass. This is useful as the imagery available for this research project is high spatial resolution only (limited number of bands). Like results from other experiments NPQI, PSR and WBI produced non-significant correlations with the measured aboveground biomass over the growing season.

The results therefore suggest that broad band vegetation indices can be used as indirect tool to estimate aboveground biomass of wheat crops. Many vegetation indices produced strong correlations with the measured biomass at different growth stages.

**Leaf area index (LAI)**

The correlation coefficient values for the relationship between the measured LAI and the forty three hyperspectral indices are given in Tables A4, A12, A18 and A24 (appendix A). Results obtained from the first experiment showed that most of the tested hyperspectral indices were significantly correlated with the measured LAI at 181 DAS. At 207 DAS, the majority of the tested hyperspectral indices gave significant correlation ($r > 0.45$). Of the three measurement dates the 225 DAS dataset produced the highest significant correlations. The strongest correlation was recorded with both GNDVI and SIPI ($r = 0.90$). $C_{green}$, $R_{800}/R_{550}$ and $R_{750}/R_{550}$ gave high significant correlation during the experiment ($r = 0.88$). Some indices such as PSI and $R_{700}/R_{670}$ had non-significant correlation with the measured LAI ($r < 0.33$).

In the second experiment (Table A12) the results showed that at the early growth stage (55 DAS) nearly all the tested hyperspectral indices were not significantly correlated with the measured LAI ($r < 0.34$). At 78 DAS more than half of the evaluated ratios significantly correlated with the measured LAI ($r > 0.35$). At 91, 103 and 127 DAS, the majority of the hyperspectral indices gave high significant correlations. The strongest correlation was recorded at 91 DAS with SIPI ($r = 0.97$). The correlation coefficients at 103 and 127 DAS were significant for most of the hyperspectral indices but lower than the values obtained at 91 DAS, this may be attributed to the decrease in chlorophyll *a* at late stages.

The results obtained from the third experiment (Scottish wheat 2006-7) had the same trend as the first experiment with this variety. Results given in Table A18 show that at 177 DAS the majority of hyperspectral indices were significantly correlated with the measured LAI and the values of the coefficient of correlation increased until reaching the maximum values at 198 and 223 DAS with $C_{green}$, $R_{800}/R_{550}$ and $GNDVI_{hyper}$ ($r = 0.90$). Some hyperspectral indices also gave high significant correlations with the measured LAI including $SR_{hyper}$, $R_{750}/R_{550}$ and $C_{NIR}$ ($r = 0.89$). It was noted that some of the tested hyperspectral indices did not give significant correlations with the measured LAI in this experiment (e.g. WI, PSI, NPQI and WBI).

In the fourth experiment (Table A24) the results showed that at early growth stage (83 DAS) most of the hyperspectral indices were not significantly correlated with the

measured LAI. At 108 DAS nearly a third of the tested hyperspectral indices exhibited significant correlations with the measured LAI ($r > 0.37$). Both the 149 and 197 DAS datasets produced better results in comparison with the previous measurements. At 197 DAS the majority of indices had significant correlations with the strongest correlation recorded with three different band ratios; $NDVI_{hyper}$, $R_{675}/R_{700}$ and RNDVI ($r = \pm 0.96$). Other hyperspectral indices such as $GNDVI_{hyper}$, $PSND_b$, $R_{695}/R_{760}$, $R_{605}/R_{760}$, $C_{green}$, $R_{750}/R_{550}$ and $R_{800}/R_{550}$ also gave strong significant correlations with the measured LAI ($r = 0.92$ to $0.94$). The wavelength of 550 nm seems to be of particular importance for examining the effects of stress in wheat as it is at this wavelength that the most obvious changes brought about by stress can be observed (chlorophyll *a* concentration, yield, biomass and plant height are all affected here). Wavelengths of 750 and 800 nm are also sensitive for predicting biophysical and biochemical properties of wheat crops.

From the results above it can be seen that a comparison of hyperspectral and broad band vegetation indices for predicting LAI shows that there is little difference between the strongest correlations from both methods. Some broad band indices such as RVI and NDVI give higher correlations in comparison to the hyperspectral indices.

**Chlorophyll *a* concentration**

The correlation coefficient values for the relationship between different hyperspectral indices and chlorophyll *a* concentration for all experiments are given in Tables A1, A7, A13 and A19 (appendix A). At early growth stages the correlation values were non-significant in all experiments (winter and spring seasons). At 73 and 125 DAS, none of the hyperspectral indices gave significant correlations with the measured chlorophyll *a* ($r < 0.30$). At 181 and 225 DAS, the majority of the indices gave significant correlations with chlorophyll *a* with the strongest correlation observed at 207 DAS with the band ratio $R_{695}/R_{670}$ ($r = 0.62$). At 181 DAS only nine vegetation indices had non-significant correlation with the measured chlorophyll *a* concentration ($r < 0.33$). WI, PSI, NWI-1, NWI-2 and WBI were not sensitive for chlorophyll *a* concentration in all growing seasons with occasional exceptions.

In the second experiment the correlation values are given in Table A7. Early signs of a significant relationship were observed at 78 DAS with nineteen indices ($r > 0.34$).

At 91 DAS thirty nine indices had a significant relationship with the measured chlorophyll *a* concentration. At 103 and 127 DAS, the majority of the hyperspectral indices produced significant correlations with the strongest correlation observed was with $PSND_{broad}$ (r = 0.68) at 127 DAS. The early prediction of chlorophyll *a* concentration in this experiment may be attributed to the short growing season (spring season) in comparison with the other winter season experiments.

In the third experiment (Scottish wheat, 2006-7) the spectroradiometry measurements were collected at 97, 135, 177, 198 and 223 DAS. At early growth stages the majority of the hyperspectral indices gave non-significant correlations with chlorophyll *a* (r < 0.35). At 177 DAS thirteen vegetation indices had low significant correlation values. At 198 and 223 DAS most of the hyperspectral vegetation indices had significant correlations with the chlorophyll *a* concentration. The strongest correlation was recorded with $R_{800}/R_{550}$ and $C_{green}$ at 198 DAS (r = 0.84). Again it seems that the wavelength 550 is particularly sensitive to changing plant properties. Four vegetation indices (WI, PSI, NPQI and WBI) gave non-significant correlations with the measured chlorophyll *a* (r < 0.30).

In the fourth experiment (Egyptian wheat variety, 2006-7 growing season), chlorophyll *a* concentration was affected by both moisture and salinity treatments in comparison to control treatments. The majority of the spectral vegetation indices produced significant correlations. At early stages most of the hyperspectral indices gave non-significant correlations with the measured chlorophyll *a* (r < 0.35). At 149 DAS more than half of the indices gave significant correlation values. At 197 DAS the majority of the forty three indices gave significant correlations. The strongest correlation was recorded at 197 DAS with the band ratio $R_{695}/R_{670}$ (r = 0.78). It is evident that the highest correlations from all experiments were found at the late growth stage. This may be due to the early senescence which occurs with stressed plants as many leaves turn dry and yellow, therefore affecting reflected spectra.

Comparing the results obtained from both broad band and hyperspectral indices the results showed no great difference between the two methods. The strongest correlation for the relationship between vegetation indices and chlorophyll *a* concentration was similar in all experiments. For example, the difference between the strongest correlation recorded with broad band ratios and hyperspectral indices was

the same in the third experiment (r = 0.84) and in two of the other experiments the difference was 0.01.

**Red edge position (REP)**

The red edge position has been calculated for all spectral data collected. Results given in Tables A25, A26, A27 and A28 (appendix A) detail the relationship between REP and the measured chlorophyll *a* concentration from Scottish and Egyptian wheat leaves in different seasons. Results demonstrated that REP is a good indicator for the concentration of chlorophyll *a*, in particular at the flowering stage. The strongest correlation was observed after the application of the required dose of nitrogen (r = 0.64, 0.69, 0.79 and 0.74 for the four experiments respectively). At early growth stages REP did not show a significant relationship with the measured chlorophyll *a* concentration. The strongest correlations were observed at 207, 103, 198 and 149 DAS in the four experiments respectively. The results suggest that the REP is a sensitive index to changes in chlorophyll *a* concentration in wheat leaves when compared to the other vegetation indices assessed. These findings are supported by other studies (Schlemer *et al*., 2005).

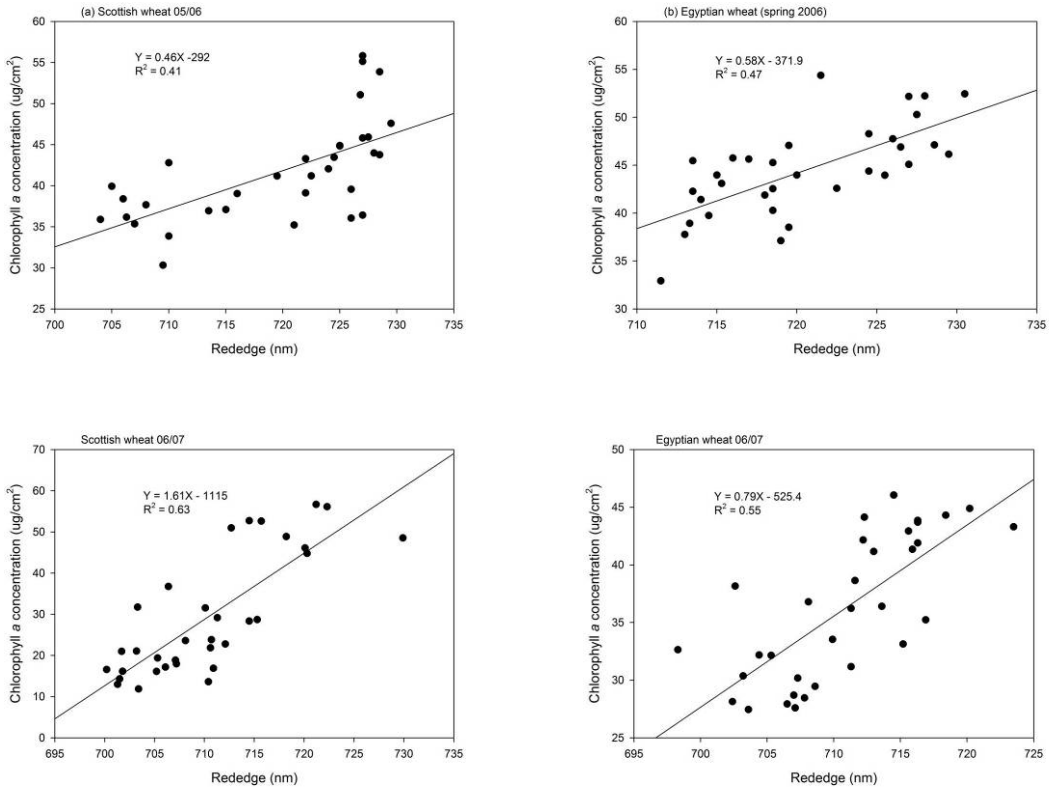


**Figure 4-16** The relationship between REP and the concentration of chlorophyll *a* extracted from Scottish and Egyptian wheat leaves in different seasons (n = 33).

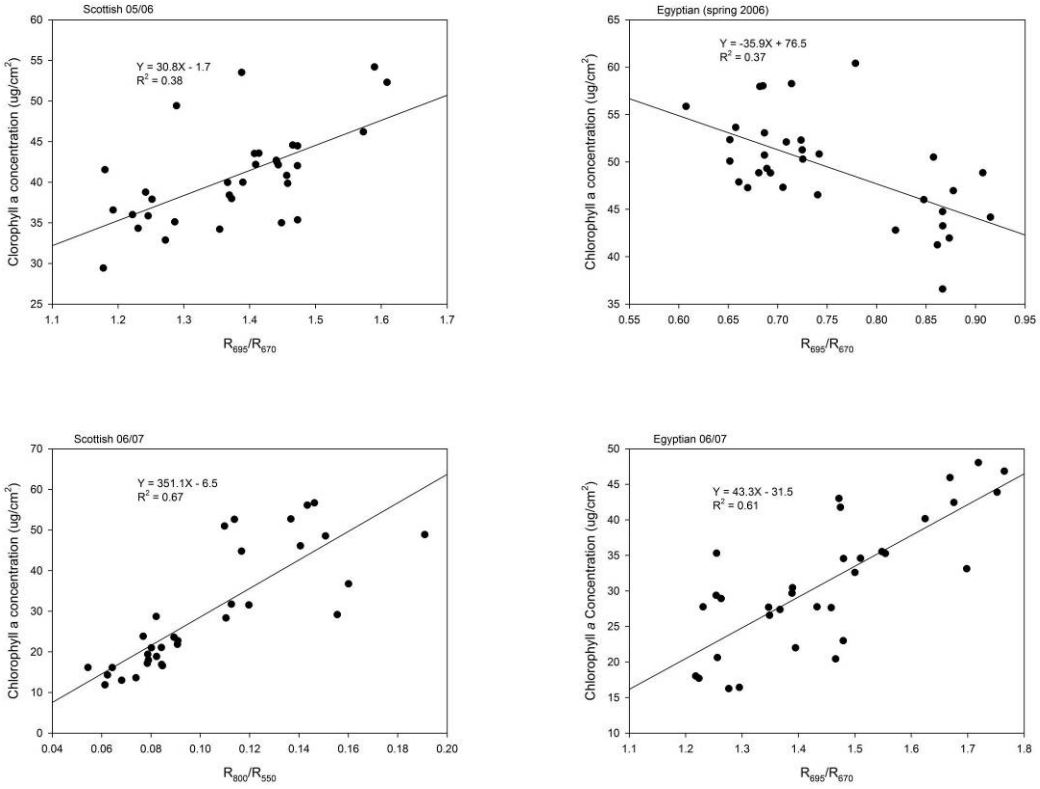


**Figure 4-17** The relationship between the band ratios $R_{695}/R_{670}$ and $R_{800}/R_{670}$ and the concentration of chlorophyll *a* from Scottish and Egyptian wheat leaves in different seasons (n = 33).

## Identifying wavelengths sensitive to chlorophyll *a* of wheat at the canopy scale

The spectral data collected in the first two experiments of Scottish and Egyptian wheat varieties using solar radiation during free-cloud days were used to develop a new index for predicting chlorophyll *a* concentration at the canopy scale. The coefficient of correlation for the relationship between reflectance and the measured chlorophyll *a* concentration for the whole spectra was calculated and plotted against wavelength (Figure 4.18). Reflectance data from 400 nm to 900 nm was used for this relationship to avoid the noisy data at the beginning and the end of the spectrum. The results given in Figure 4.18 show that the strongest correlation between reflectance and chlorophyll *a* concentration was found in two main regions: around 700 and 760 nm (r = 0.66 and 0.36 respectively). Moreover, 550 nm seems a sensitive wavelength to predict chlorophyll *a* concentration. The data obtained at 207 DAS from the first experiment with Scottish wheat gave the best result from the four experiments.

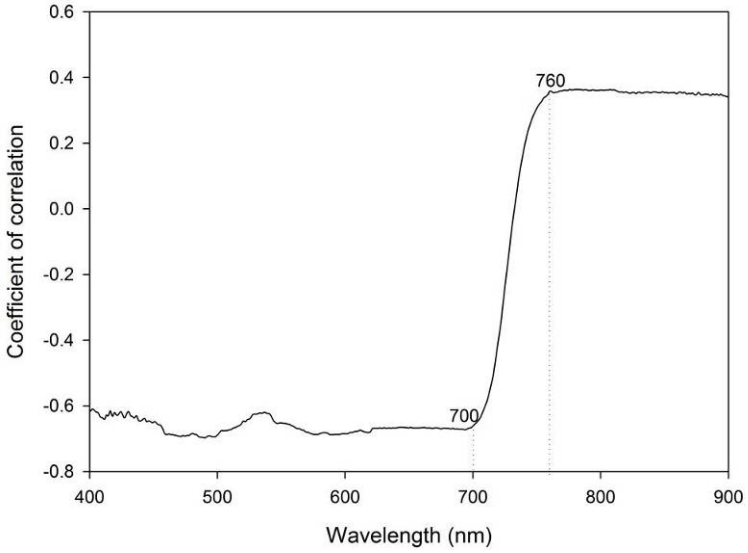


**Figure 4-18** The relationship between correlation coefficient and wavelength of the spectra collected from wheat leaves using solar radiation.

### 4.5.4 Distinguishing moisture induced stress from salinity induced stress

Both moisture and salinity stressors had a strong effect on the wheat crop in terms of total grain yield, total aboveground biomass, plant height, LAI, chlorophyll *a* and pigment concentration. To distinguish between moisture and salinity induced stress the whole spectra collected from all treatments and from each replicate were analyzed using PCA (Principle Component Analysis). This was applied to all spectra collected over the whole growing season from early growth stages (tillering) until harvest time. It has been noted that at the early growth stages it is very difficult to distinguish between moisture and salinity treatments as there is great overlap between different treatments. This may have been a result of similar spectral signatures from different treatments. However, at the early grain filling stage it becomes possible to distinguish between moisture and salinity induced stress. Despite the late distinction between moisture and salinity induced stress, these findings can be used for improving agricultural practices in the following growing seasons.

The dataset collected at the beginning of May gave the clearest differentiation between moisture and salinity induced stress in the 2005-6 growing season. PCA has the potential of distinguishing between spectra collected from healthy canopies and

spectra collected from stressed canopies but for most of the datasets, it was not possible to distinguish between moisture and salinity induced stress. The results from this analysis are given in Figures 4.19-22 for all experiments. These examples from the four experiments show the clearest distinction between moisture and salinity induced stress. The results show that at around the flowering of growth, the spectra collected from moisture induced stress tend to plot separate in one quarter of the score plot and the spectra collected from salinity induced stress plot in an opposite quarter. For example, in Figure 4.20 moisture induced stress treatments plot in the lower right corner and the salinity induced stress treatments plot in the upper right. In addition, the distinguishing between moisture and salinity induced stress is clearer for the data collected in the darkroom using controlled artificial illumination (Scottish and Egyptian wheat experiments in 2006-7 winter growing seasons).

At early growth stages all signatures from different treatments were undifferentiated, possibly as a result of similar chlorophyll *a* concentration and other pigments, and therefore similar spectral signature especially during the period of November-February. From April, the increase in day length encourages photosynthesis and therefore increases the concentration of chlorophyll *a* and pigments. Furthermore, adding the required dose of nitrogen at the beginning of March increased the concentration of chlorophyll *a*. The late distinction between salinity induced stress and moisture induced stress may be attributed to the combined effects of these stresses on the pigments and the early senescence, which occurs with moisture stress treatments. It was observed that moisture stress increased the number of dry leaves, particularly in the older ones. Moreover, the effects of moisture stress on crop physiological changes were higher in comparison to salinity stress, possibly as a result of crop tolerance to salinity.

These results showed the possibility of using PCA to differentiate between moisture and salinity induced stress at reproductive growth stages. Despite the late distinction between moisture and salinity in this research, these findings can be used for following seasons by taking informed decisions to reduce the effects of these stressors on wheat crops.

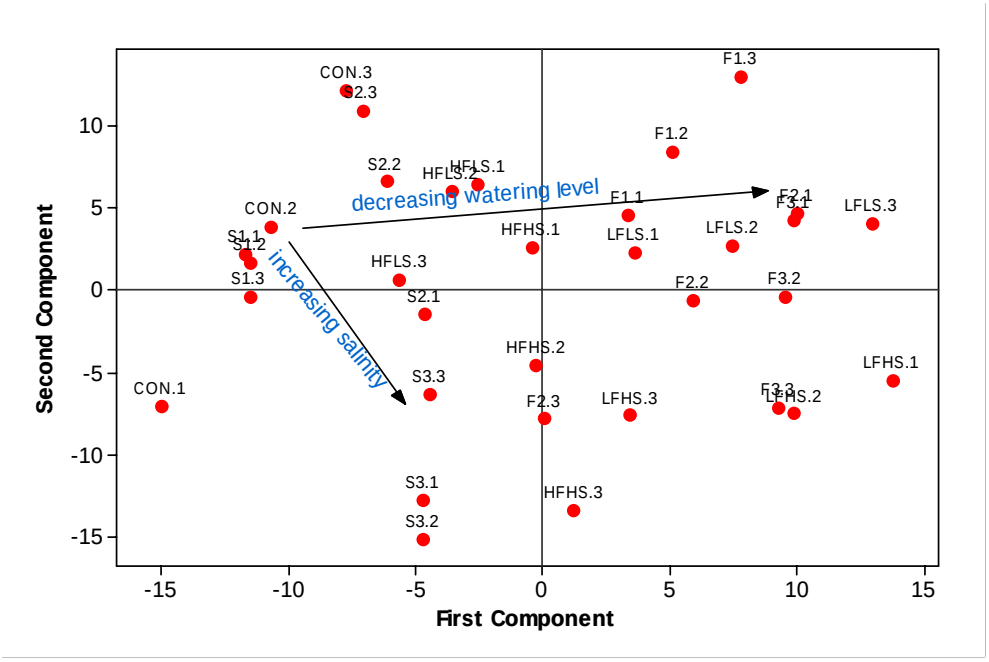


**Figure 4-19** Score plot of PCA for whole spectra collected from control, moisture and salinity induced stressed Scottish wheat canopies at 207 DAS in 2005-6 growing season (n = 33). (Treatment labels: CON-control; F1-75% FC; F2-50% FC; F3-25% FC; S1-2 dS $m^{-1}$; S2-4 dS $m^{-1}$; S3-6 dS $m^{-1}$; HFLS-0.75% FC and 2 dS $m^{-1}$; HFHS-0.75% FC and 6 dS $m^{-1}$; LFLS-0.25% FC and 2 dS $m^{-1}$; LFHS-0.25% FC and 6 dS $m^{-1}$).

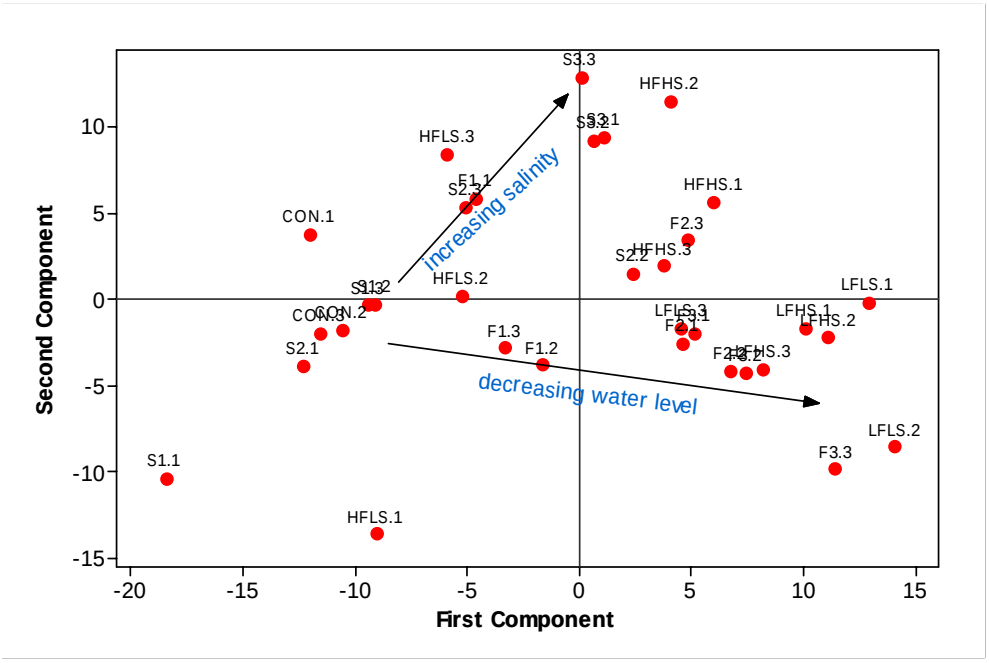


**Figure 4-20** Score plot of PCA for whole spectra collected from control, moisture and salinity induced stressed Scottish wheat canopies at 198 DAS in 2006-7 growing season (n = 33). (Treatment labels: CON-control; F1-75% FC; F2-50% FC; F3-25% FC; S1-2 dS $m^{-1}$; S2-4 dS $m^{-1}$; S3-6 dS $m^{-1}$; HFLS-0.75% FC and 2 dS $m^{-1}$; HFHS-0.75% FC and 6 dS $m^{-1}$; LFLS-0.25% FC and 2 dS $m^{-1}$; LFHS-0.25% FC and 6 dS $m^{-1}$).

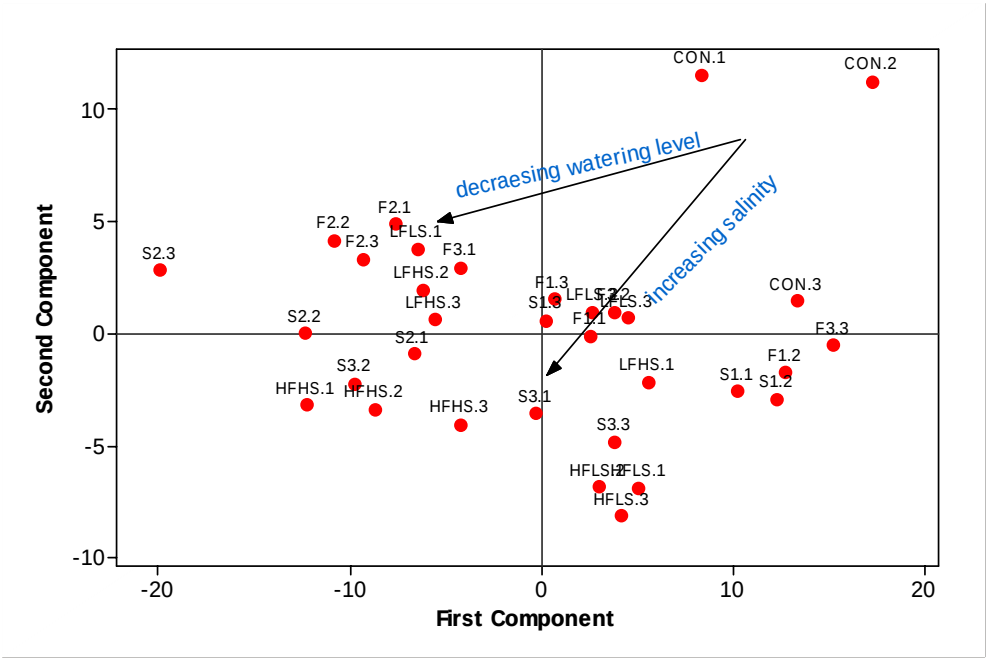


**Figure 4-21** Score plot of PCA for whole spectra collected from control, moisture and salinity induced stressed Egyptian wheat canopies at 103 DAS in spring season of 2006 (n = 33). (Treatment labels: CON-control; F1-75% FC; F2-50% FC; F3-25% FC; S1-2 dS $m^{-1}$; S2-4 dS $m^{-1}$; S3-6 dS $m^{-1}$; HFLS-0.75% FC and 2 dS $m^{-1}$; HFHS-0.75% FC and 6 dS $m^{-1}$; LFLS-0.25% FC and 2 dS $m^{-1}$; LFHS-0.25% FC and 6 dS $m^{-1}$).

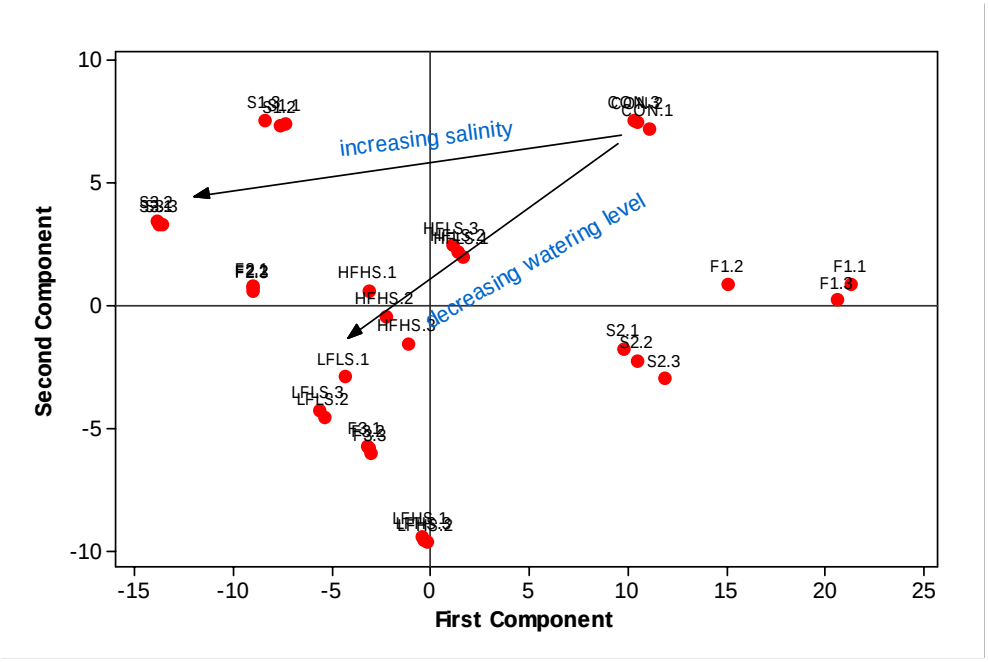


**Figure 4-22** Sore plot of PCA for whole spectra collected from control, moisture and salinity induced stressed Egyptian wheat canopies at 197 DAS in 2006-7 growing season (n = 33). (Treatment labels: CON-control; F1-75% FC; F2-50% FC; F3-25% FC; S1-2 dS $m^{-1}$; S2-4 dS $m^{-1}$; S3-6 dS $m^{-1}$; HFLS-0.75% FC and 2 dS $m^{-1}$; HFHS-0.75% FC and 6 dS $m^{-1}$; LFLS-0.25% FC and 2 dS $m^{-1}$; LFHS-0.25% FC and 6 dS $m^{-1}$).

## 4.6 Summary

The potential for using hyperspectral reflectance measurements for detecting stress in Scottish and Egyptian wheat varieties has been investigated in this chapter. More specifically the potential of remotely sensed was evaluated through controlled greenhouse experiments coupled with hyperspectral data collected to detect whether stress results from both salinity and moisture stresses in both Scottish and Egyptian wheat varieties can be distinguished. The Scottish wheat was grown in the winter season of 2005-6 and 2006-7, Egyptian wheat was grown in the spring season of 2006 and the winter season of 2006-7. The context of the research was to detect physiological changes in wheat subjected to salinity and moisture stresses through the detection of different biophysical and biochemical properties of wheat crops using remotely sensed data.

The results demonstrated that both moisture and salinity had significant effects on both biophysical and biochemical properties of wheat plants which therefore decreased total grain yield. Aboveground biomass, plant height, LAI and chlorophyll *a* were all affected by both moisture and salinity stresses. Also, results showed that calculated vegetation indices have the ability to detect changes in physiological status of wheat crops and some of these vegetation indices had a strong correlation with different biophysical and biochemical properties in wheat crops. For example, NDVI and RVI are good indicators of total grain yield and total aboveground biomass. No great difference between the coefficient of correlation values obtained using narrow band ratios (hyperspectral indices) and broad band ratios were found for predicting wheat grain yield and other properties of wheat crop. The strongest correlation for both methods was very similar in all experiments. In addition, indices calculated by transforming datasets such as the first derivative index, showed a highly significant relationship with the concentration of chlorophyll *a*. REP is a first derivative index which showed a strong correlation with the concentration of chlorophyll *a* in plant leaves ($R^2$ = 0.64, 0.69, 0.79 and 0.74 in the four experiments).

The PCA results showed that it is possible to distinguish between moisture and salinity induced stresses, but not before the flowering stage which is late in the growing season. This may be as a result of thin leaves of wheat, which may reduce the spectral response and therefore a crop with broader leaves such as maize may have a

higher response. Maize is the third most important crop in Egypt for animal fodder and recently people are starting to mix maize and wheat flour in bread manufacture. Maize leaves are broader than wheat and therefore detecting stress in maize using remotely sensed data might provide better results. The next chapter will explore the potential of using remotely sensed data in the detection of stress in maize subjected to different moisture and salinity regimes.

In summary remotely sensed data provides a robust approach for detecting plant physiological status, particularly in arid and semi-arid regions, which suffer from different types of stress such as drought and salinity stress. Furthermore, such novel techniques may be able to provide a useful tool in precision farming, which can give a better insight into plant heath and detect early signs of stress at a very early growth stage, and consequently avoid reduction in crop productivity, thus maximizing crop production in areas of the world that can ill-afford crop failure.

# 5 IN SITU SPECTRORADIOMETRY MEASUREMENTS IN MONITORING MAIZE

## 5.1 Introduction

Having demonstrated the potential for estimating grain yield and distinguishing between moisture and salinity induced stress with wheat crops in Chapter 4, this chapter extends this work to a broader leaved crop, maize. With its broader leaves, maize has the potential of increasing the spectral signal to noise ratio. In addition, it is a crop that grows in the summer season in the Nile Valley of Egypt and is perhaps subject to more intense moisture and salinity induced stress. The timing of maize crops would therefore have a better opportunity to be monitored by remote sensing and it is therefore hypothesized that *maize is more sensitive to salinity and moisture induced stress than wheat* and therefore *more sensitive at distinguishing salinity and moisture induced stress*. The greenhouse experiments described in Chapter 4 are therefore repeated for an Egyptian variety of maize (*Zea maize L*) during summer growing season of 2006-7. Both hypotheses of (i) *in situ hyperspectral measurements can predict stress in maize* and (ii) *moisture and salinity induced stress can be distinguished spectrally* are examined in this chapter.

## 5.2 Rationale

Generally, maize production is hindered by many factors including, drought, salinity, low soil fertility, nitrogen deficiency, use of non-tolerant varieties for pests and diseases, so maize production is different from place to place depending on the stressing factors. For example, in eastern and southern Africa, the annual maize production has averaged 16.2 million tones over the past two decades. During this period of time production fluctuated between 7.3 and 22.4 million tones primarily as a function of different types of stress including drought, salinity, heat stress, etc. resulting in the variability in maize production (Banziger *et al*., 2000).

Moisture stress is a key factor influencing maize production worldwide particularly sub-Saharan Africa. Drought has reduced maize productivity by 36% in the lowland areas and 21% in subtropical areas and affects around 23% of the land area (CIMMYT, 1988). Water stress affects maize productivity at different growth stages but some stages are particularly sensitive to drought including the early growth stages,

flowering and mid to late grain filling stages. The flowering stage is considered the most sensitive growth stage by drought as it reduces the capacity of developing kernels because the functioning of a key enzyme, acid invertase, is impaired (Westagte, 1997). Drought decreases maize grain yield by: (i) decreasing plant stand during the seedling stage, (ii) decreasing leaf area and therefore decreasing the rate of photosynthesis, (iii) decreasing ear and kernels and (iv) early leaf senescence during grain filling stage.

Salinity is also an important factor in decreasing maize crop productivity, particularly in arid and semi arid regions in Africa. As described in Chapter 2, Egyptian farmers use low quality water from agricultural drainage water, which is mainly saline. High salinity leads to an increase in the osmotic pressure in the root zone and makes it difficult for plants to absorb water and different nutrients. Most research on detecting stress in plants focused on the leaf scale, which ignores the effects of canopy structure and soil background. Therefore investigating the potential of remotely sensed data at canopy scale is very important to evaluate the effectiveness of different broad band and hyperspectral indices in detecting stress in crops. Many studies have shown the potential of remotely sensed data to detect stress in crops, but most of these studies were at the leaf scale. Unlike many studies, in our research reflectance measurements were collected at the canopy scale under controlled conditions.

## 5.3 Aims and objectives

This chapter assesses the potential of *in situ* hyperspectral measurements to detect and distinguish sources of stress in maize and evaluate whether salinity and moisture induced stress can be distinguished spectrally. The specific objectives of the research presented in this chapter are to:

- Grow maize under controlled greenhouse conditions.
- Subject maize plants to a range of moisture and salinity induced stress and quantify the effects of both stressors on plant growth.
- Use reflectance measurements to detect stress in maize under controlled conditions through using different hyperspectral and broad band vegetation indices.

- Establish whether salinity induced stress can be distinguished spectrally from moisture induced stress.
- Identify which spectral indices are sensitive to different crop properties.
- Identify wavelengths sensitive to stress and biochemical properties of maize.
- Consider implications for remote sensing for maize stress.

## 5.4 Experimental design and methods

### 5.4.1 Experimental design

A greenhouse-based experiment was conducted to assess the potential of *in situ* hyperspectral measurements to detect stress in maize. The same treatments of watering and water salinity used in section 4.3.1 have been used in this experiment (see Table 5.2 for more details about watering and salinity levels). The pots from the wheat crop experiments were emptied and filled with homogenised soil from the same location. The soil samples collected for chemical analysis and the results showed similar values for the different chemical elements (see Table 3.4 for more details about soil). Also, water samples were collected for analysis several times during the growing season (Table 5.1). Maize seeds were sown on 25$^{th}$ May 2007 at a density of three plants per pot. To ensure a high percentage of germination, seeds were sown at two seeds per hole and thinned to just one plant per hole after two weeks of sowing. The experiment comprised 66 pots which represent eleven different treatments of moisture and salinity (Table 5.2). To maintain moisture content within the pots at specific levels, two ways of monitoring moisture in pots were used. Pots from all treatments were weighed and the required amount of water was added to reach specific moisture content. At the same time a theta probe moisture meter was used to measure the moisture level. The theta probe was calibrated using the gravimetric method in determining moisture content. The total amount of phosphorous and potassium fertilizer was applied during soil preparation for cultivation at a rate of 60 kg ha$^{-1}$ each, but nitrogen was applied at a rate of 200 kg ha$^{-1}$ split over two doses. The first dose was applied one month after sowing and the second was just before flowering (both doses were added manually).

**Table 5-1** Chemical analysis of tap water used in this experiment.

| Sample | pH | EC, ds $m^{-1}$ | Cations, mg/l | | | | Anions mg/l | | | |
|---|---|---|---|---|---|---|---|---|---|---|
| | | | Ca | Mg | Na | K | Cl | $SO_4$ | $NO_3$ | P |
| 1 | 6.62 | 0.08 | 8.75 | 1.05 | 2.12 | 0.286 | 9.54 | 12.14 | 0.66 | 3.76 |
| 2 | 6.01 | 0.06 | 9.68 | 1.04 | 2.06 | 0.269 | 4.67 | 10.5 | 0.82 | 2.98 |
| 3 | 6.06 | 0.05 | 9.75 | 1.06 | 2.07 | 0.274 | 2.5 | 11.12 | 0.73 | 2.51 |

**Table 5-2** Different treatments of moisture and salinity levels used in this experiment (6 replicates each).

| Treatment | Salinity | Watering regime (% FC) | | | |
|---|---|---|---|---|---|
| | | 0.90 | 0.75 | 0.50 | 0.25 |
| $T_1$ | 0.05 | + | | | |
| $T_2$ | 0.05 | | + | | |
| $T_3$ | 0.05 | | | + | |
| $T_4$ | 0.05 | | | | + |
| $T_5$ | 2 | + | | | |
| $T_6$ | 4 | + | | | |
| $T_7$ | 6 | + | | | |
| $T_8$ | 6 | | + | | |
| $T_9$ | 6 | | | | + |
| $T_{10}$ | 2 | | + | | |
| $T_{11}$ | 2 | | | | + |

## 5.4.2 *In-situ* and dark room Spectroradiometry measurements

### *In-situ* measurements

The ASD FieldSpec Pro spectroradiometer (350-1050 nm) was used to measure the reflectance from maize canopy and leaves. The reflectance measurements were acquired in the same darkroom used in wheat experiments (see section 3.4.1. for more details). Spectra collection was started at very early growth stages ($V_7$) and onward during the growing season until harvest time. Each reflectance measurement comprised ten individual scans and five reflectance measurements were taken from each pot. Care was taken to minimize the influence of shadow and the white reference Spectralon panel was used before acquiring the reflectance from each pot. Figure 5.1 shows the reflectance measurements from maize canopies under artificial illumination source (two 300 W halogen lamps). The spectroradiometer was kept at specific height over the growing season.

**Figure 5-1** Measuring reflectance from maize canopy using an artificial illumination source inside the darkroom.

### 5.4.3 Spectral data analysis

The spectral reflectance data was analyzed using the same software and procedures used for the wheat. Also, the same 55 broad band and hyperspectral vegetation indices were used to predict plant physiological responses to salinity and moisture stressors. After flowering stage hyperspectral measurements were collected at the leaf scale as a result of increasing plant height to more than 2 m. Fig 5.2 shows the vegetation spectral response of maize canopy under darkroom conditions using artificial illumination source. Reflectance from maize leaves was undertaken in another darkroom (Figure 3.4) at the leaf scale. This darkroom was painted with a non reflective paint to minimise the effects of reflects from walls and ceiling. Non-reflective black cloth (reflectance < 5%) was also used underneath the instrument to minimise the reflectance from other objects around plant leaves. In this darkroom the spectrometer was kept at a constant distance of approximately 50 cm from plant leaves.

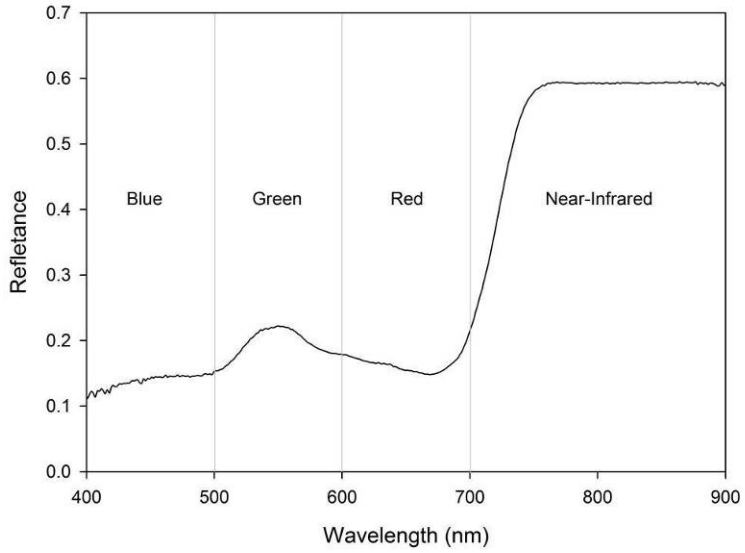


**Figure 5-2** A typical spectral vegetation spectrum obtained from maize leaves under artificial illumination source.

## 5.5 Results and discussion

### 5.5.1 Effects of moisture and salinity stress on biophysical properties of maize

#### Grain yield

The effects of moisture, salinity and moisture/salinity stress on maize grain yield were assessed through analysis of variance. Results given in Table 5.3 and depicted in Figure 5.3 show the effects of both salinity and moisture stress on maize grain yield. Both moisture and salinity stressors significantly affected maize grain yield ($R^2$ = 0.98%; p = 0.000). The highest yield of 1.86 kg $m^{-2}$ was recorded with the control treatments (high quality water with low salinity). The salinity treatments also significantly affected maize grain yield; the grain yield was negatively correlated with increasing salinity levels (p = 0.000). The lowest maize grain yield of 0.35 kg $m^{-2}$ was recorded with the low watering regime and the highest salinity (6 dS $m^{-1}$). The interaction between salinity and moisture stressors significantly affected maize grain yield (p = 0.000) with a high coefficient of determination ($R^2$ = 0.98).

**Table 5-3** P values of the analysis of variance (ANOVA) results for the effects of moisture, salinity and moisture/salinity on maize grain yield in 2007 growing season. Highlighted values are significant (P<0.05).

| Parameter | Source of stress | | | $R^2$ | $R^2_{adj}$ |
|---|---|---|---|---|---|
| | Moisture | Salinity | Moisture/salinity | | |
| Yield | 0.000 | 0.000 | 0.000 | 97.9 | 96.9 |

The reduction in maize grain yield as a result of increasing water salinity levels may be attributed to the main function of good quality water in building new cells and their elongation. It was noted that in all treatments with high salinity, the plant leaves looked twisted even with high moisture content within each pot. The explanation for that is when plants experience high salinity, the osmotic pressure in the root zone increases and therefore the ability of plants to absorb water and different nutrients from the root zone is hindered. Figure 5.3 shows the effects of both watering regime and water salinity on maize grain yield. The figure demonstrates that there is a significant positive linear relationship between watering regime and maize grain yield ($R^2$ = 0.92; p = 0.000) and a significant negative linear relationship between water salinity and maize grain yield ($R^2$ = 0.92; p = 0.000).

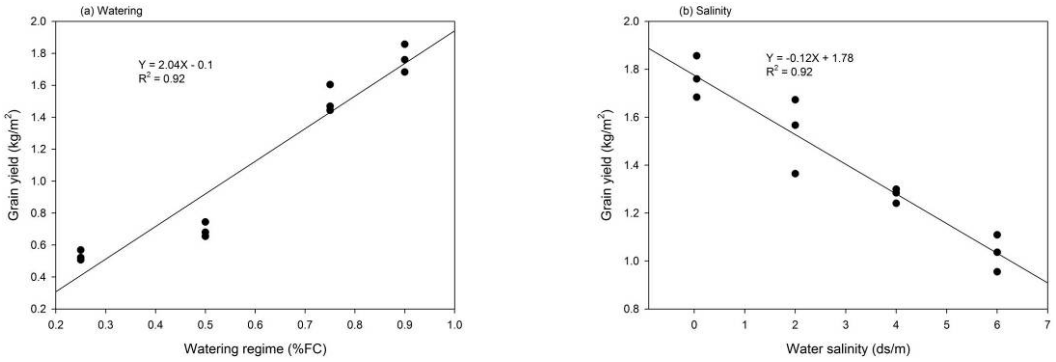


**Figure 5-3** The effects of (a) watering regime and (b) water salinity on maize grain yield in 2007 growing season (n = 12).

To predict maize grain yield under salinity and moisture stress, simple and multiple regression analyses were performed. Simple regression analysis showed that the grain yield was positively correlated with increasing moisture regime ($R^2$ = 0.92) and therefore a significant linear relationship was found between moisture treatments and maize grain yield. Also, a significant linear relationship between water salinity and

maize grain yield was observed. As mentioned above, the reduction in maize grain yield was highest in the treatments with low watering regime and high salinity level. Multiple regression analysis was then performed and the results showed that there is a high significant relationship between maize grain yield and both stressors ($R^2 = 0.88$; $p = 0.000$). Equation 5.1 shows the multiple regression equation for predicting maize grain yield:

Equation 5.1: $Y = 0.22 + 1.53W - 0.07\ S \quad R^2_{adj} = 87.7\%$

Where Y is the total grain yield (kg $m^{-2}$), W the watering regime (%FC) and S the water salinity level (dS $m^{-1}$).

**Aboveground Biomass**

Aboveground biomass was collected four times during the growing season, including harvest time. Vegetation samples were collected immediately after measuring reflectance from the maize canopies at different growth stages. Results given in Table 5.4 and illustrated in Figure 5.4 show the effects of moisture, salinity and moisture/salinity on aboveground biomass of maize. Moisture stress significantly affected the aboveground biomass ($R^2 = 0.93$) and this may be attributed to the decrease in leaf area as plants try to cope with moisture stress by twisting leaves to decrease the surface area for evaporation. The rate of photosynthesis decreases as a result and the concentration of different pigments decreases. Salinity stress also significantly affected the aboveground biomass ($R^2 = 0.91$). The highest aboveground biomass was recorded with the control treatments (highest watering regime and lowest water salinity level).

**Table 5-4** P values of the analysis of variance (ANOVA) results for the effects of moisture, salinity and salinity/moisture on aboveground biomass of maize in 2007 growing season. Highlighted values are significant ($P<0.05$).

| Parameter | Source of stress | | | $R^2$ | $R^2_{adj}$ |
|---|---|---|---|---|---|
| | Moisture | Salinity | Moisture/salinity | | |
| Biomass | 0.000 | 0.000 | 0.000 | 0.98 | 0.97 |

Aboveground biomass was negatively correlated with the salinity stress treatments as the lowest aboveground biomass was recorded with the highest level of salinity (6 dS $m^{-1}$). Again, the decrease in aboveground biomass as a result of increasing

salinity level may be attributed to the increase in osmotic pressure, which affects the rate of water and nutrient absorption from the root zone. The highest aboveground biomass of 14.7 kg $m^{-2}$ was recorded with the control treatment and the lowest aboveground biomass of 2.56 kg $m^{-2}$ was recorded with the treatment of highest salinity (6 dS $m^{-1}$) and the lowest watering regime (0.25% FC).

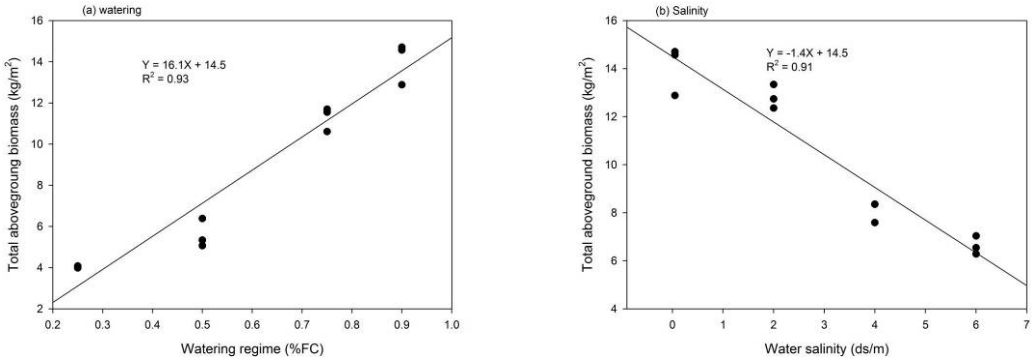


**Figure 5-4** The effects of (a) watering regime and (b) water salinity on the aboveground biomass of maize crop in 2007 growing season (n = 12).

To predict the aboveground biomass when subjected to both moisture and salinity stress, simple and multiple regression analysis were performed. The simple regression analysis demonstrated that the measured aboveground biomass was positively correlated with increasing watering level ($R^2$ = 0.93). A significant negative linear relationship was observed between aboveground biomass and water salinity ($R^2$ = 0.91). Therefore, simple regression analysis showed significant differences between the control treatment (low salinity and high watering level) and different salinity and watering levels. A multiple regression analysis was then performed to develop a regression equation to predict aboveground biomass under both moisture and salinity stress. The multiple regression analysis showed a high significant relationship between maize biomass and both stressors ($R^2$ = 0.92; p = 0.000), following is the multiple regression equation.

Equation 5.2: $B = 2.53 + 11.1\ W - 0.69\ S \quad R^2_{adj} = 79.7\%$

Where B is the total aboveground biomass (kg $m^{-2}$), W the watering regime (%FC) and S the water salinity level (dS $m^{-1}$).

## Leaf Area index (LAI)

LAI was measured immediately after measuring reflectance from the plant canopy. The results of the ANOVA for the relationship between moisture, salinity and moisture/salinity stress and LAI of maize are given in Table 5.5. Both moisture and salinity stress significantly affected the LAI at all measuring dates ($R^2 > 0.95$). Also, the interaction between moisture and salinity stress had significantly affected LAI. The decrease in LAI as a result of water salinity may be due to the effect of osmotic pressure, which affects the absorption of water and different nutrients from the root zone. The highest LAI of 3.23 was recorded at the flowering stage with control treatments and the lowest was recorded with treatment 9 (lowest watering and highest salinity).

**Table 5-5** P values of analysis of variance (ANOVA) results for the effects of moisture, salinity and moisture/salinity on leaf area index of maize crop in the 2007 growing season. Highlighted values are significant (P<0.05).

| Growth stage | Source of stress | | | $R^2$ | $R^2_{adj}$ |
|---|---|---|---|---|---|
| | Moisture | Salinity | Moisture/salinity | | |
| 65 DAS | 0.000 | 0.000 | 0.000 | 0.99 | 0.98 |
| 80 DAS | 0.000 | 0.000 | 0.000 | 0.96 | 0.96 |
| 90 DAS | 0.000 | 0.000 | 0.000 | 0.96 | 0.95 |
| 105 DAS | 0.000 | 0.000 | 0.000 | 0.97 | 0.96 |

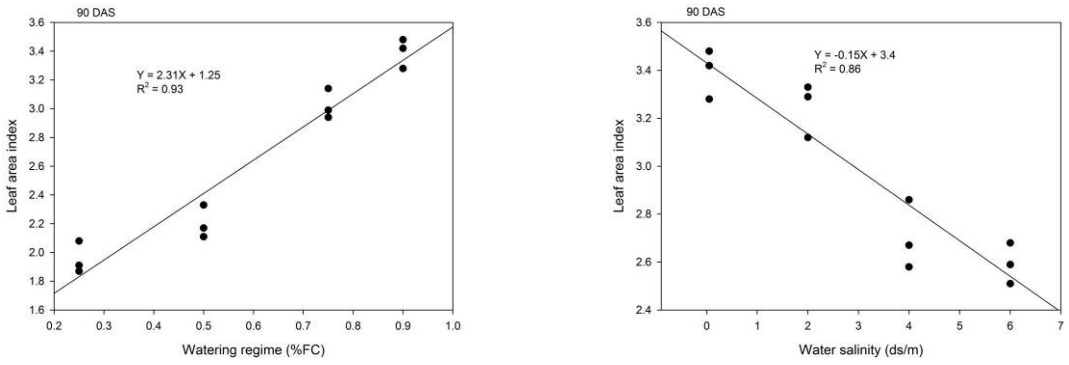


**Figure 5-5** The effects of moisture and salinity stress on LAI of maize crop at 90 DAS in 2007 growing season (n = 12).

## Plant height

Plant height of maize was measured concurrent with the acquisition of reflectance spectra as this provided a non-destructive measure. The plant height was measured until the flowering stage only as the plant height becomes constant after flowering. Analysis of Variance was applied to assess the relationship between maize plant height and moisture, salinity and moisture/salinity. Table 5.6 shows p values of the ANOVA.

The results demonstrated that moisture, salinity and their interaction significantly affected maize plant height in particular during the grain filling stage ($R^2$ = 0.98; p = 0.000). At the earliest growth stage (30 DAS), no stressor had a significant effect on maize height. At 45 DAS both moisture and salinity significantly affected the plant height, but not the combined stresses. Between 65 DAS and harvest time, all factors had a significant effect on plant height as the coefficient of determination was always greater than 0.90. Figure 5.6 shows the effects of moisture and salinity stress on maize plant height. It can be seen from the figure that there is a significant positive linear relationship between moisture regime and maize plant height ($R^2$ = 0.97; p = 0.000). Also, there is a significant negative linear relationship between plant height and water salinity ($R^2$ = 0.92; p = 0.000).

**Table 5-6** P values of analysis of variance (ANOVA) results for the effects of moisture, salinity and moisture/salinity on the plant height of maize crop in 2007 growing season. Highlighted values are significant (P<0.05).

| Growth stage | Source of stress | | | $R^2$ | $R^2_{adj}$ |
|---|---|---|---|---|---|
| | Moisture | Salinity | Moisture/salinity | | |
| 30 DAS | 1.00 | 0.952 | 0.907 | 0.06 | 0.00 |
| 45 DAS | 0.000 | 0.000 | 0.709 | 0.91 | 0.87 |
| 65 DAS | 0.000 | 0.000 | 0.000 | 0.97 | 0.96 |
| 80 DAS | 0.000 | 0.000 | 0.000 | 0.99 | 0.99 |
| 90 DAS | 0.000 | 0.000 | 0.000 | 0.98 | 0.97 |
| 105 DAS | 0.000 | 0.000 | 0.000 | 0.98 | 0.98 |

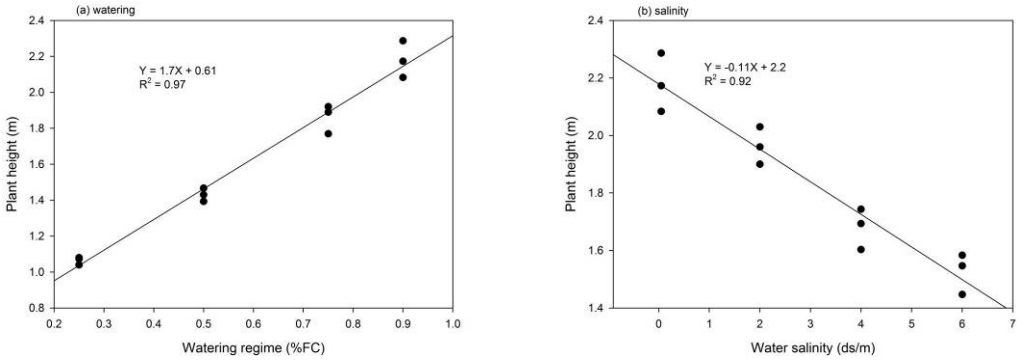


**Figure 5-6** The effects of moisture and salinity stress on plant height of maize crop at flowering stage in summer season of 2007 (n = 12).

### 5.5.2 Effects of moisture and salinity stress on chlorophyll *a* concentration of maize

Chlorophyll *a* concentration of maize leaves was measured immediately after measuring reflectance from maize canopy. ANOVA analysis was performed to assess the relationship between moisture, salinity and moisture/salinity and chlorophyll *a* concentration of maize leaves. The results for this relationship are given in Table 5.7 and depicted in Figure 5.7. At early growth stage (30 DAS) the chlorophyll *a* concentration was not affected by different treatments of moisture and salinity. At 45 DAS the concentration of chlorophyll *a* was negatively correlated with both moisture and salinity stress, but the interaction between these two stressors was non-significantly correlated with the chlorophyll *a* ($R^2$ = 0.76). Between 65 DAS and harvest time moisture, salinity and their interaction were significantly correlated with the measured chlorophyll *a* ($R^2$ = 0.94, 0.93, 0.91 and 0.96 at 65, 80, 90 and 105 DAS respectively). It should be mentioned here that the intervals between measuring dates were small because the plants were growing very fast during this period of time (mid-summer). From the flowering stage onwards reflectance was measured at the leaf scale as the plant height was very close to the spectrometer in the darkroom.

Figure 5.7 illustrates the effects of moisture and salinity on chlorophyll *a* concentration. The figure shows that water regime had a greater effect on chlorophyll *a* concentration in comparison to salinity effects. It is noted that chlorophyll *a* concentration was not affected by moisture and salinity at early stages such as grain yield, biomass and LAI; this may be attributed to the small evaporation surface.

**Table 5-7** P values of analysis of variance results for the effects of moisture, salinity and moisture/salinity on chlorophyll *a* concentration of maize leaves in summer season of 2007. Highlighted values are significant (P<0.05).

| Growth stage | Source of variation | | | $R^2$ | $R^2_{adj}$ |
|---|---|---|---|---|---|
| | Moisture | Salinity | Moisture*salinity | | |
| 30 DAS | 0.873 | 0.503 | 0.176 | 0.33 | 0.03 |
| 45 DAS | 0.00 | 0.00 | 0.142 | 0.83 | 0.76 |
| 65 DAS | 0.00 | 0.00 | 0.01 | 0.96 | 0.94 |
| 80 DAS | 0.00 | 0.00 | 0.00 | 0.95 | 0.93 |
| 90 DAS | 0.00 | 0.00 | 0.00 | 0.94 | 0.91 |
| 105 DAS | 0.00 | 0.00 | 0.00 | 0.97 | 0.96 |

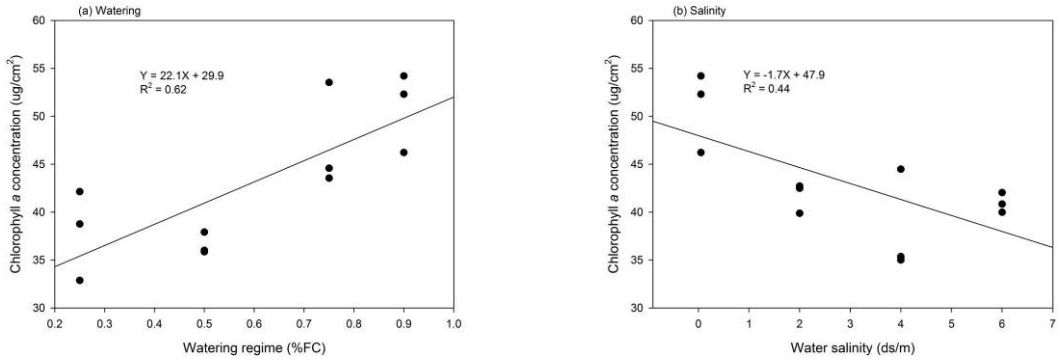


**Figure 5-7** Effects of moisture and salinity stress on chlorophyll *a* concentration extracted from maize leaves at 80 DAS in summer season of 2007 (n = 12).

The chlorophyll *a* concentration was determined also using HPLC and the results were roughly similar to those obtained using the spectrophotometer. In addition, the other pigments such as chlorophyll *b* and lutien decreased with increasing the stress level in both cases of salinity and moisture stress. This may be explained as a result of decreasing the plant ability to absorb water and basic nutrients from the root zone in both cases of stress. As mentioned before, increasing osmotic pressure in the root zone makes it difficult for plants to absorb water and nutrients and therefore plants try to cope with that by decreasing the leaf surface and consequently the rate of photosynthesis decreased, which affects pigment concentrations.

## 5.6 Reflectance measurements as a potential for predicting stress in maize

The spectral signature obtained from healthy and stressed (moisture and salinity induced stress) plants has been plotted against the wavelength as illustrated in Figure

5.8. This figure shows a typical spectral reflectance signature obtained from maize leaves subjected to both salinity and moisture stress under artificial illumination conditions. The spectral reflectance obtained from healthy plant leaves has low values in the blue region (400-520 nm) as a result of strong absorption of different pigments and chlorophylls, particularly chlorophyll *a*. Over the green region, the spectral reflectance increases until reaching the green peak, then the reflectance values decrease over the red region as a result of absorption by chlorophyll *a*. Over the NIR region the reflectance increases rapidly forming the red edge shoulder (680-730 nm).

When comparing the spectral signatures obtained from healthy plants and those obtained from stressed ones (moisture and salinity induced stress), the results demonstrated that the reflectance obtained from stressed leaves is greater than reflectance obtained from healthy plants over the blue and green regions. It can be seen that moisture stress has greatly affected the spectra in comparison to control treatment (healthy plants) as the spectral reflectance increases in blue, green and red region, which may be as a result of decreasing chlorophylls and other accessory pigments. In the NIR region, the spectral reflectance obtained from stressed canopies decreases in comparison to spectra obtained from healthy canopies as also identified by others (Serrano *et al*., 2000).

The effect of salinity stress on spectral reflectance is also noticeable as the reflectance increases in the blue, green and red region until REP shoulder, and then the reflectance values decreased over the NIR region in comparison to spectra collected from healthy plants. It is also apparent from the figure that the effects of moisture stress on spectral reflectance is higher than the effects of salinity stress; this may be due the dry edge of leaves as a result of reduced water absorption from soil, which therefore affects the spectra.

In general, the reflectance collected from stressed treatments (moisture and salinity induced stress), that have low chlorophyll concentration, showed a significant positive increase in the VIS range and significant negative increase in the NIR range. This can be explained by the effects of decreased chlorophyll and pigment absorption. Similar results were observed by Penuelas *et al*., 1997a, Wang *et al*., 2002a and 2002b.

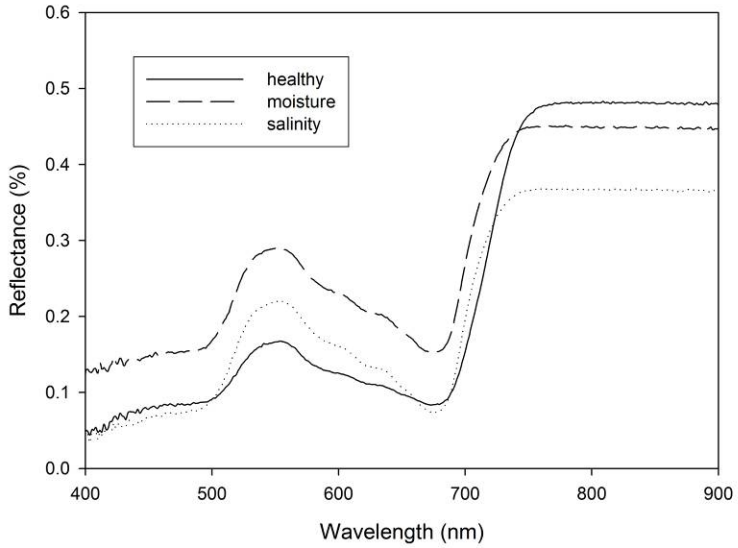


**Figure 5-8** An example of typical spectral reflectance signature obtained from maize leaves subjected to moisture and salinity stress under darkroom conditions.

## 5.6.1 Simple broad band spectral indices

### Grain yield

The correlation coefficient for the relationship between twelve broad band indices and the measured maize grain yield is given in Table B2 (appendix B). At early growth stages (30 and 45 DAS) most of the tested broad band indices were non-significantly correlated with the measured grain yield; this may be attributed to the similar spectral signature from different treatments of moisture and salinity induced stress. At 65 DAS, all tested indices were significantly correlated with the maize grain yield (r ranged between -0.55 and 0.73). At 80 DAS all indices gave highly significant correlation with the strongest correlation recorded with $GNDVI_{br}$ (r = 0.94). NDVI, SLAVI and IPVI also produced highly significant correlation values (r = 0.93). At 90 and 105 DAS, the majority of the tested broad band indices significantly correlated with the grain yield, but the correlation values were lower than those at 65 and 80 DAS; this may be due to chlorophyll degradation at late stages of the growing season. Figure 5.9 shows the relationship between maize grain yield and both $GNDVI_{br}$ and NDVI. The figure shows that both indices show a positive linear relationship with maize grain yield ($R^2$ = 0.88).

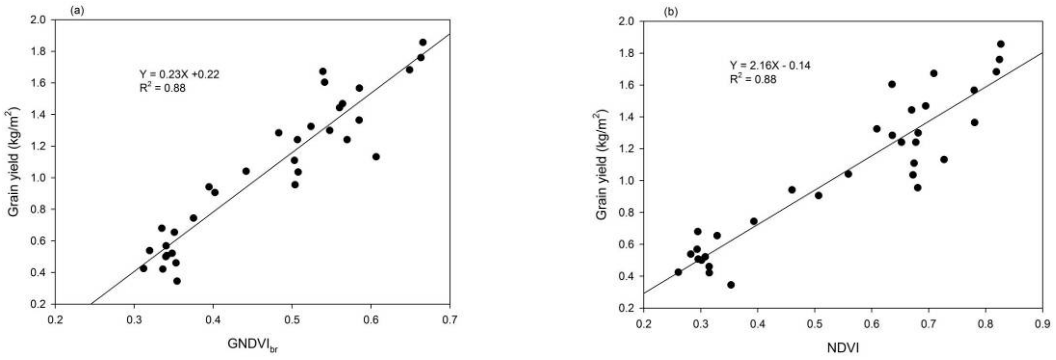


**Figure 5-9** The relationship between (a) $GNDVI_{br}$ and (b) NDVI obtained from the darkroom spertroradiometry and total grain yield of maize crop in summer season of 2007 (n = 33).

## Aboveground biomass

The coefficient of correlation for the relationship between broad band indices and the measured aboveground biomass of maize is detailed in Table B3 (appendix B). The results demonstrated that at 65 DAS all vegetation indices significantly correlated with the measured aboveground biomass ($r > 0.45$). At 80 DAS all vegetation indices significantly correlated with biomass and at this stage the correlation coefficient was higher in comparison to the previous and the subsequent dates of data collection. This may be attributed to the high chlorophyll concentration at early flowering stages. At 90 DAS, nine tested broad band indices were significant with the measured aboveground biomass. The strongest correlation was recorded with $GNDVI_{br}$ ($r = 0.85$) at 80 DAS. NDVI, RDVI and SI gave also high significant correlations ($r = 0.82$-$0.83$). VI1 often gives low correlation in comparison to the other indices during this experiment. Figure 5.10 shows the relationship between aboveground biomass and both $GNDVI_{br}$ and RDVI.

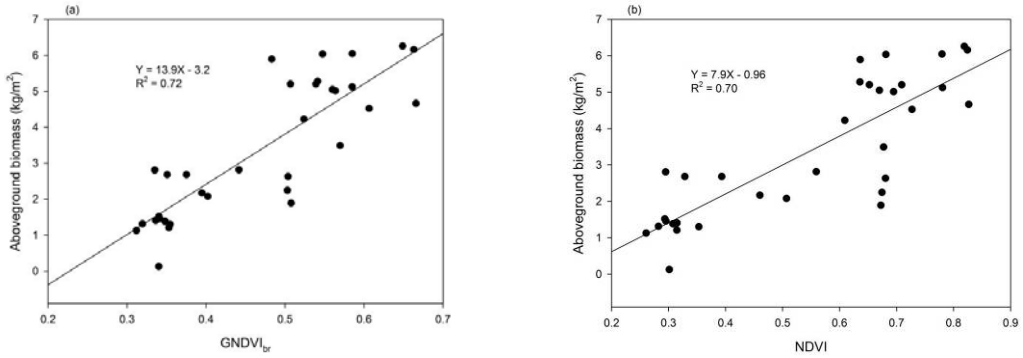


**Figure 5-10** The relationship between (a) $GNDVI_{br}$ and (b) NDVI obtained from the darkroom sectroradiometry and the measured biomass of maize crop in summer season of 2007 (n = 33).

## Plant height

Plant height was measured immediately after measuring reflectance from plant canopies at early stages or leaves at late stages of the growing season. The coefficient of correlation between maize plant height and different broad band vegetation indices are detailed in Table B4 (appendix B). At early growth stages (30 and 45 DAS) none of the tested indices were significantly correlated with the measured plant height as the correlation coefficient values ranged from -0.28 to 0.25. At 65 DAS, all indices were significantly correlated with the measured plant height. At 80 DAS all indices produced high significant correlations with the strongest correlation recorded with RVI and SI (r = 0.82). RDVI, $GNDVI_{br}$ and DVI also gave high significant correlations with the measured plant height (r = 0.78-0.80). At 90 and 105 DAS most indices gave significant correlations, but less than values at 80 DAS (canopy scale). Figure 5.11 shows the relationship between plant height and both RVI and $GNDVI_{br}$ at 80 DAS, which represents the last time of measuring reflectance at canopy scale.

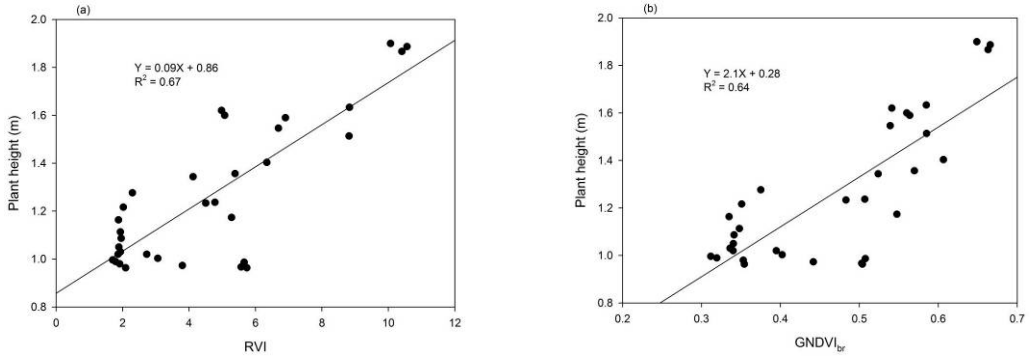


**Figure 5-11** The relationship between (a) RVI and (b) $GNDVI_{br}$ obtained from the darkroom spectroradiomtry and the plant height of maize crop in 2007 growing season (n = 33).

## Leaf Area Index (LAI)

The results for the relationship between the measured LAI and different broad band indices are given in Table B6 (appendix B). Due to low number of replicates vegetation samples were not collected at 30 and 45 DAS for determining LAI and aboveground biomass. At 65 DAS seven out of twelve indices gave significant correlations with the measured LAI. The correlation values increased with increasing the vegetation mass until 80 DAS then decreased after that. This may be attributed to senescence at the late growth stages, and also measuring reflectance at the leaf scale may be another reason for lower correlation. The strongest correlation therefore was recorded at 80 DAS with $GNDVI_{br}$ (r = 0.91). At 90 and 105 DAS most indices gave significant correlations but the correlation values were lower than that at 80 DAS which may be attributed to measuring scale. NDVI, SLAVI and IPVI also gave high significant correlations with LAI (r = 0.90).

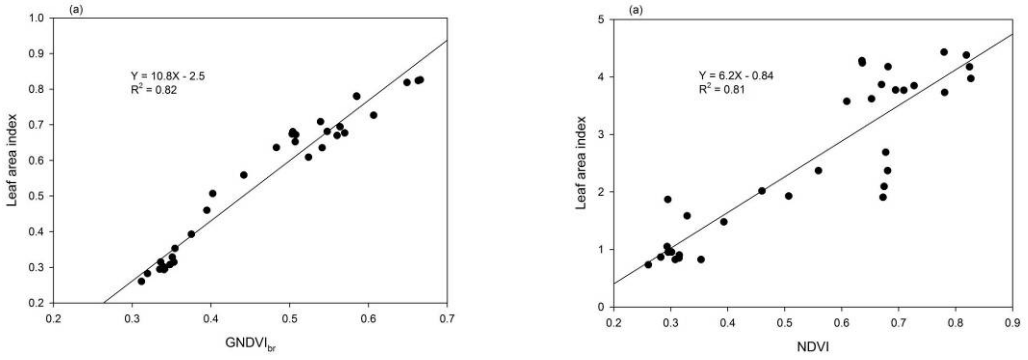


**Figure 5-12** The relationship between (a) $GNDVI_{br}$ and (b) NDVI obtained from the darkroom sectroradiometry and the leaf area index of maize crop at 80 DAS in 2007 growing season (n = 33).

## Chlorophyll *a* concentration

The relationship between different broad band vegetation indices and the concentration of chlorophyll *a* is detailed in Table B1 (appendix B). At early growth stages (30 and 45 DAS) none of the tested broad band indices gave significant correlation with the measured chlorophyll *a* (r < 0.20). No effect of moisture and salinity on plant growth at early growth stage and therefore no difference in spectral signature from different treatments. At 65 DAS most vegetation indices were significantly correlated with the measured chlorophyll *a* concentration. The highest correlations were observed at 105 DAS with the strongest correlation recorded with

DVI (r = 0.79). SAVI was also strongly correlated with the chlorophyll *a* concentration (r = 0.76). It was noted that the correlation between chlorophyll *a* concentration and different spectral vegetation indices was higher at the leaf scale than the canopy scale as shown in Table B1. The 105 DAS dataset was obtained at the leaf scale but the results at the previous dates were all at the canopy scale. Figure 5.13 shows the relationship between DVI, SAVI and the measured chlorophyll *a* concentration at 105 DAS. The figure shows a positive linear relationship between both DVI and SAVI and chlorophyll *a* concentration ($R^2$ = 0.62 and 0.58 respectively).

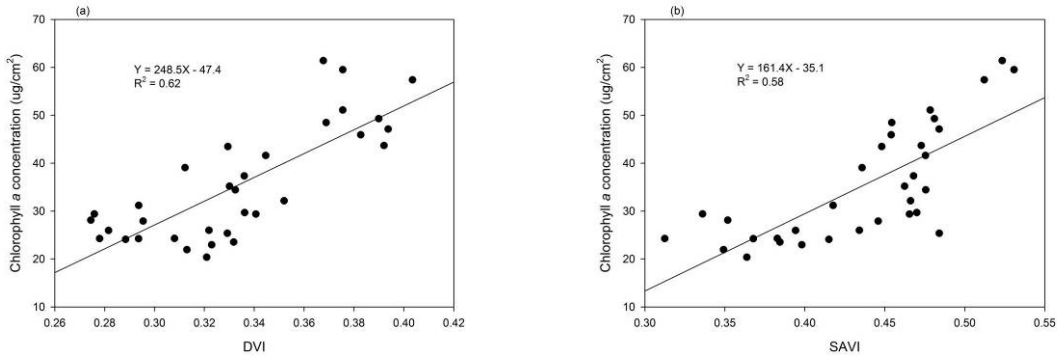


**Figure 5-13** The relationship between (a) DVI and (b) SAVI obtained from the darkroom spectroradiometry and the measured chlorophyll *a* concentration extracted from maize leaves in summer season of 2007 (n = 33).

## 5.6.2 Hyperspectral indices

### Grain yield

To detect stress in maize, forty three different hyperspectral vegetation indices were derived from darkroom spectroradiomtery data at both leaf and canopy scales. The correlation coefficients between hyperspectral indices and the measured maize grain yield are detailed in Table B2 (appendix B). The results showed that for the first two dates, the correlation values were non-significant with the majority of the forty three indices. This may have been a result of similar spectral signature from different treatments since the effects of both stressors were still very low. At 65 DAS, most of the tested hyperspectral indices gave high significant correlation with the measured grain yield. The strongest correlation was recorded at 80 DAS with 8 indices; $NDVI_{hy}$, $GNDVI_{hy}$, SIPI, $PSND_{br}$, $R_{695}/R_{760}$, $R_{605}/R_{760}$, $R_{710}/R_{760}$ and RNDVI

(r = ±0.93). At 90 and 105 DAS most hyperspectral vegetation indices produced significant correlations, but lower than observed values at 80 DAS. It was noted from the results that there was no great difference between the strongest correlation coefficient obtained using the hyperspectral and broad band ratio indices.

Figure 5.14 shows the relationship between maize grain yield and both $GNDVI_{br}$ and $R_{710}/R_{760}$ at the flowering stage. The figure shows that there is a positive linear relationship between $GNDVI_{br}$ and maize grain yield ($R^2$ = 0.86; p = 0.000). Also, there is a negative linear relationship between $R_{710}/R_{760}$ and maize grain yield ($R^2$ = 0.87; p = 0.000).

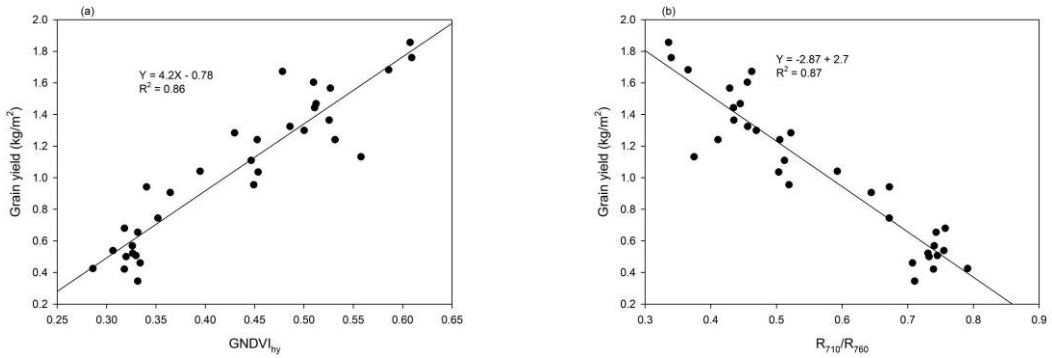


**Figure 5-14** The relationship between (a) $GNDVI_{hy}$ and (b) $R_{710}/R_{760}$ obtained from the darkroom spectroradiometry and the measured grain yield of maize at 80 DAS in 2007 growing season (n = 33).

## Aboveground biomass

The correlation coefficients for the relationship between the aboveground biomass and different hyperspectral vegetation indices derived from the darkroom at the canopy and leaf scales are given in Table B3 (appendix B). Due to low number of replicates, the aboveground biomass was collected for the first time at 65 DAS and the results showed that almost half of the hyperspectral vegetation indices gave significant correlations with the measured biomass, however, the correlation values were not high. At 80 DAS the majority of indices showed strong significant correlations with the measured biomass. The strongest correlation was recorded at 80 DAS with $GNDVI_{hy}$ and SIPI (r = 0.85). $NDVI_{hy}$, PSNDb, RNDVI, $R_{695}/R_{760}$, $R_{605}/R_{760}$ and $R_{710}/R_{760}$ also produced strong correlations (r = 0.83). However, some indices such as NPQI produced non-significant correlation with the measured biomass

throughout the growing season. Significant correlations were also recorded at 90 and 105 DAS, but most indices produced lower correlation values in comparison to 80 DAS dataset (canopy scale). This may be a result of measuring reflectance at the canopy scale, which gives better results than measuring at the leaf scale in terms of biomass. Figure 5.15 shows the relationship between $GNDVI_{br}$, $R_{710}/R_{760}$ and the measured biomass of maize. A positive linear relationship between biomass and $GNDVI_{hy}$ ($R^2 = 0.71$) is shown. Also, there is a negative linear relationship between $R_{710}/R_{760}$ and the measured aboveground biomass ($R^2 = 0.71$).

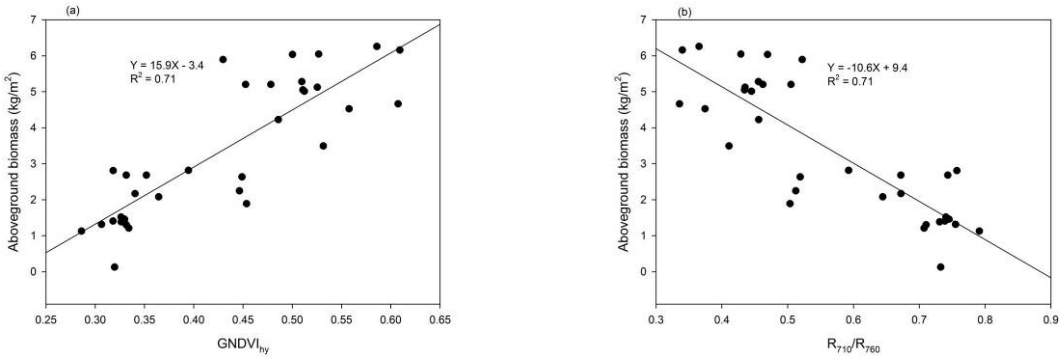


**Figure 5-15** The relationship between (a) $GNDVI_{hy}$ and (b) $R_{710}/R_{760}$ obtained from the darkroom spectroradiometry and the measured aboveground biomass of maize crop in 2007 growing season (n = 33).

## Leaf Area Index (LAI)

The correlation coefficient for the relationship between hyperspectral vegetation indices and the measured LAI of maize is given in Table B6 (appendix B) and illustrated in Figure 5.16. At 65 DAS, almost half of the hyperspectral vegetation indices demonstrated significant correlations with the measured LAI ($r \geq 0.35$). At 80 DAS the majority of the hyperspectral indices produced strong significant correlations with the measured LAI. The strongest correlation was recorded at 80 DAS (just before flowering stage) with the band ratio $R_{710}/R_{760}$ ($r = -0.91$). $NDVI_{hy}$, $GNDVI_{hy}$, SIPI, $PSND_b$, $R_{695}/R_{760}$, $R_{605}/R_{760}$ and RNDVI also produced high significant correlations (r values were 0.89 and ±0.90). At 105 DAS the correlation coefficient values were significant with almost two thirds of the hyperspectral indices but generally less than those obtained at 80 and 90 DAS, and this may be due to measuring at the leaf scale and the onset of senescence at late stages. Figure 5.16 shows the relationship between

LAI and both $R_{710}/R_{760}$ and $GNDVI_{hy}$. The graphs show that there is a negative significant linear relationship between LAI and the band ratio $R_{710}/R_{760}$ ($R^2 = 0.82$; p = 0.000). Also, there is a significant positive linear relationship between $GNDVI_{hy}$ and the measured LAI ($R^2 = 0.80$; p = 0.000).

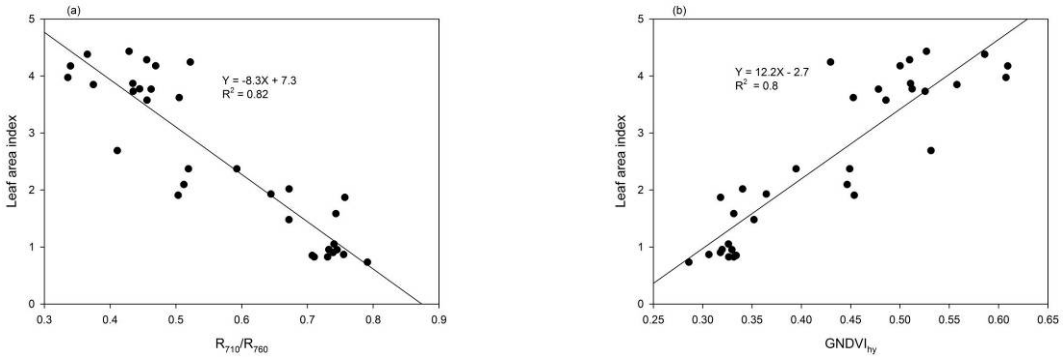


**Figure 5-16** The relationship between (a) $R_{710}/R_{760}$ and (b) $GNDVI_{hy}$ obtained from the darkroom spectroradiometry and leaf area index of maize crop at 80 DAS in 2007 growing season (n = 33).

## Plant Height

Plant height is the only biophysical property that was measured every time together with hyperspectral measurements immediately after measuring reflectance from plant canopies. The correlation coefficient for the relationship between hyperspectral vegetation indices and the measured plant height of maize is given in Table B4 (appendix B) and illustrated in Figure 5.17. At early growth stages (30 and 45 DAS), all hyperspectral vegetation indices did not show any significant correlations with the measured plant height ($r < 0.30$). At 65 DAS, almost half of the hyperspectral indices gave significant correlations with the measured plant height.

The highest correlations during the experiment were obtained from 80 DAS dataset with the strongest correlation recorded with the band ratios $R_{800}/R_{550}$ and $C_{green}$ ($r = 0.86$). $R_{750}/R_{550}$, $C_{red\ edge}$, $C_{NIR}$ and $R_{750}/R_{700}$ also produced strong significant correlations with the measured plant height ($r = 0.84$-$0.85$). The coefficient of correlation for the datasets obtained at 90 and 105 DAS had significant relationships, but generally the correlation values were less than those obtained at 80 DAS. Figure 5.17 shows a significant positive linear relationship between maize plant height and both $R_{800}/R_{550}$ and $R_{750}/R_{550}$ ($R^2 = 0.74$ and 0.73; p = 0.000 respectively). The results

suggest that 550, 750, and 850 nm wavelengths are sensitive for predicting maize plant height and other maize properties.

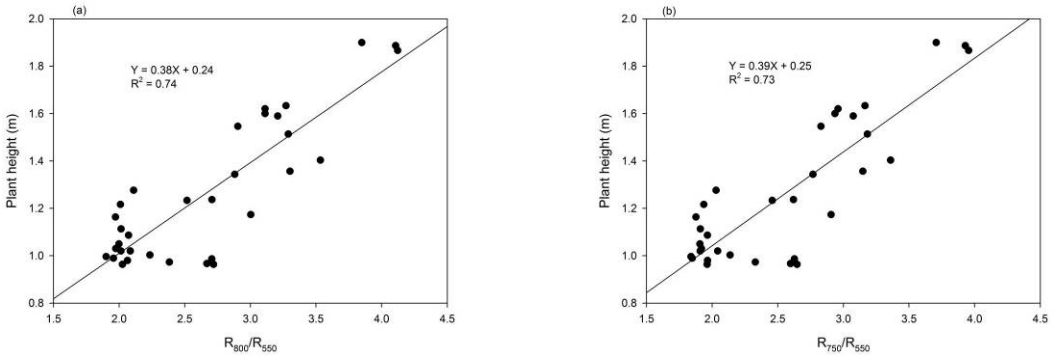


**Figure 5-17** The relationship between (a) $R_{800}/R_{550}$ and (b) $R_{750}/R_{550}$ obtained from the darkroom spectroradiometry and the plant height of maize crop at 80 DAS in 2007 growing season (n = 33).

## Chlorophyll *a* concentration

Forty three hyperspectral vegetation indices derived from darkroom measurements at both leaf and canopy scales were calculated. The correlation coefficient for the relationship between hyperspectral indices and the measured chlorophyll *a* concentration is given in Table B1 (appendix B). The results showed that at 30 and 45 DAS, none of the indices were significantly correlated with the measured chlorophyll *a* ($r < 0.34$). At 65 DAS, nineteen vegetation indices were significantly correlated with the chlorophyll *a* ($r \geq 0.35$). At 80 and 90 DAS, most of the indices significantly correlated with the chlorophyll *a* with the highest correlations obtained from 105 DAS dataset (leaf scale). The strongest correlation was recorded with $PSSR_b$ and $R_{800}$-$R_{550}$ ($r = 0.80$). The results suggest that deriving vegetation indices from reflectance measurements at the leaf scale for predicting chlorophyll *a* concentration gives better results in comparison to measuring at the canopy scale. This may be attributed to the effects of canopy structure and soil background on reflectance.

The first derivative of reflectance was also used to predict chlorophyll *a* concentration. REP has been calculated from the data obtained at the canopy scale (prior to flowering stage) and at the leaf scale (late growth stages). The results (Table B7; appendix B) exhibited that there is a significant relationship between REP and the

measured chlorophyll *a* concentration at the flowering stage. At 65 DAS, the coefficient of correlation started to be significant (r = 0.43) between the REP and the measured chlorophyll *a* concentration, and increased onwards until the late stages of vegetative growth. As many other indices, at early growth stage it is difficult to predict chlorophyll *a* concentration using REP. The strongest correlation was recorded at 105 DAS (r = 0.88) from the data obtained at the leaf scale.

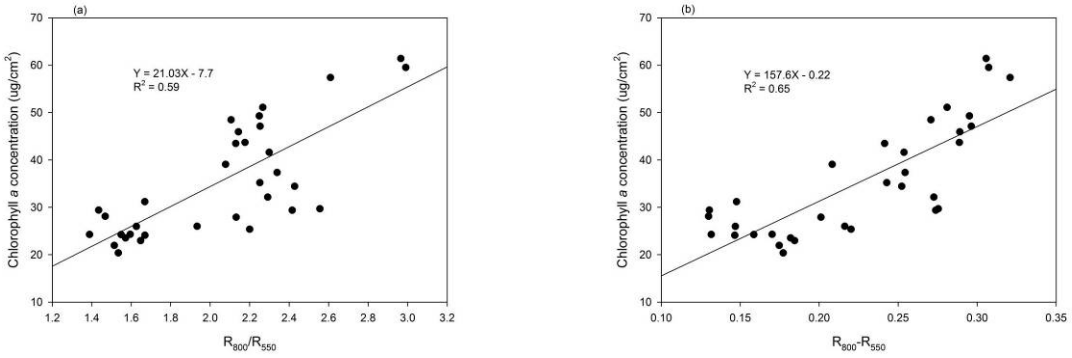


**Figure 5-18** The relationship between (a) $R_{800}/R_{550}$ and (b) R800-R550 obtained from the darkroom spectroradiometry and the chlorophyll *a* concentration extracted from maize leaves in 2007 growing season (n = 33).

Comparing the results obtained using hyperspectral and broad band vegetation indices with the results obtained using REP, the strongest correlation obtained from REP (r = 0.88) is comparable to the strongest correlation obtained using different hyperspectral and broad band indices (r = 0.80 recorded with $R_{800}$-$R_{550}$). Figure 5.19 shows the relationship between REP and the measured chlorophyll *a* concentration at different growth stages. The figure demonstrates that REP derived from hyperspectral data obtained at the leaf scale gave better results for predicting chlorophyll *a* concentration compared with those derived from data obtained at the canopy scale. For example, data collected at 105 DAS at leaf scale demonstrated strong significant correlations ($R^2$ = 0.77; p = 0.000).

It is further shown that the datasets collected under controlled conditions in the darkroom produced higher correlations with chlorophyll *a* concentration at the leaf scale in comparison to the canopy scale (Figure 5.19). However, predicting other crop properties such as aboveground biomass using vegetation indices derived from

datasets collected at the leaf scale produced lower correlations in comparison to canopy scale.

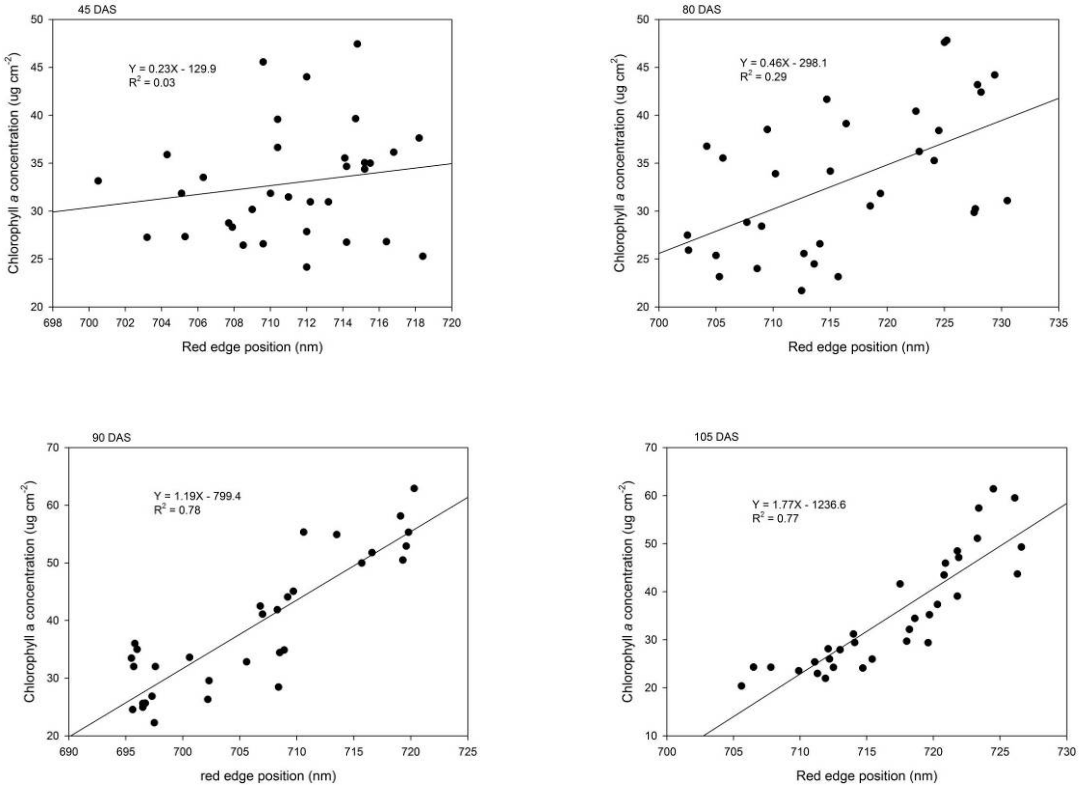


**Figure 5-19** The relationship between REP and the concentration of chlorophyll *a* extracted from maize leaves at different growth stages in summer season of 2007 (n = 33).

## Identifying wavelengths sensitive to chlorophyll *a* concentration of maize crop

The spectra obtained from the darkroom during the growing season from early growth stages until harvest time were used to identify wavelengths sensitive to chlorophyll *a* concentration. The coefficient of correlation was calculated between the reflectance values (400-900 nm) collected from different treatments and the measured chlorophyll *a* concentration, and then plotted against the wavelength (Figure 5.20). Wavelengths between 400 nm and 900 nm were used for this analysis to avoid the extreme noise at both ends of the spectrometer sampling range. High correlation values were found at three regions of the electromagnetic spectrum (550, 705 and 770 nm respectively). The highest correlation coefficient of -0.60 found at 550 nm and the other values were found at 705 and 770 nm (r = -0.55 and 0.59 respectively). These results were the best over the growing season as the highest correlation coefficient changed in response to growth stage as a result of vegetation cover and the concentration of chlorophylls. For

example, before and after applying the whole dose of nitrogen in June the concentration of chlorophyll *a* changed highly. These results in accordance with many studies as several narrow band spectral vegetation indices have been developed using wavelengths around 550 and 750 nm. The hyperspectral ratios of $R_{750}/R_{550}$, $R_{750}/R_{700}$, and $R_{800}/R_{550}$ were found to be highly correlated with chlorophyll *a* concentration (Lichtenthaler *et al*., 1996, Gitelson *et al*., 1996 and Datt, 1999).

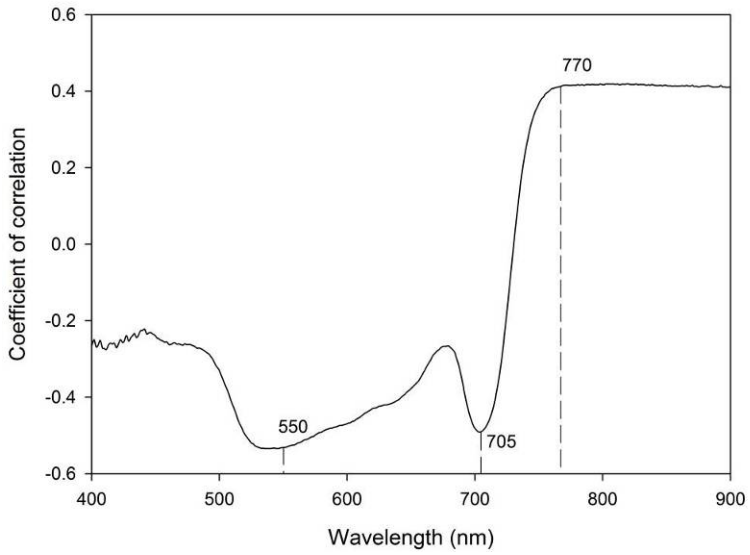


**Figure 5-20** The relationship between the correlation coefficient and wavelength of the spectra collected from maize leaves obtained under darkroom conditions.

### 5.6.3 Distinguishing moisture induced from salinity induced stress

The spectra collected at different growth stages at both canopy and leaf scales were analyzed using Principle Component Analysis (PCA). The score plot of the PCA analysis is depicted in Figure 5.21, shows that the spectra collected from healthy plants can be distinguished from the spectra collected from stressed plants (moisture and salinity induced stress), and this may be attributed to the plant water status and the concentration of different pigments. The spectra collected from treatments with high watering regime were close to each other and were plotted in one corner of the score plot. However, the spectra collected from stressed canopies or leaves tend to plot in a different quarter of the score plot whenever leaf water content and different chlorophylls become lower. The results depicted in Figure 5.21 show the score plot for the dataset of 80 DAS; the graph shows that healthy and low stressed treatments

(low salinity of 2 dS $m^{-1}$ and high watering regime of 75% FC) are plotted in the upper right corner of the score plot. It can also be noticed that all treatments that suffer from moisture stress are plotted in the lower left corner. It is further shown that most combinations of moisture and salinity are plotted in the lower left corner.

When plants reached the flowering stage some plants were over 175 cm in height, which made it difficult to measure reflectance at the canopy scale inside the darkroom because the plants were very close to the spectroradiometer. Therefore, plant leaves were collected and reflectance was measured at the leaf scale. The spectra collected at 105 DAS were used to distinguish between moisture and salinity induced stress. Figure 5.22 shows that the control and well watered treatments with low salinity are located in the upper right corner of the score plot. The figure also exhibits that most treatments that suffer from salinity are located in the lower left corner of the score plots. The moisture induced treatments are located in the upper left corner. All combinations of moisture and salinity induced stress are located in the lower right corner of the score plot. The dissimilarities between healthy treatments and stressed ones (moisture and salinity) may be attributed to the changes in biochemical and biophysical properties of maize including different pigments, plant height, biomass and LAI.

The results suggest that it is possible to distinguish between moisture and salinity induced stress from flowering stage onward. Despite the late distinction between moisture and salinity induced stress, these results can be used effectively for following growing seasons to avoid both stressors. It can be mentioned here that measuring reflectance in an actual maize field may give better results. Since reflectance can be measured at many locations with in the same field then the data can be averaged and therefore decrease the variations within the same field.

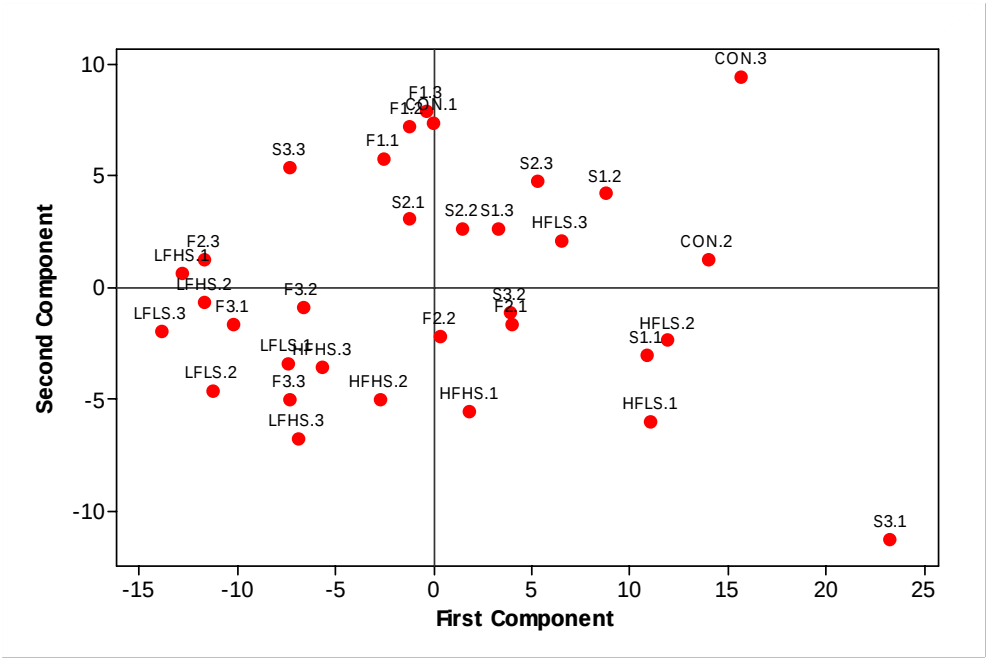


**Figure 5-21** The score plot of PCA for the spectra collected from healthy and stressed maize canopies at 80 DAS under darkroom conditions (n = 33). (Treatment labels: CON-control; F1-75% FC; F2-50% FC; F3-25% FC; S1-2 dS $m^{-1}$; S2-4 dS $m^{-1}$; S3-6 dS $m^{-1}$; HFLS-0.75% FC and 2 dS $m^{-1}$; HFHS-0.75% FC and 6 dS $m^{-1}$; LFLS-0.25% FC and 2 dS $m^{-1}$; LFHS-0.25% FC and 6 dS $m^{-1}$).

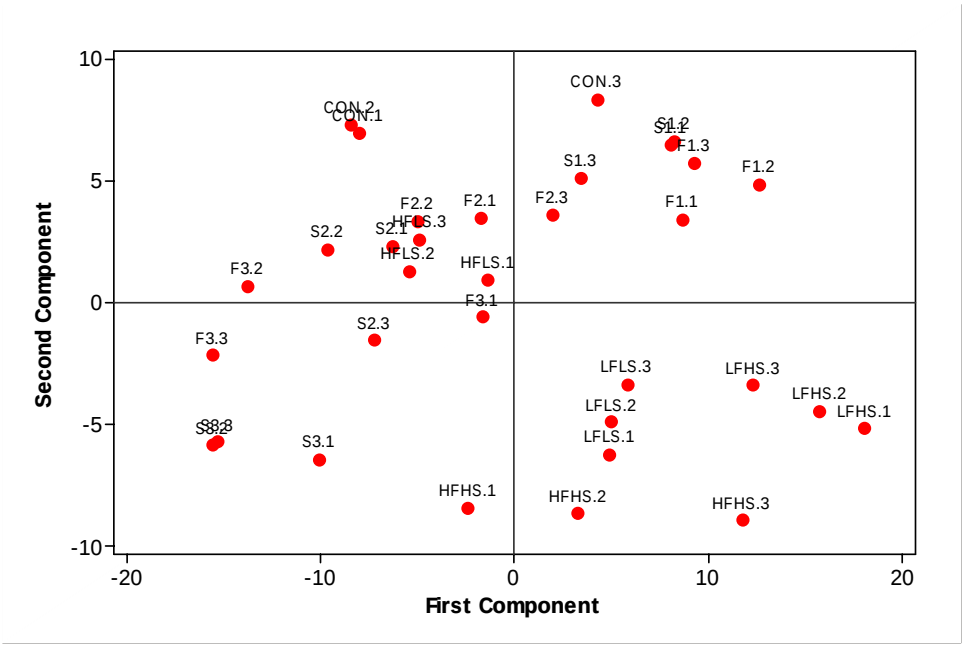


**Figure 5-22** The score plot of PCA for the spectra collected from healthy and stressed maize leaves at 105 DAS under darkroom conditions (n = 33). (Treatment labels: CON-control; F1-75% FC; F2-50% FC; F3-25% FC; S1-2 dS $m^{-1}$; S2-4 dS $m^{-1}$; S3-6 dS $m^{-1}$; HFLS-0.75% FC and 2 dS $m^{-1}$; HFHS-0.75% FC and 6 dS $m^{-1}$; LFLS-0.25% FC and 2 dS $m^{-1}$; LFHS-0.25% FC and 6 dS $m^{-1}$).

## 5.7 Summary

A greenhouse based experiment was undertaken to investigate the effects of both moisture and salinity induced stress on biophysical and biochemical properties of maize crop including grain yield, aboveground biomass, LAI, plant height, and chlorophyll *a* concentration. A time series of spectroradiometry measurement was collected to assess the potential of remotely sensed data to detect stress in maize when subjected to both salinity and moisture induced stress. Furthermore, the study aimed to distinguish between salinity and moisture induced stress spectrally. The reflectance measurements were measured at both canopy and leaf scales as the height of the darkroom was not suitable for measuring reflectance at late stages of the growing season.

Fifty five different broad band and hyperspectral vegetation indices were calculated and examined for detecting stress in maize. The results demonstrated that the strongest correlations obtained using hyperspectral and broad band vegetation indices were similar. The majority of the tested indices demonstrated strong significant correlations with different biophysical properties of maize crop including grain yield, aboveground biomass, plant height and LAI. REP was highly correlated with the concentration of chlorophyll *a* particularly after applying the required dose of nitrogen in June. The correlation values were greater than 0.80 at the flowering and grain filling stages and this may be attributed to early senescence in the stressed treatments.

PCA was applied to differentiate between moisture induced stress and salinity induced stress. The score plots of PCA showed the ability to distinguish between stressed plants and healthy plants at flowering stage. Some datasets showed the possibility to distinguish between moisture and salinity induced stress. Generally, it can be seen that PCA effectively showed the dissimilarities between healthy and stressed treatments, but it is problematic to define the source of stress at early growth stages. Measuring reflectance in an actual field may give better results as the canopy cover is greater and therefore the spectral response may be more consistent.

Therefore, remotely sensed data can be a robust technique for detecting stress in plants subjected to salinity and/or moisture stress. Detecting stress at early growth

stage could prevent reduction in grain yield and consequently maximise crop productivity. In addition, it is possible to use green, red and NIR bands derived from satellite imagery to extrapolate the data obtained using *in situ* hyperspectral measurements. Hyperspectral satellite imagery (e.g. Hyperion) is needed since it has many spectral bands (>200), which enable researchers to detect different parameters of plant health.

The results obtained above show that remotely sensed data obtained using hyperspectral measurements is a useful technique in predicting plant health status and therefore it would be beneficial if the results can be extrapolated to large scales using high spectral and spatial resolution satellite remote sensing. The next chapter will explore the ability of high resolution satellite imagery to detect stress in wheat and maize in the Nile Valley of Egypt to maximise crop productivity and use limited water and cultivated land resources more efficiently. In conclusion the results from this chapter validated the hypothesis that *in situ* hyperspectral measurements are able to detect stress in maize and even sometimes distinguish between moisture and salinity induced stress spectrally at the flowering stage.

# 6 EVALUATING SATELLITE REMOTE SENSING FOR OPTIMIZING WHEAT AND MAIZE PRODUCTION

## 6.1 Introduction

The previous two chapters (Chapter 4 and 5) have investigated the potential of *in situ* hyperspectral reflectance measurements to predict physiological changes in wheat and maize caused by moisture and salinity stress. More specifically, the aim was to detect stress through measurements of reflectance from crop canopies and to relate different spectral vegetation indices (broad band and hyperspectral indices) to changes in biophysical and biochemical properties of wheat and maize including plant height, LAI, aboveground biomass, grain yield and chlorophyll concentration. The results from these two chapters demonstrated that hyperspectral reflectance measurements have the potential to detect and even differentiate between salinity and moisture induced stress. Furthermore, the results obtained from hyperspectral and broad band vegetation indices are similar for detecting the biophysical responses to stress. This chapter extrapolates the results from Chapter 4 and 5 to the field environment to assess the ability of both *in situ* hyperspectral and high spatial resolution satellite imagery to detect stress in wheat and maize in the Nile Valley of Egypt. Here we examine the hypothesis that *in situ hyperspectral and high spatial resolution remote sensing imagery are able to detect stress in wheat and maize and even moisture induced stress can be distinguished spectrally from salinity induced stress*. In undertaking this, we establish a possible methodology for the remote sensing of crop stress in Egypt.

**Aims and Objectives**

The overall aim of this chapter is to investigate the potential of *in situ* and satellite remote sensing data to detect stress in wheat and maize in the Nile Valley of Egypt.

The specific objectives of the research presented in this chapter are to:

1. Evaluate whether the outcomes from the greenhouse experiments can be replicated in the field.

   (a) For stress detection

(b) For distinguishing moisture and salinity induced stress

2. Assess the efficiency of classification algorithms to map different crop types.

3. Having mapped individual crop types through remote sensing, predict wheat and maize biophysical and biochemical properties via remotely sensed data.

## 6.2 Methodology

### 6.2.1 Study area

The study area is located in south-west Alexandria, Egypt (latitude of 30° 55` 50`` and longitude of 29° 53` 35.6``). To have a range of stress levels in fields, three study sites were chosen, Hewaihy, Kahr and Bangar. The soil at these sites is a sandy loam with low concentration of nitrogen, as these sites have been reclaimed recently from the eastern desert. Figure 6.1 shows a map of the study sites. The majority of the fields use flood irrigation with a few farms irrigated by sprinkler or trickle irrigation, especially at the Bangar site. The weather in this area is characterised by hot summers and mild winters with respective average temperatures of 24.3ºC and 16.6ºC, average precipitation 0 and 28.3 mm per annum; average humidity 69 and 68%; and average wind speed 13.5 and 14.2 km $h^{-1}$ (The Weather Network, 2008).

Table 6.1 details the three sites and different dates of *in situ* hyperspectral survey. These sites are mainly located at the end of irrigation channel systems. The Bangar site was initially reclaimed to be irrigated by sprinkler irrigation system, but farmers gradually changed the system to flood irrigation and therefore crop requirements increased with the same amount of available water. Some fields at this site are suffering from salinity stress since farmers have used agricultural drainage water for irrigation for at least three decades. The accumulation of salts in the soil profile over this period of time affects plant health particularly sensitive crops such as maize.

**Table 6-1** Different sites and dates for the spectroradiometry survey in wheat fields in south-west Alexandria, Egypt in 2007 winter growing season.

| Site | | |
|---|---|---|
| **Kahr** | **Hewaihy** | **Bangar** |
| 11 March | 12 March | 15 March |
| 19 March | 28 March | |
| 27 March | | |


**Figure 6-1** A map showing the three study sites south-west Alexandria, Egypt (adapted from Google earth).

## 6.2.2 Field work timing

Field work was conducted in wheat fields (8-30 March) and maize fields (10-17 July) in Egypt during winter and summer seasons of 2007. The field work was timed to coincide with the acquisition of Hyperion images in both summer and winter seasons of 2006-7. March was chosen for detecting stress in wheat because the weather starts to be warmer and the grain filling stage starts in March. The middle of July was chosen for detecting stress in maize due to the high possibility of experiencing stress in maize as a result of high evapotranspiration and the shortage of water during this time. A large area is cultivated with rice in the Nile Delta, which consumes massive

amounts of water. This is why the study sites chosen tend to suffer from moisture and salinity stress. Chapter 2 outlined the typical irrigation agricultural practices for main crops in that area.

During the field work, the coordinates of 27 ground control points were collected using GPS (Global Positioning System), which represent fixed points such as intersects between roads and railway lines, bridges and roads, high ways and main drains or channels. Photographs have been taken for all these ground control points. Care was taken to ensure that this number of ground control points will cover the whole study area. During the first field visit in March to collect data in wheat fields, a time series of *in situ* hperspectral measurements was conducted to assess the physiological changes during this period of time and was undertaken during the second field visit in summer to collect data from maize field.

### 6.2.3 *In situ* hyperspectral measurements survey and sampling strategy

For wheat, an *in situ* hyperspectral survey was conducted in the study area during the winter growing season of 2007 (8-30 March) concurrent with the acquisition of Hyperion satellite imagery. The hyperspectral survey was conducted in random fields depending on the size of the field and the status of these fields in terms of stress. Basically, healthy fields were always located at the beginning of irrigation channels and the stressed fields at the end of irrigation channels. Care was taken to obtain the hyperspectral measurements at the same locations within the same fields on different measuring dates. An ASD FieldSpec hand-held spectroradiometer was used to measure reflectance from plant canopies (see Table 3.3 for the instrument technical specifications). The reflectance measurements were restricted between 10 am and 3 pm to minimize the influence of changes in solar zenith angle. Figure 6.2 shows an example of measuring reflectance in a wheat field. During the *in situ* hyperspectral survey, the sensor was kept at a constant distance from the soil surface using an iron stand of 2 m height. Vegetation samples were collected immediately after measuring reflectance from plant canopies to quantify aboveground biomass and LAI (for more details about vegetation strategy and chlorophyll analysis, see section 3.2 and 3.3). Plant height was measured following reflectance measurements from plant canopy at each location within the same field. Soil and water samples at each site were collected for chemical analysis.

**Figure 6-2** Measuring reflectance from wheat canopy under clear sky conditions during field work visit in Egypt, March 2007.

### 6.2.4 Remote sensing data acquisition

**Hyperion**

The use of Hyperion imagery was planned at the beginning of the research project as the only platform to provide hyperspectral imagery (more than 200 bands) at a suitable spatial resolution (30 m). The number of bands obtained from the spectral resolution of the Hyperion satellite enables researchers to have the ability to detect stress in crops through hyperspectal band ratios providing the potential for the *in situ* results to be replicated. For wheat in the winter season of 2007, a Hyperion scene was ordered to be acquired on 10$^{th}$ March 2007, but due to the > 99% cloud cover at this time the acquisition was rejected. For the summer season a Hyperion scene was ordered to be acquired on 15$^{th}$ of July to coincide with field work, but tasking conflicts and sensor calibration requirements resulted in no images being acquired.

**ASTER**

ASTER is a multispectral satellite with a 15 m spatial resolution. ASTER imagery also was ordered to be acquired on 5$^{th}$, 20$^{th}$ March and 5$^{th}$ April to have a time series for the crop development. Due to high percentage of cloud cover in March the

acquisition was rejected. An ASTER image was acquired on 23rd April 2007 for winter wheat for the study area, which is very late for the wheat growing season in Egypt since it is harvested during the first half of May. The radiance derived from this image was used to calculate vegetation indices, but the results showed very poor relationship between different fields of the hyperspectral survey as a result of chlorophyll degradation at this late stage.

**QuickBird**

Two QuickBird multispectral images were acquired covering wheat and maize crops. QuickBird satellite is a high spatial resolution satellite comprises four multi spectral bands (blue, green, red and near-infrared) of 2.4 m spatial resolution. The first QuickBird image of wheat fields was acquired at 09:06 h GMT on 7th April 2007 for the study area (south-west Alexandria, Egypt). The second QuickBird image of maize fields was acquired at 09:13 h GMT on 29th June 2007. Further details about QuickBird images are given in Table 6.3.

**Figure 6-3** Technical characteristics of both QuickBird images of wheat and maize fields acquired in April and June 2007 in south-west Alexandria, Egypt.

| | **7th April image** | **29th June image** |
|---|---|---|
| Satellite | QuickBird | QuickBird |
| Acquisition date | 2007-04-07 | 2007-06-29 |
| Acquisition time | 09:06 | 09:13 |
| Cloud cover | 33% | 0% |
| Off nadir angle | 13° | 22° |
| Target azimuth angle | 210° | 51° |
| Spectral bands | 4 | 4 |
| Environmental quality | 99% | 99% |
| Centre location | Lat/Lon 30.99°/29.84° | Lat/Lon 30.99°/29.84° |

**SPOT HRV**

SPOT HRV is a multispectral satellite, which gives 20 m spatial resolution with four spectral bands including blue, green, red and near infrared (see Table 2.9 for more details about the sensor specifications). Two SPOT HRV images were also planned to be acquired on 5th and 20th July concurrent with field work visit. The first SPOT HRV image of maize fields in the study area south-west Alexandria was acquired at 8.69 h GMT on 30th June 2007. The second SPOT HRV image was acquired at 9.14 h GMT

on 9th July 2007. More information about SPOT HRV satellite images are given in Table 6.4.

**Figure 6-4** Technical characteristics of both SPOT HRV images of maize fields acquired for the study area south-west Alexandria, Egypt.

| | **30th June image** | **9th July image** |
|---|---|---|
| Satellite | SPOT4 | SPOT4 |
| Instrument | HRVIR1 | HRVIR2 |
| GRS reference | 108-288 | 108-288 |
| Acquisition date | 2007-06-30 | 2007-07-09 |
| Acquisition time | 08:41:15 | 09:08:12 |
| Cloud cover | 0 | 0 |
| Orientation angle | 8.9° | 12.3° |
| Incidence angle | 28.9° | 28.9° |
| Sun angle | Azimuth: 107.6 | Azimuth: 119.8 |
| Spectral bands | 4 | 4 |
| Shift along track | 0 | 0 |
| Centre location | Lat/Lon 30.95°/29.79 | Lat/Lon 30.95°/ E29.79 |

### 6.2.5 Image processing

#### Geo Corrections

At the beginning, the row images were visually investigated for clouds and associated shadows. The QuickBird image acquired on 7th March 2007 was 33% cloud cover with associated shadows. Some of the fields of *in situ* hyperspectral survey were completely covered by these clouds and shadows. The 29th June QuickBird image was cloud free since no clouds or shadows were detected visually. ENVI v4.4 was used to geo-correct all satellite images including QuickBird, ASTER and SPOT HRV. The manual method of geo-correction was used with the available ground control points (27 fixed points). These GCPs were used on the uncorrected image to link it to these points. The 27 points nearly covered the whole scene, but it seems that the number of points was not enough. Thereafter, the method of image to image correction was used as the second QuickBird image was geo-corrected by infoterra (up to 14-meter RMSE). This routine was used for 100 points on both images until the whole image was covered and gave better results in comparison to the manual method. The transformed image was checked with the geo-corrected image and they gave approximately similar locations for each fixed point.

**Atmospheric corrections**

The main aim of atmospheric correction is to remove the effects of the atmosphere to make sure that the radiance reflected back to the sensor is the same as the radiance that would be observed at the surface by the same sensor. There are many techniques for atmospheric correction ranging from very simple methods to complex computer models. Ideally the atmospheric correction would correct the surface radiance to percentage reflectance, and thus any subsequent calibration would have greater generic value. However, the simplest method which only accounts for the influence of atmosphere on the radiance value is the dark pixel method, which does not need any additional atmospheric data. Due to the lack of information regarding the atmosphere it seems that the dark pixel is suitable to correct the images used for this research. Also, many researchers used the dark pixel method to atmospherically correct satellite imagery (Hadjimitsis and Clayton 2004, Wu, *et al*., 2005, Tyler *et al*., 2006). For example, Wu, *et al*. (2005) mentioned that the DOS (Dark Object Subtraction) technique was effective for the visible bands and produced $\rho_\lambda$ with the root mean square error (RMSE) of less than 0.01. In addition, Hadjimitsis and Clayton (2004) compared some techniques for atmospheric correction and reported that from an operational point of view the dark pixel method (which derives its input parameters from the image itself and is relatively easy to implement) is to be preferred over more sophisticated techniques that require the acquisition of atmospheric or meteorological data.

The dark pixel method is based on the assumption that there are some points on each satellite image, which are black and the reflectance from these points is nearly similar. However, the disadvantage of this approach is that the derived image is specific for that image and is difficult to apply more generally. All images in this research project were atmospherically corrected using the dark pixel method (dark pixel subtraction) in ENVI v4.4. The FLAASH module was also applied to correct SPOT HRV and QuickBird images, but the resulting images did not give useful results to apply for detecting stress in both wheat and maize.

A further attempt to deduce reflectance from satellite imagery by regression against *in situ* spectra is described in appendix D. However, the temporal difference between *in*

*situ* hyperspectral and satellite data acquisition proved problematic and no successful systematic correction could be established.

**Image classification**

The capability of remotely sensed data as a useful tool in precision agriculture was explored firstly by identifying different crops in satellite images. Prior to applying classification algorithms, images were geo-corrected, geo-referenced to the standard summer scene (the 29th June QuickBird image) and atmospherically corrected. For image classification it is sometimes important to group image pixels into different classes. It is defined as the process of grouping image pixels into classes that show similar spectral and/or textural values and assigning them to meaningful information classes. Fassanacht *et al*. (1997) divided image classification of remotely sensed data into two categories including unsupervised and supervised classifications. Both unsupervised and supervised classification algorithms were examined in this research including Maximum Likelihood (MLC), Minimum Distance (MDC) and k-means classification. MLC and MDC algorithms were chosen because they are commonly used for classifying vegetation (Shanmugam *et al*., 2006). Image classification was performed using ENVI v.4.4 (ENVI, 2003).

*Unsupervised classification*

Unsupervised classification algorithms were chosen because they do not need much information about the image being studied in terms of image features since the information classes are determined statistically by putting them in clusters by natural groupings of spectral values in the dataset. Bachmann *et al*. (2002) defined unsupervised classification as a way of assessing the spectral clusters within a dataset and determining specific areas that may overlap spectrally with others. The only specifications of the unsupervised classifications are the number of desired classes and thresholds, the number of iteration to perform and the class convergence. The most commonly used unsupervised classifications are k-means and ISODATA.

Isodata classification calculates class means evenly distributed in the data space and then iteratively clusters the remaining pixels using minimum distance techniques. In this techniques all pixels are classified to the nearest class unless a standard deviation

or distance threshold is specified, in which case some pixels may be unclassified if they do not meet the selected criteria.

K-means unsupervised classification calculates initial class means evenly distributed in the data space, and then iteratively clusters the pixels into the nearest class using a minimum distance technique. Each iteration recalculates class means and reclassifies pixels with respect to the new means. In this case all pixels are classified to the nearest class unless a standard deviation or distance threshold is specified.

*Supervised classification*

Unlike unsupervised classifiers, supervised classification needs some data to be collected for the area of interest to create spectral signature data from the imagery or import spectral signature data from laboratory or field measurements. Supervised classification depends on the collection of non-contiguous pixels may provide higher variance than polygonal pixel collection and avoid the associated autocorrelation effects, although it may not be spectrally broad enough to convey specified classes accurately. The most commonly used supervised classifications are Maximum Likelihood classification (MLC) and Minimum Distance (MDC) algorithms so they were examined in this research project. MLC assumes that the statistics for each class in each band are normally distributed and calculates the probability that a given pixel belongs to a specific class. Each pixel is assigned to the class that has the highest probability. MDC uses the mean vectors of each endmember and calculates the Euclidean distance from each unknown pixel to the mean vector for each class. All pixels are classified to the nearest class unless a standard deviation or distance threshold is specified.

## 6.3 Using *in situ* hyperspectral measurements to detect stress in wheat and maize crops

### 6.3.1 Wheat

**Aboveground biomass**

Where possible the aboveground biomass samples were collected from three locations within each field immediately after collecting the *in situ* reflectance data. The correlation coefficient for the relationship between twelve different broad band spectral vegetation indices and the measured aboveground biomass is detailed in Tables 6.2-6.4 for different study sites. Figure 6.5 shows the fields sampled within the two study sites at Hewaihy and Kahr. It is shown from the figure that some fields of the *in situ* hyperspectral survey were covered by clouds (33% cloud cover) and the associated shadows. This affected the relationship between the *in situ* hypespectral and satellite data. The results demonstrate that the dataset collected from the first study site (Kahr) showed strong correlations between most of the tested broad band indices and the measured aboveground biomass on different dates. It is noted that the majority of broad band vegetation indices had significant correlations with the measured aboveground biomass on all measuring dates of the *in situ* hyperspectral survey. The strongest correlation was recorded with NDVI, SAVI, IPVI and SLAVI on 11$^{th}$ March ($r = 0.79$), with NDVI, SAVI, SI and SLAVI on 19$^{th}$ March ($r = \pm 0.75$) and recorded with OSAVI on 27$^{th}$ March ($r = 0.83$). There was no significant correlations between VI1 and the measured biomass on two dates out of three collected from that study site. These findings concur with the results obtained from the greenhouse experiments. RVI gave higher correlations with the measured aboveground biomass, which is useful for using high spatial resolution satellite imagery with limited spectral resolution such as QuickBird (4 bands).

The results obtained from the dataset collected from the Hewaihy site are detailed in Table 6.3. The coefficient of correlation between the measured biomass and different broad band indices was non-significant for the majority of cases and this may be attributed to the variation in weather conditions throughout the day during measuring reflectance. Also, plants can not benefit equally from the application of different fertilizers. The decrease in the relationship may also be a result of the small difference in plant health within this site. The strongest correlation was recorded with RVI on

28th March (r = 0.51) and NDVI, SLAVI and IPVI on 12th March (r = 0.49). As expected VI1 produced very poor correlations with the measured aboveground biomass obtained from both 12th and 28th March.

The dataset collected from the third site (Bangar), which is nearly 20 km from the first site represents an area newly reclaimed from the desert. The irrigation system was designed initially as sprinkler irrigation, but farmers changed the system gradually to flood irrigation and consequently the crop water requirement increased. The results collected from the one-day survey at this site showed that most of the tested broad band indices significantly correlated with the measured aboveground biomass. The strongest correlation was recorded with RDVI (r = 0.85). Also, RVI and SR gave high significant correlations with the measured biomass. It is therefore noticeable that both NDVI and RVI are good indicators for predicting aboveground biomass, which as mentioned above useful when using high spatial resolution satellite imagery such as QuickBird, ASTER and SPOT HRV.

The strong correlations between different broad band vegetation indices and the measured aboveground biomass provide evidence that these indices are sensitive indicators to changes in the physiological status of wheat. Therefore, these indices can be used to estimate crop biomass and consequently a rough estimate of crop grain yield, which is closely related to aboveground biomass. The vegetation indices that produce low correlations with the measured biomass may be sensitive to other crop traits and therefore they should be examined to detect other crop parameters. For example, lignin and cellulose were not included in this research, but could be linked to those vegetation indices.

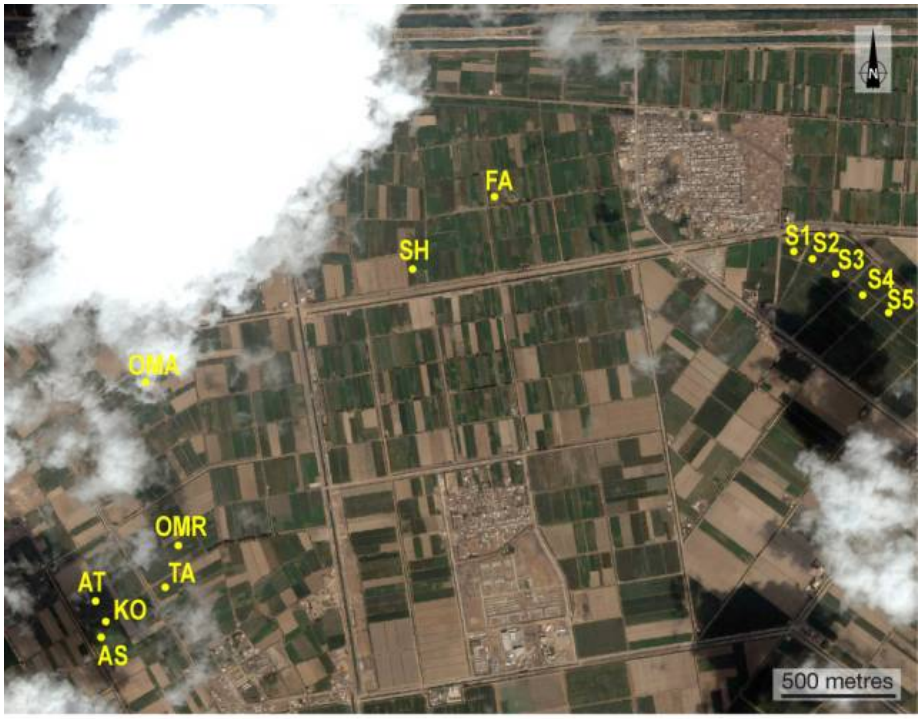


**Figure 6-5** QuickBird image acquired on 7th April 2007 showing different fields at the Hewaihy and Kahr sites south-west Alexandria, Egypt.

**Table 6-2** Coefficient of correlation for the relationship between different broad band spectral vegetation indices derived from *in situ* survey and Egyptian wheat properties collected in March 2007 at the Kahr site, south-west Alexandria, Egypt. Highlighted values are significant (P<0.05) and bold values are the strongest correlation values.

| Date | Vegetation index | Crop properties | | | |
|---|---|---|---|---|---|
| | | Chlorophyll (µg $cm^{-2}$) | Biomass (kg $m^{-2}$) | Height (m) | LAI |
| 11 March | NDVI | 0.69 | **0.79** | -0.87 | 0.73 |
| | RVI | **0.73** | 0.76 | -0.86 | **0.79** |
| | SAVI | 0.65 | **0.79** | -0.86 | 0.68 |
| | $GNDVI_{br}$ | 0.66 | 0.70 | -0.81 | 0.73 |
| | DVI | 0.59 | 0.76 | -0.82 | 0.61 |
| | SR | **0.73** | 0.75 | -0.86 | **0.79** |
| | SLAVI | 0.69 | **0.79** | -0.87 | 0.73 |
| | OSAVI | 0.68 | 0.79 | **-0.88** | 0.71 |
| | VI1 | 0.27 | 0.14 | -0.17 | -0.04 |
| | RDVI | 0.74 | 0.78 | **-0.88** | **0.79** |
| | SI | -0.67 | -0.78 | 0.86 | -0.72 |
| | IPVI | 0.69 | **0.79** | -0.87 | 0.73 |
| 19 March | NDVI | 0.84 | **0.75** | 0.86 | 0.71 |
| | RVI | 0.70 | 0.66 | **0.94** | 0.71 |
| | SAVI | **0.87** | 0.72 | 0.79 | 0.66 |
| | $GNDVI_{br}$ | 0.65 | 0.66 | 0.90 | 0.67 |
| | DVI | **0.87** | 0.69 | 0.73 | 0.63 |
| | SR | 0.70 | 0.66 | **0.94** | 0.71 |
| | SLAVI | 0.84 | **0.75** | 0.86 | 0.71 |
| | OSAVI | 0.86 | 0.74 | 0.82 | 0.68 |
| | VI1 | -0.74 | -0.62 | -0.55 | -0.48 |
| | RDVI | 0.74 | 0.69 | 0.93 | **0.72** |
| | SI | -0.85 | **-0.75** | -0.84 | -0.69 |
| | IPVI | 0.84 | **0.75** | 0.86 | 0.71 |
| 27 March | NDVI | 0.76 | 0.82 | 0.85 | 0.72 |
| | RVI | 0.78 | 0.82 | 0.85 | 0.74 |
| | SAVI | 0.79 | 0.78 | 0.69 | 0.51 |
| | $GNDVI_{br}$ | 0.79 | 0.82 | **0.87** | **0.76** |
| | DVI | 0.73 | 0.63 | 0.53 | 0.38 |
| | SR | 0.78 | 0.82 | 0.85 | 0.74 |
| | SLAVI | 0.76 | 0.82 | 0.85 | 0.72 |
| | OSAVI | **0.80** | **0.83** | 0.78 | 0.61 |
| | VI1 | -0.30 | -0.11 | 0.02 | 0.12 |
| | RDVI | 0.77 | 0.82 | 0.85 | 0.74 |
| | SI | -0.75 | -0.82 | -0.84 | -0.72 |
| | IPVI | 0.76 | 0.82 | 0.85 | 0.72 |

**Table 6-3** Coefficient of correlation for the relationship between different broad band spectral vegetation indices derived from *in situ* spectroradiometry survey and wheat crop properties collected in March 2007 at the Hewaihy site, south-west Alexandria, Egypt. Highlighted values are significant (P<0.05) and bold values are the strongest correlation values.

| Date | Vegetation index | Crop properties | | | |
|---|---|---|---|---|---|
| | | Chlorophyll (µg $cm^{-2}$) | Biomass (kg $m^{-2}$) | Height (m) | LAI |
| 12 March | NDVI | **0.52** | **0.49** | 0.47 | 0.42 |
| | RVI | 0.49 | 0.46 | **0.51** | 0.35 |
| | SAVI | 0.35 | 0.45 | 0.36 | 0.40 |
| | $GNDVI_{br}$ | 0.46 | 0.46 | 0.43 | 0.41 |
| | DVI | 0.27 | 0.43 | 0.31 | 0.38 |
| | SR | 0.49 | 0.46 | 0.50 | 0.35 |
| | SLAVI | **0.52** | **0.49** | 0.47 | 0.42 |
| | OSAVI | 0.42 | 0.47 | 0.41 | 0.41 |
| | VI1 | -0.18 | -0.43 | -0.26 | -0.37 |
| | RDVI | 0.50 | 0.47 | 0.50 | 0.37 |
| | SI | -0.51 | -0.48 | -0.45 | -0.42 |
| | IPVI | **0.52** | **0.49** | 0.47 | 0.42 |
| 28 March | NDVI | 0.45 | 0.39 | 0.81 | 0.70 |
| | RVI | **0.69** | **0.51** | 0.81 | 0.69 |
| | SAVI | 0.55 | 0.45 | 0.80 | **0.73** |
| | $GNDVI_{br}$ | 0.60 | 0.46 | **0.83** | 0.70 |
| | DVI | 0.62 | 0.49 | 0.77 | 0.72 |
| | SR | **0.69** | **0.51** | 0.81 | 0.69 |
| | SLAVI | 0.45 | 0.39 | 0.81 | 0.70 |
| | OSAVI | 0.51 | 0.43 | 0.82 | 0.72 |
| | VI1 | -0.68 | -0.48 | -0.44 | -0.49 |
| | RDVI | 0.62 | 0.49 | **0.83** | 0.71 |
| | SI | -0.40 | -0.35 | -0.79 | -0.69 |
| | IPVI | 0.45 | 0.39 | 0.81 | 0.70 |

**Table 6-4** Coefficient of correlation for the relationship between different broad band spectral vegetation indices derived from *in situ* spectroradiometry survey and wheat crop properties collected in March 2007 at the Bangar site, south-west Alexandria, Egypt. Highlighted values are significant (P<0.05) and bold values are the strongest correlation values.

| Date | Vegetation index | Crop properties | | | |
|---|---|---|---|---|---|
| | | Chlorophyll (µg $cm^{-2}$) | Biomass (kg $m^{-2}$) | Height (m) | Chlorophyll (µg $cm^{-2}$) |
| 15 March | NDVI | 0.91 | 0.81 | **0.66** | 0.85 |
| | RVI | 0.72 | 0.83 | 0.61 | **0.94** |
| | SAVI | 0.84 | -0.39 | 0.12 | -0.35 |
| | $GNDVI_{br}$ | 0.88 | 0.78 | 0.50 | 0.80 |
| | DVI | -0.17 | -0.01 | 0.12 | 0.13 |
| | SR | 0.72 | 0.83 | 0.61 | **0.94** |
| | SLAVI | 0.91 | 0.82 | **0.66** | 0.85 |
| | OSAVI | 0.88 | 0.82 | 0.60 | 0.87 |
| | VI1 | -0.55 | -0.64 | -0.21 | -0.75 |
| | RDVI | 0.80 | **0.85** | 0.64 | **0.94** |
| | SI | **-0.93** | -0.78 | -0.63 | -0.79 |
| | IPVI | 0.91 | 0.82 | **0.66** | 0.85 |

**Leaf area index (LAI)**

LAI was measured for each field at three different locations within the same field. The coefficients of correlation for the relationship between the measured LAI and different broad band vegetation indices are detailed in Tables 6.2-6.4 for the three different sites. The results for the first site demonstrate that most of the tested broad band indices derived from *in situ* spectroradiometry exhibited strongly significant correlations with the measured LAI. VI1 is the only spectral index which gave no significant correlations with the measured LAI for most datasets. RVI, SR, RDVI and $GNDVI_{br}$ gave the strongest correlations on 11$^{th}$, 19$^{th}$, and 27$^{th}$ March ($r > 0.70$). Additionally, NDVI always gave a highly significant correlation with LAI.

The coefficients of correlation for the relationship between different indices and the measured LAI at the Hewaihy site are detailed in Table 6.3. The results demonstrate that for the dataset collected on 12$^{th}$ March, none of the tested broad band indices gave significant correlations with the measured LAI since the coefficient of correlation ranged between -0.37 and 0.42. In the 28$^{th}$ March dataset, all tested broad band indices gave significant correlations with the measured LAI with the strongest correlation recorded with SAVI ($r = 0.73$). NDVI, OSAVI and RDVI also produced high significant correlations with the measured LAI ($r \geq 0.70$). The lack of strong correlations obtained from the 12$^{th}$ March dataset may be explained as a result of the small difference in crop properties or wheat is a tolerant crop to different stressors such as moisture and salinity.

The results for the Bangar site (Table 6.4) showed strong correlations between the majority of the tested indices and the measured LAI. The strongest correlation was recorded with RVI, RDVI and SR ($r = 0.94$). It is evident from the results of the three study sites that VI1 produced non-significant correlations with the measured LAI. Additionally, RVI, SR and RDVI are good indicators for predicting LAI on most measuring dates of the hyperspectral survey undertaken in the three study sites. These results concur with the results obtained from the greenhouse experiments.

**Plant height**

The correlation coefficient between different broad band indices and the measured plant height from the Hewaihy site on 12th March was not highly correlated (Table 6.3). This may be attributed to weather conditions during measuring reflectance. Moreover, the difference in plant height at different locations was rather small. Just three indices gave significant correlation with the measured plant height ($r \geq 0.50$). It was noted that this dataset did not show high correlations between different indices and the measured crop properties and the lack of strong correlation may be attributed to the small difference in these properties at different sites within this area. The correlation coefficient for the dataset collected on 28th March showed highly significant relationships between the majority of broad band indices and the measured plant height with the strongest correlation recorded with both $GNDVI_{br}$ and RDVI ($r = 0.83$). OSAVI, RVI and NDVI produced highly significant correlations ($r = 0.81$-$0.82$) with the measured plant height. At the Bangar site most vegetation indices had significant correlations with the measured plant height with the strongest correlation recorded with NDVI, IPVI and SLAVI ($r = 0.66$).

**Chlorophyll concentration**

Twenty apical leaves were sampled from each field and the SPAD chlorophyll meter was used to estimate relative chlorophyll concentration in the lab (Faculty of Agriculture, University of Alexandria, Egypt). Leaf samples were collected on 29th March following the hyperspectral survey of 27th and 28th at the Kahr and Hewaihy sites. The red edge position (REP) was estimated from *in situ* spectra collected from different sites. REP and the measured chlorophyll concentration data are detailed in Table 6.5. The coefficient of correlation for the relationship between REP and the chlorophyll concentration was calculated. A highly significant correlation between REP and the chlorophyll concentration of wheat was noticed in all datasets ($r = 0.83$), which concur with the results obtained from the greenhouse experiments. The chlorophyll concentration was determined just once during the field work visit because of the availability of the SPAD meter. The results showed that in stressed fields, REP tends to be at shorter wavelengths and at longer wavelength in healthy fields. The chlorophyll concentration was not determined at the third study site because the SPAD meter was not available. The regression analysis was performed to

determine a regression equation for predicting chlorophyll concentration using REP data as follows:

**Chlorophyll concentration = 0.992 REP-681.5**

**Table 6-5** The measured chlorophyll concentration of Egyptian wheat leaves and REP derived from the spectra collected from the same fields during field work conducted in March 2007 at different study sites south-west Alexandria, Egypt.

| site | R1 | | R2 | | R3 | |
|---|---|---|---|---|---|---|
| | Ch | RP | Ch | RP | Ch | RP |
| Salah1 | 41.3 | 725.1 | 40.9 | 721.9 | 41.1 | 722.9 |
| Salah2 | 49.2 | 729 | 46.6 | 728.9 | 47.6 | 728.6 |
| Mehlap | 42.9 | 732.4 | 44 | 731.8 | 40.9 | 731.7 |
| Atef | 46.7 | 732.5 | 45.3 | 733.4 | 43.5 | 732.5 |
| Omara | 39.8 | 724.2 | 38.2 | 721 | 39 | 724 |
| Fathy | 26.7 | 719.7 | 29.5 | 719.7 | 30.1 | 720 |
| Taha | 32.0 | 721.6 | 28.4 | 722.5 | 30.2 | 719 |
| Omran | 36.9 | 726.2 | 34.7 | 724.9 | 36.2 | 726.6 |
| Shaaban | 46.5 | 734.1 | 45.4 | 731.2 | 43.45 | 735 |
| Kosairy | 45.8 | 732.2 | 45.2 | 731.5 | 43.8 | 733.2 |
| Ashraf | 48.01 | 734.0 | 47.8 | 734.5 | 45.4 | 733.8 |
| Saber | 43.4 | 732.1 | 41.1 | 730.5 | 43.1 | 731.5 |
| **r** | | | **0.83** | | | |

Besides REP as an indicator for the chlorophyll concentration, the coefficient of correlation for the relationship between different broad band vegetation indices and the measured chlorophyll content was calculated and is detailed in Tables 6.2-6.4. At the Kahr site most vegetation indices had significant correlations with chlorophyll concentration in all datasets with the strongest correlation recorded with RVI and SR (r = 0.73) in the 11$^{th}$ dataset, with SAVI and DVI (r = 0.87) in the 19$^{th}$ dataset, and with OSAVI (r = 0.80) in the 27$^{th}$ dataset. At the Hewaihy site most vegetation indices produced significant correlations with the measured chlorophyll particularly in the 28$^{th}$ dataset. The strongest correlation was recorded with RVI and SR (r = 0.69) in 28$^{th}$ March. At the Bangar site similar results were observed as the majority of vegetation indices produced high significant correlations with the strongest recorded with SI (r = -0.93). Generally, REP gives high correlations with the measured chlorophyll concentration compared with the results obtained from different sites on different dates since some vegetation indices give high correlations on a specific day and very low correlations on others such as VI1.

The reflectance measurements obtained from these three sites were also investigated by plotting reflectance against wavelength. The average of reflectance values from each field was calculated and the dataset for each day was plotted. Figure 6.6 shows the difference between spectral responses from five different fields on 11$^{th}$ 19$^{th}$ and 27$^{th}$ March 2007. Graph 6.6 (a) shows that the spectral response obtained from the field suffering from salinity stress is different from healthy ones as the reflectance in the green and red regions is always higher than those of healthy fields. The reflectance in the NIR region is always lower than the spectral response from healthy canopies. These findings concur with the results obtained from the greenhouse based experiments.

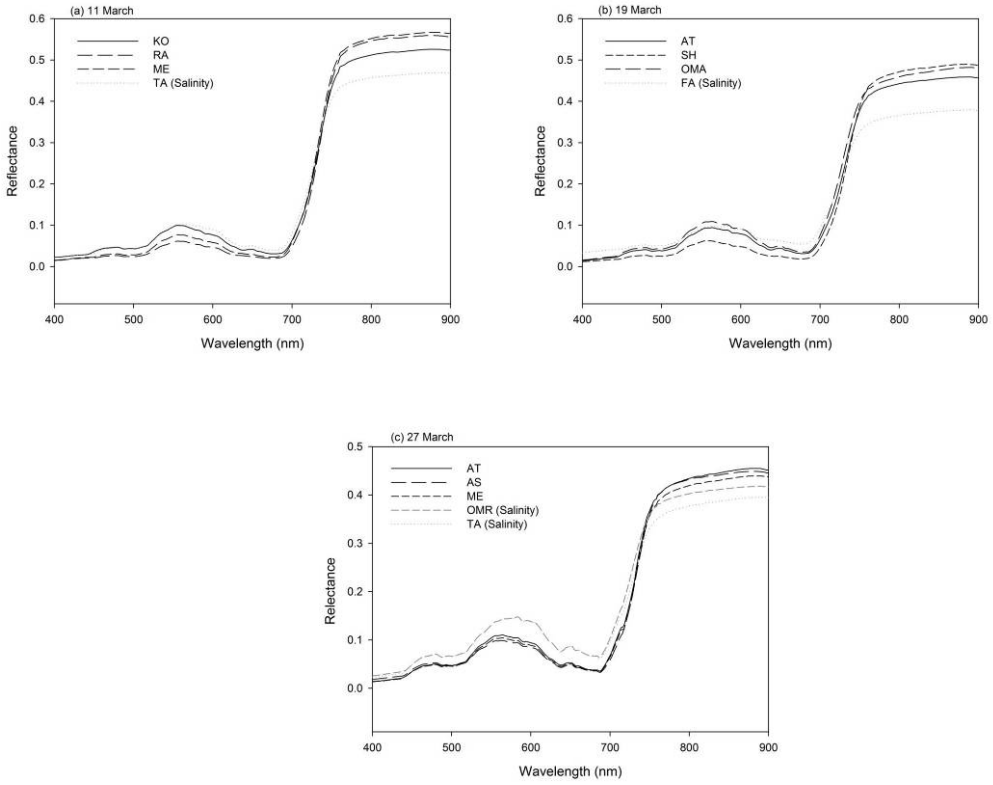


**Figure 6-6** The spectral response measured from different wheat fields at the Kahr site, south-west Alexandria, Egypt on (a) 11, (b) 19 and (c) 27 March 2007 under clear sky conditions.

The results obtained from the data collected on 19$^{th}$ March are depicted in Figure 6.6 (b); it was notable that the results had the same trend of the data collected on 11 March as the reflectance measured from stressed canopies has high reflectance in the visible region of the spectrum and over REP region exhibited low difference

especially with using the average of reflectance from each field (decrease the variations within the same field). The difference between reflectance from stressed fields and healthy fields is higher in the NIR region. The slight difference between different healthy fields may be attributed to differences in chlorophyll concentration, biomass, plant height or leaf area, which may be resulted from different sowing dates. The 27$^{th}$ March dataset depicted in Figure 6.6 (c) which shows that the spectral response from the three healthy fields and two stressed fields have similar pattern.

The second study site was nearly 5 kilometres from the previous one and *in situ* hyperspectral survey was conducted on two days (12 and 28$^{th}$ March 2007). The results obtained from this site are depicted in Figure 6.7. The reflectance from five different fields at the Hewaihy site had the same trend as the other study sites since reflectance from stressed fields was higher in the visible part of the spectrum and lower in the NIR region in comparison to the healthy fields.

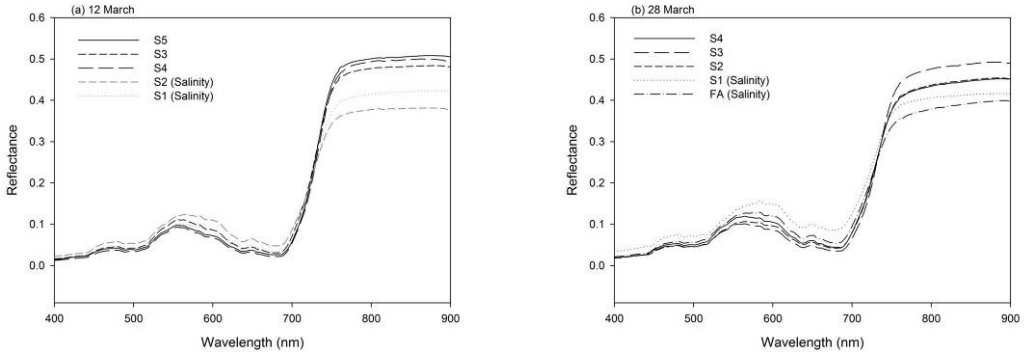


**Figure 6-7** The spectral signature obtained from five different wheat fields at the Hewaihy study site, south-west Alexandria, Egypt on (a) 12 and (b) 28 March 2007 under clear sky conditions.

The *in situ* hyperspectral survey also included a study site 20 kilometres south from the first two sites. It was chosen because of the soil texture (sandy to sandy loam) and because most fields in that area suffer from moisture stress but not salinity stress since irrigation water salinity is less than 1 dS $m^{-1}$. The reason why these fields are suffering from moisture stress is that this site reclaimed two decades ago and the irrigation system was designed initially as sprinkler irrigation, but farmers gradually changed the system to the traditional irrigation method (flood irrigation) and resultantly the amount of irrigation water is insufficient for the total cultivated area.

The spectral response from four different fields at the Bangar site and one more field a way about 10 km from that site representing a wheat field under salinity stress is depicted in Figure 6.8. The spectral response from the only healthy field is different from the other stressed fields. The reflectance pattern approximately had the same pattern as shown in the first two study sites. The high salinity in the field chosen (7 dS $m^{-1}$) greatly affected the response from plant canopies. It is shown that the reflectance obtained from the field under salinity stress is higher than those obtained from moisture stressed and healthy fields, but low reflectance in the NIR range compared with healthy fields.

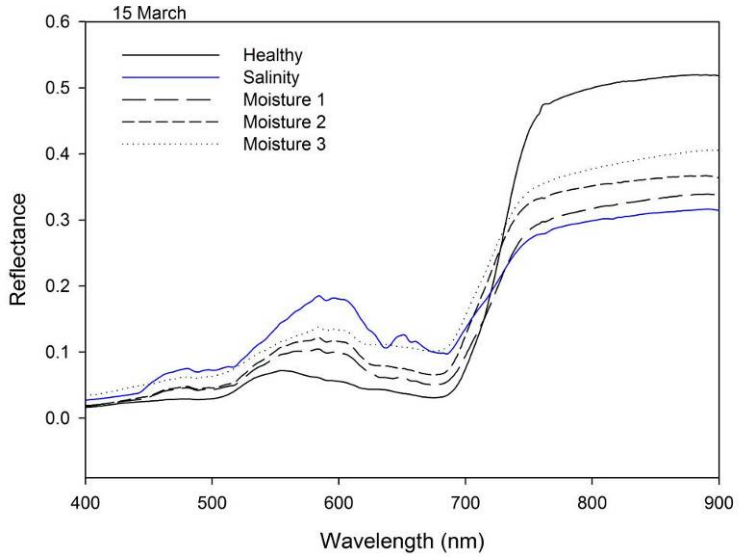


**Figure 6-8** The reflectance measurements obtained from five different wheat fields on 15 March 2007 at the Bangar site, south-west Alexandria, Egypt under clear sky conditions.

## Distinguishing between moisture and salinity induced stress

To distinguish between stressed fields and healthy fields or distinguish moisture induced stress from salinity induced stress, Principle Component Analysis (PCA) was performed on each dataset. Figures 6.9-6.13 show the score plot of the PCA for all datasets collected during *in situ* hyperspectral survey at the three different sites. As illustrated in the first three figures, which represent the first study site, the score plot shows the dissimilarities between healthy fields and fields suffering from moisture and salinity stress. In Figure 6.10 there is some overlap between salinity and moisture induced stress, which was difficult to separate and this may be attributed to the

tolerance of wheat crops to both moisture and salinity stressors. The results depicted in Figure 6.12 shows a gradient between three healthy fields and this may be attributed to the slight difference in plant height, chlorophyll concentration and LAI or aboveground biomass. This may be explained by different sowing dates, soil fertility and drainage system efficiency in each field.

The score plot of the third site's dataset is shown in Figure 6.13. It is noticeable that healthy sites are distinguished from fields suffering from moisture and salinity stress. The clear distinction at this site may be attributed to the high level of stress as the salinity level was on average over 7 dS $m^{-1}$ and moisture induced stress is apparent at this site as a result of changing irrigation system. Also, the nitrogen concentration determined in the soil at this site was low. The results sometimes show some overlap between moisture and salinity induced stress and even between different healthy fields. This may be attributed to the slight difference between healthy fields as a result of different sowing dates and the overlap between different stressors may be attributed to the tolerance of wheat to stress.

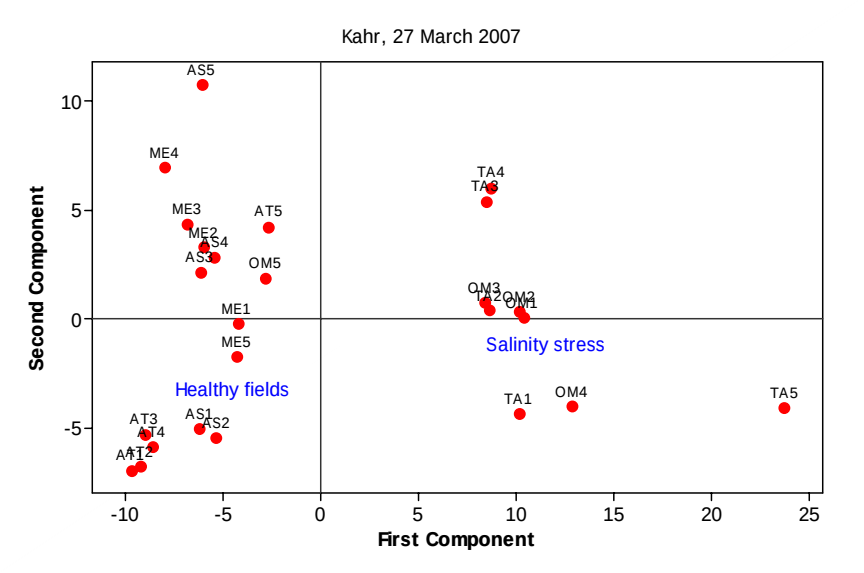


**Figure 6-9** The score plot of PCA for the spectra collected on 27 March 2007 from healthy and salinity induced stressed wheat canopies under clear sky conditions at the Kahr site (n = 20). (Site labels; TA-TAHA; ME-MEHLAP; OM-OMRAN;AS-ASHRAF;AT-ATEF).

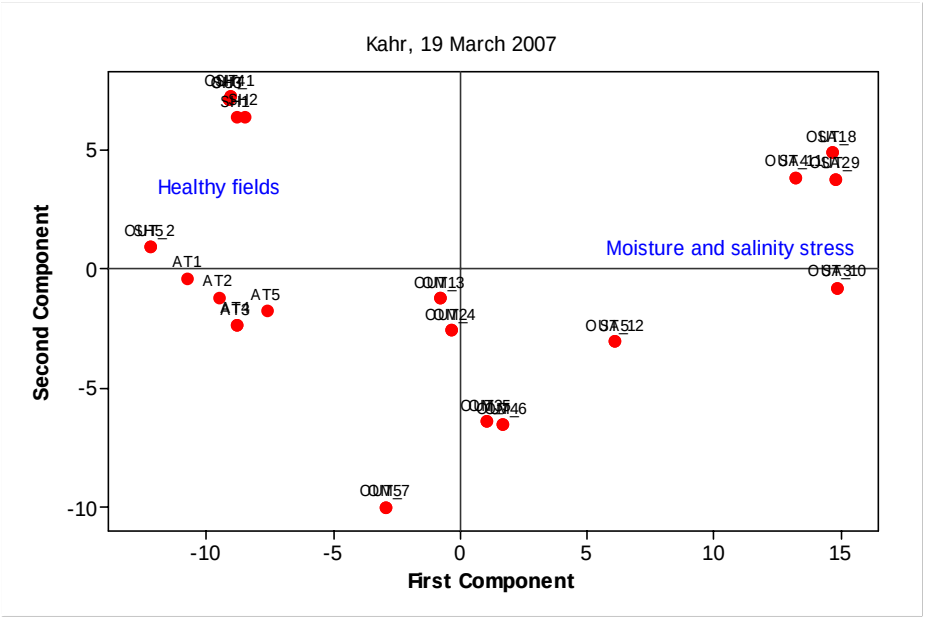


**Figure 6-10** The score plot of the Principle Component Analysis for the spectra collected on 19 March 2007 from healthy, moisture and salinity induced stressed wheat canopies under clear sky conditions at the Kahr site (n = 20). (Site labels; SH-SHAABAN; ME-MEHLAP; OM-OMRAN; OMA-OMARA;SA-SABRY;AT-ATEF).

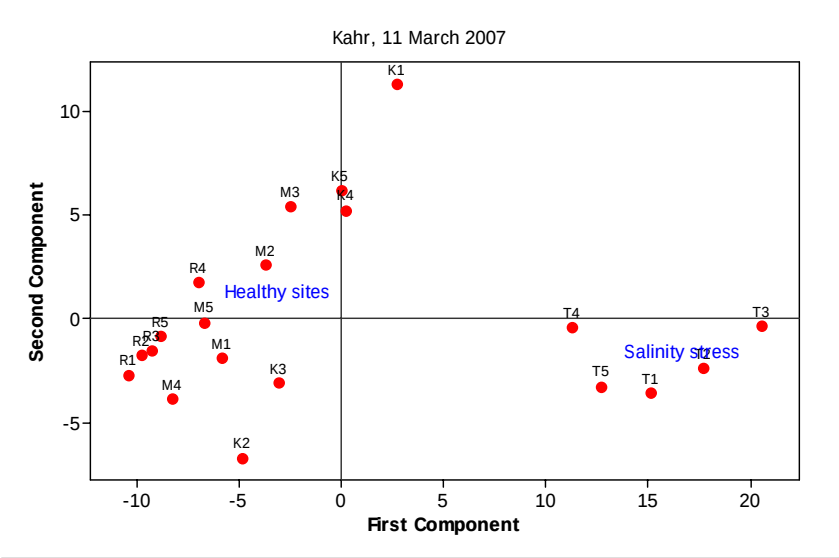


**Figure 6-11** The score plot of the Principle Component Analysis for the spectra collected on 11 March 2007 from healthy and salinity induced stressed wheat canopies under clear sky conditions at the Kahr (n = 20). (Site labels; R-RAMADAN; ME-MEHLAP; K-KOSAIRY;AS-ASHRAF;TA-TAHA).

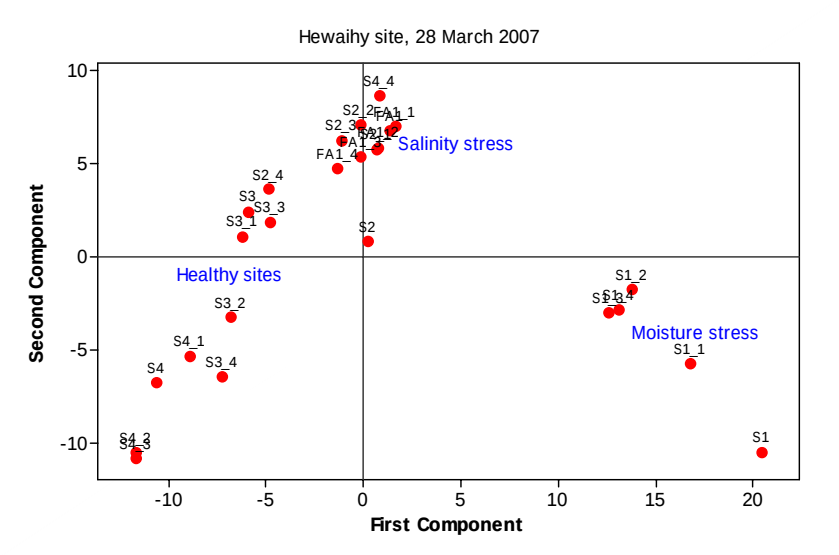


**Figure 6-12** The score plot of the Principle Component Analysis for the spectra collected on 28 March 2007 from healthy, moisture and salinity induced stressed wheat canopies under clear sky conditions at the Hewaihy site (n = 25). (Site labels; S1-ASLAH1;S2-SALAH2;S3-SALAH3;S4-SALAH4; FA-FATHY).

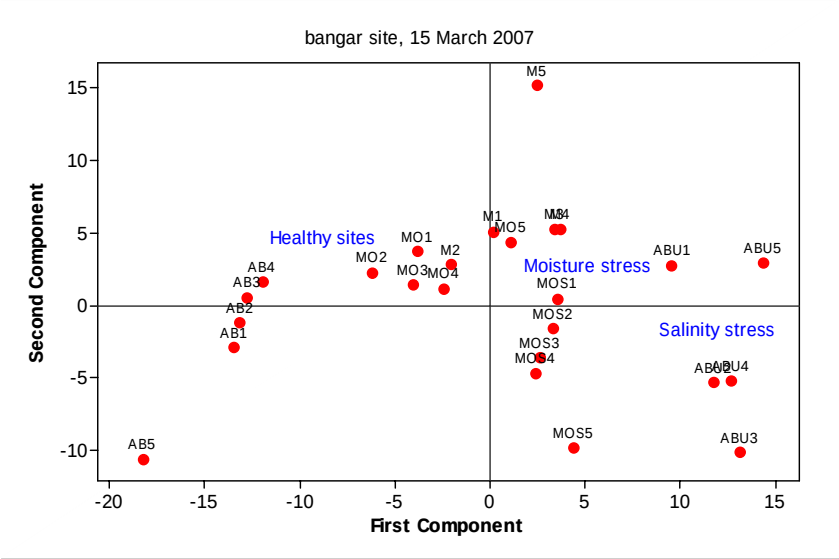


**Figure 6-13** The score plot of the Principle Component Analysis for the spectra collected from healthy and moisture and salinity induced wheat canopies under clear sky conditions in March 2007 (n = 25). (site labels; AB-ABUMASOUD2;ABU-ABUMASOUD1;MO-MOSTAFA1;M2-MOSTAFA2; MOS-MOSTAFA3).

### 6.3.2 Maize

**Aboveground biomass**

As with wheat twelve broad band vegetation indices were calculated from *in situ* hyperspectral survey. The fields within the study area were chosen according to plant health and care was taken to have a stress gradient ranging from very healthy fields to highly stressed fields. Figure 6.14 shows a QuickBird image with different fields within the study area. The correlation coefficient for the relationship between vegetation indices and different biophysical and biochemical properties of maize crops is given in Table 6.6. Strongly significant correlations between different vegetation indices and the measured biophysical and biochemical properties were observed. The 12$^{th}$ July dataset showed that eleven indices out of twelve had highly significant correlations with the measured aboveground biomass. The strongest correlation was recorded with RVI and SR ($r = 0.87$). RDVI and $GNDVI_{br}$ also produced high significant correlations with the measured aboveground biomass ($r > 0.80$).

The 14$^{th}$ July dataset had the same trend as all tested broad band indices produced highly significant correlations with biomass ($r > 0.90$) except VI1 ($r = -0.44$). The strongest correlation was recorded with RDVI ($r = 0.97$). SR, SAVI and RVI also produced very high correlations with the measured biomass ($r \geq 0.95$). As expected VI1 had the poorest correlations with the biomass ($r = -0.44$).

The 15$^{th}$ July data set showed also strong correlations between different vegetation indices and the measured biomass. The strongest correlation was recorded with RVI, SR and RDVI ($r = 0.98$). NDVI, $GNDVI_{br}$, SLAVI and IPVI also produced high significant correlations with the measured aboveground biomass ($r = 0.96$).

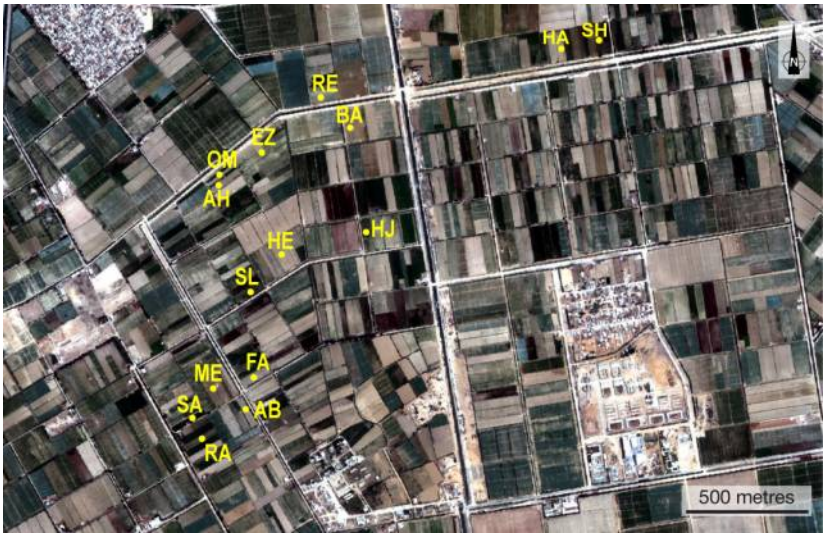


**Figure 6-14** QuickBird image showing different fields within the study area south-west Alexandria, Egypt.

To identify the optimum vegetation index, which correlate well with crop properties; data from the three-day *in situ* hyperspectral survey in maize fields was combined. The coefficient of correlation between the tested broad band indices and the measured aboveground biomass is detailed in Table 6.7. The results showed that the strongest correlation was recorded with RVI, SR and RDVI (r = 0.95) and as expected VI1 produced non-significant correlation (r = -0.37). Figure 6.15 shows the relationship between RVI and the measured biomass for the combined dataset. A strong significant linear relationship between aboveground biomass and RVI ($R^2$=0.90; p = 0.000) is shown in the figure.

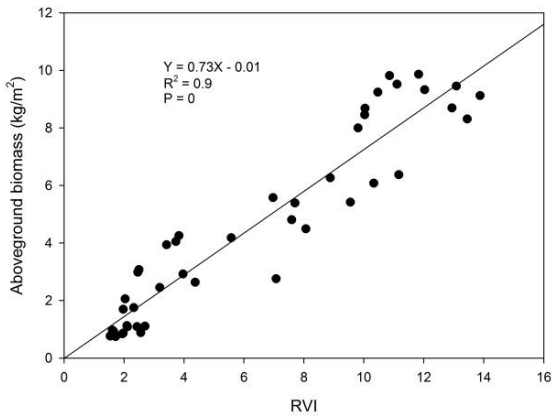


**Figure 6-15** The relationship between RVI derived from *in situ* hyperspectral survey and the measured aboveground biomass of maize collected in Egypt in July 2007 (n = 45).

**Table 6-6** Coefficient of correlation for the relationship between different broad band spectral vegetation indices and maize properties over the three-day hyperspectral survey (12-15 July 2007) in south-west Alexandria, Egypt. Highlighted values are significant (P<0.05) and bold values are the strongest correlation values.

| Date | Vegetation index | Crop properties | | | |
|---|---|---|---|---|---|
| | | Chlorophyll (µg $cm^{-2}$) | Biomass (kg $m^{-2}$) | Height (m) | LAI |
| 12 July | NDVI | 0.81 | 0.76 | 0.85 | 0.80 |
| | RVI | 0.67 | **0.87** | **0.91** | **0.85** |
| | SAVI | 0.79 | 0.72 | 0.83 | 0.76 |
| | $GNDVI_{br}$ | 0.80 | 0.81 | 0.90 | 0.83 |
| | DVI | 0.77 | 0.65 | 0.79 | 0.69 |
| | SR | 0.67 | **0.87** | **0.91** | **0.85** |
| | SLAVI | 0.78 | 0.77 | 0.84 | 0.81 |
| | OSAVI | 0.80 | 0.74 | 0.84 | 0.78 |
| | VI1 | 0.46 | 0.33 | 0.25 | 0.42 |
| | RDVI | 0.71 | 0.84 | 0.90 | 0.84 |
| | SI | **-0.83** | -0.63 | -0.76 | -0.70 |
| | IPVI | 0.78 | 0.77 | 0.84 | 0.81 |
| 14 July | NDVI | 0.89 | 0.94 | 0.93 | 0.92 |
| | RVI | **0.95** | 0.96 | **0.98** | 0.94 |
| | SAVI | 0.89 | 0.96 | 0.93 | **0.95** |
| | $GNDVI_{br}$ | 0.90 | 0.94 | 0.92 | 0.92 |
| | DVI | 0.85 | 0.94 | 0.88 | 0.94 |
| | SR | **0.95** | 0.96 | **0.98** | 0.94 |
| | SLAVI | 0.90 | 0.95 | 0.94 | 0.93 |
| | OSAVI | 0.89 | 0.95 | 0.93 | 0.94 |
| | VI1 | -0.37 | -0.44 | -0.39 | -0.50 |
| | RDVI | 0.94 | **0.97** | **0.98** | 0.94 |
| | SI | -0.76 | -0.84 | -0.82 | -0.83 |
| | IPVI | 0.90 | 0.95 | 0.94 | 0.93 |
| 15 July | NDVI | **0.97** | 0.96 | 0.97 | **0.98** |
| | RVI | 0.94 | **0.98** | **0.98** | **0.98** |
| | SAVI | **0.97** | 0.94 | 0.95 | 0.97 |
| | $GNDVI_{br}$ | **0.97** | 0.96 | 0.97 | **0.98** |
| | DVI | **0.97** | 0.90 | 0.92 | 0.95 |
| | SR | 0.94 | **0.98** | **0.98** | **0.98** |
| | SLAVI | **0.97** | 0.96 | 0.97 | **0.98** |
| | OSAVI | **0.97** | 0.95 | 0.96 | 0.97 |
| | VI1 | -0.82 | -0.61 | -0.66 | -0.73 |
| | RDVI | 0.95 | **0.98** | **0.98** | **0.98** |
| | SI | -0.96 | -0.95 | -0.96 | -0.97 |
| | IPVI | **0.97** | 0.96 | 0.97 | **0.98** |

**Table 6-7** Coefficient of correlation for the relationship between different broad band spectral vegetation indices and the combined dataset of different maize properties collected over the three-day hyperspectral survey (12-15 July 2007) in south-west Alexandria, Egypt. Highlighted values are significant (P<0.05) and bold values are the strongest correlation values.

| Date | Vegetation index | Crop properties | | | |
|---|---|---|---|---|---|
| | | Chlorophyll (µg $cm^{-2}$) | Biomass (kg $m^{-2}$) | Height (m) | LAI |
| 12-15 July | NDVI | **0.89** | 0.91 | 0.92 | 0.89 |
| | RVI | 0.86 | **0.95** | **0.96** | 0.95 |
| | SAVI | 0.87 | 0.90 | 0.90 | **0.99** |
| | $GNDVI_{br}$ | 0.88 | 0.93 | 0.93 | **0.99** |
| | DVI | 0.80 | 0.86 | 0.84 | 0.91 |
| | SR | 0.86 | **0.95** | **0.96** | 0.94 |
| | SLAVI | **0.89** | 0.91 | 0.92 | -0.95 |
| | OSAVI | 0.88 | 0.91 | 0.91 | -0.44 |
| | VI1 | -0.26 | -0.37 | -0.32 | -0.20 |
| | RDVI | 0.88 | **0.95** | **0.96** | 0.98 |
| | SI | -0.85 | -0.84 | -0.85 | -0.98 |
| | IPVI | **0.89** | 0.91 | 0.92 | -0.44 |

It is evident that maize crop is sensitive to different sources of stress such as salinity and moisture induced stress. The difference in spectral response from stressed canopies and healthy canopies may be attributed to the vegetative parameters, which are functions of many stressors. Additionally, great aboveground biomass eliminates the effects of soil background. Figure 6.16 shows two photographs for a healthy field and another field suffering from salinity stress. The photographs show the difference between plant canopies in both fields, which support the results of good correlations between different vegetation indices and aboveground biomass.

**Figure 6-16** Tow photographs showing the extremes from a very healthy maize field and another field suffering from salinity stress.

**Leaf area index of maize (LAI)**

As shown in Figure 6.16 leaf area of healthy plants completely covers the soil surface and therefore there are no effects from soil background compared with stressed plants. The correlation coefficient for the relationship between the twelve broad band vegetation indices and the measured LAI is detailed in Table 6.6 and 6.7. Vegetation indices demonstrated strong significant correlations with the measured LAI on all measuring dates. The 12$^{th}$ July dataset demonstrated that RVI and SR produced the strongest correlation with LAI (r = 0.85). The 14$^{th}$ July dataset showed that RVI and SR had high significant correlation, but the strongest correlation was recorded with SAVI (r = 0.95). This may be attributed to the advantage of SAVI in reducing the effects of soil background from stressed fields. The strongest correlation obtained from the 15$^{th}$ July dataset was recorded with RVI, NDVI, $GNDVI_{br}$, SR, SLAVI, RDVI and IPVI (r = 0.98). From the combined data it is shown that SAVI and $GNDVI_{br}$ produced the strongest correlation with the measured LAI (r = 0.99). The regression analysis was used to investigate the relationship between $GNDVI_{br}$ and the measured LAI of maize (Figure 6.17). A strong significant relationship between $GNDVI_{br}$ and the measured LAI ($R^2$ = 0.82). In all datasets VI1 produced the poorest to correlate with the measured LAI.

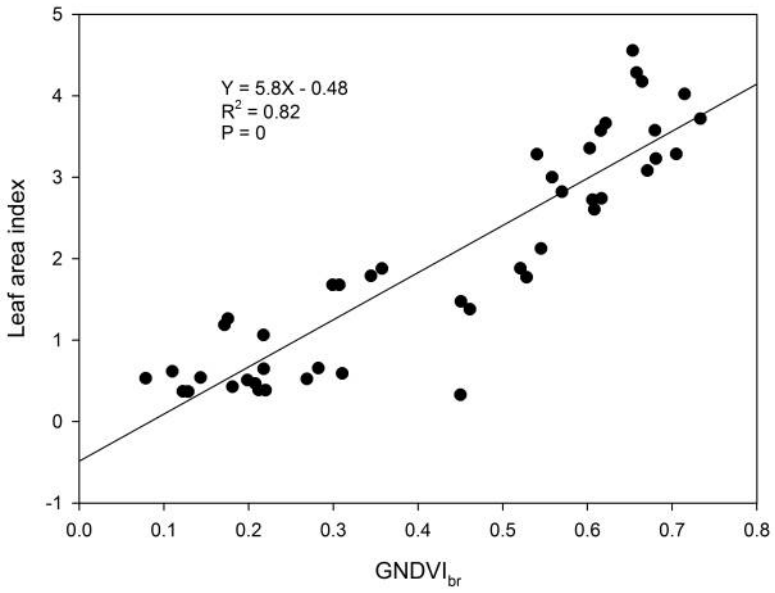


**Figure 6-17** The relationship between $GNDVI_{br}$ derived from *in situ* hyperspectral survey and the measured LAI collected from maize fields in July 2007 (n = 45).

**Plant height**

All vegetation indices demonstrated a highly significant correlation with the measured maize plant height except VI1. RVI and SR had the strongest correlation with the measured plant height on 12$^{th}$ July (r = 0.91). In the 14$^{th}$ and 15$^{th}$ July datasets RVI, SR, and RDVI produced the strongest correlations with the measured plant height (r = 0.98). Interestingly, the results obtained from the combined dataset show similar trends as the three indices produced the strongest correlation with the measured plant height (r = 0.96). The reason for strong correlations between plant height and different indices may have been a result of the large difference in plant height in stressed and healthy fields, which in turn affects the spectral response from plant canopies. Therefore, care was taken to keep constant the distance between the spectroradiometer and soil surface. Additionally, soil background may affect reflectance measurements in stressed fields. The regression analysis was performed on the combined dataset to investigate the relationship between RVI and the measured plant height (Figure 6.18). A strong significant linear relationship between plant height and RVI was observed ($R^2$ = 0.93; p = 0.000).

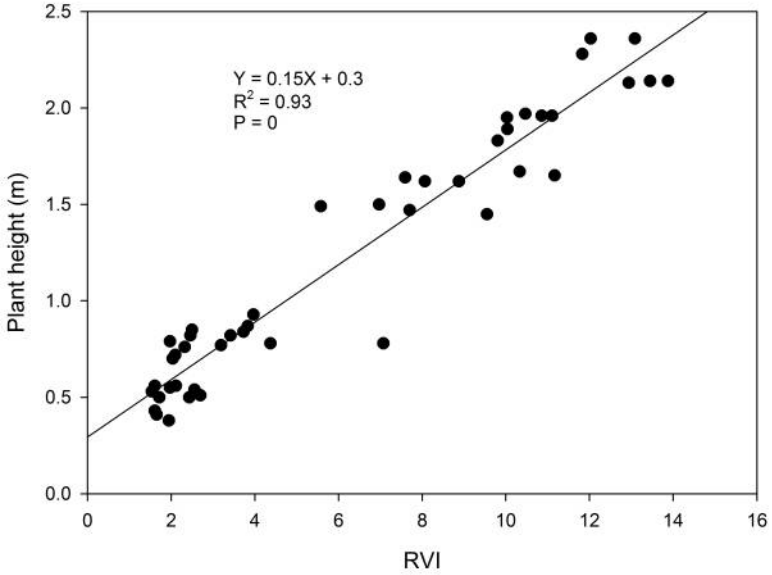


**Figure 6-18** The relationship between RVI derived from *in situ* hyperspectral survey and the measured plant height of maize crops collected in July 2007 in south-west Alexandria, Egypt (n = 45).

## Chlorophyll concentration

Apical leaf samples were collected from each field of the *in situ* hyperspectral survey and the chlorophyll concentration was measured in a lab at Alexandria University, Egypt using SPAD chlorophyll meter. From the hyperspectral survey REP was calculated as an indicator of chlorophyll and other pigments (Table 6.8). The coefficient of correlation for the relationship between REP and the measured chlorophyll concentration was calculated for each dataset and the results showed strong significant correlations between the measured chlorophyll content and REP. The combined dataset was used to assess the relationship between REP and the chlorophyll concentration. A strong correlation was observed between SPAD meter readings and REP (r = 0.80). When maize crop is subjected to moisture and salinity stress, plants try to cope by decreasing the leaf area to decrease the evaporation surface, which therefore affects the photosynthetic rate and consequently the pigment concentration.

**Table 6-8** The measured chlorophyll concentration of maize leaves and the red edge position derived from *in situ* hyperspcetral survey at different sites on 12, 14 and 15 July 2007 during the field work visit in Egypt.

| Date | site | R1 | | R2 | | R3 | |
|---|---|---|---|---|---|---|---|
| | | Ch | REP | Ch | REP | Ch | REP |
| 12 July | Saber | 48.4 | 730.6 | 50.1 | 730.9 | 49.5 | 730.1 |
| | Medhat | 50.7 | 730.6 | 47.7 | 730.4 | 49.9 | 729.5 |
| | Mehlap | 49.4 | 729.4 | 48.2 | 729.2 | 49.6 | 730.0 |
| | Abderahim | 42.16 | 724.6 | 43.25 | 725.4 | 43.1 | 726.1 |
| | Farid | 33.21 | 722.5 | 30.64 | 720.5 | 30.9 | 718 |
| 14 July | Omara | 31.5 | 718.6 | 34.3 | 718.3 | 33.2 | 719.6 |
| | Reda | 49.5 | 729.8 | 48.3 | 730.2 | 52.4 | 730.4 |
| | Eza | 34.4 | 714.3 | 31.6 | 718.9 | 33.3 | 718.3 |
| | Ahmed | 30.3 | 702 | 33.3 | 696.2 | 32.0 | 696.9 |
| | Haj | 48.4 | 728.3 | 48.2 | 730.4 | 47.1 | 729.6 |
| 15 July | Salem | 48.4 | 729.6 | 49.6 | 730.03 | 48.5 | 729.1 |
| | Helmy | 36.2 | 722 | 32.6 | 718.9 | 35.7 | 719.9 |
| | Shetaiwy | 51.0 | 730.6 | 50.6 | 730.7 | 47.6 | 728.7 |
| | Habeeb | 35.1 | 720.8 | 34.2 | 716.8 | 32.3 | 717.5 |
| | Abdelbad | 34.4 | 716.9 | 31.8 | 717.2 | 32.9 | 726.2 |

Ch is the chlorophyll concentration and REP the red edge position

Besides REP, the coefficient of correlation for the relationship between the twelve broad band vegetation indices and the measured chlorophyll concentration was calculated (Table 6.6 and 6.7). The majority of vegetation indices had strongly significant correlations with the measured chlorophyll concentration particularly in

the 15th July dataset (r > 0.80). The strongest correlation was recorded with SI (r = -0.83) on 12th July, RVI and SR (r = 0.95) on 14th July and NDVI, SAVI, $GNDVI_{br}$, DAVI, SLAVI, OSAVI and IPVI (r = 0.97) on 15th July. The combined dataset demonstrated that NDVI, SLAVI and IPVI had the strongest significant correlation with the measured chlorophyll concentration (r = 0.89). Additionally, regression analysis was performed to assess the relationship between NDVI and the measured chlorophyll concentration (Figure 6.19). A significant positive linear relationship between NDVI and the measured chlorophyll concentration ($R^2$ = 0.79; p = 0.000) is shown. NDVI seems to be sensitive indicator for chlorophyll of maize canopies. The results obtained from the combined dataset also showed that VI1 produced non-significant correlations with any maize properties.

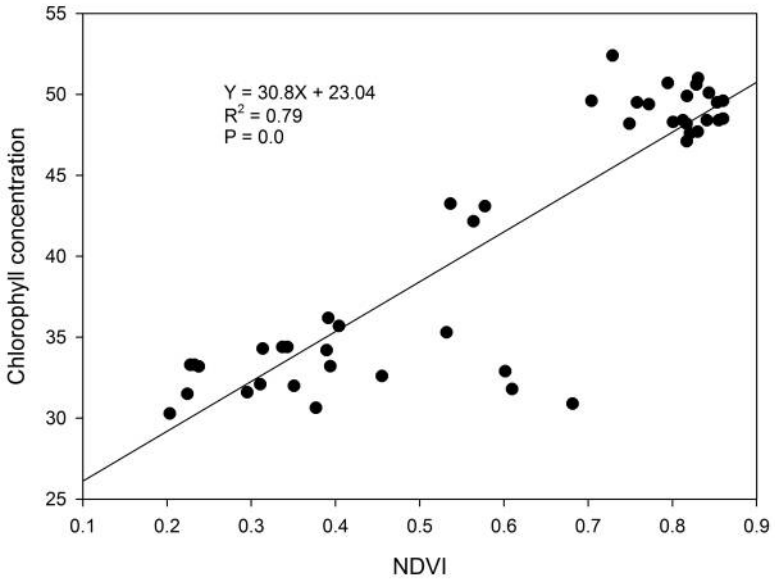


**Figure 6-19** The relationship between NDVI derived from *in situ* hyperspectral survey and the measured chlorophyll concentration collected from maize fields in July 2007 in south-west Alexandria, Egypt (n = 45).

It is evident from the results of the two field visits that most broad band vegetation indices examined in this research had strong correlations with different maize crop properties including aboveground biomass, plant height and LAI, which means the reflectance from plant canopies is a function of changes in plant biochemical and biophysical properties. A strong relationship between chlorophyll concentration and REP confirmed that REP is a good indicator for plant chlorophyll. Besides different

vegetation indices the physiological changes resulting from moisture and salinity induced stress were investigated through plotting reflectance from healthy and stressed fields in the same figures. The individual and combined datasets were used to show differences in reflectance (Figure 6.20).

As expected the results exhibited that the spectral response from maize crops gave better results in comparison to those obtained from wheat fields. This may be attributed primarily to the broader leaves of maize and there is a noticeable decrease in size as a result of both stressors. Furthermore, the high temperature in the summer season increases evapotranspiration from plants and evaporation from soil at the same time and therefore subjects plants to stress more quickly. Like the results obtained from the greenhouse experiments, the reflectance obtained from stressed canopies is higher in the green and red regions of the magnetic spectrum in comparison to reflectance obtained from healthy canopies. However, the reflectance from stressed canopies is lower in the NIR region in comparison to those obtained from healthy canopies.

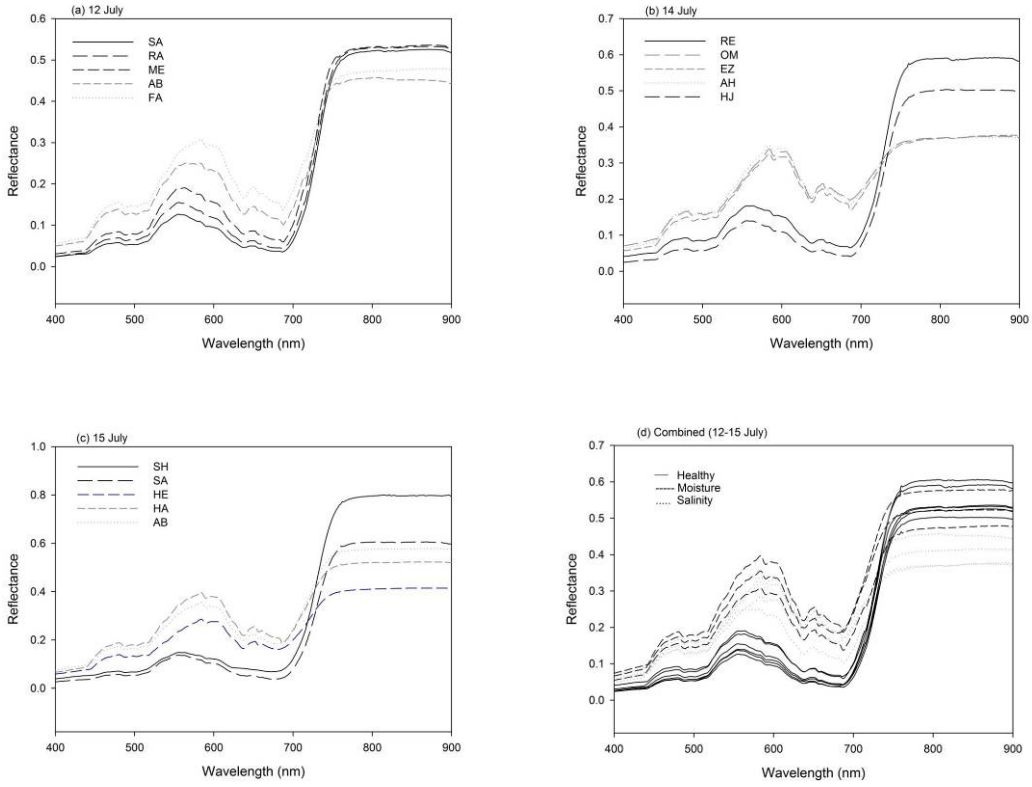


**Figure 6-20** The spectral response collected from different sites of maize crops on (a) 12th July, (b) 14th July, (c) 15th July 2007 and (d) the combined dataset of the three different dates collected under clear sky conditions.

**Distinguishing between moisture and salinity induced stress**

The Principle Component Analysis (PCA) was performed on each dataset of 12th, 14th and 15th July to show dissimilarities between reflectance from healthy and stressed fields. Figures 6.21-6.23 show the score plot of the PCA for each dataset. The 12th dataset showed that the PCA has the ability to distinguish healthy sites from those suffering from moisture and salinity stress. The dissimilarities shown between healthy fields may be a result of slight differences in biochemical and biophysical properties of maize crops. These differences may be attributed to different sowing dates, nitrogen application and moisture stress at specific growth stage. The 14th July dataset comprised one healthy field and three salinity induced fields. It is shown that the healthy field replicates tend to plot in one corner (the bottom left corner) and away from all salinity stressed fields. The 15th July dataset showed that healthy fields tend to plot in one side of the score plot (the right side of the score plot) while the stressed fields are plotted on the left side. PCA showed the ability to separate moisture induced stress from salinity induced stress particularly where large difference between healthy and stressed fields.

The results suggest that, using the technique of remotely sensed data to monitor plant health with broader leaved crops such as maize will enhance the efficiency of this technique. PCA score plots demonstrated that distinguishing between moisture and salinity induced stress is possible especially when plants are subjected to severe stress. The results further showed that distinguishing between moisture and salinity induced stress in maize is highly possible, but in wheat it needs a high stress level since wheat is a tolerant crop and mainly is grown in winter and therefore under low moisture stress. Also, the weather conditions should be considered when comparing both crops in terms of stress as maize is a summer crop and wheat is a winter crop. In this case temperature, light intensity and day length should be considered as effective parameters in plant health and therefore reflectance measurements.

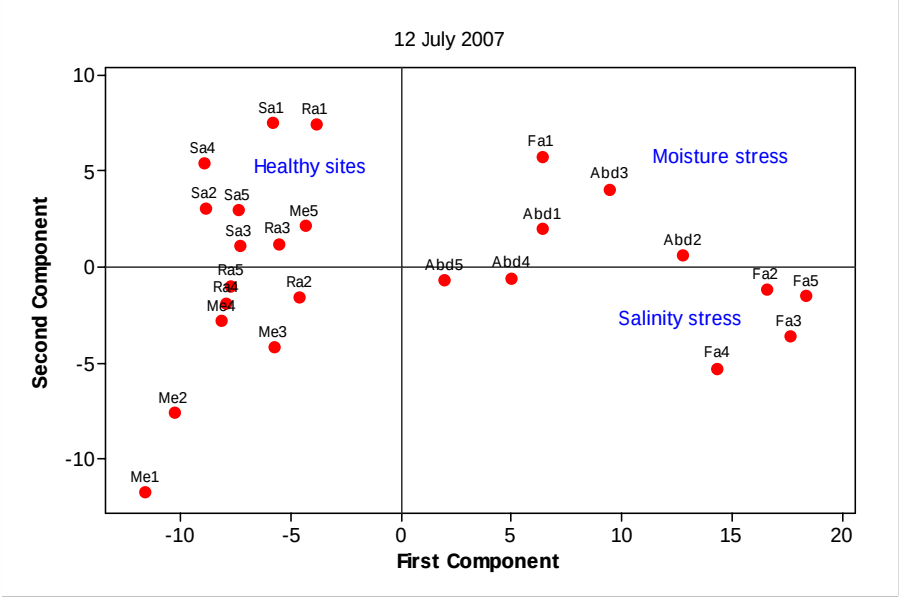


**Figure 6-21** The score plot of the Principle Component Analysis (PCA) for the spectra collected from healthy, moisture and salinity induced stressed maize canopies under clear sky conditions in summer growing season of 2007 in south-west Alexandria, Egypt (n = 25). (Site labels: Sa-Saber; Ra- Ramdan; Fa-Farid; Me-Mehlap; Abd-Abdelrahim).

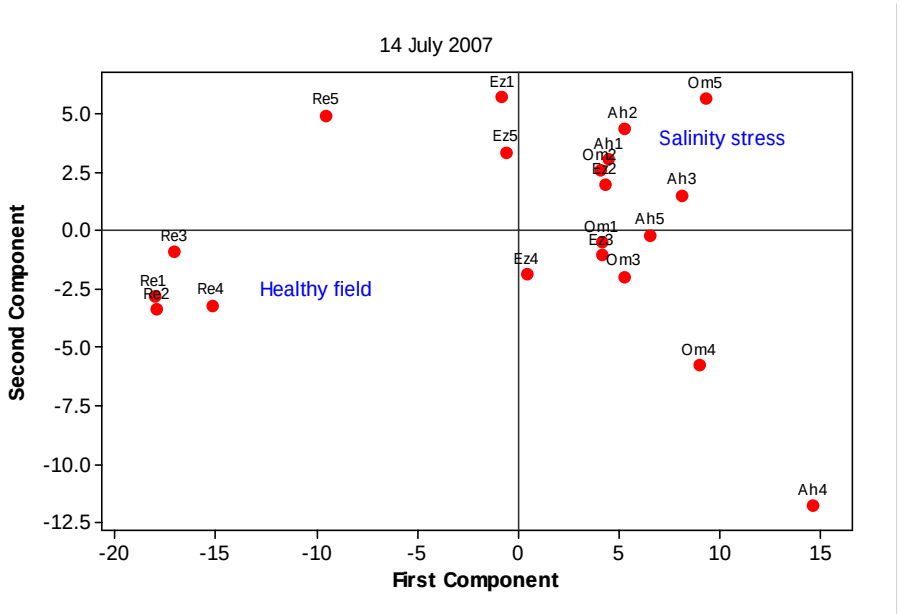


**Figure 6-22** The score plot of the Principle Component Analysis for the spectra collected from healthy and salinity induced stressed maize canopies under clear sky conditions in summer growing season of 2007 in south-west Alexandria Egypt (n = 20). (Site labels: Re-Reda; Ez-Eza; Om-Omara; Ah-Ahmed).

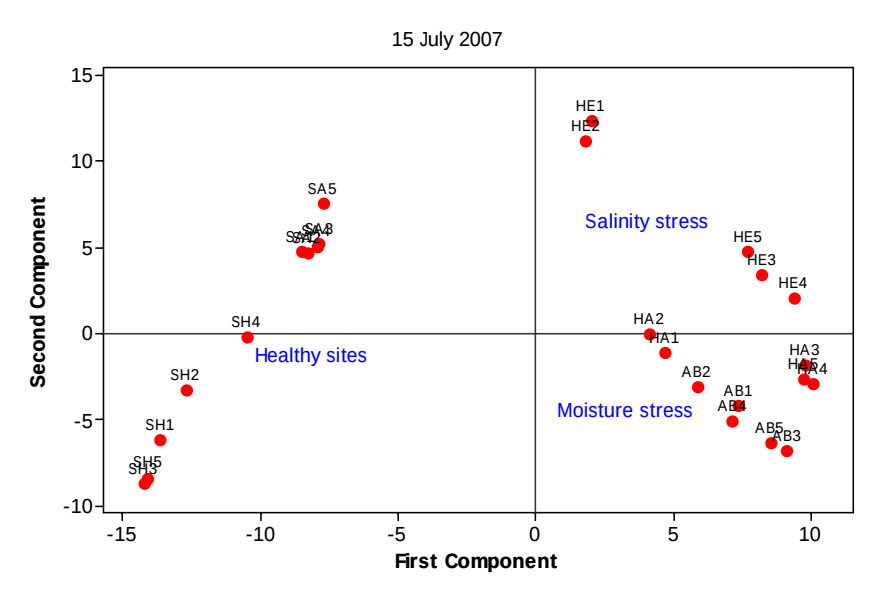


**Figure 6-23** The score plot of the Principle Component Analysis (PCA) for the spectra collected from healthy, salinity and moisture induced stressed maize canopies under clear sky conditions in summer growing season of 2007 in Egypt (n = 25). (Site labels: SH-Shetaiwy; SA-Salem; HE-Helmy; HA-Habeeb; AB-Abdelbadea).

## 6.4 Predicting Stress with high spatial resolution platforms in wheat

### 6.4.1 Introduction

Predicting different biophysical and biochemical properties of wheat crop through *in situ* and high spatial resolution satellite remote sensing is important for maximising crop production through stress detection at early growth stage. Major advances could be made in crop management if it were possible to detect physiological changes resulting from different types of stress in wheat through *in situ* and high spatial resolution satellite remote sensing. In this section the results of the analysis of QuickBird images, ASTER image and *in situ* hyperspectral measurements are described. The hypothesis of *whether high spatial resolution satellite imagery can detect stress in wheat crops* is also examined.

### 6.4.2 Spatial suitability

Both QuickBird and ASTER satellite images were evaluated in this research to detect stress in wheat. ASTER data was planned to be acquired three times; on 5$^{th}$ March, 20$^{th}$ March and 5$^{th}$ April 2007 to have a time series satellite imagery. Due to cloud cover during this period of time just one image was acquired on 23$^{rd}$ April 2007,

which was too late to encompass the wheat growing season in Egypt. Additionally, due to a lack of large fields in Egypt, using ASTER imagery in detecting stress is problematic as the majority of fields have a width less than 20 m and, as ASTER's spatial resolution is 15 m, overlap between spectral signatures from even different crops results in mixed pixels. However, using ASTER imagery could be useful in detecting stress at a regional scale. With improvements in satellite capabilities providing spatial resolution less than 10 m such as QuickBird and Ikonos imagery may provide a useful tool in precision farming. QuickBird imagery with 2.4 m spatial resolution has the potential for detecting stress and has a suitable resolution for the Egyptian farming context.

In the study area, farmers divide their fields into two or three strips each planted with different crops. In winter season they mainly grow wheat and clover while in summer they grow maize, melon and tomato. These different crops have different spectral signatures and due to the possible overlap may produce poor relationships between vegetation indices and crop properties. Therefore a single pixel may contain a mixture of crops. Figure 6.24 shows both QuickBird and ASTER images for the same study area; it is evident that obtaining pure spectra from that area using ASTER image is problematic due to issues of mixed pixels.

(a)

(b)

**Figure 6-24** QuickBird and ASTER satellite images for the same study area showing differences in pixel size.

### 6.4.3 Image classification

During field work visits notes were recorded regarding other crops in the same study site mainly clover crop. K-means unsupervised classification was performed on both QuickBird and ASTER images using ENVI v4.4. Four bands of both images (blue, green, red and near infrared) were used in this classification and 10 output classes were created. The image was investigated visually using a number of known fields as guides. The k-means classification showed the dissimilarities in spectral response from different targets including different crops, bare soil and water surfaces. The classification produced two classes for wheat crops. The two classes of wheat crops may be a result of plant health status since some fields were approaching maturation while others were still in the grain filling stage and therefore would likely have different chlorophyll and other pigment concentration. The image was reclassified using the post classification procedure in ENVI. The two wheat classes were defined and combined together in one class. It can be seen in the image that there are some misclassified pixels particularly those covered by clouds and associated shadows. The post classification technique was used to mask areas of cloud and shadow from further analysis.

Figure 6.25 shows different classes of crops as it is noticeable that the spectral signature from wheat fields is different from clover, bare soil and water. The class in red colour shows wheat fields represent the majority of fields in the image. Slight overlap between clover and wheat fields was detected after classification particularly with the very small fields. These two crops are the most common in that area as the majority of farmers grow them for production of livestock. Some other classes represent bare soil, clouds, shadows and water surfaces are defined. The figure also shows that clouds and shadows have more than one class depending on the density of both of them. When creating the training dataset for different crops, care was taken to choose them away from any clouds and shadows to decrease the effects of both of them on the spectral signature from crops.

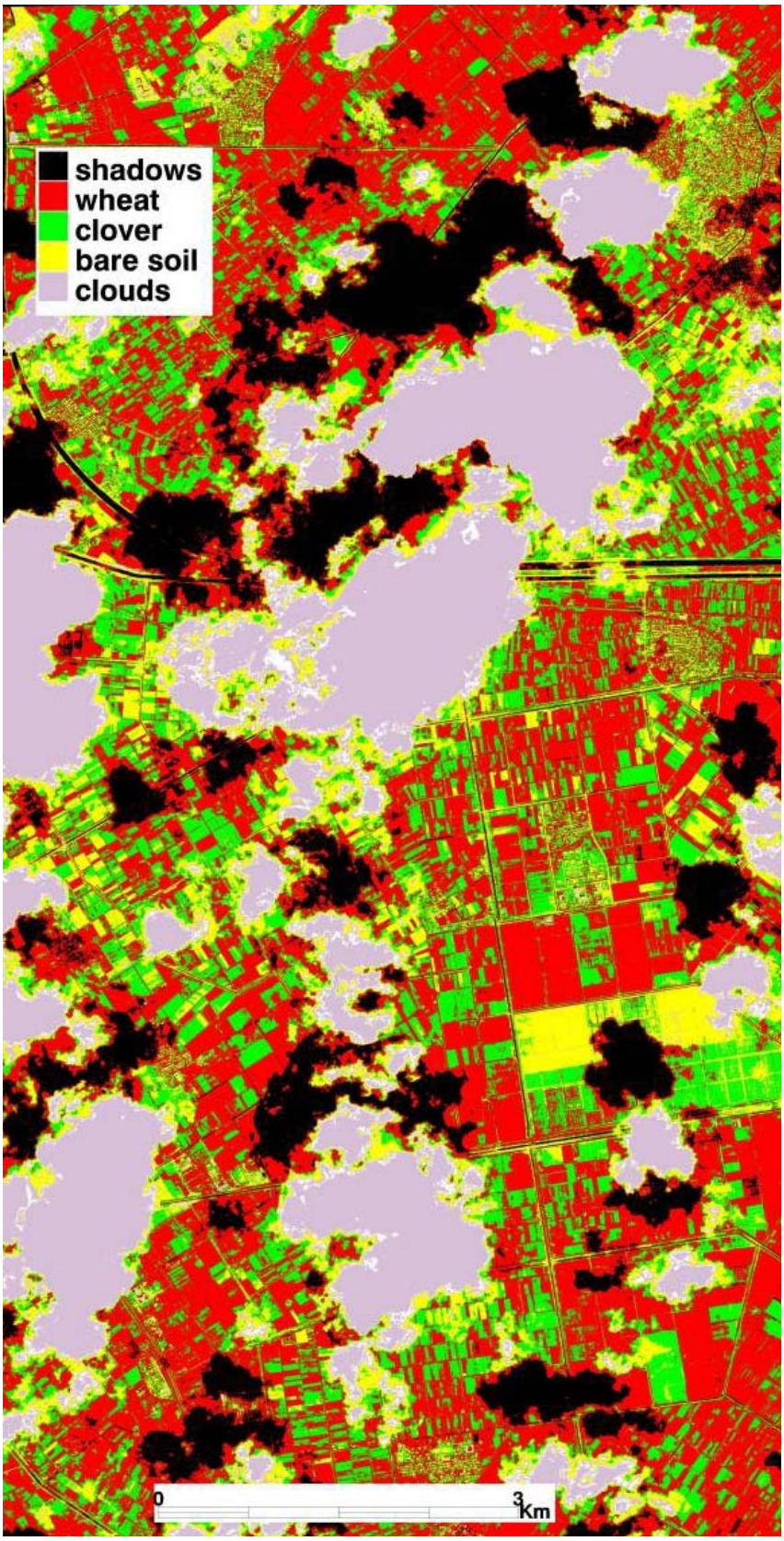


**Figure 6-25** K-means unsupervised classified QuickBird image acquired on 7th April 2007 for wheat and other crops in south-west Alexandria, Egypt.

To check the accuracy of the classification, a validation dataset was created for some fields known as wheat, clover, bare soil, or water from the hyperspectral survey. The number of pixels in the ground reference dataset varied as a result of the 33% cloud cover, which covered large number of these different pixels. The overall accuracy of the k-means unsupervised classification was calculated using a confusion matrix. It compares the location and class of each ground reference pixel with the location and the class of the corresponding pixels in the k-means classification. Confusion matrices allow the classification accuracy to be evaluated in terms of class accuracy, overall accuracy and Kappa coefficient. Table 6.9 shows the statistics of the confusion matrix including the overall accuracy, user's accuracy, producer's accuracy and Kappa coefficient. The overall accuracy of the k-means classification was slightly high of 77.4 % even with poor classification for specific targets.

The classification accuracy varied for identifying different classes ranging from 42.24% (for bare soil) to 97.60% (for wheat crops). The classification accuracy for clover and water are 94.36 and 72.45% respectively. The slight low classification accuracy for water may be a result of the spectral confusion between water and shadows. Additionally, the results give the user's and producer's accuracy for each single class. The low classification accuracy for identifying bare soil may be a result of spectral confusion between dry soils and wet soils. The moisture content in some fields may be higher in comparison to others. At this period of time some people prepare their lands to grow tomato so irrigated and non-irrigated bare soils can be found in the same time. Additionally some mixed pixels of bare soil and other crops such as clover were also detected. The lowest producer's accuracy was associated with bare soil class (42.24%), which may be a result of the spectral confusion from different moisture content in bare soils and mixed pixels. The slight lower values of Kappa coefficient for the main classes of 0.698 may be a result of many misclassified pixels. However, the k-means produced high classification accuracy it might produce too many misclassified pixels. For example the > 0.95 accuracy for identifying wheat crops may lead to high percent of misclassified pixels.

**Table 6-9** Confusion matrix results for k-means unsupervised classification of wheat and other objects in south-west Alexandria, Egypt.

| Class | Ground truth (Percent) | | | | | User's Accuracy |
|---|---|---|---|---|---|---|
| | **Wheat** | **water** | **Bare soil** | **Clover** | **total** | |
| Unclassified | 0.00 | 0.00 | 0.00 | 0.00 | 0.00 | (%) |
| Wheat | 97.60 | 25.82 | 12.65 | 4.17 | 35.09 | 69.90 |
| Water | 2.02 | 72.45 | 45.1 | 0.28 | 29.43 | 61.74 |
| Bare soil | 0.38 | 0.29 | 42.24 | 0.93 | 10.42 | 96.06 |
| Clover | 0.00 | 1.45 | 0.00 | 94.63 | 25.06 | 98.55 |
| total | 100.00 | 100.00 | 100.00 | 100.00 | 100.00 | |
| Producer's Accuracy (%) | 97.60 | 72.45 | 42.24 | 94.63 | | |
| Kappa Coefficient | **0.698** | | | | | |
| Overall Accuracy | **0.774** | | | | | |

## Supervised classification

Unlike unsupervised classification algorithms, supervised classifiers start with a training dataset by predefining the different signature for each class followed by class assignments using decision rule. Supervised classification was also performed on both images of ASTER and QuickBird. MLC and MDC algorithms were used to differentiate between different crops in the study area. Both classifiers were performed to choose the best method to classify images in terms of overall accuracy, Kappa coefficient, producer's and user's accuracy. MLC is commonly used in classifying vegetation by many authors (Mehner *et al*., 2004; Su *et al*., 2007). It assumes that the statistics for each single class in each band are normally distributed and assesses the probability that a pixel belongs to a specific class. Minimum distance (MDC) algorithm was then performed to differentiate between different classes in the images to choose the optimum classifier.

The corrected images were used to define the training dataset for fields, which are known to be wheat from the field work. Other classes such as clover, water surfaces and bare soil were considered distinct classes. The training dataset was created manually by defining a number of pixels for each class, and then the classification method was performed using the training dataset and extrapolated across the QuickBird image acquired on 7$^{th}$ March 2007. Both MDC and MLC supervised classification showed high classification accuracy for identifying different classes including the main two crops, wheat and clover. Figure 6.26 shows QuickBird

supervised classified image with the main two crops and other targets. It is noted from the classified image that the clouds and associated shadows have affected the accuracy of the classification as they did in the unsupervised one. Some misclassified fields particularly the ones covered by shadows were observed. It can be seen in the image that there is a spectral confusion between water and shadow as both are dark targets.

To evaluate the classification accuracy for both MLC and MDC, a ground reference dataset was created using radiance spectra from different classes known from the field work visit. The spectra for the ground reference dataset were manually created and were independent from the training dataset. The ground reference dataset composed at least 1000 pixels for each class. A confusion matrix was constructed to assess the overall accuracy of both algorithms (Tables 6.10 and 6.11). The overall classification accuracy for both algorithms is very high (91.77 and 88.70% for MLC and MDC, respectively).

The classification accuracy for different classes is also very high, ranging from 85.95% (for classifying clover) to 97.79 % (for classifying water) in MLC algorithm and ranging from 79.47 (for classifying clover) to 95.67 (for classifying water) in MDC algorithm. It is noticed that the only difference between these two algorithms is in identifying clover. The classification accuracy for identifying wheat crops is very high with both algorithms (> 85%). Decreases in the accuracy of classifying clover by MDC algorithm may be attributed to spectral confusion, which is due to the effects of clouds and associated shadows. The high values of Kappa coefficient (0.890 and 0.849) support the high classification accuracy for both MLC and MDC.

The results therefore suggest that MLC is a good classifier for identifying different agricultural crops. Previous studies have reported similar results showing the effectiveness of MLC to classify vegetation (Su *et al*., 2007; Pu *et al*., 2008; Wang *et al*., 2008).

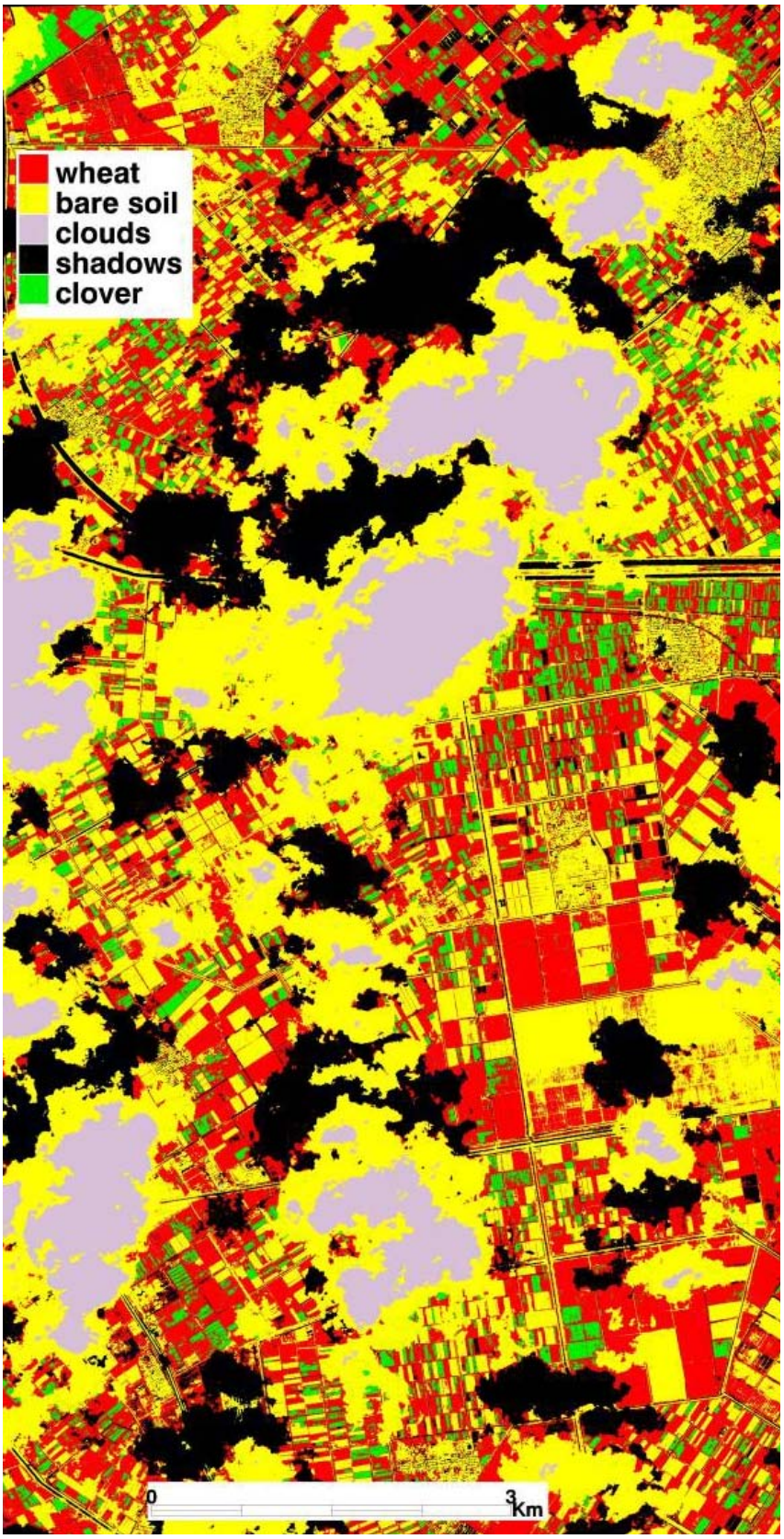


**Figure 6-26** Minimum distance supervised classification of QuickBird image acquired on 7th April 2007 for different crops in south-west Alexandria, Egypt.

Comparing the classification accuracies obtained using both unsupervised and supervised classification algorithms, it is noticeable that although k-means algorithm produced 97.6 % accuracy for classifying wheat; it produced low accuracies for both bare soil and clover crop (42.24 and 72.45% respectively), and therefore, many misclassified pixels were produced. Additionally, Kappa coefficient values are higher in supervised classification algorithms (0.890 and 0.849) in comparison to k-means classification (0.697). The low value of Kappa coefficient for using k-means is a good indicator for the many mixed pixels and therefore some of these pixels were poorly identified. Consequently, supervised classification gives better results in terms of overall accuracy, individual class classification accuracy and Kappa coefficient values. Furthermore, the user's and producer's accuracies are always higher in supervised algorithms. For example, the k-means algorithm produced a user's accuracy of 61.74% for identifying clover, which is low in comparison to MLC and MDC (90.67 and 88.03 respectively). Also, the k-means algorithm produced a user's accuracy of 69.90% for identifying wheat crops while MLC and MDC produced comparable values (96.29 and 89.20 respectively).

**Table 6-10** Confusion matrix results for maximum likelihood classification of wheat crops and other objects in south-west Alexandria, Egypt.

| **Class** | **Ground truth (Percent)** | | | | | **User's Accuracy** |
|---|---|---|---|---|---|---|
| | **Wheat** | **Clover** | **Bare soil** | **Water** | **total** | |
| Unclassified | 0 | 0 | 0 | 0 | 0.00 | (%) |
| Wheat | 90.42 | 1.28 | 2.04 | 0.00 | 22.75 | 96.29 |
| Clover | 4.26 | 85.95 | 3.99 | 0.09 | 22.63 | 90.67 |
| Bare soil | 5.32 | 11.10 | 92.46 | 2.12 | 28.92 | 84.51 |
| Water | 0.00 | 1.67 | 1.51 | 97.79 | 25.70 | 96.9 |
| Total | 100 | 100 | 100 | 100 | 100.00 | |
| Producer's Accuracy (%) | 90.42 | 85.95 | 92.46 | 97.79 | | |
| Kappa Coefficient | **0.890** | | | | | |
| Overall Accuracy(%) | **91.77** | | | | | |

**Table 6-11** Confusion matrix results for minimum distance classification of wheat crops and other objects in south-west Alexandria, Egypt.

| Class | Ground truth (Percent) | | | | | User's Accuracy |
|---|---|---|---|---|---|---|
| | **Wheat** | **Clover** | **Bare soil** | **Water** | **total** | |
| Unclassified | 0.00 | 0.00 | 0.00 | 0.00 | 0.00 | (%) |
| Wheat | 87.12 | 6.68 | 3.64 | 0.00 | 23.66 | 89.2 |
| Clover | 6.97 | 79.47 | 3.37 | 0.00 | 21.55 | 88.03 |
| Bare soil | 5.91 | 10.51 | 91.75 | 4.33 | 29.29 | 82.79 |
| Water | 0.00 | 3.34 | 1.24 | 95.67 | 25.49 | 95.58 |
| total | 100.00 | 100.00 | 100.00 | 100.00 | 100.00 | |
| Producer's Accuracy (%) | 87.12 | 79.47 | 91.75 | 95.67 | | |
| Kappa Coefficient | **0.849** | | | | | |
| Overall Accuracy | **88.70** | | | | | |

### 6.4.4 Application of vegetation indices for stress

Following the image processing (geo-correction, atmospheric correction, normalization, classification), the image was masked just to show wheat crops only using masking procedure in ENVI. Wherever possible in the image different broad band vegetation indices were derived from the corrected QuickBird image. Tables 6.12-6.15 detailed the correlation coefficient values for the relationship between different vegetation indices and the measured biophysical and biochemical properties of wheat crops. The locations of *in situ* measurements within each field were identified on the QuickBird image using the GPS coordinates. Nine pixels at each location were chosen to reduce variability, and then averaged to have the mean value of radiance. Care was taken to make sure that the location of the *in situ* measurements point is the centre of these nine pixels. The 12$^{th}$ March dataset demonstrated that the majority of vegetation indices were significantly correlated with different wheat properties. SI produced the strongest correlation with three different properties; chlorophyll concentration, aboveground biomass and plant height (r = -0.683, -0.819 and -0.654 respectively). Unexpectedly, VI1 produced the highest correlation with the measured LAI (r = 0.638). DVI produced the lowest correlations with all wheat properties except aboveground biomass (r = 0.583).

The results obtained from the 28$^{th}$ March dataset showed better results in comparison to 12$^{th}$ March dataset. This may be due to the small time difference between imagery acquisition and the time of field work data collection. Strong significant correlations were observed between broad band indices and wheat biophysical properties except plant height since the correlations were not as high as the other crop properties. This

may be attributed to the low difference in plant height between different fields of the *in situ* hyperspectral survey. SI produced the strongest correlation with the measured chlorophyll concentration (r = -0.904). RVI and SR had the strongest correlations with the measured aboveground biomass (r = 0.826). In contrast to results obtained from greenhouse experiments, VI1 has the strongest correlation with both plant height and LAI (r = 0.564 and 0.845 respectively).

Due to cloud cover and associated shadows, many fields of the *in situ* hyperspectral survey at the Kahr site were obscured and were therefore eliminated from this analysis. Some fields of *in situ* survey were in a clear part of the image and therefore different indices were derived and correlated to different wheat properties. The 27$^{th}$ March dataset was used to calculate the coefficient of correlation between wheat properties and broad band vegetation indices (Table 6.14). Strong significant correlations were recorded between all vegetation indices and wheat properties particularly biomass, plant height and LAI. RVI and SR produced the strongest correlation with chlorophyll concentration (r = 0.669). RDVI showed the strongest correlation with both biomass and LAI (r = 0.927 and 0.919 respectively). NDVI and SI produced the strongest correlation with plant height (r = 0.885 and -0.889 respectively). The correlations produced from that dataset demonstrated better results in comparison to the 12$^{th}$ March dataset as a result of the small time difference between data collection and imagery acquisition (7$^{th}$ April 2007).

To decrease variations of the effects of weather conditions on reflectance measurements, the combined dataset collected from both study sites (Kahr and Hewaihy) on 27$^{th}$ and 28$^{th}$ March 2007 was used to assess the effectiveness of different broad band indices in predicting different wheat properties (Table 6.15). Strong correlations were observed between all indices and the chlorophyll concentration with the strongest recorded with SI (r = -0.864). In contrast to the 27$^{th}$ dataset, RVI and SR produced the lowest correlation with the measured chlorophyll concentration. NDVI again showed a strong significant relationships with the measured chlorophyll producing similar correlations to SI (r = 0.863). It is further noticed from individual and combined datasets that SI and NDVI produced similar results with different wheat properties. DVI produced the strongest correlation with the measured biomass, plant height and LAI (r = 0.850, 0.656 and 0.811 respectively).

However, from individual datasets DVI sometimes demonstrates low relationships with different crop properties. This may be attributed to the strong correlations between DVI and different indices obtained from the 27th dataset. It can be seen that SI always give highly strong correlations with the measured chlorophyll. For example, SI produced the strongest correlation in three datasets out of four including the combined dataset. It is therefore evident that no single index produces the strongest correlation in all datasets and the relationship between different indices and crop properties changes from one dataset to another.

**Table 6-12** Coefficient of correlation for the relationship between different broad band spectral vegetation indices derived from QuickBird image and wheat biophysical and biochemical properties data collected on 12th March 2007 at the Hewaihy site in south-west Alexandria, Egypt. Highlighted values are significant (P<0.05) and bold values are the strongest correlation values.

| Date | Vegetation index | Crop properties | | | |
|---|---|---|---|---|---|
| | | Chlorophyll (µg $cm^{-2}$) | Biomass (kg $m^{-2}$) | Height (m) | LAI |
| 12 March | NDVI | 0.676 | 0.816 | 0.636 | 0.576 |
| | RVI | 0.613 | 0.762 | 0.509 | 0.621 |
| | SAVI | 0.676 | 0.815 | 0.636 | 0.576 |
| | $GNDVI_{br}$ | 0.671 | 0.797 | 0.618 | 0.597 |
| | DVI | 0.353 | 0.583 | 0.245 | 0.419 |
| | SR | 0.613 | 0.762 | 0.509 | 0.621 |
| | SLAVI | 0.676 | 0.816 | 0.636 | 0.576 |
| | OSAVI | 0.676 | 0.816 | 0.636 | 0.576 |
| | VI1 | 0.626 | 0.767 | 0.535 | **0.638** |
| | RDVI | 0.502 | 0.702 | 0.418 | 0.503 |
| | SI | **-0.683** | **-0.819** | **-0.654** | -0.569 |
| | IPVI | 0.676 | 0.816 | 0.636 | 0.576 |

**Table 6-13** Coefficient of correlation for the relationship between different broad band spectral vegetation indices derived from QuickBird image and wheat biophysical and biochemical properties data collected on 28th March 2007 at the Hewaihy site in south-west Alexandria, Egypt. Highlighted values are significant (P<0.05) and bold values are the strongest correlation values.

| Date | Vegetation index | Crop properties | | | |
|---|---|---|---|---|---|
| | | Chlorophyll (µg $cm^{-2}$) | Biomass (kg $m^{-2}$) | Height (m) | LAI |
| 28 March | NDVI | 0.893 | 0.788 | 0.539 | 0.795 |
| | RVI | 0.679 | **0.826** | 0.552 | 0.841 |
| | SAVI | 0.893 | 0.788 | 0.539 | 0.794 |
| | $GNDVI_{br}$ | 0.880 | 0.766 | 0.513 | 0.779 |
| | DVI | 0.744 | 0.739 | 0.431 | 0.691 |
| | SR | 0.679 | **0.826** | 0.552 | 0.841 |
| | SLAVI | 0.893 | 0.788 | 0.539 | 0.795 |
| | OSAVI | 0.893 | 0.788 | 0.539 | 0.794 |
| | VI1 | 0.747 | 0.824 | **0.564** | **0.845** |
| | RDVI | 0.830 | 0.775 | 0.491 | 0.753 |
| | SI | **-0.904** | -0.753 | -0.504 | -0.761 |
| | IPVI | 0.893 | 0.788 | 0.539 | 0.795 |

**Table 6-14** Coefficient of correlation for the relationship between different broad band spectral vegetation indices derived from QuickBird image and wheat biophysical and biochemical properties data collected on 12th March 2007 at the Kahr site in south-west Alexandria, Egypt. Highlighted values are significant (P<0.05) and bold values are the strongest correlation values.

| Date | Vegetation index | Crop properties | | | |
|---|---|---|---|---|---|
| | | Chlorophyll (µg cm$^{-2}$) | Biomass (kg m$^{-2}$) | Height (m) | LAI |
| 27 March | NDVI | 0.627 | 0.905 | 0.885 | 0.894 |
| | RVI | **0.669** | 0.839 | 0.811 | 0.884 |
| | SAVI | 0.627 | 0.905 | 0.885 | 0.894 |
| | $GNDVI_{br}$ | 0.627 | 0.884 | 0.836 | 0.884 |
| | DVI | 0.498 | 0.919 | 0.856 | 0.916 |
| | SR | **0.669** | 0.839 | 0.811 | 0.884 |
| | SLAVI | 0.627 | 0.904 | 0.885 | 0.894 |
| | OSAVI | 0.627 | 0.904 | 0.885 | 0.894 |
| | VI1 | 0.666 | 0.829 | 0.797 | 0.878 |
| | RDVI | 0.544 | **0.927** | 0.873 | **0.919** |
| | SI | -0.619 | -0.908 | **-0.889** | -0.889 |
| | IPVI | 0.627 | 0.905 | 0.885 | 0.894 |

**Table 6-15** Coefficient of correlation for the relationship between different broad band spectral vegetation indices derived from QuickBird image and wheat biophysical and biochemical properties data collected on 27th and 28th March 2007 (combined) in south-west Alexandria, Egypt. Highlighted values are significant (P<0.05) and bold values are the strongest correlation values.

| Date | Vegetation index | Crop properties | | | |
|---|---|---|---|---|---|
| | | Chlorophyll (µg cm$^{-2}$) | Biomass (kg m$^{-2}$) | Height (m) | LAI |
| 27-28 March | NDVI | 0.863 | 0.689 | 0.588 | 0.677 |
| | RVI | 0.696 | 0.706 | 0.616 | 0.665 |
| | SAVI | 0.863 | 0.689 | 0.588 | 0.677 |
| | $GNDVI_{br}$ | 0.836 | 0.654 | 0.557 | 0.623 |
| | DVI | 0.747 | **0.850** | **0.656** | **0.811** |
| | SR | 0.696 | 0.706 | 0.616 | 0.665 |
| | SLAVI | 0.863 | 0.688 | 0.588 | 0.677 |
| | OSAVI | 0.863 | 0.688 | 0.587 | 0.677 |
| | VI1 | 0.718 | 0.665 | 0.594 | 0.607 |
| | RDVI | 0.826 | 0.810 | 0.649 | 0.781 |
| | SI | **-0.864** | -0.649 | -0.541 | -0.652 |
| | IPVI | 0.863 | 0.689 | 0.588 | 0.677 |

The combined dataset was also used to investigate the relationship between broad band vegetation indices derived from *in situ* hyperspectral survey and the same broad band indices derived from the QuickBird satellite imagery (Figure 6.27). Regression analysis showed that there is a significant positive linear relationship between NDVI derived from *in situ* hyperspectral and NDVI derived from QuickBird satellite image ($R^2$ = 0.61; p = 0.000). From both individual datasets and the combined dataset, NDVI would appear to be a good indicator for detecting stress in crops. The decrease

in the relationship may have been a result of the 10 days difference between *in situ* survey and imagery acquisition since the crops were at late stage of the growing season and one week difference may change crop properties particularly chlorophyll concentration. Furthermore, as shown in Table 6.3 that the two QuickBird images for wheat and maize were acquired at 13° and 22° off nadir whilst hyperspectral data acquired at nadir viewing angle and therefore affects the reflectance from plant canopies. Also, both images were acquired at mid morning while hyperspectral data collected around midday, which in turn affect the comparison.

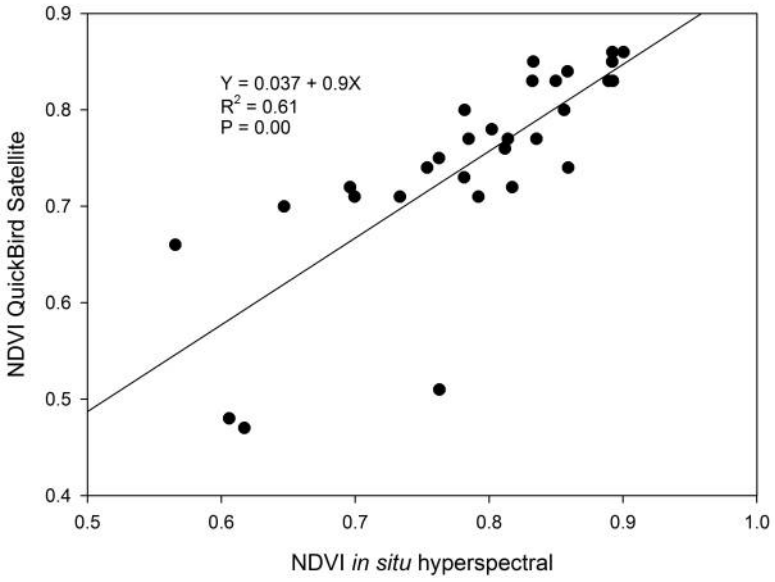


**Figure 6-27** The relationship between NDVI derived from *in situ* hyperspectral survey and NDVI derived from QuickBird image collected from wheat fields in south-west Alexandria, Egypt (n = 30).

To extrapolate the results on a large scale, NDV and DVI maps were created using the classified QuickBird image (Figure C1 and C2; appendix C). Both maps were created first for the whole image including all classes then masked just for wheat crops via the created training dataset. Some wheat fields known from the field work visit were used to create the training dataset for wheat crops. The band math then was run to create NDVI and DVI maps for the whole scene. Figure C1 shows that there is no specific trend for decreasing NDVI over the whole scene, which as mentioned before as a result of different agricultural practices including different sowing dates, nitrogen fertilization rate, moisture and salinity induced stress. NDVI map shows the dissimilarities in plant health over the whole cultivated area. Fields in red colour shows the healthy ones in terms of biomass, chlorophyll, plant height and LAI. It is

further shown that some areas in purple colour are suffering from stress and therefore produce lower NDVI values in comparison to other areas as shown in the same figure since the stressed area is suffering from salinity stress or nutrient deficiency.

The regression analysis was performed on the data collected during hyperspectral survey to calculate regression equations for predicting biophysical and biochemical properties of wheat including biomass, chlorophyll, plant height and LAI. The indices produced the strongest correlations with each property were used to calculate these equations. Due to high sensitivity of NDVI to chlorophyll and DVI to LAI, plant height and biomass, they were used to calculate regression equations as follows:

| | | | |
|---|---|---|---|
| Equation 6.1 | LAI = -0.17 + 0.004 DVI | $R^2 = 0.66$ | p = 0.000 |
| Equation 6.2 | Plant height = 0.28 + 0.001 DVI | $R^2 = 0.48$ | p = 0.000 |
| Equation 6.3 | Biomass = -0.59 + 0.01 DVI | $R^2 = 0.72$ | p = 0.000 |
| Equation 6.4 | Chlorophyll = 14.8 + 34.3 NDVI | $R^2 = 0.75$ | p = 0.000 |

The regression equations then were used in ENVI to create maps for predicting different biochemical and biophysical properties of wheat (Figures 6.28 and 6.29). The decrease in the relationship between *in situ* data and satellite data may be attributed to the time difference between them; even with a one week difference in March and April as plants are approaching maturation and chlorophyll concentration can be changed markedly. Additionally, the cloud cover and shadows affected this relationship by covering some fields used for the *in situ* hyperspectral survey.

The two calibrated maps for chlorophyll concentration and biomass demonstrate that there is no specific trend for stress across the whole area. This can be attributed to different agricultural practices throughout the area. However, it can be noticed in the calibrated image that some large fields have high values of both chlorophyll concentration and biomass as a result of using similar agricultural practices including; sowing dates, nitrogen fertilization rate, plant protection schedule and consequently high vegetation cover, which lead to high productivity. The maps also showed that the fields at the top of the image have high values of both chlorophyll and biomass as a result of using high quality water directly from the main irrigation channel.

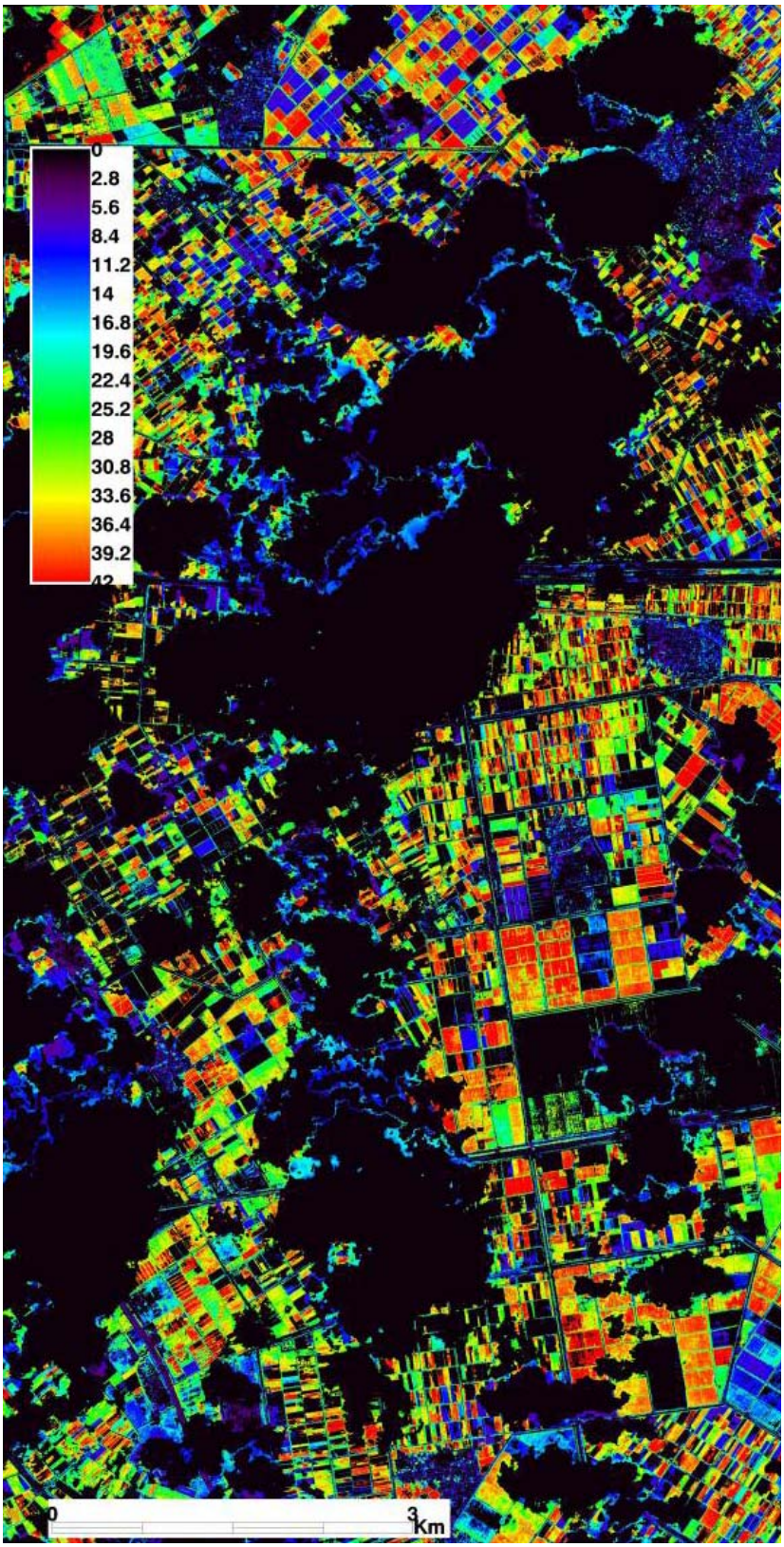


**Figure 6-28** classified QuickBird (NDVI) image acquired on 7th April calibrated to chlorophyll concentration of wheat crops in south-west Alexandria, Egypt.

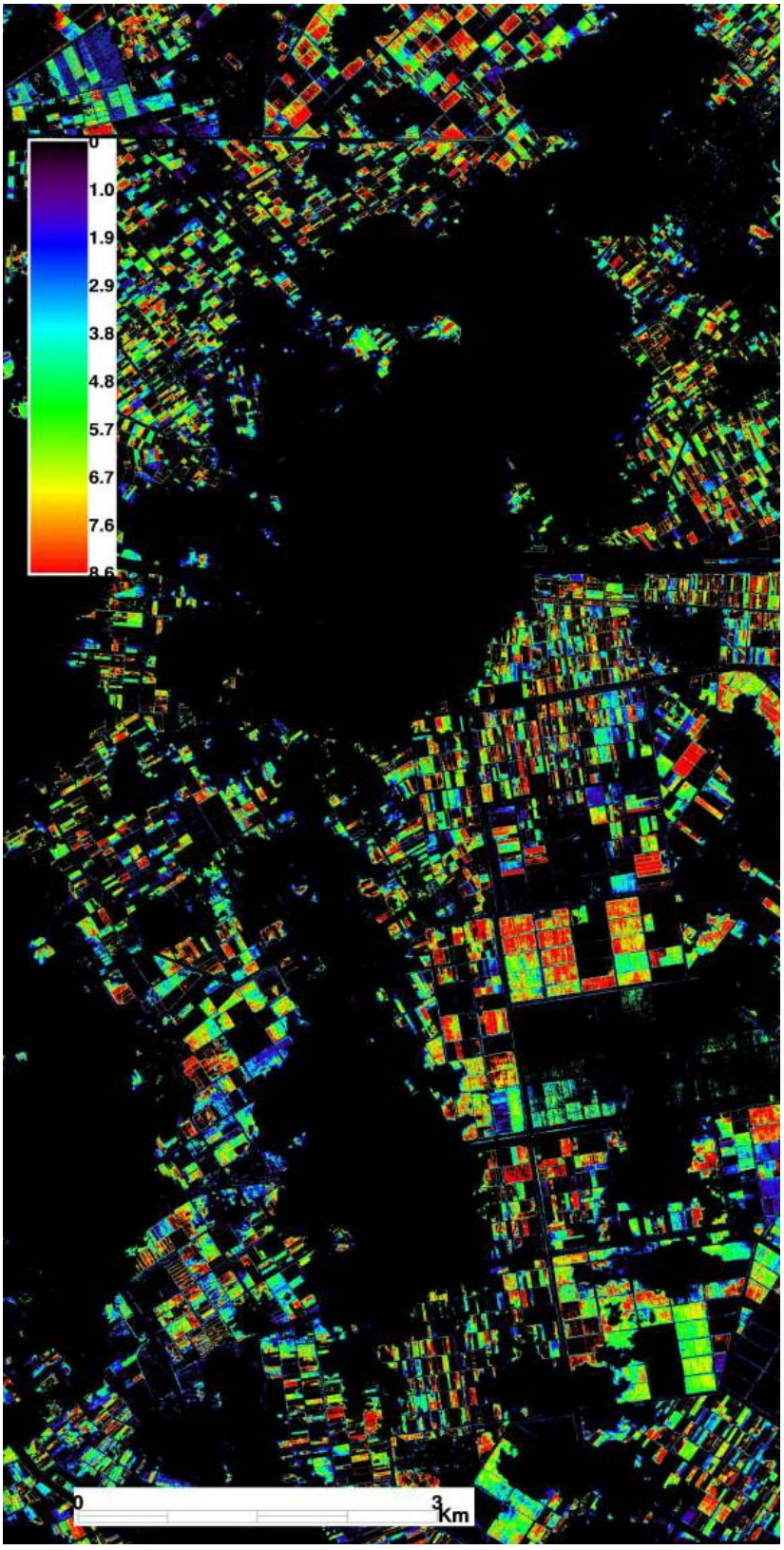


**Figure 6-29** classified QuickBird (DVI) image acquired on 7th April calibrated to aboveground biomass of wheat crops in south-west Alexandria, Egypt.

Figures 6.30 and 6.31 show a significant positive relationship between NDVI and the measured chlorophyll concentration ($R^2$ = 0.75; p = 0.000). A strong positive linear relationship is also shown in Figure 6.32 between DVI and the measured biomass ($R^2$ = 0.72; p = 0.000). The results obtained using QuickBird satellite imagery demonstrated that both NDVI and SI are sensitive indicators of the chlorophyll concentration (often give higher correlations with the measured chlorophyll in comparison to other indices). Unexpectedly, RVI values from satellite imagery did not produce high correlations with the measured biomass and therefore do not match the results obtained by *in situ* hyperspectral survey.

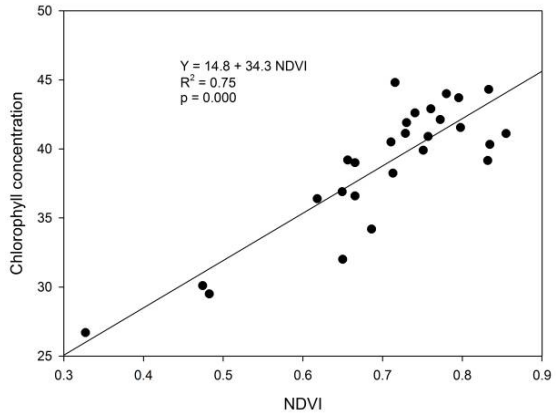


**Figure 6-30** The relationship between NDVI derived from the QuickBird image acquired on 7th April 2007 and the measured chlorophyll concentration (SPAD measures) collected in south-west Alexandria, Egypt (n = 27).

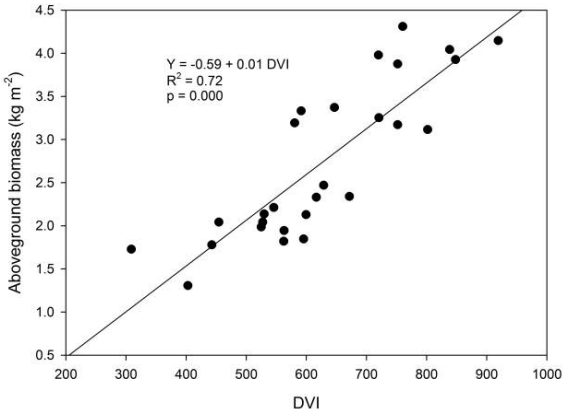


**Figure 6-31** The relationship between DVI derived from the QuickBird image acquired on 7th April 2007 and the measured aboveground biomass collected in south-west Alexandria, Egypt (n = 27)

Figure 6.32 shows an example of NDVI for stressed and healthy areas, which are very close, but irrigated from two different channels. The healthy fields belong to one

farmer who applies the same agricultural practices; same sowing date, fertilization rate, same wheat variety and irrigation intervals. The other side shows some small fields, which are owned by many farmers who use different agricultural practices. Generally these fields are suffering from stress (mainly salinity) since that area is irrigated with saline water for more than 20 years. It can also be seen in Figure 6.32 that there is a gradient in NDVI values in the healthy area and this may be attributed to a slight moisture stress. Furthermore, the permeability and the drainage conditions may differ from place to place within the same area depending on distance to the main drains, which in turn affect moisture level in the root zone.

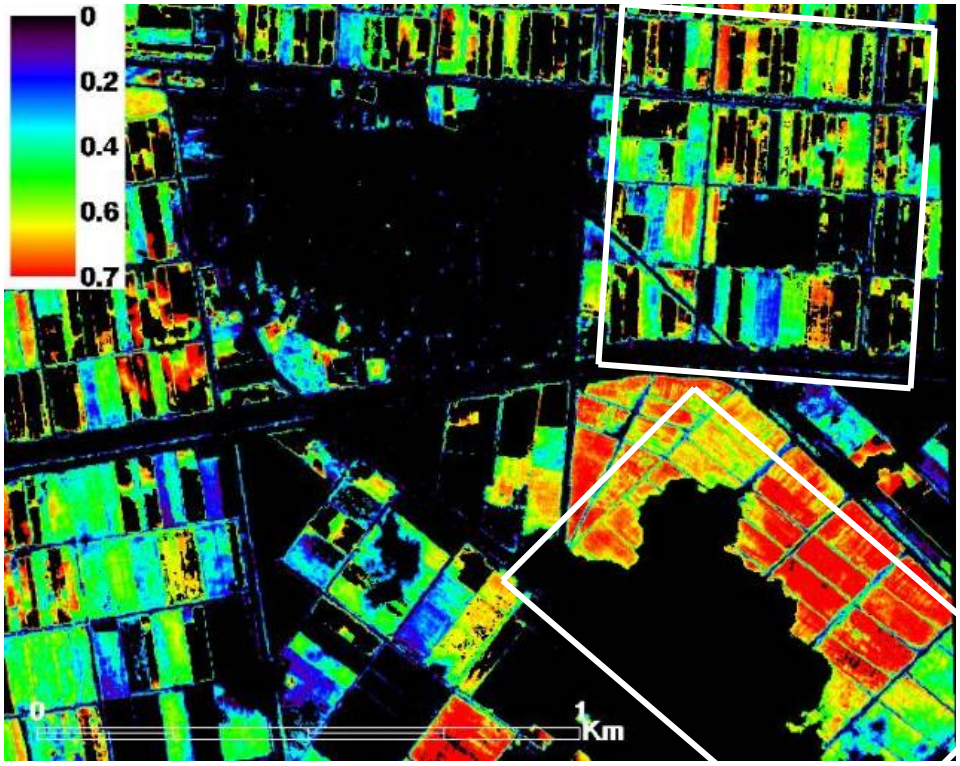


**Figure 6-32** An example of NDVI derived from QuickBird image for two stressed and healthy areas within the study site, south-west Alexandria, Egypt.

## 6.5 Predicting Stress with high spatial resolution platforms in maize crop

### 6.5.1 Introduction

The potential of *in situ* hyperspectral and high spatial resolution satellite remote sensing to monitor maize crop health are investigated in this section through calculating different broad band vegetation indices. More specifically, investigating whether remotely sensed data is able to detect moisture and salinity stress in maize crops in the Nile Valley of Egypt or not. The classification methods used and extrapolating results across the whole satellite image is also described. We are examining the third hypothesis of this research assessing *whether high spatial resolution satellite imagery can detect stress in maize or not*.

### 6.5.2 Spatial suitability

A SPOT HRV image was acquired for the same study area on 9$^{th}$ July 2007 and this image was evaluated to be used for detecting stress in maize fields at a regional scale. The results showed that in such a small field system it is problematic to use SPOT HRV satellite images to detect stress in maize within a field scale; since most of the fields in that area have width less than 20 m, and therefore the mixed pixels from different crops make the analysis of crop stress difficult. It is also difficult to remove overlap between pixels from different fields, which sometimes have different crops and therefore different spectral signatures. However, using SPOT HRV imagery for detecting stress at a regional scale may provide a better understanding about stress trends with reasonable cost.

A QuickBird image was acquired on 29$^{th}$ June 2007 for the study area in south-west Alexandria, Egypt. The 2.4 m resolution image was examined to map stress at a local scale. The first QuickBird image acquired on 7$^{th}$ April 2007 showed the possibility to detect stress in wheat at a local scale. A combined approach of using higher and medium spatial resolution images (QuickBird and SPOT HRV) could provide better insight about stress at both local and regional scales. Figure 6.33 shows the difference in pixel size between QuickBird image and SPOT HRV image for the same study area as a result of each image resolution.

(a)

(b)

**Figure 6-33** Two satellite images of (a) QuickBird and (b) SPOT HRV showing the difference between them in pixel size and the details shown from each image.

### 6.5.3 Image classification

**Unsupervised classification**

Classification algorithms were used to identify different crops particularly maize, then assessing the potential of remotely sensed data to detect stress in maize. Unsupervised classification algorithms were chosen since some studies showed their effectiveness in classifying vegetation (Yang *et al*., 2006a and 2006b). K-means unsupervised classification was performed on both QuickBird and SPOT HRV images using ENVI v4.4. Four bands of both images (blue, green, red and near infrared) were used in this classification and 10 output classes were created. The classified images produced more than one class for maize crops as a result of stress and different growth stages. The post classification in ENVI was used to combine them in one class. The classified image was reclassified to merge classes representing just one class for each target. The image was investigated visually using a number of known fields as guide. Farmers in the study area grow maize after winter season crops such as wheat and clover. Some farmers prefer to keep clover as much as they can to feed cattle so they sow maize in the middle of June. The earlier sowing date for maize in that area is around middle of May following the harvest of wheat crops. This explains why there are different growth stages at the same time. In summer season, two weeks are enough for maize crop to progress to another growth stage with great difference in plant height. Figure 6.34 shows the final unsupervised classified QuickBird image, which shows different classes- maize in red, water in cyan, melon in blue, tomato in green, bare soil in yellow.

It can be seen from the QuickBird classified image that most of the cultivated area is maize. Most farmers grow maize because it is not costly in terms of fertilizers, pesticide and fungicide. Some bare soils were misclassified and overlap occurs with tomato or maize at the very early stage, which may be a result of mixed pixels or spectral confusion from similar spectral characteristics. Soil moisture content also varies from field to field depending on many factors such as permeability, distance from main drains and distance from irrigation channels, irrigation intervals and drains system efficiency and therefore affects the spectral signature. Crops such as tomato or maize at early growth stage may be misclassified as a result of the effects of soil

background on reflected energy from both soil surface and vegetation, which leads to mixed pixels.

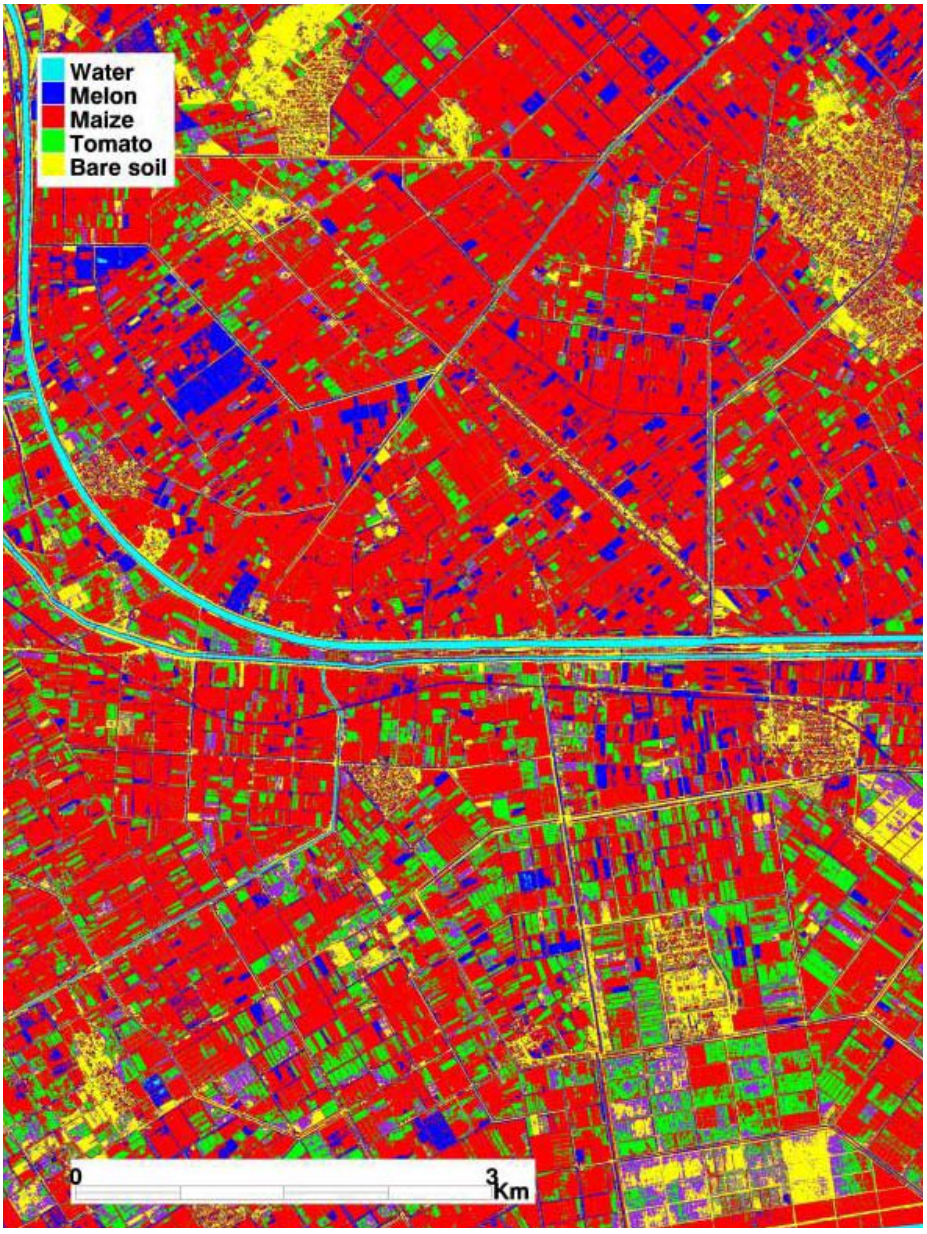


**Figure 6-34** K-means unsupervised classification of the QuickBird image acquired on 29th June 2007 for maize and other crops in south-west Alexandria, Egypt.

The overall accuracy of the K-means unsupervised classification was calculated using a confusion matrix. This was calculated using the original QuickBird image by defining the fields, which they are known as maize during the field work visit. Also,

other classes such as melon, tomato, bare soil and water surfaces were considered as different classes. A confusion matrix was applied following the same routine explained for wheat images. Table 6.16 shows the statistics of the confusion matrix including the overall accuracy, Kappa coefficient and the individual classification accuracy for each class. The results show that the classification accuracy is generally high (80.62%). However, the classification accuracies derived for various classes are different ranging from 58.12 (for tomato fields) to 94.13% (for water surfaces). The classification accuracy for maize crops is very high (93.46). The low accuracy derived for tomato crop may be attributed to many mixed pixels. This may be explained by the spectral confusion between tomato and other targets on the ground or to the mixed pixels between tomato and bare soil. Additionally, the growth stage of tomato may be another factor that leads to the spectral confusion since at early growth stage the vegetation cover is very low and the soil background affects the classification accuracy. It is also notable that the lowest producer's accuracy was associated with tomato crop, which shows that the ground reference data for tomato crop were not accurately defined. The classification accuracy is supported by high kappa coefficient value of 0.758. An accuracy of 93.46% in maize identification may lead to many misclassified pixels as the associated user's accuracy for maize crop is low (61.91%) in comparison to other targets.

**Table 6-16** Confusion matrix results for the k-means unsupervised classification of maize and other objects in south-west Alexandria, Egypt.

| **Class** | **Ground truth (Percent)** | | | | | | **User's** |
|---|---|---|---|---|---|---|---|
| | **Maize** | **Tomato** | **Melon** | **Bare soil** | **Water** | **Total** | **Accuracy** |
| Unclassified | 0 | 0 | 0 | 0 | 0 | 0 | (%) |
| Maize | 93.46 | 41.88 | 3.6 | 0.67 | 1.67 | 26.56 | 61.91 |
| Tomato | 6.09 | 58.12 | 2.43 | 0.96 | 32.32 | 20.63 | 59.90 |
| Melon | 0.23 | 0.00 | 93.77 | 3.94 | 0.00 | 19.97 | 95.73 |
| Bare soil | 0.23 | 0.00 | 0.00 | 66.01 | 0.29 | 13.39 | 99.80 |
| Water | 0.00 | 0.00 | 0.19 | 0.00 | 94.13 | 19.46 | 99.26 |
| Total | 100 | 100 | 100 | 100 | 100 | 100 | |
| Producer's Accuracy (%) | 93.46 | 58.12 | 93.77 | 94.13 | 66.01 | | |
| Kappa Coefficient | **0.758** | | | | | | |
| Overall Accuracy | **80.62%** | | | | | | |

**Supervised classification**

Unlike unsupervised classification, supervised algorithms start with creating a training dataset then run the classification procedures. From the hyperspectral survey coupled with the QuickBird imagery acquisition, different crops, bare soil and water surfaces were identified. A training dataset was created using spectra derived from the defined classes to run both MLC and MDC algorithms. The training dataset comprised at least 1000 pixels for each class. MLC produced a very high overall accuracy (93.67%), which is the highest among all three classification algorithms (k-means, MLC and MDC). MDC also produced high overall accuracy of 89.94% associated with high Kappa coefficient of 0.874. MLC and MDC algorithms produced high classification accuracies in comparison to k-means unsupervised classification (80.62%).

Although the classification accuracy obtained using unsupervised classifications was high, the accuracy for each class varied and was very low for tomato crop. Figure 6.35 shows the supervised classified QuickBird image showing different crops. The class in red colour shows maize fields, which is distinct among all classes. The other distinct crops over the whole scene are tomato and melon in green and blue colours, respectively. Some mixed pixels were detected in the image particularly the very small fields close to each other with different crops. Sometimes the spectral confusion occurs as a result of plant health status since there are some very healthy and very stressed fields. For example, some farmers do not follow the correct agricultural rotations (growing the same crop every season), which affect crop health indirectly even when applying the optimum rates of nitrogen, seed rate, crop variety, optimum sowing date and irrigation interval.

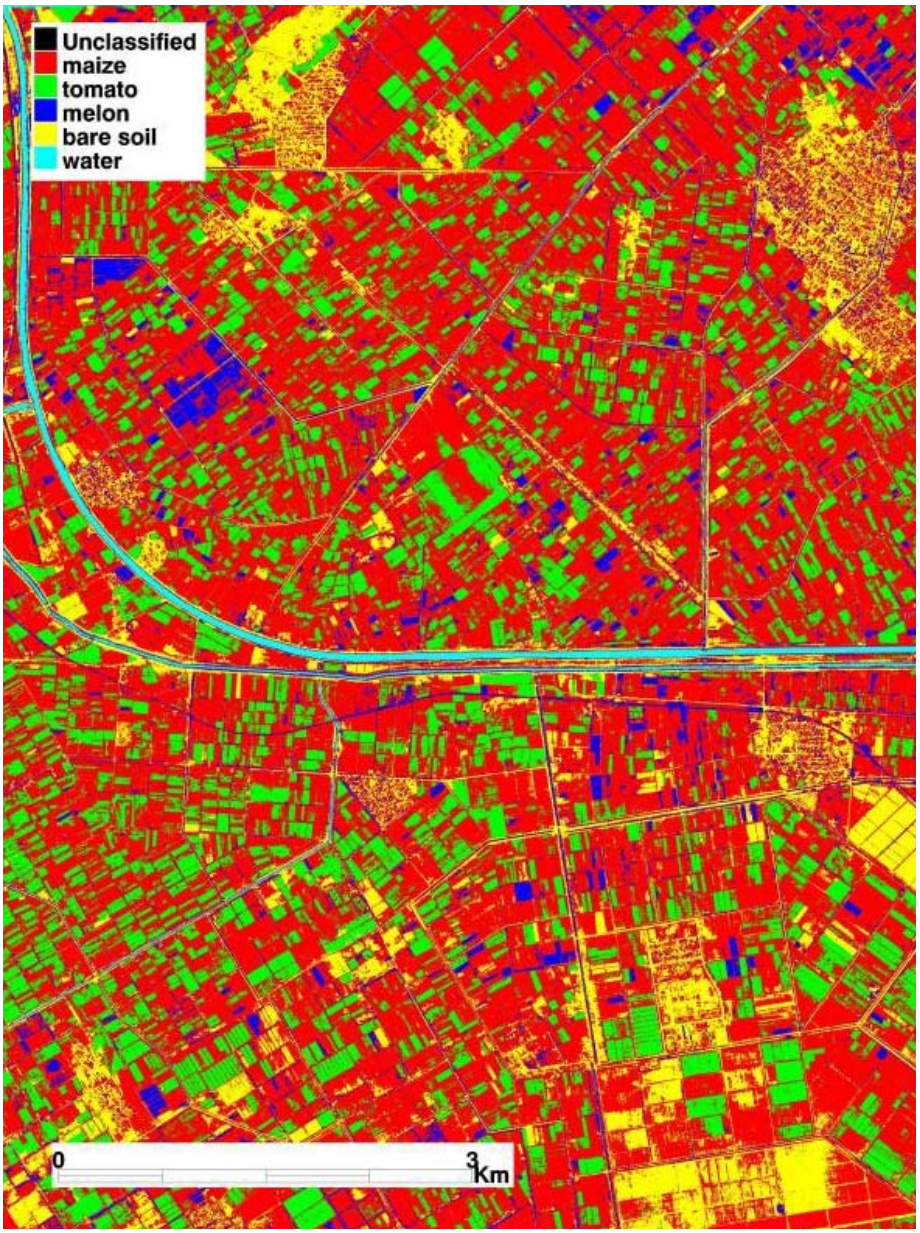


**Figure 6-35** Minimum distance supervised classification of QuickBird image acquired on 29th June 2007 for maize and other crops in south-west Alexandria, Egypt.

To evaluate the classification methods, a confusion matrix was derived from both MLC and MDC classifications of the QuickBird imagery by identifying a validation dataset, which was independent from the training dataset. The validation dataset composed at least 1000 pixels for each class. The results of the confusion matrix showed that the overall classification accuracy derived from MLC for all different classes is high ranging from 89.87 (for maize) to 96.79% (for water surfaces) and from 85.10 (for tomato crop) to 96.71% (bare soil) with MDC classifier. User's and producer's accuracy were high in both MLC and MDC (> 0.85) supporting the high overall accuracy.

It is further noticed that the lowest classification accuracy obtained from k-means unsupervised classification was observed with the tomato crop. The user's and producer's accuracies were also very high (> 80%) with all classes in both MLC and MDC. It can also be seen that the classification accuracy for identifying maize crops using MLC and MDC was very high (> 0.80) with high classification accuracies for other classes. Although k-means classifier produced very high classification accuracy for maize (93.46), it produced very low accuracy for identifying tomato. This leads to many misclassified pixels and therefore low overall accuracy. Consequently, unsupervised classification produced very high accuracy for identifying maize fields, but the overall accuracy and classification accuracy for individual classes are lower in comparison to supervised classification algorithms (Table 6.16, 6.17 and 6.18). Furthermore, Kappa coefficient values in supervised algorithms are comparable to those obtained from k-means classifier.

The results suggest that supervised classification algorithms showed high overall accuracy and individual classification accuracy in the same time for identifying various classes. The low classification accuracy for tomato may have been a result of wide furrows that farmers use for growing tomato, which are sometimes around 1 meter in width so at early growth stages most of the soil is bare and there is strong possibility of background effects.

It can be seen from the confusion matrix results that the overall accuracy and the individual classification accuracy for identifying different classes are higher for summer season imagery than those obtained from winter season imagery which, may be a result of the effects of clouds and associated shadows on classification accuracy. Moreover, Kappa coefficient values for summer season imagery were comparable to those of winter season imagery. The spectral confusion resulted from both clouds and associated shadows affecting the overall accuracy and other parameters. For example, too many water pixels were identified as shadow, which therefore led to many mixed pixels in the image.

**Table 6-17** Confusion matrix results for MLC algorithm of maize and other crops in south-west Alexandria, Egypt.

| Class | Ground truth (Percent) | | | | | | User's |
|---|---|---|---|---|---|---|---|
| | **Maize** | **Tomato** | **Melon** | **Bare soil** | **Water** | **Total** | **Accuracy** |
| Unclassified | 0.00 | 0.00 | 0.00 | 0.00 | 0.00 | 0.00 | (%) |
| Maize | 89.87 | 4.66 | 5.1 | 4.07 | 0.00 | 20.81 | 86.70 |
| Tomato | 3.28 | 93.67 | 1.67 | 0.19 | 0.00 | 19.98 | 94.82 |
| Melon | 2.06 | 0.19 | 92.40 | 0.00 | 0.09 | 19.25 | 97.55 |
| Bare soil | 4.78 | 1.49 | 0.46 | 95.74 | 3.12 | 20.60 | 90.40 |
| Water | 0.00 | 0.00 | 0.37 | 0.00 | 96.79 | 19.36 | 99.61 |
| Total | 100 | 100 | 100 | 100 | 100 | 100.00 | |
| Producer's Accuracy (%) | 89.87 | 93.67 | 92.4 | 95.74 | 96.79 | | |
| Kappa Coefficient | **0.921** | | | | | | |
| Overall Accuracy | **93.67%** | | | | | | |

**Table 6-18** Confusion matrix results for MDC algorithm of maize and other crops in south-west Alexandria, Egypt.

| Class | Ground truth (Percent) | | | | | | User's |
|---|---|---|---|---|---|---|---|
| | **Maize** | **Tomato** | **Melon** | **Bare soil** | **Water** | **Total** | **Accuracy** |
| Unclassified | 0.00 | 0.00 | 0.00 | 0.00 | 0.00 | 0.00 | (%) |
| Maize | 84.43 | 11.64 | 7.60 | 3.19 | 0.38 | 21.54 | 78.67 |
| Tomato | 10.69 | 85.10 | 1.30 | 0.10 | 0.00 | 19.64 | 87.63 |
| Melon | 0.94 | 0.00 | 91.10 | 0.00 | 5.67 | 19.83 | 93.35 |
| Bare soil | 3.94 | 3.26 | 0.00 | 96.71 | 1.32 | 20.53 | 91.65 |
| Water | 0.00 | 0.00 | 0.00 | 0.00 | 92.63 | 18.46 | 100.00 |
| Total | 100.00 | 100.00 | 100.00 | 100.00 | 100.00 | 100.00 | |
| Producer's Accuracy (%) | 84.43 | 85.10 | 91.10 | 96.71 | 92.63 | | |
| Kappa Coefficient | **0.874** | | | | | | |
| Overall Accuracy (%) | **89.94** | | | | | | |

Before calculating vegetation indices and to convert radiance obtained from QuickBird image to reflectance; the reflectance obtained from the three-day *in situ* hyperspectral survey (combined dataset) and the radiance obtained from the QuickBird satellite image were used for regression analysis to convert radiance to reflectance. The results of the regression analysis showed significant relationships in band 1, 2 and 3 ($R^2$ = 0.65, 0.66 and 0.65 respectively). However, the relationship was very poor in the NIR (band 4) with a very low coefficient of determination of 0.02 (p = 0.380). Due to this poor relationship in the NIR region, this method for converting radiance to reflectance is not useful since band 4 is very important to calculate most broad band vegetation indices. The results therefore suggest that

converting radiance to reflectance needs a lot of reflectance measurements from fixed ground control points to be dependable for conversion.

### 6.5.4 Application of vegetation indices for stress

Twelve broad band vegetation indices were derived from the QuickBird satellite image acquired on 29th June 2007. The coefficient of correlation for the relationships between different indices and both biophysical and biochemical properties of maize crops collected from the study area is detailed in Tables 6.19-6.22. The data collected on 12th, 14th and 15th July were used separately. Then the combined dataset from the three day survey was used to investigate the potential of different broad band indices to detect stress in maize crops. The results from the 12th July dataset demonstrated that all vegetation indices produced high significant correlations for predicting biomass, LAI and plant height. Unexpectedly, RVI produced non-significant correlation with the measured chlorophyll concentration. SI produced the highest correlations to predict chlorophyll, plant height and LAI (r = -0.669, -0.966 and -0.943 respectively). Strong correlations were also observed between both $GNDVI_{br}$ and NDVI and different crop properties. NDVI, SAVI, OSAVI and IPVI produced the strongest correlation for predicting aboveground biomass (r = 0.98).

The 14th July dataset demonstrated similar results for predicting chlorophyll concentration as the highest correlation was also recorded with SI (r = -0.719). All vegetation indices were significantly correlated with different crop properties. The strongest correlations for predicting biomass, plant height, and LAI were recorded with NDVI (r = 0.874, 0.876 and 0.804 respectively). It can be noticed from different tables that some indices produce approximately similar correlations for predicting crop properties. For example, GNDVIbr, SAVI, OSAVI and IPVI produced similar correlations to NDVI for predicting biomass, plant height and LAI.

The 15th July dataset showed very strong correlations between all vegetation indices and maize biophysical and biochemical properties (r > 0.90). $GNDVI_{br}$ gave the strongest correlation with the measured chlorophyll concentration while SI produced the strongest correlations with the measured biomass, plant height and LAI (r = -0.980, -0.991 and 0.970 respectively). It can be seen that $GNDVI_{br}$ and NDVI produced approximately similar correlations with different maize properties. The combined dataset from the three-day survey was used to choose the best index for

predicting each crop property (see Table 6.22). As expected SI produced the strongest correlation with the measured chlorophyll concentration (r = -0.785). $GNDVI_{br}$ produced the strongest correlation with the measured biomass, plant height and LAI (0.914, 0.926 and 0.892 respectively). NDVI produced approximately similar results obtained with $GNDVI_{br}$.

From both individual and the combined datasets, it is further noticed that $GNDVI_{br}$ is a sensitive indicator of different maize crop properties. It is shown in Table 6.22 that NDVI and $GNDVI_{br}$ produced similar correlations with different maize properties. The strong relationships between different indices and maize properties may have been a result of the sensitivity of maize crops to stress and therefore large differences between healthy and stressed fields. Generally the majority of vegetation indices produced strong correlations with maize properties.

Comparing the results derived from *in situ* hyperspectral survey and QuickBird satellite image, it is shown in Tables 6.7 and 6.22 that NDVI derived from both datasets demonstrated strong significant correlations with chlorophyll concentration. $GNDVI_{br}$ derived from both datasets produced high significant correlations with maize biophysical properties. The majority of indices derived from both datasets were significantly correlated with each other. The only exception was VI1 derived from *in situ* data since it produced non-significant correlations with maize crops while gave significant correlations with QuickBird satellite data.

**Table 6-19** Coefficient of correlation for the relationship between different broad band vegetation indices derived from QuickBird image and maize biophysical and biochemical properties data collected on 12th July 2007 in south-west Alexandria, Egypt. Highlighted values are significant (P<0.05) and bold values are the strongest correlation values.

| Date | Vegetation index | Crop properties | | | |
|---|---|---|---|---|---|
| | | Chlorophyll | Biomass | Height | LAI |
| 12July | NDVI | **0.602** | **0.983** | 0.942 | 0.933 |
| | RVI | 0.429 | 0.932 | 0.839 | 0.862 |
| | SAVI | 0.602 | **0.983** | 0.942 | 0.933 |
| | $GNDVI_{br}$ | 0.623 | 0.981 | 0.952 | 0.934 |
| | DVI | 0.561 | 0.978 | 0.924 | 0.922 |
| | SR | 0.429 | 0.932 | 0.839 | 0.862 |
| | SLAVI | 0.602 | **0.983** | 0.942 | 0.933 |
| | OSAVI | 0.602 | **0.983** | 0.942 | 0.933 |
| | VI1 | 0.476 | 0.951 | 0.871 | 0.886 |
| | RDVI | 0.584 | 0.981 | 0.934 | 0.929 |
| | SI | **-0.669** | -0.979 | **-0.966** | **-0.943** |
| | IPVI | 0.602 | **0.983** | 0.942 | 0.933 |

**Table 6-20** Coefficient of correlation for the relationship between different broad band vegetation indices derived from QuickBird image and maize biophysical and biochemical properties data collected on 14th July 2007 in south-west Alexandria, Egypt. Highlighted values are significant (P<0.05) and bold values are the strongest correlation values.

| Date | Vegetation index | Crop properties | | | |
|---|---|---|---|---|---|
| | | Chlorophyll | Biomass | Height | LAI |
| 14 July | NDVI | 0.709 | **0.874** | **0.876** | **0.804** |
| | RVI | 0.639 | 0.854 | 0.836 | 0.763 |
| | SAVI | 0.709 | **0.874** | **0.876** | **0.804** |
| | $GNDVI_{br}$ | 0.693 | **0.874** | 0.871 | 0.798 |
| | DVI | 0.712 | 0.817 | 0.844 | 0.769 |
| | SR | 0.639 | 0.854 | 0.836 | 0.763 |
| | SLAVI | 0.709 | **0.874** | **0.876** | **0.804** |
| | OSAVI | 0.709 | **0.874** | **0.876** | **0.804** |
| | VI1 | 0.639 | 0.860 | 0.841 | 0.767 |
| | RDVI | 0.716 | 0.853 | 0.866 | 0.793 |
| | SI | **-0.719** | -0.856 | -0.869 | -0.799 |
| | IPVI | 0.709 | **0.874** | **0.876** | **0.804** |

**Table 6-21** Coefficient of correlation for the relationship between different broad band vegetation indices derived from QuickBird image and maize biophysical and biochemical properties collected on 15th July 2007 in south-west Alexandria, Egypt. Highlighted values are significant (P<0.05) and bold values are the strongest correlation values.

| Date | Vegetation index | Crop properties | | | |
|---|---|---|---|---|---|
| | | Chlorophyll | Biomass | Height | LAI |
| 15 July | NDVI | 0.969 | 0.975 | 0.987 | 0.963 |
| | RVI | 0.956 | 0.946 | 0.964 | 0.933 |
| | SAVI | 0.969 | 0.975 | 0.987 | 0.963 |
| | $GNDVI_{br}$ | **0.970** | 0.977 | 0.987 | 0.964 |
| | DVI | 0.936 | 0.935 | 0.974 | 0.921 |
| | SR | 0.956 | 0.946 | 0.964 | 0.934 |
| | SLAVI | 0.969 | 0.975 | 0.987 | 0.962 |
| | OSAVI | 0.969 | 0.975 | 0.987 | 0.963 |
| | VI1 | 0.962 | 0.955 | 0.969 | 0.942 |
| | RDVI | 0.956 | 0.959 | 0.984 | 0.946 |
| | SI | -0.965 | **-0.980** | **-0.991** | **-0.969** |
| | IPVI | 0.969 | 0.975 | 0.987 | 0.963 |

**Table 6-22** Coefficient of correlation for the relationship between different broad band vegetation indices derived from QuickBird image and maize biophysical and biochemical properties collected on 12-15th July 2007 in south-west Alexandria, Egypt. Highlight values are significant (P<0.05) and bold values are the strongest correlation values.

| Date | Vegetation index | Crop properties | | | |
|---|---|---|---|---|---|
| | | Chlorophyll | Biomass | Height | LAI |
| 12-15 July Combined | NDVI | 0.754 | 0.909 | 0.919 | 0.889 |
| | RVI | 0.585 | 0.788 | 0.799 | 0.794 |
| | SAVI | 0.754 | 0.909 | 0.919 | 0.889 |
| | $GNDVI_{br}$ | 0.759 | **0.914** | **0.926** | **0.892** |
| | DVI | 0.722 | 0.857 | 0.882 | 0.849 |
| | SR | 0.585 | 0.788 | 0.799 | 0.794 |
| | SLAVI | 0.754 | 0.909 | 0.919 | 0.889 |
| | OSAVI | 0.754 | 0.909 | 0.919 | 0.889 |
| | VI1 | 0.644 | 0.844 | 0.852 | 0.838 |
| | RDVI | 0.742 | 0.888 | 0.905 | 0.874 |
| | SI | **-0.785** | -0.909 | **-0.926** | -0.889 |
| | IPVI | 0.754 | 0.909 | 0.919 | 0.889 |

To extrapolate the results obtained from the *in situ* hyperspectral survey and QuickBird imagery, NDVI, SI and $GNDVI_{br}$ maps were created from the QuickBird image using the band math procedure in ENVI (Figures C3-5). Following the image being classified; the derived maps were then masked just to have these areas containing maize crops. Some fields known as maize from the fieldwork visit were used to create ground reference dataset of maize then used to mask the image to show maize fields only. $GNDVI_{br}$ map shows the dissimilarities between healthy and stressed fields over the whole area. It can be seen from the image that the main irrigation canal at the middle of the image nearly divides the site into two areas. The upper area represents fields which are irrigated directly from this canal without using any type of pumping stations and therefore irrigation water is available all the time. However, the area below this canal is irrigated from small channels, which are supplied with water by irrigation pumping stations and consequently water is not available all the time.

It can be further seen from $GNDVI_{br}$ map that healthy maize fields have greater $GNDVI_{br}$ values which coloured in red. Few fields in the upper half were coloured in purple producing low values of $GNDVI_{br}$ (>0.25) as a result of sub-optimum agricultural practices. However, at least one third of the lower half is coloured in purple giving $GNDVI_{br}$ values less than 0.25 which is obvious evident for stress in that area particularly the right bottom corner. This area is suffering from severe

moisture stress every summer since a massive amount of water is consumed by rice crops in the Nile Valley and Delta (0.59 million hectare), which therefore decrease the water flow in main canals nationwide especially the ends of these canals. It can also be seen in the above mentioned figures that the upper left corner of the lower half produced high values of $GNDVI_{br}$ in comparison to the rest of that half. This can be attributed to the source of irrigation water since that area is also irrigated directly from the main canal. The regression equations for the relationship between biophysical properties of maize and $GNDVI_{br}$ were calculated to extrapolate the results across the study area (figure 6.36).

The regression analysis was performed between $GNDVI_{br}$ as a sensitive index for different maize properties and biophysical and biochemical properties of maize including biomass, plant height, LAI and chlorophyll concentration. The combined dataset from the three-day survey was used for this analysis.

| | | |
|---|---|---|
| Biomass = -1.33 + 16.9 $GNDVI_{br}$ | $R^2 = 0.84$ | p = 0.000 |
| LAI = -0.42 + 6.87 $GNDVI_{br}$ | $R^2 = 0.80$ | p = 0.000 |
| Plant height = 0.03 + 3.44 $GNDVI_{br}$ | $R^2 = 0.86$ | p = 0.000 |
| Chlorophyll = 29.1 + 34.9 $GNDVI_{br}$ | $R^2 = 0.58$ | p = 0.000 |

A strong positive linear relationship between $GNDVI_{br}$ and the measured aboveground biomass is shown in Figure 6.38 ($R^2 = 0.84$; p = 0.000). $GNDVI_{br}$ also showed a significant relationship with the chlorophyll concentration ($R^2 = 0.58$). The decrease in the relationship between chlorophyll concentration and different vegetation indices may be a result of the time difference between field sampling and satellite imagery acquisition. The two weeks difference can make a great change in maize properties particularly chlorophyll concentration. For example, when a farmer applies a dose of nitrogen to crops it significantly changes the chlorophyll concentration especially if it is the first dose and crops are suffering from nitrogen deficiency.

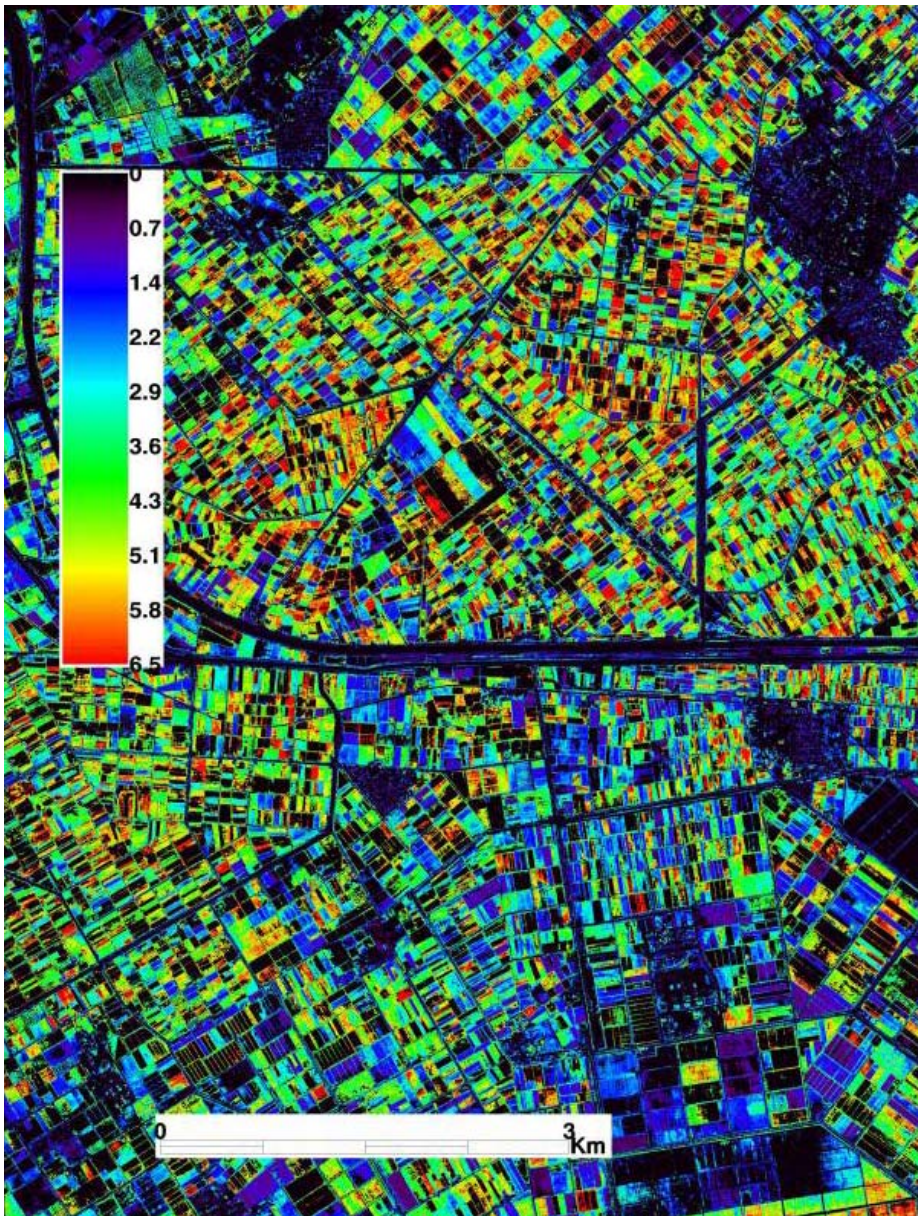


**Figure 6-36** classified QuickBird (GNDVI) image acquired on 29th June calibrated to Aboveground biomass of maize crops in south-west Alexandria, Egypt.

Also, SI map was used to create a map for predicting chlorophyll concentration. The regression analysis was performed to determine the regression equation between SI and chlorophyll concentration and extrapolate the results across the whole image. Figure 6.37 show a map for predicting chlorophyll concentration for maize crops in the study area south-west Alexandria.

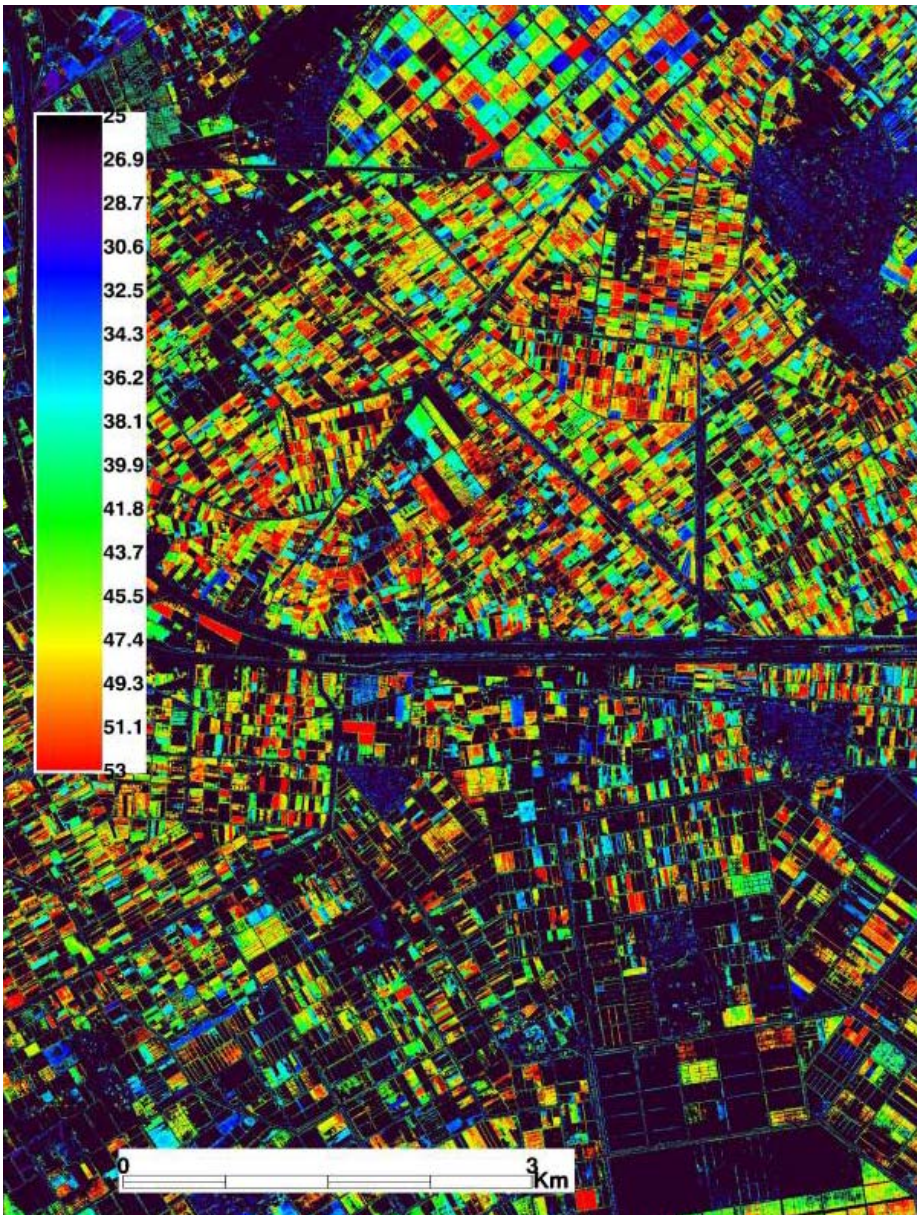


**Figure 6-37** classified QuickBird (SI) image acquired on 29th June calibrated to chlorophyll concentration of maize crops in south-west Alexandria, Egypt.

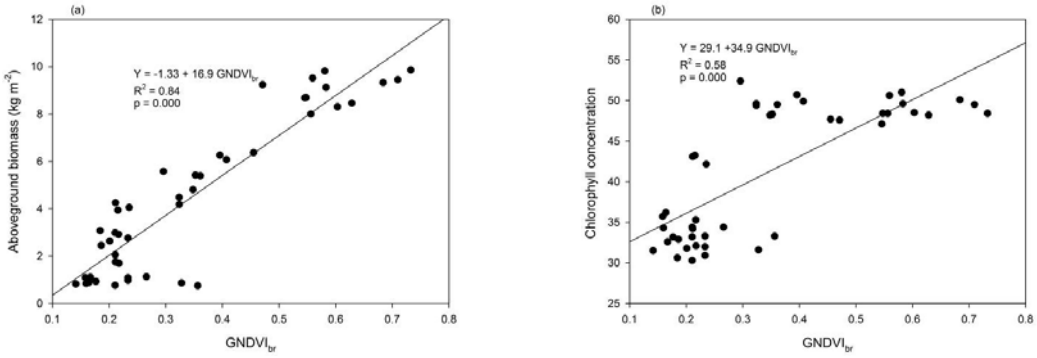


**Figure 6-38** The relationship between $GNDVI_{br}$ derived from QuickBird image and (a) aboveground biomass of maize and (b) chlorophyll concentration of maize leaves collected in south-west Alexandria, Egypt (n = 45).

The relationship between *in situ* hyperspectral measurements and satellite data was investigated through regression analysis. The combined dataset collected during the three-day survey was used for this analysis. $GNDVI_{br}$ was derived from both *in situ* and QuickBird satellite imagery for same fields then the regression analysis was performed to determine the regression equation between $GNDVI_{br}$ derived from both datasets (Figure 6.39). A significant linear relationship between $GNDVI_{br}$ obtained from both platforms is shown ($R^2 = 0.75$; $p = 0.000$). Some outliers which may be due to changes in weather conditions during measuring reflectance were detected. It should be mentioned that maize crops in south-west Alexandria grow very quickly during July and August and therefore great differences exist in plant properties including plant height, leaf area and biomass. During July and August, temperatures are at their maximum and as a result the evapotranspiration increases.

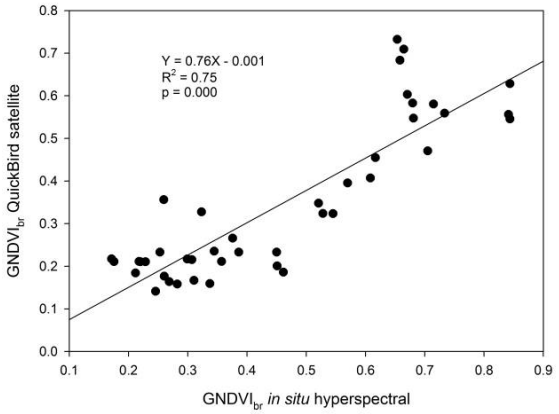


**Figure 6-39** The relationship between $GNDVI_{br}$ derived from *in situ* hyperspectral measurements and $GNDVI_{br}$ derived from QuickBird satellite image (n = 45).

## 6.6 Stress detection at regional scales

In order to detect stress at a regional scale the SPOT HRV image acquired on 9th July was used to extrapolate the results across south-west Alexandria, Egypt. As mentioned before, the spatial resolution of SPOT HRV image (20 m) produced some mixed pixels particularly from small fields. The classified SPOT HRV image (Figure 6.40) was used to assess trends in plant stress across the whole region. Following image processing, the image was classified using k-means unsupervised classification. Then two classes of maize and two of bare soil were combined in one class each using post classification in ENVI. Applying supervised classification algorithms is problematic since it is difficult to create a training datasets for maize crops due to mixed pixel effects. The image then was masked just for maize crop using image masking procedure.

NDVI map was created using the masked image to predict plant health in the whole region. It is noticed that stress is obvious at the edge of the cultivated area and plant health increases towards the Delta centre. It can be seen that the values of NDVI increase gradually from the far west and south west to inside the Delta. This can be attributed to many factors; firstly, the study area is a newly reclaimed area, which was originally desert and soil fertility is very low in comparison to the old Valley and Delta. People try to overcome this deficiency by adding manure and chemical fertilizers. Secondly, most fields in that area suffer from moisture stress particularly during the summer season due to the large area cultivated for rice, which consumes a massive amount of the available water. Furthermore, the weather conditions in that area may affect plant health since it is close to an extensive area of desert (the West Desert).

Interestingly, it is noticeable that there are some circular patches of very healthy fields and they are quite large. These fields are owned by private companies, which follow the optimum agricultural practices. They are irrigated using a sprinkler irrigation system called centre pivot which is capable of irrigating between 50-100 hectare circular areas depending on the length of the system. Chemicals such as fungicides and pesticides are applied through irrigation system so the chemicals are distributed uniformly. Also, fertilizers are applied to fields through the system to insure high fertilization use efficiency over the whole field and therefore low spatial variability.

The results suggest that using satellite remote sensing to detect stress in crops in large field-system will be a highly effective tool since large fields enable researchers to have fewer mixed pixels and therefore pure spectral signatures for training and the ground-reference datasets. This will decrease the variation within the same field and therefore increase the classification accuracy obtained by different algorithms. In addition, although lacking spatial detection within and across small fields, the broad underlying trends can still be observed. Improvements in remote sensing capabilities in terms of spectral and spatial resolution and the number of bands seem to increase the efficiency of this technique to detect stress in crops. For example, satellite images of less than 1 m spatial resolution with sufficient number of spectral bands in such a small-field system can be very beneficial in distinguishing between moisture and salinity stress.

In a large-field system, using a high spectral resolution satellite imagry such as Hyperion (more than 200 spectral bands) would increase the ability of this technique to show dissimilarities between different fields as a result of changes in physiological properties of plants and even distinguish between different sources of stress. The *in situ* hyperspectral measurements demonstrated that there are wavelengths sensitive to specific types of stress such as moisture stress (Penuelas *et al*., 1997b). In this context, Hyperion satellite imagery would be very useful in distinguishing different sources of stress. Improvements in Hyperion satellite specifications in terms of spatial resolution seem to be very beneficial in detecting stress and even distinguishing between different types of stress.

The new generation of hyperspectral satellites, VENUS and HyspIRI, with high spectral capabilities may provide useful information in detection stress at regional scale. Moreover, this will enhance the capability of distinguishing sources of stress such as moisture and salinity induced stress.

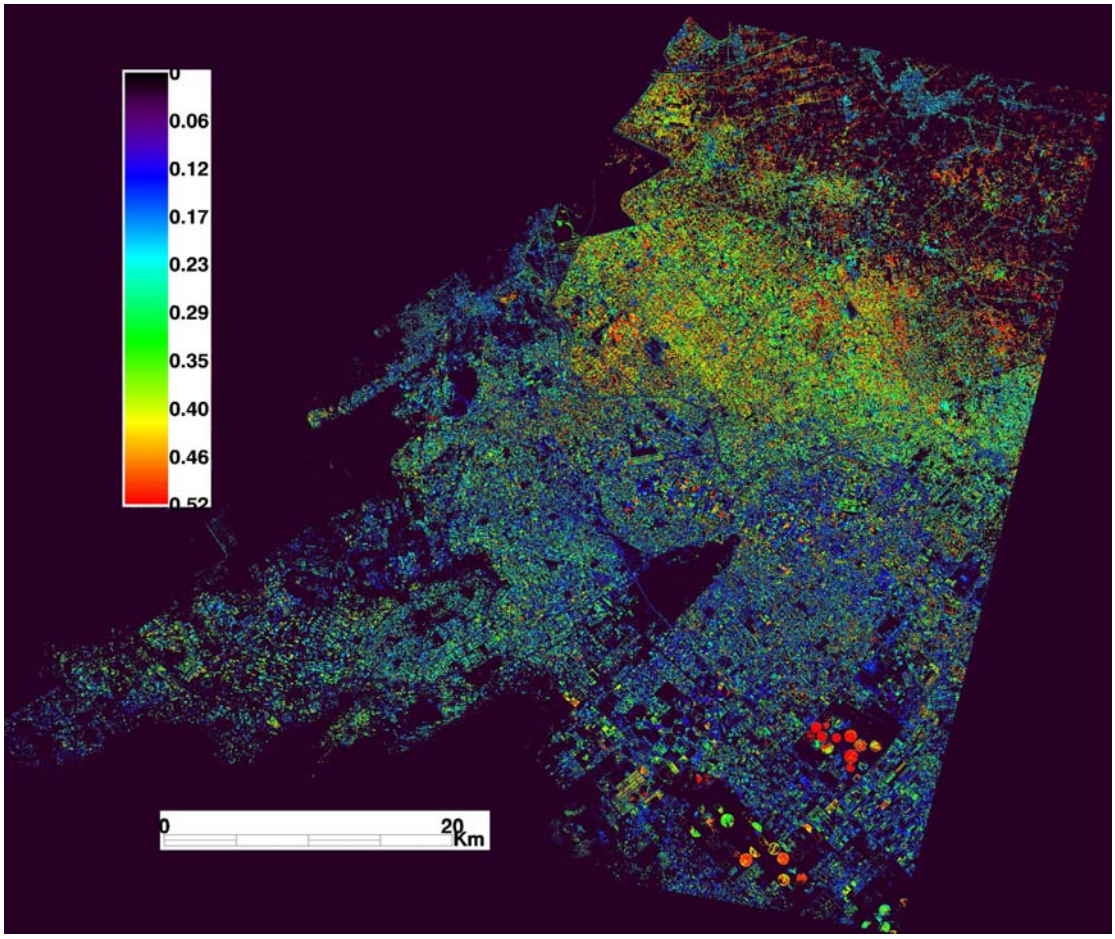


**Figure 6-40** A NDVI map derived from SPOT HRV image acquired on 9th July 2007 in south-west Alexandria, Egypt.

## 6.7 Summary

The potential of remotely sensed data, both ground based and satellite based, to detect stress in wheat and maize was investigated in this chapter. *In situ* hyperspectral survey was undertaken twice in summer and winter seasons of 2007 at a study area south-west Alexandria, Egypt. High spatial resolution satellite imagery including QuickBird, ASTER and SPOT HRV were used for this research to detect stress at local and regional scales to extrapolate the results obtained by *in situ* hyperspectral survey. High spectral resolution satellite imagery (Hyperion) was planned and requested two times for both winter and summer season crops, but there was no imagery available due to weather conditions in winter season of 2007 and tasking conflicts and sensor calibration requirements in summer season of 2007.

Green, red and NIR ratios were derived from both *in situ* hyperspectral and QuickBird satellite images to evaluate the efficiency of remotely sensed data in detecting stress in wheat and maize crops. Twelve broad band spectral vegetation indices were derived from *in situ* hyperspectral measurements and the results demonstrated that the majority of the twelve vegetation indices had significant correlations with the measured biophysical and biochemical properties of both wheat and maize. Reflectance measurements showed variations between healthy fields and fields suffering moisture and salinity stress, particularly with maize crops. In addition, the results obtained using the principle component analysis showed the potential to distinguish between moisture and salinity induced stress in maize crop as a broader leaved crop. However, some overlap occurred between salinity and moisture induced stress with spectra collected from wheat fields.

To extrapolate the results derived from *in situ* hyperspectral survey, high spatial resolution satellite images were used. Vegetation indices from satellite image were evaluated to define the best indices to create maps for detecting different wheat and maize properties. NDVI, SI and $GNDVI_{br}$ demonstrated strong significant correlations with different crop properties. The results collected for maize crop showed that the correlation coefficient between crop properties and vegetation indices derived from both *in situ* and satellite platforms were significant at most dates of measurements. The coefficient of correlation for the relationship between NDVI derived from *in situ* hyperspectral and NDVI derived from QuickBird image was usually significant ($r > 0.75$). The results also demonstrated the possibility of using satellite data to detect stress in wheat. As a tolerant crop grown in winter season, the correlations between NDVI and crop properties were significant, but distinguishing between moisture and salinity stress always associated with some overlap. As expected the results obtained for maize gave better results compared with those of wheat due to the sensitivity of maize to different stressors.

High spectral satellite remote sensing imagery (Hyperion) is needed for distinguishing moisture and salinity induced stress since Hyperion satellite imagery has more than 200 spectral bands, which provide the ability to calculate different hyperspectral vegetation indices and detect wavelengths sensitive to both moisture and salinity stressors. Furthermore, a combined approach of high and moderate spatial resolution

satellite images can give good indicator about stress trends at both local and regional scales. However, high spatial resolution satellite imagery can not distinguish between moisture and salinity induced stress spectrally due to limited number of spectral bands. Some other satellite images such as Hyperion and HyspIRI can be used to distinguish between the two types of stress.

It can be concluded that remote sensing has the potential to be a robust technique in detecting stress in agronomic crops particularly arid and semi arid regions since most crops suffer from some types of stress such as moisture and salinity stress. In addition, remote sensing may provide a useful tool to assess the demand for redesigning irrigation systems in countries such as Egypt and therefore expanding the cultivated area to tackle the rapid population growth. The research in this chapter succeeded in proving the hypothesis that *in situ* and high spatial resolution remote sensing imagery can predict stress in maize and wheat through predicting changes in biophysical and biochemical properties of both crops.

# 7 DISCUSSION AND CONCLUSIONS

## 7.1 Introduction

The main objective of most agronomists is to increase crop productivity to sustain the massive worldwide increase in population. However, increasing crop productivity is hindered by many stress factors including drought, salinity, pollution, fertilizer deficiency and disease. Monitoring crop health by sample-point technique is tedious, laborious and a costly process. There is therefore a demand to improve the monitoring of plant status at a large scale to achieve greater productivity. Remote sensing and precision farming are relatively new techniques used in the field of agronomy to target resource and improve crop production (Brisco *et al*., 1998). In this context, remote sensing has the potential of providing much valuable information on crop stress and its management in Egypt.

Salinity and drought are major inhibitors to crop production and increasing efforts to remotely detect the effects of both moisture and salinity induced stress for irrigation management are important in semi arid and arid environments. A few studies have shown the ability of remote sensing technology to detect the impacts of water and salinity stress on crop yields (Poss *et al*., 2006). Research and technology advances in the field of remote sensing have greatly enhanced the ability to detect and quantify physical and biological stresses that affect the productivity of agricultural crops (Hong *et al*., 2007). Before launching the first generation of high spatial resolution IKONOS and QuickBird satellite imagers in 1999 and 2001, satellite imagery had limited use in precision farming as a result of coarse spatial resolution, long revisit period and slow data delivery (Yang *et al*., 2006b). In this context, this thesis examines the efficacy of implementing remote sensing to detect stress in wheat and maize crops in the Nile Valley of Egypt. The chapter addresses each of the hypotheses outlined in Chapter 2 (see section 2.6).

### 7.1 The association between crop productivity and moisture and salinity stress

The first hypothesis tested in this research was *moisture and salinity induced stress affect crop grain yield.*

Moisture and salinity stressors are inhibitors of crop productivity. The results from this research showed that both moisture and salinity stress had significantly affected different agronomic parameters of both wheat and maize crops including; grain yield, biomass, plant height, LAI and chlorophyll concentration. Multiple regression analysis showed strong and significant relationships between wheat grain yield and both moisture and salinity induced stress ($R^2 > 0.85$ in the four experiments of wheat). The watering regime of 25% FC reduced wheat grain yield by 78, 69, 61, and 58% in the 2005-6, 2006 and 2006-7 growing seasons with biggest impact on Scottish wheat in the 2005-6. Salinity level of 6 dS $m^{-1}$ decreased wheat grain yield by 46, 26, 45, and 40% in the 2005-6, 2006 and 2006-7 growing seasons respectively. The decrease in wheat grain yield can be attributed to the effects of both stressors on all agronomic parameters. During the vegetative growth, plant height, leaf area, and tiller number were affected by both moisture and salinity and therefore the aboveground biomass was also decreased. Multiple regression analysis also showed strong significant relationships between aboveground biomass and both moisture and salinity stress ($R^2 > 0.80$ in all experiments). Furthermore, both stressors had significantly affected LAI, chlorophyll concentration and plant height.

Similar significant relationships were also observed between maize crop yield and both moisture and salinity stressors. Regression analysis demonstrated that moisture and salinity had significantly affected maize grain yield ($R^2 = 0.88$; $p = 0.000$). The highest stress level of moisture and salinity reduced maize yield by 69 and 42% respectively. Also, both stressors had significantly affected aboveground biomass of maize particularly at late stages ($R^2 = 0.91$; $p = 0.000$). Moisture and salinity stress also affected LAI, plant height and chlorophyll concentration ($R^2 > 0.90$; $p = 0.000$). The strong relationships between both stressors and maize may be attributed to the apparent differences between healthy and stressed treatments. It was further noticed that the effects of stress on maize crops were higher in comparison to wheat crops. This can perhaps be explained by the great differences in climatic conditions between summer and winter and therefore the stress level. The broad leaves of maize are likely

to increase the evapotranspiration rate and subsequently any stress greatly affects plant health. Furthermore, wheat crops are tolerant of stress while maize is considered a sensitive crop to different stressors.

These results concur with what is generally known about plant response to moisture and salinity induced stress. Under moisture stress, absorbing nutrients by roots from soil is reduced by decreasing the rate of diffusion of nutrients from the soil matrix to the absorbing root surface (Pinkerton and Simpson, 1986). Nutrient transport from roots to shoots is also limited as a result of low transpiration rates and impaired active transport and membrane permeability (Kramer and Boyer, 1995). Under moderate water stress, partial stomatal closure, which reduces $H_2O$ transpiration and the $CO_2$ available for C fixation, may occur for several hours a day. Plants experiencing moderate stress may not wilt or have photochemical activity impaired (Souza *et al*., 2004). With increasing levels of water deficiency, the plant increasingly appears wilted and the actual photochemical activity of chlorophyll can be reduced (Souza *et al*., 2004).

Previous studies have documented the effects of moisture and salinity on crop productivity. Drought is one of the major limitations to food production worldwide and one of the major stress factors during the maturation and ripening of cereals in many production areas (Barnabas *et al*., 2008). They also stated that plants respond to drought stress at the molecular, cellular and physiological levels depending on the species and genotype, the length and the severity of water loss, stage of development, the organ and cell type and the sub-cellular compartment. Furthermore, they reported that periods of water stress during the grain filling stage caused large yield losses.

High salinity in the soil can result in physiological drought even with high moisture content in the soil profile. The plants wilt because the ability of roots to absorb water and different nutrients is very weak. Under salinity stress conditions, soil contains high levels of the following ratios $Na^+/Ca^{+2}$, $Na^+/K^+$, $Ca^{+2}/Mg^{+2}$ and $Cl^-/NO_3^-$, resulting in specific ion toxicity (Grattan and Grieve, 1999). Salinity always impairs the distribution of macro and micronutrients along the growing leaves of maize (Neves-Piestuna and Bernstein, 2005; Hu *et al*., 2007) and wheat (Hu *et al*., 2000) thereby affecting the rate of growing tissues.

In wheat, final grain yield is affected by the number of tillers, spikes, grain per spike and grain weight. These yield components may be affected by different types of stress. For example, Mass and Poss (1989) in studying the effects of salinity on wheat grain yield; concluded that salinity affected the tiller and spikelet number and therefore greatly affected the final grain yield. During vegetative growth, different agronomic parameters including tiller number, leaf number and LAI decreased with increasing salinity levels (El-Hendawy, 2004).

In conclusion, the experimental work presented here has been undertaken under controlled conditions in terms of temperature, watering interval, irrigation regime and fertilization rates. This eliminates the environmental factors that affect crops in actual fields particularly the amount of rainfall for wheat crops during winter season. The results obtained from this research showed that water having low salinity (2 ds $m^{-1}$) can be used for watering tolerant crops such as wheat with only slight effects on grain yield. This implies that the estimated amount of agricultural drainage water in Egypt (17 billion $m^3$) could be used to extend the cropped area by at least 25% and therefore increases crop production to tackle the problem of rapid population growth.

## 7.2 Using *in situ* measurements in detecting stress in crops

### 7.2.1 Wheat crop

The second tested hypothesis was *in situ hypertspectral measurements can detect stress in crops.*

The experimental work outlined in Chapter 4 and 5 demonstrated the effectiveness of vegetation indices in predicting different biophysical and biochemical properties of wheat. Due to changes in the relationship between different vegetation indices and crop properties over the growing season, the correlation values were ranked for all experiments to choose the optimum index for predicting different biophysical and biochemical properties of wheat. Generally, grain yield was highly correlated with specific vegetation indices at specific growth stages and poorly correlated with others. Poor correlations between different vegetation indices and wheat grain yield were recorded at early growth stages. In the four experiments, milk stage seems the best growth stage to predict wheat grain yield. Ranking showed that the optimum hyperspectral index to detect wheat grain yield is $R_{725}/R_{675}$. In the meantime, RVI and

SR were ranked the best broad band vegetation indices for predicting wheat yield. A strong significant correlation was observed between RVI and wheat yield for the first two experiments (r = 0.91 and 0.96 for the 2005-6 winter season and 2006 spring season respectively).

Ranking also further showed that RDVI is a sensitive indicator for predicting aboveground biomass of wheat. It produced the best index to correlate with wheat biomass in the first two experiments of the Scottish and Egyptian wheat (r = 0.92 and 0.98 for the winter season 2006-7 and spring season 2006). Additionally, RVI was the fourth best index to predict aboveground biomass of the Scottish and Egyptian wheat (r > 0.90). Moreover, RVI was ranked the optimum index for predicting chlorophyll *a* concentration for all wheat experiments. The strongest correlation between RVI and chlorophyll *a* concentration was recorded in the 2006-7 growing season of the Scottish wheat (r = 0.82). Specific indices produced strong correlations at a specific stage, but poor correlations over the growing season. For example, OSAVI produced the highest correlation with the measured chlorophyll *a* concentration (r = 0.84), but lower correlations over the growing season. REP is also a sensitive indicator for chlorophyll *a* concentration in comparison to the majority of the tested broad band and hyperspectral vegetation indices with the strongest correlation of 0.79 recorded in the third experiment.

Other studies have documented the possibility of using remotely sensed data to predict grain yield and other crop properties under different stresses using spectral vegetation indices. Most studies investigated the potential of remotely sensed data at the leaf scale under controlled conditions eliminating the effects of canopy structure. For example, at the leaf scale Marti *et al*. (2007) investigated the possibility of using NDVI to predict wheat biomass and grain yield at early stages, and found that NDVI at milk-grain stage was well correlated to final grain yield and biomass of wheat. Some attempts have been made to detect crop properties under salinity stress. For example, Wang *et al*. (2002a) concluded that canopy spectral reflectance in the NIR region of the spectrum was reduced incrementally with increasing salinity level. Also, Penuelas *et al*. (1997a) reported that changes in barley biophysical properties resulted from salinity stress can be determined with remote sensing technique. Our research examined the potential of remotely sensed data at the canopy scale under controlled

conditions to detect stress in wheat and maize. We have shown that at the canopy scale stress can be detected using both hyperspectral and broad band vegetation indices. Moreover, crop yield can be estimated through remotely sensed data.

Babar *et al*. (2006) employed different vegetation indices at the leaf scale as a potential indirect technique to predict wheat grain yield; they concluded that measuring reflectance at heading and grain filling stages appear to be the most suitable time to differentiate genotypes for wheat grain yield. They also found that RNDVI, GNDVI and SR showed significant positive correlations with grain yield at heading and the grain filling stages in three years cases. Royo *et al*. (2003) investigated the effectiveness of vegetation indices in predicting wheat grain yield and concluded that milk-grain stage shown to be the most appropriate developmental stage for yield assessment. In contrast, other studies demonstrated that the best time to predict wheat grain yield was recorded at maturation not at booting, heading, anthesis or milk-grain stages (Aparicio *et al*., 2000). They also found that RNDVI was correlated well with wheat grain yield. However, the work presented here at the canopy scale has shown that the milk stage seems the best stage for predicting grain yield.

### 7.2.2 Maize crop

Maize is a broader leaved crop than wheat and is therefore assumed to be a crop more susceptible to different types of stress. We hypothesized that *the spectral signature from maize canopy will be greatly affected by physiological changes resulting from both moisture and salinity stress and more so than wheat*. As a sensitive crop, maize needs to be monitored efficiently to manage areas of stress and avoid reduction in crop productivity. The experimental work detailed in Chapter 5 established a strong relationship between maize properties and both broad band and hyperspectral vegetation indices. In this research, 55 hyperspectral and broad band vegetation indices have been examined to predict maize properties under moisture and salinity induced stress. Strong correlations between many vegetation indices and different biophysical and biochemical properties of maize were observed. There was no specific index to predict a crop parameter over the growing season. As a result the coefficient of correlation for the relationship between different vegetation indices and the measured crop properties at different growth stages was ranked to choose the

optimum index for predicting each maize property. $C_{rededge}$ was the optimum vegetation index to predict chlorophyll *a* concentration in maize crop. As mentioned in Chapter 5 the wavelength 550 nm is sensitive to many maize properties. Ranking also showed that the band ratios $R_{750}/R_{550}$ and $R_{800}/R_{550}$ are sensitive for predicting chlorophyll *a* concentration. These two indices were also ranked among the best five indices for predicting maize plant height.

$R_{750}/R_{550}$ was also ranked the fourth best index among 55 indices for predicting maize grain yield. The best ranked index for predicting maize yield was the band ratio $R_{695}/R_{760}$. $GNDVI_{br}$ ranked the most sensitive broad band index for predicting aboveground biomass and LAI. These findings are supported by other studies, for example Shanahan *et al*., (2001) reported that $GNDVI_{br}$ had the strongest correlation with maize grain yield at mid-grain filling stage, which can be used to produce relative yield maps. It is further shown that some vegetation indices produced higher correlations at specific growth stages, but in general poor relationships for the whole growing season. For example, VI1 gave the strongest correlation at 80 DAS at the canopy scale ($r = -0.62$) although it produced non-significant correlations on four dates out of six ($r < 0.20$). $C_{rededge}$ was recorded the optimum index to correlate with chlorophyll *a* concentration of maize leaves. Similar results were obtained by Gitelson *et al*. (2005) as they proposed three different indices to predict chlorophyll concentration, $C_{green}$, $C_{rededge}$ and $C_{NIR}$.

Quantifying crop productivity in cereals is considered a priority in most research programmes (Steinmetz *et al*., 1990) due to urgent need for different grain crops to tackle the rapid increase in population growth worldwide (Rudorff *et al*., 1996). Increased efforts are therefore needed to detect the effects of moisture and salinity induced stress in maize since some studies have shown the potential of remotely sensed data in monitoring maize health status (Blackmer *et al*., 1996; Osborne *et al*., 2002b; Daughtry *et al*., 2000; Hong *et al*., 2007; Wu *et al*., 2007c). However, most research in agricultural crops focused on detecting moisture and nitrogen deficiency stress. Our studies focused on using remotely sensed data in detecting moisture and salinity stress and distinguishing between them spectrally. Previous studies reported the effectiveness or remotely sensed data to detect stress in crops. For example, chlorophyll *a* concentration (Gitelson and Merzlyak, 1996; Cuttler and Curran, 2000;

Sims and Gamon, 2003), Pest damage (Yang *et al*., 2005; Mirik *et al*., 2007; Genc *et al.,* 2008), salinity induced stress (Penuelas *et al*., 1997a; Wang *et al*., 2002a; Wang *et al*., 2002b), pollution stress (Davids and Tyler, 2003) nitrogen deficiency (Osborne, 2004; Schlemmer *et al*., 2005; Reyniers and Vrindts, 2006; Clay *et al*., 2006; Tartachnyk and Rademacher, 2006; Hong *et al*., 2007 ) and moisture stress ( Penuelas and Inoue, 1999; Osborne *et al*., 2002b; Bahrun *et al*., 2003; Ozturk and Aydin, 2004; Tilling *et al*., 2007). The results therefore suggest that spectral vegetation indices derived from hyperspectral measurements can be used successfully to predict wheat and maize properties.

The results further demonstrated that vegetation indices performed inconsistently over the growing season in both wheat and maize crops. There is no specific vegetation index that gives strong correlations with a crop property over the growing season. It is therefore clear that more work is needed to validate the effectiveness of using vegetation indices as a non-destructive tool to predict crop properties.

To the best of the author's knowledge, this research is the first to investigate the potential of remotely sensed data to detect stress in wheat and maize resulting from the combined effects of moisture and salinity stress. Moreover, most scientists who are working to detect stress in crops measure reflectance at the leaf scale (basically apical leaves) ignoring the effects of canopy structure on reflectance measurements, which are arguably important in terms of satellite remote sensing imagery. In this research, measurements at both leaf and canopy scales were used to assess the differences between healthy and stressed plants.

### 7.2.3 Comparison between broad band and hyperspectral vegetation indices in detecting stress in wheat and maize

The sub-hypothesis tested and outlined in Chapters 4 and 5 was *hyperspectral vegetation indices are more sensitive to physiological changes in plant status resulting from stress than broad band vegetation indices*. Twelve broad band and forty three hyperspectral vegetation indices have been examined in this research to detect the biophysical and biochemical properties of wheat and maize. The results demonstrated that there are no great differences between broad band and hyperspectral vegetation indices under both natural and artificial illumination

conditions. The strongest correlations obtained using both hyperspectral and broad band indices were similar in most cases.

The results demonstrated slight differences between broad band and hyperspectral vegetation indices. In all experiments of wheat and maize crops some hyperspectral indices produced slightly higher correlations with a crop parameter than broad band indices. For example, $R_{800}$-$R_{550}$ produced the highest correlations with chlorophyll *a* concentration of maize at the leaf and canopy scales (r = 0.80 and 0.63 respectively), while the highest correlations from broad band indices were obtained with $GNDVI_{br}$ (r = 0.79 and 0.61). Similar to these results, Elvide and Chen (1995) investigated the potential of hyperspectral and broad band vegetation indices in monitoring rooted pinyon pine canopy with five different gravel backgrounds; they reported that hyperspectral vegetation indices had only slightly better accuracy than broad band vegetation indices. Deriving vegetation indices from a dataset measured at the leaf scale produced higher correlations with chlorophyll *a* in comparison to the data collected at the canopy scale. At the leaf scale, the variation in plant architecture is ignored and the effects of different parameters of weather are also ignored. Furthermore, most researchers collect apical leaves and do not consider the effects of leaves at lower levels of the canopy, which contribute to the spectral reflectance. Measuring reflectance from plant canopies under controlled illumination in this research appear to be much more representative for the general plant health rather than specific part of these plants.

### 7.2.4 Distinguishing between moisture and salinity induced stress

The third hypothesis tested in this research was *moisture and salinity induced stress can be distinguished spectrally.*

PCA score plots showed that moisture induced stress in wheat can be distinguished from salinity induced stress at the grain filling stage, but these results are too late for remediation. At the grain filling stage it is too late to take a decision to reduce the effects of stress and avoid crop yield reductions. However, these findings are considered important implications for the following growing seasons and the decision makers can make informed decisions to avoid stress in this area by means of re-designing irrigation system and following optimum agricultural practices. Re-

designing irrigation systems will provide the optimum crop water requirements and consequently increase water use efficiency.

In addition, hyperspectral survey coupled with the acquisition time of satellite imagery showed the possibility of distinguishing between fields suffering from moisture and salinity stress particularly when the stress levels were high (Figures 6.12 and 6.13). However, when the stress level was low overlap between both stressors was detected. Hyperspectral measurements showed that reflectance in the green and red regions of the spectrum in fields with salinity induced stress was always lower than in those with moisture stress. The same trend was also observed in the NIR region as reflectance obtained from fields with moisture induced stress was always higher than those obtained from fields with salinity induced stress (Figure 6.8).

Further work in investigating plant changes as a result of increasing soil salinity is required to validate these findings, and assess exactly which parameters are susceptible to each type of stress and therefore distinguish between these two stressors as early as possible. Other crop properties such as lignin and cellulose should be investigated under both moisture and salinity stress and whether these parameters affect reflectance from plant canopies and/or leaves. Furthermore, use of the SWIR region of the spectrum may provide useful information about plant stress.

## 7.3 Using satellite remote sensing in detecting and differentiating stress

The fourth hypothesis tested in this research was *high spatial resolution satellite remote sensing imagery can detect stress in wheat and maize crops at both local and regional scales at early stages and therefore help maximise crop productivity.*

*In situ* hyperspectral measurements have been documented in the literature as a useful potential tool to predict different biophysical and biochemical crop properties. Due to the lack of spectral and spatial resolution capabilities of satellites in 1980s and 1990s, it was not common to use satellite imagery in detecting crop stress. With the launching of the first hyperspectral satellite (Hyperion) on board Earth Observing-1 by NASA in 2000, the use of hyperspectral data has increased.

### 7.3.1 Identifying crop types (classification)

Different classification algorithms were performed to identify different crops within the study area. Both unsupervised and supervised classification methods were used in this research to choose the most robust classifier for images to identify different crops. K-means of unsupervised classification is widely used in classifying vegetation (Bachmann, 2002; Yang *et al*., 2006a; Yang *et al*., 2006b). Therefore, it was performed on all images of this research. The results showed that k-means classification produced classified image of wheat with slightly high overall accuracy of 77.4%, but produced low classification accuracies for specific classes. The existence of clouds and associated shadows might affect the accuracy of this method and many mixed pixels were detected. For example, the classification accuracy for identifying bare soil was very low (42.24%), which means it was poorly identified. The low accuracy may be attributed to differences in the moisture content of bare soils and also the spectral confusion resulting from the very small plants in some fields. Some farmers grow tomatoes in March; the plants are very small and are grown in very wide furrows (0.8-1 m). This results in many mixed pixels in the classified image.

MLC and MDC supervised classification algorithms were also performed on all images. Many researchers showed the effectiveness of supervised classifiers in the literature for mapping vegetation (Jahne, 1991; Richardes, 1993; Foody *et al*., 1992; Su *et al*., 2007). Our results showed that MLC produced the highest accuracy for identifying wheat crops. The overall accuracy derived from the confusion matrix was very high (> 90%) with associated high Kappa coefficient supporting the high overall accuracy. Although MDC algorithm produced high overall accuracy (88.7%), the classification accuracy to identify a specific class was less compared with the results obtained using MLC. Both classifiers produced two distinct crops, wheat and clover, for the winter image, which are the most commonly grown crops in that area. The results suggest that supervised classification algorithms are advantageous in comparison to k-means classifier.

Similar to the results in this research, many researchers have shown that MLC has high accuracies for mapping vegetation. Pu *et al*. (2008) found that MLC produced high overall accuracy for classifying vegetation in a forest using airborne CASI data.

Wang *et al*. (2008) compared three classification methods (feed-forward neural network classifier), Clustering-Based Neural Network classifier (CBNN) and MLC for discriminating mangrove canopies in the Caribbean coast of Panama using IKONOS data. They concluded that CBNN and MLC presented the best classification accuracy. In contrast, Bagan *et al*. (2008) compared Self Organizing Map (SOM) neural network with MLC for classifying ASTER data and found that using all band combinations of VIS, VNIR, SWIR and TIR, SOM produced higher classification accuracy in comparison to MLC. The implementation of a neural network approach to classification is an area worthy of future investigation in the Egyptian context.

### 7.3.2 Detecting stress in wheat

Having classified the image for a specific crop type, the crop status influenced by stress could be examined. QuickBird and ASTER images were used in this research project to assess the potential of high spatial resolution remote sensing images to detect stress in wheat. The only available ASTER image was acquired at the end of April 2007, which is very late for wheat crops in Egypt and consequently no significant correlations were found between vegetation indices derived from the ASTER image and the different biophysical and biochemical properties of wheat crops in the three study sites.

The 2.4 m resolution QuickBird imagery acquired on 7$^{th}$ April 2007 was also examined to detect stress in wheat in the same study area. Most vegetation indices derived from QuickBird imagery demonstrated highly significant correlations with different biophysical and total chlorophyll concentrations of wheat. Strong correlation values were observed between chlorophyll concentration and both SI and NDVI ($r = \pm 0.86$). DVI produced the strongest relationships with biomass, plant height and LAI ($r = 0.85$, 0.66 and 0.81 respectively). From individual datasets NDVI produced strong relationships with different crop properties.

Within the QuickBird image there were no systematic spatial trends for crop stress. However, the stressed areas could be related to different agricultural practices. Furthermore, tolerance of wheat crops to stress may be another reason for that since wheat is a tolerant crop in comparison to other crops such as maize. However, stress can be detected in the image for specific areas, which suffer from severe stress (Figure 6.32).

Comparing the results obtained from *in situ* hyperspectral survey and QuickBird image, a significant positive correlation was observed between vegetation indices derived from *in situ* hyperspectral measurements and the same indices derived from QuickBird satellite imagery. The time difference between *in situ* hyperspectral survey and acquisition time for QuickBird image however, may influence the comparisons. Furthermore, the clouds and associated shadows may affect the spectral signature from some fields. Additionally, illumination changes due to cloud cover during *in situ* hyperspectral survey may be another reason for this decrease. These factors may have contributed to the scatter in the comparison, but nevertheless a robust comparison was demonstrated.

### 7.3.3 Differentiating stress

Wheat was chosen at the start of this research as the most important crop for Egypt. The results obtained from the four greenhouse experiments of the Scottish and Egyptian wheat varieties demonstrated that the distinction between moisture and salinity induced stress occurs late in the growing season. Close to the flowering stage it was possible to distinguish between the two types of stress spectrally. PCA successfully demonstrated the potential of distinguishing between healthy and stressed fields and even between moisture and salinity induced stress using *in situ* hyperspectral measurements collected during field visits for both wheat and maize (see Figures 6.9-13 and Figures 6.21-23). This concurred with the results of the greenhouse experiments.

Due to limited spectral resolution of the QuickBird satellite imagery, it was not possible to differentiate between different sources of stress from the spectral signatures. The four bands of QuickBird imagery were used to calculate the most commonly used vegetation indices to detect stress in both wheat and maize crops. Distinguishing between moisture and salinity induced stress needs hyperspectral satellite imagery such as Hyperion or similar platforms, which provides more than 200 spectral bands. However, using this type of imagery will be restricted by the small-field system and many mixed pixels in the image will be problematic. Therefore, co-operation between the Egyptian Government and farmers is very important to tackle this problem, specifically, to sow crops at the same time and have larger areas cultivated with the same crop.

Other investigations encourage subtle changes in the spectral response have also demonstrated that direct comparison with broad band reflectance is very limited. However, decorrelating spectral information through PCA analysis can sometimes provide subtle information on spectral change. For example, Tyler *et al*. (2006) demonstrated the potential of Landsat TM and ETM imagery to map chlorophyll *a* concentration in Lake Balaton and concluded that chlorophyll *a* concentration cannot be mapped directly from raw image data. However, the mixture modelling approach can provide a robust technique for mapping chlorophyll *a* in open fresh water in the presence of heterogeneous suspended sediment concentrations, which tend to dominate the reflectance characteristics. In this context, the addition of the shortwave infrared (SWIR) may provide useful information on plant canopy structure (Gong *et al*., 2003; Twele *et al*., 2008; Wang *et al*., 2008).

Using a mixture modelling approach may provide a way forward for distinguishing moisture and salinity induced stress. Some studies have shown the possibility of estimating sub-pixel abundance by means of multivariate regression (Rainey *et al*., 2003). Among few different soft classification algorithms, mixture modelling was considered the most suitable technique because it does not need too much ground reference data (Bastin, 1997), however, it may also be worth exploring the Artificial Neural Network (ANN) approach in future research. Mixture modelling may therefore be applied in mapping crops to detect stress using high spectral resolution remote sensing imagery and solve the mixed pixels resulting from the small field system.

## 7.4 Using remote sensing in detecting and differentiating stress in Maize crops

### 7.4.1 Identifying crop types (classification)

To differentiate between different crops and even between healthy and stressed fields, both unsupervised and supervised classification algorithms were performed on QuickBird and SPOT HRV images to identify different crops. K-means unsupervised classification demonstrated slightly higher overall accuracy (80.62%) associated with high Kappa coefficient (0.758). However, the classification accuracy for identifying tomato crops was very low (58.12%). As mentioned in section 6.5.3 the low classification accuracy may have been a result of the spectral confusion produced from other crops during their early growth stage. Also, some mixed pixels occur as a

result of very low vegetation cover at early growth stages since more than 80% of soil is bare. At early growth stages, tomato has low vegetation cover and the crop may be classified as bare soil or melon since both crops are grown on wide furrows approximately at the same time following a clover crop.

Supervised classification algorithms demonstrated high overall accuracy associated with high Kappa coefficient values. As with the wheat imagery the MLC produced the highest overall accuracy of 93.67% with high associated Kappa coefficient of 0.921. Although MDC produced high overall accuracy of 89.94%, the classification accuracy for identifying maize was less (84.43%) in comparison to MLC (89.87%). The decrease in classification accuracy to identify maize crops using MDC may have been a result of different growth stages and therefore different biophysical and biochemical properties. MLC demonstrated very high user's and producer's accuracies (> 0.85). In conclusion, supervised classification algorithms provided better results in comparison to k-means in terms of overall accuracy, Kappa coefficient and individual classification accuracies for different classes. Results from our research are supported by previous studies that demonstrated high accuracy of MLC algorithm to classify vegetation (Bagan *et al*., 2008; Wang *et al*., 2008). MLC is commonly used technique for the classification of vegetation. Shanmugam *et al*. (2006) concluded that MLC produced higher accuracies in comparison to unsupervised classifier. However, they established a decrease in the classification accuracy of both ISODATA and MLC with increasing number of classes being identified. Other studies showed that although hard classification techniques such as MLC give high accuracy, it produced too many mixed pixels and therefore the mixed pixels identified as the most similar class. These studies demonstrated that soft classification techniques such as linear spectral mixture modelling or ANN approach could produce accurate vegetation maps comparable to those obtained using hard classification techniques and needs to be explored in future work in the Nile Valley of Egypt.

### 7.4.2 Detecting stress in maize

To detect dissimilarities between healthy and stressed fields in south-west Alexandria at local and regional scales, QuickBird and SPOT HRV images were examined in this research project to detect stress in maize. The 20 m resolution SPOT HRV image had the same problem as the ASTER image in the winter season since the spatial

resolution is similar to a field's width resulting in great overlap between pixels from different fields with different crops and therefore different spectral signatures. However, the SPOT HRV image produced an overview picture to understand the stress in the whole region (Figure 6.40). It also shows that the newly reclaimed land at the Bangar site suffers from stress as a result of using sub-optimum agricultural practices particularly changes from sprinkler irrigation to the traditional irrigation method (flood irrigation). Moreover, the figure shows several fields irrigated by centre pivot system, which have very high NDVI values as indicator of larger biomass. The sandy to sandy loam soils in that area have a high infiltration rate and therefore massive amount of water is lost through deep percolation. The SPOT HRV image gave a clear understanding about the stress at a regional scale, which can be used as an indicator for reconsidering irrigation system design in the whole country.

The 2.4 m resolution QuickBird image was also used to derive broad band vegetation indices to detect stress at a local scale. Twelve broad band vegetation indices were calculated using the red and near infrared bands derived from the corrected image. Strong correlations between different biochemical and biophysical properties of maize and the majority of vegetation indices were observed. From individual datasets it can be seen that NDVI had strong correlations with different maize properties ($r > 0.90$). Results also showed that NDVI and SI had strong correlations with all maize properties. $GNDVI_{br}$ produced the strongest correlations with biomass, height and LAI ($r = 0.914$, 0.926 and 0.892 respectively). NDVI produced similar correlations obtained by $GNDVI_{br}$ with biomass, height and LAI.

A strong relationship between $GNDVI_{br}$ derived from *in situ* and $GNDVI_{br}$ derived from satellite image was observed. Figure 6.39 shows a linear significant relationship between $GNDVI_{br}$ obtained from both datasets ($R^2 = 0.75$). The decrease in this relationship may have been a result of the temporal difference between *in situ* hyperspectral survey and QuickBird acquisition time.

$GNDVI_{br}$ and SI calibrated maps derived from the QuickBird images were used to create maps for predicting aboveground biomass and chlorophyll concentration (Figures 6.36 and 6.37 respectively). $GNDVI_{br}$ map showed that the study area is split into two halves and most fields of the upper half have high $GNDVI_{br}$ values. Most fields in the lower half have low values of biomass and chlorophyll, which is evidence

for stress from both moisture and salinity. When farmers suffer from shortage of fresh water they use agricultural drainage water to irrigate their crops. In this case moisture, nitrogen and salinity stress are closely linked since farmers generally can not add the required amount of nitrogen on time and wait until fresh irrigation water becomes available. Broadly, the $GNDVI_{br}$ demonstrated that stressed fields are distributed throughout the image, which may be attributed to different agricultural practices in each field. In conclusion, a specific trend for crop stress was shown in different calibrated maps of maize properties and therefore QuickBird satellite imagery successfully identified stressed areas at local scale in south-west Alexandria.

## 7.5 Implication within Egypt's Agricultural system

### 7.5.1 High spatial resolution and coverage

The small field system in Egypt is a result of changing the system of communism to capitalism in the 1990s. The Egyptian Government sold the landmass to a large number of farmers. Farmers usually have less than one hectare particularly in the Nile Delta and Valley. Monitoring these small fields individually with satellite remote sensing imagery with a spatial resolution of more than 10 m is problematic. However, high spatial resolution satellite images such as SPOT HRV and ASTER may provide a better understanding about stress at regional scales. New satellite sensors with spatial resolution less than 5 m such as QuickBird and IKONOS are very useful in such system to detect stress within a field and/or at a local scale. The results of our research showed that at field and local scales QuickBird imagery was able to differentiate between healthy and stressed fields particularly maize crops since the stress in some fields was apparent in comparison to wheat crop. However, these satellite sensors have limited spectral capabilities, which in turn restrict the use of these satellite platforms in differentiating different types of stress such as salinity and moisture, but would be used for targeting more detailed investigation.

In this research QuickBird satellite images showed the possibility of detecting stress at the local scale, but applying this type of imagery at a regional scale will be very costly. Alternatively, using a combined approach of high spatial resolution satellite imagery with moderate spatial resolution imagery such as SPOT HRV or ASTER will give a general idea about stressed areas in the Nile Valley and Delta at a reasonable cost. It can be seen in Figure 6.40 that SPOT HRV imagery showed the possibility of

detecting stress at a regional scale and identifying areas of good irrigation practices. From this imagery stressed areas can be identified and targeted using higher resolution satellite imagery such as QuickBird. SPOT HRV imagery showed that the Bangar site has the lowest values of NDVI as a result of using poor irrigation practices. Interestingly, the same figure showed that there are some large fields near the Bangar site that have very high values of NDVI, which is an indicator of very healthy maize crops within the same stressed area. Consequently, QuickBird and SPOT HRV together could give a better understanding about stress at both local and regional scales at a reasonable cost as well as policing agricultural practices, providing a mean for costing the return in crop yield against the cost of improved irrigation management and enable a forecast of future crop yields.

### 7.5.2 High spectral resolution

This research has shown that high spectral resolution remote sensing of spectroradiometry data has the potential of providing important crop monitoring information, especially in distinguishing between salinity and moisture induced stress. However, currently the Hyperion satellite platform is the only system that approaches the specification required to monitor and distinguish different sources of stress within Egyptian field systems. Unfortunately, Hyperion is a research tool and no other platform is currently available to provide suitable monitoring requirements. However, as illustrated with the SPOT HRV image, the slightly poorer spatial resolution (20 m) may still be sufficient to provide a broader understanding of sources of stress across field system, if not within. Additionally, the hyperspectral infrared imager (HyspIRI; 2013-2016) would be effective satellite imagery in detecting stress at a regional scale since it provides images at 400-2500 nm with 45 m spatial resolution. Using this imager with the new advances in detectors, optics and electronics could acquire images with 210 spectral bands in the above mentioned range. As documented in the literature the SWIR may provide useful data in detecting stress in crops. Other crop properties such as lignin and cellulose could be estimated using the SWIR range. In the next 5 years, the proposed VENUS and HyspIRI platforms could provide suitable spectral capabilities and consequently enhance the ability to differentiate sources of stress.

However, the implementation of *in situ* hyperspectral measurements in conjunction with SPOT HRV imagery to target field campaigns may provide an effective compromise in understanding the sources of stresses in specific field systems. However, the effectiveness of this type of implementation is clearly an area requiring further research.

To apply high spectral satellite remote sensing imagery such as Hyperion or similar platforms needs co-operation between the Government and farmers in Egypt. The Government is now establishing a new agricultural development in a valley called Toshki in southern Egypt. The project aims to reclaim over a million hectares of land and is expected to be irrigated from the Nile, which therefore affects the availability of water for the Nile Valley and the Delta. In this considerable area it would be easy to use high spatial and spectral satellite remote sensing for different purposes in agricultural fields. The high summer temperature in this area (>40°C) results in high evapotranspiration rates and hence high crop water requirements.

### 7.5.3 Predicting crop yield

Maximising crop production at minimum cost is very important for farmers. Mapping and predicting yield at an early growth stage is therefore essential for farmers to take decisions to improve their agricultural practices. Monitoring plant status by means of remotely sensed data will enable farmers to maintain optimal levels of soil moisture and nutrients and avoid overuse of different chemicals, which potentially contaminate soil and water. A further advantage is the possibility to quantify the amount of grain needed to satisfy population demand. It is therefore evident that using satellite imagery could be a robust tool in site specific management in the Nile Valley and the Nile Delta of Egypt.

Different vegetation indices derived from both hyperspectral and satellite based systems showed strong correlations with different maize and wheat properties. QuickBird satellite imagery successfully mapped the spatial variability of aboveground biomass, which is closely linked to crop grain yield. Grain yield can therefore be predicted using this type of satellite imagery. Successful mapping of agricultural grain crops at early stages will provide a useful tool to detect areas suffering from stress and therefore enable remediation to be implemented to increase yield. Avoiding and managing crop stress in the Nile Valley may increase and even

double crop productivity, which is crucial to a country like Egypt to sustain the rapid population growth.

Detecting stressed areas can help manage limited water and land resources more efficiently. For example, SPOT HRV scene showed that using centre pivot irrigation system led to high biomass, which was an indicator of crop status in comparison to near fields (the Bangar site) irrigated by conventional irrigation method. Although the cost of this type of irrigation system is initially high, in the long term it will be very economical in terms of crop productivity and resource use. The centre pivot irrigation systems have very high irrigation efficiency since they provide plants with the required amounts of water, fertilizers and chemicals. The high efficiency of this system will save at least 30% of irrigation water (deep percolation losses) and consequently this amount can be used to expand the cultivated area.

Similar to the results obtained in this research, previous studies showed the possibility of using satellite imagery to predict crop properties. High spatial resolution imagery offers new opportunities for crop management (Yang *et al*., 2006a). They concluded that cotton yield was successfully mapped using both QuickBird and airborne images. In a sorghum field experiment, Yang *et al*. (2006b) established a strong significant relationship between sorghum grain yield and both datasets of QuickBird and airborne images. Reyniers and Vrindts (2006) also established a strong correlation between NDVI derived from both Ikonos and multispectral radiometer and nitrogen variability in a wheat field under various seeding densities and nitrogen application rates. Wu *et al*. (2007a and 2007b) utilised QuickBird satellite images to estimate chlorophyll concentration and LAI of potato and maize canopies and showed the possibility of using this type of imagery to detect crop properties. The results obtained from our research showed the potential of QuickBird images to detect stress at local scale, however, cloud interference and high cost of these images could limit the use of them in making timely management decisions (Wu *et al*., 2007a). High spatial resolution satellite imagery has the potential for mapping crop growth variability and identifying problem areas within fields (Yang *et al*., 2006b). The results therefore suggest that QuickBird satellite images could provide useful data to detect stress at both within field and local scales. Moreover, SPOT HRV and/or ASTER images could give a general insight about stress trends at regional scales at a cheap cost in the same time.

## 7.6 Key findings

### 7.6.1 Hypotheses

1. *Moisture and salinity induced stress greatly affected wheat and maize grain yield*.

It has been demonstrated that the grain yield of both wheat and maize crops were significantly affected by both moisture and salinity stress in all greenhouse experiments. Wheat was less affected by both stressors than maize, hence maize would benefit from being grown in less stressed areas less likely to experience these stresses.

2. *In situ hyperspectral measurements are able to detect stress in wheat and maize resulting from moisture and salinity stress.*

The results showed that broad band and hyperspectral vegetation indices derived from *in situ* spectroradiometry measurements can detect stress as well as various biophysical and biochemical properties of maize and wheat. Different indices strongly correlated with the grain yield of both wheat and maize.

3. *Moisture induced stress and salinity induced stress can be distinguished spectrally*.

The analysis showed that for the first time that moisture and salinity induced stress can be distinguished in wheat and maize. PCA of the hyperspectral data (400 nm-900 nm) successfully showed the dissimilarities between plants affected by moisture and salinity induced stress particularly at the grain filling stage in wheat and at the flowering stage in maize. At early stages, overlap between moisture and salinity stress was detected. Despite the late distinction between the two stressors, these results can be used as a reference for following seasons.

4. *High spatial resolution remote sensing imagery can detect stress in wheat and maize at local and regional scales and therefore contribute to maximising crop productivity*.

This hypothesis has been proven since both QuickBird and SPOT HRV images successfully mapped and detected stress in wheat and maize. The processed

images showed for the first time the extent of crop stress at both regional and local scales. In addition, QuickBird image data strongly correlated with maize and wheat biomass, which is closely linked with grain yield. It is therefore possible to map and estimate grain yield during the growing season through remotely sensed data.

### 7.6.2 Redesigning irrigation system

There is a clear need to redesign the irrigation system as the SPOT HRV image showed that the newly reclaimed areas at the Bangar site are suffering from severe moisture stress, particularly at the border between cultivated land and the west desert. Furthermore, the soil in this site had low fertility due to very low nitrogen concentration. Additionally, the sandy to sandy loam texture leads to a high infiltration rate, which results in massive water losses through deep percolation. Soils with such specifications need much more efficient agricultural practices.

The 9$^{th}$ July SPOT HRV image showed that the centre pivot irrigation system produced the highest vegetation cover for maize crops in south-west Alexandria since it has high irrigation efficiency. Crops are provided with the optimum amount of water, chemicals and fertilizers. Keeping water losses at a minimum and reducing the risk of soils and surface water contamination.

### 7.6.3 The spatial perspective on stress

Our research also demonstrated the ability to distinguish between healthy and stressed areas and even identify different crops within field system through the combined approach of ground and satellite based platforms. The results highlight the importance of crop choice in maximising productivity in areas experiencing stress. For example wheat crop showed high tolerance to both moisture and salinity and therefore can be successfully grown in such areas. Sensitive crops such as maize should be grown in less stressed areas near the main irrigation canals (e.g. Mynofia and Dakahlia).

It is also further shown that crop grain yield can be effectively estimated through remotely sensed data before crop maturation. Predicting different biophysical and biochemical properties of crops, which are closely linked with crop yield, can increase crop productivity by avoiding stress at specific growth stages (e.g. grain filling stage).

Moreover, applying efficient irrigation systems will increase crop productivity and increase water use efficiency (the amount of grain per unit area in; e.g. kg $m^{-1}$).

Some farmers grow rice crops in sandy and sandy loam soils (high infiltration rate), which is not allawed due to limited water resources. As a result, the Egyptian Government introduced a penalty to farmers who grow rice in such soils. Using remote sensing technique as a useful tool for policing areas of rice crops will deter farmers from growing rice in these areas. Remote sensing therefore would be a useful quick tool to target these fields and can be a robust policing tool to identify contrary irrigation practices.

### 7.6.4 Distinguishing sources of stress

The research presented in this thesis showed the potential of *in situ* hyperspectral measurements to detect stress and even distinguish between moisture and salinity induced stress. PCA successfully showed dissimilarities in plant responses resulting from moisture and salinity stress. Due to limitations in spectral resolution of high spatial resolution images, it is difficult to distinguish between moisture and salinity induced stress. However, new platforms such as VENUS and HyspIRI with high spectral resolution (more than 200 spectral bands) can enhance the ability of remote sensing imagery to detect stress in crops and even distinguish sources of stress at a regional scale. In addition, Hyperion can provide reliable satellite imagery to differentiate sources of stress.

These new platforms can provide decision makers with better understanding about areas, which suffer from moisture and/or salinity induced stress, and consequently, take informed decisions to follow the right irrigation policy. For example, areas suffering from salinity stress can be flooded with fresh water for two or three times to reduce the salinity effects on plants. Moreover, areas irrigated using trickle irrigation system sometimes suffer from slight salinity stress as a result of partial-wet zones, which can be identified using these hyperspectral platforms and consequently take a quick decision to solve the problem and avoid yield reductions.

### 7.6.5 Contribution

Chapter 4, 5 and 6 demonstrated the potential of detecting stress in wheat and maize crops using both *in situ* hyperspectral and satellite remote sensing data. Importantly,

the data have shown for the first time the spatial extent of stress across a portion of the Nile Delta. This has illustrated the considerable potential for improving crop yield and the framework for better management of water and land resources. From this spatial context it may be possible to undertake a cost benefit analysis of the cost of improving irrigation system compared with the improvement in crop yield. At this scale there is clear need for the government in formulating policy and regulations to stimulate this type of development.

The remote sensing data have demonstrated that a substantial improvement in crop productivity can be gained by redesigning irrigation systems to those such as the centre pivot system and forms of drip irrigation. As new areas become developed (e.g. Toshki and Sinai in southern and northern Egypt) and pressures from population and climate change, this type of modification will become a priority for Egypt. In this context, remote sensing has the potential of forecasting crop yield and targeting areas requiring attention and policing. This type of monitoring can be performed by SPOT HRV and QuickBird or similar platforms. Mapping south-west Alexandria by SPOT HRV satellite established a decreasing stress trend from the edge of cultivated land to inside the Nile Delta which is a sign of shortage of water and poor agricultural practices in this area or may have been a result of combined effects of both salinity and moisture stressors. In addition, identifying the area occupied by each crop will be very useful in determining the amount of water required for the whole regions, and thus assessing the size of irrigation channels required to supply the sufficient irrigation water. Newly reclaimed areas in Toshki and Sainai will affect water resources for the existing cultivated land in the Nile Valley and Delta, so accurate techniques of crop monitoring such as remote sensing are crucial.

The application of high spatial resolution remotely sensed data in monitoring agricultural crops as a precision farming tool has many benefits for wheat and maize growers. Firstly, by detecting stress at early stages informed decisions can be made to improve agricultural practices. Secondly, remotely sensed data can be used to predict grain yield and thereby provide a rough estimate of the potential income. In addition, remotely sensed data can reduce inputs for agricultural production by providing accurate data for optimising seed rates and application rates for fertilisers, fungicide and pesticides. Finally, lowering application rates (fertilizers, fungicide, pesticide and

seeds) and input costs tend to lead to an increase in overall income and would be useful for extending the area of cultivated land.

As the pressure on water resources increases and climate change further influences water availability, issues of salinity induced stress may also become more important. The ability of hyperspectral platforms to distinguish moisture and salinity stress is a particularly novel finding from this research. In the immediate future, this type of analysis may be performed from *in situ* data.

In conclusion, mapping crop health in an area like south-west Alexandria by means of remotely sensed data can be used efficiently to make informed decisions in site specific management. The valuable information obtained by SPOT HRV images can be used as a policing tool for detecting prohibited agricultural practices. Both QuickBird and SPOT HRV images produced representative maps of crop stress at local and regional scales. However, remote sensing data collection in this research has been restricted by some limitations, which are now being summarized.

### 7.6.6 Limitations

- The commercial availability of high spectral resolution satellite imagery (Hyperion) was a problem. However, this kind of satellite imagery may provide agronomists with better understanding for detecting changes in plant physiology resulting from different stressors.

- Weather conditions in winter restricted the acquisition of satellite imagery particularly high spectral resolution (Hyperion). Owing to problems with Hyperion, other images had to be acquired resulting in a large time difference between *in situ* measurements and satellite image acquisition. In this research *in situ* data was collected approximately 10 days before the acquisition of QuickBird satellite imagery, which decrease the relationship between both datasets.

- Small-field systems in Egypt make it problematic to use satellite imagery with spatial resolutions greater than 10 m. Overlap between spectral signatures from different fields with different crops leads to poor relationships between different crop properties and spectral datasets.

- Time series satellite imagery was needed for monitoring wheat crop development throughout the growing season to detect stress as early as possible and avoid reduction in crop productivity. Platforms with high revisit cycles would resolve this issue since new platforms provide images with 2-3 revisit cycles. Due to the weather conditions in winter, there is no guarantee for image acquisition since sometimes the cloud cover is over 75%.

- The only available QuickBird image for winter wheat crop in south-west Alexandria was associated with 33% cloud cover and consequently many fields of the *in situ* hyperspectral survey were covered by clouds and associated shadows. This restricted the comparison between *in situ* hyperspectral and satellite data.

- Assistance from farmers during field work visits was very limited as some farmers refused to provide vegetation samples. To increase cooperativeness local farmers in Egypt should be notified and trained by local authorities regarding scientific research and new technologies.

- There was a lack of equipment to extract chlorophylls and pigments during field work visits, hence, the chlorophyll concentration was determined by a SPAD meter which only provides a relative measure for total chlorophyll.

- Different sowing dates for maize crops in south-west Alexandria sometimes hindered the distinction between moisture and salinity induced stress. Farmers grow maize in that area following wheat and clover, which are harvested at different times.

### 7.6.7 Future work

The results obtained from this thesis suggest that both *in situ* hyperspectral and high spatial satellite remote sensing can be used to detect different biophysical and biochemical properties in wheat and maize. However, distinguishing different types of stress at early stages is still problematic and some improvements may lead to a better understanding of the changes in plant physiological status. For example, using ground-based instruments with shortwave Infrared band may lead to better results

regarding stress. In this context, there are some improvements to enhance the future work which can be summarized as follow:

- Investigating spectral signatures from different crops and assessing the ability to distinguish different signatures for different crops.

- Characterising spectral properties for the same crop at different sites with various soil and climatic conditions.

- Investigating spectral signatures from the same crops under different irrigation systems such as sprinkler, trickle and flood irrigation and assessing the efficiency of irrigation system from hyperspectral datasets.

- Use of *in situ* hyperspectral measurements including shortwave Infrared band, which might be useful in identifying wave bands sensitive to moisture and salinity stress.

- Using hyperspectral satellite imagery (Hyperion, VENUS and HyspIRI) with low visit cycles to detect stress in different crops and identify wavelengths sensitive to physiological changes resulting from moisture and salinity stress.

- High spatial and spectral resolution satellite remote sensing need to be evaluated for detecting stress in different crops.

- Assessing the potential for the innovative use of remotely sensed data in detecting stress in crops resulting from other factors in particular pollution. Recently farmers in Egypt have been burning the residues of their crops after harvesting, especially rice straw, which produces serious air pollution during the summer season every year. Remote sensing imagery could identify accurately the polluted areas and subsequently take actions against farmers who do not follow the regulations could be implemented.

- Another source of pollution which results from discharging industrial effluent into the River Nile needs to be investigated as many heavy metals are released from factories on both sides of the river. These metals could be causing stress in agricultural crops. Monitoring water quality in the Nile by remote sensing

imagery in this case could produce accurate maps of water quality identifying the main areas of pollution.

### 7.6.8 Final conclusion

Monitoring crop health in the Nile Valley of Egypt is based on traditional methods of sample-point techniques. As a result of rapid population growth but little increase in the amount of water and cultivated land, there is an urgent need for new technologies to increase and even double crop productivity in the Nile Valley of Egypt. The use of new technologies such as remote sensing is still restricted in the field of agriculture in the Nile Valley. The small-field system hinders the application of remote sensing techniques at an individual level since it would be costly for every farmer who owns less than one hectare to monitor his crops health by satellite imagery. However, cooperation between farmers and the Government will be very useful for applying this technology. Growing one crop in the same area following the same agricultural practices including ploughing, crop variety, nitrogen rate, irrigation interval, plant protection methods and sowing date will make it easier to utilise remote sensing techniques to detect stress in this area and resultantly enhance crop productivity.

The combined approach of using high and moderate spatial resolution satellite remote sensing such as QuickBird and SPOT HRV can give a better understanding about stress at both local and regional scales. Due to limited spectral resolution of these satellite images, it is difficult to distinguish different sources of stress. However, this may be resolved in the next 5 years with the launch of new satellite systems (VENUS, 2010 and HyspIRI, 2013-2016) with high spectral resolution and low revisit cycles. The results obtained from this research established the possibility to detect stress in south-west Alexandria by mapping different crop properties using both QuickBird and SPOT HRV images. Moreover, *in situ* Hyperspectral remotely sensed data demonstrated the ability to distinguish between moisture and salinity induced stress spectrally. High spectral resolution imagery (Hyperion or similar platforms) is therefore a reliable satellite imagery to achieve this task at a regional scale.

This research project has demonstrated the high efficiency of high spatial resolution remote sensing imagery to detect stress in wheat and maize by predicting different plant parameters such as LAI, biomass, plant height and chlorophyll concentration. Using this technique in the Nile Valley will maximise the efficiency of water use and

decrease input costs (pesticides, fungicides, fertilizers, seeds and irrigation). Remote sensing can therefore be used as a useful, quick and cost-effective tool in precision farming and regional analysis giving timely information about crops in specific areas and thereby providing valuable data for decision makers.

# REFERENCES


Adams, M. L., Philpot, W. D. and Norvell, W. A. (1999). Yellowness index: an application of spectral second derivatives to estimate chlorosis of leaves in stressed vegetation. *Int. J. Remote Sens*., 20: 3663-3675.

Aloy, M. (1992). Effect of different levels of salinity on yield and yield components of six varieties of barley. Proc.2nd Congress, European Society of Agronomy, Warwick, UK.

Alscher, R. G., Cumming, J. R. and Allen, N. S. (1990). Stress responses in plants: Adaptation and acclimation mechanisms, Plant Biology, ISBN 0-471-56810-4, Wiley-Liss, Inc. 12:6-7.

Ambast, S. K., Keshari, A. K. and Gosain, A. K. (2002). Satellite remote sensing to support management of irrigation systems: concepts and approaches. *Irrigation and Drainage*, vol. 51: 25-39.

Amer, M. H., El-Guindy, S. and Rafla, W. (1989). Economic justification of drainage projects in Egypt. In: Amer, M. H., Ridder, N. A., (Eds.), Land drainage in Egypt. Drainage Research Institute, Cairo, pp 327-339.

Aparicio, N., Villegas, D., Araus, J. L., Casadesus, J. and Royo, C. (2002). Relationship between growth traits and spectral vegetation indices in durum wheat. *Crop Science* 42: 1547-1555.

Aparicio, N., Villegas, D., Casadesus, J., Araus, J. L. and Royo, C. (2000). Spectral Vegetation Indices as Non Destructive Tools for Determining Durum Wheat Yield. *Agron. J*. 92: 83-91.

Araus, J. L., Casadesus, J. and Bort, J. (2001). Recent tools for the screening of physiological traits determining yield. P. 59-77. In M.P. Reynolds, J. I. Ortiz-Monasterio and A. Mcnab (Eds.) Application of physiology in wheat breeding. CIMMYT, Mexico.

Asrar, G., Kanemasu, E. T. and Yoshida, M. (1985). Estimates of leaf area index from spectral reflectance of wheat under different cultural practices and solar angle. *Remote Sensing of Environment* 17: 1-11.

Ayers, R. S. and Westcot, D. W. (1985). Water quality for agriculture. FAO Irrigation and Drainage paper No. 29, Rome, pp 174.

Babar, M. A., Reynolds, M. P., van Ginkel, M., Klatt, A. R., Raun, W. R. and Stone, M. L. (2006). Spectral reflectance indices as a potential indirect selection criteria for wheat yield under irrigation. *Crop Sci*. 46: 578-588.

Bachmann, C. M., Donato, T. F., Lamela, G. M., Rhea, W. J., Bettenhausen, M. H., Fusina, R. A., Du Bois, K. R., Porter, J. H. and Truitt, B. R. (2002). Automatic classification of land cover on Smith Island, VA, using hymap imagery. *IEEE Transactions on Geosciences and Remote Sensing* 40, 2313-2330.

Bagan, H., Wang, Q., Watanabe, M., Karneyarna, S. and Bao, Y. (2008). Land-cover classification using ASTER multi-band combinations based on wavelet fusion and SOM neural network. *Photogrammetric Engineering and Remote Sensing* 74(3): 333-342.

Bahrun, A., Mogensen, V. O. and Jensen, C. R. (2003). Water stress detection in field-grown maize by using spectral vegetation index. *Communications in Soil Science and Plant Analysis* 34(1): 65-79.

Ball, D. F. (1964). Loss-on-ignition as an estimate of organic matter and organic carbon in non-calcareous soils. *Journal of Soil Science* 15: 84-92.

Ball, M.C. (1988). Salinity tolerance in mangroves, *Aegceras corniculatum* and *Avicennia marina*. I. Water use in relation to growth, carbon partitioning and salt tolerance. *Aust. J. Plant Physiol*. 15: 447-464.

Bannari, A., Khurshid, K. S., Staenz, K. and Schwarz, J. (2008). Potential of Hyperion EO-1 hyperspectral data for wheat crop chlorophyll content estimation. *Canadian Journal of Remote Sensing* 34: 139-157.

Bannari, A., Morin, D., Bonn, F. and Huete, A. R. (1995). A review of vegetation indices. *Remote Sens. Rev*. 13: 95-120.

Banziger, M. and Diallo, A. O. (2004). Progress in developing drought and N stress tolerant maize cultivars for eastern and southern Africa. Pp. 189-194 In D.K. Friesen

and A.F.E. Palmer (eds). Integrated approaches to higher maize productivity in the new millennium. Proceeding of the 7th eastern and southern Africa regional maize conference, 5-11 February 2002. CIMMYT/KARI, Nairobi, Kenya.

Banziger, M., Edmeads, G. O., Beck, D. and Bellon, M. (2000). Breeding for drought and nitrogen stress tolerance in maize. From theory to practice. CIMMYT, Mexico City.

Barnabas, B., Jager, K. and Feher, A. (2008). The effect of drought and heat stress on reproductive process in cereals. *Cell and Environment* 31: 11-38.

Barnes, E. M., Moran, M. S., Pinter Jr, P. J. and Clarke, T. R. (1996). Multispectral remote sensing and site-specific agriculture: Examples of current technology and future possibilities. Proceeding of the 3rd international conference on precision agriculture.

Barnes, J. D., Balaguer, L., Manrique, E., Elvira, S. and Davison, A. W. (1992). A Reappraisal of the Use of Dmso for the extraction and determination of chlorophyll *a* and chlorophyll *b* in lichens and Higher plants. *Environmental and Experimental Botany* 32: 85-100.

Bastin, L. (1997). Comparison of fussy c-means classification, linear mixture modelling and MLC probabilities as tools for unmixing coarse pixels. *International Journal of remote sensing* 18: 3629-3648.

Bausch, W. C. and Duke, H. R. (1996). Remote sensing of plant nitrogen status in corn. *Transactions of the ASAE* 39: 1869-1875.

Blackburn, G. A. (1998). Quantifying chlorophylls and carotenoids at leaf and canopy scales: an evaluation of some hyperspectral approaches. *Remote sens. Envi.* 66: 273-285.

Blackmer, T. M., Schepers, J. S. and Varvel, G. E. (1994). Light reflectance compared with other nitrogen stress measurements in corn leaves. *Agronomy Journal* 86: 934-938.

Blackmer, T. M., Schepers, J. S., Varvel, G. E. and Walter-Shea, E. A. (1996). Nitrogen deficiency detection using reflected shortwave radiation from irrigated corn canopies. *Agronomy Journal* 88: 1-5.

Bresler, E., McNael B. L. and Carter, D. L. (1982). Saline and sodic soils: Principles, Dynamic Modelling, 236 pp. Springer-Verlag, Berlin.

Brisco, B., Brown, R. J., Hirose, T., McNairn, H. and Staenz, K. (1998). Precision agriculture and the role of remote sensing: a review. *Canadian Journal of Remote Sensing* 24: 315-327.

Broge, N. H. and Leblanc, E. (2001). Comparing prediction power and stability of broadband and hyperspectral vegetation indices for estimation of green leaf area index and canopy chlorophyll density. *Remote Sensing of Environment* 76: 156-172.

Buermann, W., Dong, J., Zeng, X., Myneni, R. B. and Dickinson, R. E. (2001). Evaluation of the utility of satellite-based vegetation leaf area index data for climate simulations. *Journal of Climate* 14: 3536-3551.

Buschmann, C., Langsdorf, G. and Lichtenthaler, H. K. (2000). Imaging of the blue, green, and red fluorescence emission of plants: an overview. *Photosynthetica* 38(4): 483-491.

Buschmann, C. and Nagel, E. (1993). In vivo spectroscopy and internal optics of leaves as basis for remote sensing of vegetation. *International Journal of Remote sensing* 14: 711-722.

Campbell, J. B. (1996). Introduction of remote sensing. 2nd ed. The Guilford Press, London.

Carter, G. A. (1991). Primary and secondary effects of water content on the spectral reflectance of leaves. *American journal of botany* 78: 916-924.

Carter, G. A. (1993). Responses of leaf spectral reflectance to plant stress. *American Journal of botany* 80(3): 239-243.

Carter, G. A. (1994). Ratios of leaf reflectance in narrow wavebands as indicators of plant stress. *International journal of remote sensing* 15(3): 697-703.

Carter, G. A., Cibula, W. G. and Miller, R. L. (1996). Narrow-band reflectance imagery compared with thermal imagery for early detection of plant stress. *J. Plant Physiol*. 148: 515-522.

Carter, G. A. and Miller, R. L. (1994). Early detection of plant stress by digital imaging within narrow stress-sensitive wavebands. *Remote Sensing of Environment* 50: 295-302.

Casady,W. W. and Palm, H. L. (2002). Precision agriculture, remote sensing and ground truthing. University of Missouri-Colombia EQ 453 (www.muextension.missouri.edu/xplor/).

Chaney, W. R. (2000). Yellow polar and drought. Retrieved from http://www.fnr.purdue.edu/inwood/yellowpo.htm accessed on 14th July 2008.

Chappelle, E. W., Kim, M. S. and Mcmurtry, J. E. (1992). Ratio Analysis of Reflectance Spectra (Rars)–an Algorithm for the Remote Estimation of the Concentration of Chlorophyll-a, Chlorophyll-b, and Carotenoids in Soybean Leaves. *Remote Sensing of Environment* 39: 239-247.

CIMMYT, (1988). Change for the better: CIMMYT 1988 Annual report. CIMMYT, Mexico City.

Claassen, M. M. and Shaw, R. H. (1970) Water deficit effects on corn. I. Grain components. *Agronomy Journal* 62: 652-655.

Clay, D. E., Kim, K., Chang, J., Clay, S. and Dalsted, K. (2006). Characterising water and nitrogen stress in corn using remote sensing. *Agronomy Journal* 98: 579-587.

Clevers, J. G. P. W. (1986). Application of remote sensing to agricultural field trails. Wageningen agricultural university papers 86-4, the Netherlands.

Clevers, J. G. P. W. (1997). A simplified approach for yield prediction of sugar beet based on optical remote sensing data. *Remote sensing of Environment* 61: 221-228.

Clutterbuck, B. J. and Simpson, K. (1978). The interactions of water and fertiliser nitrogen in effects on growth pattern and yield of potatoes. *Journal of Agricultural Science, Cambridge* 91: 161-172.

Congalton, R. G. and Green, K. (1999). Assessing the accuracy of remotely sensed data: Principles and practices, Lewis Publishers.

Crippen, E. R. (1990). Calculating the vegetation index faster. *Remote Sensing of Environment* 34: 71-73.

Curran, P. J. (1989). Remote sensing of foliar chemistry. *Remote sensing of Environment* 30(3): 271-278.

Cutler, M. E. J. (2000). Specular and anisotropic reflectance effects on the relationship between remotely sensed data and wheat canopy chlorophyll concentration. *Aspects of Applied Biology* 60: 115-122.

Datt, B. (1998). Remote Sensing of Chlorophyll a, Chlorophyll b, Chlorophyll a+b, and Total Carotenoid Content in Eucalyptus Leaves. *Remote Sensing of Environment* 66: 111-121.

Datt, B. (1999). Visible/Near Infrared reflectance and chlorophyll content in Eucalyptus leaves. *International Journal of Remote Sensing* 20: 2741-2759.

Daughtry, C. S. T., Walthall, C. L., Kim, M. S., Brown de Colstoun, E. and McMurtrey, J. E. (2000). Estimating corn leaf chlorophyll concentration from leaf and canopy reflectance. *Remote Sensing of Environment* 74: 229-239.

Davids, C. and Tyler, A. N. (2003). Detecting contamination-induced tree stress within the Chernobyl exclusion zone. *Remote Sensing of Environment* 85: 30-38.

Eck, H. V. (1986). Effects of water deficit on yield, yield components, and water use efficiency of irrigated corn. *Agronomy Journal* 78: 1035-1040

Edmeades, G. O., Balanos, J. and Laffite, H. R. (1992). Progress of breeding for drought tolerance in maize, p. 93-111 In Wilkinson, D. (ed). Proceeding of the 47$^{th}$ annual corn and sorghum industrial research conference. 1992 ASTA, Washington DC.

Ehleringer, J. R. and Forseth, I. N. (1989). Durinal leaf movements and productivity in canopies. In (Russell, G.; Marshall, B. and Jarvis, P.G., eds.): Plant canopies: their growth, form and function. Cambridge University Press, pp 180.

Eid, H. and Saleh, M. (1992). Modelling of climate change impacts on Egyptian Agriculture, unpublished manuscript, international institute for applied systems analysis, Laxenburg, Austria pp 15.

El-Hendawy, S. E. (2004). Salinity tolerance in Egyptian spring wheat genotypes. PhD. Thesis, dept. fur Pflanzenwissenschaften, Technische Universitat Munchen.

El-Lakany, M. H., Hassan, M. N., Ahmad, A. M. and Mounir, M. (1986). Salt affected soils and marshes in Egypt; their possible use for forages and fuel production. *Reclamation and Revegetation Res*. 5: 49-58.

El-Raey, M., Nasr, S., Frihi, S., Desouki, S. and Dewidar, K. (1995). Potential impacts of accelerated sea-level rise on Alexandria Governorate, *Egypt J.,Coastal Res*. 14: 190-204.

Elvidge, C. D. and Chen, Z. (1995). Comparisons of broad band and narrow band red and near infrared vegetation indices. *Remote Sensing of Environment* 54: 38-48.

Elvidge, C. D. and Lyon, R. J. P. (1985). Influence of rock-soil spectral variation on the assessment of green biomass, *Remote Sensing of Environment* 17: 265-269.

El-Wakeel, A. F. and El-Mowelhi, N. M. (1993). Reuse of drainage water on farm with reference to soil properties, crop production and heavy metal contents in plant tissues and dairy products. *Egypt J. Agric. Res.* 71 (4): 845-861.

ENVI (2003). ENVI: A user guide, Colorado, USA: RSI ENVI.

FAO, (2005). Fertilizer use by crop in Egypt. Food and Agriculture Organization of the united nations, Rome.

Fassnacht, K. S., Gower, S. T., MacKenzie, M. D., Nordheim, E. V. and Lillesand, T.M. (1997). Estimating the leaf area index of north central Wisconsin forests using the Landsat Thematic Mapper. *Remote Sensing of Environment* 61: 229-245.

Fernandez, S., Vidal, D. and Simon, E. and Sole-Sugranes, L. (1994). Radiometric characteristics of *triticum aestivum* cv. Astral under water and N stress. *International Journal of Remote* Sensing 15 (9): 1867-1884.

Filella, I. and Penuelas, J. (1994). The red edge position and shape as indicators of plant chlorophyll content, biomass and hydric status. *International journal of remote sensing* 15(7): 1459-1470.

Filella, I., Serrano, L., Serra, J. and Penuelas, J. (1995). Evaluating wheat nitrogen status with canopy reflectance indices and discriminate analysis. *Crop science* 35: 1400-1405.

Fitter, A. H. and Hay, R. K. M. (1981). Environmental physiology of plants, Academic Press, pp. 124-125.

Flowers, T. J., Garcia, A., Koyama, M. and Yeo, A. R. (1997). Breeding for salt tolerance in crop plants-the role of molecular biology. *Acta. Physiol. Plantar*. 19: 427-433.

Foody, G. M., Campbell, N. A, Trodd, N. M. and Wood, T. F. (1992). Derivation and applications of probabilistic measures of class membership from the maximum likelihood classification. *Photogrammetric Engineering & Remote Sensing* 58: 1335-1341.

Franke, J. and Menz, G. (2006). Detection of fungal infection in wheat with high-resolution multispectral data. Proc. of SPIE vol. 6298: 1-8.

Friedle, M. A., Michlaelsen, J., Davis, F., Walker, H. and Shimel, D. S. (1994). Estimating grassland biomass and leaf area index using ground and satellite data. *International Journal of Remote Sensing* 15: 1401-1420.

Galvao, L. S., Ponzoni, F. J., Epiphanio, J. C. N., Rundorff, B. F. T. and Formaggio, A. R. (2004). Sun and view angle effects on NDVI determination of land cover types in the Brazilian Amazon region with hyperspectral data. *International Journal of Remote Sensing* 25(10): 1861-1879.

Gamon, J. A., Field, C. B., Goulden, M. L., Griffin, K. L., Hartley, A. E., Joel, G., Penuelas, J. and Valentini, R. (1995). Relationships between NDVI, canopy structure and photosynthesis in three Californian vegetation types. *Ecol.Appl*. 5(1): 28-41

Gamon, J. A., Penuelas, J. and Field, C. B. (1992). A narrow-waveband spectral index that tracks diurnal changes in photosynthetic efficiency. *Remote sensing of Environment* 41: 35-44.

Gamon, J. A., Serrano, L. and Surfus, J. S. (1997). The photochemical reflectance index: an optical indicator of photosynthetic radiation use efficiency across species, functional types, and nutrient levels. Oecologia 112: 492-501.

Gao, B. C. (1996). NDWI-a normalized difference water index for remote sensing of vegetation liquid water from space. *Remote sensing of Environment* 58: 257-266.

Gao, B. C. and Goetz, A. F. H. (1992). A linear spectral matching technique for retrieving equivalent water thickness and biochemical constituents of green vegetation, Proc. of the third Airborn Annual JPL Geosciences workshop (AVIRIS, TIMS and AIRSAR), Jet Propulsion Laboratory, Pasadena, CA.

Genc, H., Genc, L., Turhan, H., Smith, S. E. and Nation, J. L. (2008). Vegetation indices as indicators of damage by the sunn pest (Hemiptera: Scutelleridae) to field grown wheat. *African Journal of Biotechnology* 7(2): 173-180.

Gitelson, A. A., Buschmann, C. and Lichtenthaler, H. K. (1999). The chlorophyll fluorescence ratio F735/F700 as an accurate measure of the chlorophyll content in plants. *Remote sensing of Environment* 69: 296-302.

Gitelson, A. A., Kaufman, Y. J. and Merzlyak, M. N. (1996). Use of a green channel in remote sensing of global vegetation from EOS-MODIS. *Remote Sensing of Environment* 58: 289-298.

Gitelson, A. A., Kaufman, Y., Stark, R. and Rundquist, D. (2002). Novel algorithms for remote estimation of vegetation fraction, *Remote sensing of Environment* 80: 76-87.

Gitelson, A. A. and Myrzlyak, M. N. (1994). Quantitative estimation of chlorophyll-*a* using reflectance spectra: experiments with autumn chestnut and maple leaves. *J. Photochem. Photobiol B: Biol*. 22: 247-252.

Gitelson, A. A. and Merzlyak, M. N. (1996). Spectra Reflectance changes Associated with Autumn Senescence of *Aesculus-Hippocastanum* L. and *Acer-Platanoides* L. Leaves – Spectral Features and Relation to Chlorophyll Estimation. *Journal of Plant Physiology* 148: 494-500.

Gitelson, A. A., Vina, A., Rundquist, D. C., Ciganda, V. and Arkebauer, T. J. (2005). Remote estimation of canopy chlorophyll content in crops. Geophys. Res. Lett. 32: L08403 doi: 10.1029/2005GL022688.

Goel, P. K., Prasher, S. O., Landry, J. A., Patel, R. M., Bonnell, R. B., Viau, A. A. and Miller, J. R. (2003). Potential of airborne hyperspectral remote sensing to detect nitrogen deficiency and weed infestation in corn. *Computers and Electronics in Agriculture* 38: 99-124.

Gong, P., Pu, R. L., Biging, G. S. and Larrieu, M. R. (2003). Estimation of forest leaf area index using vegetation indices derived from Hyperion hyperspectral data. *IEEE Transactions on Geoscience and Remote Sensing* 41: 1355-1362.

Gonzalez, C. E. A. (1998). Water management in America. *Water Resources Development* 14: 289-291.

Gooding, M. J. and Davies, W. P. (1997). Wheat production and utilization. Congress, Washington DC, USA.

Gopala Pillai, S., Tian, L. and Beal, J. (1998). Detection of nitrogen stress in corn using digital aerial imaging. ASAE Annual International Meeting, Paper No. 983030, ASAE, 2950 Niles Road, St. Joseph, MI 49085-9659.

Gorham, J. (1992). Salt tolerance in plants. *Sci. Progr*. 76: 273-285.

Graeff, S. and Claupein, W. (2007). Identification and discrimination of water stress in wheat leaves (*Triticum aestivum L.*) by means of reflectance measurements. *Irrigation Science* 26: 61-70.

Grattan, S. R. and Grieve, C. M. (1999). Salinity mineral nutrient relations in horticulture crops. *Sci. Hortic*. 78: 127-157

Greenway, H. and Munns, R. (1980). Mechanism of salt tolerance in non-halophytes. *Ann. Rev. Plant physiology* 31: 149-190.

Guiducci, M., Antognoni, A. and Benincasa, P. (1993). Movimento del fogliame, intercettazione e utilizzazione della luce in colture diverse in funzione della disponibilita idrica. *Rivista di Agronomia* 27: 392-397.

Hadjimitsis, D. G. and Clayton, C. R. I. (2004). An assessment of the effectiveness of atmospheric correction algorithms through the remote sensing of some reservoirs. *International Journal of Remote Sensing* 25 (18): 3651-3674.

Hamza, W. and Mason, S. (2004). Water availability and food security challenges in Egypt. International forum on food security under water scarcity in the Middle-East: Problems and solutions, Como, Italy, 24-27 Nov.

Hoffman, G. J., Mead, R. M., Ziska, L. H., Francois, L. E. and Gatlin P. B. (1986). Salt tolerance of mature plum trees yield. Water Management Research Laboratory Annual Report, USDA, Fresno, CA, pp 62-63.

Hong, S.-D., Schepers, J. S., Francis, D. D. and Schlemmer, M. R. (2007). Comparisons of ground-based remote sensors for evaluation of corn biomass affected by nitrogen stress. *Communications in Soil Science and Plant Analysis* 38: 2209-2226.

Hu, Y., Burucs, Z., Tucher, S. V. and Schmidhalter, U. (2007). Short-term effects of drought and salinity on mineral nutrient distribution along growing leaves of maize seedlings. *Environmental and Experimental Botany* 60: 268-275.

Hu, Y. and Schmidhalter, U. (1998). Spatial distribution and net deposition rates of mineral elements in the elongating wheat (Triticum aestivum L.) leaf under saline soil conditions. *Planta* 204: 212-219.

Hu, Y., Von Tucher, S. and Schmidhalter, U. (2000). Spatial distribution and net deposition rates of Fe, Mn and Zn in the elongating leaves of wheat under saline soil conditions. Aust. J. *Plant Physiology* 27: 53-59.

Huete, A. R. (1988). A Soil-Adjusted Vegetation Index (SAVI), *Remote Sensing of Environment* 25: 295-309.

Huete, A. R., Post, D. F. and Jackson, R. D. (1984). Soil spectral effects on 4-space vegetation discrimination. *Remote Sensing of Environment* 15: 155-165.

Inoue, Y. (2003). Remote Sensing and GIS for spatial assessment of Agro-Ecosystem: [online] http://147.46.223.123/Database/2003_symposium/proceeding/Inoue.pdf. Accessed in June 2007.

Jackson, R. D., Slater, P. N. and Pinter, P. J. (1983). Discrimination of growth and water stress in wheat by various vegetation indices through clear and turbid atmospheres. *Remote Sensing of Environment* 25: 295-309.

Jago, R. A., Cutler, M. E. J. and Curran, P. J. (1999). Estimating canopy chlorophyll concentration from field and airborne spectra. *Remote Sensing Environment* 68: 217-224.

Jahne, B. (1991). Digital image processing. 219-230 in. Springer-Verlag, New York.

Jiang, Y., Carrow, R. N. and Duncan, R. R. (2003). Correlation analysis procedures for canopy spectral reflectance data of Seashore Paspalum under Traffic stress. *J. Amer. Soc. Hort. Sci.* 13: 187-208.

Jones, H. G. (1999). Use of infrared thermometry for estimation of stomatal conductance as a possible aid to irrigation scheduling. *Agricultural and Forest Meteorology* 95: 139-149.

Jordan, C. F. (1969). Derivation of leaf area index from quality of light on the forest floor. *Ecology* 50: 663-666.

Kattenberg, A., Giorgi, F., Grassl, H., Meehl, G. A., Mitchell, J. F. B., Stouffer, R. J., Tokioka, T., Weaver, A. J. and Wigley, T. M. L. (1996). Climate model; projection of future climate. In: climate change 1995: the Science of Climate Change. Contribution of working group I to the second assessment report of the intergovernmental Panel on climate change. Cambridge University Press, Cambridge, United Kingdom and New York, NY, USA, pp. 285-357.

Klapp, E. (1967). Lehrbuch des Acker-und Pllanzenbaues 6. Auflage, Berlin.

Knipling, E. B. (1970). Physical and physiological basis for the reflectance of visible and near infrared radiation from vegetation. *Remote Sensing of Environment* 1: 155-159.

Kramer, P. J. and Boyer, J. S. (1995). Water relations of plants and soils. Academic Press Inc., San Diego.

Lamb, D.W. and Brown, R. B. (2001). Remote sensing and mapping of weeds in crops. *Journal of Agricultural Engineering Research* 78(2): 117-125.

Larcher, W. (1995). Physiological Plant Ecology, Third Edition, Springer-Verlag Berlin Heidelberg.

Le Maire, G., Francois, C. and Dufrene, E. (2004). Towardes universal broad leaf chlorophyll indices using PROSPECT simulated database and hyperspectral reflectance measurements. *Remote Sensing of Environment* 89: 1-28.

Lemaire, G. and Gastal, F. (1997). N uptake and distribution in plant canopies. In: G. Lemaire (Ed.), Diagnosis of the nitrogen status in crops, Springer-Verlag, Heidelberg, Germany, 3-43.

Li, F., Gnyp, M. L., Jia, L., Miao, Y., Yu, Z., Koppe, W., Bareth, G., Chen, X. and Zhang, F. (2008). Estimating N status of winter wheat using a handheld spectrometer in the North China Plain. *Field Crops Research* 106: 77-85.

Lichtenthaler, H. K. (1987). Chlorophylls and carotenoids: Pigments of photosynthetic biomembranes. *Methods in Enzymology* 148: 349-382.

Lichtenthaler, H. K., Gitelson, A. A. and Lang, M. (1996). Non destructive determination of chlorophyll content of leaves of a green and an aurea mutant of tobacco by reflectance measurements. *Journal of plant physiology* 148: 483-493.

Lillesand, T. M. and Kiefer, R. W. (2000). Remote Sensing and image Interpretation. 4th edition. John Wiley & Sons, Inc., New York.

Liu, L., Wang, J., Hunge, W., Zhao, C., Zhang, B. and Tong, Q. (2004). Estimating winter wheat plant water content using red edge parameters. *International Journal of Remote Sensing* 25 (17): 3331-3342.

Longenecker, D. E. and Lyerly, P. J. (1974). Control of soluble salts in farming and gardening. Texas A&M University system, Collage Station. June, pp 36.

Lord, D., Desjardins, R. L. and Dube, P. A. (1985b). Influence of wind on crop canopy reflectance measurements. *Remote Sensing of Environment* 18(2): 113-123.

Lord, D., Desjardins, R. L. and Dube, P. A. (1988). Sun angle effects on the red and Near-Infrared reflectance of five different crop canopies. *Canadian Journal of Remote Sensing* 14: 46-55.

Lord, D., Desjardins, R. L., Dube, P. A. and Brach, E. J. (1985a). Variations of crop canopy spectral reflectance measurements under changing sky conditions. *Photogrammetric Engineering and Remote Sensing* 51: 689-695.

Lu, Y. L., Li, S. K., Xie, R. Z., Gao, S. J., Wang, K. R., Wang, G. and Xiao, C. H. (2005). Estimating wheat grain protein content from ground-based hyperspectral data using an improved detecting method. IGARSS: *IEEE International Geoscience and Remote Sensing Symposium*, Vols 1-8, Proceedings: 1871-1874.

Lymburner, L., Beggs, P. J. and Jacobson, C. R. (2000). Estimation of canopy-average surface-specific leaf area using Landsat TM data. *Photogrametric Engineering & Remote Sensing* 66:183-191.

Maccioni, A., Agati, G. and Mazzinghi, P. (2001). New vegetation indices for remote measurement of chlorophylls based on leaf directional reflectance spectra. *Journal of Photochemistry and Photobiology B-Biology* 61: 52-61.

Major, D. J., Baret, F. and Guyot, G. (1990). A ration vegetation index adjusted for soil brightness. *International Journal of Remote Sensing* 11: 727-740.

Malthus, T. J. and Madeira, A. C. (1993). High resolution spectroradiometry: spectral reflectance of field bean leaves infected by *Botrytis fibac*. *Remote Sensing of Environment* 45: 107-116.

Marti, J., Bort, J., Salfer, G. A. and Araus, J. L. (2007). Can wheat yield be assessed by early measurements of Normalized Difference Vegetation Index. *Annals of Applied Biology* 150: 253-257.

Mass, E. V. and Poss, J. A. (1989). Salt sensitivity of cowpea at various growth stages. *Irri . Sci*. 10: 313-320.

Mehner, H., Cutler, M., Fairbairn, D. and Thompson, G. (2004). Remote sensing of upland vegetation: the potential of high spatial resolution satellite sensors. *Global Ecology and Biogeography* 13: 359-369.

Michelakis, N., Vougioucalou, E. and Clapaki, G. (1993). Water use, wetted soil volume, root distribution and yield of avocado under drip irrigation. *Agricultural Water Management* 24: 119-131.

Mickelson, Jr., John, G., Civco, D. L., Silander, Jr. and John, A. (1998). Responses of spectral indices to variations in vegetation cover and soil background. *Photogrammetric Engineering and Remote Sensing* 64(9): 915-921.

Mirik, M., Michels, G., Kassymzhanova, G. J., Mirik, S. and Elliott, N. C. (2007). Reflectance characteristics of Russian wheat aphid (*Hemiptera: Aphididae*) stress and abundance in winter wheat. Comp.Electr. Agric. 57: 123-134.

Moran, M. S. (2000). New imaging sensor technologies suitable for agricultural management. Aspects of Applied Biology, 60. *Remote Sensing in Agriculture*, 1-10.

Moran, M. S., Clarke, T. R., Inoue, Y. and Vidal, A. (1994). Estimating crop water deficit using the relation between surface air temperature and spectral vegetation index. *Remote sensing of Environment* 49 (3): 246-263.

Moran, M. S., Inoue, Y. and Barnes, E. M. (1997). Opportunities and limitations for image based remote sensing in precision crop management. *Remote Sensing of Environment* 61: 319-346.

Moran, M. S., Vidal, A., Troufleau, D., Qi, J., Clarke, T. R., Pinter, P. J., Mitchell, T. A., Inoue, Y. and Neale, C. M. U. (1997). Combining multifrequency microwave and optical data for crop management. *Remote sensing of Environment* 61: 96-109.

Musick, J. T. and Dusek, D. A. (1980). Irrigated corn yield response to water. *Trans. ASAE* 23: 92-98.

NASA 2005: Online: http://earthobservatory.nasa.gov/library/RemoteSensing Accessed on 18th July 2008.

Neumann, R. M. (1995). Inhibition of root growth by salinity stress: toxicity or adaptive biophysical response? In: Baluska, F. Ciamporova, M., Gasparikova, O., and Barlow, P.W., (Eds), Structure and Function of roots: Developments in Plant and Soil Sciences. *Kluwer Academic Publishers, Netherlands*: 299-304.

Neves-Piestun, B. G. and Bernstein, N. (2005). Salinity-induced changes in the nutritional status of expanding cells may impact leaf growth inhibition in maize. *Funct. Plant Biol*. 32: 141-152.

Nicholls, R. and Leatherman, S. (1995). Global sea level rise, in Strzepek, K. and Smith, J. (eds.), as climate changes, International Impacts and Implications, Cambridge University Press, Cambridge, pp 92.

Nilsson, H. E. (1991) Hand-held radiometry and IR-thermography of plant disease in field plot experiments. *International journal of Remote Sensing* 12(3): 545-557.

Oron, G. (1993). Recycling drainage water in San-Joaquin valley. *California Journal and Drainage Engineering Division, ASCE* 119: 265-285.

Osborne, L. S., Schepers, J. S., Francis, D. D. and Schlemmer, M. R. (2002a). Detecting Phosphorus and Nitrogen Deficiencies in Corn Using Radiance Measurements. *Agronomy Journal* 94: 1215-1221.

Osborne, L. S., Schepers, J. S., Francis, D. D. and Schlemmer, M. R. (2002b). Use of spectral radiance to estimate in-season biomass and grain yield in nitrogen and water stressed corn. *Crop Science* 42: 165-171.

Osborne, L. S., Schepers, J. S. and Schlemmer, M. R. (2004). Detecting Nitrogen and Phosphorus stress in corn using Multi-Spectral Imagery. *Communications in soil science and plant analysis* 35(3-4): 505-516

Ozturk, A. and Aydin, F. (2004). Effect of water stress at various growth stages on some quality characteristics of winter wheat. *Agronomy Journal and Crop Science* 190: 93-99.

Paolo, E. and Rinaldi, M. (2008). Yield response of corn to irrigation and nitrogen fertilization in a Mediterranean environment. *Field Crops Research* 105: 202-210.

Parkes, I. (1997). Earth Observation Science: AATSR. Retrieved from http://www.le.ac.uk/CWIS/AD/PH/PHE/pheasr_4html.

Pattey, E., Strachan, I. B., Boisvert, J. B., Desjardins, R. L. and McLaughlin, N. B. (2001). Detecting effects of nitrogen rate and weather on corn growth using micrometeorological and hyperspectral reflectance measurements. *Agricultural and forest meteorology* 108: 85-99.

Pearson, R. L. and Miller, L. D. (1972). Remote mapping of standing crop biomass for estimation of the productivity of the shortgrass prairie, Pawnee National Grassland, Colorado. In: proceeding of the 8th international symposium on Remote Sensing of Environment, ERIM International (pp. 1357-1381) (Ann Arbor, MI, USA)

Penuelas, J. and Filella, I. (1998). Visible and near-infrared reflectance techniques for diagnosing plant physiological status. *Trends in plant science* 3(4): 151-156.

Penuelas, J., Filella, I., Biel, C. and Serrno, L. and Save, R. (1993). The reflectance at the 950-970 nm region as an indicator of plant water status. *International journal of remote sensing* 14 (10): 1887-1905.

Penuelas, J., Filella, I. and Gamon, J. A. (1995). Assessment of photosynthetic radiation-use efficiency with spectral reflectance. *New Phytolgist* 131: 291-296.

Penuelas, J., Filella, I., Sav, R. and Serrno, L. (1996). Cell wall elasticity and water index (R970/R900) in wheat under different nitrogen availabilities. *International Journal of Remote Sensing* 17: 373-382.

Penuelas, J., Gamon, J. A. Ferdeen, A. L., Merino, J. and Field, C. B. (1994). Reflectance indices associated with physiological changes in nitrogen and water limited sunflower leaves. *Remote sensing Environment* 48: 135-146.

Penuelas, J. and Inoue, Y. (1999). Reflectance indices indicative of changes in water and pigment contents of peanut and wheat leaves. *Photosynthetic* 36(3): 355-360.

Penuelas, J., Isla, R., Filella, I. and Araus, J. L. (1997a). Visible and near-infrared reflectance assessment of salinity effects on barley. *Crop Science* 37: 198-202.

Penuelas, J., Pinol, J., Ogaya, R. and Filella, I. (1997b). Estimation of plant water concentration by the reflectance water index WI ($R_{900}/R_{970}$). *International Journal of Remote Sensing* 13: 2869-2872.

Penuelas, J., Save, R., Marfa, O. and Serrno, L. (1992). Remotely measured canopy temperature of greenhouse strawberries as indicator of water status and yield under mild and very mild water stress conditions. *Agricultural and Forest Meteorology* 58: 63-77.

Pessarkali, M. and Huber, J. T. (1991). Biomass production and protein synthesis by alfalfa under salt stress. *J. Plant Nutr*. 14: 283-293.

Pinkerton, A. and Simpson, J. R. (1986). Interactions of surface drying and subsurface nutrients affecting plant-growth on acidic soil profiles from an old pasture. *Aust. J. Exp. Agric.* 26: 681-689.

Pinter, P. J., Jerry, C. R, Jerry, L. H. and Galen, F. H. (2003).The Agricultural Research Service's Remote Sensing Program: An Example of Interagency Collaboration. *Photogrammetric Engineering and Remote Sensing* 8: 953-957.

Pinter, P. J., Zipoli, G., Maracchi, G. and Reginato, R. J. (1987). Influence of topography and sensor view angles on NIR/red ratio and greenness vegetation indices of wheat. *International Journal of Remote Sensing* 8: 953-957.

Poss, J. A., Russell, W. B. and Grieve, C. M. (2006). Estimating yield of salt-and water-stressed forages with remote sensing in the visible and near infrared. *J. Environ. Qual.* 35: 1060-1071.

Prasad, B., Carver, B. F., Stone, M. L., Babar, M. A., Raun, W. R. and Klatt, A. R. (2007). Potential use of spectral reflectance indices as a selection tool for grain yield in winter wheat under Great Plains conditions. *Crop Science* 47: 1426-1440.

Pu, R., Kelly, M., Anderson, G. L. and Gong, P. (2008). Using CASI hyperspectral imagery to detect mortality and vegetation stress associated with hardwood forest disease. *Photogrammetric Engineering and Remote Sensing* 74(1): 65-76.

Rainey, M. P., Tyler, A. N., Bryant, R. G., Gilvear, D. J. (2000). The influence of surface and interstitial moisture on the spectral characteristics of intertidal sediments: implications for airborne image acquisition and processing. *International Journal of Remote Sensing* 21 (16): 3025-3038.

Rainey, M. P., Tyler, A. N., Gilvear, D. J., Bryant, R. G. and McDonald, P. (2003). Mapping intertidal estuarine sediment grain size distribution through airborne remote sensing. *Remote Sensing of Environment* 86: 480-490.

Rains, G. C. and Thomas, D. L. (2000). Precision farming – and introduction. Georgia Bulletin 1186, the world web-site http://www.ces.uga.edu/pubcd/B1186.htm.

Ranson, K. J., Daughtry, C. S. T., Biehl, L. L. and Bauer, M. E. (1985). Sun-view angle effects on reflectance factors of corn canopies, *Remote Sensing of Environment* 18(2): 147-161.

Raun, W. R., Solie, J. B., Johnson, G. V., Stone, M. L., Lukina, E. V., Thomson, W. E. and Schepers, J. S. (2001). In-season prediction of potential grain yield in winter wheat using canopy reflectance. *Agronomy Journal* 93: 131-138.

Rawlins, S. L. (1996). Moving from precision to prescription farming: the next plateau, in proceeding of the 3rd international conference on precision agriculture, (Robert, P. C.; Rust, R. H. and Larson, W. E. eds), 425-432 Madison, Wisconsin, ASA, CSSA, SSSA, pp 283-294.

Reujean, J. and Breon, F. (1995). Estimating PAR absorbed by vegetation from bidirectional from reflectance measurements. *Remote Sensing of Environment* 51: 375-384.

Reyniers, M. and Vrindts, E. (2006). Measuring wheat nitrogen status from space and ground-based platform. *International Journal of Remote Sensing* 27(3): 549-567.

Reyniers, M. Vrindts, E. and De Baerdemaeker, J. (2004). Optical measurement of crop cover for yield prediction of wheat. *Biosystem Engineering* 89: 383-394.

Rhoades, J. D., Kandiah, A. and Mashali, A. M. (1992). The use of saline water for crop production. FAO irrigation and drainage paper No. 48, Rome, pp 133.

Richards, J. A. (1993). Remote sensing digital image analysis. Springer-Verlag, New York.

Riedell, W. E. and Blackmer, T. M. (1999). Leaf reflectance spectra of cereal aphid-damage wheat. *Crop Science* 39(6): 1835-1840.

Riedell, W. E., Hesler, L. S., Obsorne, S. and Blackmer, T. M. (2000). Remote sensing of insect damage in wheat. Proceeding of fifth International Conference on Precision Agriculture (CD), July 16-19, 2000. Bloomington, MN, USA.

Ritchie, S. W., Hanway, J. J. and Benson, G. O. (1992). How a corn plant develops. Special Report NO. 48. Iowa State University, pp 21.

Rodriguez, I. R. and Miller, G. L. (2000). Using near infrared reflectance spectroscopy to schedule nitrogen applications on dwarf-type bermudagrasses. *Agronomy Journal* 92: 423-427.

Rondeaux, G., Steven, M. and Baret, F. (1996). Optimization of soil-adjusted vegetation indices. *Remote Sensing of Environment* 55: 95-107.

Rouse, J. W., Haas, Jr. R. H., Deering, D. W., Schell, J. A. and Harlan, J. C. (1974). Monitoring the vernal advancement and retro gradation (green wave effect) of natural vegetation; NASA/GSFC Type III final report, Greenbelt, MD. pp 371.

Rouse, J. W., Haas, Jr. R. H., Schell, J. A. and Deering, D. W. (1973). Monitoring vegetation systems in the Great Plains with ERTS. In: N. SP-351, (Ed.) pp. 309-317. Washington: NASA.

Rowell, D. L. (1994). Soil Science methods and applications. Longman group UK Limited.

Royo, C., Aparicio, N., Villegas, D., Casadesus, J., Monnveux, P. and Araus, J. L. (2003). Usefulness of spectral reflectance indices as durum wheat yield predictors under contrasting Mediterranean conditions. *International Journal of Remote Sensing* 24: 4403-4419.

Rudorff, B. F. T., Mulchi, C. L., Daughtry, C. S. T. and Lee, E. H. (1996). Growth, radiation use efficiency, and canopy reflectance of wheat and corn grown under elevated ozone and carbon dioxide atmospheres. *Remote sensing of Environment* 55: 163-173.

Saltveit, M. E. Jr. and Moris, L. L. (1990). Overview of chilling injury of horticultural crops. 3-15. In: Ed. C. Y. Wang. Chilling Injury of Horticulture Crops. CRC Press, Boca Raton.

Satellite imaging corporation (2008): Accessed online on 19 September 2008: http://www.satimagingcrop.com/satellite-sensors

Schepers, J. S., Blackmer, T. M., Wilhelm, W. W. and Resende, M. (1996). Transmittance and reflectance measurements of corn leaves from plant with different nitrogen and water supply. *Journal of Plant Physiology* 148: 523-529.

Schlemmer, M. R., Francis, D. D., Shanahan, J. F. and Schepers, J. S. (2005). Remotely measuring chlorophyll content in corn leaves with differing nitrogen levels and relative water content. *Agronomy Journal* 97: 106-112.

Schneider, A. D. and Howell, T. A. (1998). LEPA and spray irrigation of corn-Southern High Plains. *Trans. ASAE* 41(5): 1391-1396.

Serrano, L., Filella, I. and Peuelas, J. (2000). Remote sensing of biomass and yield of winter wheat under different nitrogen supplies. *Crop Science* 40: 723-731.

Shanahan, J. F., Schepers, J. S. Francis, D. D., Varvel, G. E., Wilhelm, W. W., Tringe, J. M., Schlemmer, M. R. and Major, D. J. (2001). Use of remote sensing imagery to estimate corn grain yield. *Agronomy Journal* 93: 583-589.

Shanmugam, P., Ahn, Y. H. and Sanjeevi, S. (2006). A comparison of the classification of wetland characteristics by linear spectral mixture modelling and

traditional hard classifiers on multispectral remotely sensed imagery in southern India. *Ecological Modelling* 194: 379-394.

Sims, D. A. and Gamon, J. A. (2003). Estimation of vegetation water content and photosynthetic tissue area from spectral reflectance: a comparison of indices based on liquid water and chlorophyll absorption features. *Remote sensing of Environment* 84: 526-537.

Souza, R. P., Machado, E. C., Silva, J. A. B., Lagoa, A. M. M. A. and Silveira, J. A. G. (2004). Photosynthetic gas exchange, chlorophyll fluorescence, and some associated metabolic changes in cowpea (*Vigna unguiculata*) during water stress and recovery. *Environ. Exp. Bot*. 51: 45-56.

Starks, P. J., Zhao, D., Phillips, W. A. and Coleman, S. W. (2006). Development of Canopy Reflectance Algorithms for Real-Time Prediction of Bermudagrass Pasture Biomass and Nutritive Values. *Crop Science* 46: 927-934.

Staub, J. E. (1990). Screening of the US cucumber Germplasm Collection for Heat Stress Tolerance. Cucurbit Genetics Cooperative Report, 13: 4-7.

Steinmetz, S., Guerif, M., Delecolle, R. and Baret, F. (1990). Spectral estimates of the absorbed photosynthetically active radiation and light-use efficiency of a winter wheat crop subjected to N and water deficiencies. *International Journal of Remote Sensing* 11: 1797-1808.

Steven, M. D. (1993). Satellite remote sensing for agricultural management: opportunities and logistic constraints. *ISPRS Journal of photogrammetry and Remote Sensing* 48 (4): 29-34.

Stone, M. L., Raun, W. R., Johnson, G. V., Solie, J. B., Whitney, R. W., Sembiring, H., Laruffa, J. M. and Lukina, E. V. (1997). Sensing nitrogen deficiencies in winter wheat and bermudagrass. *Better Crops* 81(4): 15-19.

Stone, M. L., Solie, J. B., Raun, W. R., Whitney, R. W., Taylor, S. L. and Ringer, J. D. (1996). Use of spectral radiance for correcting in-season fertilizer nitrogen deficiencies in winter wheat. *Transactions of the American Society of Agricultural Engineers* 39(5): 1623-1631.

Stoskopf, N. C. (1992). Cereal Grain Crops. Reston publishing company, Virginia.

Strachan, I. B., Pattey, E. and Boisvert, J. B. (2002). Impact of nitrogen and environmental conditions on corn as detected by hyperspectral reflectance. *Remote Sensing of Environment* 80: 213-224.

Su, L. H., Chopping, M. J., Rango, A., Maronchik, J. V. and Peters, D. P. C. (2007). Support Vector Machines for recognition of semi-arid vegetation types using Misr Multi-Angle Imagery. *Remote Sensing of Environment* 107: 299-331.

Tartachnyk, I. I. and Rademacher, I. (2006). Distinguishing nitrogen deficiency and fungal infection of winter wheat by laser-induced fluorescence. *Precision Agric*. 7: 281-293.

Teillet, P. M. Staenz, K. and Williams, D. J. (1997). Effects of spectral, spatial and radiometric characteristics on remote sensing vegetation indices of forested regions. *Remote Sensing of Environment* 61: 139-149.

Thenkabail, P. S., Ward, A. D. and Lyon, J. G. (1995). Landsat-5 Thematic Mapper models of soybean and corn crop characteristics. *International Journal of Remote Sensing* 15: 49-58.

The Texas A&M University System: Irrigation water quality Standards and salinity management: accessed online on 15 March 2008: http://tcebookstore.org

Thirkawala, S., Weersink, A., Kachanoski, G. and Fox, G. (1999). Economic feasibility of variable rate technology for nitrogen on corn. *American Journal of Agricultural Economics* 81: 914-927.

Tian, Q. and Tong, Q. Pu, R., Guo, X. and Zhao, C. (2001). Spectroscopic determination of wheat water status using 1650-1850 nm spectral absorption features. *International Journal of Remote Sensing* 22(12): 2329-2338.

Tian, Y., Zhang, Y., Knyazikhin, Y., Myneni, R. B., Glassy, J. M., Dedieu, G. and Running, S. W. (2000). Prototyping of MODIS LAI and FPAR algorithm with LASUR and LANDSAT data. *IEEE Transactions on Geoscience and Remote Sensing* 38: 2387-2401.

Tilling, A. K, Leary, G. J., Ferwerda, J. G., Jones, S. D., Fitzgerald, G. J., Rodriguez, D. and Belford, R. (2007). Remote sensing of nitrogen and water stress in wheat. *Field Crops Research* 104: 77-85.

Toler, R. W., Smith, B. D., and Harlan, J. C. (1981). Use of aerial colour infrared photography to evaluate crop disease. *Plant Disease* 65: 24-31.

Tucker, C. J. (1979). Red and Photographic infrared linear combination for monitoring vegetation. *Remote Sensing of Environment* 8: 127-150.

Tucker, C. J. and Sellers, P. J. (1986). Satellite remote sensing of primary production. *International Journal of Remote Sensing* 7: 1395-1416.

Twele, A., Erasmi, S. and Kappas, M. (2008). Spatially explicit estimation of leaf area index using EO-1 Hyperion and landsat ETM+data: Implications of spectral bandwidth and shortwave infrared data on prediction accuracy in a tropical montane environment. *Gioscience and Remote Sensing* 45 (2): 229-248.

Tyler, A. N., Svab, E., Preston, T., Presing, M. and Kovacs, W. A. (2006). Remote Sensing of the water quality of shallow lakes: A mixture modelling approach to quantifying phytoplankton in water characterized by high-suspended sediment. *International Journal of Remote Sensing* 27(8): 1521-1537.

Vina, A. (2003). Remote detection of Biophysical Properties of Plant Canopies. [Online]: http://calamps.unl.edu/snrscoq/SNRS_Colloquium_2002_Andres_Vina.ppt.

Vouillot, M. O., Huet, P. and Boissard, P. (1998). Early detection of N deficiency in a wheat crop using physiological and radiometric methods. *Agronomie* 18: 117-130.

Wang, D., Poss, J. A., Donovan, T. J., Shannon, M. C. and Lesch, S. M. (2002a). Biophysical properties and biomass production of elephant grass under saline condition. *Journal of Arid Environments* 52: 447-456.

Wang, D., Wilson, C. and Shannon, M. C. (2002b). Interpretation of salinity and irrigation effects on soybean canopy reflectance in visible and near infrared spectrum domain. *International Journal of Remote Sensing* 23(5): 811-824.

Wang, F. M., Huang J. F., Xu, J. F. and Wang, X. Z. (2008). Wavebands selection for rice information extraction based on spectral bands inter-correlation. *Specrtoscopy and Spectral Analysis* 28(5): 1098-1101.

Wang, L., Silvan-Cardenas, J. L. and Sousa, W. P. (2008). Neural network classification on mangrove species from multi-seasonal ikonos imagery. *Photogrammetric Engineering and Remote Sensing* 74(7): 921-927.

Weather Network 2008. Online: http://www.theweathernetwork.com/statistics/C01411/egxx0001

Wheeler, T. R., Hong, T. D., Ellis, R. H., Batts, G. R., Morison, J. I. L. and Hadley, P. (1996). The duration and rate of grain growth, and harvest index, of wheat (*Triticum aestivum*) in response to temperature and CO2. *Journal of Experimental Botany* 47: 623-630.

Wibberley, E. J. (1989). Cereal husbandry. Farming press, Ipswich, pp 258.

Wright, S. W., Jeffrey, S. W., Mantoura, R. F. C., Llewellyn, C. A., Bjornland, T., Repeta, D. and Welschmeyer, N. (1991). Improved HPLC method for the analysis of chlorophylls and carotenoids from marine-phytoplankton. *Marine Ecology-Progress Series* 77: 183-196.

Wu, J., Schepers, J. S., Francis, D. D. and Schlemmer, M. R. (2007c). Comparison of ground-based remote sensors for evaluation of corn biomass affected by nitrogen stress. *Communication in Soil Science and Plant Analysis* 38: 2209-2226.

Wu, J., Wang, D. and Bauer, M. E. (2005). Image-based atmospheric correction of QuickBird imagery of Minnesota cropland. *Remote Sensing of Environment* 99(3): 315-325.

Wu, J., Wang, D. and Bauer, M. E. (2007b). Assessing broadband vegetation indices and QuickBird data in estimating leaf area index of corn and potato canopies. *Field Crops Research* 102: 33-42.

Wu, J., Wang, D., Rosen, C. J. and Bauer, M. B. (2007a). Comparison of petiole nitrate concentration, SPAD chlorophyll readings, and QuickBird satellite imagery in detecting nitrogen status of potato canopies. *Field Crops Research* 101: 96-103.

Xu, H. R., Ying, Y. B., Fu, X. P. and Zhu, S. P. (2007). Near-infrared Spectroscopy in detecting leaf miner damage on tomato leaf. *Biosystems Engineering* 96(4): 447-454.

Yang, C., Everitt, J. H. and Bradford, J. M. (2006a). Comparisons of QuickBird satellite imagery and airborne imagery for mapping grain sorghum yield patterns. *Precision Agriculture* 7: 33-44.

Yang, C., Everitt, J. H. and Bradford, J. M. (2006b). Evaluating high-resolution QuickBird satellite imagery for estimating cotton yield. *Transactions of the ASABE* 49 (5): 1599-1606.

Yang, C.-M., Lee, Y.-J., Hong, K.-Y. and Hsu, F.-H. (2007). Estimation of forage production of Nilegrass using vegetation reflectance. *Crop Science* 47: 1647-1651.

Yang, Z., Rao, M. N., Elliott, N. C., Kindler, S. D. and Popham, T. W. (2005). Using ground-based multispectral radiometry to detect stress in wheat caused by greenbug (Homoptera Aphididiae) infestation. *Computers and Electronics in Agriculture* 47(2): 121-135.

Yefremenko, V. V., Moshkov, A. V., Semenov, A. A. and Chimitdorzhiyez, T. N. (1998). Use of false colour scanner imagery to detect vegetation stress. *GIS Science and Remote Sensing* 35: 218-226.

Zadoks, J. C. Chang, T. T. and Konzak, C. F. (1974). A decimal code for the growth stages of cereals. *Weed research, Oxford* 14: 415-421.

Zaidi, P. H., Srinivasan, G., Cordova, H. S. and Sanchez, C. (2004). Grains from improvement for mid-season drought tolerance in tropical maize (*Zea mays* L.). *Field Crops Research* 89: 135-152.

# APPENDIX A

**Table A1**- Coefficient of correlation for the relationship between different vegetation indices and chlorophyll *a* concentration of Scottish wheat obtained at different DAS in the 2005-06 growing season. Highlighted values are significant (P<0.05) and bold values are the strongest correlations.

| Scale | Vegetation index | Chlorophyll *a* concentration (µg cm$^{-2}$) | | | | |
|---|---|---|---|---|---|---|
| | | 73 DAS | 125 DAS | 181 DAS | 207 DAS | 225 DAS |
| Broad band | NDVI | -0.01 | 0.11 | 0.56 | 0.51 | 0.50 |
| | RVI | 0.00 | 0.19 | **0.57** | 0.55 | 0.55 |
| | SAVI | -0.08 | -0.05 | 0.53 | 0.56 | 0.49 |
| | GNDVI br | 0.01 | 0.10 | 0.55 | 0.52 | 0.55 |
| | DVI | -0.07 | -0.11 | 0.50 | 0.55 | 0.45 |
| | SR | 0.00 | 0.19 | **0.57** | 0.55 | 0.55 |
| | SLAVI | -0.01 | 0.11 | 0.56 | 0.51 | 0.50 |
| | OSAVI | -0.07 | 0.00 | 0.55 | 0.55 | 0.49 |
| | VI1 | 0.08 | 0.14 | -0.46 | -0.46 | -0.14 |
| | RDVI | 0.00 | 0.17 | **0.57** | 0.54 | 0.54 |
| | SI | 0.01 | -0.10 | -0.55 | -0.51 | -0.48 |
| | IPVI | -0.01 | 0.11 | 0.56 | 0.51 | 0.50 |
| Hyper | WI | 0.04 | 0.19 | -0.29 | -0.29 | -0.24 |
| | PSI | -0.06 | 0.00 | 0.14 | -0.27 | -0.09 |
| | NWI-1 | -0.08 | 0.11 | -0.48 | -0.24 | -0.29 |
| | NWI-2 | -0.13 | 0.09 | -0.54 | -0.24 | -0.30 |
| | NDVI hy | -0.01 | 0.10 | 0.56 | 0.51 | 0.48 |
| | GNDVI hy | 0.02 | 0.09 | 0.54 | 0.52 | 0.56 |
| | SIPI | -0.04 | 0.06 | 0.54 | 0.53 | 0.51 |
| | SRPI | 0.05 | 0.28 | 0.37 | 0.46 | 0.46 |
| | NPCI | -0.02 | -0.22 | -0.43 | -0.44 | -0.44 |
| | NPQI | -0.12 | 0.23 | -0.21 | 0.17 | 0.35 |
| | PSSRb | -0.07 | -0.10 | 0.50 | 0.55 | 0.47 |
| | PSNDb | 0.02 | 0.11 | 0.56 | 0.51 | 0.51 |
| | Rshoulder | -0.08 | -0.13 | 0.48 | 0.50 | 0.32 |
| | C420 | 0.08 | 0.15 | -0.06 | 0.30 | 0.45 |
| | NDI | -0.07 | -0.11 | 0.50 | 0.55 | 0.45 |
| | SR hyper | 0.01 | 0.21 | 0.57 | 0.56 | 0.54 |
| | R800-R550 | -0.07 | -0.10 | 0.51 | 0.57 | 0.52 |
| | R800/R550 | 0.02 | 0.12 | 0.53 | 0.54 | 0.59 |
| | R695/R760 | 0.02 | -0.12 | -0.56 | -0.49 | -0.49 |
| | R605/R760 | 0.01 | -0.11 | -0.56 | -0.51 | -0.51 |
| | R710/R760 | -0.04 | -0.12 | -0.55 | -0.48 | -0.52 |
| | R695/R670 | 0.02 | 0.08 | 0.52 | **0.62** | 0.38 |
| | R550 | -0.09 | -0.20 | 0.23 | -0.33 | -0.49 |
| | R675/R700 | -0.01 | -0.09 | -0.56 | -0.58 | -0.41 |
| | R675/(R700*R650) | 0.08 | 0.17 | -0.21 | 0.28 | 0.57 |
| | R672/(R55*R708) | 0.07 | 0.03 | -0.47 | -0.32 | -0.01 |
| | R672/R550 | 0.01 | -0.11 | -0.56 | -0.50 | -0.39 |
| | R860/(R550*R708) | 0.10 | 0.21 | 0.06 | 0.39 | 0.56 |
| | R750/R550 | 0.02 | 0.12 | 0.55 | 0.54 | 0.59 |
| | R750/R700 | 0.02 | 0.18 | 0.56 | 0.51 | 0.56 |
| | R725/R675 | 0.01 | 0.19 | 0.58 | 0.55 | 0.51 |
| | (R850-R710)/(R850-R680) | 0.08 | 0.12 | 0.47 | 0.41 | 0.59 |
| | (R780-R710)/(R780-R680) | 0.08 | 0.12 | 0.48 | 0.41 | 0.58 |
| | R700-R670 | -0.09 | -0.20 | 0.32 | 0.29 | -0.27 |
| | RNDVI | 0.00 | 0.09 | 0.56 | 0.51 | 0.48 |
| | PSR | 0.00 | -0.20 | -0.44 | -0.47 | -0.43 |
| | WBI | -0.03 | 0.16 | -0.40 | -0.32 | -0.26 |
| | SIPI | -0.03 | -0.09 | -0.52 | -0.48 | -0.41 |
| | YI | 0.00 | 0.08 | 0.11 | -0.35 | -0.42 |
| | VI2 | 0.08 | 0.15 | -0.46 | -0.46 | -0.15 |
| | Cgreen | 0.02 | 0.12 | 0.53 | 0.54 | 0.59 |
| | Cred edge | 0.02 | 0.18 | 0.54 | 0.51 | 0.56 |
| | C NIR | 0.06 | 0.11 | 0.42 | 0.50 | 0.55 |

**Table A2**- Coefficient of correlation for the relationship between different vegetation indices and grain yield of Scottish wheat obtained at different DAS in the 2005-06 growing season. Highlighted values are significant (P<0.05) and bold values are the strongest correlations.

| Scale | Vegetation index | Grain yield (kg $m^{-2}$) | | | | |
|---|---|---|---|---|---|---|
| | | 73 DAS | 125 DAS | 181 DAS | 207 DAS | 225 DAS |
| Broad band | NDVI | 0.07 | 0.28 | 0.35 | 0.76 | 0.88 |
| | RVI | 0.11 | 0.33 | 0.35 | 0.84 | **0.91** |
| | SAVI | -0.15 | 0.30 | 0.40 | 0.71 | 0.86 |
| | GNDVI br | 0.15 | 0.18 | 0.34 | 0.76 | **0.91** |
| | DVI | -0.15 | 0.30 | 0.41 | 0.64 | 0.79 |
| | SR | 0.11 | 0.33 | 0.35 | 0.84 | **0.91** |
| | SLAVI | 0.07 | 0.28 | 0.35 | 0.76 | 0.88 |
| | OSAVI | -0.12 | 0.30 | 0.39 | 0.74 | 0.87 |
| | VI1 | 0.16 | -0.29 | -0.40 | -0.40 | -0.28 |
| | RDVI | 0.10 | 0.32 | 0.36 | 0.83 | **0.91** |
| | SI | -0.06 | -0.27 | -0.35 | -0.74 | -0.86 |
| | IPVI | 0.07 | 0.28 | 0.35 | 0.76 | 0.88 |
| Hyper | WI | 0.20 | -0.13 | -0.18 | -0.52 | -0.75 |
| | PSI | -0.10 | 0.13 | -0.02 | -0.09 | -0.13 |
| | NWI-1 | -0.16 | 0.14 | -0.29 | -0.56 | -0.77 |
| | NWI-2 | -0.04 | 0.10 | -0.33 | -0.56 | -0.78 |
| | NDVI hy | 0.08 | 0.29 | 0.35 | 0.76 | 0.87 |
| | GNDVI hy | 0.19 | 0.15 | 0.32 | 0.75 | 0.91 |
| | SIPI | 0.05 | 0.26 | 0.33 | 0.77 | 0.90 |
| | SRPI | 0.10 | 0.11 | 0.20 | 0.75 | 0.84 |
| | NPCI | 0.09 | -0.20 | -0.28 | -0.71 | -0.78 |
| | NPQI | -0.11 | -0.21 | -0.07 | 0.58 | 0.66 |
| | PSSRb | -0.15 | 0.30 | 0.41 | 0.64 | 0.80 |
| | PSNDb | 0.06 | 0.27 | 0.35 | 0.76 | 0.89 |
| | Rshoulder | -0.16 | 0.29 | 0.41 | 0.48 | 0.56 |
| | C420 | 0.23 | -0.12 | -0.06 | 0.59 | 0.71 |
| | NDI | -0.15 | 0.30 | 0.41 | 0.64 | 0.79 |
| | SR hyper | 0.13 | 0.36 | 0.34 | 0.85 | 0.90 |
| | R800-R550 | -0.13 | 0.29 | 0.42 | 0.62 | 0.84 |
| | R800/R550 | 0.22 | 0.16 | 0.30 | 0.78 | 0.92 |
| | R695/R760 | -0.16 | -0.24 | -0.35 | -0.74 | -0.87 |
| | R605/R760 | -0.15 | -0.24 | -0.37 | -0.75 | -0.87 |
| | R710/R760 | -0.33 | -0.16 | -0.32 | -0.74 | -0.89 |
| | R695/R670 | 0.02 | 0.38 | 0.40 | 0.88 | 0.79 |
| | R550 | -0.25 | 0.24 | 0.28 | -0.61 | -0.75 |
| | R675/R700 | 0.00 | -0.35 | -0.39 | -0.85 | -0.82 |
| | R675/(R700*R650) | 0.25 | -0.22 | -0.23 | 0.66 | 0.88 |
| | R672/(R55*R708) | 0.24 | -0.33 | -0.36 | -0.26 | -0.24 |
| | R672/R550 | 0.07 | -0.35 | -0.39 | -0.78 | -0.78 |
| | R860/(R550*R708) | 0.31 | -0.13 | -0.09 | 0.71 | 0.89 |
| | R750/R550 | 0.18 | 0.17 | 0.32 | 0.78 | **0.93** |
| | R750/R700 | 0.14 | 0.23 | 0.32 | 0.80 | 0.91 |
| | R725/R675 | 0.10 | 0.39 | 0.39 | 0.84 | 0.89 |
| | (R850-R710)/(R850-R680) | 0.33 | 0.04 | 0.21 | 0.66 | 0.86 |
| | (R780-R710)/(R780-R680) | 0.31 | 0.06 | 0.22 | 0.66 | 0.87 |
| | R700-R670 | -0.22 | 0.29 | 0.35 | 0.06 | -0.19 |
| | RNDVI | 0.05 | 0.29 | 0.35 | 0.76 | 0.87 |
| | PSR | 0.12 | -0.20 | -0.29 | -0.70 | -0.79 |
| | WBI | 0.24 | -0.06 | -0.24 | -0.57 | -0.77 |
| | SIPI | -0.08 | -0.24 | -0.33 | -0.69 | -0.78 |
| | YI | -0.28 | 0.34 | 0.08 | -0.49 | -0.71 |
| | VI2 | 0.17 | -0.29 | -0.40 | -0.37 | -0.27 |
| | Cgreen | 0.22 | 0.16 | 0.30 | 0.78 | 0.92 |
| | Cred edge | 0.18 | 0.21 | 0.30 | 0.80 | 0.91 |
| | C NIR | 0.33 | 0.03 | 0.13 | 0.74 | 0.89 |

**Table A3**- Coefficient of correlation for the relationship between different vegetation indices and aboveground biomass of Scottish wheat obtained at different DAS in the 2005-06 growing season. Highlighted values are significant (P<0.05) and bold values are the strongest correlations.

| Scale | Vegetation index | Aboveground biomass (kg m$^{-2}$) | | |
|---|---|---|---|---|
| | | 181 DAS | 207 DAS | 225 DAS |
| Broad band | NDVI | 0.44 | 0.79 | 0.91 |
| | RVI | 0.44 | 0.83 | 0.91 |
| | SAVI | 0.44 | 0.71 | 0.88 |
| | GNDVI br | 0.43 | 0.79 | **0.92** |
| | DVI | 0.43 | 0.62 | 0.81 |
| | SR | 0.44 | 0.83 | 0.91 |
| | SLAVI | 0.44 | 0.79 | 0.91 |
| | OSAVI | 0.44 | 0.76 | 0.90 |
| | VI1 | -0.41 | -0.35 | -0.28 |
| | RDVI | 0.44 | 0.83 | **0.92** |
| | SI | -0.43 | -0.78 | -0.89 |
| | IPVI | 0.44 | 0.79 | 0.91 |
| Hyper | WI | -0.25 | -0.61 | -0.71 |
| | PSI | 0.04 | -0.01 | -0.13 |
| | NWI-1 | -0.37 | -0.60 | -0.76 |
| | NWI-2 | -0.42 | -0.61 | -0.78 |
| | NDVI hy | 0.43 | 0.79 | 0.90 |
| | GNDVI hy | 0.41 | 0.78 | **0.92** |
| | SIPI | 0.41 | 0.81 | **0.92** |
| | SRPI | 0.29 | 0.78 | 0.87 |
| | NPCI | -0.35 | -0.70 | -0.80 |
| | NPQI | -0.07 | 0.55 | 0.68 |
| | PSSRb | 0.44 | 0.62 | 0.82 |
| | PSNDb | 0.43 | 0.79 | 0.91 |
| | Rshoulder | 0.42 | 0.44 | 0.56 |
| | C420 | -0.04 | 0.58 | 0.72 |
| | NDI | 0.43 | 0.62 | 0.81 |
| | SR hyper | 0.43 | 0.83 | 0.90 |
| | R800-R550 | 0.44 | 0.60 | 0.85 |
| | R800/R550 | 0.39 | 0.79 | **0.92** |
| | R695/R760 | -0.44 | -0.78 | -0.90 |
| | R605/R760 | -0.46 | -0.78 | -0.90 |
| | R710/R760 | -0.42 | -0.78 | -0.91 |
| | R695/R670 | 0.45 | 0.86 | 0.83 |
| | R550 | 0.25 | -0.67 | -0.77 |
| | R675/R700 | -0.45 | -0.84 | -0.86 |
| | R675/(R700*R650) | -0.20 | 0.70 | 0.87 |
| | R672/(R55*R708) | -0.39 | -0.19 | -0.26 |
| | R672/R550 | -0.45 | -0.78 | -0.81 |
| | R860/(R550*R708) | 0.00 | 0.73 | 0.87 |
| | R750/R550 | 0.41 | 0.79 | **0.92** |
| | R750/R700 | 0.42 | 0.80 | 0.90 |
| | R725/R675 | 0.47 | 0.82 | 0.89 |
| | (R850-R710)/(R850-R680) | 0.32 | 0.72 | 0.86 |
| | (R780-R710)/(R780-R680) | 0.33 | 0.72 | 0.87 |
| | R700-R670 | 0.32 | -0.01 | -0.13 |
| | RNDVI | 0.44 | 0.79 | 0.90 |
| | PSR | -0.37 | -0.71 | -0.82 |
| | WBI | -0.30 | -0.64 | -0.75 |
| | SIPI | -0.42 | -0.73 | -0.83 |
| | YI | 0.11 | -0.54 | -0.73 |
| | VI2 | -0.41 | -0.32 | -0.26 |
| | Cgreen | 0.39 | 0.79 | **0.92** |
| | Cred edge | 0.40 | 0.81 | 0.90 |
| | C NIR | 0.25 | 0.79 | 0.90 |

**Table A4-** Coefficient of correlation for the relationship between different vegetation indices and LAI of Scottish wheat at different DAS in the 2005-06 growing season. Highlighted values are significant ($P<0.05$) and bold values are the strongest correlations.

| Scale | Vegetation index | Leaf Area Index | | |
|---|---|---|---|---|
| | | 181 DAS | 207 DAS | 225 DAS |
| Broad band | NDVI | 0.55 | 0.76 | 0.85 |
| | RVI | 0.57 | 0.76 | 0.81 |
| | SAVI | 0.48 | 0.64 | 0.82 |
| | GNDVI br | 0.53 | 0.78 | **0.90** |
| | DVI | 0.46 | 0.53 | 0.74 |
| | SR | 0.57 | 0.76 | 0.81 |
| | SLAVI | 0.55 | 0.76 | 0.85 |
| | OSAVI | 0.51 | 0.71 | 0.84 |
| | VI1 | -0.42 | -0.23 | -0.21 |
| | RDVI | 0.57 | 0.77 | 0.84 |
| | SI | -0.55 | -0.75 | -0.85 |
| | IPVI | 0.55 | 0.76 | 0.85 |
| Hyper | WI | -0.17 | -0.65 | -0.56 |
| | PSI | 0.24 | -0.12 | 0.00 |
| | NWI-1 | -0.49 | -0.62 | -0.63 |
| | NWI-2 | -0.53 | -0.64 | -0.64 |
| | NDVI hy | 0.55 | 0.76 | 0.84 |
| | GNDVI hy | 0.52 | 0.78 | **0.90** |
| | SIPI | 0.53 | 0.80 | **0.90** |
| | SRPI | 0.36 | 0.74 | 0.81 |
| | NPCI | -0.42 | -0.62 | -0.67 |
| | NPQI | -0.18 | 0.46 | 0.68 |
| | PSSRb | 0.46 | 0.52 | 0.75 |
| | PSNDb | 0.56 | 0.76 | 0.85 |
| | Rshoulder | 0.43 | 0.33 | 0.49 |
| | C420 | -0.10 | 0.49 | 0.57 |
| | NDI | 0.46 | 0.53 | 0.74 |
| | SR hyper | 0.56 | 0.76 | 0.79 |
| | R800-R550 | 0.46 | 0.51 | 0.81 |
| | R800/R550 | 0.51 | 0.79 | 0.88 |
| | R695/R760 | -0.55 | -0.75 | -0.84 |
| | R605/R760 | -0.54 | -0.76 | -0.87 |
| | R710/R760 | -0.53 | -0.76 | -0.85 |
| | R695/R670 | 0.58 | 0.79 | 0.78 |
| | R550 | 0.21 | -0.74 | -0.79 |
| | R675/R700 | -0.57 | -0.77 | -0.79 |
| | R675/(R700*R650) | -0.09 | 0.74 | 0.82 |
| | R672/(R55*R708) | -0.41 | -0.04 | -0.16 |
| | R672/R550 | -0.58 | -0.71 | -0.71 |
| | R860/(R550*R708) | 0.16 | 0.76 | 0.81 |
| | R750/R550 | 0.52 | 0.78 | 0.88 |
| | R750/R700 | 0.54 | 0.75 | 0.80 |
| | R725/R675 | 0.60 | 0.73 | 0.80 |
| | (R850-R710)/(R850-R680) | 0.42 | 0.75 | 0.82 |
| | (R780-R710)/(R780-R680) | 0.43 | 0.74 | 0.83 |
| | R700-R670 | 0.32 | -0.11 | -0.11 |
| | RNDVI | 0.56 | 0.76 | 0.84 |
| | PSR | -0.42 | -0.65 | -0.71 |
| | WBI | -0.32 | -0.68 | -0.60 |
| | SIPI | -0.50 | -0.70 | -0.78 |
| | YI | 0.20 | -0.64 | -0.72 |
| | VI2 | -0.42 | -0.20 | -0.20 |
| | Cgreen | 0.51 | 0.79 | 0.88 |
| | Cred edge | 0.53 | 0.76 | 0.80 |
| | C NIR | 0.36 | 0.81 | 0.84 |

**Table A5**- Coefficient of correlation for the relationship between different vegetation indices and leaf water content of Scottish wheat obtained at different DAS in the 2005-06 growing season. Highlighted values are significant (P<0.05) and bold values are the strongest correlations.

| Scale | Vegetation index | Leaf water content (%) | | |
|---|---|---|---|---|
| | | 181 DAS | 207 DAS | 225 DAS |
| Broad band | NDVI | 0.43 | 0.82 | **0.92** |
| | RVI | 0.42 | 0.81 | 0.85 |
| | SAVI | 0.39 | 0.78 | 0.89 |
| | GNDVI br | 0.41 | 0.79 | **0.92** |
| | DVI | 0.39 | 0.70 | 0.82 |
| | SR | 0.42 | 0.81 | 0.85 |
| | SLAVI | 0.43 | 0.82 | **0.92** |
| | OSAVI | 0.41 | 0.81 | 0.91 |
| | VI1 | -0.37 | -0.46 | -0.29 |
| | RDVI | 0.42 | 0.83 | 0.89 |
| | SI | -0.43 | -0.81 | **-0.92** |
| | IPVI | 0.43 | 0.82 | **0.92** |
| Hyper | WI | -0.09 | -0.59 | -0.71 |
| | PSI | 0.07 | 0.04 | -0.22 |
| | NWI-1 | -0.30 | -0.51 | -0.78 |
| | NWI-2 | -0.36 | -0.52 | -0.80 |
| | NDVI hy | 0.42 | 0.82 | 0.91 |
| | GNDVI hy | 0.40 | 0.78 | 0.91 |
| | SIPI | 0.40 | 0.81 | 0.91 |
| | SRPI | 0.30 | 0.81 | 0.90 |
| | NPCI | -0.35 | -0.75 | -0.81 |
| | NPQI | -0.07 | 0.55 | 0.69 |
| | PSSRb | 0.39 | 0.70 | 0.82 |
| | PSNDb | 0.43 | 0.81 | 0.92 |
| | Rshoulder | 0.37 | 0.54 | 0.56 |
| | C420 | -0.04 | 0.63 | 0.73 |
| | NDI | 0.39 | 0.70 | 0.82 |
| | SR hyper | 0.40 | 0.81 | 0.85 |
| | R800-R550 | 0.39 | 0.68 | 0.84 |
| | R800/R550 | 0.37 | 0.75 | 0.87 |
| | R695/R760 | -0.43 | -0.80 | **-0.92** |
| | R605/R760 | -0.44 | -0.80 | **-0.92** |
| | R710/R760 | -0.41 | -0.79 | **-0.92** |
| | R695/R670 | 0.44 | 0.86 | 0.83 |
| | R550 | 0.21 | -0.60 | -0.75 |
| | R675/R700 | -0.43 | -0.86 | -0.87 |
| | R675/(R700*R650) | -0.13 | 0.63 | 0.84 |
| | R672/(R55*R708) | -0.36 | -0.33 | -0.27 |
| | R672/R550 | -0.44 | -0.83 | -0.82 |
| | R860/(R550*R708) | 0.05 | 0.65 | 0.83 |
| | R750/R550 | 0.39 | 0.75 | 0.88 |
| | R750/R700 | 0.40 | 0.80 | 0.86 |
| | R725/R675 | 0.44 | 0.81 | 0.85 |
| | (R850-R710)/(R850-R680) | 0.31 | 0.71 | 0.87 |
| | (R780-R710)/(R780-R680) | 0.33 | 0.70 | 0.89 |
| | R700-R670 | 0.28 | 0.13 | -0.09 |
| | RNDVI | 0.43 | 0.82 | **0.92** |
| | PSR | -0.36 | -0.76 | -0.84 |
| | WBI | -0.15 | -0.62 | -0.75 |
| | SIPI | -0.41 | -0.78 | -0.87 |
| | YI | 0.19 | -0.45 | -0.71 |
| | VI2 | -0.37 | -0.43 | -0.26 |
| | Cgreen | 0.37 | 0.75 | 0.87 |
| | Cred edge | 0.38 | 0.80 | 0.86 |
| | C NIR | 0.23 | 0.78 | 0.89 |

**Table A6**- Coefficient of correlation for the relationship between different vegetation indices and plant height of Scottish wheat obtained at different DAS in the 2005-06 growing season. Highlighted values are significant (P<0.05) and bold values are the strongest correlations.

| Scale | Vegetation index | Plant height (m) | | | | |
|---|---|---|---|---|---|---|
| | | 73 DAS | 125 DAS | 181 DAS | 207 DAS | 225 DAS |
| Broad band | NDVI | -0.30 | 0.46 | 0.55 | 0.85 | **0.88** |
| | RVI | -0.28 | 0.45 | 0.51 | 0.82 | 0.84 |
| | SAVI | -0.40 | 0.37 | 0.53 | 0.77 | 0.85 |
| | GNDVI br | -0.33 | 0.45 | 0.54 | 0.85 | 0.91 |
| | DVI | -0.40 | 0.35 | 0.51 | 0.68 | 0.79 |
| | SR | -0.28 | 0.45 | 0.51 | 0.82 | 0.84 |
| | SLAVI | -0.30 | 0.46 | 0.55 | 0.85 | **0.88** |
| | OSAVI | -0.39 | 0.41 | 0.55 | 0.82 | 0.87 |
| | VI1 | 0.40 | -0.32 | -0.48 | -0.40 | -0.29 |
| | RDVI | -0.29 | 0.46 | 0.52 | 0.84 | 0.87 |
| | SI | 0.30 | -0.46 | -0.55 | -0.84 | -0.87 |
| | IPVI | -0.30 | 0.46 | 0.55 | 0.85 | **0.88** |
| Hyper | WI | -0.07 | -0.06 | -0.11 | -0.70 | -0.62 |
| | PSI | 0.00 | 0.16 | 0.01 | -0.07 | -0.20 |
| | NWI-1 | -0.04 | -0.08 | -0.39 | -0.56 | -0.70 |
| | NWI-2 | -0.15 | -0.11 | -0.46 | -0.59 | -0.71 |
| | NDVI hy | -0.24 | 0.44 | 0.54 | 0.85 | 0.86 |
| | GNDVI hy | -0.29 | 0.44 | 0.53 | 0.84 | **0.91** |
| | SIPI | -0.20 | 0.44 | 0.54 | 0.86 | 0.90 |
| | SRPI | 0.21 | 0.14 | 0.29 | 0.83 | 0.83 |
| | NPCI | -0.05 | -0.19 | -0.34 | -0.73 | -0.74 |
| | NPQI | -0.01 | -0.21 | -0.10 | 0.51 | 0.67 |
| | PSSRb | -0.40 | 0.36 | 0.51 | 0.67 | 0.80 |
| | PSNDb | -0.29 | 0.48 | 0.54 | 0.85 | 0.88 |
| | Rshoulder | -0.40 | 0.33 | 0.49 | 0.49 | 0.56 |
| | C420 | 0.20 | -0.03 | -0.14 | 0.60 | 0.67 |
| | NDI | -0.40 | 0.35 | 0.51 | 0.68 | 0.79 |
| | SR hyper | -0.22 | 0.44 | 0.50 | 0.82 | 0.83 |
| | R800-R550 | -0.40 | 0.37 | 0.51 | 0.66 | 0.84 |
| | R800/R550 | -0.27 | 0.41 | 0.49 | 0.81 | 0.89 |
| | R695/R760 | 0.30 | -0.48 | -0.55 | -0.84 | -0.87 |
| | R605/R760 | 0.28 | -0.49 | -0.57 | -0.84 | -0.89 |
| | R710/R760 | 0.19 | -0.47 | -0.52 | -0.84 | -0.88 |
| | R695/R670 | -0.08 | 0.33 | 0.53 | 0.86 | 0.78 |
| | R550 | -0.37 | 0.12 | 0.28 | -0.71 | -0.75 |
| | R675/R700 | 0.16 | -0.35 | -0.55 | -0.87 | -0.81 |
| | R675/(R700*R650) | 0.29 | -0.06 | -0.26 | 0.70 | 0.83 |
| | R672/(R55*R708) | 0.35 | -0.27 | -0.49 | -0.20 | -0.20 |
| | R672/R550 | 0.21 | -0.34 | -0.53 | -0.81 | -0.74 |
| | R860/(R550*R708) | 0.26 | 0.11 | 0.01 | 0.73 | 0.83 |
| | R750/R550 | -0.29 | 0.42 | 0.51 | 0.81 | 0.89 |
| | R750/R700 | -0.32 | 0.45 | 0.49 | 0.82 | 0.84 |
| | R725/R675 | -0.22 | 0.44 | 0.54 | 0.81 | 0.83 |
| | (R850-R710)/(R850-R680) | -0.35 | 0.38 | 0.39 | 0.79 | 0.86 |
| | (R780-R710)/(R780-R680) | -0.27 | 0.40 | 0.41 | 0.79 | 0.86 |
| | R700-R670 | -0.36 | 0.19 | 0.39 | 0.03 | -0.12 |
| | RNDVI | -0.24 | 0.44 | 0.55 | 0.85 | 0.87 |
| | PSR | -0.04 | -0.18 | -0.36 | -0.75 | -0.76 |
| | WBI | -0.16 | -0.06 | -0.25 | -0.72 | -0.67 |
| | SIPI | 0.18 | -0.34 | -0.49 | -0.81 | -0.80 |
| | YI | -0.44 | 0.42 | 0.11 | -0.60 | -0.68 |
| | VI2 | 0.39 | -0.32 | -0.48 | -0.37 | -0.28 |
| | Cgreen | -0.27 | 0.41 | 0.49 | 0.81 | 0.89 |
| | Cred edge | -0.31 | 0.45 | 0.47 | 0.82 | 0.84 |
| | C NIR | -0.28 | 0.33 | 0.31 | 0.85 | 0.87 |

**Table A7**- Coefficient of correlation for the relationship between different vegetation indices and chlorophyll *a* of Egyptian wheat obtained at different DAS in spring season 2006. Highlighted values are significant (P<0.05) and bold values are the strongest correlations.

| Scale | Vegetation index | Chlorophyll *a* concentration (µg cm$^{-2}$) | | | | |
|---|---|---|---|---|---|---|
| | | 57 DAS | 78 DAS | 91 DAS | 103 DAS | 127 DAS |
| Broad band | NDVI | -0.01 | 0.38 | 0.58 | 0.59 | 0.68 |
| | RVI | 0.02 | 0.42 | 0.58 | 0.59 | 0.68 |
| | SAVI | 0.09 | 0.39 | 0.60 | 0.62 | **0.69** |
| | GNDVI br | -0.01 | 0.10 | 0.50 | 0.58 | 0.31 |
| | DVI | 0.11 | 0.38 | 0.60 | 0.54 | 0.67 |
| | SR | 0.02 | 0.42 | 0.58 | 0.59 | 0.68 |
| | SLAVI | -0.01 | 0.38 | 0.58 | 0.59 | 0.68 |
| | OSAVI | 0.05 | 0.40 | 0.59 | 0.62 | **0.69** |
| | VI1 | -0.15 | -0.35 | -0.56 | -0.16 | -0.49 |
| | RDVI | 0.01 | 0.41 | 0.58 | 0.60 | 0.68 |
| | SI | 0.02 | -0.37 | -0.58 | -0.58 | -0.68 |
| | IPVI | -0.01 | 0.38 | 0.58 | 0.59 | 0.68 |
| Hyper | WI | 0.34 | 0.26 | -0.18 | -0.37 | -0.40 |
| | PSI | -0.10 | 0.40 | 0.52 | 0.46 | 0.24 |
| | NWI-1 | 0.04 | 0.17 | -0.48 | -0.23 | -0.39 |
| | NWI-2 | 0.05 | 0.18 | -0.49 | -0.32 | -0.37 |
| | NDVI hy | -0.03 | 0.40 | 0.58 | 0.60 | 0.67 |
| | GNDVI hy | 0.01 | 0.07 | 0.47 | 0.57 | 0.29 |
| | SIPI | 0.02 | 0.42 | 0.58 | 0.62 | 0.64 |
| | SRPI | -0.12 | 0.04 | 0.57 | 0.37 | -0.04 |
| | NPCI | 0.06 | -0.02 | -0.57 | -0.46 | 0.28 |
| | NPQI | -0.27 | -0.46 | 0.34 | -0.05 | -0.53 |
| | PSSRb | 0.13 | 0.39 | 0.60 | 0.51 | 0.65 |
| | PSNDb | 0.02 | 0.43 | 0.58 | 0.59 | **0.68** |
| | Rshoulder | 0.14 | 0.35 | 0.58 | 0.25 | 0.49 |
| | C420 | 0.05 | -0.05 | 0.46 | 0.13 | -0.54 |
| | NDI | 0.11 | 0.38 | 0.60 | 0.54 | 0.67 |
| | SR hyper | 0.00 | 0.44 | 0.57 | 0.60 | 0.66 |
| | R800-R550 | 0.12 | 0.31 | 0.57 | 0.43 | 0.34 |
| | R800/R550 | 0.01 | 0.09 | 0.48 | 0.58 | 0.28 |
| | R695/R760 | -0.01 | -0.45 | -0.57 | -0.58 | -0.61 |
| | R605/R760 | 0.04 | -0.11 | -0.52 | -0.58 | -0.35 |
| | R710/R760 | -0.09 | -0.50 | -0.55 | -0.56 | -0.61 |
| | R695/R670 | -0.15 | 0.00 | 0.62 | 0.62 | 0.57 |
| | R550 | 0.15 | 0.25 | 0.01 | -0.20 | 0.32 |
| | R675/R700 | 0.15 | -0.15 | -0.61 | -0.62 | -0.66 |
| | R675/(R700*R650) | -0.06 | -0.09 | 0.38 | 0.27 | -0.30 |
| | R672/(R55*R708) | -0.03 | -0.33 | -0.64 | -0.42 | -0.51 |
| | R672/R550 | 0.01 | -0.40 | -0.61 | -0.59 | -0.31 |
| | R860/(R550*R708) | -0.04 | -0.04 | 0.42 | 0.42 | -0.06 |
| | R750/R550 | 0.04 | 0.09 | 0.48 | 0.58 | 0.29 |
| | R750/R700 | 0.10 | 0.47 | 0.55 | 0.58 | 0.59 |
| | R725/R675 | -0.05 | 0.39 | 0.58 | 0.61 | 0.65 |
| | (R850-R710)/(R850-R680) | 0.31 | 0.52 | 0.39 | 0.38 | -0.58 |
| | (R780-R710)/(R780-R680) | 0.30 | 0.52 | 0.42 | 0.39 | -0.57 |
| | R700-R670 | 0.02 | 0.03 | 0.58 | 0.26 | 0.62 |
| | RNDVI | -0.02 | 0.36 | 0.58 | 0.60 | 0.67 |
| | PSR | 0.07 | -0.02 | -0.58 | -0.45 | 0.29 |
| | WBI | 0.14 | 0.12 | -0.19 | -0.31 | -0.37 |
| | SIPI | 0.01 | -0.32 | -0.56 | -0.53 | -0.61 |
| | YI | 0.26 | 0.32 | 0.35 | 0.43 | 0.04 |
| | VI2 | -0.14 | -0.33 | -0.56 | -0.12 | -0.45 |
| | Cgreen | 0.01 | 0.09 | 0.48 | 0.58 | 0.28 |
| | Cred edge | 0.09 | 0.48 | 0.55 | 0.58 | 0.61 |
| | C NIR | 0.20 | 0.51 | 0.47 | 0.55 | 0.47 |

**Table A8**- Coefficient of correlation for the relationship between different vegetation indices and grain yield of Egyptian wheat obtained at different DAS in spring season of 2006. Highlighted values are significant (P<0.05) and bold values are the strongest correlations.

| Scale | Vegetation index | Grain yield (kg $m^{-2}$) | | | | |
|---|---|---|---|---|---|---|
| | | 57 DAS | 78 DAS | 91 DAS | 103 DAS | 127 DAS |
| Broad band | NDVI | 0.20 | 0.71 | 0.95 | 0.90 | 0.78 |
| | RVI | 0.23 | 0.72 | **0.96** | 0.93 | 0.78 |
| | SAVI | 0.13 | 0.73 | 0.94 | 0.78 | 0.76 |
| | GNDVI br | 0.26 | 0.20 | 0.91 | 0.87 | 0.20 |
| | DVI | 0.11 | 0.71 | 0.92 | 0.58 | 0.78 |
| | SR | 0.23 | 0.72 | **0.96** | 0.93 | 0.78 |
| | SLAVI | 0.20 | 0.71 | 0.95 | 0.90 | 0.78 |
| | OSAVI | 0.15 | 0.76 | 0.95 | 0.86 | 0.78 |
| | VI1 | -0.05 | -0.66 | -0.78 | 0.01 | -0.42 |
| | RDVI | 0.22 | 0.72 | **0.96** | 0.93 | 0.78 |
| | SI | -0.19 | -0.71 | -0.94 | -0.88 | -0.78 |
| | IPVI | 0.20 | 0.71 | 0.95 | 0.90 | 0.78 |
| Hyper | WI | 0.02 | 0.49 | -0.49 | -0.74 | -0.71 |
| | PSI | -0.22 | 0.59 | 0.41 | 0.70 | 0.35 |
| | NWI-1 | 0.20 | 0.30 | -0.73 | -0.49 | -0.69 |
| | NWI-2 | 0.18 | 0.30 | -0.81 | -0.67 | -0.67 |
| | NDVI hy | 0.19 | 0.73 | 0.94 | 0.90 | 0.81 |
| | GNDVI hy | 0.29 | 0.14 | 0.87 | 0.87 | 0.16 |
| | SIPI | 0.16 | 0.82 | 0.93 | 0.87 | 0.72 |
| | SRPI | 0.14 | -0.02 | 0.94 | 0.67 | 0.13 |
| | NPCI | -0.24 | 0.11 | -0.96 | -0.79 | 0.32 |
| | NPQI | -0.18 | -0.52 | 0.62 | 0.11 | -0.64 |
| | PSSRb | 0.12 | 0.72 | 0.92 | 0.55 | 0.71 |
| | PSNDb | 0.23 | 0.75 | 0.95 | 0.89 | 0.76 |
| | Rshoulder | 0.06 | 0.66 | 0.84 | 0.10 | 0.43 |
| | C420 | 0.34 | -0.31 | 0.87 | 0.39 | -0.62 |
| | NDI | 0.11 | 0.71 | 0.92 | 0.58 | 0.78 |
| | SR hyper | 0.22 | 0.73 | **0.97** | 0.94 | 0.80 |
| | R800-R550 | 0.13 | 0.58 | 0.90 | 0.42 | 0.28 |
| | R800/R550 | 0.30 | 0.16 | 0.87 | 0.89 | 0.18 |
| | R695/R760 | -0.25 | -0.80 | -0.94 | -0.87 | -0.76 |
| | R605/R760 | -0.24 | -0.30 | -0.92 | -0.88 | -0.26 |
| | R710/R760 | -0.30 | -0.77 | -0.94 | -0.87 | -0.66 |
| | R695/R670 | 0.00 | 0.18 | 0.93 | 0.93 | 0.64 |
| | R550 | -0.05 | 0.49 | -0.26 | -0.52 | 0.29 |
| | R675/R700 | -0.02 | -0.47 | -0.96 | -0.92 | -0.79 |
| | R675/(R700*R650) | 0.17 | -0.26 | 0.77 | 0.68 | -0.14 |
| | R672/(R55*R708) | 0.02 | -0.71 | -0.88 | -0.38 | -0.55 |
| | R672/R550 | -0.10 | -0.71 | -0.91 | -0.90 | -0.51 |
| | R860/(R550*R708) | 0.22 | -0.19 | 0.86 | 0.84 | -0.04 |
| | R750/R550 | 0.31 | 0.16 | 0.87 | 0.89 | 0.21 |
| | R750/R700 | 0.32 | 0.75 | 0.96 | 0.91 | 0.74 |
| | R725/R675 | 0.16 | 0.72 | **0.97** | 0.94 | 0.81 |
| | (R850-R710)/(R850-R680) | 0.30 | 0.65 | 0.85 | 0.66 | -0.72 |
| | (R780-R710)/(R780-R680) | 0.36 | 0.67 | 0.87 | 0.68 | -0.67 |
| | R700-R670 | -0.03 | 0.30 | 0.68 | 0.10 | 0.75 |
| | RNDVI | 0.20 | 0.70 | 0.95 | 0.90 | 0.81 |
| | PSR | -0.24 | 0.11 | -0.96 | -0.76 | 0.33 |
| | WBI | -0.15 | 0.27 | -0.59 | -0.67 | -0.67 |
| | SIPI | -0.21 | -0.42 | -0.89 | -0.81 | -0.79 |
| | YI | -0.03 | 0.52 | 0.08 | 0.73 | 0.02 |
| | VI2 | -0.05 | -0.64 | -0.77 | 0.06 | -0.38 |
| | Cgreen | 0.30 | 0.16 | 0.87 | 0.89 | 0.18 |
| | Cred edge | 0.31 | 0.75 | 0.96 | 0.91 | 0.73 |
| | C NIR | 0.36 | 0.64 | 0.89 | 0.87 | 0.38 |

**Table A9**- Coefficient of correlation for the relationship between different vegetation indices and aboveground biomass of Egyptian wheat obtained at different DAS in spring season of 2006. Highlighted values are significant (P<0.05) and bold values are the strongest correlations.

| Scale | Vegetation index | Aboveground biomass (kg $m^{-2}$) | | | | |
|---|---|---|---|---|---|---|
| | | 57 DAS | 78 DAS | 91 DAS | 103 DAS | 127 DAS |
| Broad band | NDVI | 0.10 | 0.72 | 0.97 | 0.91 | 0.87 |
| | RVI | 0.13 | 0.72 | 0.97 | 0.91 | 0.87 |
| | SAVI | 0.04 | 0.77 | 0.96 | 0.81 | 0.84 |
| | GNDVI br | 0.14 | 0.24 | 0.91 | 0.91 | 0.21 |
| | DVI | 0.03 | 0.74 | 0.94 | 0.61 | 0.85 |
| | SR | 0.13 | 0.72 | 0.97 | 0.91 | 0.87 |
| | SLAVI | 0.10 | 0.72 | 0.97 | 0.91 | 0.87 |
| | OSAVI | 0.05 | 0.80 | 0.97 | 0.88 | 0.86 |
| | VI1 | 0.00 | -0.68 | -0.81 | -0.01 | -0.47 |
| | RDVI | 0.12 | 0.72 | **0.98** | 0.92 | 0.87 |
| | SI | -0.08 | -0.72 | -0.96 | -0.90 | -0.87 |
| | IPVI | 0.10 | 0.72 | 0.97 | 0.91 | 0.87 |
| Hyper | WI | -0.01 | 0.49 | -0.55 | -0.71 | -0.73 |
| | PSI | -0.28 | 0.58 | 0.46 | 0.68 | 0.43 |
| | NWI-1 | 0.24 | 0.29 | -0.79 | -0.57 | -0.71 |
| | NWI-2 | 0.23 | 0.33 | -0.85 | -0.74 | -0.68 |
| | NDVI hy | 0.08 | 0.74 | 0.97 | 0.91 | 0.89 |
| | GNDVI hy | 0.17 | 0.18 | 0.87 | 0.91 | 0.18 |
| | SIPI | 0.05 | 0.85 | 0.96 | 0.92 | 0.82 |
| | SRPI | 0.10 | -0.03 | 0.95 | 0.66 | 0.13 |
| | NPCI | -0.17 | 0.13 | -0.96 | -0.72 | 0.38 |
| | NPQI | -0.16 | -0.51 | 0.55 | 0.02 | -0.66 |
| | PSSRb | 0.04 | 0.75 | 0.94 | 0.58 | 0.79 |
| | PSNDb | 0.12 | 0.77 | 0.97 | 0.91 | 0.86 |
| | Rshoulder | 0.00 | 0.69 | 0.86 | 0.13 | 0.47 |
| | C420 | 0.31 | -0.34 | 0.84 | 0.31 | -0.70 |
| | NDI | 0.03 | 0.74 | 0.94 | 0.61 | 0.85 |
| | SR hyper | 0.12 | 0.74 | 0.97 | 0.91 | 0.89 |
| | R800-R550 | 0.05 | 0.61 | 0.91 | 0.45 | 0.30 |
| | R800/R550 | 0.18 | 0.18 | 0.86 | 0.92 | 0.19 |
| | R695/R760 | -0.14 | -0.81 | -0.96 | -0.89 | -0.85 |
| | R605/R760 | -0.12 | -0.34 | -0.93 | -0.90 | -0.29 |
| | R710/R760 | -0.19 | -0.78 | -0.96 | -0.89 | -0.79 |
| | R695/R670 | -0.08 | 0.17 | 0.93 | 0.89 | 0.68 |
| | R550 | -0.06 | 0.51 | -0.22 | -0.52 | 0.34 |
| | R675/R700 | 0.06 | -0.47 | -0.97 | -0.91 | -0.85 |
| | R675/(R700*R650) | 0.18 | -0.32 | 0.76 | 0.66 | -0.19 |
| | R672/(R55*R708) | 0.09 | -0.73 | -0.91 | -0.37 | -0.62 |
| | R672/R550 | -0.02 | -0.68 | -0.94 | -0.89 | -0.57 |
| | R860/(R550*R708) | 0.21 | -0.22 | 0.86 | 0.83 | -0.06 |
| | R750/R550 | 0.19 | 0.17 | 0.87 | 0.92 | 0.21 |
| | R750/R700 | 0.22 | 0.75 | **0.98** | 0.91 | 0.83 |
| | R725/R675 | 0.07 | 0.73 | 0.97 | 0.91 | 0.89 |
| | (R850-R710)/(R850-R680) | 0.26 | 0.67 | 0.86 | 0.71 | -0.75 |
| | (R780-R710)/(R780-R680) | 0.31 | 0.67 | 0.88 | 0.73 | -0.71 |
| | R700-R670 | -0.09 | 0.32 | 0.71 | 0.10 | 0.79 |
| | RNDVI | 0.09 | 0.70 | 0.97 | 0.91 | 0.89 |
| | PSR | -0.16 | 0.13 | -0.95 | -0.70 | 0.39 |
| | WBI | -0.19 | 0.30 | -0.62 | -0.65 | -0.68 |
| | SIPI | -0.11 | -0.37 | -0.92 | -0.82 | -0.86 |
| | YI | -0.03 | 0.52 | 0.14 | 0.74 | 0.06 |
| | VI2 | 0.00 | -0.66 | -0.80 | 0.05 | -0.42 |
| | Cgreen | 0.18 | 0.18 | 0.86 | 0.92 | 0.19 |
| | Cred edge | 0.21 | 0.76 | 0.97 | 0.91 | 0.83 |
| | C NIR | 0.30 | 0.67 | 0.91 | 0.90 | 0.48 |

**Table A10**- Coefficient of correlation for the relationship between different vegetation indices and leaf water content of Egyptian wheat obtained at different DAS in spring season of 2006. Highlighted values are significant (P<0.05) and bold values are the strongest correlations.

| Scale | Vegetation index | Leaf water content (%) | | | | |
|---|---|---|---|---|---|---|
| | | 57 DAS | 78 DAS | 91 DAS | 103 DAS | 127DAS |
| Broad band | NDVI | -0.24 | 0.08 | 0.97 | 0.94 | 0.89 |
| | RVI | -0.22 | 0.04 | 0.88 | 0.90 | 0.88 |
| | SAVI | -0.26 | 0.02 | 0.96 | 0.79 | 0.83 |
| | GNDVI br | -0.23 | -0.01 | 0.88 | 0.94 | 0.12 |
| | DVI | -0.25 | 0.00 | 0.95 | 0.57 | 0.85 |
| | SR | -0.22 | 0.04 | 0.88 | 0.90 | 0.88 |
| | SLAVI | -0.24 | 0.08 | 0.97 | 0.94 | 0.89 |
| | OSAVI | -0.27 | 0.04 | 0.97 | 0.89 | 0.87 |
| | VI1 | 0.21 | 0.01 | -0.84 | 0.04 | -0.45 |
| | RDVI | -0.23 | 0.05 | 0.93 | 0.93 | 0.89 |
| | SI | 0.25 | -0.08 | **-0.98** | -0.94 | -0.90 |
| | IPVI | -0.24 | 0.08 | 0.97 | 0.94 | 0.89 |
| Hyper | WI | -0.08 | 0.12 | -0.56 | -0.74 | -0.72 |
| | PSI | -0.09 | 0.08 | 0.51 | 0.69 | 0.52 |
| | NWI-1 | -0.12 | 0.16 | -0.75 | -0.54 | -0.71 |
| | NWI-2 | -0.05 | 0.15 | -0.84 | -0.71 | -0.69 |
| | NDVI hy | -0.24 | 0.07 | **0.97** | 0.94 | 0.93 |
| | GNDVI hy | -0.23 | -0.02 | 0.84 | 0.93 | 0.08 |
| | SIPI | -0.30 | 0.05 | 0.97 | 0.94 | 0.82 |
| | SRPI | 0.03 | 0.05 | 0.95 | 0.69 | 0.19 |
| | NPCI | 0.04 | -0.01 | -0.91 | -0.74 | 0.36 |
| | NPQI | 0.39 | 0.16 | 0.47 | 0.09 | -0.64 |
| | PSSRb | -0.24 | 0.00 | 0.95 | 0.54 | 0.75 |
| | PSNDb | -0.24 | 0.10 | **0.97** | 0.94 | 0.86 |
| | Rshoulder | -0.22 | -0.01 | 0.88 | 0.07 | 0.43 |
| | C420 | 0.16 | 0.13 | 0.79 | 0.35 | -0.68 |
| | NDI | -0.25 | 0.00 | 0.95 | 0.57 | 0.85 |
| | SR hyper | -0.21 | 0.03 | 0.89 | 0.89 | 0.92 |
| | R800-R550 | -0.24 | -0.02 | 0.90 | 0.40 | 0.18 |
| | R800/R550 | -0.21 | -0.04 | 0.81 | 0.92 | 0.07 |
| | R695/R760 | 0.21 | -0.12 | **-0.97** | -0.93 | -0.93 |
| | R605/R760 | 0.21 | -0.02 | -0.92 | -0.94 | -0.22 |
| | R710/R760 | 0.19 | -0.12 | -0.96 | -0.92 | -0.85 |
| | R695/R670 | -0.19 | -0.11 | 0.86 | 0.87 | 0.63 |
| | R550 | -0.16 | 0.01 | -0.12 | -0.57 | 0.42 |
| | R675/R700 | 0.24 | 0.03 | -0.95 | -0.92 | -0.86 |
| | R675/(R700*R650) | 0.16 | 0.02 | 0.68 | 0.73 | -0.18 |
| | R672/(R55*R708) | 0.23 | -0.06 | -0.93 | -0.33 | -0.68 |
| | R672/R550 | 0.21 | -0.10 | -0.95 | -0.91 | -0.67 |
| | R860/(R550*R708) | 0.08 | -0.01 | 0.79 | 0.89 | -0.11 |
| | R750/R550 | -0.22 | -0.04 | 0.81 | 0.93 | 0.10 |
| | R750/R700 | -0.21 | 0.09 | 0.93 | 0.92 | 0.90 |
| | R725/R675 | -0.21 | 0.03 | 0.89 | 0.90 | 0.92 |
| | (R850-R710)/(R850-R680) | -0.06 | 0.11 | 0.84 | 0.72 | -0.81 |
| | (R780-R710)/(R780-R680) | -0.08 | 0.11 | 0.87 | 0.75 | -0.77 |
| | R700-R670 | -0.24 | -0.09 | 0.76 | 0.05 | 0.74 |
| | RNDVI | -0.24 | 0.07 | **0.97** | 0.94 | 0.92 |
| | PSR | 0.03 | -0.02 | -0.93 | -0.73 | 0.37 |
| | WBI | -0.09 | 0.11 | -0.67 | -0.68 | -0.69 |
| | SIPI | 0.23 | -0.11 | **-0.97** | -0.87 | -0.92 |
| | YI | -0.11 | 0.07 | 0.19 | 0.76 | 0.18 |
| | VI2 | 0.21 | 0.02 | -0.83 | 0.09 | -0.37 |
| | Cgreen | -0.21 | -0.04 | 0.81 | 0.92 | 0.07 |
| | Cred edge | -0.20 | 0.08 | 0.93 | 0.92 | 0.89 |
| | C NIR | -0.17 | 0.02 | 0.93 | 0.91 | 0.46 |

**Table A11**- Coefficient of correlation for the relationship between different vegetation indices and plant height of Egyptian wheat obtained at different DAS in spring season of 2006. Highlighted values are significant (P<0.05) and bold values are the strongest correlations.

| Scale | Vegetation index | Plant height (m) | | | | |
|---|---|---|---|---|---|---|
| | | 57 DAS | 78 DAS | 91 DAS | 103 DAS | 127 DAS |
| Broad band | NDVI | 0.19 | 0.68 | **0.93** | 0.85 | 0.84 |
| | RVI | 0.18 | 0.68 | 0.88 | 0.86 | 0.84 |
| | SAVI | -0.10 | 0.56 | **0.93** | 0.74 | 0.82 |
| | GNDVI br | 0.09 | 0.23 | 0.88 | 0.84 | 0.18 |
| | DVI | -0.15 | 0.52 | 0.92 | 0.54 | 0.84 |
| | SR | 0.18 | 0.68 | 0.88 | 0.86 | 0.84 |
| | SLAVI | 0.19 | 0.68 | **0.93** | 0.85 | 0.84 |
| | OSAVI | 0.00 | 0.61 | **0.93** | 0.82 | 0.84 |
| | VI1 | 0.30 | -0.43 | -0.82 | 0.05 | -0.51 |
| | RDVI | 0.19 | 0.68 | 0.91 | 0.87 | 0.84 |
| | SI | -0.20 | -0.68 | **-0.93** | -0.84 | -0.84 |
| | IPVI | 0.19 | 0.68 | **0.93** | 0.85 | 0.84 |
| Hyper | WI | 0.13 | 0.37 | -0.65 | -0.69 | -0.69 |
| | PSI | 0.06 | 0.56 | 0.50 | 0.65 | 0.47 |
| | NWI-1 | -0.13 | 0.15 | -0.75 | -0.63 | -0.66 |
| | NWI-2 | -0.09 | 0.18 | -0.86 | -0.78 | -0.63 |
| | NDVI hy | 0.23 | 0.70 | 0.93 | 0.86 | 0.87 |
| | GNDVI hy | 0.09 | 0.18 | 0.85 | 0.84 | 0.15 |
| | SIPI | 0.10 | 0.76 | **0.94** | 0.85 | 0.83 |
| | SRPI | 0.48 | 0.12 | 0.89 | 0.66 | 0.06 |
| | NPCI | -0.40 | 0.02 | -0.86 | -0.70 | 0.44 |
| | NPQI | 0.25 | -0.38 | 0.41 | 0.06 | -0.71 |
| | PSSRb | -0.17 | 0.54 | 0.92 | 0.50 | 0.78 |
| | PSNDb | 0.18 | 0.74 | 0.93 | 0.85 | 0.84 |
| | Rshoulder | -0.28 | 0.45 | 0.86 | 0.07 | 0.50 |
| | C420 | 0.32 | -0.14 | 0.72 | 0.28 | -0.73 |
| | NDI | -0.15 | 0.52 | 0.92 | 0.54 | 0.84 |
| | SR hyper | 0.22 | 0.70 | 0.88 | 0.86 | 0.86 |
| | R800-R550 | -0.19 | 0.45 | 0.89 | 0.37 | 0.27 |
| | R800/R550 | 0.10 | 0.18 | 0.83 | 0.85 | 0.15 |
| | R695/R760 | -0.23 | -0.78 | -0.93 | -0.83 | -0.84 |
| | R605/R760 | -0.12 | -0.30 | -0.90 | -0.84 | -0.24 |
| | R710/R760 | -0.21 | -0.80 | -0.93 | -0.82 | -0.79 |
| | R695/R670 | 0.18 | 0.09 | 0.84 | 0.86 | 0.61 |
| | R550 | -0.36 | 0.25 | -0.17 | -0.51 | 0.42 |
| | R675/R700 | -0.20 | -0.37 | -0.91 | -0.87 | -0.81 |
| | R675/(R700*R650) | 0.38 | -0.04 | 0.67 | 0.64 | -0.25 |
| | R672/(R55*R708) | 0.17 | -0.49 | -0.87 | -0.35 | -0.66 |
| | R672/R550 | -0.26 | -0.64 | -0.89 | -0.85 | -0.57 |
| | R860/(R550*R708) | 0.39 | 0.01 | 0.80 | 0.80 | -0.13 |
| | R750/R550 | 0.08 | 0.17 | 0.83 | 0.86 | 0.17 |
| | R750/R700 | 0.18 | 0.75 | 0.91 | 0.86 | 0.82 |
| | R725/R675 | 0.20 | 0.65 | 0.88 | 0.86 | 0.85 |
| | (R850-R710)/(R850-R680) | -0.05 | 0.75 | 0.85 | 0.57 | -0.71 |
| | (R780-R710)/(R780-R680) | -0.01 | 0.76 | 0.88 | 0.61 | -0.68 |
| | R700-R670 | -0.18 | 0.02 | 0.71 | 0.08 | 0.73 |
| | RNDVI | 0.21 | 0.66 | 0.93 | 0.86 | 0.86 |
| | PSR | -0.41 | 0.03 | -0.88 | -0.69 | 0.45 |
| | WBI | 0.05 | 0.16 | -0.76 | -0.66 | -0.64 |
| | SIPI | -0.34 | -0.44 | -0.90 | -0.78 | -0.85 |
| | YI | -0.34 | 0.39 | 0.09 | 0.64 | 0.15 |
| | VI2 | 0.30 | -0.42 | -0.81 | 0.10 | -0.44 |
| | Cgreen | 0.10 | 0.18 | 0.83 | 0.85 | 0.15 |
| | Cred edge | 0.20 | 0.75 | 0.91 | 0.86 | 0.83 |
| | C NIR | 0.14 | 0.74 | 0.91 | 0.82 | 0.51 |

**Table A12**- Coefficient of correlation for the relationship between different vegetation indices and LAI of Egyptian wheat obtained at different DAS in spring season of 2006. Highlighted values are significant (P<0.05) and bold values are the strongest correlations.

| Scale | Vegetation index | Leaf Area Index | | | | |
|---|---|---|---|---|---|---|
| | | 57 DAS | 78 DAS | 91 DAS | 103 DAS | 127 DAS |
| Broad band | NDVI | 0.03 | 0.63 | **0.96** | 0.91 | 0.83 |
| | RVI | 0.07 | 0.64 | 0.91 | 0.90 | 0.82 |
| | SAVI | 0.08 | 0.67 | **0.96** | 0.81 | 0.82 |
| | GNDVI br | 0.11 | 0.14 | 0.90 | 0.91 | 0.23 |
| | DVI | 0.09 | 0.64 | 0.95 | 0.62 | 0.83 |
| | SR | 0.07 | 0.63 | 0.91 | 0.90 | 0.82 |
| | SLAVI | 0.03 | 0.63 | **0.96** | 0.91 | 0.84 |
| | OSAVI | 0.06 | 0.70 | **0.96** | 0.88 | 0.83 |
| | VI1 | -0.10 | -0.60 | -0.85 | -0.03 | -0.51 |
| | RDVI | 0.05 | 0.64 | 0.94 | 0.91 | 0.84 |
| | SI | -0.02 | -0.63 | **-0.96** | -0.90 | -0.84 |
| | IPVI | 0.03 | 0.63 | **0.96** | 0.91 | 0.84 |
| Hyper | WI | 0.12 | 0.51 | -0.52 | -0.64 | -0.57 |
| | PSI | -0.23 | 0.65 | 0.49 | 0.64 | 0.41 |
| | NWI-1 | 0.37 | 0.32 | -0.78 | -0.64 | -0.56 |
| | NWI-2 | 0.32 | 0.38 | -0.87 | -0.75 | -0.53 |
| | NDVI hy | 0.01 | 0.66 | 0.96 | 0.91 | 0.85 |
| | GNDVI hy | 0.14 | 0.09 | 0.86 | 0.90 | 0.20 |
| | SIPI | 0.05 | 0.76 | **0.97** | 0.92 | 0.79 |
| | SRPI | -0.08 | -0.07 | 0.93 | 0.65 | 0.07 |
| | NPCI | 0.02 | 0.18 | -0.89 | -0.74 | 0.38 |
| | NPQI | -0.41 | -0.50 | 0.42 | 0.06 | -0.61 |
| | PSSRb | 0.10 | 0.65 | 0.95 | 0.59 | 0.76 |
| | PSNDb | 0.06 | 0.70 | 0.95 | 0.91 | 0.82 |
| | Rshoulder | 0.10 | 0.60 | 0.89 | 0.15 | 0.50 |
| | C420 | 0.12 | -0.31 | 0.72 | 0.34 | -0.67 |
| | NDI | 0.09 | 0.64 | 0.95 | 0.62 | 0.83 |
| | SR hyper | 0.04 | 0.66 | 0.91 | 0.90 | 0.83 |
| | R800-R550 | 0.12 | 0.50 | 0.92 | 0.46 | 0.29 |
| | R800/R550 | 0.14 | 0.08 | 0.84 | 0.91 | 0.19 |
| | R695/R760 | -0.05 | -0.76 | -0.95 | -0.90 | -0.82 |
| | R605/R760 | -0.05 | -0.22 | -0.93 | -0.91 | -0.31 |
| | R710/R760 | -0.11 | -0.76 | -0.94 | -0.89 | -0.78 |
| | R695/R670 | -0.17 | 0.02 | 0.91 | 0.87 | 0.63 |
| | R550 | 0.06 | 0.49 | -0.15 | -0.49 | 0.39 |
| | R675/R700 | 0.14 | -0.32 | -0.96 | -0.91 | -0.81 |
| | R675/(R700*R650) | 0.05 | -0.27 | 0.67 | 0.65 | -0.25 |
| | R672/(R55*R708) | 0.03 | -0.67 | -0.92 | -0.39 | -0.63 |
| | R672/R550 | 0.06 | -0.67 | -0.93 | -0.89 | -0.51 |
| | R860/(R550*R708) | 0.08 | -0.21 | 0.79 | 0.83 | -0.10 |
| | R750/R550 | 0.16 | 0.07 | 0.84 | 0.91 | 0.21 |
| | R750/R700 | 0.16 | 0.71 | 0.93 | 0.91 | 0.79 |
| | R725/R675 | -0.02 | 0.62 | 0.92 | 0.90 | 0.83 |
| | (R850-R710)/(R850-R680) | 0.33 | 0.70 | 0.79 | 0.66 | -0.77 |
| | (R780-R710)/(R780-R680) | 0.34 | 0.71 | 0.82 | 0.69 | -0.76 |
| | R700-R670 | -0.04 | 0.19 | 0.80 | 0.14 | 0.74 |
| | RNDVI | 0.02 | 0.61 | 0.96 | 0.91 | 0.85 |
| | PSR | 0.03 | 0.18 | -0.91 | -0.71 | 0.40 |
| | WBI | -0.06 | 0.31 | -0.61 | -0.59 | -0.53 |
| | SIPI | -0.01 | -0.38 | -0.93 | -0.84 | -0.83 |
| | YI | 0.10 | 0.56 | 0.17 | 0.73 | 0.10 |
| | VI2 | -0.10 | -0.57 | -0.84 | 0.02 | -0.45 |
| | Cgreen | 0.14 | 0.08 | 0.84 | 0.91 | 0.19 |
| | Cred edge | 0.14 | 0.71 | 0.93 | 0.90 | 0.80 |
| | C NIR | 0.35 | 0.69 | 0.88 | 0.87 | 0.48 |

**Table A13**- Coefficient of correlation for the relationship between different vegetation indices and chlorophyll *a* concentration of Scottish wheat obtained at different DAS in the 2006-07 growing season. Highlighted values are significant (P<0.05) and bold values are the strongest correlations.

| Scale | Vegetation index | Chlorophyll *a* concentration (µg cm$^{-2}$) | | | | |
|---|---|---|---|---|---|---|
| | | 97DAS | 135 DAS | 177 DAS | 198 DAS | 223 DAS |
| Broad band | NDVI | -0.11 | 0.31 | -0.42 | 0.80 | 0.61 |
| | RVI | -0.08 | 0.32 | -0.38 | 0.83 | 0.69 |
| | SAVI | -0.09 | 0.29 | -0.12 | **0.84** | 0.59 |
| | GNDVI br | -0.11 | 0.36 | -0.36 | 0.83 | 0.60 |
| | DVI | -0.07 | 0.28 | -0.08 | 0.83 | 0.57 |
| | SR | -0.08 | 0.32 | -0.37 | 0.83 | 0.69 |
| | SLAVI | -0.11 | 0.31 | -0.42 | 0.80 | 0.61 |
| | OSAVI | -0.10 | 0.30 | -0.19 | **0.84** | 0.60 |
| | VI1 | -0.01 | -0.24 | -0.08 | -0.78 | -0.38 |
| | RDVI | -0.09 | 0.32 | -0.39 | 0.83 | 0.65 |
| | SI | 0.12 | -0.31 | 0.43 | -0.78 | -0.57 |
| | IPVI | -0.11 | 0.31 | -0.42 | 0.80 | 0.61 |
| Hyper | WI | 0.03 | 0.18 | -0.01 | -0.16 | -0.25 |
| | PSI | -0.24 | -0.25 | -0.13 | 0.09 | -0.03 |
| | NWI-1 | -0.02 | 0.08 | 0.13 | -0.60 | -0.28 |
| | NWI-2 | -0.02 | 0.11 | 0.23 | -0.52 | -0.28 |
| | NDVI hy | -0.11 | 0.30 | -0.43 | 0.80 | 0.59 |
| | GNDVI hy | 0.02 | 0.34 | -0.34 | 0.83 | 0.59 |
| | SIPI | -0.11 | 0.52 | -0.08 | 0.59 | 0.47 |
| | SRPI | -0.02 | 0.13 | -0.17 | 0.65 | 0.58 |
| | NPCI | 0.00 | -0.01 | 0.03 | -0.62 | -0.51 |
| | NPQI | -0.19 | -0.03 | -0.04 | -0.11 | 0.01 |
| | PSSRb | -0.08 | 0.28 | -0.07 | 0.83 | 0.59 |
| | PSNDb | -0.12 | 0.30 | -0.42 | 0.81 | 0.62 |
| | Rshoulder | 0.01 | 0.24 | 0.07 | 0.79 | 0.40 |
| | C420 | 0.08 | 0.26 | -0.04 | 0.30 | -0.09 |
| | NDI | -0.07 | 0.28 | -0.08 | 0.83 | 0.57 |
| | SR hyper | -0.06 | 0.29 | -0.41 | 0.82 | 0.68 |
| | R800-R550 | 0.04 | 0.28 | -0.02 | 0.82 | 0.54 |
| | R800/R550 | 0.02 | 0.37 | -0.30 | **0.84** | 0.65 |
| | R695/R760 | 0.08 | -0.31 | 0.40 | -0.78 | -0.57 |
| | R605/R760 | 0.11 | -0.30 | 0.44 | -0.79 | -0.58 |
| | R710/R760 | 0.07 | -0.34 | 0.43 | -0.80 | -0.59 |
| | R695/R670 | -0.17 | 0.16 | -0.41 | 0.54 | 0.56 |
| | R550 | -0.01 | -0.20 | 0.34 | -0.37 | -0.32 |
| | R675/R700 | 0.04 | -0.30 | 0.28 | -0.73 | -0.55 |
| | R675/(R700*R650) | -0.16 | 0.30 | -0.32 | 0.48 | 0.56 |
| | R672/(R55*R708) | 0.14 | -0.16 | 0.28 | -0.75 | -0.23 |
| | R672/R550 | 0.12 | -0.29 | 0.43 | -0.79 | -0.58 |
| | R860/(R550*R708) | -0.04 | 0.40 | -0.43 | 0.79 | 0.69 |
| | R750/R550 | 0.02 | 0.35 | -0.30 | 0.83 | 0.65 |
| | R750/R700 | -0.07 | 0.32 | -0.41 | 0.83 | 0.68 |
| | R725/R675 | -0.02 | 0.28 | -0.38 | 0.79 | 0.66 |
| | (R850-R710)/(R850-R680) | 0.01 | 0.44 | -0.04 | 0.72 | 0.54 |
| | (R780-R710)/(R780-R680) | 0.11 | 0.44 | -0.08 | 0.73 | 0.59 |
| | R700-R670 | -0.19 | 0.22 | 0.01 | 0.35 | 0.31 |
| | RNDVI | -0.14 | 0.31 | -0.46 | 0.78 | 0.60 |
| | PSR | 0.07 | 0.03 | 0.11 | -0.47 | -0.43 |
| | WBI | -0.01 | 0.19 | 0.18 | -0.23 | -0.02 |
| | SIPI | 0.33 | -0.28 | 0.14 | -0.60 | -0.45 |
| | YI | 0.16 | 0.34 | 0.30 | 0.35 | 0.44 |
| | VI2 | -0.02 | -0.25 | -0.09 | -0.78 | -0.35 |
| | Cgreen | 0.02 | 0.37 | -0.30 | **0.84** | 0.65 |
| | Cred edge | -0.07 | 0.33 | -0.41 | 0.83 | 0.68 |
| | C NIR | -0.07 | 0.41 | -0.24 | 0.88 | 0.65 |

**Table A14**- Coefficient of correlation for the relationship between different vegetation indices and grain yield of the Scottish wheat at different DAS in the 2006-07 growing season. Highlighted values are significant (P<0.05) and bold values are the strongest correlations.

| Scale | Vegetation index | Grain yield (kg $m^{-2}$) | | | | |
|---|---|---|---|---|---|---|
| | | 97DAS | 135 DAS | 177 DAS | 198 DAS | 223 DAS |
| Broad band | NDVI | 0.54 | 0.53 | 0.61 | 0.90 | 0.45 |
| | RVI | 0.65 | 0.61 | 0.64 | 0.88 | 0.58 |
| | SAVI | 0.28 | 0.60 | 0.35 | 0.89 | 0.52 |
| | GNDVI br | 0.49 | 0.56 | 0.54 | **0.92** | 0.42 |
| | DVI | 0.17 | 0.60 | 0.29 | 0.88 | 0.54 |
| | SR | 0.65 | 0.61 | 0.64 | 0.88 | 0.58 |
| | SLAVI | 0.54 | 0.53 | 0.61 | 0.90 | 0.45 |
| | OSAVI | 0.42 | 0.59 | 0.43 | 0.91 | 0.50 |
| | VI1 | 0.24 | -0.57 | -0.13 | -0.79 | -0.56 |
| | RDVI | 0.62 | 0.59 | 0.63 | 0.90 | 0.51 |
| | SI | -0.51 | -0.50 | -0.61 | -0.88 | -0.39 |
| | IPVI | 0.54 | 0.53 | 0.61 | 0.90 | 0.45 |
| Hyper | WI | -0.04 | -0.04 | -0.02 | -0.11 | -0.12 |
| | PSI | -0.74 | -0.42 | 0.13 | 0.03 | 0.15 |
| | NWI-1 | -0.17 | -0.08 | -0.03 | -0.58 | -0.37 |
| | NWI-2 | -0.05 | -0.05 | -0.21 | -0.52 | -0.50 |
| | NDVI hy | 0.54 | 0.51 | 0.59 | 0.90 | 0.44 |
| | GNDVI hy | 0.62 | 0.60 | 0.48 | **0.92** | 0.40 |
| | SIPI | 0.25 | 0.70 | -0.02 | 0.61 | 0.36 |
| | SRPI | 0.42 | 0.26 | 0.29 | 0.74 | 0.34 |
| | NPCI | -0.30 | -0.16 | -0.19 | -0.69 | -0.53 |
| | NPQI | 0.18 | -0.18 | 0.06 | -0.17 | 0.10 |
| | PSSRb | 0.17 | 0.60 | 0.29 | 0.88 | 0.55 |
| | PSNDb | 0.55 | 0.53 | 0.58 | 0.91 | 0.45 |
| | Rshoulder | -0.22 | 0.57 | 0.14 | 0.80 | 0.56 |
| | C420 | 0.68 | 0.14 | 0.18 | 0.44 | 0.03 |
| | NDI | 0.17 | 0.60 | 0.29 | 0.88 | 0.54 |
| | SR hyper | 0.66 | 0.59 | 0.60 | 0.87 | 0.58 |
| | R800-R550 | 0.07 | 0.61 | 0.22 | 0.86 | 0.54 |
| | R800/R550 | 0.63 | 0.66 | 0.48 | **0.92** | 0.49 |
| | R695/R760 | -0.53 | -0.50 | -0.62 | -0.88 | -0.38 |
| | R605/R760 | -0.49 | -0.48 | -0.62 | -0.89 | -0.39 |
| | R710/R760 | -0.44 | -0.52 | -0.62 | -0.89 | -0.41 |
| | R695/R670 | 0.58 | 0.56 | 0.54 | 0.70 | 0.51 |
| | R550 | -0.54 | -0.25 | -0.24 | -0.54 | 0.20 |
| | R675/R700 | -0.66 | -0.58 | -0.64 | -0.82 | -0.44 |
| | R675/(R700*R650) | 0.08 | 0.29 | 0.07 | 0.63 | 0.12 |
| | R672/(R55*R708) | -0.66 | -0.37 | -0.55 | -0.72 | -0.46 |
| | R672/R550 | -0.59 | -0.45 | -0.57 | -0.85 | -0.49 |
| | R860/(R550*R708) | 0.58 | 0.55 | 0.46 | 0.88 | 0.40 |
| | R750/R550 | 0.67 | 0.65 | 0.50 | **0.92** | 0.48 |
| | R750/R700 | 0.52 | 0.60 | 0.57 | 0.90 | 0.55 |
| | R725/R675 | 0.74 | 0.61 | 0.67 | 0.85 | 0.57 |
| | (R850-R710)/(R850-R680) | -0.12 | 0.52 | 0.21 | 0.77 | 0.31 |
| | (R780-R710)/(R780-R680) | -0.07 | 0.51 | 0.27 | 0.79 | 0.31 |
| | R700-R670 | 0.29 | 0.55 | 0.33 | 0.40 | 0.42 |
| | RNDVI | 0.55 | 0.54 | 0.64 | 0.89 | 0.45 |
| | PSR | -0.09 | -0.08 | 0.09 | -0.58 | -0.54 |
| | WBI | -0.08 | -0.04 | -0.26 | -0.23 | 0.02 |
| | SIPI | -0.04 | -0.37 | -0.14 | -0.72 | -0.23 |
| | YI | 0.03 | 0.50 | 0.08 | 0.47 | 0.10 |
| | VI2 | 0.28 | -0.57 | -0.11 | -0.79 | -0.55 |
| | Cgreen | 0.63 | 0.66 | 0.48 | **0.92** | 0.49 |
| | Cred edge | 0.48 | 0.61 | 0.55 | 0.90 | 0.55 |
| | C NIR | 0.32 | 0.61 | 0.37 | **0.92** | 0.49 |

**Table A15**- Coefficient of correlation for the relationship between different vegetation indices and plant height of Scottish wheat at different DAS in the 2006-07 growing season. Highlighted values are significant (P<0.05) and bold values are the strongest correlations.

| Scale | Vegetation index | Plant height (m) | | | | |
|---|---|---|---|---|---|---|
| | | 97DAS | 135 DAS | 177 DAS | 198 DAS | 223 DAS |
| Broad band | NDVI | 0.25 | 0.84 | 0.83 | 0.91 | 0.39 |
| | RVI | 0.21 | 0.79 | 0.86 | 0.86 | 0.50 |
| | SAVI | 0.03 | 0.77 | 0.51 | 0.85 | 0.43 |
| | GNDVI br | 0.17 | 0.88 | 0.74 | **0.92** | 0.35 |
| | DVI | 0.04 | 0.74 | 0.44 | 0.83 | 0.44 |
| | SR | 0.21 | 0.79 | 0.86 | 0.86 | 0.50 |
| | SLAVI | 0.25 | 0.84 | 0.83 | 0.91 | 0.39 |
| | OSAVI | 0.12 | 0.81 | 0.60 | 0.88 | 0.41 |
| | VI1 | 0.24 | -0.62 | -0.20 | -0.72 | -0.39 |
| | RDVI | 0.23 | 0.83 | 0.85 | 0.89 | 0.44 |
| | SI | -0.26 | -0.82 | -0.82 | -0.91 | -0.33 |
| | IPVI | 0.25 | 0.84 | 0.83 | 0.91 | 0.39 |
| Hyper | WI | -0.22 | -0.08 | -0.16 | -0.20 | -0.08 |
| | PSI | -0.03 | 0.04 | 0.32 | 0.12 | 0.03 |
| | NWI-1 | -0.19 | -0.24 | 0.04 | -0.47 | -0.21 |
| | NWI-2 | -0.16 | -0.19 | -0.08 | -0.39 | -0.30 |
| | NDVI hy | 0.27 | 0.83 | 0.79 | 0.91 | 0.39 |
| | GNDVI hy | 0.15 | 0.89 | 0.70 | 0.91 | 0.32 |
| | SIPI | 0.05 | 0.79 | 0.38 | 0.66 | 0.26 |
| | SRPI | 0.06 | 0.48 | 0.26 | 0.83 | 0.41 |
| | NPCI | 0.06 | -0.25 | -0.08 | -0.78 | -0.50 |
| | NPQI | -0.34 | 0.01 | -0.11 | -0.13 | 0.07 |
| | PSSRb | 0.01 | 0.74 | 0.45 | 0.83 | 0.44 |
| | PSNDb | 0.23 | 0.84 | 0.79 | **0.92** | 0.39 |
| | Rshoulder | -0.23 | 0.63 | 0.23 | 0.73 | 0.39 |
| | C420 | 0.07 | 0.50 | 0.28 | 0.38 | 0.03 |
| | NDI | 0.04 | 0.74 | 0.44 | 0.83 | 0.44 |
| | SR hyper | 0.23 | 0.79 | 0.79 | 0.85 | 0.51 |
| | R800-R550 | -0.08 | 0.73 | 0.38 | 0.81 | 0.41 |
| | R800/R550 | 0.19 | 0.87 | 0.71 | 0.89 | 0.41 |
| | R695/R760 | -0.23 | -0.82 | -0.81 | -0.90 | -0.33 |
| | R605/R760 | -0.30 | -0.84 | -0.79 | -0.91 | -0.32 |
| | R710/R760 | -0.16 | -0.83 | -0.71 | -0.91 | -0.36 |
| | R695/R670 | 0.11 | 0.70 | 0.57 | 0.74 | 0.39 |
| | R550 | -0.25 | -0.57 | -0.39 | -0.64 | 0.05 |
| | R675/R700 | -0.28 | -0.76 | -0.77 | -0.82 | -0.35 |
| | R675/(R700*R650) | 0.18 | 0.64 | 0.22 | 0.73 | 0.25 |
| | R672/(R55*R708) | -0.27 | -0.46 | -0.71 | -0.64 | -0.30 |
| | R672/R550 | -0.33 | -0.76 | -0.78 | -0.86 | -0.45 |
| | R860/(R550*R708) | 0.23 | 0.80 | 0.65 | 0.89 | 0.41 |
| | R750/R550 | 0.18 | 0.86 | 0.71 | 0.88 | 0.41 |
| | R750/R700 | 0.20 | 0.82 | 0.79 | 0.88 | 0.49 |
| | R725/R675 | 0.22 | 0.79 | 0.83 | 0.84 | 0.48 |
| | (R850-R710)/(R850-R680) | -0.41 | 0.70 | 0.00 | 0.77 | 0.38 |
| | (R780-R710)/(R780-R680) | -0.44 | 0.70 | 0.08 | 0.80 | 0.32 |
| | R700-R670 | -0.03 | 0.57 | 0.34 | 0.37 | 0.27 |
| | RNDVI | 0.20 | 0.85 | 0.82 | 0.91 | 0.39 |
| | PSR | -0.37 | -0.06 | 0.16 | -0.68 | -0.50 |
| | WBI | -0.32 | -0.03 | -0.34 | -0.29 | 0.03 |
| | SIPI | -0.14 | -0.72 | -0.34 | -0.79 | -0.20 |
| | YI | 0.21 | 0.59 | 0.14 | 0.53 | 0.05 |
| | VI2 | 0.21 | -0.63 | -0.20 | -0.72 | -0.38 |
| | Cgreen | 0.19 | 0.87 | 0.71 | 0.89 | 0.41 |
| | Cred edge | 0.21 | 0.83 | 0.78 | 0.89 | 0.49 |
| | C NIR | -0.13 | 0.83 | 0.34 | 0.91 | 0.44 |

**Table A16**- Coefficient of correlation for the relationship between different vegetation indices and aboveground biomass of Scottish wheat at different DAS in the 2006-07 growing season. Highlighted values are significant (P<0.05) and bold values are the strongest correlations.

| Scale | Vegetation index | Aboveground biomass ((kg $m^{-2}$) | | |
|---|---|---|---|---|
| | | 177 DAS | 198 DAS | 223 DAS |
| Broad band | NDVI | 0.49 | 0.88 | 0.39 |
| | RVI | 0.57 | 0.86 | 0.51 |
| | SAVI | 0.57 | 0.88 | 0.47 |
| | GNDVI br | 0.53 | **0.90** | 0.37 |
| | DVI | 0.57 | 0.86 | 0.49 |
| | SR | 0.57 | 0.86 | 0.51 |
| | SLAVI | 0.49 | 0.88 | 0.39 |
| | OSAVI | 0.56 | 0.89 | 0.44 |
| | VI1 | -0.55 | -0.79 | -0.52 |
| | RDVI | 0.55 | 0.88 | 0.45 |
| | SI | -0.47 | -0.86 | -0.34 |
| | IPVI | 0.49 | 0.88 | 0.39 |
| Hyper | WI | -0.07 | -0.11 | -0.15 |
| | PSI | -0.48 | 0.01 | 0.12 |
| | NWI-1 | -0.06 | -0.58 | -0.32 |
| | NWI-2 | -0.03 | -0.52 | -0.47 |
| | NDVI hy | 0.47 | 0.87 | 0.39 |
| | GNDVI hy | 0.57 | 0.91 | 0.35 |
| | SIPI | 0.65 | 0.59 | 0.30 |
| | SRPI | 0.27 | 0.73 | 0.28 |
| | NPCI | -0.18 | -0.68 | -0.45 |
| | NPQI | -0.20 | -0.16 | 0.09 |
| | PSSRb | 0.57 | 0.86 | 0.50 |
| | PSNDb | 0.49 | 0.89 | 0.40 |
| | Rshoulder | 0.55 | 0.80 | 0.52 |
| | C420 | 0.12 | 0.42 | 0.00 |
| | NDI | 0.57 | 0.86 | 0.49 |
| | SR hyper | 0.55 | 0.85 | 0.52 |
| | R800-R550 | 0.59 | 0.85 | 0.49 |
| | R800/R550 | 0.62 | 0.90 | 0.43 |
| | R695/R760 | -0.46 | -0.86 | -0.33 |
| | R605/R760 | -0.45 | -0.87 | -0.34 |
| | R710/R760 | -0.48 | -0.87 | -0.36 |
| | R695/R670 | 0.52 | 0.66 | 0.44 |
| | R550 | -0.23 | -0.51 | 0.21 |
| | R675/R700 | -0.53 | -0.78 | -0.37 |
| | R675/(R700*R650) | 0.24 | 0.59 | 0.09 |
| | R672/(R55*R708) | -0.35 | -0.72 | -0.42 |
| | R672/R550 | -0.40 | -0.83 | -0.44 |
| | R860/(R550*R708) | 0.49 | 0.86 | 0.35 |
| | R750/R550 | 0.62 | 0.90 | 0.43 |
| | R750/R700 | 0.57 | 0.88 | 0.50 |
| | R725/R675 | 0.58 | 0.83 | 0.50 |
| | (R850-R710)/(R850-R680) | 0.46 | 0.77 | 0.32 |
| | (R780-R710)/(R780-R680) | 0.47 | 0.79 | 0.30 |
| | R700-R670 | 0.51 | 0.39 | 0.36 |
| | RNDVI | 0.50 | 0.87 | 0.40 |
| | PSR | -0.14 | -0.57 | -0.46 |
| | WBI | -0.03 | -0.24 | -0.02 |
| | SIPI | -0.33 | -0.70 | -0.21 |
| | YI | 0.47 | 0.44 | 0.03 |
| | VI2 | -0.55 | -0.79 | -0.51 |
| | Cgreen | 0.62 | 0.90 | 0.43 |
| | Cred edge | 0.58 | 0.88 | 0.50 |
| | C NIR | 0.54 | **0.92** | 0.45 |

**Table A17**- Coefficient of correlation for the relationship between different vegetation indices and leaf water content of Scottish wheat at different DAS in the 2006-07 growing season. Highlighted values are significant (P<0.05) and bold values are the strongest correlations.

| Scale | Vegetation index | Leaf water content (%) | | |
|---|---|---|---|---|
| | | 177 DAS | 198 DAS | 223 DAS |
| Broad band | NDVI | 0.85 | **0.92** | 0.31 |
| | RVI | 0.76 | 0.86 | 0.43 |
| | SAVI | 0.73 | 0.83 | 0.36 |
| | GNDVI br | 0.88 | 0.89 | 0.26 |
| | DVI | 0.69 | 0.80 | 0.37 |
| | SR | 0.76 | 0.86 | 0.43 |
| | SLAVI | 0.85 | **0.92** | 0.31 |
| | OSAVI | 0.78 | 0.87 | 0.34 |
| | VI1 | -0.55 | -0.68 | -0.35 |
| | RDVI | 0.81 | 0.90 | 0.37 |
| | SI | -0.84 | -0.91 | -0.25 |
| | IPVI | 0.85 | **0.92** | 0.31 |
| Hyper | WI | -0.15 | -0.09 | -0.24 |
| | PSI | 0.08 | 0.25 | 0.08 |
| | NWI-1 | -0.22 | -0.47 | -0.24 |
| | NWI-2 | -0.19 | -0.42 | -0.35 |
| | NDVI hy | 0.85 | 0.91 | 0.30 |
| | GNDVI hy | 0.89 | 0.87 | 0.24 |
| | SIPI | 0.74 | 0.68 | 0.19 |
| | SRPI | 0.54 | 0.75 | 0.34 |
| | NPCI | -0.29 | -0.67 | -0.47 |
| | NPQI | -0.07 | -0.14 | 0.09 |
| | PSSRb | 0.68 | 0.80 | 0.37 |
| | PSNDb | 0.85 | 0.91 | 0.30 |
| | Rshoulder | 0.56 | 0.69 | 0.36 |
| | C420 | 0.54 | 0.45 | 0.00 |
| | NDI | 0.69 | 0.80 | 0.37 |
| | SR hyper | 0.77 | 0.84 | 0.44 |
| | R800-R550 | 0.67 | 0.76 | 0.35 |
| | R800/R550 | 0.85 | 0.86 | 0.33 |
| | R695/R760 | -0.84 | -0.90 | -0.24 |
| | R605/R760 | -0.86 | -0.89 | -0.23 |
| | R710/R760 | -0.85 | -0.89 | -0.27 |
| | R695/R670 | 0.71 | 0.80 | 0.36 |
| | R550 | -0.64 | -0.63 | 0.11 |
| | R675/R700 | -0.75 | -0.87 | -0.29 |
| | R675/(R700*R650) | 0.71 | 0.75 | 0.16 |
| | R672/(R55*R708) | -0.38 | -0.67 | -0.30 |
| | R672/R550 | -0.75 | -0.91 | -0.39 |
| | R860/(R550*R708) | 0.84 | 0.89 | 0.31 |
| | R750/R550 | 0.85 | 0.86 | 0.33 |
| | R750/R700 | 0.81 | 0.88 | 0.41 |
| | R725/R675 | 0.76 | 0.86 | 0.42 |
| | (R850-R710)/(R850-R680) | 0.70 | 0.70 | 0.33 |
| | (R780-R710)/(R780-R680) | 0.70 | 0.73 | 0.26 |
| | R700-R670 | 0.48 | 0.43 | 0.24 |
| | RNDVI | 0.86 | **0.92** | 0.31 |
| | PSR | -0.09 | -0.56 | -0.50 |
| | WBI | -0.09 | -0.14 | -0.12 |
| | SIPI | -0.75 | -0.79 | -0.11 |
| | YI | 0.53 | 0.47 | 0.10 |
| | VI2 | -0.55 | -0.67 | -0.34 |
| | Cgreen | 0.85 | 0.86 | 0.33 |
| | Cred edge | 0.81 | 0.88 | 0.41 |
| | C NIR | 0.83 | 0.86 | 0.35 |

**Table A18**- Coefficient of correlation for the relationship between different vegetation indices and LAI of the Scottish wheat at different DAS in the 2006-07 growing season. Highlighted values are significant (P<0.05) and bold values are the strongest correlations.

| Scale | Vegetation index | Leaf Area Index | | |
|---|---|---|---|---|
| | | 177 DAS | 198 DAS | 223 DAS |
| Broad band | NDVI | 0.42 | 0.86 | 0.86 |
| | RVI | 0.52 | 0.88 | 0.83 |
| | SAVI | 0.48 | 0.86 | 0.78 |
| | GNDVI br | 0.39 | 0.87 | **0.90** |
| | SR | 0.52 | 0.88 | 0.83 |
| | SLAVI | 0.42 | 0.86 | 0.86 |
| | OSAVI | 0.46 | 0.87 | 0.82 |
| | VI1 | -0.48 | -0.76 | -0.63 |
| | RDVI | 0.47 | 0.89 | 0.86 |
| | SI | -0.37 | -0.84 | -0.84 |
| | IPVI | 0.42 | 0.86 | 0.86 |
| Hyperspec | WI | -0.12 | -0.22 | -0.12 |
| | PSI | 0.02 | 0.06 | 0.08 |
| | NWI-1 | -0.24 | -0.59 | -0.18 |
| | NWI-2 | -0.36 | -0.49 | -0.13 |
| | NDVI hy | 0.42 | 0.86 | 0.85 |
| | GNDVI hy | 0.36 | 0.87 | **0.90** |
| | SIPI | 0.29 | 0.64 | 0.81 |
| | SRPI | 0.38 | 0.75 | 0.49 |
| | NPCI | -0.52 | -0.72 | -0.25 |
| | NPQI | -0.04 | -0.09 | 0.02 |
| | DVI | 0.50 | 0.85 | 0.75 |
| | PSSRb | 0.50 | 0.84 | 0.75 |
| | PSNDb | 0.42 | 0.86 | 0.86 |
| | Rshoulder | 0.48 | 0.77 | 0.64 |
| | C420 | 0.06 | 0.38 | 0.54 |
| | NDI | 0.50 | 0.85 | 0.75 |
| | SR hyper | 0.53 | 0.89 | 0.82 |
| | R800-R550 | 0.48 | 0.83 | 0.74 |
| | R800/R550 | 0.43 | **0.90** | **0.90** |
| | R695/R760 | -0.37 | -0.83 | -0.84 |
| | R605/R760 | -0.37 | -0.84 | -0.86 |
| | R710/R760 | -0.40 | -0.85 | -0.85 |
| | R695/R670 | 0.43 | 0.70 | 0.70 |
| | R550 | 0.14 | -0.54 | -0.59 |
| | R675/R700 | -0.40 | -0.82 | -0.77 |
| | R675/(R700*R650) | 0.14 | 0.61 | 0.69 |
| | R672/(R55*R708) | -0.40 | -0.69 | -0.45 |
| | R672/R550 | -0.48 | -0.82 | -0.77 |
| | R860/(R550*R708) | 0.38 | 0.86 | 0.85 |
| | R750/R550 | 0.43 | 0.89 | 0.89 |
| | R750/R700 | 0.50 | 0.87 | 0.85 |
| | R725/R675 | 0.51 | 0.86 | 0.82 |
| | (R850-R710)/(R850-R680) | 0.37 | 0.73 | 0.72 |
| | (R780-R710)/(R780-R680) | 0.33 | 0.75 | 0.71 |
| | R700-R670 | 0.33 | 0.39 | 0.55 |
| | RNDVI | 0.42 | 0.85 | 0.86 |
| | PSR | -0.54 | -0.58 | -0.01 |
| | WBI | -0.02 | -0.28 | -0.10 |
| | SIPI | -0.27 | -0.68 | -0.73 |
| | YI | 0.02 | 0.48 | 0.65 |
| | VI2 | -0.47 | -0.76 | -0.63 |
| | Cgreen | 0.43 | 0.90 | **0.90** |
| | Cred edge | 0.51 | 0.88 | 0.86 |
| | C NIR | 0.48 | 0.89 | 0.87 |

**Table A19**- Coefficient of correlation for the relationship between different vegetation indices and chlorophyll *a* concentration of the Egyptian wheat at different DAS in the 2006-07 growing season. Highlighted values are significant (P<0.05) and bold values are the strongest correlation.

| Scale | Vegetation index | Chlorophyll *a* concentration (µg cm$^{-2}$) | | | | |
|---|---|---|---|---|---|---|
| | | 83 DAS | 108 DAS | 130 DAS | 149 DAS | 197 DAS |
| Broad band | NDVI | 0.06 | 0.24 | -0.28 | 0.67 | 0.72 |
| | RVI | 0.45 | 0.24 | -0.34 | 0.27 | 0.73 |
| | SAVI | 0.04 | 0.06 | -0.30 | 0.60 | 0.77 |
| | GNDVI br | 0.08 | -0.32 | -0.28 | -0.31 | 0.70 |
| | DVI | 0.13 | 0.09 | -0.30 | 0.10 | 0.74 |
| | SR | 0.39 | 0.24 | -0.34 | 0.10 | 0.73 |
| | SLAVI | 0.24 | 0.24 | -0.28 | 0.10 | 0.72 |
| | OSAVI | 0.05 | 0.09 | -0.31 | 0.66 | **0.79** |
| | VI1 | 0.13 | -0.02 | 0.26 | 0.52 | -0.69 |
| | RDVI | 0.12 | 0.24 | -0.32 | 0.47 | 0.74 |
| | SI | 0.08 | -0.24 | 0.27 | 0.17 | -0.69 |
| | IPVI | -0.15 | 0.24 | -0.28 | 0.50 | 0.72 |
| Hyper | WI | 0.10 | 0.24 | 0.59 | -0.22 | -0.19 |
| | PSI | 0.17 | -0.35 | 0.13 | 0.16 | 0.22 |
| | NWI-1 | 0.15 | 0.15 | -0.31 | 0.04 | -0.31 |
| | NWI-2 | 0.16 | 0.27 | -0.30 | 0.02 | -0.31 |
| | NDVI hy | 0.07 | 0.21 | -0.33 | 0.64 | 0.73 |
| | GNDVI hy | 0.19 | 0.19 | -0.21 | -0.10 | 0.70 |
| | SIPI | -0.05 | 0.34 | -0.03 | 0.31 | 0.69 |
| | SRPI | 0.15 | -0.18 | 0.10 | 0.04 | 0.36 |
| | NPCI | 0.05 | 0.18 | -0.08 | 0.60 | -0.25 |
| | NPQI | 0.03 | -0.09 | -0.04 | 0.61 | -0.17 |
| | PSSRb | 0.18 | 0.10 | -0.28 | -0.05 | 0.75 |
| | PSNDb | 0.13 | 0.22 | -0.18 | 0.39 | 0.72 |
| | Rshoulder | -0.07 | 0.03 | -0.27 | -0.59 | 0.70 |
| | C420 | -0.13 | -0.19 | -0.31 | -0.63 | 0.18 |
| | NDI | -0.08 | 0.09 | -0.30 | -0.47 | 0.74 |
| | SR hyper | -0.01 | 0.19 | -0.42 | 0.59 | 0.75 |
| | R800-R550 | 0.20 | 0.10 | -0.27 | -0.31 | 0.75 |
| | R800/R550 | -0.02 | 0.19 | -0.18 | -0.68 | 0.73 |
| | R695/R760 | -0.18 | -0.23 | 0.30 | 0.19 | -0.70 |
| | R605/R760 | -0.10 | 0.10 | 0.32 | -0.46 | -0.70 |
| | R710/R760 | -0.01 | 0.19 | 0.19 | -0.63 | -0.70 |
| | R695/R670 | -0.22 | 0.61 | -0.14 | 0.47 | **0.78** |
| | R550 | 0.13 | -0.03 | -0.19 | 0.41 | 0.40 |
| | R675/R700 | 0.07 | -0.47 | 0.28 | 0.47 | -0.73 |
| | R675/(R700*R650) | 0.02 | -0.22 | 0.19 | 0.66 | -0.21 |
| | R672/(R55*R708) | 0.16 | -0.27 | 0.35 | 0.00 | -0.72 |
| | R672/R550 | 0.29 | -0.30 | 0.31 | -0.01 | -0.69 |
| | R860/(R550*R708) | 0.12 | -0.12 | 0.15 | 0.07 | 0.13 |
| | R750/R550 | 0.05 | 0.13 | -0.25 | 0.64 | 0.73 |
| | R750/R700 | 0.08 | 0.02 | -0.35 | 0.16 | 0.71 |
| | R725/R675 | 0.37 | 0.39 | -0.34 | 0.23 | 0.74 |
| | (R850-R710)/(R850-R680) | -0.05 | -0.29 | 0.14 | -0.65 | 0.58 |
| | (R780-R710)/(R780-R680) | -0.11 | 0.01 | 0.07 | -0.02 | 0.59 |
| | R700-R670 | 0.06 | 0.34 | -0.20 | 0.67 | 0.57 |
| | RNDVI | 0.10 | 0.48 | -0.24 | 0.21 | 0.72 |
| | PSR | -0.20 | 0.15 | -0.27 | 0.12 | -0.04 |
| | WBI | -0.19 | 0.25 | 0.39 | 0.11 | -0.06 |
| | SIPI | 0.05 | 0.35 | 0.03 | 0.63 | -0.62 |
| | YI | -0.07 | -0.09 | -0.13 | -0.67 | 0.34 |
| | VI2 | 0.06 | -0.05 | 0.26 | 0.67 | -0.68 |
| | Cgreen | 0.13 | 0.19 | -0.18 | 0.39 | 0.73 |
| | Cred edge | 0.07 | 0.09 | -0.31 | 0.46 | 0.71 |
| | C NIR | 0.12 | -0.55 | -0.10 | 0.06 | 0.64 |

**Table A20**- Coefficient of correlation for the relationship between different vegetation indices and grain yield of Egyptian wheat at different DAS in the 2006-07 growing season. Highlighted values are significant (P<0.05) and bold values are the strongest correlations.

| Scale | Vegetation index | Grain yield (kg $m^{-2}$) | | | | |
|---|---|---|---|---|---|---|
| | | 83 DAS | 108 DAS | 130 DAS | 149 DAS | 197 DAS |
| Broad band | NDVI | 0.23 | 0.55 | 0.43 | 0.79 | 0.93 |
| | RVI | -0.11 | 0.60 | 0.42 | 0.79 | 0.91 |
| | SAVI | 0.21 | 0.26 | -0.13 | 0.25 | 0.90 |
| | GNDVI br | 0.18 | 0.55 | 0.28 | 0.68 | 0.92 |
| | DVI | 0.25 | 0.20 | -0.18 | 0.21 | 0.85 |
| | SR | -0.10 | 0.60 | 0.42 | 0.79 | 0.91 |
| | SLAVI | -0.16 | 0.55 | 0.42 | 0.79 | 0.93 |
| | OSAVI | 0.22 | 0.29 | -0.05 | 0.35 | **0.94** |
| | VI1 | 0.27 | -0.19 | 0.34 | -0.03 | -0.77 |
| | RDVI | 0.25 | 0.59 | 0.43 | 0.80 | 0.93 |
| | SI | 0.27 | -0.53 | -0.42 | -0.78 | -0.91 |
| | IPVI | 0.00 | 0.55 | 0.42 | 0.79 | 0.93 |
| Hyper | WI | -0.05 | 0.20 | 0.00 | 0.29 | -0.40 |
| | PSI | 0.06 | -0.53 | 0.14 | -0.22 | 0.38 |
| | NWI-1 | 0.24 | -0.30 | -0.19 | -0.04 | -0.46 |
| | NWI-2 | 0.24 | -0.13 | -0.06 | -0.03 | -0.44 |
| | NDVI hy | 0.24 | 0.07 | 0.35 | 0.78 | **0.94** |
| | GNDVI hy | 0.26 | 0.62 | 0.27 | 0.62 | 0.93 |
| | SIPI | -0.42 | 0.16 | 0.73 | 0.37 | 0.87 |
| | SRPI | 0.24 | -0.06 | 0.15 | 0.52 | 0.59 |
| | NPCI | 0.21 | 0.11 | -0.05 | -0.28 | -0.45 |
| | NPQI | 0.20 | -0.24 | -0.24 | 0.19 | -0.27 |
| | PSSRb | 0.25 | 0.28 | -0.17 | 0.20 | 0.86 |
| | PSNDb | 0.23 | 0.47 | 0.40 | 0.79 | 0.92 |
| | Rshoulder | -0.23 | 0.20 | -0.33 | 0.04 | 0.78 |
| | C420 | -0.31 | 0.18 | -0.07 | 0.32 | 0.15 |
| | NDI | -0.24 | 0.20 | -0.18 | 0.21 | 0.85 |
| | SR hyper | 0.29 | 0.13 | 0.33 | 0.78 | 0.92 |
| | R800-R550 | 0.27 | 0.37 | -0.20 | 0.13 | 0.85 |
| | R800/R550 | -0.27 | 0.59 | 0.26 | 0.59 | 0.93 |
| | R695/R760 | -0.35 | -0.55 | -0.36 | -0.72 | -0.91 |
| | R605/R760 | -0.30 | -0.36 | -0.31 | -0.78 | -0.91 |
| | R710/R760 | -0.20 | -0.13 | -0.13 | -0.62 | -0.93 |
| | R695/R670 | -0.30 | 0.32 | 0.41 | 0.74 | 0.92 |
| | R550 | 0.25 | -0.10 | -0.56 | -0.28 | 0.40 |
| | R675/R700 | 0.20 | -0.43 | -0.55 | -0.80 | -0.92 |
| | R675/(R700*R650) | 0.23 | -0.17 | 0.46 | 0.22 | -0.11 |
| | R672/(R55*R708) | -0.46 | -0.15 | -0.09 | -0.53 | -0.84 |
| | R672/R550 | -0.47 | -0.11 | -0.44 | -0.75 | -0.89 |
| | R860/(R550*R708) | 0.30 | 0.10 | 0.64 | 0.55 | 0.32 |
| | R750/R550 | 0.23 | 0.61 | 0.28 | 0.60 | 0.93 |
| | R750/R700 | -0.05 | 0.58 | 0.26 | 0.67 | 0.91 |
| | R725/R675 | -0.23 | 0.60 | 0.44 | 0.83 | 0.91 |
| | (R850-R710)/(R850-R680) | -0.19 | 0.19 | -0.23 | 0.08 | 0.84 |
| | (R780-R710)/(R780-R680) | -0.09 | 0.62 | -0.07 | 0.06 | 0.85 |
| | R700-R670 | 0.23 | 0.16 | -0.17 | 0.15 | 0.64 |
| | RNDVI | 0.25 | 0.63 | 0.45 | 0.76 | 0.93 |
| | PSR | -0.26 | -0.08 | -0.14 | 0.17 | -0.08 |
| | WBI | -0.26 | 0.26 | -0.23 | 0.23 | -0.23 |
| | SIPI | 0.22 | 0.56 | -0.31 | -0.75 | -0.82 |
| | YI | -0.24 | 0.51 | 0.59 | 0.18 | 0.47 |
| | VI2 | 0.23 | -0.19 | 0.33 | -0.02 | -0.76 |
| | Cgreen | 0.23 | 0.59 | 0.26 | 0.59 | 0.93 |
| | Cred edge | 0.18 | 0.57 | 0.25 | 0.67 | 0.90 |
| | C NIR | -0.02 | -0.34 | -0.08 | 0.18 | 0.89 |

**Table A21**- Coefficient of correlation for the relationship between different vegetation indices and aboveground biomass of Egyptian wheat at DAS in the 2006-07 growing season. Highlighted values are significant (P<0.05) and bold values are the strongest correlations.

| Scale | Vegetation index | Aboveground biomass (kg $m^{-2}$) | | | | |
|---|---|---|---|---|---|---|
| | | 83 DAS | 108 DAS | 130 DAS | 149 DAS | 197 DAS |
| Broad band | NDVI | 0.26 | 0.57 | 0.37 | 0.78 | 0.92 |
| | RVI | -0.09 | 0.61 | 0.37 | 0.77 | 0.92 |
| | SAVI | 0.24 | 0.29 | -0.18 | 0.23 | 0.89 |
| | GNDVI br | 0.20 | 0.51 | 0.22 | 0.67 | 0.91 |
| | DVI | 0.27 | 0.22 | -0.22 | 0.19 | 0.84 |
| | SR | -0.11 | 0.62 | 0.37 | 0.77 | 0.92 |
| | SLAVI | -0.18 | 0.56 | 0.37 | 0.78 | 0.92 |
| | OSAVI | 0.24 | 0.32 | -0.10 | 0.33 | **0.94** |
| | VI1 | 0.29 | -0.21 | 0.37 | -0.02 | -0.76 |
| | RDVI | 0.28 | 0.60 | 0.37 | 0.78 | **0.94** |
| | SI | 0.29 | -0.55 | -0.37 | -0.77 | -0.90 |
| | IPVI | 0.01 | 0.56 | 0.37 | 0.78 | 0.92 |
| Hyper | WI | -0.06 | 0.29 | 0.00 | 0.27 | -0.36 |
| | PSI | 0.09 | -0.54 | 0.11 | -0.23 | 0.36 |
| | NWI-1 | 0.26 | -0.29 | -0.23 | -0.04 | -0.43 |
| | NWI-2 | 0.27 | -0.10 | -0.09 | -0.04 | -0.38 |
| | NDVI hy | 0.26 | 0.09 | 0.30 | 0.77 | **0.93** |
| | GNDVI hy | 0.28 | 0.67 | 0.21 | 0.61 | 0.92 |
| | SIPI | -0.42 | 0.16 | 0.74 | 0.36 | 0.89 |
| | SRPI | 0.26 | -0.09 | 0.12 | 0.48 | 0.54 |
| | NPCI | 0.24 | 0.12 | -0.03 | -0.26 | -0.37 |
| | NPQI | 0.22 | -0.28 | -0.19 | 0.19 | -0.25 |
| | PSSRb | 0.27 | 0.30 | -0.21 | 0.18 | 0.85 |
| | PSNDb | 0.26 | 0.43 | 0.35 | 0.77 | 0.91 |
| | Rshoulder | -0.25 | 0.23 | -0.36 | 0.03 | 0.77 |
| | C420 | -0.33 | 0.20 | -0.08 | 0.25 | 0.17 |
| | NDI | -0.26 | 0.22 | -0.22 | 0.19 | 0.84 |
| | SR hyper | 0.31 | 0.14 | 0.28 | 0.78 | **0.93** |
| | R800-R550 | 0.29 | 0.40 | -0.24 | 0.11 | 0.84 |
| | R800/R550 | -0.29 | 0.63 | 0.21 | 0.58 | **0.93** |
| | R695/R760 | -0.36 | -0.55 | -0.31 | -0.71 | -0.90 |
| | R605/R760 | -0.32 | -0.37 | -0.25 | -0.77 | -0.90 |
| | R710/R760 | -0.22 | -0.08 | -0.08 | -0.63 | -0.91 |
| | R695/R670 | -0.32 | 0.38 | 0.38 | 0.74 | **0.93** |
| | R550 | 0.28 | -0.09 | -0.57 | -0.30 | 0.39 |
| | R675/R700 | 0.22 | -0.49 | -0.49 | -0.79 | -0.93 |
| | R675/(R700*R650) | 0.25 | -0.22 | 0.47 | 0.23 | -0.12 |
| | R672/(R55*R708) | -0.45 | -0.20 | -0.03 | -0.51 | -0.84 |
| | R672/R550 | -0.42 | -0.14 | -0.39 | -0.73 | -0.88 |
| | R860/(R550*R708) | 0.32 | 0.07 | 0.64 | 0.56 | 0.31 |
| | R750/R550 | 0.26 | 0.66 | 0.22 | 0.60 | **0.93** |
| | R750/R700 | -0.06 | 0.56 | 0.20 | 0.65 | 0.91 |
| | R725/R675 | -0.22 | 0.66 | 0.38 | 0.82 | 0.92 |
| | (R850-R710)/(R850-R680) | -0.21 | 0.16 | -0.23 | 0.08 | 0.82 |
| | (R780-R710)/(R780-R680) | -0.09 | 0.60 | -0.09 | 0.06 | 0.83 |
| | R700-R670 | 0.26 | 0.21 | -0.19 | 0.14 | 0.63 |
| | RNDVI | 0.27 | 0.66 | 0.40 | 0.75 | 0.92 |
| | PSR | -0.28 | -0.14 | -0.18 | 0.21 | -0.06 |
| | WBI | -0.28 | 0.34 | -0.24 | 0.22 | -0.18 |
| | SIPI | 0.25 | 0.62 | -0.27 | -0.74 | -0.79 |
| | YI | -0.26 | 0.48 | 0.55 | 0.15 | 0.53 |
| | VI2 | 0.26 | -0.22 | 0.36 | -0.01 | -0.75 |
| | Cgreen | 0.26 | 0.63 | 0.21 | 0.58 | 0.93 |
| | Cred edge | 0.20 | 0.55 | 0.19 | 0.65 | 0.91 |
| | C NIR | -0.02 | -0.42 | -0.12 | 0.17 | 0.87 |

**Table A22**- Coefficient of correlation for the relationship between different vegetation indices and leaf water content at different DAS in the 2006-07 growing season. Highlighted values are significant (P<0.05) and bold values are the strongest correlations.

| Scale | Vegetation index | Leaf water content (%) | | | | |
|---|---|---|---|---|---|---|
| | | 83 DAS | 108 DAS | 130 DAS | 149 DAS | 197 DAS |
| Broad band | NDVI | 0.19 | 0.54 | 0.28 | 0.62 | 0.75 |
| | RVI | -0.09 | 0.57 | 0.29 | 0.62 | **0.80** |
| | SAVI | 0.17 | 0.20 | -0.17 | 0.18 | 0.72 |
| | GNDVI br | 0.11 | 0.38 | 0.18 | 0.57 | 0.75 |
| | DVI | 0.22 | 0.14 | -0.20 | 0.16 | 0.66 |
| | SR | -0.19 | 0.58 | 0.29 | 0.62 | **0.80** |
| | SLAVI | -0.26 | 0.54 | 0.28 | 0.62 | 0.75 |
| | OSAVI | 0.18 | 0.24 | -0.11 | 0.26 | 0.76 |
| | VI1 | 0.22 | -0.13 | 0.33 | -0.01 | -0.59 |
| | RDVI | 0.21 | 0.56 | 0.29 | 0.63 | **0.80** |
| | SI | 0.21 | -0.52 | -0.28 | -0.61 | -0.72 |
| | IPVI | -0.02 | 0.54 | 0.28 | 0.62 | 0.75 |
| Hyper | WI | -0.04 | 0.41 | 0.00 | 0.22 | -0.18 |
| | PSI | 0.17 | -0.43 | 0.11 | -0.31 | 0.20 |
| | NWI-1 | 0.22 | -0.15 | -0.26 | -0.01 | -0.19 |
| | NWI-2 | 0.22 | 0.02 | -0.14 | -0.01 | -0.13 |
| | NDVI hy | 0.19 | 0.14 | 0.24 | 0.63 | 0.75 |
| | GNDVI hy | 0.24 | 0.70 | 0.18 | 0.58 | 0.76 |
| | SIPI | -0.31 | 0.19 | 0.68 | 0.46 | 0.73 |
| | SRPI | 0.22 | -0.16 | 0.22 | 0.29 | 0.33 |
| | NPCI | 0.17 | 0.21 | -0.16 | -0.12 | -0.18 |
| | NPQI | 0.16 | -0.26 | 0.00 | 0.08 | -0.22 |
| | PSSRb | 0.23 | 0.18 | -0.19 | 0.15 | 0.68 |
| | PSNDb | 0.20 | 0.30 | 0.27 | 0.66 | 0.75 |
| | Rshoulder | -0.18 | 0.14 | -0.32 | 0.02 | 0.60 |
| | C420 | -0.25 | 0.07 | -0.12 | 0.10 | 0.23 |
| | NDI | -0.20 | 0.14 | -0.20 | 0.16 | 0.66 |
| | SR hyper | 0.23 | 0.17 | 0.23 | 0.65 | **0.80** |
| | R800-R550 | 0.26 | 0.32 | -0.22 | 0.10 | 0.67 |
| | R800/R550 | -0.20 | 0.66 | 0.17 | 0.57 | 0.79 |
| | R695/R760 | -0.29 | -0.42 | -0.25 | -0.57 | -0.72 |
| | R605/R760 | -0.25 | -0.32 | -0.19 | -0.63 | -0.72 |
| | R710/R760 | -0.16 | 0.04 | -0.07 | -0.54 | -0.73 |
| | R695/R670 | -0.31 | 0.48 | 0.31 | 0.62 | 0.78 |
| | R550 | 0.21 | -0.21 | -0.50 | -0.29 | 0.25 |
| | R675/R700 | 0.17 | -0.66 | -0.41 | -0.69 | -0.75 |
| | R675/(R700*R650) | 0.18 | -0.30 | 0.34 | 0.13 | -0.06 |
| | R672/(R55*R708) | -0.28 | -0.22 | 0.03 | -0.34 | -0.67 |
| | R672/R550 | -0.16 | -0.21 | -0.30 | -0.55 | -0.70 |
| | R860/(R550*R708) | 0.25 | 0.13 | 0.58 | 0.53 | 0.28 |
| | R750/R550 | 0.19 | 0.70 | 0.18 | 0.57 | **0.80** |
| | R750/R700 | -0.04 | 0.41 | 0.15 | 0.52 | 0.77 |
| | R725/R675 | -0.15 | 0.75 | 0.32 | 0.69 | **0.80** |
| | (R850-R710)/(R850-R680) | -0.16 | 0.08 | -0.19 | 0.12 | 0.63 |
| | (R780-R710)/(R780-R680) | -0.11 | 0.43 | -0.06 | 0.13 | 0.65 |
| | R700-R670 | 0.19 | 0.17 | -0.17 | 0.11 | 0.47 |
| | RNDVI | 0.21 | 0.60 | 0.32 | 0.61 | 0.75 |
| | PSR | -0.24 | -0.22 | -0.18 | 0.26 | -0.06 |
| | WBI | -0.24 | 0.47 | -0.23 | 0.27 | 0.00 |
| | SIPI | 0.18 | 0.64 | -0.33 | -0.62 | -0.57 |
| | YI | -0.19 | 0.28 | 0.38 | 0.04 | 0.57 |
| | VI2 | 0.19 | -0.12 | 0.31 | -0.01 | -0.58 |
| | Cgreen | 0.20 | 0.66 | 0.17 | 0.57 | 0.79 |
| | Cred edge | 0.15 | 0.40 | 0.15 | 0.53 | 0.77 |
| | C NIR | -0.09 | -0.51 | -0.08 | 0.21 | 0.68 |

**Table A23**- Coefficient of correlation for the relationship between different vegetation indices and plant height of Egyptian wheat at different DAS in the 2006-07 growing season. Highlighted values are significant (P<0.05) and bold values are the strongest correlations.

| Scale | Vegetation index | Plant height (m) | | | | |
|---|---|---|---|---|---|---|
| | | 83 DAS | 108 DAS | 130 DAS | 149 DAS | 197 DAS |
| Broad band | NDVI | -0.06 | 0.12 | 0.42 | 0.76 | 0.90 |
| | RVI | 0.12 | 0.07 | 0.44 | 0.74 | 0.91 |
| | SAVI | -0.05 | 0.07 | -0.02 | 0.22 | 0.89 |
| | GNDVI br | -0.08 | 0.04 | 0.31 | 0.65 | 0.90 |
| | DVI | -0.06 | 0.05 | -0.06 | 0.17 | 0.84 |
| | SR | 0.04 | 0.07 | 0.44 | 0.74 | 0.91 |
| | SLAVI | 0.03 | 0.12 | 0.42 | 0.76 | 0.90 |
| | OSAVI | -0.06 | 0.08 | 0.05 | 0.32 | 0.93 |
| | VI1 | -0.06 | -0.06 | 0.19 | 0.00 | -0.76 |
| | RDVI | -0.10 | 0.09 | 0.44 | 0.76 | **0.93** |
| | SI | -0.08 | -0.14 | -0.42 | -0.76 | -0.88 |
| | IPVI | 0.02 | 0.12 | 0.42 | 0.76 | 0.90 |
| Hyper | WI | -0.02 | 0.35 | -0.15 | 0.34 | -0.43 |
| | PSI | -0.23 | -0.15 | 0.12 | -0.18 | 0.32 |
| | NWI-1 | -0.06 | 0.31 | -0.02 | 0.08 | -0.48 |
| | NWI-2 | -0.06 | 0.39 | 0.11 | 0.06 | -0.46 |
| | NDVI hy | -0.06 | 0.01 | 0.37 | 0.75 | 0.92 |
| | GNDVI hy | -0.06 | 0.21 | 0.32 | 0.57 | 0.91 |
| | SIPI | 0.12 | 0.14 | 0.69 | 0.27 | 0.87 |
| | SRPI | -0.06 | -0.05 | 0.14 | 0.54 | 0.54 |
| | NPCI | -0.05 | 0.06 | -0.09 | -0.29 | -0.43 |
| | NPQI | -0.05 | -0.13 | -0.15 | 0.06 | -0.24 |
| | PSSRb | -0.07 | 0.05 | -0.05 | 0.16 | 0.85 |
| | PSNDb | -0.09 | 0.00 | 0.39 | 0.75 | 0.90 |
| | Rshoulder | 0.05 | 0.06 | -0.18 | 0.01 | 0.77 |
| | C420 | 0.01 | 0.34 | -0.13 | 0.35 | 0.20 |
| | NDI | 0.03 | 0.05 | -0.06 | 0.17 | 0.84 |
| | SR hyper | -0.04 | -0.05 | 0.37 | 0.74 | **0.93** |
| | R800-R550 | -0.05 | 0.13 | -0.07 | 0.09 | 0.84 |
| | R800/R550 | 0.08 | 0.25 | 0.30 | 0.53 | **0.93** |
| | R695/R760 | 0.12 | -0.05 | -0.40 | -0.70 | -0.88 |
| | R605/R760 | 0.07 | -0.01 | -0.34 | -0.75 | -0.88 |
| | R710/R760 | 0.03 | 0.15 | -0.17 | -0.59 | -0.91 |
| | R695/R670 | 0.02 | 0.05 | 0.31 | 0.70 | 0.91 |
| | R550 | -0.09 | -0.07 | -0.42 | -0.30 | 0.40 |
| | R675/R700 | -0.05 | -0.21 | -0.53 | -0.76 | -0.91 |
| | R675/(R700*R650) | -0.05 | -0.15 | 0.24 | 0.25 | -0.13 |
| | R672/(R55*R708) | 0.11 | -0.12 | -0.13 | -0.49 | -0.84 |
| | R672/R550 | 0.16 | -0.11 | -0.43 | -0.71 | -0.87 |
| | R860/(R550*R708) | -0.06 | 0.03 | 0.55 | 0.53 | 0.32 |
| | R750/R550 | -0.06 | 0.22 | 0.32 | 0.55 | 0.93 |
| | R750/R700 | -0.02 | -0.01 | 0.29 | 0.62 | 0.92 |
| | R725/R675 | 0.21 | 0.19 | 0.45 | 0.78 | 0.91 |
| | (R850-R710)/(R850-R680) | 0.04 | -0.23 | -0.23 | 0.06 | 0.82 |
| | (R780-R710)/(R780-R680) | -0.18 | -0.09 | -0.05 | 0.04 | 0.83 |
| | R700-R670 | -0.06 | 0.06 | -0.08 | 0.14 | 0.62 |
| | RNDVI | -0.06 | 0.07 | 0.42 | 0.74 | 0.91 |
| | PSR | 0.06 | -0.02 | -0.22 | 0.21 | -0.12 |
| | WBI | 0.06 | 0.31 | -0.35 | 0.25 | -0.22 |
| | SIPI | -0.05 | 0.24 | -0.39 | -0.78 | -0.77 |
| | YI | 0.06 | -0.06 | 0.50 | 0.12 | 0.42 |
| | VI2 | -0.06 | -0.06 | 0.18 | 0.01 | -0.76 |
| | Cgreen | -0.09 | 0.25 | 0.30 | 0.53 | 0.93 |
| | Cred edge | -0.05 | 0.04 | 0.28 | 0.61 | 0.91 |
| | C NIR | -0.18 | -0.12 | 0.03 | 0.15 | 0.89 |

**Table A24**- Coefficient of correlation for the relationship between different vegetation indices and LAI of Egyptian wheat at different DAS in the 2006-07 growing season. Highlighted values are significant ($P<0.05$) and bold values are the strongest correlations.

| Scale | Vegetation index | Leaf Area Index | | | | |
|---|---|---|---|---|---|---|
| | | 83 DAS | 108 DAS | 130 DAS | 149 DAS | 197 DAS |
| Broad band | NDVI | 0.20 | 0.46 | 0.4 | 0.82 | **0.96** |
| | RVI | -0.23 | 0.51 | 0.39 | 0.81 | 0.89 |
| | SAVI | 0.18 | 0.17 | -0.2 | 0.16 | 0.84 |
| | GNDVI br | 0.23 | 0.47 | 0.22 | 0.64 | 0.95 |
| | DVI | 0.23 | 0.12 | -0.25 | 0.13 | 0.78 |
| | SR | -0.26 | 0.52 | 0.39 | 0.81 | 0.89 |
| | SLAVI | -0.27 | 0.46 | 0.4 | 0.82 | **0.96** |
| | OSAVI | 0.19 | 0.20 | -0.11 | 0.26 | 0.90 |
| | VI1 | 0.25 | -0.10 | 0.41 | 0.07 | -0.69 |
| | RDVI | 0.24 | 0.50 | 0.39 | 0.82 | 0.93 |
| | SI | 0.27 | -0.44 | -0.4 | -0.81 | -0.95 |
| | IPVI | -0.10 | 0.46 | 0.4 | 0.82 | **0.96** |
| Hyper | WI | 0.06 | 0.22 | 0.08 | 0.30 | -0.49 |
| | PSI | 0.04 | -0.41 | 0.09 | -0.05 | 0.55 |
| | NWI-1 | 0.21 | -0.28 | -0.28 | -0.13 | -0.57 |
| | NWI-2 | 0.22 | -0.14 | -0.17 | -0.11 | -0.51 |
| | NDVI hy | 0.21 | 0.04 | 0.31 | 0.80 | **0.96** |
| | GNDVI hy | 0.25 | 0.52 | 0.18 | 0.53 | 0.94 |
| | SIPI | -0.52 | 0.08 | 0.74 | 0.38 | 0.92 |
| | SRPI | 0.21 | 0.02 | 0.19 | 0.47 | 0.67 |
| | NPCI | 0.18 | 0.04 | -0.1 | -0.22 | -0.46 |
| | NPQI | 0.16 | -0.28 | -0.19 | 0.14 | -0.41 |
| | PSSRb | 0.23 | 0.20 | -0.23 | 0.12 | 0.79 |
| | PSNDb | 0.22 | 0.40 | 0.39 | 0.83 | 0.95 |
| | Rshoulder | -0.20 | 0.12 | -0.4 | -0.06 | 0.70 |
| | C420 | -0.27 | 0.15 | 0.1 | 0.38 | -0.02 |
| | NDI | -0.19 | 0.12 | -0.25 | 0.13 | 0.78 |
| | SR hyper | 0.27 | 0.10 | 0.28 | 0.80 | 0.89 |
| | R800-R550 | 0.26 | 0.26 | -0.28 | 0.04 | 0.78 |
| | R800/R550 | -0.25 | 0.49 | 0.18 | 0.54 | 0.92 |
| | R695/R760 | -0.38 | -0.46 | -0.31 | -0.74 | -0.94 |
| | R605/R760 | -0.29 | -0.38 | -0.27 | -0.81 | -0.94 |
| | R710/R760 | -0.16 | -0.17 | -0.11 | -0.61 | -0.93 |
| | R695/R670 | -0.33 | 0.29 | 0.51 | 0.76 | 0.91 |
| | R550 | 0.24 | -0.14 | -0.61 | -0.41 | 0.31 |
| | R675/R700 | 0.16 | -0.33 | -0.54 | -0.90 | **-0.96** |
| | R675/(R700*R650) | 0.19 | -0.06 | 0.57 | 0.37 | 0.01 |
| | R672/(R55*R708) | -0.49 | -0.10 | -0.08 | -0.49 | -0.81 |
| | R672/R550 | -0.60 | -0.11 | -0.45 | -0.83 | -0.93 |
| | R860/(R550*R708) | 0.28 | 0.15 | 0.63 | 0.65 | 0.39 |
| | R750/R550 | 0.20 | 0.51 | 0.19 | 0.55 | 0.92 |
| | R750/R700 | 0.07 | 0.50 | 0.23 | 0.69 | 0.89 |
| | R725/R675 | -0.37 | 0.50 | 0.43 | 0.89 | 0.89 |
| | (R850-R710)/(R850-R680) | -0.14 | 0.27 | -0.2 | 0.03 | 0.82 |
| | (R780-R710)/(R780-R680) | -0.06 | 0.58 | -0.07 | -0.04 | 0.83 |
| | R700-R670 | 0.20 | 0.08 | -0.19 | 0.05 | 0.58 |
| | RNDVI | 0.22 | 0.53 | 0.47 | 0.79 | **0.96** |
| | PSR | -0.24 | 0.01 | -0.2 | 0.09 | 0.00 |
| | WBI | -0.24 | 0.29 | -0.14 | 0.20 | -0.33 |
| | SIPI | 0.19 | 0.50 | -0.29 | -0.82 | -0.82 |
| | YI | -0.21 | 0.40 | 0.57 | 0.25 | 0.50 |
| | VI2 | 0.20 | -0.11 | 0.39 | 0.08 | -0.69 |
| | Cgreen | 0.22 | 0.49 | 0.18 | 0.54 | 0.92 |
| | Cred edge | 0.14 | 0.50 | 0.22 | 0.69 | 0.89 |
| | C NIR | 0.00 | -0.28 | -0.2 | 0.11 | 0.89 |

**Table A25**- The relationship between the rededge position and the measured chlorophyll *a* concentration extracted from Scottish wheat leaves collected at DAS in the 2005-06 growing season. Highlighted values are significant (P<0.05) and bold value is the strongest correlations.

| Treatment | Replicates | Days after sowing | | | | | | | | | |
|---|---|---|---|---|---|---|---|---|---|---|---|
| | | 73 DAS | | 125 DAS | | 181 DAS | | 207 DAS | | 225 DAS | |
| | | Rededge | Chl *a* | Rededge | Chl *a* | Rededge | Chl *a* | Rededge | Chl *a* | Rededge | Chl *a* |
| T1 | R1 | 717.5 | 34.27 | 721.7 | 37.75 | 726.1 | 53.54 | 728.5 | 53.87 | 728.7 | 52.30 |
| | R2 | 718 | 35.83 | 717.1 | 38.47 | 729 | 49.94 | 727 | 55.83 | 729.2 | 54.21 |
| | R3 | 716.5 | 35.30 | 721 | 36.03 | 728.4 | 47.23 | 729.5 | 47.60 | 728 | 46.21 |
| T2 | R1 | 719 | 34.95 | 720.9 | 41.38 | 725.8 | 52.20 | 727.5 | 45.93 | 719.1 | 44.59 |
| | R2 | 717 | 34.89 | 717.4 | 40.19 | 727.3 | 44.19 | 725 | 44.85 | 719.4 | 43.54 |
| | R3 | 718.5 | 28.95 | 713.3 | 35.25 | 726.1 | 42.51 | 727 | 55.13 | 720.2 | 53.53 |
| T3 | R1 | 718.5 | 31.40 | 712 | 40.06 | 727.1 | 41.80 | 713.5 | 36.95 | 705.4 | 35.87 |
| | R2 | 719 | 32.49 | 713 | 39.39 | 727.8 | 37.67 | 716 | 39.05 | 703.3 | 37.91 |
| | R3 | 718 | 31.87 | 717.3 | 39.61 | 724.9 | 35.94 | 715 | 37.10 | 702.4 | 36.02 |
| T4 | R1 | 718 | 27.67 | 706.2 | 44.93 | 722.9 | 28.95 | 710 | 33.86 | 696.1 | 32.88 |
| | R2 | 718 | 26.58 | 709 | 41.47 | 724.4 | 30.91 | 705 | 39.93 | 696.6 | 38.77 |
| | R3 | 719 | 26.11 | 714.4 | 39.65 | 724.6 | 29.28 | 706 | 38.40 | 700.9 | 42.14 |
| T5 | R1 | 716.5 | 27.72 | 713.9 | 39.36 | 727.1 | 52.10 | 728 | 43.99 | 729.2 | 42.71 |
| | R2 | 717 | 26.91 | 716 | 37.53 | 728.4 | 52.45 | 728.5 | 43.77 | 727.9 | 42.49 |
| | R3 | 717.5 | 31.46 | 715.5 | 36.78 | 727.1 | 49.35 | 726.8 | 51.07 | 728.1 | 39.87 |
| T6 | R1 | 718.9 | 30.23 | 714 | 37.07 | 723.6 | 49.04 | 726 | 36.06 | 725.6 | 35.01 |
| | R2 | 719 | 29.70 | 716.4 | 40.57 | 725 | 46.20 | 727 | 36.43 | 725.3 | 35.37 |
| | R3 | 717.5 | 32.38 | 714 | 34.77 | 728.4 | 43.84 | 727 | 45.81 | 725.1 | 44.48 |
| T7 | R1 | 718 | 31.53 | 712.5 | 40.55 | 726.1 | 40.52 | 722.5 | 41.20 | 720.1 | 40.00 |
| | R2 | 716.5 | 30.84 | 711.5 | 40.23 | 727.6 | 41.46 | 724 | 42.07 | 721.3 | 40.84 |
| | R3 | 716.5 | 27.44 | 708 | 38.77 | 725.1 | 42.71 | 722 | 43.30 | 722.6 | 42.04 |
| T8 | R1 | 717 | 33.39 | 705.5 | 39.28 | 723 | 26.52 | 709.5 | 30.34 | 695.4 | 29.45 |
| | R2 | 717 | 31.68 | 703.6 | 35.92 | 724.9 | 27.04 | 706.3 | 36.17 | 695.2 | 35.12 |
| | R3 | 716.5 | 31.97 | 702.5 | 43.90 | 724.7 | 27.81 | 704 | 35.89 | 697.8 | 49.41 |
| T9 | R1 | 718 | 30.71 | 713.5 | 41.82 | 728.8 | 37.81 | 722 | 39.12 | 719.1 | 37.98 |
| | R2 | 718.5 | 29.75 | 718.4 | 39.14 | 725 | 38.70 | 719.5 | 41.18 | 720.5 | 39.98 |
| | R3 | 717 | 32.51 | 702.4 | 41.28 | 726.8 | 39.74 | 721 | 35.23 | 722.5 | 34.21 |
| T10 | R1 | 718.5 | 36.09 | 709 | 44.36 | 725.2 | 26.46 | 707 | 35.36 | 698.1 | 34.33 |
| | R2 | 717.5 | 36.25 | 711.2 | 40.13 | 723.6 | 29.55 | 708 | 37.68 | 699.3 | 36.58 |
| | R3 | 719 | 29.32 | 709.5 | 39.11 | 723.4 | 28.30 | 710 | 42.80 | 699.6 | 41.55 |
| T11 | R1 | 719 | 36.58 | 718.6 | 43.67 | 727.5 | 46.26 | 725 | 44.89 | 718.5 | 43.58 |
| | R2 | 718.5 | 38.01 | 719.5 | 41.38 | 724.9 | 43.79 | 724.5 | 43.46 | 717.4 | 42.19 |
| | R3 | 718.5 | 35.73 | 717.7 | 34.01 | 728.4 | 42.27 | 726 | 39.57 | 716.3 | 38.42 |
| r | | **0.07** | | **-0.28** | | 0.59 | | **0.64** | | 0.47 | |

**Table A26**- The relationship between the rededge position and the measured chlorophyll *a* concentration extracted from Egyptian wheat leaves collected at different Das in spring season of 2006. Highlighted values are significant (P<0.05) and bold values are the strongest correlations.

| Treatment | Replicates | Days after sowing | | | | | | | | | |
|---|---|---|---|---|---|---|---|---|---|---|---|
| | | 57 DAS | | 78 DAS | | 91 DAS | | 103 DAS | | 127 DAS | |
| | | Rededge | Chl *a* | Rededge | Chl *a* | Rededge | Chl *a* | Rededge | Chl *a* | Rededge | Chl *a* |
| T1 | R1 | 698.5 | 30.46 | 720.5 | 32.64 | 720.5 | 48.59 | 730.5 | 52.44 | 726 | 58.27 |
| | R2 | 699.5 | 31.54 | 719.5 | 34.13 | 719.5 | 50.73 | 729.5 | 46.15 | 730 | 51.28 |
| | R3 | 700 | 29.94 | 719 | 33.62 | 719 | 53.01 | 728.6 | 47.12 | 730.5 | 52.36 |
| T2 | R1 | 699.5 | 29.31 | 719.5 | 33.28 | 719.5 | 48.16 | 724.5 | 48.28 | 724.5 | 53.65 |
| | R2 | 699.5 | 32.1 | 718 | 33.23 | 718 | 45.62 | 727 | 45.08 | 728 | 50.09 |
| | R3 | 700 | 30.4 | 719.5 | 27.57 | 719.5 | 50.42 | 727.5 | 50.28 | 727.5 | 55.87 |
| T3 | R1 | 700.5 | 29.45 | 717 | 29.90 | 712 | 42.07 | 721.5 | 54.38 | 721.5 | 60.42 |
| | R2 | 699 | 28.47 | 715.5 | 30.94 | 715.5 | 42.80 | 719.5 | 38.52 | 719.5 | 42.80 |
| | R3 | 698.5 | 31.54 | 713 | 30.35 | 713 | 43.12 | 719 | 37.13 | 719 | 41.25 |
| T4 | R1 | 702 | 28.46 | 719 | 26.35 | 699.5 | 47.38 | 718.5 | 40.29 | 713 | 44.77 |
| | R2 | 698 | 28.9 | 716.5 | 25.31 | 703 | 40.66 | 715 | 43.98 | 714.5 | 48.87 |
| | R3 | 699.5 | 31.2 | 713.8 | 29.06 | 701.5 | 39.19 | 714.5 | 39.75 | 712 | 44.17 |
| T5 | R1 | 700.5 | 30.61 | 718 | 32.38 | 718 | 49.75 | 728 | 52.23 | 728 | 58.03 |
| | R2 | 700 | 30.58 | 718.5 | 34.56 | 718.5 | 50.09 | 727 | 52.17 | 729 | 57.97 |
| | R3 | 698.5 | 31.2 | 717.5 | 29.96 | 717.5 | 48.84 | 725.5 | 43.96 | 727.5 | 48.84 |
| T6 | R1 | 699.5 | 29.87 | 717 | 28.79 | 717 | 41.65 | 722.5 | 42.59 | 723 | 47.33 |
| | R2 | 698 | 30.7 | 718 | 28.28 | 718 | 50.27 | 720 | 43.98 | 724 | 48.87 |
| | R3 | 699 | 31.45 | 718.5 | 30.84 | 718.5 | 52.93 | 719.5 | 47.07 | 724.5 | 52.30 |
| T7 | R1 | 699.5 | 28.74 | 717 | 30.03 | 717 | 40.80 | 718 | 41.88 | 720.5 | 46.54 |
| | R2 | 701.5 | 29.45 | 718 | 29.37 | 718 | 49.63 | 718.5 | 45.27 | 719 | 50.30 |
| | R3 | 699 | 28.46 | 718.5 | 26.13 | 718.5 | 51.37 | 716 | 45.76 | 718.5 | 50.84 |
| T8 | R1 | 701.5 | 30.21 | 717.5 | 26.89 | 711.5 | 49.29 | 717 | 45.65 | 718.5 | 50.72 |
| | R2 | 701.5 | 30.67 | 713 | 30.18 | 713 | 47.82 | 715.3 | 43.10 | 719.5 | 47.89 |
| | R3 | 700 | 29.65 | 715 | 30.45 | 715 | 47.01 | 718.5 | 42.56 | 717 | 47.29 |
| T9 | R1 | 699.5 | 28.94 | 715.5 | 25.38 | 699 | 41.56 | 711.5 | 32.93 | 709 | 36.59 |
| | R2 | 700 | 30.61 | 718 | 28.34 | 701 | 42.29 | 713 | 37.78 | 711.5 | 41.97 |
| | R3 | 699.5 | 30.54 | 714.6 | 28.94 | 702.5 | 40.18 | 713.5 | 45.46 | 708.5 | 50.51 |
| T10 | R1 | 700.5 | 31.26 | 717.5 | 34.37 | 717.5 | 50.45 | 726.5 | 46.90 | 726.5 | 52.11 |
| | R2 | 700.5 | 31.02 | 718 | 34.52 | 718 | 47.30 | 726 | 47.76 | 725 | 53.06 |
| | R3 | 698.5 | 29.57 | 718 | 27.93 | 718 | 48.69 | 724.5 | 44.38 | 723.5 | 49.32 |
| T11 | R1 | 699 | 28.69 | 716.3 | 25.99 | 703.5 | 41.61 | 714 | 41.42 | 714 | 46.02 |
| | R2 | 698.5 | 29.64 | 717 | 27.87 | 700.5 | 46.63 | 713.3 | 38.93 | 715.5 | 43.25 |
| | R3 | 699 | 30.21 | 716.9 | 27.18 | 700 | 39.37 | 713.5 | 42.27 | 711 | 46.97 |
| **r** | | **-0.04** | | **0.26** | | **0.67** | | **0.69** | | **0.66** | |

**Table A27**- The relationship between the rededge position and the measured chlorophyll *a* concentration extracted from Scottish wheat leaves collected at different DAS in the 2006-07 growing season. Highlighted values are significant (P<0.05) and bold values are the strongest correlations.

| Treatment | Replicates | Days after sowing | | | | | | | | | |
|---|---|---|---|---|---|---|---|---|---|---|---|
| | | 97 DAS | | 135 DAS | | 177 DAS | | 198 DAS | | 223 DAS | |
| | | Rededge | Chl *a* | Rededge | Chl *a* | Rededge | Chl *a* | Rededge | Chl *a* | Rededge | Chl *a* |
| T1 | R1 | 713.1 | 32.64 | 721.7 | 35.28 | 721.3 | 53.54 | 722.3 | 56.11 | 726.5 | 52.30 |
| | R2 | 714.8 | 34.13 | 717.1 | 35.95 | 714.6 | 49.94 | 721.2 | 56.70 | 728 | 54.21 |
| | R3 | 721.5 | 33.62 | 721 | 33.68 | 719.9 | 47.23 | 729.9 | 48.53 | 728.6 | 46.21 |
| T2 | R1 | 715.7 | 33.28 | 720.9 | 38.68 | 716.1 | 52.20 | 712.7 | 50.98 | 719.3 | 44.59 |
| | R2 | 719.9 | 33.23 | 717.4 | 37.56 | 716 | 44.19 | 715.7 | 52.64 | 721.8 | 43.54 |
| | R3 | 710.6 | 27.57 | 713.3 | 32.94 | 717 | 42.51 | 720.3 | 44.81 | 724.5 | 53.53 |
| T3 | R1 | 707 | 29.90 | 698.3 | 37.44 | 713.6 | 51.80 | 712.1 | 22.76 | 721.3 | 35.87 |
| | R2 | 714.2 | 30.94 | 719 | 36.81 | 716 | 37.67 | 710.6 | 21.87 | 719.2 | 37.91 |
| | R3 | 715.2 | 30.35 | 717.3 | 37.02 | 713 | 35.94 | 715.3 | 28.72 | 721.5 | 36.02 |
| T4 | R1 | 711 | 26.35 | 716.2 | 41.99 | 705.2 | 28.95 | 710.9 | 16.89 | 718.3 | 32.88 |
| | R2 | 707.6 | 25.31 | 698.7 | 38.76 | 703.1 | 30.91 | 707.1 | 18.88 | 719.5 | 38.77 |
| | R3 | 706.2 | 24.86 | 714.4 | 37.05 | 708.1 | 29.28 | 707.2 | 17.98 | 716.6 | 42.14 |
| T5 | R1 | 718.3 | 26.40 | 713.9 | 36.78 | 719.7 | 52.10 | 718.2 | 48.88 | 728.3 | 42.71 |
| | R2 | 719.7 | 25.63 | 699.2 | 35.08 | 718.1 | 52.45 | 714.5 | 52.74 | 727.4 | 42.49 |
| | R3 | 716.6 | 29.96 | 699 | 34.37 | 707.7 | 49.35 | 720.1 | 46.10 | 724.4 | 39.87 |
| T6 | R1 | 719.1 | 28.79 | 700 | 34.64 | 713.6 | 49.04 | 711.3 | 29.17 | 722.7 | 35.01 |
| | R2 | 715.4 | 28.28 | 698.8 | 37.91 | 711 | 46.20 | 708.1 | 23.61 | 724.8 | 35.37 |
| | R3 | 720.5 | 30.84 | 704.3 | 32.49 | 712.2 | 43.84 | 703.3 | 31.76 | 721.9 | 44.48 |
| T7 | R1 | 719.1 | 30.03 | 698.4 | 37.90 | 712.6 | 40.52 | 710.7 | 23.84 | 716.8 | 40.00 |
| | R2 | 717.2 | 29.37 | 699.9 | 37.60 | 711.6 | 41.46 | 705.3 | 19.39 | 720.4 | 40.84 |
| | R3 | 716.5 | 26.13 | 698.9 | 36.24 | 717.5 | 42.71 | 701.7 | 21.01 | 716.8 | 42.04 |
| T8 | R1 | 711.5 | 31.80 | 698.4 | 36.71 | 712.2 | 26.52 | 710.4 | 13.62 | 716.4 | 29.45 |
| | R2 | 702.4 | 30.18 | 703.6 | 33.57 | 712.1 | 27.04 | 701.5 | 14.33 | 711.6 | 35.12 |
| | R3 | 708.1 | 30.45 | 721.3 | 41.03 | 714.8 | 27.81 | 703.2 | 21.06 | 714.3 | 49.41 |
| T9 | R1 | 721 | 29.25 | 719.6 | 39.09 | 703 | 37.81 | 701.3 | 13.00 | 715.7 | 37.98 |
| | R2 | 718 | 28.34 | 718.4 | 36.58 | 707.1 | 38.70 | 703.4 | 11.88 | 713.9 | 39.98 |
| | R3 | 719.2 | 30.97 | 699.3 | 38.58 | 712.2 | 39.74 | 706.1 | 17.21 | 715 | 34.21 |
| T10 | R1 | 719.7 | 34.37 | 719 | 41.46 | 714.5 | 26.46 | 706.4 | 36.74 | 724.3 | 34.33 |
| | R2 | 715.4 | 34.52 | 717.2 | 37.50 | 717.5 | 29.55 | 710.1 | 31.55 | 723.6 | 36.58 |
| | R3 | 718.2 | 27.93 | 719.5 | 36.55 | 715.1 | 28.30 | 714.5 | 28.35 | 722.6 | 41.55 |
| T11 | R1 | 716.3 | 34.83 | 718.6 | 40.81 | 712 | 46.26 | 701.8 | 16.14 | 715.8 | 43.58 |
| | R2 | 713.2 | 36.20 | 719.5 | 38.68 | 710.4 | 43.79 | 705.2 | 16.13 | 717.6 | 42.19 |
| | R3 | 713.6 | 34.03 | 717.7 | 31.78 | 711.2 | 42.27 | 700.2 | 16.58 | 719.7 | 38.42 |
| **r** | | **0.19** | | **0.20** | | **0.38** | | **0.79** | | **0.36** | |

**Table A28**- The relationship between the rededge position and the measured chlorophyll *a* concentration extracted from Egyptian wheat leaves collected at different DAS in the 2006-07 growing season. Highlighted values are significant (P<0.05) and bold values are the strongest correlations.

| Treatment | Replicates | Days after sowing | | | | | | | | | |
|---|---|---|---|---|---|---|---|---|---|---|---|
| | | 97 DAS | | 135 DAS | | 177 DAS | | 198 DAS | | 223 DAS | |
| | | Rededge | Chl *a* | Rededge | Chl *a* | Rededge | Chl *a* | Rededge | Chl *a* | Rededge | Chl *a* |
| T1 | R1 | 699.5 | 28.38 | 704 | 32.64 | 716.4 | 38.45 | 714.5 | 46.06 | 719.6 | 48.06 |
| | R2 | 701.8 | 29.71 | 701.8 | 34.13 | 712.7 | 35.11 | 720.2 | 44.89 | 723.1 | 43.89 |
| | R3 | 693 | 29.26 | 704 | 33.62 | 714.4 | 37.48 | 716.3 | 43.85 | 721.1 | 46.85 |
| T2 | R1 | 704.1 | 29.95 | 704.1 | 33.28 | 711.2 | 36.75 | 715.6 | 42.94 | 718.7 | 45.94 |
| | R2 | 699.1 | 29.90 | 703 | 33.23 | 708.5 | 32.13 | 713 | 41.16 | 719.8 | 40.16 |
| | R3 | 698.3 | 27.82 | 698.3 | 27.57 | 710.7 | 33.51 | 712.3 | 44.13 | 722.5 | 33.13 |
| T3 | R1 | 704.1 | 28.91 | 704.1 | 29.90 | 708.2 | 29.91 | 716.9 | 35.23 | 718.7 | 27.38 |
| | R2 | 699 | 27.84 | 699 | 30.94 | 704.2 | 26.17 | 711.6 | 38.64 | 717.2 | 27.71 |
| | R3 | 696.3 | 27.32 | 698.5 | 30.35 | 709.5 | 25.26 | 708.1 | 36.80 | 716.2 | 26.58 |
| T4 | R1 | 702.6 | 29.71 | 702.6 | 26.35 | 702.5 | 26.50 | 707 | 28.70 | 713.6 | 20.63 |
| | R2 | 697.7 | 28.78 | 697.7 | 25.31 | 701.5 | 23.01 | 711.3 | 31.18 | 713.4 | 16.27 |
| | R3 | 703.3 | 26.38 | 699 | 24.86 | 700 | 28.25 | 704.4 | 32.19 | 706.2 | 35.31 |
| T5 | R1 | 701.8 | 28.76 | 701.8 | 26.40 | 711.4 | 33.96 | 718.4 | 44.31 | 718.5 | 42.45 |
| | R2 | 700.7 | 30.06 | 700.7 | 25.63 | 713 | 28.23 | 716.3 | 41.90 | 718.1 | 35.28 |
| | R3 | 703.1 | 26.96 | 703.1 | 29.96 | 711.4 | 33.43 | 723.5 | 43.30 | 724 | 35.53 |
| T6 | R1 | 696.3 | 29.91 | 696.3 | 28.79 | 707 | 27.65 | 713.6 | 36.41 | 719.2 | 34.56 |
| | R2 | 695.1 | 28.45 | 695.1 | 28.28 | 709 | 18.40 | 715.2 | 33.14 | 715.6 | 23.00 |
| | R3 | 696.6 | 27.76 | 696.6 | 30.84 | 702.3 | 27.68 | 711.3 | 36.24 | 718 | 34.60 |
| T7 | R1 | 700.5 | 27.02 | 700.5 | 30.03 | 708.3 | 22.12 | 702.6 | 38.16 | 711.3 | 27.66 |
| | R2 | 695.3 | 30.43 | 695.3 | 29.37 | 705.9 | 22.21 | 698.3 | 32.64 | 709.4 | 27.76 |
| | R3 | 698 | 26.52 | 698 | 26.13 | 704.2 | 23.75 | 709.9 | 33.54 | 710.7 | 29.68 |
| T8 | R1 | 701.9 | 28.62 | 701.9 | 31.80 | 710.1 | 16.35 | 705.3 | 32.15 | 709.5 | 20.43 |
| | R2 | 697.7 | 27.16 | 697.7 | 30.18 | 705.2 | 17.60 | 707.3 | 30.19 | 714.2 | 22.00 |
| | R3 | 700.3 | 27.40 | 700.3 | 30.45 | 709.8 | 24.36 | 703.2 | 30.37 | 713.2 | 30.45 |
| T9 | R1 | 706.6 | 26.32 | 706.6 | 29.25 | 700.1 | 14.18 | 707.8 | 28.47 | 707.4 | 17.72 |
| | R2 | 700.9 | 29.50 | 700.9 | 28.34 | 703.9 | 14.43 | 706.5 | 27.94 | 707.7 | 18.03 |
| | R3 | 699.9 | 27.87 | 699.9 | 30.97 | 704 | 22.21 | 708.6 | 29.47 | 705 | 27.76 |
| T10 | R1 | 699 | 30.93 | 699 | 34.37 | 710.2 | 34.41 | 712.2 | 42.16 | 718.7 | 43.01 |
| | R2 | 705.8 | 31.07 | 705.8 | 34.52 | 708.2 | 33.42 | 716.3 | 43.70 | 720 | 41.77 |
| | R3 | 702.1 | 30.14 | 702.1 | 27.93 | 706 | 26.09 | 715.9 | 41.35 | 716.8 | 32.61 |
| T11 | R1 | 697.8 | 31.35 | 697.8 | 34.83 | 705.2 | 13.15 | 702.4 | 28.14 | 709.2 | 16.44 |
| | R2 | 695.4 | 32.58 | 698.4 | 36.20 | 700.9 | 23.51 | 707.1 | 27.60 | 712.2 | 29.39 |
| | R3 | 703.2 | 30.63 | 703.2 | 34.03 | 702.4 | 23.14 | 703.6 | 27.46 | 703.5 | 28.92 |
| **r** | | **-0.11** | | **0.26** | | **0.61** | | **0.74** | | **0.63** | |

# APPENDIX B

**Table B1**- Coefficient of correlation for the relationship between different vegetation indices and chlorophyll *a* concentration of an Egyptian maize variety at different DAS in summer season of 2007. Highlighted values are significant (P<0.05) and bold values are the strongest correlations.

| Scale | Vegetation index | chlorophyll *a* concentration (µg cm$^{-2}$) | | | | | |
|---|---|---|---|---|---|---|---|
| | | 30 DAS | 45 DAS | 65 DAS | 80 DAS | 90 DAS | 105 DAS |
| Braod band | NDVI | 0.02 | 0.16 | 0.38 | 0.47 | 0.51 | 0.58 |
| | RVI | -0.05 | 0.17 | 0.52 | 0.59 | 0.46 | 0.59 |
| | SAVI | -0.18 | 0.10 | 0.38 | 0.60 | 0.03 | 0.76 |
| | GNDVI br | -0.03 | 0.13 | 0.47 | 0.53 | 0.56 | 0.72 |
| | DVI | -0.17 | 0.08 | 0.38 | 0.61 | -0.02 | **0.79** |
| | SR | -0.05 | 0.17 | 0.52 | 0.59 | 0.46 | 0.59 |
| | SLAVI | 0.02 | 0.16 | 0.38 | 0.47 | 0.51 | 0.58 |
| | OSAVI | -0.16 | 0.11 | 0.38 | 0.57 | 0.13 | 0.67 |
| | VI1 | 0.19 | -0.05 | -0.35 | **-0.62** | 0.16 | -0.05 |
| | RDVI | -0.02 | 0.17 | 0.48 | 0.55 | 0.49 | 0.59 |
| | SI | -0.05 | -0.16 | -0.34 | -0.44 | -0.50 | -0.58 |
| | IPVI | 0.02 | 0.16 | 0.38 | 0.47 | 0.51 | 0.58 |
| Hyper | WI | 0.17 | 0.10 | -0.06 | -0.08 | -0.26 | -0.51 |
| | PSI | -0.07 | -0.12 | 0.28 | 0.42 | 0.00 | 0.26 |
| | NWI-1 | 0.18 | 0.34 | -0.21 | -0.32 | 0.02 | -0.53 |
| | NWI-2 | 0.20 | 0.33 | -0.19 | -0.31 | -0.28 | -0.57 |
| | NDVI hy | 0.07 | 0.08 | 0.34 | 0.45 | 0.49 | 0.50 |
| | GNDVI hy | 0.12 | 0.14 | 0.47 | 0.54 | 0.58 | 0.75 |
| | SIPI | -0.10 | 0.05 | 0.36 | 0.43 | 0.27 | 0.48 |
| | SRPI | 0.18 | -0.09 | 0.29 | 0.34 | 0.74 | 0.20 |
| | NPCI | -0.15 | 0.06 | -0.24 | -0.31 | -0.77 | -0.06 |
| | NPQI | -0.03 | -0.07 | -0.31 | -0.24 | -0.23 | -0.09 |
| | PSSRb | -0.20 | 0.12 | 0.39 | 0.62 | -0.02 | **0.80** |
| | PSNDb | -0.06 | 0.19 | 0.41 | 0.47 | 0.52 | 0.63 |
| | Rshoulder | -0.20 | 0.05 | 0.36 | 0.63 | -0.14 | 0.41 |
| | C420 | 0.17 | 0.01 | 0.28 | -0.40 | 0.51 | 0.22 |
| | NDI | -0.17 | 0.08 | 0.38 | 0.61 | -0.02 | 0.79 |
| | SR hyper | 0.00 | 0.10 | 0.50 | 0.57 | 0.40 | 0.47 |
| | R800-R550 | -0.18 | 0.13 | 0.43 | 0.63 | -0.03 | **0.80** |
| | R800/R550 | 0.06 | 0.14 | 0.51 | 0.58 | 0.55 | 0.77 |
| | R695/R760 | 0.03 | -0.19 | -0.36 | -0.45 | -0.56 | -0.63 |
| | R605/R760 | 0.07 | -0.17 | -0.40 | -0.47 | -0.53 | -0.66 |
| | R710/R760 | 0.12 | -0.13 | -0.44 | -0.50 | -0.69 | -0.72 |
| | R695/R670 | -0.04 | -0.08 | 0.33 | 0.49 | 0.13 | -0.35 |
| | R550 | -0.21 | -0.05 | 0.07 | 0.53 | -0.36 | -0.53 |
| | R675/R700 | -0.07 | -0.07 | -0.26 | -0.46 | -0.38 | 0.36 |
| | R675/(R700*R650) | 0.19 | 0.08 | -0.11 | -0.37 | 0.58 | 0.51 |
| | R672/(R55*R708) | 0.20 | 0.01 | -0.19 | -0.46 | -0.10 | 0.60 |
| | R672/R550 | 0.07 | -0.04 | -0.23 | -0.42 | -0.46 | 0.36 |
| | R860/(R550*R708) | 0.22 | 0.10 | 0.14 | 0.06 | 0.72 | 0.65 |
| | R750/R550 | 0.10 | 0.14 | 0.50 | 0.58 | 0.57 | 0.76 |
| | R750/R700 | -0.06 | 0.18 | 0.49 | 0.57 | 0.61 | 0.69 |
| | R725/R675 | -0.03 | 0.13 | 0.46 | 0.57 | 0.32 | 0.19 |
| | (R850-R710)/(R850-R680) | -0.25 | 0.11 | 0.32 | 0.35 | 0.33 | 0.71 |
| | (R780-R710)/(R780-R680) | -0.24 | 0.11 | 0.33 | 0.45 | 0.38 | 0.71 |
| | R700-R670 | -0.16 | -0.04 | 0.11 | 0.50 | -0.24 | -0.58 |
| | RNDVI | -0.03 | 0.13 | 0.34 | 0.46 | 0.50 | 0.51 |
| | PSR | 0.16 | -0.25 | -0.17 | -0.28 | -0.76 | -0.06 |
| | WBI | 0.21 | 0.16 | -0.06 | 0.03 | -0.34 | -0.52 |
| | SIPI | -0.20 | -0.13 | -0.14 | -0.29 | -0.63 | -0.32 |
| | YI | -0.09 | 0.22 | 0.40 | 0.51 | 0.07 | 0.39 |
| | VI2 | 0.20 | -0.06 | -0.35 | -0.62 | 0.16 | -0.13 |
| | Cgreen | 0.06 | 0.14 | 0.51 | 0.58 | 0.55 | 0.77 |
| | Cred edge | -0.08 | 0.17 | 0.50 | 0.57 | 0.62 | 0.70 |
| | C NIR | 0.11 | 0.07 | 0.42 | 0.51 | 0.40 | 0.78 |

**Table B2** - Coefficient of correlation for the relationship between different vegetation indices and grain yield of an Egyptian maize variety at different DAS in summer season of 2007. Highlighted values are significant (P<0.05) and bold values are the strongest correlations.

| Scale | Vegetation index | Grain yield (kg $m^{-2}$) | | | | | |
|---|---|---|---|---|---|---|---|
| | | 30 DAS | 45 DAS | 65 DAS | 80 DAS | 90 DAS | 105 DAS |
| Broad band | NDVI | 0.06 | 0.00 | 0.54 | 0.93 | 0.75 | 0.50 |
| | RVI | 0.06 | 0.04 | 0.73 | 0.89 | 0.67 | 0.50 |
| | SAVI | -0.34 | -0.17 | 0.58 | 0.87 | 0.30 | 0.62 |
| | GNDVI br | 0.03 | 0.10 | 0.64 | **0.94** | 0.67 | 0.58 |
| | DVI | -0.38 | -0.22 | 0.59 | 0.84 | 0.24 | 0.62 |
| | SR | 0.06 | 0.04 | 0.73 | 0.89 | 0.67 | 0.50 |
| | SLAVI | 0.06 | 0.00 | 0.54 | 0.93 | 0.75 | 0.50 |
| | OSAVI | -0.32 | -0.15 | 0.57 | 0.90 | 0.39 | 0.56 |
| | VI1 | 0.40 | 0.21 | -0.55 | -0.77 | -0.10 | 0.03 |
| | RDVI | 0.06 | 0.02 | 0.68 | 0.92 | 0.71 | 0.50 |
| | SI | -0.06 | 0.01 | -0.50 | -0.92 | -0.75 | -0.50 |
| | IPVI | 0.06 | 0.00 | 0.54 | 0.93 | 0.75 | 0.50 |
| Hyper | WI | 0.04 | 0.48 | 0.09 | -0.40 | -0.40 | -0.67 |
| | PSI | 0.02 | -0.45 | 0.46 | 0.61 | 0.28 | 0.35 |
| | NWI-1 | 0.36 | 0.12 | -0.41 | -0.56 | -0.11 | -0.58 |
| | NWI-2 | 0.42 | 0.28 | -0.39 | -0.68 | -0.44 | -0.62 |
| | NDVI hy | 0.02 | -0.24 | 0.50 | **0.93** | 0.74 | 0.48 |
| | GNDVI hy | 0.02 | 0.15 | 0.63 | **0.93** | 0.60 | 0.60 |
| | SIPI | -0.34 | 0.30 | 0.48 | **0.93** | 0.53 | 0.51 |
| | SRPI | -0.03 | -0.41 | 0.30 | 0.76 | 0.84 | 0.08 |
| | NPCI | -0.03 | 0.41 | -0.26 | -0.62 | -0.83 | 0.15 |
| | NPQI | 0.24 | -0.42 | 0.03 | -0.06 | -0.22 | -0.25 |
| | PSSRb | -0.37 | -0.15 | 0.60 | 0.83 | 0.24 | 0.61 |
| | PSNDb | 0.21 | 0.10 | 0.60 | **0.93** | 0.74 | 0.51 |
| | Rshoulder | -0.41 | -0.21 | 0.57 | 0.78 | 0.11 | 0.27 |
| | C420 | 0.29 | -0.35 | 0.14 | -0.37 | 0.42 | -0.01 |
| | NDI | -0.38 | -0.22 | 0.59 | 0.84 | 0.24 | 0.62 |
| | SR hyper | 0.06 | -0.18 | 0.72 | 0.88 | 0.62 | 0.45 |
| | R800-R550 | -0.42 | -0.10 | 0.64 | 0.80 | 0.21 | 0.63 |
| | R800/R550 | -0.13 | 0.10 | 0.67 | 0.90 | 0.58 | 0.62 |
| | R695/R760 | -0.02 | -0.11 | -0.55 | **-0.93** | -0.78 | -0.51 |
| | R605/R760 | 0.03 | -0.07 | -0.57 | **-0.93** | -0.74 | -0.52 |
| | R710/R760 | 0.39 | -0.04 | -0.62 | **-0.93** | -0.79 | -0.56 |
| | R695/R670 | -0.33 | -0.21 | 0.47 | 0.80 | 0.39 | -0.13 |
| | R550 | -0.40 | -0.23 | 0.21 | 0.57 | -0.11 | -0.47 |
| | R675/R700 | -0.27 | 0.01 | -0.37 | -0.89 | -0.66 | 0.15 |
| | R675/(R700*R650) | 0.41 | 0.22 | -0.22 | -0.10 | 0.41 | 0.38 |
| | R672/(R55*R708) | 0.25 | 0.22 | -0.31 | -0.80 | -0.39 | 0.43 |
| | R672/R550 | -0.04 | 0.18 | -0.37 | -0.90 | -0.73 | 0.19 |
| | R860/(R550*R708) | 0.36 | 0.17 | 0.14 | 0.46 | 0.63 | 0.51 |
| | R750/R550 | 0.07 | 0.07 | 0.67 | 0.91 | 0.62 | 0.61 |
| | R750/R700 | 0.00 | -0.03 | 0.72 | 0.92 | 0.76 | 0.54 |
| | R725/R675 | 0.14 | 0.04 | 0.66 | 0.88 | 0.58 | 0.25 |
| | (R850-R710)/(R850-R680) | -0.48 | 0.11 | 0.41 | 0.28 | 0.08 | 0.53 |
| | (R780-R710)/(R780-R680) | -0.52 | 0.18 | 0.44 | 0.56 | 0.15 | 0.53 |
| | R700-R670 | -0.39 | -0.13 | 0.23 | 0.75 | 0.04 | -0.43 |
| | RNDVI | -0.12 | -0.02 | 0.50 | **0.93** | 0.75 | 0.47 |
| | PSR | -0.05 | -0.13 | -0.14 | -0.59 | -0.82 | 0.15 |
| | WBI | 0.04 | 0.44 | -0.01 | -0.29 | -0.49 | -0.71 |
| | SIPI | 0.20 | 0.21 | -0.19 | -0.86 | -0.83 | -0.17 |
| | YI | -0.11 | 0.16 | 0.57 | 0.64 | 0.33 | 0.22 |
| | VI2 | 0.43 | 0.20 | -0.55 | -0.77 | -0.09 | -0.04 |
| | Cgreen | -0.13 | 0.10 | 0.67 | 0.90 | 0.58 | 0.62 |
| | Cred edge | -0.12 | 0.01 | 0.73 | 0.92 | 0.76 | 0.55 |
| | C NIR | 0.07 | -0.03 | 0.52 | 0.80 | 0.28 | 0.62 |

**Table B3-** Coefficient of correlation for the relationship between different vegetation indices and the aboveground biomass of an Egyptian maize variety at different DAS in summer season of 2007. Highlighted values are significant (P<0.05) and bold values are the strongest correlations.

| Scale | Vegetation index | Aboveground biomass (kg $m^{-2}$) | | | |
|---|---|---|---|---|---|
| | | 65 DAS | 80 DAS | 90 DAS | 105 DAS |
| Broad band | NDVI | 0.49 | 0.83 | 0.63 | 0.51 |
| | RVI | 0.67 | 0.79 | 0.53 | 0.50 |
| | SAVI | 0.54 | 0.78 | 0.14 | 0.68 |
| | GNDVI br | 0.60 | **0.85** | 0.59 | 0.62 |
| | DVI | 0.54 | 0.74 | 0.09 | 0.72 |
| | SR | 0.67 | 0.79 | 0.53 | 0.50 |
| | SLAVI | 0.49 | 0.83 | 0.63 | 0.51 |
| | OSAVI | 0.52 | 0.81 | 0.24 | 0.59 |
| | VI1 | -0.51 | -0.68 | 0.06 | -0.05 |
| | RDVI | 0.63 | 0.82 | 0.58 | 0.51 |
| | SI | -0.45 | -0.83 | -0.63 | -0.51 |
| | IPVI | 0.49 | 0.83 | 0.63 | 0.51 |
| Hyper | WI | 0.00 | -0.42 | -0.45 | -0.54 |
| | PSI | 0.37 | 0.60 | 0.14 | 0.23 |
| | NWI-1 | -0.30 | -0.52 | -0.06 | -0.45 |
| | NWI-2 | -0.28 | -0.62 | -0.40 | -0.48 |
| | NDVI hy | 0.44 | 0.83 | 0.62 | 0.46 |
| | GNDVI hy | 0.59 | **0.85** | 0.55 | 0.65 |
| | SIPI | 0.42 | **0.85** | 0.40 | 0.45 |
| | SRPI | 0.25 | 0.62 | 0.80 | 0.14 |
| | NPCI | -0.21 | -0.51 | -0.79 | 0.01 |
| | NPQI | 0.05 | 0.16 | -0.29 | -0.19 |
| | PSSRb | 0.56 | 0.73 | 0.08 | 0.71 |
| | PSNDb | 0.55 | 0.83 | 0.63 | 0.54 |
| | Rshoulder | 0.52 | 0.69 | -0.04 | 0.38 |
| | C420 | 0.18 | -0.40 | 0.43 | 0.12 |
| | NDI | 0.54 | 0.74 | 0.09 | 0.72 |
| | SR hyper | 0.66 | 0.77 | 0.48 | 0.43 |
| | R800-R550 | 0.59 | 0.71 | 0.06 | 0.72 |
| | R800/R550 | 0.63 | 0.81 | 0.53 | 0.66 |
| | R695/R760 | -0.49 | -0.83 | -0.67 | -0.54 |
| | R605/R760 | -0.52 | -0.84 | -0.63 | -0.57 |
| | R710/R760 | -0.59 | -0.84 | -0.74 | -0.62 |
| | R695/R670 | 0.40 | 0.70 | 0.25 | -0.26 |
| | R550 | 0.18 | 0.53 | -0.25 | -0.46 |
| | R675/R700 | -0.31 | -0.80 | -0.52 | 0.27 |
| | R675/(R700*R650) | -0.16 | -0.15 | 0.52 | 0.40 |
| | R672/(R55*R708) | -0.27 | -0.73 | -0.25 | 0.48 |
| | R672/R550 | -0.32 | -0.80 | -0.61 | 0.29 |
| | R860/(R550*R708) | 0.15 | 0.41 | 0.67 | 0.53 |
| | R750/R550 | 0.63 | 0.82 | 0.55 | 0.65 |
| | R750/R700 | 0.67 | 0.82 | 0.66 | 0.58 |
| | R725/R675 | 0.60 | 0.78 | 0.41 | 0.19 |
| | (R850-R710)/(R850-R680) | 0.43 | 0.27 | 0.18 | 0.61 |
| | (R780-R710)/(R780-R680) | 0.45 | 0.53 | 0.25 | 0.61 |
| | R700-R670 | 0.19 | 0.67 | -0.11 | -0.48 |
| | RNDVI | 0.44 | 0.83 | 0.63 | 0.46 |
| | PSR | -0.10 | -0.46 | -0.79 | 0.01 |
| | WBI | -0.09 | -0.36 | -0.55 | -0.59 |
| | SIPI | -0.12 | -0.76 | -0.77 | -0.27 |
| | YI | 0.54 | 0.63 | 0.17 | 0.28 |
| | VI2 | -0.51 | -0.68 | 0.06 | -0.13 |
| | Cgreen | 0.63 | 0.81 | 0.53 | 0.66 |
| | Cred edge | 0.68 | 0.81 | 0.66 | 0.59 |
| | C NIR | 0.50 | 0.73 | 0.32 | 0.69 |

**Table B4-** Coefficient of correlation for the relationship between different vegetation indices and the plant height of an Egyptian maize variety at different DAS in summer season of 2007. Highlighted values are significant (P<0.05) and bold values are the strongest correlations.

| Scale | Vegetation index | Plant height (m) | | | | | |
|---|---|---|---|---|---|---|---|
| | | 30 DAS | 45 DAS | 65 DAS | 80 DAS | 90 DAS | 105 DAS |
| Broad band | NDVI | -0.05 | -0.25 | 0.39 | 0.71 | 0.72 | 0.55 |
| | RVI | -0.07 | -0.25 | 0.57 | **0.82** | 0.65 | 0.55 |
| | SAVI | -0.12 | -0.27 | 0.39 | 0.77 | 0.29 | 0.69 |
| | GNDVI br | -0.09 | -0.13 | 0.55 | 0.80 | 0.71 | 0.65 |
| | DVI | -0.11 | -0.25 | 0.39 | 0.78 | 0.24 | 0.70 |
| | SR | -0.07 | -0.25 | 0.57 | **0.82** | 0.65 | 0.55 |
| | SLAVI | -0.05 | -0.25 | 0.39 | 0.71 | 0.72 | 0.55 |
| | OSAVI | -0.12 | -0.28 | 0.38 | 0.76 | 0.39 | 0.63 |
| | VI1 | 0.11 | 0.21 | -0.35 | -0.75 | -0.09 | 0.01 |
| | RDVI | -0.06 | -0.25 | 0.52 | 0.78 | 0.68 | 0.55 |
| | SI | 0.04 | 0.25 | -0.35 | -0.67 | -0.72 | -0.55 |
| | IPVI | -0.05 | -0.25 | 0.39 | 0.71 | 0.72 | 0.55 |
| Hyper | WI | -0.14 | -0.02 | 0.05 | -0.47 | -0.44 | -0.64 |
| | PSI | 0.08 | -0.07 | 0.27 | 0.52 | 0.21 | 0.30 |
| | NWI-1 | -0.01 | 0.14 | -0.23 | -0.49 | -0.17 | -0.61 |
| | NWI-2 | -0.04 | 0.12 | -0.21 | -0.54 | -0.47 | -0.64 |
| | NDVI hy | 0.00 | -0.27 | 0.34 | 0.69 | 0.71 | 0.51 |
| | GNDVI hy | -0.06 | -0.12 | 0.56 | 0.82 | 0.67 | 0.67 |
| | SIPI | 0.00 | -0.01 | 0.35 | 0.74 | 0.49 | 0.54 |
| | SRPI | 0.02 | -0.16 | 0.26 | 0.53 | 0.82 | 0.14 |
| | NPCI | -0.05 | 0.14 | -0.22 | -0.47 | -0.80 | 0.09 |
| | NPQI | -0.02 | -0.01 | 0.04 | 0.20 | -0.25 | -0.20 |
| | PSSRb | -0.14 | -0.26 | 0.40 | 0.78 | 0.23 | 0.70 |
| | PSNDb | -0.15 | -0.18 | 0.45 | 0.71 | 0.73 | 0.58 |
| | Rshoulder | -0.11 | -0.22 | 0.36 | 0.75 | 0.11 | 0.32 |
| | C420 | -0.02 | 0.09 | 0.29 | -0.16 | 0.44 | 0.07 |
| | NDI | -0.11 | -0.25 | 0.39 | 0.78 | 0.24 | 0.70 |
| | SR hyper | -0.02 | -0.29 | 0.55 | 0.80 | 0.59 | 0.48 |
| | R800-R550 | -0.12 | -0.25 | 0.45 | 0.79 | 0.22 | 0.71 |
| | R800/R550 | -0.09 | -0.14 | 0.59 | **0.86** | 0.64 | 0.70 |
| | R695/R760 | 0.07 | 0.17 | -0.40 | -0.68 | -0.76 | -0.57 |
| | R605/R760 | 0.24 | 0.19 | -0.45 | -0.70 | -0.74 | -0.59 |
| | R710/R760 | 0.05 | 0.17 | -0.53 | -0.77 | -0.83 | -0.64 |
| | R695/R670 | 0.11 | -0.13 | 0.31 | 0.60 | 0.32 | -0.19 |
| | R550 | -0.08 | -0.08 | 0.03 | 0.50 | -0.13 | -0.52 |
| | R675/R700 | -0.01 | 0.12 | -0.20 | -0.64 | -0.59 | 0.23 |
| | R675/(R700*R650) | 0.07 | 0.08 | -0.01 | -0.16 | 0.43 | 0.45 |
| | R672/(R55*R708) | 0.04 | 0.17 | -0.13 | -0.55 | -0.33 | 0.52 |
| | R672/R550 | -0.05 | 0.18 | -0.20 | -0.62 | -0.66 | 0.26 |
| | R860/(R550*R708) | 0.07 | 0.03 | 0.29 | 0.45 | 0.66 | 0.59 |
| | R750/R550 | -0.13 | -0.15 | 0.59 | 0.85 | 0.67 | 0.69 |
| | R750/R700 | -0.05 | -0.19 | 0.58 | 0.84 | 0.76 | 0.61 |
| | R725/R675 | -0.03 | -0.18 | 0.49 | 0.77 | 0.52 | 0.25 |
| | (R850-R710)/(R850-R680) | -0.11 | -0.07 | 0.45 | 0.56 | 0.20 | 0.62 |
| | (R780-R710)/(R780-R680) | 0.02 | -0.06 | 0.47 | 0.72 | 0.27 | 0.62 |
| | R700-R670 | -0.03 | -0.09 | 0.06 | 0.56 | 0.00 | -0.50 |
| | RNDVI | 0.03 | -0.23 | 0.34 | 0.69 | 0.71 | 0.51 |
| | PSR | 0.08 | -0.02 | -0.14 | -0.43 | -0.81 | 0.09 |
| | WBI | -0.13 | -0.04 | 0.00 | -0.45 | -0.52 | -0.67 |
| | SIPI | -0.08 | 0.04 | -0.10 | -0.56 | -0.80 | -0.22 |
| | YI | -0.17 | -0.11 | 0.42 | 0.80 | 0.30 | 0.30 |
| | VI2 | 0.11 | 0.21 | -0.35 | -0.75 | -0.10 | -0.06 |
| | Cgreen | -0.09 | -0.14 | 0.59 | **0.86** | 0.64 | 0.70 |
| | Cred edge | -0.04 | -0.17 | 0.59 | 0.84 | 0.76 | 0.62 |
| | C NIR | -0.05 | -0.11 | 0.52 | 0.85 | 0.41 | 0.71 |

**Table B5-** Coefficient of correlation for the relationship between different vegetation indices and the plant water content of maize leaves at different DAS in summer season of 2007. Highlighted values are significant (P<0.05) and bold values are the strongest correlations.

| Scale | Vegetation index | Plant water content (%) | | | |
|---|---|---|---|---|---|
| | | 65 DAS | 80 DAS | 90 DAS | 105 DAS |
| Broad band | NDVI | 0.37 | 0.48 | **0.75** | 0.39 |
| | RVI | 0.57 | 0.56 | 0.66 | 0.38 |
| | SAVI | 0.38 | 0.60 | 0.39 | 0.49 |
| | GNDVI br | 0.53 | 0.48 | 0.59 | 0.45 |
| | DVI | 0.37 | 0.60 | 0.34 | 0.49 |
| | SR | 0.57 | 0.56 | 0.66 | 0.38 |
| | SLAVI | 0.37 | 0.48 | **0.75** | 0.39 |
| | OSAVI | 0.37 | 0.58 | 0.47 | 0.44 |
| | VI1 | -0.34 | -0.61 | -0.21 | 0.04 |
| | RDVI | 0.52 | 0.54 | 0.70 | 0.39 |
| | SI | -0.33 | -0.46 | **-0.75** | -0.39 |
| | IPVI | 0.37 | 0.48 | **0.75** | 0.39 |
| Hyper | WI | -0.02 | 0.09 | -0.45 | -0.57 |
| | PSI | 0.30 | 0.54 | 0.35 | 0.22 |
| | NWI-1 | -0.20 | -0.20 | -0.15 | -0.47 |
| | NWI-2 | -0.17 | -0.34 | -0.47 | -0.50 |
| | NDVI hy | 0.32 | 0.48 | 0.76 | 0.37 |
| | GNDVI hy | 0.53 | 0.47 | 0.49 | 0.47 |
| | SIPI | 0.33 | 0.39 | 0.57 | 0.42 |
| | SRPI | 0.22 | 0.31 | 0.76 | 0.04 |
| | NPCI | -0.19 | -0.30 | -0.71 | 0.17 |
| | NPQI | 0.02 | -0.29 | -0.31 | -0.21 |
| | PSSRb | 0.39 | 0.60 | 0.33 | 0.48 |
| | PSNDb | 0.44 | 0.50 | 0.73 | 0.39 |
| | Rshoulder | 0.35 | 0.61 | 0.22 | 0.21 |
| | C420 | 0.15 | -0.53 | 0.26 | -0.04 |
| | NDI | 0.37 | 0.60 | 0.34 | 0.49 |
| | SR hyper | 0.55 | 0.57 | 0.63 | 0.35 |
| | R800-R550 | 0.43 | 0.59 | 0.29 | 0.50 |
| | R800/R550 | 0.56 | 0.48 | 0.47 | 0.50 |
| | R695/R760 | -0.37 | -0.47 | **-0.77** | -0.38 |
| | R605/R760 | -0.41 | -0.47 | -0.72 | -0.40 |
| | R710/R760 | -0.49 | -0.46 | -0.72 | -0.44 |
| | R695/R670 | 0.35 | 0.58 | 0.48 | -0.07 |
| | R550 | 0.04 | 0.66 | 0.05 | -0.38 |
| | R675/R700 | -0.21 | -0.53 | -0.69 | 0.11 |
| | R675/(R700*R650) | -0.01 | -0.54 | 0.24 | 0.28 |
| | R672/(R55*R708) | -0.10 | -0.61 | -0.50 | 0.35 |
| | R672/R550 | -0.19 | -0.49 | -0.76 | 0.16 |
| | R860/(R550*R708) | 0.28 | -0.14 | 0.45 | 0.41 |
| | R750/R550 | 0.55 | 0.48 | 0.52 | 0.49 |
| | R750/R700 | 0.55 | 0.50 | 0.70 | 0.42 |
| | R725/R675 | 0.51 | 0.57 | 0.60 | 0.19 |
| | (R850-R710)/(R850-R680) | 0.44 | 0.08 | -0.06 | 0.42 |
| | (R780-R710)/(R780-R680) | 0.45 | 0.23 | 0.01 | 0.41 |
| | R700-R670 | 0.08 | 0.63 | 0.18 | -0.33 |
| | RNDVI | 0.32 | 0.49 | 0.76 | 0.37 |
| | PSR | -0.10 | -0.26 | -0.72 | 0.17 |
| | WBI | -0.09 | 0.25 | -0.53 | -0.62 |
| | SIPI | 0.00 | -0.35 | -0.82 | -0.10 |
| | YI | 0.46 | 0.17 | 0.41 | 0.16 |
| | VI2 | -0.34 | -0.62 | -0.21 | -0.02 |
| | Cgreen | 0.56 | 0.48 | 0.47 | 0.50 |
| | Cred edge | 0.56 | 0.49 | 0.69 | 0.43 |
| | C NIR | 0.51 | 0.36 | 0.17 | 0.50 |

**Table B6**- Coefficient of correlation for the relationship between different vegetation indices and the LAI of an Egyptian maize variety at different DAS in summer season of 2007. Highlighted values are significant (P<0.05) and bold values are the strongest correlations.

| Scale | Vegetation index | Leaf area index | | | |
|---|---|---|---|---|---|
| | | 65 DAS | 80 DAS | 90 DAS | 105 DAS |
| Broad band | NDVI | 0.32 | 0.90 | 0.85 | 0.49 |
| | RVI | 0.54 | 0.82 | 0.81 | 0.48 |
| | SAVI | 0.37 | 0.80 | 0.82 | 0.63 |
| | GNDVI br | 0.52 | **0.91** | 0.9 | 0.60 |
| | DVI | 0.38 | 0.76 | 0.74 | 0.63 |
| | SR | 0.54 | 0.82 | 0.81 | 0.48 |
| | SLAVI | 0.32 | 0.90 | 0.85 | 0.49 |
| | OSAVI | 0.34 | 0.85 | 0.84 | 0.56 |
| | VI1 | -0.35 | -0.69 | -0.21 | 0.01 |
| | RDVI | 0.48 | 0.87 | 0.84 | 0.49 |
| | SI | -0.28 | -0.89 | -0.85 | -0.49 |
| | IPVI | 0.32 | 0.90 | 0.85 | 0.49 |
| Hyper | WI | -0.10 | -0.39 | -0.56 | -0.61 |
| | PSI | 0.20 | 0.57 | 0 | 0.34 |
| | NWI-1 | -0.11 | -0.53 | -0.63 | -0.50 |
| | NWI-2 | -0.08 | -0.65 | -0.64 | -0.53 |
| | NDVI hy | 0.26 | 0.89 | 0.84 | 0.44 |
| | GNDVI hy | 0.54 | 0.90 | 0.9 | 0.62 |
| | SIPI | 0.25 | 0.90 | 0.9 | 0.45 |
| | SRPI | 0.23 | 0.73 | 0.81 | 0.13 |
| | NPCI | -0.20 | -0.62 | -0.67 | 0.05 |
| | NPQI | 0.06 | 0.10 | 0.68 | -0.17 |
| | PSSRb | 0.40 | 0.74 | 0.75 | 0.64 |
| | PSNDb | 0.40 | 0.89 | 0.85 | 0.53 |
| | Rshoulder | 0.36 | 0.70 | 0.49 | 0.30 |
| | C420 | 0.29 | -0.41 | 0.57 | 0.10 |
| | NDI | 0.38 | 0.76 | 0.74 | 0.63 |
| | SR hyper | 0.53 | 0.81 | 0.79 | 0.40 |
| | R800-R550 | 0.45 | 0.72 | 0.81 | 0.66 |
| | R800/R550 | 0.57 | 0.86 | 0.88 | 0.62 |
| | R695/R760 | -0.33 | -0.90 | -0.84 | -0.53 |
| | R605/R760 | -0.38 | -0.90 | -0.87 | -0.55 |
| | R710/R760 | -0.50 | **-0.91** | -0.85 | -0.59 |
| | R695/R670 | 0.24 | 0.74 | 0.78 | -0.24 |
| | R550 | 0.01 | 0.51 | -0.79 | -0.48 |
| | R675/R700 | -0.11 | -0.85 | -0.79 | 0.24 |
| | R675/(R700*R650) | 0.07 | -0.08 | 0.82 | 0.40 |
| | R672/(R55*R708) | -0.05 | -0.78 | -0.16 | 0.47 |
| | R672/R550 | -0.13 | -0.86 | -0.71 | 0.27 |
| | R860/(R550*R708) | 0.31 | 0.48 | 0.81 | 0.51 |
| | R750/R550 | 0.56 | 0.86 | 0.88 | 0.62 |
| | R750/R700 | 0.55 | 0.86 | 0.8 | 0.55 |
| | R725/R675 | 0.46 | 0.81 | 0.8 | 0.19 |
| | (R850-R710)/(R850-R680) | 0.52 | 0.28 | 0.82 | 0.58 |
| | (R780-R710)/(R780-R680) | 0.52 | 0.56 | 0.83 | 0.58 |
| | R700-R670 | 0.02 | 0.69 | -0.11 | -0.48 |
| | RNDVI | 0.26 | 0.90 | 0.84 | 0.45 |
| | PSR | -0.12 | -0.58 | -0.71 | 0.05 |
| | WBI | -0.15 | -0.32 | -0.6 | -0.67 |
| | SIPI | -0.03 | -0.84 | -0.78 | -0.21 |
| | YI | 0.42 | 0.61 | -0.72 | 0.29 |
| | VI2 | -0.35 | -0.69 | -0.2 | -0.06 |
| | Cgreen | 0.57 | 0.86 | 0.88 | 0.62 |
| | Cred edge | 0.56 | 0.86 | 0.8 | 0.56 |
| | C NIR | 0.55 | 0.78 | 0.84 | 0.63 |

**Table B7**- The relationship between the rededge position and the measured chlorophyll *a* concentration extreacted from Egyptian maize leaves collecteed at different DAS in summer season of 2007. Highlighted values are significant (P<0.05) and bold values are the strongest correlations.

| Treatment | Replicates | Days after sowing | | | | | | | | | | | |
|---|---|---|---|---|---|---|---|---|---|---|---|---|---|
| | | 30 DAS | | 45 DAS | | 65 DAS | | 80 DAS | | 90 DAS | | 105 | |
| | | Rededge | Chl a | Rededge | Chl a | Rededge | Chl a | Rededge | Chl a | Rededge | Chl a | Rededge | Chl a |
| T1 | R1 | 707.7 | 40.77 | 714.8 | 47.45 | 726.1 | 45.07 | 729.4 | 44.20 | 720.3 | 62.91 | 724.5 | 61.41 |
| | R2 | 704.4 | 37.53 | 710.4 | 39.58 | 721 | 42.60 | 725 | 47.61 | 719.1 | 58.12 | 726.1 | 59.52 |
| | R3 | 704.6 | 41.63 | 712 | 44.02 | 722.7 | 41.82 | 727.9 | 43.20 | 719.8 | 55.31 | 723.4 | 57.40 |
| T2 | R1 | 702.7 | 40.23 | 706.3 | 33.53 | 722.1 | 43.15 | 725.2 | 47.82 | 719.6 | 52.92 | 721.8 | 48.48 |
| | R2 | 706.8 | 38.69 | 715.2 | 35.06 | 721.6 | 40.80 | 728.2 | 42.41 | 719.3 | 50.49 | 720.9 | 45.94 |
| | R3 | 705.1 | 36.67 | 712.2 | 30.96 | 720.2 | 41.30 | 722.5 | 40.43 | 716.6 | 51.79 | 726.3 | 43.68 |
| T3 | R1 | 709.2 | 40.47 | 705.3 | 27.34 | 711.9 | 36.50 | 715 | 34.17 | 708.4 | 28.47 | 719.6 | 29.39 |
| | R2 | 707.1 | 37.73 | 714.2 | 26.76 | 712.4 | 35.20 | 718.5 | 30.55 | 705.6 | 32.84 | 718 | 29.70 |
| | R3 | 708.7 | 35.68 | 716.4 | 26.82 | 712.1 | 33.14 | 719.4 | 31.84 | 708.5 | 34.45 | 718.2 | 32.16 |
| T4 | R1 | 712.6 | 40.64 | 708.5 | 26.45 | 711.8 | 30.15 | 730.5 | 31.09 | 702.3 | 29.56 | 712.2 | 26.00 |
| | R2 | 704.6 | 39.61 | 713.2 | 30.96 | 714.2 | 29.41 | 727.6 | 29.86 | 700.6 | 33.63 | 711.1 | 25.39 |
| | R3 | 711.7 | 38.55 | 715.2 | 34.38 | 708.2 | 32.66 | 727.7 | 30.24 | 702.2 | 26.31 | 713 | 27.92 |
| T5 | R1 | 708.8 | 35.30 | 716.8 | 36.14 | 721.3 | 39.15 | 724.5 | 38.41 | 715.7 | 49.98 | 726.6 | 49.30 |
| | R2 | 708.7 | 41.01 | 714.7 | 39.65 | 721.8 | 40.64 | 716.4 | 39.13 | 710.6 | 55.35 | 721.9 | 47.14 |
| | R3 | 707.1 | 41.29 | 709.6 | 45.56 | 723.2 | 141.30 | 714.7 | 41.66 | 713.5 | 54.90 | 723.3 | 51.11 |
| T6 | R1 | 711.3 | 42.17 | 710.4 | 36.64 | 712.6 | 37.30 | 710.2 | 33.90 | 708.3 | 41.87 | 720.3 | 37.36 |
| | R2 | 716.4 | 40.77 | 704.3 | 35.89 | 715 | 36.40 | 704.2 | 36.77 | 708.9 | 34.89 | 718.6 | 34.44 |
| | R3 | 714.8 | 37.11 | 715.5 | 35.00 | 717.4 | 38.15 | 705.6 | 35.54 | 709.7 | 45.09 | 721.8 | 39.07 |
| T7 | R1 | 714.8 | 39.10 | 707.7 | 28.77 | 702 | 37.33 | 702.6 | 25.92 | 697.6 | 32.02 | 715.4 | 25.97 |
| | R2 | 712 | 37.53 | 700.5 | 33.15 | 705.1 | 34.56 | 712.7 | 25.58 | 696.7 | 25.67 | 714.7 | 24.12 |
| | R3 | 705.9 | 37.73 | 710 | 31.85 | 703.5 | 37.19 | 714.1 | 26.58 | 696 | 35.00 | 714 | 31.20 |
| T8 | R1 | 705.4 | 35.47 | 705.1 | 31.85 | 705 | 30.25 | 713.6 | 24.49 | 695.5 | 33.49 | 712.1 | 28.12 |
| | R2 | 717.6 | 40.84 | 703.2 | 27.26 | 701.3 | 27.90 | 705.3 | 23.15 | 695.7 | 32.02 | 714.1 | 29.42 |
| | R3 | 714.1 | 34.76 | 709.6 | 26.58 | 701.8 | 29.25 | 712.5 | 21.71 | 695.6 | 24.57 | 707.8 | 24.29 |
| T9 | R1 | 711.9 | 41.60 | 712 | 27.85 | 711.2 | 26.46 | 715.7 | 23.15 | 696.5 | 25.63 | 711.9 | 21.96 |
| | R2 | 709.2 | 38.55 | 712 | 24.16 | 709.3 | 22.95 | 708.6 | 24.01 | 695.8 | 36.03 | 705.6 | 20.39 |
| | R3 | 703.3 | 37.73 | 718.4 | 25.29 | 710.6 | 24.03 | 707.7 | 28.83 | 696.5 | 24.94 | 709.9 | 23.54 |
| T10 | R1 | 701.7 | 39.95 | 714.1 | 35.54 | 721.5 | 33.76 | 709.5 | 38.51 | 707 | 41.11 | 720.8 | 43.48 |
| | R2 | 707.8 | 40.87 | 718.2 | 37.63 | 714 | 35.75 | 724.1 | 35.27 | 706.8 | 42.52 | 719.7 | 35.20 |
| | R3 | 712.5 | 41.63 | 714.2 | 34.66 | 712.8 | 32.92 | 722.8 | 36.22 | 709.2 | 44.09 | 717.5 | 41.63 |
| T11 | R1 | 707.5 | 36.16 | 707.9 | 28.32 | 709 | 26.91 | 709 | 28.43 | 697.5 | 22.27 | 712.5 | 24.25 |
| | R2 | 710.5 | 34.55 | 709 | 30.17 | 713.4 | 28.66 | 705 | 25.38 | 696.5 | 25.63 | 706.5 | 24.32 |
| | R3 | 707.5 | 39.61 | 711 | 31.47 | 707.9 | 29.90 | 702.5 | 27.50 | 697.3 | 26.86 | 711.3 | 22.99 |
| r | | **0.08** | | **0.17** | | **0.43** | | **0.54** | | **0.88** | | **0.87** | |

# APPENDIX C

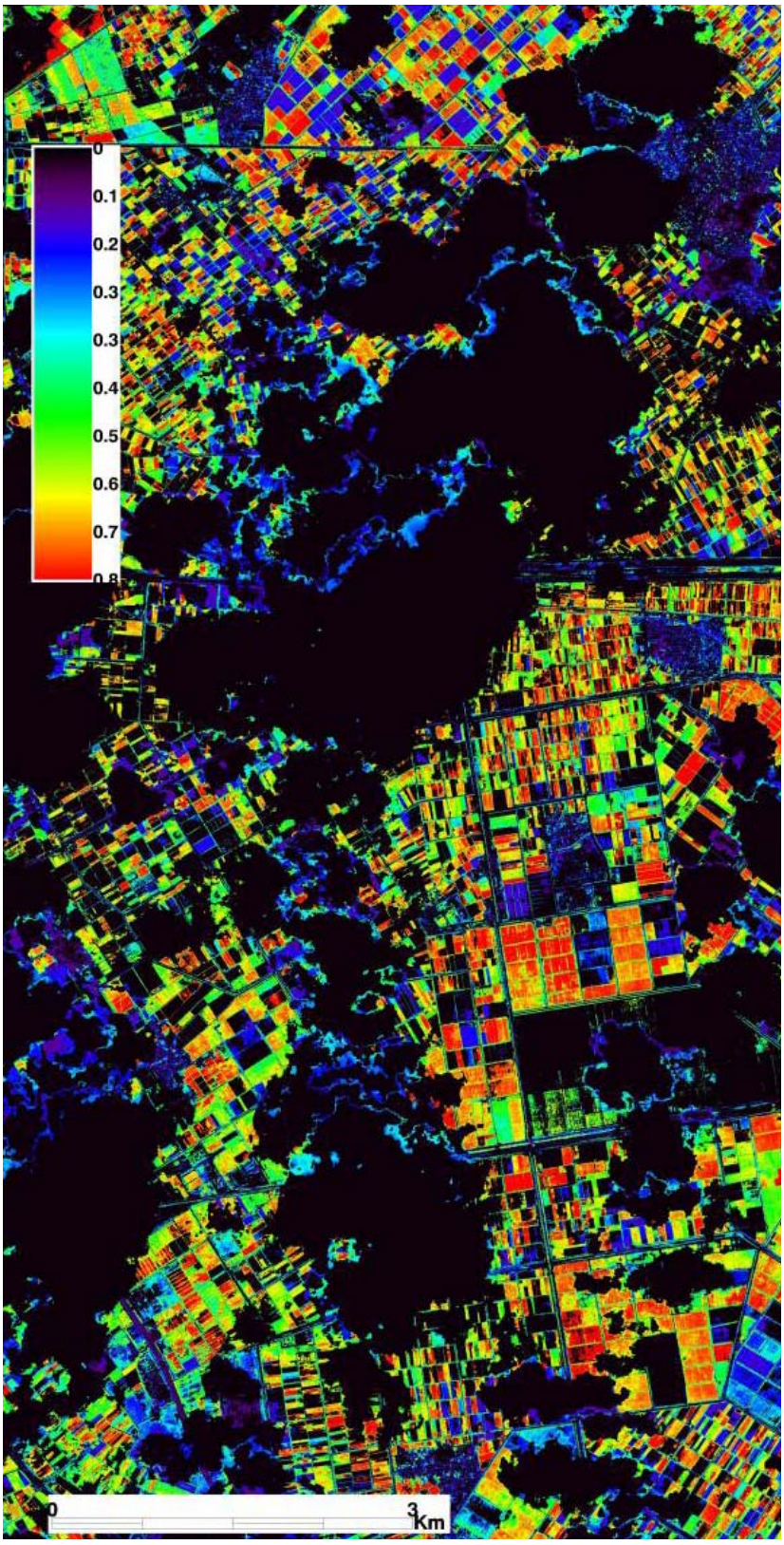


**Figure C1**: NDVI map derived from QuickBird image acquired on 7th April 2007 for wheat crops in south-west Alexandria, Egypt.

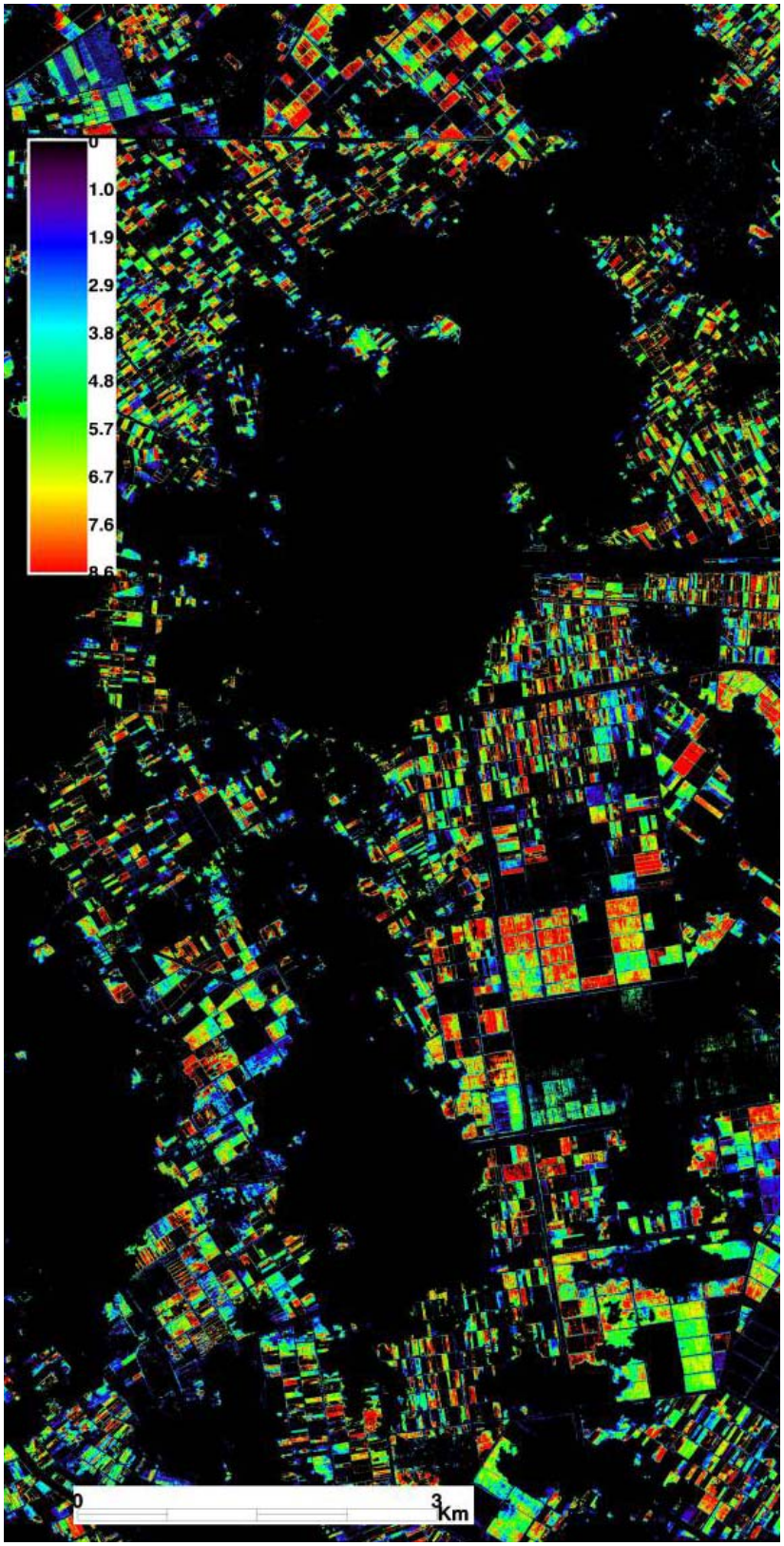


**Figure C2:** DVI map derived from QuickBird image acquired on 7th April for wheat crops in south-west Alexandria, Egypt.

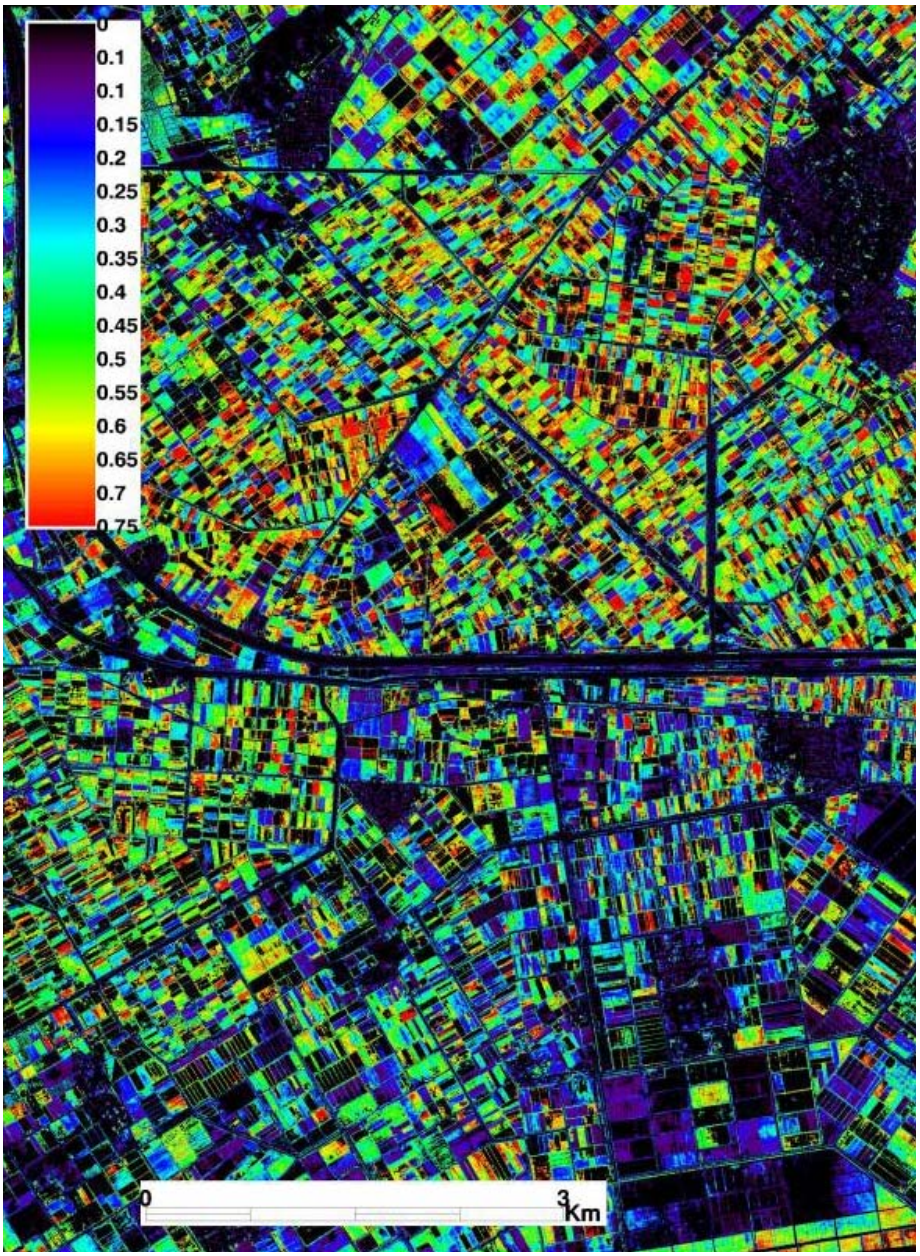


**Figure C3:** NDVI map derived from QuickBird image acquired on 29th June for maize crops in south-west Alexandria, Egypt.

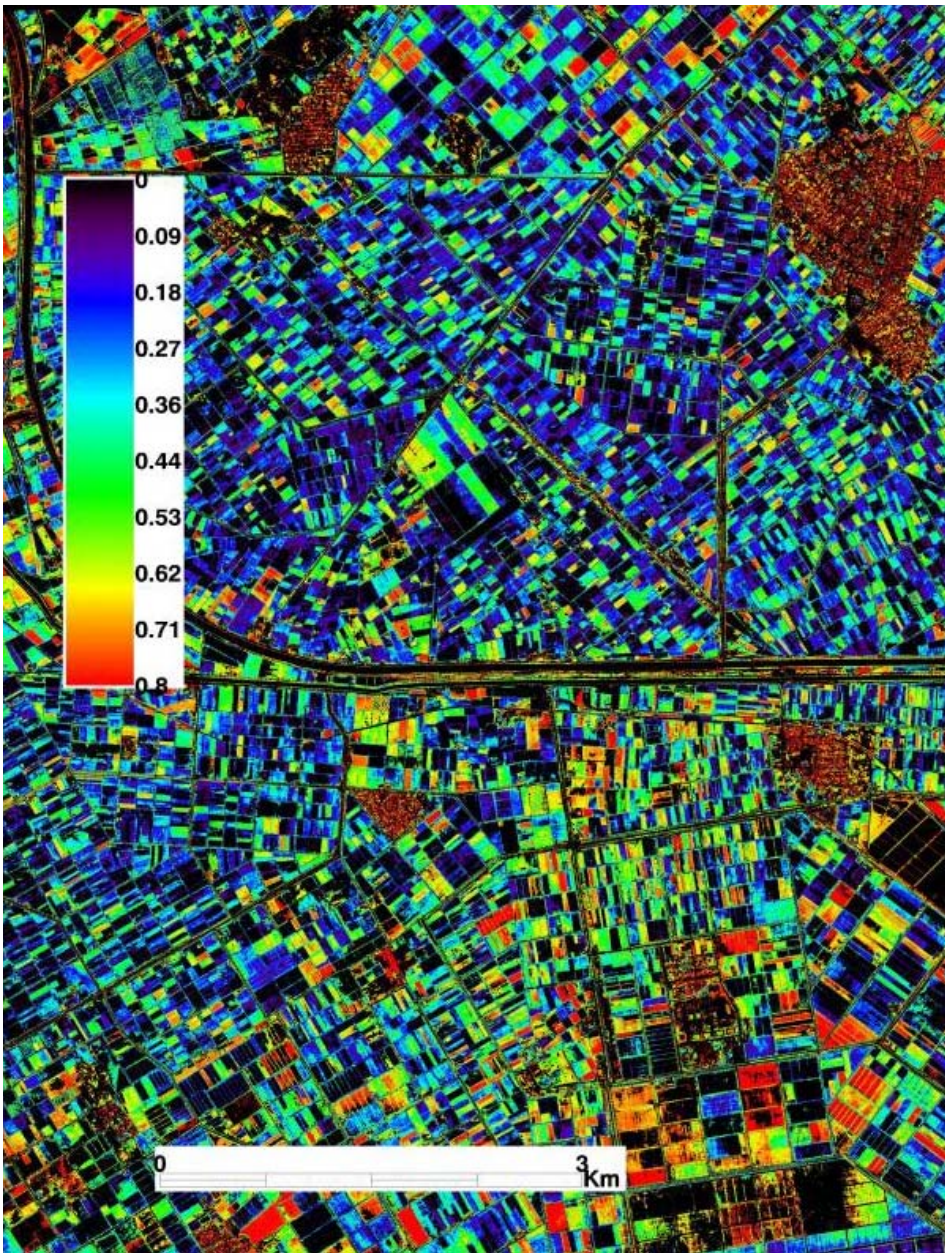


**Figure C4:** SI map derived from QuickBird image acquired on 29th June for maize crops in south-west Alexandria, Egypt.

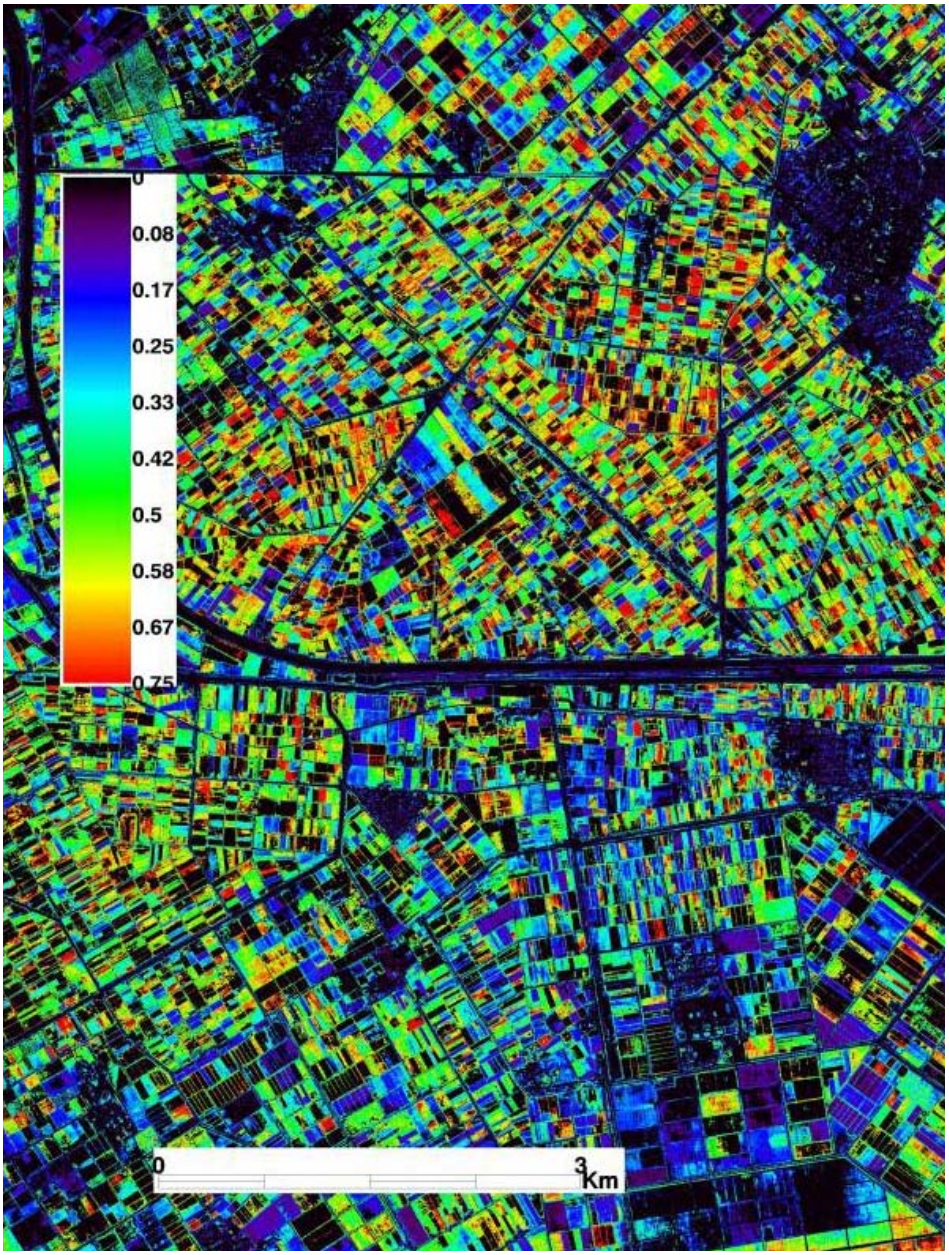


**Figure C5:** $GNDVI_{br}$ map derived from QuickBird image acquired on 29th June for maize crops in south-west Alexandria, Egypt.

# APPENDIX D

## Converting radiance to reflectance

Following the simple dark pixel subtraction technique, an attempt was made to convert radiance to reflectance by matching pixels with *in situ* spectra. Radiance in each band from the QuickBird image was derived via specific ROIs in ENVI. The reflectance obtained from *in situ* hyperspectral survey at each location within the same field was averaged to simulate the bands of QuickBird image (four spectral bands). The dataset collected from the Hewaihy site on 28$^{th}$ March was used for this analysis since at the Kahr site more than half of the fields of *in situ* hyperspectral survey were covered by clouds and associated shadows. The regression analysis was performed to investigate the relationship between reflectance and radiance in every band. The results showed non-significant relationships between reflectance obtained from *in situ* hyperspectral survey and radiance obtained from QuickBird satellite image as p values were non-significant in bands 1, 3, and 4 ($p = 0.41$, 0.37, 0.89 respectively) and very low coefficient of determination values in these three bands ($R^2 = 0.050$, 0.060, and 0.002). Only band 3 data gave low significant relationship ($R^2 = 0.37$; $p = 0.017$).

The regression analysis was also performed on the dataset collected from the Hewaihy site on the 12$^{th}$ March. Same trends of the 28$^{th}$ dataset were observed as the coefficient of determination values was 0.001, 0.230, 0.090, and 0.05 in bands 1, 2, 3, and 4 respectively. Figure 6.25 shows the relationship between reflectance derived from *in situ* hyperspectral measurements and radiance derived from QuickBird satellite image in different band. The results therefore suggest that it is difficult to convert radiance to reflectance through the relationship between reflectance obtained from *in situ* hyperspectral and radiance obtained from QuickBird satellite image. Lots of reflectance data from many fixed ground control points such as roads are needed to convert radiance to reflectance.

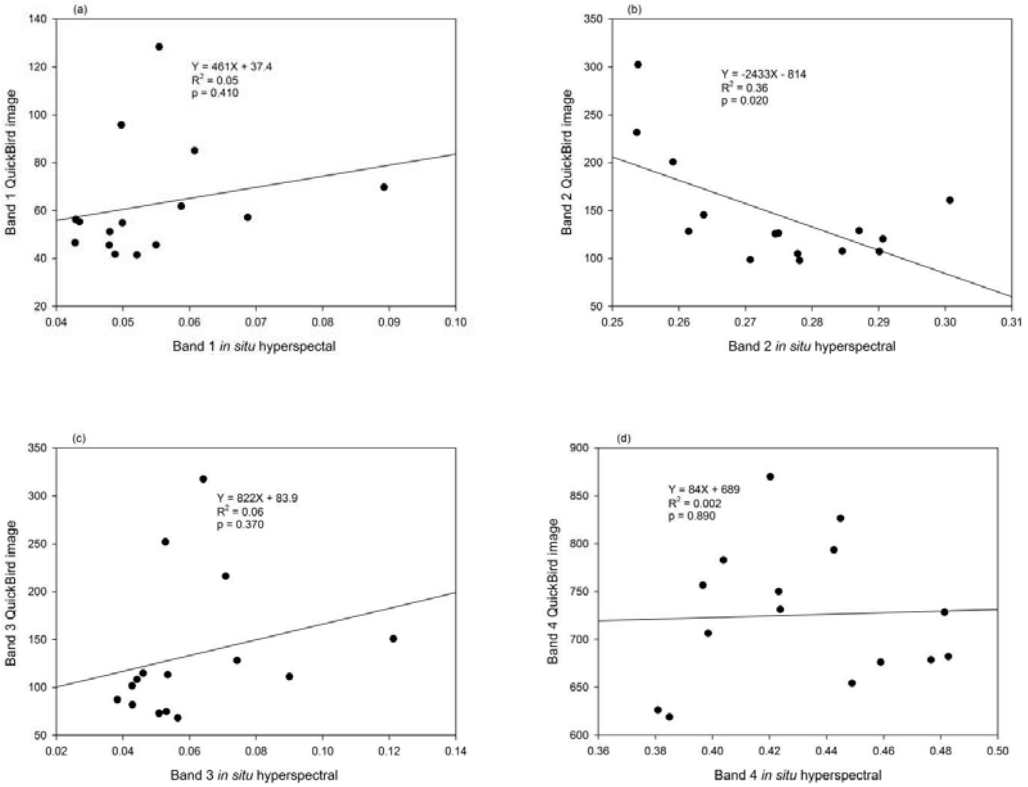


**Figure D1:** The relationship between reflectance obtained from *in situ* hyperspectral survey and radiance obtained from QuickBird satellite image in (a) band 1, (b) band 2, (c) band 3 and (d) band 4 (n = 15).